Stem Cells International

Engineering Cell Systems

Lead Guest Editor: Tiago Fernandes
Guest Editors: Ricardo Baptista and Howard Kim

Engineering Cell Systems

Stem Cells International

Engineering Cell Systems

Lead Guest Editor: Tiago Fernandes
Guest Editors: Ricardo Baptista and Howard Kim

Editorial Board

Contents

Hindawi
Stem Cells International
Volume 2019, Article ID 4685137, 3 pages
https://doi.org/10.1155/2019/4685137

Editorial
Engineering Cell Systems

Tiago G. Fernandes[1,2] **Ricardo P. Baptista,**[3] **and Howard Kim**[4]

[1]*iBB-Institute for Bioengineering and Biosciences and Department of Bioengineering, Instituto Superior Técnico, Universidade de Lisboa, Av. Rovisco Pais, 1049-001 Lisbon, Portugal*
[2]*The Discoveries Centre for Regenerative and Precision Medicine (Lisbon Campus), Instituto Superior Técnico, Universidade de Lisboa, Av. Rovisco Pais, 1049-001 Lisbon, Portugal*
[3]*Cell and Gene Therapy Catapult, 12th floor Guy's Hospital, Great Maze Pond, London SE1 9RT, UK*
[4]*The New York Stem Cell Foundation, New York, USA*

Correspondence should be addressed to Tiago G. Fernandes; tfernandes@tecnico.ulisboa.pt

Received 20 March 2019; Accepted 20 March 2019; Published 2 June 2019

The term "engineering cell systems" can be used to describe the application of engineering principles to the understanding of biological systems, solve biological problems, and ultimately contribute to the translation of new therapeutic approaches into clinical practice [1, 2]. Eventually, for the widespread use of stem cells in biomedical applications, it will be essential to recognize the complexity and the dynamics of stem cell systems, and therefore, the application of engineering principles will become crucial to the understanding of important biological questions, ranging from the cell level to the whole organism [3, 4]. This interesting concept is based on truly interdisciplinary methodologies and integrates contributions from multiple scientific and technological fields.

Currently, one can easily identify several key technologies that are gaining substantial attention in this area. Among these, we can find novel bioprocesses for the maintenance and expansion of human stem cells, as well as their differentiated progeny [5–7], and micro-/nanofabrication to produce tissue-like substitutes [8]. Moreover, these technologies should be developed with the objective of being implemented under Good Manufacturing Practice (GMP) conditions, in order to facilitate their translation to the clinic [9]. Several contributions featured in this special issue focus their attentions on these topics. Particularly, S. Dakhore et al. review current strategies for human pluripotent stem cell (hPSC) culture and discuss the challenges associated with the development of appropriate conditions to promote large-scale, quality-controlled expansion of hPSCs. On the same note, F. C. Paccola Mesquita et al. present an interesting study on the use of a closed hollow-fiber system that provides the necessary environment to scale up production of hPSCs while maintaining their stemness. They also demonstrate that laminin 521 can be used to promote the attachment of cells in the hollow-fiber reactor, resulting in a greater yield of viable hPSCs when compared with vitronectin. These results highlight the potential of such culture systems to yield high cell numbers in controlled environments, particularly when the scarcity of the initial cell population is an issue. Both contributions of A. T. Serra et al. and K. Chen et al. also tackle such questions by using microcarriers and spontaneously formed spheroids to expand cancer stem cells and compact bone-derived cells, respectively.

Another important objective of the field is the elucidation of the mechanisms that will allow the generation of functional human tissue-like substitutes [3, 6, 10]. To this end, mechanotransduction is of paramount importance, since this process may strongly influence cell fate and, thus, augment the precision of the differentiation of hPSCs into specific cell types, like cardiomyocytes. In this special issue, R. Santoro et al. review the main integrin-dependent mechanisms and

signaling pathways involved in mechanotransduction, with particular emphasis in the cardiovascular field, focusing on biomaterial-based *in vitro* models of hPSC differentiation into cardiomyocytes. Generically, human morphogenesis is a complex process involving distinct microenvironmental and physical signals that are manipulated in space and time to give rise to complex tissues and organs. The development of organoids from hPSCs represents one reliable system to modeling such events, and T. P. Silva et al. review the main bioengineering methods used to promote the self-organization of stem cells, including assembly, patterning, and morphogenesis *in vitro*, contributing to tissue-like structure formation.

Other emerging topics of this area include the development of cellular products based on innovative scaffolds for the cultivation of stem/progenitor cells [11, 12] and controlled-release particles to program the differentiation of stem cells [13, 14]. In this special issue, M. Haagdorens et al. describe a collagen-like peptide biomaterial for tissue engineering of the cornea, while W. Qin et al. present a drug delivery system, consisting of calcium phosphate cement-containing chitosan with controlled release of metformin, to promote cell viability and odontogenic differentiation of human dental pulp cells, favoring dentin regeneration. In fact, stimuli-responsive materials, also known as smart materials, can change their structure and, consequently, original behavior in response to external or internal stimuli. D. K. Patel et al. also address this topic and review the physiochemical properties of graphene and graphene-based hybrid materials for stimuli-responsive drug delivery, tissue engineering, and antimicrobial applications. Additionally, taking advantage of the strong tropism that stem cells exhibit towards tumors, different researchers have proposed them as attractive candidates for targeted drug delivery in cancer treatment with minimal side effects. In this special issue, P. Wang and A. Aguirre describe the latest stem cell-based approaches for the treatment of cancer and also summarize the emerging imaging techniques being applied for monitoring anticancer stem cell therapy. This known tropism of certain stem cell populations to chronic tissue damage is typically complemented by regulatory effects on the immune microenvironment. Certain cells can regulate the immune microenvironment during tissue repair and provide a good "soil" for tissue regeneration. H. Li et al. discuss the regulation of immune cells by mesenchymal stem cells in the local tissue microenvironment and the subsequent tissue damage repair mechanisms.

Finally, the development of *in vitro* tests for toxicity, cell differentiation, genomic stability of expanded cells, and biocompatibility can profit from these scientific and technological advancements [4, 9, 15], and several contributions to this special issue focus on discussing these issues and the implications of these novel technologies for cell therapies, regeneration, and precision medicine.

Conflicts of Interest

The editors declare no conflicts of interest regarding the publication of the special issue.

Acknowledgments

The guest editorial team would like to express gratitude to all the authors for their interest in selecting this special issue as a venue for disseminating their scholarly work. The editors also wish to thank the anonymous reviewers for their careful reading of the manuscripts submitted to this special issue collection and their many insightful comments and suggestions.

Tiago G. Fernandes
Ricardo P. Baptista
Howard Kim

References

[1] C. M. Madl, S. C. Heilshorn, and H. M. Blau, "Bioengineering strategies to accelerate stem cell therapeutics," *Nature*, vol. 557, no. 7705, pp. 335–342, 2018.

[2] M. Tewary, N. Shakiba, and P. W. Zandstra, "Stem cell bioengineering: building from stem cell biology," *Nature Reviews Genetics*, vol. 19, no. 10, pp. 595–614, 2018.

[3] E. Lau, D. T. Paik, and J. C. Wu, "Systems-wide approaches in induced pluripotent stem cell models," *Annual Review of Pathology: Mechanisms of Disease*, vol. 14, no. 1, pp. 395–419, 2019.

[4] Y. Y. Lipsitz, P. Bedford, A. H. Davies, N. E. Timmins, and P. W. Zandstra, "Achieving efficient manufacturing and quality assurance through synthetic cell therapy design," *Cell Stem Cell*, vol. 20, no. 1, pp. 13–17, 2017.

[5] S. M. Badenes, T. G. Fernandes, C. A. V. Rodrigues, M. M. Diogo, and J. M. S. Cabral, "Microcarrier-based platforms for *in vitro* expansion and differentiation of human pluripotent stem cells in bioreactor culture systems," *Journal of Biotechnology*, vol. 234, pp. 71–82, 2016.

[6] M. H. Kim and M. Kino-Oka, "Bioprocessing strategies for pluripotent stem cells based on Waddington's epigenetic landscape," *Trends in Biotechnology*, vol. 36, no. 1, pp. 89–104, 2018.

[7] G. M. C. Rodrigues, C. A. V. Rodrigues, T. G. Fernandes, M. M. Diogo, and J. M. S. Cabral, "Clinical-scale purification of pluripotent stem cell derivatives for cell-based therapies," *Biotechnology Journal*, vol. 10, no. 8, pp. 1103–1114, 2015.

[8] C. C. Miranda, T. G. Fernandes, M. M. Diogo, and J. M. S. Cabral, "Towards multi-organoid systems for drug screening applications," *Bioengineering*, vol. 5, no. 3, p. 49, 2018.

[9] Y. Y. Lipsitz, N. E. Timmins, and P. W. Zandstra, "Quality cell therapy manufacturing by design," *Nature Biotechnology*, vol. 34, no. 4, pp. 393–400, 2016.

[10] I. Heemskerk, K. Burt, M. Miller et al., "Rapid changes in morphogen concentration control self-organized patterning in human embryonic stem cells," *Elife*, vol. 8, 2019.

[11] T. B. Bertucci and G. Dai, "Biomaterial engineering for controlling pluripotent stem cell fate," *Stem Cells International*, vol. 2018, Article ID 9068203, 12 pages, 2018.

[12] Y. Ma, M. Lin, G. Huang et al., "3D spatiotemporal mechanical microenvironment: a hydrogel-based platform for guiding stem cell fate," *Advanced Materials*, vol. 30, no. 49, article 1705911, 2018.

[13] P. Jayaraman, C. Gandhimathi, J. R. Venugopal, D. L. Becker, S. Ramakrishna, and D. K. Srinivasan, "Controlled release of

drugs in electrosprayed nanoparticles for bone tissue engineering," *Advanced Drug Delivery Reviews*, vol. 94, pp. 77–95, 2015.

[14] J. L. Madrigal, R. Stilhano, and E. A. Silva, "Biomaterial-guided gene delivery for musculoskeletal tissue repair," *Tissue Engineering Part B: Reviews*, vol. 23, no. 4, pp. 347–361, 2017.

[15] C. C. Miranda, T. G. Fernandes, S. N. Pinto, M. Prieto, M. M. Diogo, and J. M. S. Cabral, "A scale out approach towards neural induction of human induced pluripotent stem cells for neurodevelopmental toxicity studies," *Toxicology Letters*, vol. 294, pp. 51–60, 2018.

Hindawi
Stem Cells International
Volume 2019, Article ID 8469012, 13 pages
https://doi.org/10.1155/2019/8469012

Research Article

Spontaneously Formed Spheroids from Mouse Compact Bone-Derived Cells Retain Highly Potent Stem Cells with Enhanced Differentiation Capability

Kai Chen,[1] Xianqi Li,[1,2,3] Ni Li,[1] Hongwei Dong,[1] Yiming Zhang,[4] Michiko Yoshizawa,[1,2] and Hideaki Kagami[1,2,3,5]

[1]*Department of Hard Tissue Research, Graduate School of Oral Medicine, Matsumoto Dental University, Shiojiri 399-0781, Japan*
[2]*Department of Oral and Maxillofacial Surgery, School of Dentistry, Matsumoto Dental University, Shiojiri 399-0781, Japan*
[3]*Institute for Oral Science, Matsumoto Dental University, Shiojiri 399-0781, Japan*
[4]*Department of Stomatology, Shanghai Tenth People's Hospital, Tongji University School of Medicine, Shanghai 200072, China*
[5]*Department of General Medicine, IMSUT Hospital, Institute of Medical Science, University of Tokyo, Tokyo 108-8639, Japan*

Correspondence should be addressed to Hideaki Kagami; hideaki.kagami@mdu.ac.jp

Received 19 October 2018; Revised 26 February 2019; Accepted 10 March 2019; Published 5 May 2019

Guest Editor: Tiago Fernandes

The results from our recent study showed the presence of two distinct spheroid-forming mechanisms, i.e., spontaneous and mechanical. In this study, we focused on the spontaneously formed spheroids, and the character of spontaneously formed spheroids from mouse compact bone-derived cells (CBDCs) was explored. Cells from (C57BL/6J) mouse leg bones were isolated, and compact bone-derived cells were cultured after enzymatic digestion. Spontaneous spheroid formation was achieved on a culture plate with specific water contact angle as reported. The expression levels of embryonic stem cell markers were analyzed using immunofluorescence and quantitative reverse transcription polymerase chain reaction. Then, the cells from spheroids were induced into osteogenic and neurogenic lineages. The spontaneously formed spheroids from CBDCs were positive for ES cell markers such as SSEA1, Sox2, Oct4, and Nanog. Additionally, the expressions of fucosyltransferase 4/FUT4 (SSEA1), Sox2, and Nanog were significantly higher than those in monolayer cultured cells. The gene expression of mesenchymal stem cell markers was almost identical in both spheroids and monolayer-cultured cells, but the expression of Sca-1 was higher in spheroids. Spheroid-derived cells showed significantly higher osteogenic and neurogenic marker expression than monolayer-cultured cells after induction. Spontaneously formed spheroids expressed stem cell markers and showed enhanced osteogenic and neurogenic differentiation capabilities than cells from the conventional monolayer culture, which supports the superior stemness.

1. Introduction

Somatic stem cells have a great potential for use in tissue repair and regeneration. Among them, mesenchymal stem cells (MSCs) have been widely used not only for basic research but also for clinical applications such as bone tissue engineering [1, 2]. Two-dimensional (2D) culture of adherent cells has been used as a standard technique for the in vitro expansion of MSCs, which is a relatively easy and generally accepted protocol [3, 4]. However, some reports have indicated the immediate loss of characteristic features of stem cells during culture, such as homing ability, replication capability, colony-forming efficiency, and differentiation capability [5–9]. To overcome these shortcomings, the potential of novel cell culture protocols has been explored [10–15].

One important breakthrough of somatic stem cell culture was the discovery of a floating culture, which was first reported for neural stem cells [16]. The presence of neural stem cells has been questioned for the long term. However, they were isolated from the embryonic brain using this novel culture protocol, which enabled selective, elongated survival

and expansion of neural stem cells as spheroids [16–19]. Thereafter, this technique has been applied to the selective culture of various somatic stem cells, including mesenchymal stem cells [20–23]. Compared with traditional 2D cell culture, spheroids are a form of three-dimensional (3D) culture and are regarded for their ability to replicate the physiological environment for cells, thus better preserving the characteristics of somatic stem cells [24, 25]. The limitation of 3D culture includes the limited growth for mesenchymal stem cells [26] and low culture efficiency when the spheroid formed spontaneously [27].

There are several different approaches to generate spheroids (e.g., spinner flask method, liquid overlay method, and hanging drop method) [28, 29]. However, the differences among spheroids, obtained from different culture protocols, have yet to be shown. In this study, spheroid formation was achieved under static conditions on a plate with a specific water contact angle, which is around 90°. Because spheroid formation with this method occurs spontaneously, we designate this type of spheroid as a spontaneously formed spheroid [27]. Although the difference between spontaneously formed spheroids and mechanically formed spheroids (such as the spinner flask method) is not well known, spontaneously formed spheroids ideally consist of a purer stem cell population because spheroid formation starts from stem cells only, which possess the ability to proliferate enough to form spheroids. On the other hand, mechanically formed spheroids may contain various types of cells due to the forced aggregation of surrounding cells [27, 30]. However, most of the reported studies did not pay attention on the difference of those two methods, and in particular, the character of spontaneously formed spheroids with mesenchymal stem cells has not been well understood.

The most well studied and widely used cell source for mesenchymal stem cells is bone marrow mesenchymal stem cells (BMMSCs). However, some recent reports have shown that compact bone-derived cells (CBDCs) are a superior cell source compared with BMMSCs because CBDCs possess a higher proliferation and pluripotent differentiation capability [31–36]. In this study, we focused on spontaneously formed spheroids from CBDCs to characterize their potential as a somatic stem cell source. To our knowledge, this is the first report on spontaneously formed spheroids and spheroid-forming cells from mouse CBDCs.

2. Materials and Methods

All procedures for experiments in this study were performed in accordance with the guidelines laid down by the National Institutes of Health (NIH) in the USA, regarding the care and use of animals for experimental procedures, and approved by the Matsumoto Dental University Committee on Intramural Animal Use (No. 289).

2.1. Preparation of Mouse CBDCs. The cultivation protocol for CBDCs was conducted according to the protocol in our previous publication with some modifications [31]. Briefly, male C57BL/6J mice (3 weeks old, SLC Japan, Hamamatsu, Japan) were sacrificed with an overdose of anesthesia. The femurs and tibiae were disconnected from the trunk, and soft tissues were removed from the bone surface thoroughly. Epiphyses were cut, and bone marrow was flushed out using a syringe and 27-gauge needle with culture medium consisting of α-minimum essential medium with glutamine and phenol red (α-MEM, Wako Pure Chemical Industries Ltd., Osaka, Japan), supplemented with 1% penicillin-streptomycin-amphotericin B solution (Biological Industries Israel Beit Haemek Ltd., Kibbutz Beit Haemek, Israel). After the bone color became pale, the bones were placed in phosphate-buffered saline (PBS; Wako Pure Chemical Industries Ltd., Osaka, Japan) and were carefully cut into 1~2 mm fragments with scissors. Then, the bone chips were transferred into a 50 ml centrifuge tube containing 20 ml of PBS with 0.25% collagenase (Wako Pure Chemical Industries Ltd., Osaka, Japan) and 20% fetal bovine serum (FBS; Biowest, France). The tube was placed in a shaking incubator at 37°C with a shaking speed of 90 rpm. After 45 minutes of incubation, the cells were collected and transferred to another tube through a 40 μm cell strainer (Falcon®, Corning, NY, USA). The tube was centrifuged for 5 minutes at 300 g at 4°C. The supernatant was removed, and the cell pellet was gently resuspended in α-MEM supplemented with 10% FBS, 1% penicillin-streptomycin-amphotericin solution, and 10 ng/ml recombinant human basic-fibroblast growth factor (bFGF; PeproTech, Rocky Hill, NJ, USA), which were used as the basic culture medium. The cell suspension was seeded into a culture dish (Falcon®, Corning, USA) at a density of $5.5 \times 10^5/\text{cm}^2$. Bone chips were collected and placed in a 30×15 mm cell culture dish with 2 ml of basal culture medium to collect additional cells. The primary cells were cultured at 37°C in a 5% CO_2 humidified incubator. The medium was changed every three days. When the cells reached 70-80% confluence, the cells were detached with 0.25% trypsin-EDTA (Gibco: Life Technologies, Carlsbad, CA, USA) and subcultured in a new culture dish at a density of 1.5×10^4 cells/cm^2 until subconfluent.

Table 1: Immunofluorescence staining antibody reagent list.

Antibody	Dilution	Product no. and manufacturer
Primary antibodies		
SSEA1 (mouse monoclonal)	1 : 100	ab16285, Abcam
Sox2 (rabbit polyclonal)	1 : 250	ab97959, Abcam
Oct4 (rabbit polyclonal)	1 : 250	ab19857, Abcam
Nanog (rabbit polyclonal)	1 : 100	ab80892, Abcam
βIII-tubulin (mouse monoclonal)	1 : 250	ab87087, Abcam
Nestin (mouse monoclonal)	1 : 500	ab6142, Abcam
Secondary antibodies		
IgM Alexa Fluor 488 (goat anti-mouse)	1 : 200	ab150121, Abcam
IgG Alexa Fluor 647 (goat anti-rabbit)	1 : 500	ab150079, Abcam
IgG Alexa Fluor 488 (goat anti-mouse)	1 : 500	ab150113, Abcam

Table 2: Quantitative reverse transcription-PCR primer set list.

Primer	Direction	Sequence (5′-3′)
β-Actin	Forward	CATCCGTAAAGACCTCTATGCCAAC
	Reverse	ATGGAGCCACCGATCCACA
Glyceraldehyde-3-phosphate dehydrogenase (GAPDH)	Forward	GGTGTGAACCACGAGAAA
	Reverse	TGAAGTCGCAGGAGACAA
Sox2/sex determining region Y (SRY)-box 2	Forward	GTTCTAGTGGTACGTTAGGCGCTTC
	Reverse	TCGCCCGGAGTCTAGCTCTAAATA
Fucosyltransferase 4 (FUT4·SSEA1)	Forward	GCAGGGCCCAAGATTAACTGAC
	Reverse	AAGCGCCTGGGCCTAAGAA
Octamer-binding transcription factor 4 (Oct4)	Forward	CAGACCACCATCTGTCGCTTC
	Reverse	AGACTCCACCTCACACGGTTCTC
Nanog	Forward	TGCCAGTGATTTGGAGGTGAA
	Reverse	ATTTCACCTGGTGGAGTCACAGAG
Hypoxia-inducible factors 2α (HIF-2α)	Forward	CAGTACTCCCACAGGCCTGACTAAC
	Reverse	GACTGTCACACCGCTGCCATA
CD105	Forward	CTGCCAATGCTGTGCGTGAA
	Reverse	GCTGGAGTCGTAGGCCAAGT
CD44	Forward	CAAGCCACTCTGGGATTGGTC
	Reverse	GGCAAGCAATGTCCTACCACAAC
CD29	Forward	CCATGCCAGGGACTGACAGA
	Reverse	GAGCTTGATTCCAATGGTCCAGA
Stem cell antigen-1 (Sca-1)	Forward	TTGCCTTTATAGCCCCTGCT
	Reverse	GTCATGAGCAGCAATCCACA
Kruppel-like factor 4 (KLF4)	Forward	AACATGCCCGGACTTACAAA
	Reverse	TTCAAGGGAATCCTGGTCTTC
Transcription factor Sp7/osterix (OSX)	Forward	AGGCCTTTGCCAGTGCCTA
	Reverse	GCCAGATGGAAGCTGTGAAGA
Bone sialoprotein (BSP)	Forward	GAGACGGCGATAGTTCC
	Reverse	AGTGCCGCTAACTCAA
Dentin matrix protein 1 (DMP1)	Forward	AGTGAGTCATCAGAAGAAAGTCAAGC
	Reverse	CTATACTGGCCTCTGTCGTAGCC
Microtubule-associated protein 2 (MAP2)	Forward	CAGTTTGGCTGAAGGTAGCTGAA
	Reverse	CACATCTGTGTGAGTGTGTGTGGA
Nestin	Forward	GAGGTGTCAAGGTCCAGGATGTC
	Reverse	ACACCGTCTCTAGGGCAGTTACAA
Nerve growth factor receptor (NGFR)/P75NTR	Forward	TCTGATGGAGTCGGGCTAATGTC
	Reverse	CCACAAATGCCCTGTGGCTA
Neuronal differentiation (NeuroD)	Forward	CAAAGCCACGGATCAATCTTC
	Reverse	TGTACGCACAGTGGATTCGTTTC

2.2. CBDC Spheroid Formation. The method of spheroid formation was conducted according to the protocol in our previous publication [27]. Briefly, passage 2 CBDCs were resuspended in basic culture medium and transferred to a 55×17 mm low-adhesion culture dish (AS ONE, Osaka, Japan) at a density of 1.5×10^4 cells/cm^2 for spheroid formation, incubated at 37°C in a 5% CO_2 humidified incubator. The density was optimized in our preliminary experiments (data not shown). The size and number of spheroids were observed using an inverted microscope (Olympus IX70, Olympus Optical Co. Ltd., Tokyo, Japan) at 12, 24, and 72 hours. At each observation time point, the size of spheroids was measured using 6 randomly selected fields (100x magnification) of a culture plate in 5 independent experiments. The photomicrographs were taken and used to measure the diameters of spheroids using the Olympus cellSens Standard 1.15

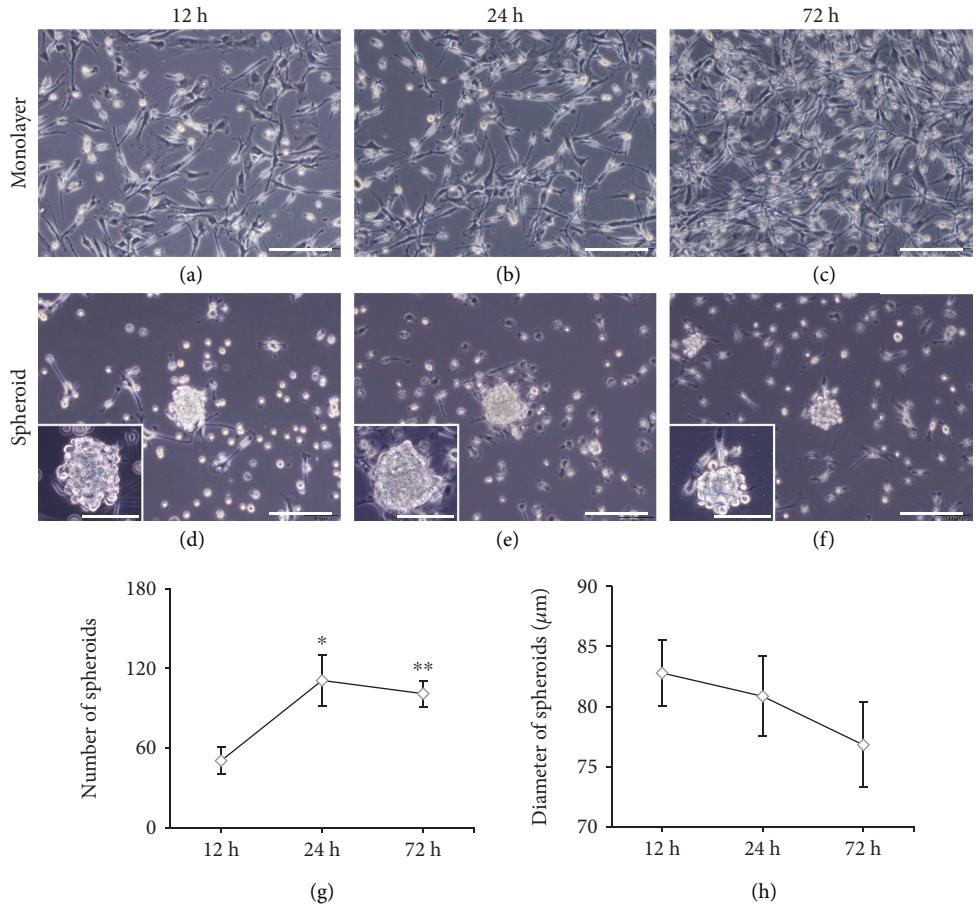

Figure 1: Spontaneous spheroid formation of CBDCs. On a conventional monolayer culture plate, adhered CBDCs showed fibroblast-like morphology and stable growth (a–c). On spheroid-forming plates, CBDCs began to form spheroids at 12 hours (d) and were maintained during the observation period (e and f). The number of spheroids peaked at 24 hours and then plateaued. The change in spheroid number between 24 hours and 72 hours was not statistically significant but was significant between 12 hours and 24 hours ($P < 0.05$) and also between 12 hours and 72 hours ($P < 0.01$), $N = 5$ (g). The average diameter of spheroids decreased gradually during the time course without statistically significant changes, $N = 30$ (h). Scale bars = 100 μm. Data are represented as the mean ± SEM. $^{*}P < 0.05$ and $^{**}P < 0.01$.

software. The number of spheroids was counted using a phase-contrast microscope at 40x magnification, which covered the entire plate.

2.3. Osteogenic and Neurogenic Induction of CBDCs. After 24 hours of spheroid formation, the spheroids were transferred into new conventional culture dishes to allow the spheroids to attach and spread on the bottom of the culture dish to grow as a monolayer. When CBDCs in monolayer culture or spheroids reached 50-60% confluence, the basic culture medium was replaced with osteogenic induction medium (basic culture medium, supplemented with 100 nM dexamethasone (Sigma-Aldrich, St. Louis, MO, USA), 50 μM L-ascorbic acid phosphate (Wako Pure Chemical Industries, Ltd.), and 10 mM glycerol phosphate disodium salt hydrate (Sigma-Aldrich)) or neurogenic induction medium (basic culture medium, supplemented with 50 ng/ml recombinant nerve growth factor, 50 ng/ml recombinant brain-derived neurotrophic factor, and 10 ng/ml recombinant NT-3 (all three reagents from PeproTech, Rock Hill, NJ, USA)). During the induction process, the media were changed every two days.

2.4. Alkaline Phosphatase (ALP) Activity Assay. After 7 days of osteogenic induction, ALP activity was measured to confirm osteogenic induction. Noninduced cells were used as a control, which were continuously cultured in basic culture medium. An enzymatic assay (cell counting kit-8 (CCK-8); Dojindo Laboratories, Kumamoto, Japan) and p-nitrophenyl phosphate (SIGMAFAST™ p-Nitrophenyl Phosphate Tablet; Sigma-Aldrich Co. LLC.) were used to evaluate cell proliferation and ALP activity according to the manufacturer's instructions. Formazan was measured at 450 nm, and p-nitrophenyl phosphate was quantified at 405 nm using an iMark™ Microplate Absorbance Reader (Bio-Rad Laboratories, Hercules, CA, USA).

2.5. Immunofluorescence Microscopy. Immunofluorescence staining was performed with embryonic stem cell markers. Spheroids were collected 24 hours after seeding to the low-adhesion plate and solidified in iPGell (Genostaff, Tokyo,

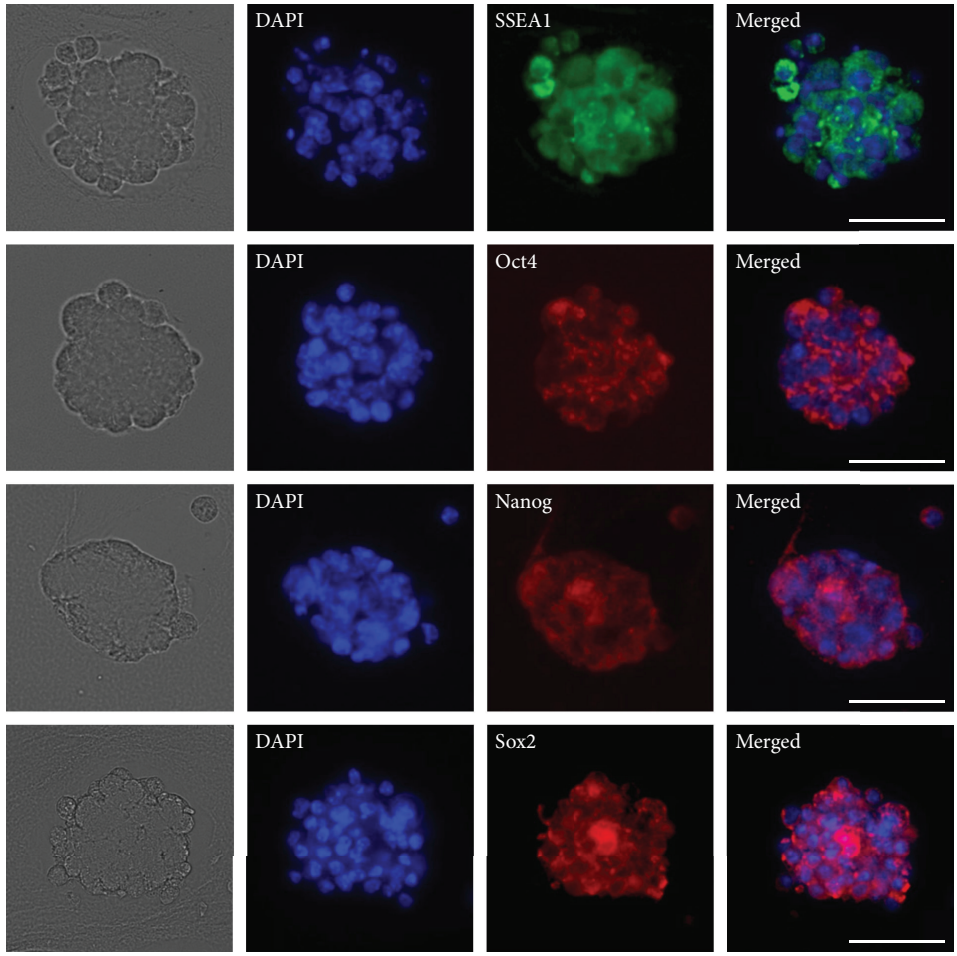

Figure 2: Immunofluorescence staining of spontaneously formed spheroids. CBDCs were cultured in spheroid-forming conditions for 24 h, and paraffin sections of spheroids were immunostained with primary antibodies specific for SSEA1, Oct4, Nanog, and Sox2 (corresponding to the first horizontal to the fourth horizontal). The positive reaction was distributed among almost all spheroid-forming cells. DAPI (4′,6-diamidino-2-phenylindole) was used for nuclear staining. Scale bars = 50 μm.

Japan) according to the manufacturer's instructions, fixed with 4% paraformaldehyde in phosphate buffer, embedded in paraffin, and sectioned at a thickness of 8 μm, as previously described [31]. Sections were permeabilized and blocked with 5% BSA, 5% goat serum, and 0.5% Triton X-100 in PBS. After incubation with primary antibodies overnight at 4°C, the sections were washed with PBS three times, followed by incubation with the respective secondary antibodies for 2 hours. Nuclei were counterstained with 4′,6-diamidino-2-phenylindole solution (Fluoroshield Mounting Medium with DAPI, ab104139, Abcam) for 30 min.

To confirm neurogenic induction, immunofluorescence staining for neural cell markers was performed after 14 days of induction. CBDCs from monolayer culture and spheroids were fixed with 4% paraformaldehyde in phosphate buffer for 20 minutes at room temperature followed by washing three times with PBS. The cells were treated with 5% BSA, 5% goat serum, and 0.5% Triton X-100 in PBS for 25 minutes at room temperature to permeate and block nonspecific binding of the antibodies. Primary antibodies were incubated with cells overnight at 4°C. After rinsing three times with PBS, the cells were incubated with the respective secondary antibodies for 2 hours at room temperature in dark and then washed three times with PBS. Nuclei were counterstained with DAPI for 30 min. The antibodies used are summarized in Table 1.

All fluorescent imaging was taken with a fluorescence microscope (Keyence BZ-X710, Keyence, Osaka, Japan) with 20x or 40x objective magnification. Cells incubated with secondary antibodies, without primary antibody incubation, served as a negative control.

2.6. RNA Extraction and qRT-PCR. qRT-PCR was performed to determine the expression levels of stem cell markers, osteogenic and neurogenic markers in spheroids, and CBDCs from spheroids or monolayer culture. Briefly, total RNA was extracted using the TRIzol reagent (Ambion®; Life Technologies, Carlsbad, CA, USA). After quantification of total RNA with a spectrophotometer (NanoDrop® ND-1000, Thermo Fisher Scientific, Waltham, MA, USA), RNA samples were reverse transcribed into complementary

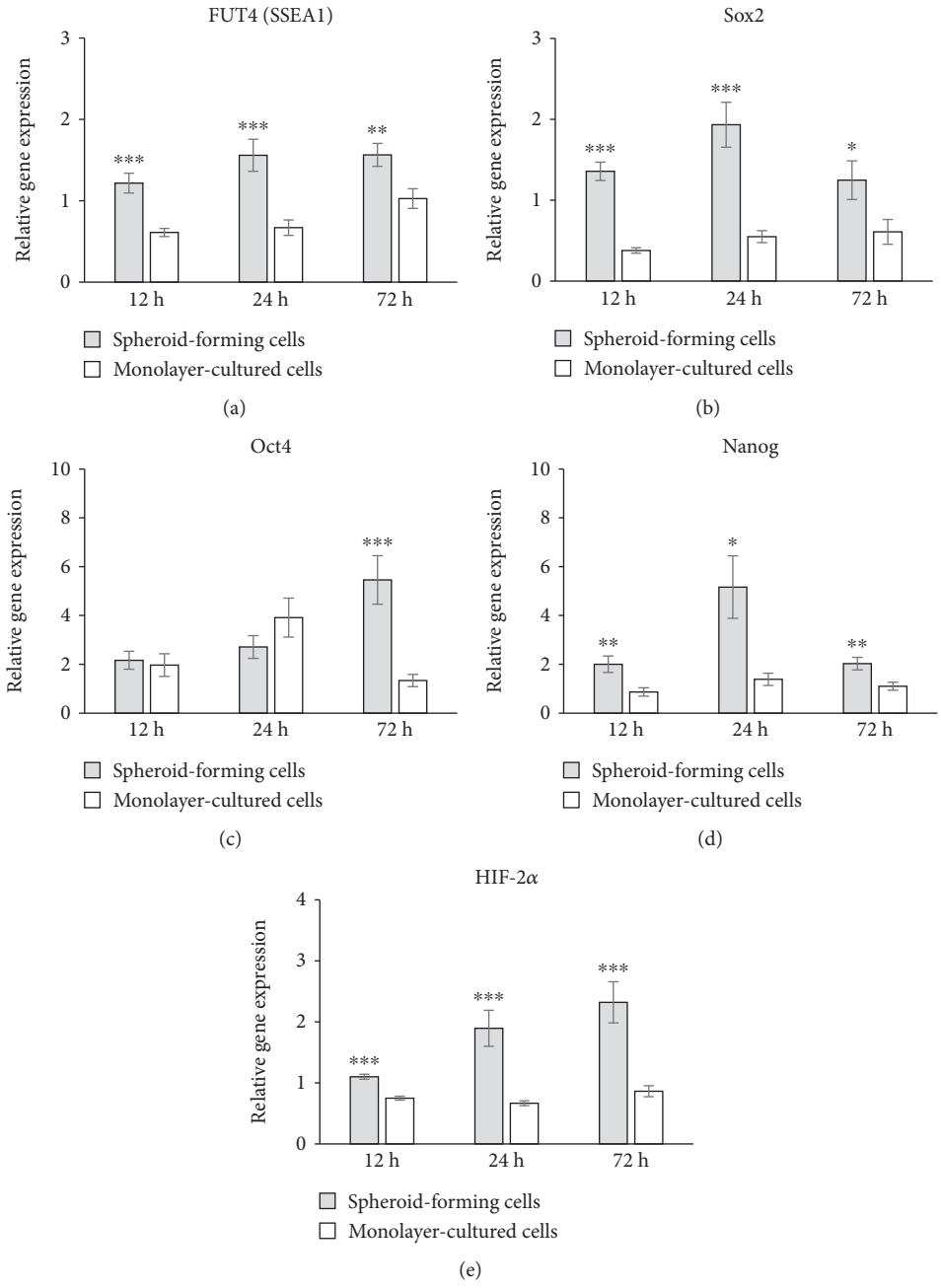

Figure 3: The expression of stem cell markers and HIF in spheroid-forming cells and monolayer-cultured cells. The relative expression of FUT4 (SSEA1) (a), Sox2 (b), Nanog (d), and HIF-2α (e) was significantly higher in spheroid-forming cells at any time point examined. The expression of Oct4 (c) in spheroids was significantly higher than that of monolayer-cultured cells at 72 hours. Data are represented as the mean ± SEM. (a and b) $N = 5$. (c) $N = 4$. (d) $N = 6$. (e) $N = 3$. $^{*}P < 0.05$, $^{**}P < 0.01$, and $^{***}P < 0.001$.

DNA (cDNA) using oligo (dT)12–18 primers (Life Technologies), dNTPs (Toyobo Co. Ltd., Osaka, Japan), and ReverTra Ace® (Toyobo Co. Ltd.) according to the manufacturer's instructions. qRT-PCR was performed in a thermal cycler (Thermal Cycler Dice Real Time System II TP-900, Takara Bio, Japan) using the SYBR Premix Ex TaqII reagent (Takara Bio, Kusatsu, Japan) according to the manufacturer's protocol. Primer sets (Sigma-Aldrich Co.) used for the PCR experiment are listed in Table 2.

2.7. Statistical Analyses. The results are presented as the means ± standard error of the means (SEM). Statistical analyses were conducted using Student's t-test between two groups. A P value of less than 0.05 was considered statistically significant.

3. Results

3.1. The Generation of Spontaneous Spheroids from CBDCs. When mouse CBDCs were seeded into a conventional plastic

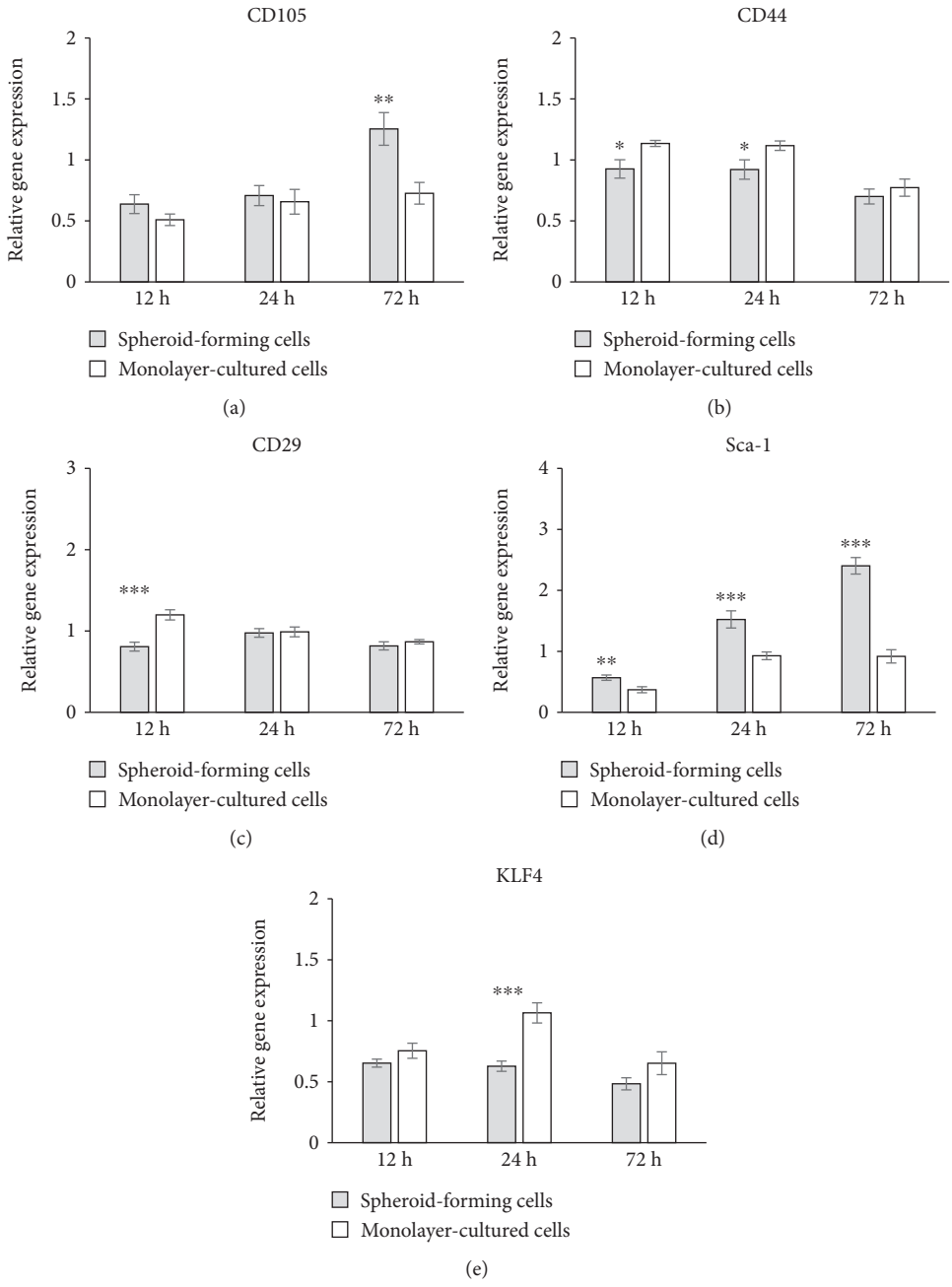

Figure 4: The expression of MSC markers in spheroid-forming cells and monolayer-cultured cells. The relative expression of CD105 (a), CD44 (b), CD29 (c), and KLF4 (e) was at close levels between spheroid-forming cells and monolayer-cultured cells, except for the individual observation time point. The relative expression of Sca-1 (d) showed a higher expression in spheroids than monolayer-cultured cells at all time points examined. Data are represented as the mean ± SEM. (a, d, and e) $N = 4$. (b and c) $N = 3$. $^{*}P < 0.05$, $^{**}P < 0.01$, and $^{***}P < 0.001$.

culture dish at passage 2, the cells adhered to the tissue culture plastic and showed fibroblast-like morphology after 12 hours (Figure 1(a)). The growth of CBDCs was stable, and the cell density increased after 24 hours (Figure 1(b)) and nearly reached confluence after 72 hours (Figure 1(c)). At 12 hours after seeding onto the low-adhesion culture plate, CBDCs began to form multicellular aggregates, which gradually became spheroids (Figure 1(d)). The spheroids were maintained during the observation period (Figure 1(e) and (f)). There were some spheroids that reattached on the dish and lost their spheroid morphology. However, no obvious cell death in spheroids was observed. The number of spheroids increased from 12 to 24 hours after cell seeding. The number of spheroids at 24 hours was significantly larger than that at 12 hours ($P < 0.05$). Then, the number of spheroids plateaued (Figure 1(g)). The average diameter of spheroids decreased gradually over time, but the difference was not significant (Figure 1(h)).

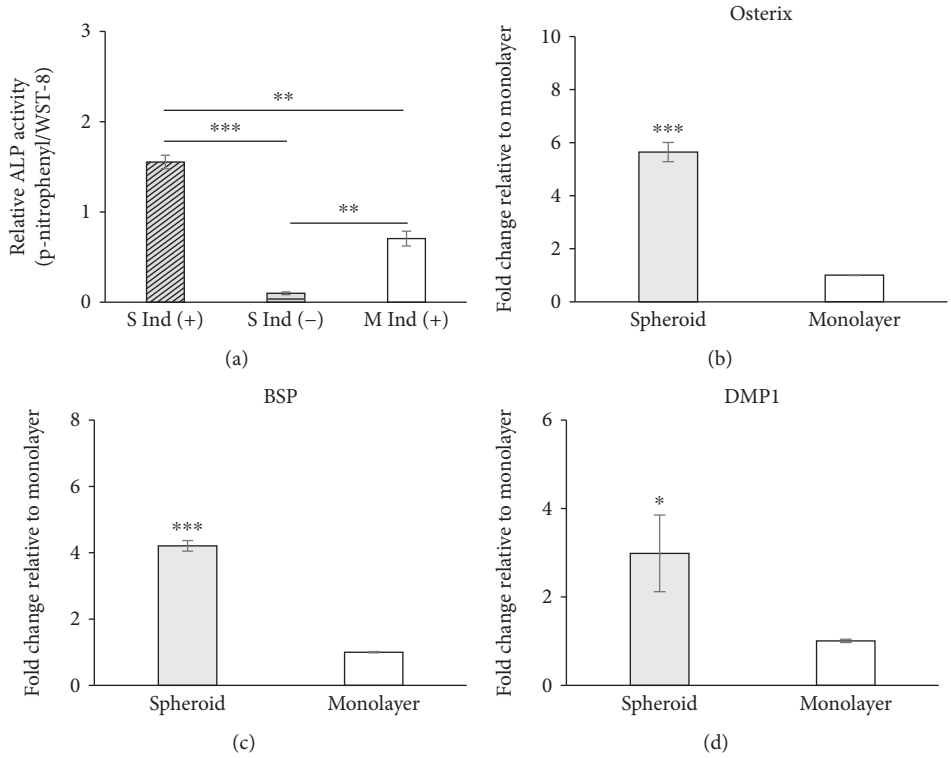

Figure 5: Osteogenic capability of spheroids. Monolayer-cultured CBDCs and spheroid-derived cells were incubated with osteogenic induction medium for 7 days. ALP assay data showed that induced spheroid-derived cells have significantly increased ALP activity compared with induced monolayer cells (a). qRT-PCR data showed that induced spheroid-derived cells expressed higher levels of osteogenic-related genes, such as osterix, BSP, and DMP1, with statistical significance (b–d). Data are represented as the mean ± SEM. ALP assay, $N = 3$; qRT-PCR, $N = 3$. $^{*}P < 0.05$, $^{**}P < 0.01$, and $^{***}P < 0.001$.

3.2. The Expression of Stem Cell Markers in Spheroids. The immunofluorescence results showed that the spheroids were positive for embryonic stem cell (ES cell) markers such as SSEA1, Oct4, Nanog, and Sox2, and the staining was exclusive to spheroid-forming cells. Positive cells were observed in almost all spheroids and evenly distributed for all examined ES cell markers (Figure 2).

The results from qRT-PCR showed that the relative expression of FUT4 (SSEA1) (Figure 3(a)), Sox2 (Figure 3(b)), and Nanog (Figure 3(d)) was significantly higher in spheroids at any time point examined. The expression of Oct4 in spheroids was significantly higher than that of monolayer-cultured cells at 72 hours (Figure 3(c)). The expressions of all those ES cell markers were detected up to 120 hours (data not shown). The expression of HIF-2α in spheroids was significantly higher than that of monolayer-cultured cells at 12, 24, and 72 hours (Figure 3(e)).

On the other hand, the expressions of MSC markers such as CD105, CD44, CD29, and KLF4 were almost identical between spheroids and monolayer-cultured cells (Figures 4(a)–4(c) and 4(e)), except for Sca-1, which showed a higher expression in spheroids than monolayer-cultured cells at all time points examined (Figure 4(d)).

3.3. Osteogenic Induction. An ALP assay and qRT-PCR were performed to confirm the osteogenic induction at day 7. ALP activity was significantly higher in the induced groups than in the noninduced group for both monolayer and spheroid-derived cells (Figure 5(a)). The ALP activity of induced spheroid-derived cells was significantly higher than that of induced monolayer-cultured cells ($P < 0.01$).

The relative osteogenic marker gene expression levels were analyzed using qRT-PCR. The relative expression level of osterix in spheroid-derived cells was 5.65-fold higher than that in monolayer-cultured cells (Figure 5(b)). Similarly, the expression levels of BSP and DMP1 were higher than those in monolayer-cultured cells, and the differences were 4.21-fold and 2.98-fold greater, respectively (Figures 5(c) and 5(d)).

3.4. Neurogenic Induction In Vitro. The qRT-PCR results showed that spheroid-derived cells had a significantly higher Nestin expression (2.35-fold) after 2 weeks of neurogenic induction (Figure 6(a)). The expression of MAP2 and NGRF in induced spheroid-derived cells was 2.62- and 2.38-fold higher than that in induced monolayer cells, respectively (Figures 6(b) and 6(c)). The expression of NeuroD in induced spheroid-derived cells was also significantly higher (3.10-fold) than that in induced monolayer cells (Figure 6(d)).

Furthermore, immunocytochemical analysis was performed to examine the distribution of the neural cell marker proteins in induced spheroid-derived cells and monolayer-cultured cells. Immunofluorescent images showed that the expression of Nestin and βIII-tubulin was observed with neuronal-like morphology only in spheroid-derived cells,

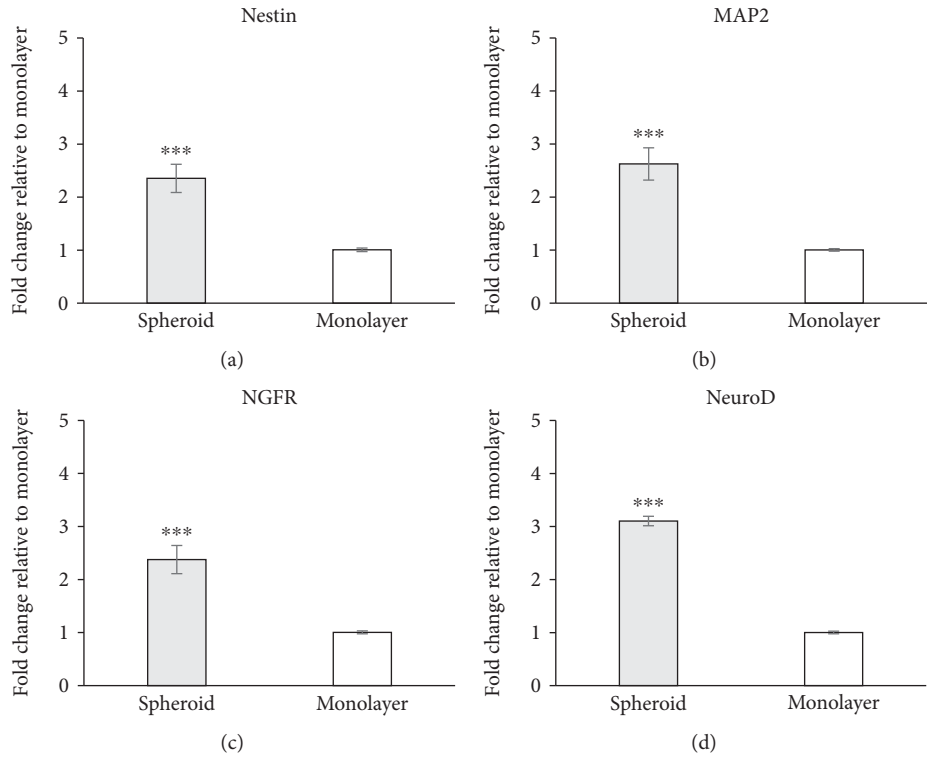

Figure 6: Expression of neurogenic-related genes in induced spheroid-derived and monolayer-cultured cells. Spheroid-derived cells and monolayer cells were cultured with neurogenic induction medium for 2 weeks. The expression of Nestin (a), MAP2 (b), NGFR (c), and NeuroD (d) in spheroid-derived cells was more than 2-fold higher than that in monolayer-cultured cells. Data are represented as the mean ± SEM, $N = 4$, and $^{***}P < 0.001$.

though the ratio of positive cells was relatively small (0.13% and 0.053% for Nestin and βIII-tubulin, respectively) (Figure 7(a)). In contrast, monolayer-cultured cells showed no positive staining for either Nestin or βIII-tubulin (Figure 7(b)).

4. Discussion

Spheroid formation from CBDCs was observed as early as 12 hours and peaked at 24 hours. Compared with spontaneous spheroid formation from neural cells and skin-derived cells, it occurs relatively early. Because our spheroid-forming method utilizes low-adhesion culture dishes, the early spheroid formation from CBDCs might reflect the relatively low adherence of spheroid-forming cells (possibly somatic stem cells) from CBDCs compared with those from neural- or skin-derived cells. To support this idea, the average size of spheroids from CBDCs (80.14 ± 19.27 micrometers in diameter) was smaller than that from skin-derived cells (approximately 100 micrometers). The spheroid diameter decreased over time. This finding might be due to the condensation of spheroid-forming cell aggregates, which was also observed in spheroids from other cell sources, such as periodontal ligament-derived cells [37].

To the best of our knowledge, this is the first study showing the expression of ES cell markers in CBDCs. Spheroids from CBDCs are positive for SSEA1, Oct4, Nanog, and Sox2, which suggests that the spheroid-forming cells from CBDCs are highly potent stem cells. The qRT-PCR results confirmed this result, and the expression of stemness markers such as FUT4, which encodes the SSEA1, Nanog, and Sox2 in spheroids, was significantly higher in spheroid-forming cells than in monolayer cells. At present, it is not fully understood why spheroid formation can switch on the expression of those ES cell markers. Although spontaneous spheroid formation is a process of selective culture of pluripotent stem cells, it may not fully explain the immediate increase in ES cell marker gene expression in spheroids. One possibility is the dedifferentiation of stem (or more differentiated) cells. It has been noted that the spheroid culture condition could restore MSCs to a more primitive status and cause epigenetic changes. For example, it was reported that spheroids from hMSCs showed higher miR-489, miR-370, and miR-433 levels, which play important roles in maintaining the quiescent state of adult stem cells [38–40]. Guo et al. also showed that the change in the histone H3K9 acetylation status changes in spheroids, which may also alter the epigenetic status of spheroid-forming cells [38]. Hypoxia-inducible factor (HIF) is a master transcription factor of hypoxia-associated genes, and HIF-2α is reported as one of the factors affecting the pluripotency of MSCs [41]. Although the size of spheroid from CBDCs is relatively small, the inside of spheroids might be hypoxic. This idea was supported by the higher expression of HIF-2α shown in this study. The

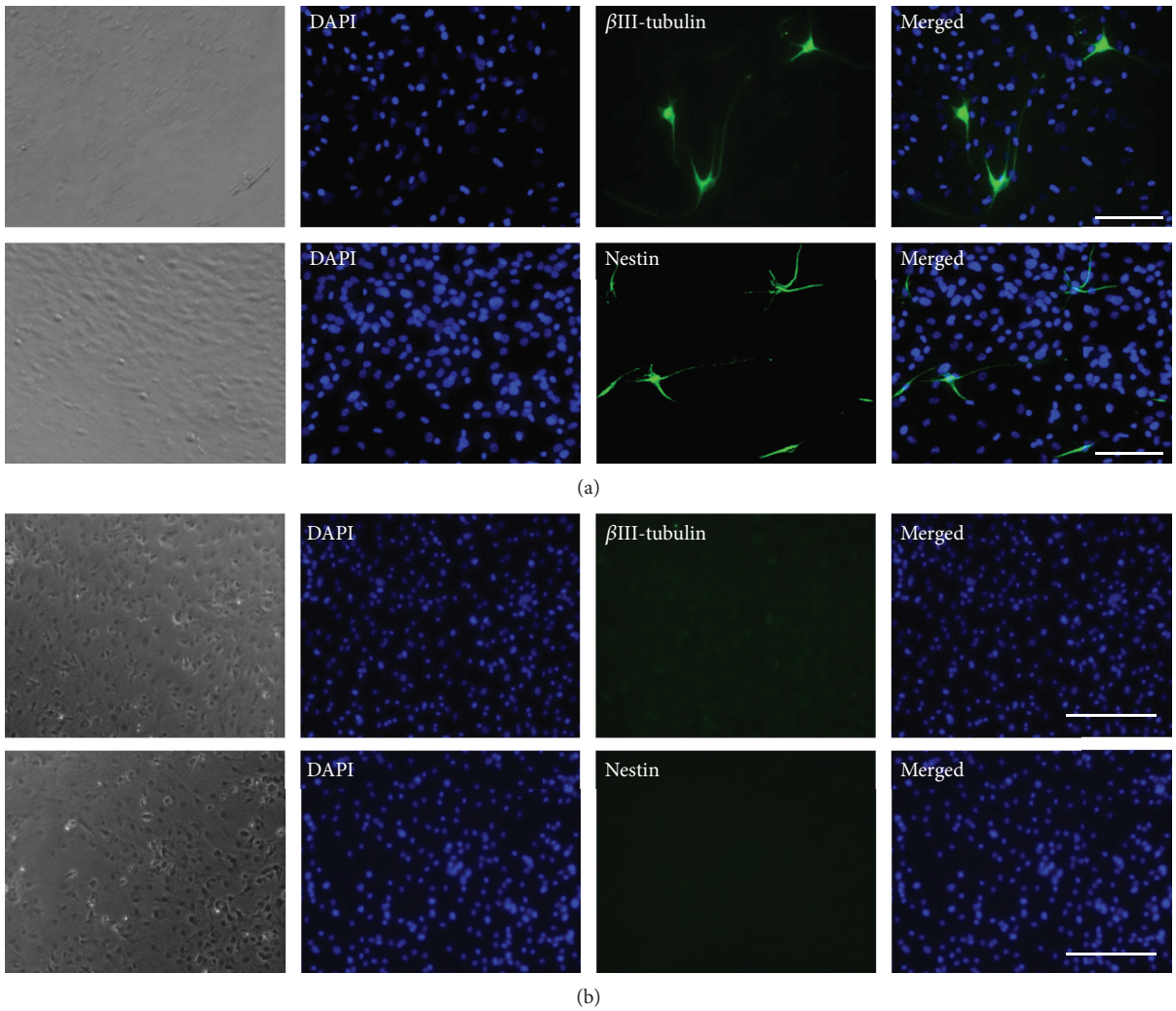

Figure 7: Immunofluorescence staining of neurogenic-induced spheroid-derived and monolayer-cultured CBDCs. After 2 weeks of neurogenic induction, spheroid-derived cells and monolayer-cultured cells were confirmed by immunofluorescence staining. The expression of Nestin and βIII-tubulin was observed with neural cell-like morphology only in spheroid-derived cells (a). In contrast, monolayer-cultured cells showed no positive staining for both Nestin and βIII-tubulin (b). DAPI (4′,6-diamidino-2-phenylindole) was used for nuclear staining. Scale bars = 50 μm.

hypoxic condition and the subsequent induction of HIF might be another mechanism that affects the stemness of spheroid-forming cells [4].

In contrast to ES cell markers, the expression of MSC markers is almost identical between spheroid-forming cells and monolayer-cultured cells, which confirmed reports from the previous publications regarding MSCs derived from periodontal ligament cells [37]. One exception was Sca-1, which showed a higher expression in spheroids than monolayer-cultured cells. Sca-1 was originally identified as a marker for hematopoietic stem cells [42, 43], and Sca-1-positive cells are known to have high plasticity, such as the potential to differentiate into cardiomyocytes [44]. Thus, a higher expression of Sca-1 in spontaneously formed spheroids might also reflect a higher plasticity.

In terms of MSCs from bone marrow and adipose tissue, spheroids have been reported to possess enhanced anti-inflammatory, angiogenic, and tissue regenerative effects after transplantation compared with monolayer-cultured cells [45–47]. However, the nature of spheroid-forming cells from MSCs has been investigated only recently, and the information is limited. Furthermore, there was no report on spheroid-forming cells from CBDCs. In parallel with the higher expression of ES cell marker genes in spheroid-forming cells from CBDCs, they showed a higher osteogenic differentiation capability and a higher expression of osteogenic marker genes such as BSP, osterix, and DMP1 than those of monolayer-cultured cells. This phenomenon shows the potential usefulness of spheroid-forming cells from CBDCs for future clinical applications in bone tissue engineering.

In this study, we also investigated the neurogenic differentiation capability of spheroid-derived cells from CBDCs. Immunofluorescence staining showed that the spheroid-derived cells express Nestin and βIII-tubulin with neuron-like morphology after neurogenic induction, while they are

negative in the monolayer-cultured cells. In accordance with the immunofluorescence staining data, the results of qRT-PCR confirmed the higher gene expression of Nestin, MAP2, NGFR, and NeuroD in spheroid-derived cells compared with monolayer-cultured cells. These findings would pave the way for future usage of spheroid-forming cells from CBDCs for neurodegenerative disorders.

Although the results from the current study showed the potential usefulness of spontaneously formed spheroids from CBDCs, there are remaining works toward the clinical application. First, the feasibility of spontaneous spheroid formation should be tested with human cells. Second, the efficiency of spheroid generation needs to be tested. One of the advantages of our protocol is the relatively higher efficiency, since the spontaneous spheroids can be formed from monolayer-cultured cells even after passages. This means a relatively large number of cells are available for spheroid formation, which may allow the production of clinical scale cells from CBDCs. Since spontaneous spheroids possess superior functions compared with monolayer-cultured cells, it might be reasonable to expect a higher homing ability, replication capability, colony-forming efficiency and differentiation capability. Further studies are required to understand the functional aspects of spontaneous spheroids from CBDCs.

Both safety and efficacy are the important issues for clinical application. Although the spontaneous spheroids exhibit ES cell markers, the results from our preliminary in vivo transplantation experiment showed no teratoma formation, which supports the relative safe nature of spontaneous spheroid-derived cells (data not shown). Efficiency of this method with human cells should be confirmed further toward clinical applications.

5. Conclusions

Mouse CBDCs can spontaneously form spheroids on a low-adhesion culture plate. The spheroid-forming cells showed a higher gene expression of stem cell marker genes and enhanced osteogenic and neurogenic differentiation capability than cells from conventional monolayer culture systems. Although the direct comparison of spontaneously and mechanically formed spheroids was not performed, our data support the enhanced stemness of spontaneously formed spheroids, thus indicating the usefulness for future clinical applications, such as bone regeneration therapy and treatment of neurodegenerative disorders.

Data Availability

The data used to support the findings of this study are included within the article.

Conflicts of Interest

The authors declare no competing interests.

Acknowledgments

The authors wish to thank Professor Wang Raorao at Tenth People's Hospital of Tongji University for his generous support to KC and Ms. Michiko Sato for her excellent technical assistance. This work was supported in part by a Grant-in-Aid for Scientific Research (JSPS KAKENHI Grant Numbers JP16H05546, JP16K15815, and JP15K11230).

Supplementary Materials

The results from flow cytometry of CBDCs for mesenchymal stem cell markers and hematopoietic cell markers. CBDCs at passage 1 were analyzed. CBDCs were positive for mesenchymal stem cell markers including CD29, CD105, CD51, and Sca-1 and negative for CD45 and CD11b. *(Supplementary Materials)*

References

[1] Y. Yamada, S. Nakamura, K. Ito et al., "Injectable bone tissue engineering using expanded mesenchymal stem cells," *Stem Cells*, vol. 31, no. 3, pp. 572–580, 2013.

[2] H. Kagami, H. Agata, M. Inoue et al., "The use of bone marrow stromal cells (bone marrow-derived multipotent mesenchymal stromal cells) for alveolar bone tissue engineering: basic science to clinical translation," *Tissue Engineering Part B: Reviews*, vol. 20, no. 3, pp. 229–232, 2014.

[3] Y. Yamaguchi, J. Ohno, A. Sato, H. Kido, and T. Fukushima, "Mesenchymal stem cell spheroids exhibit enhanced in-vitro and in-vivo osteoregenerative potential," *BMC Biotechnology*, vol. 14, no. 1, p. 105, 2014.

[4] Z. Cesarz and K. Tamama, "Spheroid culture of mesenchymal stem cells," *Stem Cells International*, vol. 2016, Article ID 9176357, 11 pages, 2016.

[5] W. J. C. Rombouts and R. E. Ploemacher, "Primary murine MSC show highly efficient homing to the bone marrow but lose homing ability following culture," *Leukemia*, vol. 17, no. 1, pp. 160–170, 2003.

[6] K. Stenderup, J. Justesen, C. Clausen, and M. Kassem, "Aging is associated with decreased maximal life span and accelerated senescence of bone marrow stromal cells," *Bone*, vol. 33, no. 6, pp. 919–926, 2003.

[7] A. Banfi, A. Muraglia, B. Dozin, M. Mastrogiacomo, R. Cancedda, and R. Quarto, "Proliferation kinetics and differentiation potential of ex vivo expanded human bone marrow stromal cells: implications for their use in cell therapy," *Experimental Hematology*, vol. 28, no. 6, pp. 707–715, 2000.

[8] F. Sugiura, H. Kitoh, and N. Ishiguro, "Osteogenic potential of rat mesenchymal stem cells after several passages," *Biochemical and Biophysical Research Communications*, vol. 316, no. 1, pp. 233–239, 2004.

[9] H. Agata, I. Asahina, N. Watanabe et al., "Characteristic change and loss of in vivo osteogenic abilities of human bone marrow stromal cells during passage," *Tissue Engineering Part A*, vol. 16, no. 2, pp. 663–673, 2010.

[10] A. Abbott, "Cell culture: Biology's new dimension," *Nature*, vol. 424, no. 6951, pp. 870–872, 2003.

[11] S. Levenberg, N. F. Huang, E. Lavik, A. B. Rogers, J. Itskovitz-Eldor, and R. Langer, "Differentiation of human embryonic stem cells on three-dimensional polymer scaffolds,"

Proceedings of the National Academy of Sciences of the United States of America, vol. 100, no. 22, pp. 12741–12746, 2003.

[12] J. E. Frith, B. Thomson, and P. G. Genever, "Dynamic three-dimensional culture methods enhance mesenchymal stem cell properties and increase therapeutic potential," *Tissue Engineering Part C: Methods*, vol. 16, no. 4, pp. 735–749, 2010.

[13] J. H. Ylostalo, T. J. Bartosh, A. Tiblow, and D. J. Prockop, "Unique characteristics of human mesenchymal stromal/-progenitor cells pre-activated in 3-dimensional cultures under different conditions," *Cytotherapy*, vol. 16, no. 11, pp. 1486–1500, 2014.

[14] B. N. Cavalcanti, B. D. Zeitlin, and J. E. Nör, "A hydrogel scaffold that maintains viability and supports differentiation of dental pulp stem cells," *Dental Materials*, vol. 29, no. 1, pp. 97–102, 2013.

[15] J. De Waele, K. Reekmans, J. Daans, H. Goossens, Z. Berneman, and P. Ponsaerts, "3D culture of murine neural stem cells on decellularized mouse brain sections," *Biomaterials*, vol. 41, pp. 122–131, 2015.

[16] B. A. Reynolds and S. Weiss, "Generation of neurons and astrocytes from isolated cells of the adult mammalian central nervous system," *Science*, vol. 255, no. 5052, pp. 1707–1710, 1992.

[17] C. Lois and A. Alvarez-Buylla, "Proliferating subventricular zone cells in the adult mammalian forebrain can differentiate into neurons and glia," *Proceedings of the National Academy of Sciences of the United States of America*, vol. 90, no. 5, pp. 2074–2077, 1993.

[18] A. Gritti, E. A. Parati, L. Cova et al., "Multipotential stem cells from the adult mouse brain proliferate and self-renew in response to basic fibroblast growth factor," *The Journal of Neuroscience*, vol. 16, no. 3, pp. 1091–1100, 1996.

[19] L. J. Richards, T. J. Kilpatrick, and P. F. Bartlett, "De novo generation of neuronal cells from the adult mouse brain," *Proceedings of the National Academy of Sciences of the United States of America*, vol. 89, no. 18, pp. 8591–8595, 1992.

[20] T. J. Bartosh and J. H. Ylostalo, "Preparation of anti-inflammatory mesenchymal stem/precursor cells (MSCs) through sphere formation using hanging-drop culture technique," *Current Protocols in Stem Cell Biology*, vol. 28, no. 1, pp. 2B.6.1–2B.6.23, 2014.

[21] S. I. Lee, Y. Ko, and J. B. Park, "Evaluation of the osteogenic differentiation of gingiva-derived stem cells grown on culture plates or in stem cell spheroids: comparison of two- and three-dimensional cultures," *Experimental and Therapeutic Medicine*, vol. 14, no. 3, pp. 2434–2438, 2017.

[22] S. Kanao, N. Ogura, K. Takahashi et al., "Capacity of human dental follicle cells to differentiate into neural cells *in vitro*," *Stem Cells International*, vol. 2017, Article ID 8371326, 10 pages, 2017.

[23] M. Belicchi, F. Pisati, R. Lopa et al., "Human skin-derived stem cells migrate throughout forebrain and differentiate into astrocytes after injection into adult mouse brain," *Journal of Neuroscience Research*, vol. 77, no. 4, pp. 475–486, 2004.

[24] W. Mueller-Klieser, "Three-dimensional cell cultures: from molecular mechanisms to clinical applications," *American Journal of Physiology-Cell Physiology*, vol. 273, no. 4, pp. C1109–C1123, 1997.

[25] T. M. Achilli, J. Meyer, and J. R. Morgan, "Advances in the formation, use and understanding of multi-cellular spheroids," *Expert Opinion on Biological Therapy*, vol. 12, no. 10, pp. 1347–1360, 2012.

[26] A. C. Tsai, Y. Liu, X. Yuan, and T. Ma, "Compaction, fusion, and functional activation of three-dimensional human mesenchymal stem cell aggregate," *Tissue Engineering Part A*, vol. 21, no. 9-10, pp. 1705–1719, 2015.

[27] X. Li, N. Li, K. Chen, S. Nagasawa, M. Yoshizawa, and H. Kagami, "Around 90° contact angle of dish surface is a key factor in achieving spontaneous spheroid formation," *Tissue Engineering Part C: Methods*, vol. 24, no. 10, pp. 578–584, 2018.

[28] W. Mueller-Klieser, "Multicellular spheroids. A review on cellular aggregates in cancer research," *Journal of Cancer Research and Clinical Oncology*, vol. 113, no. 2, pp. 101–122, 1987.

[29] R. Foty, "A simple hanging drop cell culture protocol for generation of 3D spheroids," *Journal of Visualized Experiments*, vol. 6, no. 51, article e2720, 2011.

[30] J. M. Kelm and M. Fussenegger, "Microscale tissue engineering using gravity-enforced cell assembly," *Trends in Biotechnology*, vol. 22, no. 4, pp. 195–202, 2004.

[31] Y. Zhang, X. Li, T. Chihara et al., "Comparing immunocompetent and immunodeficient mice as animal models for bone tissue engineering," *Oral Diseases*, vol. 21, no. 5, pp. 583–592, 2015.

[32] H. Zhu, Z. K. Guo, X. X. Jiang et al., "A protocol for isolation and culture of mesenchymal stem cells from mouse compact bone," *Nature Protocols*, vol. 5, no. 3, pp. 550–560, 2010.

[33] Y. Cai, T. Liu, F. Fang, C. Xiong, and S. Shen, "Comparisons of mouse mesenchymal stem cells in primary adherent culture of compact bone fragments and whole bone marrow," *Stem Cells International*, vol. 2015, Article ID 708906, 8 pages, 2015.

[34] B. Corradetti, F. Taraballi, S. Powell et al., "Osteoprogenitor cells from bone marrow and cortical bone: understanding how the environment affects their fate," *Stem Cells and Development*, vol. 24, no. 9, pp. 1112–1123, 2015.

[35] J. S. Fernandez-Moure, B. Corradetti, P. Chan et al., "Enhanced osteogenic potential of mesenchymal stem cells from cortical bone: a comparative analysis," *Stem Cell Research & Therapy*, vol. 6, no. 1, p. 203, 2015.

[36] D. Blashki, M. B. Murphy, M. Ferrari, P. J. Simmons, and E. Tasciotti, "Mesenchymal stem cells from cortical bone demonstrate increased clonal incidence, potency, and developmental capacity compared to their bone marrow–derived counterparts," *Journal of Tissue Engineering*, vol. 7, 2016.

[37] Y. Moritani, M. Usui, K. Sano et al., "Spheroid culture enhances osteogenic potential of periodontal ligament mesenchymal stem cells," *Journal of Periodontal Research*, vol. 53, no. 5, pp. 870–882, 2018.

[38] L. Guo, Y. Zhou, S. Wang, and Y. Wu, "Epigenetic changes of mesenchymal stem cells in three-dimensional (3D) spheroids," *Journal of Cellular and Molecular Medicine*, vol. 18, no. 10, pp. 2009–2019, 2014.

[39] L. Guo, R. C. H. Zhao, and Y. Wu, "The role of microRNAs in self-renewal and differentiation of mesenchymal stem cells," *Experimental Hematology*, vol. 39, no. 6, pp. 608–616, 2011.

[40] T. H. Cheung, N. L. Quach, G. W. Charville et al., "Maintenance of muscle stem-cell quiescence by microRNA-489," *Nature*, vol. 482, no. 7386, pp. 524–528, 2012.

[41] K. Drela, A. Sarnowska, P. Siedlecka et al., "Low oxygen atmosphere facilitates proliferation and maintains undifferentiated

state of umbilical cord mesenchymal stem cells in an hypoxia inducible factor-dependent manner," *Cytotherapy*, vol. 16, no. 7, pp. 881–892, 2014.

[42] S. Okada, H. Nakauchi, K. Nagayoshi, S. Nishikawa, Y. Miura, and T. Suda, "In vivo and in vitro stem cell function of c-kit- and Sca-1-positive murine hematopoietic cells," *Blood*, vol. 80, no. 12, pp. 3044–3050, 1992.

[43] G. J. Spangrude, S. Heimfeld, and I. Weissman, "Purification and characterization of mouse hematopoietic stem cells," *Science*, vol. 241, no. 4861, pp. 58–62, 1988.

[44] K. Matsuura, T. Nagai, N. Nishigaki et al., "Adult cardiac Sca-1-positive cells differentiate into beating cardiomyocytes," *Journal of Biological Chemistry*, vol. 279, no. 12, pp. 11384–11391, 2004.

[45] T. J. Bartosh, J. H. Ylostalo, A. Mohammadipoor et al., "Aggregation of human mesenchymal stromal cells (MSCs) into 3D spheroids enhances their antiinflammatory properties," *Proceedings of the National Academy of Sciences of the United States of America*, vol. 107, no. 31, pp. 13724–13729, 2010.

[46] N. C. Cheng, S. Y. Chen, J. R. Li, and T. H. Young, "Short-term spheroid formation enhances the regenerative capacity of adipose-derived stem cells by promoting stemness, angiogenesis, and chemotaxis," *Stem Cells Translational Medicine*, vol. 2, no. 8, pp. 584–594, 2013.

[47] N. C. Cheng, S. Wang, and T. H. Young, "The influence of spheroid formation of human adipose-derived stem cells on chitosan films on stemness and differentiation capabilities," *Biomaterials*, vol. 33, no. 6, pp. 1748–1758, 2012.

Hindawi
Stem Cells International
Volume 2019, Article ID 4508470, 17 pages
https://doi.org/10.1155/2019/4508470

Review Article

Design Principles for Pluripotent Stem Cell-Derived Organoid Engineering

Teresa P. Silva,[1,2,3] João P. Cotovio,[1,2] Evguenia Bekman,[1,2,3] Maria Carmo-Fonseca,[2,3] Joaquim M. S. Cabral,[1,2] and Tiago G. Fernandes[1,2]

[1]*Department of Bioengineering and iBB-Institute for Bioengineering and Biosciences, Instituto Superior Técnico, Universidade de Lisboa, Av. Rovisco Pais, 1049-001 Lisboa, Portugal*
[2]*The Discoveries Centre for Regenerative and Precision Medicine, Lisbon Campus, Universidade de Lisboa, Lisboa, Portugal*
[3]*Instituto de Medicina Molecular, Faculdade de Medicina, Universidade de Lisboa, Av Prof Egas Moniz, Edificio Egas Moniz, 1649-028 Lisboa, Portugal*

Correspondence should be addressed to Tiago G. Fernandes; tfernandes@tecnico.ulisboa.pt

Received 18 October 2018; Revised 12 February 2019; Accepted 24 February 2019; Published 18 April 2019

Academic Editor: Alexander Kleger

Human morphogenesis is a complex process involving distinct microenvironmental and physical signals that are manipulated in space and time to give rise to complex tissues and organs. Advances in pluripotent stem cell (PSC) technology have promoted the *in vitro* recreation of processes involved in human morphogenesis. The development of organoids from human PSCs represents one reliable source for modeling a large spectrum of human disorders, as well as a promising approach for drug screening and toxicological tests. Based on the "self-organization" capacity of stem cells, different PSC-derived organoids have been created; however, considerable differences between *in vitro*-generated PSC-derived organoids and their *in vivo* counterparts have been reported. Advances in the bioengineering field have allowed the manipulation of different components, including cellular and noncellular factors, to better mimic the *in vivo* microenvironment. In this review, we focus on different examples of bioengineering approaches used to promote the self-organization of stem cells, including assembly, patterning, and morphogenesis *in vitro*, contributing to tissue-like structure formation.

1. Introduction

The application of the biomimicry concept, defined as the imitation of biological systems, has contributed to a significant innovation in regenerative medicine during the last years. This concept is usually associated with new approaches that aim to achieve the recapitulation of the natural form or function, natural processes, or natural systems [1, 2]. In the bioengineering field, efforts have been made to mimic the natural forms and functions of the human body *in vitro*, from the molecular to the cellular level, in an attempt to recreate the highest complexity level, the organism.

Recently, with the discovery of the ability of pluripotent stem cells (PSCs) to coordinate various key signals and to recapitulate different structures as seen *in vivo*, including tissue- and mini organ-like structures, our knowledge about human development and morphogenesis in healthy and disease contexts has been greatly improved [3, 4]. With the recapitulation of human organogenesis *in vitro*, the concept "organoid" emerged. In 1946, the "organoid" term was employed for the first time to define a tumor-derived mass isolated from a human tissue [5]. Subsequently, all tissue masses resultant from transplants were defined as "organoids" [6, 7], and the concept evolved to include cultures that were generated from dissociation and aggregation of animal- and tissue-derived cells [8–10]. With the recent advances in human PSC expansion culture and direct differentiation, the "organoid" definition followed the same evolution, nowadays referring to an *in vitro* 3D multicellular structure containing different cell types with self-organization, as seen

Table 1: Bioengineering approaches to control cell organization into PSC-derived organoids.

Self-organization control	Self-assembly	Scaffold-free approaches	Hanging drop method		[73–77]
			V-bottomed and round-bottomed multiwell plates		
			Microwells		
		Scaffold for imposing external and internal architecture	Nanotopography	Electrospinning	[88]
				Electron beam	
				Selective etching	
				Nanoimprinting	
			3D printing	Nozzle	[93, 94, 96, 188]
				Laser	
				Inkjet	
		Manipulation of organoid assembly	DNA-programmed assembly of cells		[100, 101]
			3D bioprinting	Inkjet bioprinting	[102–110, 112, 113, 189]
				Microextrusion systems	
				Laser-based direct-write techniques	
			Synthetic ECM	Adhesion peptides	[146–148]
				Peptide substrates	
				Combined hydrogels	
	Self-patterning and self-morphogenesis	Spatiotemporal control of mechanical signals	DNA-directed assembly of shape-controlled units		[149]
			Light-mediated patterning		[150, 151]
			pH-mediated patterning		[152]
			Supramolecular "host-guest" interactions		[153]
			Enzymatic reaction-mediated patterning		[154]
		Spatiotemporal control of morphogen diffusion	Light-mediated patterning		[160, 161]
			Microfluidic systems		[163, 167]
			Micro/nanoparticles		[170–172]

in human tissues, typically derived from stem cells [2]. Frequently, organoids display spherical or irregular shapes in suspension or are embedded in different types of matrices [11].

The recreation of functional and structural mimicry within the organoid requires a minimal number of design components inspired on the original biological system. These include cellular and noncellular parameters, such as cell type and microenvironmental and physical parameters, as well as the resulting internal and external interactions, like cell-cell, cell-matrix, and cell-microenvironment [12]. The ultimate goal is to reestablish some of the features of human tissues, particularly the presence of different cell types to recapitulate the multicellular heterogeneity, and to control the microenvironment to recreate a high level of organization, promoting organoid maturation to achieve tissue functionality [11]. Thus, the application of bioengineering strategies to manipulate cellular and noncellular components may become a powerful tool to direct 3D human organoid morphogenesis.

The remarkable progress in organoid generation has provided the possibility to use these novel platforms for understanding human development and the complex processes involved in organogenesis. The use of organoids in drug screening and toxicological testing could also improve the safety and efficiency of drugs before reaching clinical trials, making the drug development process more cost-effective. Lastly, disease-derived organoids could also offer a valuable platform to study the mechanisms involved in disease manifestation and to identify possible therapeutic targets.

Here, we review distinct bioengineering approaches to direct the stem cell commitment and further self-organization of cells, recapitulating tissue morphogenesis *in vitro*. First, the self-organization capacity of cells is explored based on cell-cell and cell-matrix interactions. Afterwards, as self-organization is based on three different cell-associated capacities, including self-assembly, self-patterning, and self-morphogenesis, we highlight examples of bioengineering methodologies to control the initial state and the spatiotemporal positioning of cells and, lastly, the growth and remodeling of multicellular aggregates to achieve complex structures (Table 1).

2. Self-Organization in PSC-Derived Organoids

The ability of human PSCs to produce highly organized structures that reproduce features similar to the embryo and adult tissues was first detected in the teratomas formed after the injection of human embryonic stem cells (ESCs) in immune-deficient mice (reviewed in [13]). The "self-organization" capacity involves three different categories: first, the control of relative cell position, named "self-assembly";

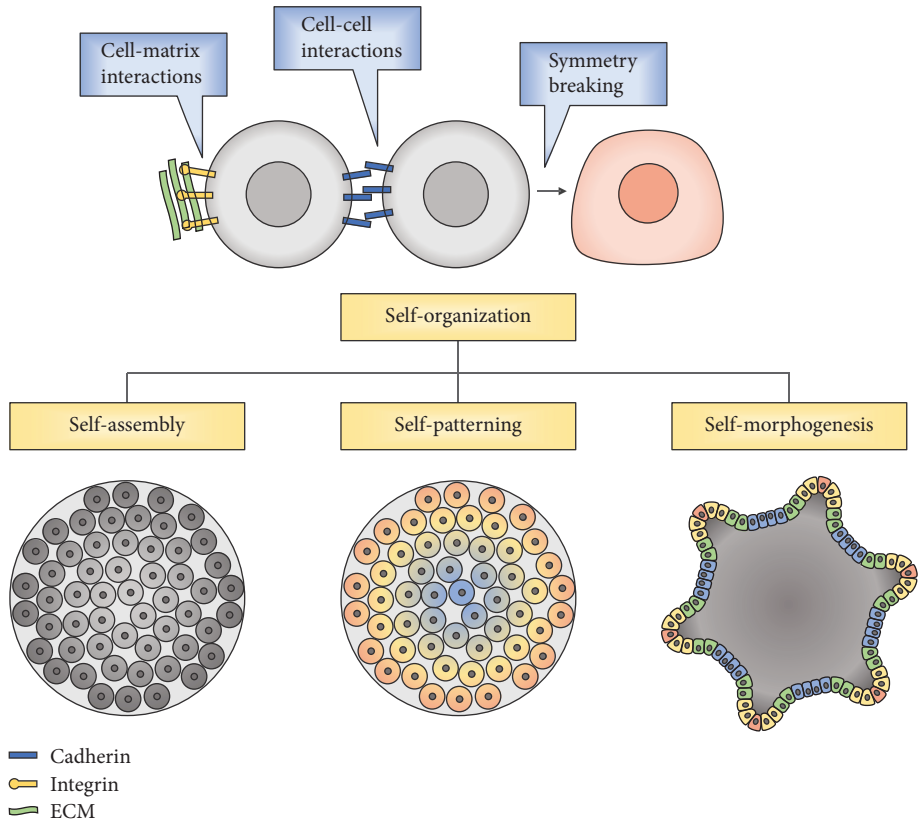

Figure 1: In tissue morphogenesis, the self-organization capacity of cells is achieved by a multicellular process involving cell-cell and cell-matrix interactions, as well as symmetry breaking. This capacity includes a combination of self-assembly, self-patterning, and self-morphogenesis capacities, which involves the control of the cell position, spatiotemporal control of cell stage, and control of tissue mechanics.

second, the spatiotemporal control of the cell stage, defined as "self-patterning"; and lastly, the capacity to promote deformation, growth, and remodeling, which is termed "self-morphogenesis" (Figure 1) [14]. This intrinsic ability of organization is strongly dependent of the physical and morphological properties of cells, the autologous and exogenous signals that they receive, and also the mechanical features of the system.

2.1. Cell-Cell Adhesive Interactions. During embryogenesis, cell-cell interactions play a critical role in the dynamic changes of cell sorting, arrangement, and migration that originate different tissue morphologies. The adhesive forces between cells are crucial for the assembly and organization into a 3D structure. The most important and global mechanism of cell adhesive interactions is mediated by cadherins, which are Ca^{2+}-dependent transmembrane proteins that facilitate homophilic cell-cell adhesion by their extracellular domains, whereas the intracellular domain interacts with their partner proteins, the catenins (reviewed in [15]). Following cell-cell adhesion, a protein complex is formed composed by the catenin polypeptide of α-, β- or γ-catenins (reviewed in [16]). Subsequently, α-catenin mediates physical interaction to the actin cytoskeleton, demonstrating that cadherins can also guide cell cytoskeletal anchoring [17, 18]. Different cadherins are expressed in different tissues, and the best-studied are the classical vertebrate cadherins, including N-cadherin, highly expressed in the neuronal tissue [19, 20], and E-cadherin, mostly expressed in epithelial cells [21]. Nonclassical cadherins can be found in other human tissues, for instance, VE-cadherin, which is the vascular-endothelial cadherin [22], and R-cadherin, expressed in the retinal tissue [19].

During morphogenesis, different mechanisms involving cadherins appear to influence cell sorting and therefore alter the spatial organization of cells. The expression of different types of cadherins in different cell types promotes the selective recognition and connection of cells expressing the same type of cadherin leading to cell sorting and separation into different tissues [23–25]. For instance, N-cadherin expression in neural cells allows the separation from epithelial cells that express E-cadherin (Figure 2(a)) [26]. In other cases, independently of the cadherin type expression, cell sorting is also observed based on differential levels of cadherin expression [25, 27, 28]. The epithelial-mesenchymal transition (EMT), the reverse of epithelization, is a strong example of the self-assembly capacity of cells mediated by cadherin expression and regulation (Figure 2(b)) [29]. This process is achieved by altering cell-cell contact and promoting cell migration. In particular, E-cadherin is downregulated during the transition to the mesenchymal state, leading to the decrease of cell-cell interactions [30, 31]. Simultaneously,

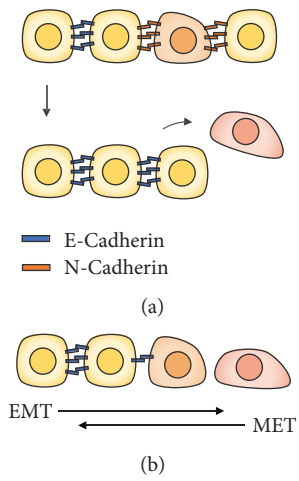

Figure 2: Cadherin involvement in tissue morphogenesis. (a) Cell sorting based on differential expression of distinct cadherins. (b) Epithelial-mesenchymal transition (EMC) and its reverse (MET), an example of self-assembly capacity mediated by differential cadherin expression and regulation.

an alteration on cellular signaling profiles and a remodulation of the cytoskeleton is observed, allowing cell migration (reviewed in [32]).

In addition, other physiological factors that interact with cadherin-mediated signaling can influence cell sorting independently of cadherin expression. During development, an anterior-posterior axis is created leading to the formation of compartment boundaries. Although epithelial cells express high levels of E-cadherin, selective adhesion is observed creating different boundaries in response to Hedgehog (Hh) signaling [33, 34]. Activation of Hh expression in posterior cells conduces to diffusion of signals across the anterior-posterior boundary that determine the sorting of some anterior cells next to the boundary, which are not capable of receiving Hh and are sorted toward the posterior region [34]. Besides that, the dynamic regulation of cadherin adhesions may drive cell rearrangements and migration. By breaking and reforming cadherin adhesive bonds, the convergent extension movements contribute to tissue morphogenesis by changing the local cellular arrangement with respect to neighboring cells [35, 36].

Besides the important function of cadherins during morphogenesis, their critical role in cell aggregate formation and further differentiation was already demonstrated. By inhibition of E-cadherin-mediated adhesion, the agglomeration of ESCs in cell aggregates is prevented as well as their differentiation [37–39]. Hence, technologies to control stem cell differentiation by manipulating cell-cell interactions have been created. For example, surface engineering by immobilization of cadherins has been used to manipulate cadherin-mediated signaling pathways and thus direct stem cell fate decisions [40, 41]. Moreover, it was demonstrated that not only does the immobilization of cadherins mediate stem cell differentiation but the interaction with adjacent cells also has an important role in patterning particular cell types. The incorporation of certain progenitor cells allows the addition of specific cell-cell interactions that mimic *in vivo* conditions and manipulate differentiation processes. For example, coculture with organ-matched mesenchymal cells allows the proliferation of progenitor cells, without differentiation, giving rise to progenitors that were able to efficiently produce large numbers of specific differentiated cells [42].

2.2. Cell-Matrix Interactions. Not only do cell-cell interactions provide important signals in the cell niche but other structural, physical, electrical, or biochemical signals present in the complex microenvironment during embryonic development also affect cell fate decisions (reviewed in [43]). The extracellular matrix (ECM) is an important component that gives the structural support to the cell niche and also contributes for mediating signaling for cell migration, retention, and polarization [44, 45]. The ECM is composed primarily by glycosaminoglycans and fibrous proteins that are secreted by the cells to generate their own physical scaffold (reviewed in [43]). Cells interact with ECM molecules via integrins, which are cell adhesion receptors, regulating cellular behavior (reviewed in [46]).

Integrins present a family of heterodimeric transmembrane glycoproteins where heterodimers are composed of non-covalently connected α and β subunits [47]. In vertebrates, 24 different heterodimers resulting from different assemblies of 18 α subunits and 8 β subunits have been described. Based on their subunit composition, integrins can be classified in different subgroups. Under certain conditions, each cell type exhibits a specific integrin signature, including the subgroup and quantity of integrins (reviewed in [48]). However, this is a dynamic process, and both the developmental stage and microenvironmental conditions can change the integrin repertoire (reviewed in [49]). While the extracellular domain of integrins interacts with components of ECM, including fibronectin, laminin, and collagens, the intracellular domain links to cytoskeletal and regulatory proteins, such as α-actinin, filamin, calreticulin, and cytohesin (reviewed in [50]). It is also known that the same component of ECM interacts with different integrin receptors, and in the same way, a specific integrin receptor may recognize different ECM components (reviewed in [48]).

The role of integrins during embryogenesis has been extensively studied, and the data accumulated so far are already enough to place integrins as important players in fertilization, cell migration in gastrulation, adhesion in embryo implantation, and generation of different organ systems, like the nervous system (reviewed in [50]). Additionally, it was already shown that the composition of ECM is able to influence ESC behavior in the development of 3D structures as well as their differentiation. For example, fibronectin was reported to strongly stimulate endothelial and vascular cell differentiation, while laminin promotes the generation of beating cardiomyocytes [51]. The matrix that is most commonly used for PSC differentiation and generation of different types of organoids is Matrigel, which is a gelatinous protein mixture extracted from Engelbreth-Holm-Swarm mouse sarcoma cells [52, 53], prone to lot-to-lot variation. There are few studies that try to address the exact mechanism by which Matrigel supports organoid development. Although the manipulation of integrin signaling to

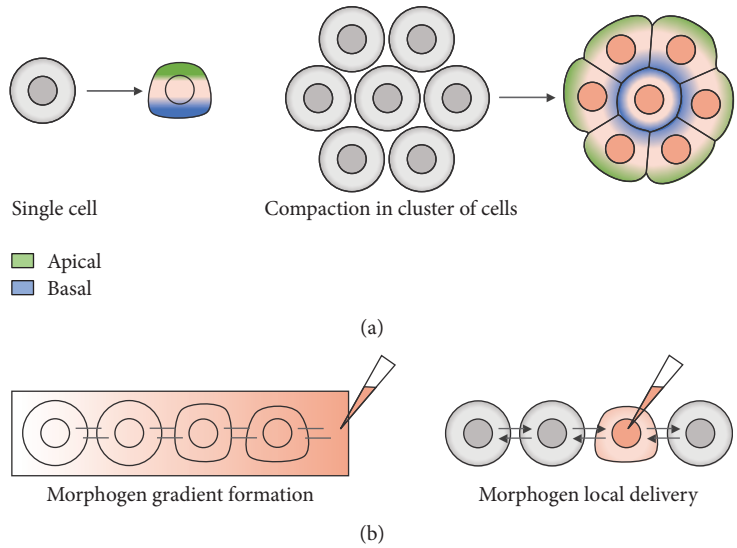

Figure 3: Symmetry breaking process. (a) Symmetry breaking *in vivo* is observed at the single-cell level and multicellular level, involving a process of compaction. (b) Different approaches for symmetry breaking *in vitro*, using microfluidic approaches to create a morphogen gradient or local delivery of morphogens.

direct stem cell fate is still very difficult, some groups have been studying the involvement of specific integrins in PSC differentiation, with a focus on identification of ECM components directly interacting with a specific integrin subgroup and promoting selective endoderm [54], mesoderm [55], or ectoderm [56] differentiation.

In addition to these chemical cues from the ECM, mechanical and physical stimuli, like porosity and stiffness, also exert their influence on cellular commitment [57]. The matrix stiffness can be sensed by cells through mechanoreceptors that also include integrins, regulating cellular behavior (reviewed in [58]). While intermediate substrate stiffness favors the endodermal lineage, softer substrates originate ectodermal tissues [59]. It was also demonstrated that mesodermal differentiation is very sensitive to mechanical properties of the ECM [60]. While soft substrates enhance mesoderm commitment, stiff matrices induce only minimal mesoderm differentiation [60]. In this latter study, authors showed that on a soft substrate, human ESCs present β-catenin accumulation at cell-cell adhesions leading to enhanced WNT signaling and subsequent WNT-dependent mesoderm differentiation. In contrast, stiff materials promote the integrin-dependent β-catenin degradation and thus inhibit mesoderm commitment [60]. Therefore, by playing with biochemical components of the ECM, as well as its mechanical and physical parameters, cell proliferation and differentiation can be manipulated in the 3D microenvironments.

2.3. Breaking Symmetry. Symmetry breaking is a pivotal phenomenon in animal development that precedes pattern formation, allowing the generation of higher morphological and functional specialization. *In vivo*, symmetry is broken at the single-cell level, where the cellular cytoskeleton and membrane-associated proteins are redistributed to create apicobasal polarity (Figure 3(a)). For example, while integrins accumulate at the basal side of the cell, a ring of actin filaments is formed at the apical side. The actin ring contraction can drive apical constriction leading to cell shape alteration and epithelial sheet bending (reviewed in [61, 62]). In addition, symmetry breaking also occurs at the multicellular level, as seen in the early mouse embryo. This morphological event called compaction transforms the embryo from a loose cluster of spherical nonpolarized cells into a tightly packed mass, in which cell-cell contacts are strengthened and cell polarization is achieved (Figure 3(a)). Several mechanisms are involved in the compaction process: cell-cell adhesive interactions, involving the redistribution of E-cadherin; cortical tension, generated by actomyosin network contractility determining the cell shape; and extension of long membrane protrusions (reviewed in [63, 64]).

The precise molecular and physical features, as well as the precise timing in which symmetry breaking occurs, are still poorly understood. Some events appear to be cell-autonomous, depending on the asymmetric gene expression in embryonic cells, and others appear to be caused by morphogen gradients. In fact, symmetry breaking can be achieved by an initially homogeneous morphogen distribution, which can turn into a concentration gradient due to reaction-diffusion [65]. In a reaction-diffusion model, the self-organization capacity of cells leads to symmetry breaking activated by a stochastic disturbance of the system without a requirement of a dominant "master factor" [66]. Therefore, cell characteristics, including gene expression and cell polarity, and local interactions between cells can by themselves be responsible for lineage establishment. Reported studies already demonstrated that a uniform aggregate of stem cells is capable to originate a high level of organization, comparable to what is observed in native tissues [67–69]. Some organoid models with minimal but sufficient complexity are able to undergo spontaneous symmetry breaking in the absence of spatial cues. In this case, a specific pattern is created including

rostral-caudal polarization in cortical organoids [67], anterior-posterior patterning in 3D gastruloids [68, 70, 71], and dorsal-ventral patterning in neural tube organoids [69, 72]. Therefore, symmetry breaking events can be attained *in vitro* by the addition of a single morphogen, through a diffusion-reaction mechanism, or by using more sophisticated bioengineering approaches to create symmetry breaking based on local morphogen delivery (Figure 3(b)).

3. Controlled Assembly of PSCs

The generation of organoids starts by promoting the assembly of PSCs into a 3D structure. Similar to the human embryo, the earliest cell fate decision is based on the spatial orientation of cells (reviewed in [64]). Therefore, methodologies to control cell arrangement during the initial organoid assembly can affect further morphogenesis induction. The assembly process can be achieved based on the self-assembly properties of cells in a scaffold-free tissue engineering approach or by using different bioengineering strategies to direct and control the arrangement of cells.

3.1. Scaffold-Free Approaches. The generation of organoids in a scaffold-free manner is based on the "self-organization" property of stem cells, in which cells have the ability to assemble in a 3D structure. Different methodologies have been applied to form 3D aggregates of PSCs, with the embryoid body (EB) formation by the hanging drop method the first to be used for the production of homogeneous cell aggregates. This technique is based on gravity to force the cells to aggregate and consists of creating small drops of a medium with cells suspended on a lid [73]. To overcome the manipulation limitations that could disturb the EBs, this technique was adapted to V-bottomed and round-bottomed multiwell plates, in which cells are forced to rapidly aggregate by applying a rotational force [74]. However, this methodology does not avoid the individual manipulation of the cell aggregates. Therefore, different microwells fabricated by lithographic techniques have been used to simultaneously generate 100s to 1000s of cell aggregates by centrifugation, allowing the scaling up of the multiwell plate technique [75–77]. In addition, microfluidic channels have also been used for the continuous formation of cell aggregates, being a powerful tool for high-throughput applications [78].

In these scaffold-free methodologies, the most important parameter to be controlled is the size of the generated aggregates. It was demonstrated that the size of the cell niche influences the differentiation trajectories because of its impact on the microenvironmental parameters, including the spatial gradient of soluble molecules, and cell-cell and cell-matrix interactions [79, 80]. Thus, since variations in cell number are translated to different aggregate sizes, controlling the cell aggregate size can influence the signaling pathways conducing to a more efficient commitment and differentiation. In fact, different research groups have been optimizing the aggregate diameter to improve the mesoderm or neuroectodermal induction, achieving higher yields of cardiac and neuronal cells [81–83].

More recently, Xie et al. reported that not only the size of cell aggregates can influence the differentiation toward different lineages but also the self-assembly kinetics. The study showed that the aggregation kinetics altered the EB structure; in particular, slower kinetics originated EBs with higher porosity facilitating the exposure of cells to growth factors. Ultimately, faster aggregation appears to favor ectodermal commitment whereas slower aggregation promotes mesoendodermal differentiation [84].

3.2. Scaffolds for Imposing External and Internal Architecture. Cellular organization within an engineering tissue involves the assembly of cells into a specific arrangement for mimicking the architecture of the native tissue. To mimic the *in vivo* physical and biochemical properties of the tissue microenvironment, different matrices can be used, including those from natural sources or artificially synthesized. A specific architecture can be externally imposed by using different approaches to manipulate the tissue shape, like molds and scaffolds. For example, microcontact printing can provide different molds from different materials like agarose, polydimethylsiloxane, or polyacrylamide, with minimal adhesive properties, only to force cells to aggregate and acquire a specific shape [85, 86]. Besides that, this technique can be used to introduce some functionalization by directly depositing proteins or ECM components onto a partially polymerized substrate [87]. Furthermore, the control of the shape, size, space, and organizational symmetry of nanometer-scale features in different biomaterials has been achieved by using different nanolithography strategies. Among different nanotopography approaches, the electrospinning allows the formation of nanofibrous substrates from natural or synthetic polymers, while electron-beam, selective etching, and nanoimprinting have been used to create nanopits, nanopillars, or nanochannels on various materials. By applying these different approaches, the natural dimensions of basement-membrane fibers and pore sizes can be reached allowing to mimic the porosity of the natural ECM (reviewed in [88]).

The scaffolds used for imposing the external shape and mimicking the natural ECM mostly have a fixed morphology. However, human development starts on a microscale, and considerable morphologic changes have to occur to achieve the final morphogenesis. Therefore, it is very important to try to dynamically control the organoid morphology in order to reach a correct tissue-like organization. The application of different types of hydrogels has been able to improve the control of the 3D microscale morphology of organoids. Hydrogels are hydrophilic 3D polymeric networks with natural or synthetic origin that are insoluble due to the presence of chemical or physical crosslinks [89, 90]. The internal structure of the hydrogel can be manipulated by using different techniques, including 3D printing [91] and sacrificial molding [92], which can possibly regulate the morphology of the generated structures.

In the last years, significant improvements have been made concerning mechanical performance and functionality in the 3D printing of hydrogels. There are different reported hydrogel composite 3D printing techniques that allow to fabricate complex and highly customizable scaffold structures,

including nozzle-based, laser-based, and inkjet-based 3D printing systems (reviewed in [93]). The nozzle-based 3D printing is the most used approach, in which viscous liquids or melted polymers are forced to extrude out of a nozzle, syringe, or orifice in order to sequentially build a 3D structure based on a predesigned path created by computer modeling. Recently, Hinton et al. reported an adaptable and cost-effective nozzle-based 3D printing, termed freeform reversible embedding of suspended hydrogels (FRESH), that uses a thermo-reversible support bath to enable deposition of hydrogels. Based on 3D imaging data from whole organs, FRESH is able to print scaffolds with complex internal and external architectures, including a 3D CAD model of the embryonic heart [94], demonstrating a valuable applicability in organogenesis. In addition, the laser-based 3D printing systems are also capable of building 3D structures in photo-treatable hydrogels under the deposition of laser energy, normally UV light, into specific designed patterns [95]. Finally, inkjet printing is a noncontact printing technique used to create ink droplets onto a material platform (reviewed in [96]). Even though biological molecules and structures are fragile and sensitive, this approach appears to be appropriate to introduce biological modification on generated scaffolds, since it already was successfully used to transfer biomolecules like nucleic acids to solid supports [97].

Miller et al. were the first to report the generation of cylindrical networks within different hydrogels by using 3D filament networks of carbohydrate glass as a sacrificial template [92]. Therefore, they were able to pattern vascular networks into 3D tissue constructs by molding channels. Following this study, this sacrificial molding technique was also used by other groups to create internal cavities of micro- to macroscale dimensions within a variety of hydrogel materials by applying different molds, including calcium alginate and polyvinyl alcohol (PVOH) templates [98, 99]. Briefly, the sacrificial molding technique is based on encapsulating a dissolvable or degradable material within a second hydrogel material. After the composite hydrogel formation, the internal sacrificial material is removed and a hydrogel with defined internal architecture is created. This internal architecture manipulation in the hydrogels provides an important tool not only to create vascularized tissues but also for organoid encapsulation, in which the internal spaces allow the growth, deformation, and remodeling of the organoids to generate a defined morphology.

3.3. Bioengineering Approaches to Manipulate Organoid Assembly. Several bioengineering approaches have been applied to guide cell assembly in order to achieve a desired cell arrangement and organoid shape. In 2015, Todhunter et al. reported a DNA-programmed assembly of cells (DPAC), in which size, shape, composition, and spatial heterogeneity is programmed, thereby recreating the multicellular organization of organoids [100]. In DPAC, 2D DNA-patterned substrates are used to guide cellular organization by presenting complimentary lipid-modified oligonucleotides. After this programmed assembly, a DNase treatment is performed to release a well-organized cell aggregate, followed by encapsulation within ECM gels [100, 101].

As previously described for fabrication of scaffold structures, 3D printing techniques have also been applied to control cell assembly by the deposition of single or multiple types of cells with different supportive matrices. This type of bioprinting methodology involves different approaches, like inkjet bioprinting, microextrusion systems, and laser-based direct-write techniques, in which different actuation methods are applied (reviewed in [102]). In inkjet bioprinting, two different actuation methods are used, piezoelectric and thermal, whereby either acoustic waves or thermal forces, respectively, are used to prepare liquid droplets. While in the thermal approach a variable size of droplets is obtained, in the piezoelectric technology, regular and equal sizes are generated [103, 104]. This is a low-cost technology with high resolution and printing speed; however, it has some limitations regarding the type of materials that can be printed. Although some thermal and mechanical stress can be introduced to the cells, this technology was already successfully applied to different mammalian cell printing with a viability above 85% [104]. On the other hand, the microextrusion technique is derived from the modification of inkjet printers, which are pressure-assisted robotic apparatus that can extrude cell-laden hydrogels by pneumatic or mechanical dispensing onto a substrate (reviewed in [105, 106]). Human chondrocytes and osteogenic progenitors in combination with an alginate hydrogel were already extruded by using a pneumatic syringe dispenser, demonstrating the ability to create 3D structures with high cell viability [107].

The laser-based direct-write technique is the most applied bioprinting technology. This technique uses a laser beam that is focused on a support layer underlying a cell-containing matrix on the donor print ribbon, forcing its rapid volatilization and allowing the cell to be transferred onto an adjacently localized receiving substrate (reviewed in [108]). High cell viabilities have been reported using this technique, due to low shear stress, and its high resolution allows single-cell deposition, yielding scaffold-free 3D cell constructs [109]. For cell-based applications, the most common laser-based techniques are biological laser processing (BioLP), matrix-assisted pulsed laser evaporation direct writing (MAPLE-DW), laser-induced forward transfer (LIFT), absorbing film-assisted laser-induced forward transfer (AFA-LIFT), and laser-guided direct writing (LG-DW) (reviewed in [108]). MAPLE-DW was successfully used to deposit patterns of different cell types onto and within the Matrigel, demonstrating that spatial coherence can be achieved [110, 111]. Furthermore, human osteosarcoma cells were printed by BioLP and transferred into the Matrigel, producing a 3D cellular construct with 95% of cell viability [112]. This method was later improved reaching 100% viable cells and single-cell resolution [113]. Thus, a high control in cell assembly is reached, allowing to manipulate cellular arrangement and composition within an organoid with a defined 3D microscale morphology.

4. Directed Organoid Patterning and Morphogenesis

The knowledge about the signaling pathways involved in pluripotency maintenance, as well as the generation of

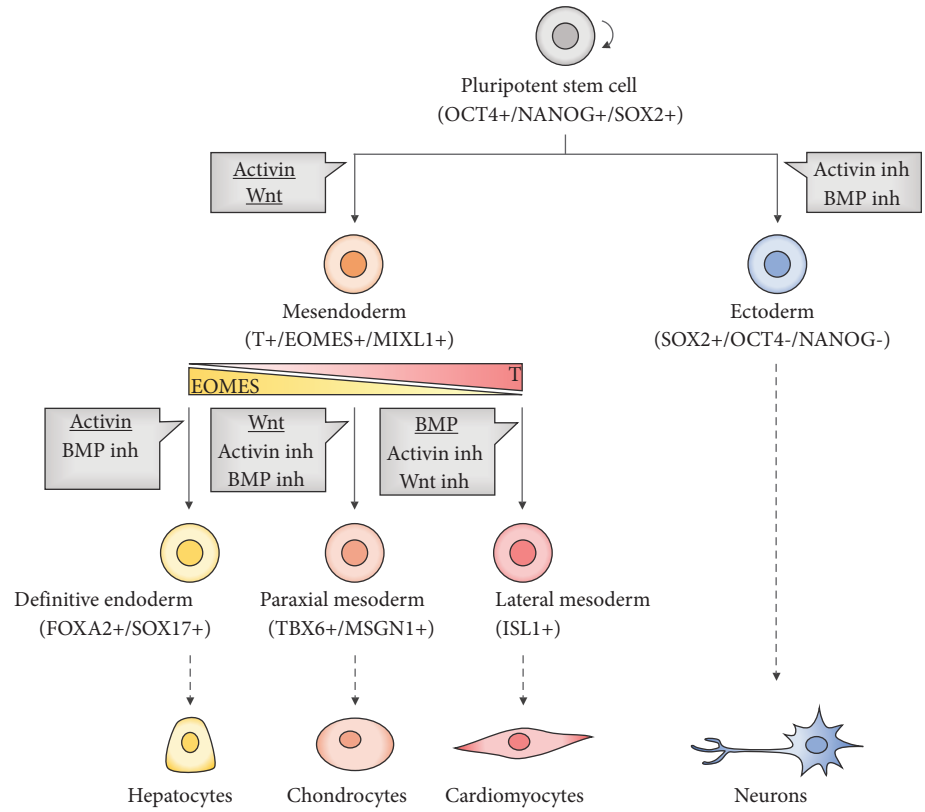

Figure 4: Lineage specification from PSCs. Ectoderm induction is achieved by dual SMAD inhibition, whereas mesendodermal differentiation is based on the activation of dual SMAD regulators and WNT signaling. Dashed arrows represent examples of different cell types achieved by manipulating specific lineage differentiation.

different germ layers, has allowed the manipulation and control of PSC commitment to different lineages and further differentiation into specific cell types. For instance, neuroectoderm commitment is easily achieved by manipulating TGFβ signaling [114]. The most efficient method for neural induction from PSCs is the dual SMAD inhibition of BMP and activin signaling (Figure 4), which are antagonized by Noggin and Lefty, respectively [114, 115]. Other chemical antagonists have been used to promote BMP signaling inhibition, like Dorsomorphin and LDN-193189, blocking the commitment towards the trophectoderm [115, 116]. For nodal/activin signaling inhibition, a chemical antagonist SB431542 is efficient to prevent the mesendodermal differentiation by blocking the TGFβ signaling [115, 117].

Oppositely, the activation of dual SMAD regulators, as well as the WNT signaling, appears to be critical for the initial mesendoderm commitment, giving rise to Brachyury$^+$ (T)/EOMES$^+$/MIXL1$^+$ cells [118, 119]. Following mesendoderm induction, by manipulating the levels of T and EOMES, further differentiation towards the mesoderm or endoderm can be specified (Figure 4) [120]. T action seems to be important for the mesodermal fate, repressing endodermal differentiation [120]. On the other hand, high levels of EOMES are essential for the expression of endoderm markers (FOXA2 and SOX17) [121]. While activin leads to the development of a population with higher expression of FOXA2, resulting in endoderm specification, WNT activation generates cells with lower expression of FOXA2, important for the mesoderm fate [122]. Interestingly, although BMP is not required for the mesendoderm commitment, alone, it is capable of inducing the development of a population with low expression of FOXA2 [119, 123]. In mesodermal specification, WNT and BMP signals induce bifurcation of two mesoderm subtypes, the paraxial and the lateral mesoderm, respectively [124]. While WNT appears to be important for mesoderm specification and further generation of chondrocytes, the inhibition of WNT signaling is essential to promote cardiac differentiation [124–126].

On the other hand, after the establishment of the activin-induced definitive endoderm, various cell populations can arise, such as hepatocytes and pancreatic cells. BMP and WNT signaling pathways have an important role in the generation of the pancreatic lineage, while the specification of insulin-producing cells can be achieved by FGF signaling [127, 128]. The combination of FGF and BMP4 signaling is related with hepatic fate specification [129].

Based on the manipulation of the previously described signaling pathways, as well as on the "self-organization" capacity of stem cells, organoids from different lineages have been produced including the brain, kidney, liver, pancreas, lung, and gut [3, 130–134]. Eiraku et al. were the first to demonstrate the ability of PSCs to self-organize in the cortical tissue and recapitulate embryonic brain development [135]. Later, Lancaster et al. were able to direct human PSC differentiation into different cerebral cortex regions and apply this technique for disease modeling [3]. A variety of well-

organized neuronal organoids was later reported, including forebrain-, midbrain-, hypothalamus-, and cerebellum-like structures [136–139]. In addition to brain organoids, by directing PSCs towards the intermediate mesoderm, organoids that recapitulate the first trimester of the human fetal kidney were also generated. These organoids present individual nephron-like structures segmented into distal and proximal tubules surrounded by endothelia and renal interstitium, demonstrating a well-organized structure [133]. These are some examples of the ability to recapitulate human organogenesis *in vitro* from PSCs by the addition of only a few signaling cues. However, differences between native organ- and PSC-derived organoids can still be observed. This can result from inappropriate selection of microenvironmental cues or static signaling presentation in both space and time. Therefore, a higher spatiotemporal control is required to achieve closer similarity to the native microenvironment.

4.1. Bioengineering Approaches for Spatiotemporal Control of Mechanical Signals. As previously demonstrated, the mechanical properties of the cellular microenvironment strongly influence cell differentiation, as well as cellular proliferation and apoptosis [60, 140, 141]. Additionally, such mechanical features are specific for different organs, or even within the same organ, different components present distinct mechanical properties, allowing the modulation of cellular behavior and promoting multicomponent organogenesis [142, 143]. Subsequently, for organoid generation, the spatial modulation of mechanical features is a critical issue that can be achieved by generating composite hydrogels. For instance, the functionalization of traditional hydrogels, such as the Matrigel or collagen, with synthetic ECM analogs allows to manipulate the mechanical properties [144, 145]. The incorporation of adhesion peptides permits to manipulate mobility, since long peptide tethers lead to cell attachment and spreading, whereas short peptide tethers induce cell adhesion resistance, resulting in cell clustering [146]. Also, the incorporation of peptide substrates that are susceptible to enzymatic cleavage can also modulate hydrogel degradation by cells and therefore promote cell migration [147]. A modular design of silk protein-based porous scaffolds was also used to produce combined hydrogels, recreating the six-layered architecture of the human cortex. The reported approach consisted of an adhesive-free assembly of concentric units to create the modular structures based on a jigsaw puzzle-like cutting process. In this way, different layers were populated with distinct types of neurons, and a functional 3D cortical tissue construction was reached [148]. An alternative route to produce complex structures with composite hydrogels is a DNA-directed assembly of shape-controlled units. This technique presents the same principle as previously described to cell assembly, consisting in the enrichment of different blocks with circle DNA strand "glues." Based on the complementarity of each DNA block, a programmable assembly of complex macroscale structures can be achieved [149].

In addition to the reported technologies that allow the spatial modulation of mechanical features, further temporal guidance is possible to be generated by light-mediated patterning. The formation of photodegradable hydrogels by incorporating photolabile moieties within the network backbone of a hydrogel, like poly(ethylene glycol), makes the manipulation of the physical features of the ECM possible by using the light of different wavelengths. Upon light exposure, the local network crosslink density decreases and the hydrogel is cleaved, resulting in changes in physical properties, including stiffness, water content, diffusivity, or complete erosion, even in the presence of cells [150]. In contrast to this local softening, the presence of a photoinitiator originates additional crosslinking after the exposure to ultraviolet light, providing local stiffening [151].

In addition to light-patterning, other approaches have been applied for tuning the stiffness of hydrogels by using a combination of a pH-sensitive poly(2-(diisopropylamino)ethyl methacrylate) (PDPA) and biocompatible poly(2-(methacryloyloxy)ethyl phosphorylcholine) (PMPC) [152]. With the careful adjustment of the pH, the hydrogel film elasticity could be reversibly modulated allowing for the stiffening or softening of the material and for the temporal dynamic manipulation of cell adhesion/detachment [152]. This reversibly tunable stiffness can also be reached in cell-laden hydrogels based on supramolecular "host-guest" interactions. In this reported method, the stiffness is manipulated by noncovalent and reversible host-guest interactions between pendant "host" motifs, which are present in the primary hydrogel network and soluble polymers. Thus, when these soluble polymers are added, additional physical crosslinks are formed resulting in increased hydrogel crosslinking density and elastic modulus [153]. Hydrogels can also be dynamically stiffened by using enzymatic reactions, in which a peptide linker with additional amino acid residues that are susceptible to a specific enzyme catalyzation is created. After enzyme exposure, a specific dimer formation is achieved leading to additional crosslinks and final stiffening of the cell-laden hydrogel [154].

Therefore, based on these techniques, a spatiotemporal patterning of the mechanical features is straightforwardly reached. And by manipulating the matrix stiffness, the growth of neighboring tissues and consequently the mechanical confinement as seen *in vivo* could be mimicked in the organoid microenvironment [155].

4.2. Bioengineering Approaches for Spatiotemporal Control of Morphogen Diffusion. Morphogens are molecules that are able to coordinate organ growth and patterning, establishing a graded concentration distribution and eliciting distinct cellular responses in a dose-dependent manner. They can be either cytoplasmatic proteins, able to promote a diffusion gradient within the cell, or secreted signaling molecules [156]. The gradient of these signaling molecules appears to direct tissue patterning during embryogenesis [157, 158]. The formation of specific structures can be induced by gradients of signaling molecules produced by the neighboring cells and leading to differential gene expression, tissue patterning, and morphogenesis [159]. *In vitro*, various morphogens, including small molecules, growth factors, and hormones, have been used to regulate cell fate within the organoids. Furthermore, advances in the bioengineering

field allowed for the spatiotemporal control of the morphogen gradients within the organoid making possible to instruct the correct morphogenesis.

As already mentioned above, light-mediated patterning approaches present also a promising application to control morphogenic signals in both space and time. Biomolecules can be introduced within the hydrogel at a desired location, protected by a photodegradable moiety [160, 161]. At the proper timing, light exposure leads to a specific photoreleasing of the biomolecule. Beyond the spatial and temporal delivery control, for a given light exposure, the amount of biomolecule that is released can be predicted [161]. Additionally, the use of microfluidic systems or micro/nanoparticles allows an efficient spatiotemporal control of morphogen gradients. Lithographic techniques can be used for the production of channels to create functional microfluidic structures within hydrogels. Given the hydrodynamic properties of microchannels, following the initial homogeneous distribution of biomolecules inside the channels, a concentration gradient is formed by adjusting the flow rate. The delivered biomolecules can be changed over time within the scaffold, and the temporal modulation of these molecules can be achieved across the entire network in a spatially uniform manner [162]. These microfluidic devices were already successfully used to modulate neural tube patterning *in vitro*. Uzel et al. reported a microfluidic design to create orthogonal linear gradients in a 3D cell-embedded scaffold [163]. The authors used the reported device to generate gradients of retinoic acid (RA) and SAG, an agonist of the sonic hedgehog (SHH) [164], across a 3D collagen hydrogel with mouse ESC-derived aggregates [163]. Since RA has a caudalizing effect on the neuroepithelium and SHH is secreted in the most ventral part of the neural tube [165, 166], a combinatorial effect of these two morphogens specifies progenitor cells into caudal and ventral identities leading to the subsequent formation of ventral spinal cord neurons [163]. A similar approach was also used by Demers et al. In addition to RA and SHH signaling, they introduced a BMP4 gradient in a microfluidic device capable of mimicking the dorsal patterning of the neuroepithelium [167]. During neural differentiation, dorsal-ventral identity is achieved by establishment of opposing gradients of SHH and BMP, whereas the orthogonal delivery of the RA gradient allows the generation of the rostral-caudal axis [167]. These two different studies demonstrated the ability to generate temporally controlled morphogen gradients that allow the spatial patterning in stem cell-derived 3D structures.

Thus, the use of microfluidics can provide a transorganoid morphogen gradient, along with the immobilization of biomolecules in the biomaterial for spatial control [168]. In fact, direct integration of biomolecules into the scaffold allows to manipulate cell attachment, migration, and fate, but when combined with a delivery vehicle, like micro/nanoparticles, the controlled release of biomolecules is possible, allowing the generation of spatial gradients [169]. Mahoney and Saltzman were the first to assemble cells with the controlled release of polymeric microparticles to develop tissues with programmable synthetic extracellular microenvironments [170]. This technology was later applied to promote the controlled release of morphogens within organoids [171]. Degradable PLGA microspheres, containing RA, were incorporated within ESC-derived aggregates to achieve a controlled morphogen presentation and cystic spheroid formation [171]. An efficient cell differentiation and morphogenesis by the generation of structures that resemble the early mouse embryos (E6.75), with an exterior visceral endoderm enveloping an epiblast-like layer, was demonstrated [171]. Moreover, the combination of microparticles that present different kinetic releases allows a controlled and sequential morphogen presentation and therefore predetermine the time course of delivery and accomplish an efficient induction [172]. These approaches represent a versatile tool to create morphogen gradients that provide an accurate spatiotemporal regulation, being capable of inducing the symmetry breaking necessary for correct organoid morphogenesis.

5. Scaling Up of Organoid Generation

Other parameters, beyond biochemical signals and physical properties of ECM, should be considered for organoid generation, including sufficient nutrient and oxygen supply. The organoid size increases with the complexity of the generated structures, and it can range from 200 μm to 4 mm [14]. Larger organoids usually present diffusion limitations making it hard to mimic some developmental features [173]. Based on the physics of diffusion, cell density, and the lower range of reported metabolic consumption rates for oxygen, cerebral organoids can achieve a maximal diameter of 1.4 mm without presenting central necrosis [174]. However, the predicted diameter is based only on the low metabolic activity present in the organoids, since spontaneous neural activity is infrequent [174]. The use of a dynamic system, like a spinning bioreactor, is able to support organoid growth due to an efficient transport of nutrients and oxygen diffusion, allowing the maintenance of large-size organoids, with about 4 mm, that efficiently recapitulate the cerebral structure [3]. In fact, bioreactors have been largely applied to expand and differentiate PSCs toward mesodermal, endodermal, and ectodermal lineages, without structural cellular arrangement within the stem cell-derived 3D aggregates [175–179]. The protocols for organoid generation using bioreactors typically involve initial commitment in static conditions and further embedding of the organoids within a hydrogel, followed by transferring organoids to the bioreactor [3, 180–182]. This methodology limits the potential scale-up and the application of organoid culture in high-throughput processes for drug discovery and toxicology studies. Recently, a new platform was reported that allows capsule production through electrospraying using a Matrigel core, yielding robust capsules with microenvironmental support and organoid growth through the generation of an outer alginate shell that protects the cell-Matrigel core [183]. However, the generation of controlled size aggregates and further differentiation into well-organized organoids using bioreactors, in a continuous process, remains a challenge. Moreover, how the bioreactor design can affect the organization and morphogenesis of the organoid is still poorly understood.

6. Conclusions and Future Challenges

The powerful self-organization capacity of PSCs has been demonstrated thought the *in vitro* generation of different mini organ-like structures, only by providing some critical cues. Therefore, *in vitro* morphogenesis recapitulation can provide significant insights for regenerative medicine, disease modeling, and drug screening applications. However, uncontrolled organogenesis can produce nonconsistent organoid anatomy and variable cellular composition, in which some cell types, as well as functional features, may be missing. The application of engineering methodologies to instruct organoid organization allows the better mimicking of human morphogenesis. In this review, we focused on distinct bioengineering approaches to achieve high levels of cellular organization within PSC-derived organoids, by controlling the initial cell position, spatiotemporal cellular stage, and remodeling of generated tissue.

3D recapitulation of human tissues offers the opportunity to better understand the biological systems, being a necessary reliable analysis of the organoids, with full characterization of the structure and function. However, only few methodologies allow the identification of the phenotype and morphogenesis without destroying the 3D organization of an organoid, by using advanced microscopy approaches. For example, using a clearing method, the scattering of tissues can be reduced and the structure becomes more transparent, enhancing deep light penetration into the tissues and imaging of deep structures [184]. In fact, with light-sheet microscopy, a 3D image is generated by scanning plane-by-plane through the sample, allowing deeper visualization in tissues with high spatiotemporal resolution [185]. In addition to imaging techniques, robust methods to evaluate the functionality of the generated 3D structures should be developed. For instance, electrophysiology is used to characterize the function of cardiomyocytes and neurons, since they are electrically excitable. Nevertheless, these techniques only permit the use of single cells (patch clamp) and monolayers (microelectrode arrays). Some adaptations have been made to record physiological parameters in the 3D constructs. In order to evaluate the functionality of the generated neuronal network in an intact system, the patch clamp has been performed in organoid sections [139, 186]. However, better methodologies for assessing the functional properties of whole organoids are needed.

In addition to the described challenges in the assessment of function and structure of organoids, our ability to generate organoids from PSCs has also been subjected to some limitations [187]. Firstly, there is a need to produce a significant number of organoids to use in high-throughput applications, as well as larger organoids are required to better recapitulate the anatomy seen in human tissues. Secondly, since PSC-derived organoids tend to form tissues reminiscent of human embryonic development, there is also the need to enhance the functionality of the generated tissues in order to produce more mature organoids. Attempts to overcome these challenges have been made, and organoids still have great potential to be used in biological and therapeutic studies aimed at better understanding human development and disease manifestation and at providing critical insights about effective therapies for several disorders.

Conflicts of Interest

The authors declare that there is no conflict of interest regarding the publication of this article.

Acknowledgments

T.P. Silva and J.P. Cotovio acknowledge FundaÇão para a Ciência e a Tecnologia (FCT; Portugal, http://www.fct.pt) for the financial support through individual grants: SFRH/BD/105773/2014 and PD/BD135500/2018, respectively. Funding was also received from FCT through grant: UID/BIO/04565/2013. Funding was received from projects cofunded by FEDER (POR Lisboa 2020—Programa Operacional Regional de Lisboa PORTUGAL 2020) and FCT through grant PAC-PRECISE LISBOA-01-0145-FEDER-016394 and CEREBEX Generation of Cerebellar Organoids for Ataxia Research grant LISBOA-01-0145-FEDER-029298. Funding was also received from the European Union's Horizon 2020 Research and Innovation programme, under the Grant Agreement number 739572—The Discoveries Centre for Regenerative and Precision Medicine H2020-WIDESPREAD-01-2016-2017.

References

[1] G. Zhang, "Biomimicry in biomedical research," *Organogenesis*, vol. 8, no. 4, pp. 101-102, 2012.

[2] M. Simunovic and A. H. Brivanlou, "Embryoids, organoids and gastruloids: new approaches to understanding embryogenesis," *Development*, vol. 144, no. 6, pp. 976–985, 2017.

[3] M. A. Lancaster, M. Renner, C. A. Martin et al., "Cerebral organoids model human brain development and microcephaly," *Nature*, vol. 501, no. 7467, pp. 373–379, 2013.

[4] Y. Sasai, "Next-generation regenerative medicine: organogenesis from stem cells in 3D culture," *Cell Stem Cell*, vol. 12, no. 5, pp. 520–530, 2013.

[5] E. Smith and W. J. Cochrane, "Cystic organoid teratoma; report of a case," *Canadian Medical Association Journal*, vol. 55, no. 2, p. 151, 1946.

[6] W. R. Waddell, "Organoid differentiation of the fetal lung-a histologic study of the differentiation of mammalian fetal lung in utero and in transplants," *Archives of Pathology*, vol. 47, no. 3, pp. 227–247, 1949.

[7] Y. Yoshida, V. Hilborn, and A. E. Freeman, "Fine structural identification of organoid mouse lung cells cultured on a pigskin substrate," *In Vitro*, vol. 16, no. 11, pp. 994–1006, 1980.

[8] A. Elkasaby, D. Xu, C. Schroter-Kermani, and H. J. Merker, "Morphology, differentiation and matrix production of liver cells in organoid cultures (high density cultures) of fetal rat livers," *Histology and Histopathology*, vol. 6, no. 2, pp. 217–228, 1991.

[9] R. D. Ridgeway, J. W. Hamilton, and R. R. MacGregor, "Characteristics of bovine parathyroid cell organoids in culture," *In Vitro Cellular & Developmental Biology*, vol. 22, no. 2, pp. 91–99, 1986.

[10] C. Schröter-Kermani, N. Hinz, P. Risse, B. Zimmermann, and H. J. Merker, "The extracellular matrix in cartilage organoid culture: biochemical, immunomorphological and electron microscopic studies," *Matrix*, vol. 11, no. 6, pp. 428–441, 1991.

[11] Y. R. Lou and A. W. Leung, "Next generation organoids for biomedical research and applications," *Biotechnology Advances*, vol. 36, no. 1, pp. 132–149, 2018.

[12] X. Yin, B. E. Mead, H. Safaee, R. Langer, J. M. Karp, and O. Levy, "Engineering stem cell organoids," *Cell Stem Cell*, vol. 18, no. 1, pp. 25–38, 2016.

[13] S. A. Przyborski, "Differentiation of human embryonic stem cells after transplantation in immune-deficient mice," *Stem Cells*, vol. 23, no. 9, pp. 1242–1250, 2005.

[14] Y. Li, C. Xu, and T. Ma, "In vitro organogenesis from pluripotent stem cells," *Organogenesis*, vol. 10, no. 2, pp. 159–163, 2014.

[15] B. M. Gumbiner, "Cell adhesion: the molecular basis of tissue architecture and morphogenesis," *Cell*, vol. 84, no. 3, pp. 345–357, 1996.

[16] P. J. Marie, E. Haÿ, D. Modrowski, L. Revollo, G. Mbalaviele, and R. Civitelli, "Cadherin-mediated cell-cell adhesion and signaling in the skeleton," *Calcified Tissue International*, vol. 94, no. 1, pp. 46–54, 2014.

[17] D. L. Rimm, E. R. Koslov, P. Kebriaei, C. D. Cianci, and J. S. Morrow, "Alpha 1(E)-catenin is an actin-binding and -bundling protein mediating the attachment of F-actin to the membrane adhesion complex," *Proceedings of the National Academy of Sciences of the United States of America*, vol. 92, no. 19, pp. 8813–8817, 1995.

[18] M. Itoh, A. Nagafuchi, S. Moroi, and S. Tsukita, "Involvement of ZO-1 in cadherin-based cell adhesion through its direct binding to α catenin and actin filaments," *Journal of Cell Biology*, vol. 138, no. 1, pp. 181–192, 1997.

[19] M. Matsunaga, K. Hatta, A. Nagafuchi, and M. Takeichi, "Guidance of optic nerve fibres by N-cadherin adhesion molecules," *Nature*, vol. 334, no. 6177, pp. 62–64, 1988.

[20] N. Uchida, Y. Honjo, K. R. Johnson, M. J. Wheelock, and M. Takeichi, "The catenin/cadherin adhesion system is localized in synaptic junctions bordering transmitter release zones," *Journal of Cell Biology*, vol. 135, no. 3, pp. 767–779, 1996.

[21] Y. Kimura, H. Matsunami, T. Inoue et al., "Cadherin-11 expressed in association with mesenchymal morphogenesis in the head, somite, and limb bud of early mouse embryos," *Developmental Biology*, vol. 169, no. 1, pp. 347–358, 1995.

[22] K. Venkiteswaran, K. Xiao, S. Summers et al., "Regulation of endothelial barrier function and growth by VE-cadherin, plakoglobin, and β-catenin," *American Journal of Physiology-Cell Physiology*, vol. 283, no. 3, pp. C811–C821, 2002.

[23] S. C. Suzuki, T. Inoue, Y. Kimura, T. Tanaka, and M. Takeichi, "Neuronal circuits are subdivided by differential expression of type-II classic cadherins in postnatal mouse brains," *Molecular and Cellular Neurosciences*, vol. 9, no. 5–6, pp. 433–447, 1997.

[24] S. R. Price, N. V. De Marco Garcia, B. Ranscht, and T. M. Jessell, "Regulation of motor neuron pool sorting by differential expression of type II cadherins," *Cell*, vol. 109, no. 2, pp. 205–216, 2002.

[25] D. R. Friedlander, R. M. Mège, B. A. Cunningham, and G. M. Edelman, "Cell sorting-out is modulated by both the specificity and amount of different cell adhesion molecules (CAMs) expressed on cell surfaces," *Proceedings of the National Academy of Sciences of the United States of America*, vol. 86, no. 18, pp. 7043–7047, 1989.

[26] P. Katsamba, K. Carroll, G. Ahlsen et al., "Linking molecular affinity and cellular specificity in cadherin-mediated adhesion," *Proceedings of the National Academy of Sciences of the United States of America*, vol. 106, no. 28, pp. 11594–11599, 2009.

[27] D. Duguay, R. A. Foty, and M. S. Steinberg, "Cadherin-mediated cell adhesion and tissue segregation: qualitative and quantitative determinants," *Developmental Biology*, vol. 253, no. 2, pp. 309–323, 2003.

[28] D. Godt and U. Tepass, "Drosophila oocyte localization is mediated by differential cadherin-based adhesion," *Nature*, vol. 395, no. 6700, pp. 387–391, 1998.

[29] E. D. Hay and A. Zuk, "Transformations between epithelium and mesenchyme: normal, pathological, and experimentally induced," *American Journal of Kidney Diseases*, vol. 26, no. 4, pp. 678–690, 1995.

[30] A. Cano, M. A. Pérez-Moreno, I. Rodrigo et al., "The transcription factor Snail controls epithelial-mesenchymal transitions by repressing E-cadherin expression," *Nature Cell Biology*, vol. 2, no. 2, pp. 76–83, 2000.

[31] R. Moore, W. Tao, Y. Meng, E. R. Smith, and X.-X. Xu, "Cell adhesion and sorting in embryoid bodies derived from N- or E-cadherin deficient murine embryonic stem cells," *Biology Open*, vol. 3, no. 2, pp. 121–128, 2014.

[32] S. Lamouille, J. Xu, and R. Derynck, "Molecular mechanisms of epithelial-mesenchymal transition," *Nature Reviews Molecular Cell Biology*, vol. 15, no. 3, pp. 178–196, 2014.

[33] C. Dahmann and K. Basler, "Opposing transcriptional outputs of hedgehog signaling and engrailed control compartmental cell sorting at the *Drosophila* A/P boundary," *Cell*, vol. 100, no. 4, pp. 411–422, 2000.

[34] U. Tepass, D. Godt, and R. Winklbauer, "Cell sorting in animal development: signalling and adhesive mechanisms in the formation of tissue boundaries," *Current Opinion in Genetics and Development*, vol. 12, no. 5, pp. 572–582, 2002.

[35] Y. Zhong, W. M. Brieher, and B. M. Gumbiner, "Analysis of C-cadherin regulation during tissue morphogenesis with an activating antibody," *Journal of Cell Biology*, vol. 144, no. 2, pp. 351–359, 1999.

[36] B. M. Gumbiner, "Epithelial morphogenesis," *Cell*, vol. 69, no. 3, pp. 385–387, 1992.

[37] A. Dasgupta, R. Hughey, P. Lancin, L. Larue, and P. V. Moghe, "E-Cadherin synergistically induces hepatospecific phenotype and maturation of embryonic stem cells in conjunction with hepatotrophic factors," *Biotechnology and Bioengineering*, vol. 92, no. 3, pp. 257–266, 2005.

[38] S. M. Dang, S. Gerecht-Nir, J. Chen, J. Itskovitz-Eldor, and P. W. Zandstra, "Controlled, scalable embryonic stem cell differentiation culture," *Stem Cells*, vol. 22, no. 3, pp. 275–282, 2004.

[39] E. Y. L. Fok and P. W. Zandstra, "Shear-controlled single-step mouse embryonic stem cell expansion and embryoid body-based differentiation," *Stem Cells*, vol. 23, no. 9, pp. 1333–1342, 2005.

[40] B. L. Beckstead, D. M. Santosa, and C. M. Giachelli, "Mimicking cell-cell interactions at the biomaterial-cell interface for control of stem cell differentiation," *Journal*

of Biomedical Materials Research-Part A, vol. 79, no. 1, pp. 94–103, 2006.

[41] S. Alimperti and S. T. Andreadis, "CDH2 and CDH11 act as regulators of stem cell fate decisions," *Stem Cell Research*, vol. 14, no. 3, pp. 270–282, 2015.

[42] J. B. Sneddon, M. Borowiak, and D. A. Melton, "Self-renewal of embryonic-stem-cell-derived progenitors by organ-matched mesenchyme," *Nature*, vol. 491, no. 7426, pp. 765–768, 2012.

[43] F. Gattazzo, A. Urciuolo, and P. Bonaldo, "Extracellular matrix: a dynamic microenvironment for stem cell niche," *Biochimica et Biophysica Acta-General Subjects*, vol. 1840, no. 8, pp. 2506–2519, 2014.

[44] C. D. Hartman, B. C. Isenberg, S. G. Chua, and J. Y. Wong, "Extracellular matrix type modulates cell migration on mechanical gradients," *Experimental Cell Research*, vol. 359, no. 2, pp. 361–366, 2017.

[45] D. M. Bryant, J. Roignot, A. Datta et al., "A molecular switch for the orientation of epithelial cell polarization," *Developmental Cell*, vol. 31, no. 2, pp. 171–187, 2014.

[46] K. R. Legate, S. A. Wickström, and R. Fässler, "Genetic and cell biological analysis of integrin outside-in signaling," *Genes and Development*, vol. 23, no. 4, pp. 397–418, 2009.

[47] J. W. Tamkun, D. W. DeSimone, D. Fonda et al., "Structure of integrin, a glycoprotein involved in the transmembrane linkage between fibronectin and actin," *Cell*, vol. 46, no. 2, pp. 271–282, 1986.

[48] M. Barczyk, S. Carracedo, and D. Gullberg, "Integrins," *Cell and Tissue Research*, vol. 339, no. 1, pp. 269–280, 2010.

[49] C. M. Meighan and J. E. Schwarzbauer, "Temporal and spatial regulation of integrins during development," *Current Opinion in Cell Biology*, vol. 20, no. 5, pp. 520–524, 2008.

[50] T. Darribére, M. Skalski, H. Cousin, A. Gaultier, C. Montmory, and D. Alfandari, "Integrins: regulators of embryogenesis," *Biology of the Cell*, vol. 92, no. 1, pp. 5–25, 2000.

[51] S. Battista, D. Guarnieri, C. Borselli et al., "The effect of matrix composition of 3D constructs on embryonic stem cell differentiation," *Biomaterials*, vol. 26, no. 31, pp. 6194–6207, 2005.

[52] H. K. Kleinman and G. R. Martin, "Matrigel: basement membrane matrix with biological activity," *Seminars in Cancer Biology*, vol. 15, no. 5, pp. 378–386, 2005.

[53] R. W. Orkin, P. Gehron, E. McGoodwin, G. R. Martin, T. Valentine, and R. Swarm, "A murine tumor producing a matrix of basement membrane," *The Journal of Experimental Medicine*, vol. 145, no. 1, pp. 204–220, 1977.

[54] Z. Farzaneh, M. Pakzad, M. Vosough, B. Pournasr, and H. Baharvand, "Differentiation of human embryonic stem cells to hepatocyte-like cells on a new developed xeno-free extracellular matrix," *Histochemistry and Cell Biology*, vol. 142, no. 2, pp. 217–226, 2014.

[55] S. Sa, L. Wong, and K. E. McCloskey, "Combinatorial fibronectin and laminin signaling promote highly efficient cardiac differentiation of human embryonic stem cells," *BioResearch Open Access*, vol. 3, no. 4, pp. 150–161, 2014.

[56] Y. Li, M. Liu, Y. Yan, and S. T. Yang, "Neural differentiation from pluripotent stem cells: the role of natural and synthetic extracellular matrix," *World Journal of Stem Cells*, vol. 6, no. 1, pp. 11–23, 2014.

[57] N. D. Evans, C. Minelli, E. Gentleman et al., "Substrate stiffness affects early differentiation events in embryonic stem cells," *European Cells and Materials*, vol. 18, pp. 1–14, 2009.

[58] J. D. Humphrey, E. R. Dufresne, and M. A. Schwartz, "Mechanotransduction and extracellular matrix homeostasis," *Nature Reviews Molecular Cell Biology*, vol. 15, no. 12, pp. 802–812, 2014.

[59] J. Zoldan, E. D. Karagiannis, C. Y. Lee, D. G. Anderson, R. Langer, and S. Levenberg, "The influence of scaffold elasticity on germ layer specification of human embryonic stem cells," *Biomaterials*, vol. 32, no. 36, pp. 9612–9621, 2011.

[60] L. Przybyla, J. N. Lakins, and V. M. Weaver, "Tissue mechanics orchestrate Wnt-dependent human embryonic stem cell differentiation," *Cell Stem Cell*, vol. 19, no. 4, pp. 462–475, 2016.

[61] C. Pohl, "Cytoskeletal symmetry breaking and chirality: from reconstituted systems to animal development," *Symmetry*, vol. 7, no. 4, pp. 2062–2107, 2015.

[62] A. J. Spracklen and M. Peifer, "Actin and apical constriction: some (re)-assembly required," *Developmental Cell*, vol. 35, no. 6, pp. 662–664, 2015.

[63] M. D. White, S. Bissiere, Y. D. Alvarez, and N. Plachta, "Mouse embryo compaction," *Current Topics in Developmental Biology*, vol. 120, pp. 235–258, 2016.

[64] A. I. Mihajlović and A. W. Bruce, "The first cell-fate decision of mouse preimplantation embryo development: integrating cell position and polarity," *Open Biology*, vol. 7, no. 11, 2017.

[65] S. C. van den Brink, P. Baillie-Johnson, T. Balayo et al., "Symmetry breaking, germ layer specification and axial organisation in aggregates of mouse embryonic stem cells," *Development*, vol. 141, no. 22, pp. 4231–4242, 2014.

[66] S. Wennekamp, S. Mesecke, F. Nédélec, and T. Hiiragi, "A self-organization framework for symmetry breaking in the mammalian embryo," *Nature Reviews Molecular Cell Biology*, vol. 14, no. 7, pp. 452–459, 2013.

[67] N. Takata, E. Sakakura, M. Eiraku, T. Kasukawa, and Y. Sasai, "Self-patterning of rostral-caudal neuroectoderm requires dual role of Fgf signaling for localized Wnt antagonism," *Nature Communications*, vol. 8, no. 1, article 1339, 2017.

[68] S. M. Morgani, J. J. Metzger, J. Nichols, E. D. Siggia, and A. K. Hadjantonakis, "Micropattern differentiation of mouse pluripotent stem cells recapitulates embryo regionalized cell fate patterning," *eLife*, vol. 7, article e32839, 2018.

[69] K. Ishihara, A. Ranga, M. P. Lutolf, E. M. Tanaka, and A. Meinhardt, "Reconstitution of a patterned neural tube from single mouse embryonic stem cells," *Methods in Molecular Biology*, vol. 1597, pp. 43–55, 2017.

[70] D. A. Turner, M. Girgin, L. Alonso-Crisostomo et al., "Anteroposterior polarity and elongation in the absence of extra-embryonic tissues and of spatially localised signalling in gastruloids: mammalian embryonic organoids," *Development*, vol. 144, no. 21, pp. 3894–3906, 2017.

[71] Y. C. Poh, J. Chen, Y. Hong et al., "Generation of organized germ layers from a single mouse embryonic stem cell," *Nature Communications*, vol. 5, no. 1, article 4000, 2014.

[72] A. Meinhardt, D. Eberle, A. Tazaki et al., "3D reconstitution of the patterned neural tube from embryonic stem cells," *Stem Cell Reports*, vol. 3, no. 6, pp. 987–999, 2014.

[73] H. Kurosawa, T. Imamura, M. Koike, K. Sasaki, and Y. Amano, "A simple method for forming embryoid body

from mouse embryonic stem cells," *Journal of Bioscience and Bioengineering*, vol. 96, no. 4, pp. 409–411, 2003.

[74] E. S. Ng, R. P. Davis, L. Azzola, E. G. Stanley, and A. G. Elefanty, "Forced aggregation of defined numbers of human embryonic stem cells into embryoid bodies fosters robust, reproducible hematopoietic differentiation," *Blood*, vol. 106, no. 5, pp. 1601–1603, 2005.

[75] M. D. Ungrin, C. Joshi, A. Nica, C. Bauwens, and P. W. Zandstra, "Reproducible, ultra high-throughput formation of multicellular organization from single cell suspension-derived human embryonic stem cell aggregates," *PLoS One*, vol. 3, no. 2, article e1565, 2008.

[76] H. C. Moeller, M. K. Mian, S. Shrivastava, B. G. Chung, and A. Khademhosseini, "A microwell array system for stem cell culture," *Biomaterials*, vol. 29, no. 6, pp. 752–763, 2008.

[77] J. C. Mohr, J. J. de Pablo, and S. P. Palecek, "3-D microwell culture of human embryonic stem cells," *Biomaterials*, vol. 27, no. 36, pp. 6032–6042, 2006.

[78] Y. S. Torisawa, B. H. Chueh, D. Huh et al., "Efficient formation of uniform-sized embryoid bodies using a compartmentalized microchannel device," *Lab on a Chip*, vol. 7, no. 6, pp. 770–776, 2007.

[79] C. L. Bauwens, R. Peerani, S. Niebruegge et al., "Control of human embryonic stem cell colony and aggregate size heterogeneity influences differentiation trajectories," *Stem Cells*, vol. 26, no. 9, pp. 2300–2310, 2008.

[80] R. Peerani, B. M. Rao, C. Bauwens et al., "Niche-mediated control of human embryonic stem cell self-renewal and differentiation," *The EMBO Journal*, vol. 26, no. 22, pp. 4744–4755, 2007.

[81] V. C. Chen, J. Ye, P. Shukla et al., "Development of a scalable suspension culture for cardiac differentiation from human pluripotent stem cells," *Stem Cell Research*, vol. 15, no. 2, pp. 365–375, 2015.

[82] H. Fonoudi, H. Ansari, S. Abbasalizadeh et al., "A universal and robust integrated platform for the scalable production of human cardiomyocytes from pluripotent stem cells," *Stem Cells Translational Medicine*, vol. 4, no. 12, pp. 1482–1494, 2015.

[83] C. C. Miranda, T. G. Fernandes, J. F. Pascoal et al., "Spatial and temporal control of cell aggregation efficiently directs human pluripotent stem cells towards neural commitment," *Biotechnology Journal*, vol. 10, no. 10, pp. 1612–1624, 2015.

[84] A. W. Xie, B. Y. K. Binder, A. S. Khalil et al., "Controlled self-assembly of stem cell aggregates instructs pluripotency and lineage bias," *Scientific Reports*, vol. 7, no. 1, article 14070, 2017.

[85] J. Youssef, A. K. Nurse, L. B. Freund, and J. R. Morgan, "Quantification of the forces driving self-assembly of three-dimensional microtissues," *Proceedings of the National Academy of Sciences of the United States of America*, vol. 108, no. 17, pp. 6993–6998, 2011.

[86] J. Dahlmann, G. Kensah, H. Kempf et al., "The use of agarose microwells for scalable embryoid body formation and cardiac differentiation of human and murine pluripotent stem cells," *Biomaterials*, vol. 34, no. 10, pp. 2463–2471, 2013.

[87] L. Filipponi, P. Livingston, O. Kašpar, V. Tokárová, and D. V. Nicolau, "Protein patterning by microcontact printing using pyramidal PDMS stamps," *Biomedical Microdevices*, vol. 18, p. 9, 2016.

[88] W. L. Murphy, T. C. McDevitt, and A. J. Engler, "Materials as stem cell regulators," *Nature Materials*, vol. 13, no. 6, pp. 547–557, 2014.

[89] S. Van Vlierberghe, P. Dubruel, and E. Schacht, "Biopolymer-based hydrogels as scaffolds for tissue engineering applications: a review," *Biomacromolecules*, vol. 12, no. 5, pp. 1387–1408, 2011.

[90] O. Wichterle and D. Lím, "Hydrophilic gels for biological use," *Nature*, vol. 185, no. 4706, pp. 117-118, 1960.

[91] P. J. Su, Q. A. Tran, J. J. Fong, K. W. Eliceiri, B. M. Ogle, and P. J. Campagnola, "Mesenchymal stem cell interactions with 3D ECM modules fabricated via multiphoton excited photochemistry," *Biomacromolecules*, vol. 13, no. 9, pp. 2917–2925, 2012.

[92] J. S. Miller, K. R. Stevens, M. T. Yang et al., "Rapid casting of patterned vascular networks for perfusable engineered three-dimensional tissues," *Nature Materials*, vol. 11, no. 9, pp. 768–774, 2012.

[93] T.-S. Jang, H.-D. Jung, H. M. Pan, W. T. Han, S. Chen, and J. Song, "3D printing of hydrogel composite systems: recent advances in technology for tissue engineering," *International Journal of Bioprinting*, vol. 4, no. 1, p. 126, 2018.

[94] T. J. Hinton, Q. Jallerat, R. N. Palchesko et al., "Three-dimensional printing of complex biological structures by freeform reversible embedding of suspended hydrogels," *Science Advances*, vol. 1, no. 9, article e1500758, 2015.

[95] C. A. DeForest and K. S. Anseth, "Cytocompatible click-based hydrogels with dynamically tunable properties through orthogonal photoconjugation and photocleavage reactions," *Nature Chemistry*, vol. 3, no. 12, pp. 925–931, 2011.

[96] X. Cui, T. Boland, D. D. D'Lima, and M. K. Lotz, "Thermal inkjet printing in tissue engineering and regenerative medicine," *Recent Patents on Drug Delivery & Formulation*, vol. 6, no. 2, pp. 149–155, 2012.

[97] T. Goldmann and J. S. Gonzalez, "DNA-printing: utilization of a standard inkjet printer for the transfer of nucleic acids to solid supports," *Journal of Biochemical and Biophysical Methods*, vol. 42, no. 3, pp. 105–110, 2000.

[98] X. Y. Wang, Z. H. Jin, B. W. Gan, S. W. Lv, M. Xie, and W. H. Huang, "Engineering interconnected 3D vascular networks in hydrogels using molded sodium alginate lattice as the sacrificial template," *Lab on a Chip*, vol. 14, no. 15, pp. 2709–2716, 2014.

[99] A. Tocchio, M. Tamplenizza, F. Martello et al., "Versatile fabrication of vascularizable scaffolds for large tissue engineering in bioreactor," *Biomaterials*, vol. 45, pp. 124–131, 2015.

[100] M. E. Todhunter, N. Y. Jee, A. J. Hughes et al., "Programmed synthesis of three-dimensional tissues," *Nature Methods*, vol. 12, no. 10, pp. 975–981, 2015.

[101] M. E. Todhunter, R. J. Weber, J. Farlow, N. Y. Jee, A. E. Cerchiari, and Z. J. Gartner, "Fabrication of 3-D reconstituted organoid arrays by DNA-programmed assembly of cells (DPAC)," *Current Protocols in Chemical Biology*, vol. 8, no. 3, pp. 147–178, 2016.

[102] E. Garreta, R. Oria, C. Tarantino et al., "Tissue engineering by decellularization and 3D bioprinting," *Materials Today*, vol. 20, no. 4, pp. 166–178, 2017.

[103] M. Nakamura, A. Kobayashi, F. Takagi et al., "Biocompatible inkjet printing technique for designed seeding of individual living cells," *Tissue Engineering*, vol. 11, no. 11–12, pp. 1658–1666, 2005.

[104] R. E. Saunders, J. E. Gough, and B. Derby, "Delivery of human fibroblast cells by piezoelectric drop-on-demand inkjet printing," *Biomaterials*, vol. 29, no. 2, pp. 193–203, 2008.

[105] C. Mandrycky, Z. Wang, K. Kim, and D. H. Kim, "3D bioprinting for engineering complex tissues," *Biotechnology Advances*, vol. 34, no. 4, pp. 422–434, 2016.

[106] S. V. Murphy and A. Atala, "3D bioprinting of tissues and organs," *Nature Biotechnology*, vol. 32, no. 8, pp. 773–785, 2014.

[107] N. E. Fedorovich, W. Schuurman, H. M. Wijnberg et al., "Biofabrication of osteochondral tissue equivalents by printing topologically defined, cell-laden hydrogel scaffolds," *Tissue Engineering Part C: Methods*, vol. 18, no. 1, pp. 33–44, 2012.

[108] N. R. Schiele, D. T. Corr, Y. Huang, N. A. Raof, Y. Xie, and D. B. Chrisey, "Laser-based direct-write techniques for cell printing," *Biofabrication*, vol. 2, no. 3, article 032001, 2010.

[109] N. R. Schiele, R. A. Koppes, D. T. Corr et al., "Laser direct writing of combinatorial libraries of idealized cellular constructs: biomedical applications," *Applied Surface Science*, vol. 255, no. 10, pp. 5444–5447, 2009.

[110] T. M. Patz, A. Doraiswamy, R. J. Narayan et al., "Three-dimensional direct writing of B35 neuronal cells," *Journal of Biomedical Materials Research-Part B Applied Biomaterials*, vol. 78B, no. 1, pp. 124–130, 2006.

[111] A. Doraiswamy, R. J. Narayan, M. L. Harris, S. B. Qadri, R. Modi, and D. B. Chrisey, "Laser microfabrication of hydroxyapatite-osteoblast-like cell composites," *Journal of Biomedical Materials Research-Part A*, vol. 80, no. 3, pp. 635–643, 2007.

[112] J. A. Barron, B. J. Spargo, and B. R. Ringeisen, "Biological laser printing of three dimensional cellular structures," *Applied Physics A: Materials Science and Processing*, vol. 79, no. 4-6, pp. 1027–1030, 2004.

[113] J. A. Barron, D. B. Krizman, and B. R. Ringeisen, "Laser printing of single cells: statistical analysis, cell viability, and stress," *Annals of Biomedical Engineering*, vol. 33, no. 2, pp. 121–130, 2005.

[114] I. K. Suzuki and P. Vanderhaeghen, "Is this a brain which I see before me? Modeling human neural development with pluripotent stem cells," *Development*, vol. 142, no. 18, pp. 3138–3150, 2015.

[115] S. M. Chambers, C. A. Fasano, E. P. Papapetrou, M. Tomishima, M. Sadelain, and L. Studer, "Highly efficient neural conversion of human ES and iPS cells by dual inhibition of SMAD signaling," *Nature Biotechnology*, vol. 27, no. 3, pp. 275–280, 2009.

[116] C. E. Sanvitale, G. Kerr, A. Chaikuad et al., "A new class of small molecule inhibitor of BMP signaling," *PLoS One*, vol. 8, no. 4, article e62721, 2013.

[117] N. J. Laping, E. Grygielko, A. Mathur et al., "Inhibition of transforming growth factor (TGF)-β1-induced extracellular matrix with a novel inhibitor of the TGF-β type I receptor kinase activity: SB-431542," *Molecular Pharmacology*, vol. 62, no. 1, pp. 58–64, 2002.

[118] X. Lian, J. Zhang, K. Zhu, T. J. Kamp, and S. P. Palecek, "Insulin inhibits cardiac mesoderm, not mesendoderm, formation during cardiac differentiation of human pluripotent stem cells and modulation of canonical Wnt signaling can rescue this inhibition," *Stem Cells*, vol. 31, no. 3, pp. 447–457, 2013.

[119] C. E. Murry and G. Keller, "Differentiation of embryonic stem cells to clinically relevant populations: lessons from embryonic development," *Cell*, vol. 132, no. 4, pp. 661–680, 2008.

[120] T. Faial, A. S. Bernardo, S. Mendjan et al., "Brachyury and SMAD signalling collaboratively orchestrate distinct mesoderm and endoderm gene regulatory networks in differentiating human embryonic stem cells," *Development*, vol. 142, no. 12, pp. 2121–2135, 2015.

[121] A. K. K. Teo, S. J. Arnold, M. W. B. Trotter et al., "Pluripotency factors regulate definitive endoderm specification through eomesodermin," *Genes and Development*, vol. 25, no. 3, pp. 238–250, 2011.

[122] P. Gadue, T. L. Huber, P. J. Paddison, and G. M. Keller, "Wnt and TGF-beta signaling are required for the induction of an in vitro model of primitive streak formation using embryonic stem cells," *Proceedings of the National Academy of Sciences of the United States of America*, vol. 103, no. 45, pp. 16806–16811, 2006.

[123] M. C. Nostro, X. Cheng, G. M. Keller, and P. Gadue, "Wnt, activin, and BMP signaling regulate distinct stages in the developmental pathway from embryonic stem cells to blood," *Cell Stem Cell*, vol. 2, no. 1, pp. 60–71, 2008.

[124] K. M. Loh, A. Chen, P. W. Koh et al., "Mapping the pairwise choices leading from pluripotency to human bone, heart, and other mesoderm cell types," *Cell*, vol. 166, no. 2, pp. 451–467, 2016.

[125] X. Lian, C. Hsiao, G. Wilson et al., "Robust cardiomyocyte differentiation from human pluripotent stem cells via temporal modulation of canonical Wnt signaling," *Proceedings of the National Academy of Sciences of the United States of America*, vol. 109, no. 27, pp. E1848–E1857, 2012.

[126] E. Trompouki, T. V. Bowman, L. N. Lawton et al., "Lineage regulators direct BMP and Wnt pathways to cell-specific programs during differentiation and regeneration," *Cell*, vol. 147, no. 3, pp. 577–589, 2011.

[127] M. Johannesson, A. Ståhlberg, J. Ameri, F. W. Sand, K. Norrman, and H. Semb, "FGF4 and retinoic acid direct differentiation of hESCs into PDX1-expressing foregut endoderm in a time- and concentration-dependent manner," *PLoS One*, vol. 4, no. 3, article e4794, 2009.

[128] M. C. Nostro, F. Sarangi, S. Ogawa et al., "Stage-specific signaling through TGFβ family members and WNT regulates patterning and pancreatic specification of human pluripotent stem cells," *Development*, vol. 138, no. 7, pp. 1445–1445, 2011.

[129] V. Gouon-Evans, L. Boussemart, P. Gadue et al., "BMP-4 is required for hepatic specification of mouse embryonic stem cell-derived definitive endoderm," *Nature Biotechnology*, vol. 24, no. 11, pp. 1402–1411, 2006.

[130] J. Spence, C. Mayhew, S. Rankin et al., "Directed differentiation of human pluripotent stem cells into intestinal tissue *in vitro*," *Nature*, vol. 470, no. 7332, pp. 105–109, 2011.

[131] B. R. Dye, P. H. Dedhia, A. J. Miller et al., "A bioengineered niche promotes in vivo engraftment and maturation of pluripotent stem cell derived human lung organoids," *eLife*, vol. 5, article e19732, 2016.

[132] T. Takebe, R. R. Zhang, H. Koike et al., "Generation of a vascularized and functional human liver from an iPSC-derived organ bud transplant," *Nature Protocols*, vol. 9, no. 2, pp. 396–409, 2014.

[133] M. Takasato, P. X. Er, H. S. Chiu et al., "Kidney organoids from human iPS cells contain multiple lineages and model

human nephrogenesis," *Nature*, vol. 526, no. 7574, pp. 564–568, 2015.

[134] Y. Kim, H. Kim, U. H. Ko et al., "Islet-like organoids derived from human pluripotent stem cells efficiently function in the glucose responsiveness *in vitro* and *in vivo*," *Scientific Reports*, vol. 6, no. 1, article 35145, 2016.

[135] M. Eiraku, K. Watanabe, M. Matsuo-Takasaki et al., "Self-organized formation of polarized cortical tissues from ESCs and its active manipulation by extrinsic signals," *Cell Stem Cell*, vol. 3, no. 5, pp. 519–532, 2008.

[136] E. Karzbrun, A. Kshirsagar, S. R. Cohen, J. H. Hanna, and O. Reiner, "Human brain organoids on a chip reveal the physics of folding," *Nature Physics*, vol. 14, no. 5, pp. 515–522, 2018.

[137] X. Qian, F. Jacob, M. M. Song, H. N. Nguyen, H. Song, and G. Ming, "Generation of human brain region–specific organoids using a miniaturized spinning bioreactor," *Nature Protocols*, vol. 13, no. 3, pp. 565–580, 2018.

[138] K. Muguruma, A. Nishiyama, H. Kawakami, K. Hashimoto, and Y. Sasai, "Self-organization of polarized cerebellar tissue in 3D culture of human pluripotent stem cells," *Cell Reports*, vol. 10, no. 4, pp. 537–550, 2015.

[139] J. Jo, Y. Xiao, A. X. Sun et al., "Midbrain-like organoids from human pluripotent stem cells contain functional dopaminergic and neuromelanin-producing neurons," *Cell Stem Cell*, vol. 19, no. 2, pp. 248–257, 2016.

[140] P. M. Gilbert, K. L. Havenstrite, K. E. G. Magnusson et al., "Substrate elasticity regulates skeletal muscle stem cell self-renewal in culture," *Science*, vol. 329, no. 5995, pp. 1078–1081, 2010.

[141] C. M. Nelson, R. P. Jean, J. L. Tan et al., "Emergent patterns of growth controlled by multicellular form and mechanics," *Proceedings of the National Academy of Sciences of the United States of America*, vol. 102, no. 33, pp. 11594–11599, 2005.

[142] A. J. Engler, S. Sen, H. L. Sweeney, and D. E. Discher, "Matrix elasticity directs stem cell lineage specification," *Cell*, vol. 126, no. 4, pp. 677–689, 2006.

[143] J. I. Lopez, I. Kang, W. K. You, D. M. McDonald, and V. M. Weaver, "*In situ* force mapping of mammary gland transformation," *Integrative Biology*, vol. 3, no. 9, pp. 910–921, 2011.

[144] B. J. Gill, D. L. Gibbons, L. C. Roudsari et al., "A synthetic matrix with independently tunable biochemistry and mechanical properties to study epithelial morphogenesis and EMT in a lung adenocarcinoma model," *Cancer Research*, vol. 72, no. 22, pp. 6013–6023, 2012.

[145] M. Ehrbar, A. Sala, P. Lienemann et al., "Elucidating the role of matrix stiffness in 3D cell migration and remodeling," *Biophysical Journal*, vol. 100, no. 2, pp. 284–293, 2011.

[146] W. Kuhlman, I. Taniguchi, L. G. Griffith, and A. M. Mayes, "Interplay between PEO tether length and ligand spacing governs cell spreading on RGD-modified PMMA-g-PEO comb copolymers," *Biomacromolecules*, vol. 8, no. 10, pp. 3206–3213, 2007.

[147] G. P. Raeber, M. P. Lutolf, and J. A. Hubbell, "Molecularly engineered PEG hydrogels: a novel model system for proteolytically mediated cell migration," *Biophysical Journal*, vol. 89, no. 2, pp. 1374–1388, 2005.

[148] M. D. Tang-Schomer, J. D. White, L. W. Tien et al., "Bioengineered functional brain-like cortical tissue," *Proceedings of the National Academy of Sciences of the United States of America*, vol. 111, no. 38, pp. 13811–13816, 2014.

[149] H. Qi, M. Ghodousi, Y. du et al., "DNA-directed self-assembly of shape-controlled hydrogels," *Nature Communications*, vol. 4, no. 1, p. 2275, 2013.

[150] A. M. Kloxin, A. M. Kasko, C. N. Salinas, and K. S. Anseth, "Photodegradable hydrogels for dynamic tuning of physical and chemical properties," *Science*, vol. 324, no. 5923, pp. 59–63, 2009.

[151] M. Guvendiren and J. A. Burdick, "Stiffening hydrogels to probe short- and long-term cellular responses to dynamic mechanics," *Nature Communications*, vol. 3, no. 1, p. 792, 2012.

[152] H. Y. Yoshikawa, F. F. Rossetti, S. Kaufmann et al., "Quantitative evaluation of mechanosensing of cells on dynamically tunable hydrogels," *Journal of the American Chemical Society*, vol. 133, no. 5, pp. 1367–1374, 2011.

[153] H. Shih and C. C. Lin, "Tuning stiffness of cell-laden hydrogel via host-guest interactions," *Journal of Materials Chemistry B*, vol. 4, no. 29, pp. 4969–4974, 2016.

[154] H. Y. Liu, T. Greene, T. Y. Lin, C. S. Dawes, M. Korc, and C. C. Lin, "Enzyme-mediated stiffening hydrogels for probing activation of pancreatic stellate cells," *Acta Biomaterialia*, vol. 48, pp. 258–269, 2017.

[155] N. Gjorevski, A. Ranga, and M. P. Lutolf, "Bioengineering approaches to guide stem cell-based organogenesis," *Development*, vol. 141, no. 9, pp. 1794–1804, 2014.

[156] J. L. Christian, "Morphogen gradients in development: from form to function," *Wiley Interdisciplinary Reviews: Developmental Biology*, vol. 1, no. 1, pp. 3–15, 2012.

[157] F. Crick, "Diffusion in embryogenesis," *Nature*, vol. 225, no. 5231, pp. 420–422, 1970.

[158] L. Wolpert, "Positional information and the spatial pattern of cellular differentiation," *Journal of Theoretical Biology*, vol. 25, no. 1, pp. 1–47, 1969.

[159] P. Muller, K. W. Rogers, S. R. Yu, M. Brand, and A. F. Schier, "Morphogen transport," *Development*, vol. 140, no. 8, pp. 1621–1638, 2013.

[160] R. G. Wylie, S. Ahsan, Y. Aizawa, K. L. Maxwell, C. M. Morshead, and M. S. Shoichet, "Spatially controlled simultaneous patterning of multiple growth factors in three-dimensional hydrogels," *Nature Materials*, vol. 10, no. 10, pp. 799–806, 2011.

[161] C. A. DeForest and K. S. Anseth, "Photoreversible patterning of biomolecules within click-based hydrogels," *Angewandte Chemie-International Edition*, vol. 51, no. 8, pp. 1816–1819, 2012.

[162] N. W. Choi, M. Cabodi, B. Held, J. P. Gleghorn, L. J. Bonassar, and A. D. Stroock, "Microfluidic scaffolds for tissue engineering," *Nature Materials*, vol. 6, no. 11, pp. 908–915, 2007.

[163] S. G. M. Uzel, O. C. Amadi, T. M. Pearl, R. T. Lee, P. T. C. So, and R. D. Kamm, "Simultaneous or sequential orthogonal gradient formation in a 3D cell culture microfluidic platform," *Small*, vol. 12, no. 5, pp. 612–622, 2016.

[164] J. K. Chen, J. Taipale, K. E. Young, T. Maiti, and P. A. Beachy, "Small molecule modulation of smoothened activity," *Proceedings of the National Academy of Sciences of the United States of America*, vol. 99, no. 22, pp. 14071–14076, 2002.

[165] E. Dessaud, A. P. McMahon, and J. Briscoe, "Pattern formation in the vertebrate neural tube: a sonic hedgehog

morphogen-regulated transcriptional network," *Development*, vol. 135, no. 15, pp. 2489–2503, 2008.

[166] M. Maden, "Retinoic acid in the development, regeneration and maintenance of the nervous system," *Nature Reviews Neuroscience*, vol. 8, no. 10, pp. 755–765, 2007.

[167] C. J. Demers, P. Soundararajan, P. Chennampally et al., "Development-on-chip: *in vitro* neural tube patterning with a microfluidic device," *Development*, vol. 143, no. 11, pp. 1884–1892, 2016.

[168] C. R. Marti-Figueroa and R. S. Ashton, "The case for applying tissue engineering methodologies to instruct human organoid morphogenesis," *Acta Biomaterialia*, vol. 54, pp. 35–44, 2017.

[169] S. Van Rijt and P. Habibovic, "Enhancing regenerative approaches with nanoparticles," *Journal of the Royal Society Interface*, vol. 14, no. 129, p. 20170093, 2017.

[170] M. J. Mahoney and W. M. Saltzman, "Transplantation of brain cells assembled around a programmable synthetic microenvironment," *Nature Biotechnology*, vol. 19, no. 10, pp. 934–939, 2001.

[171] R. L. Carpenedo, A. M. Bratt-Leal, R. A. Marklein et al., "Homogeneous and organized differentiation within embryoid bodies induced by microsphere-mediated delivery of small molecules," *Biomaterials*, vol. 30, no. 13, pp. 2507–2515, 2009.

[172] P. N. Dang, N. Dwivedi, L. M. Phillips et al., "Controlled dual growth factor delivery from microparticles incorporated within human bone marrow-derived mesenchymal stem cell aggregates for enhanced bone tissue engineering via endochondral ossification," *Stem Cells Translational Medicine*, vol. 5, no. 2, pp. 206–217, 2016.

[173] A. P. Van Winkle, I. D. Gates, and M. S. Kallos, "Mass transfer limitations in embryoid bodies during human embryonic stem cell differentiation," *Cells, Tissues, Organs*, vol. 196, no. 1, pp. 34–47, 2012.

[174] R. J. McMurtrey, "Analytic models of oxygen and nutrient diffusion, metabolism dynamics, and architecture optimization in three-dimensional tissue constructs with applications and insights in cerebral organoids," *Tissue Engineering Part C: Methods*, vol. 22, no. 3, pp. 221–249, 2016.

[175] C. Kropp, H. Kempf, C. Halloin et al., "Impact of feeding strategies on the scalable expansion of human pluripotent stem cells in single-use stirred tank bioreactors," *Stem Cells Translational Medicine*, vol. 5, no. 10, pp. 1289–1301, 2016.

[176] C. C. Miranda, T. G. Fernandes, M. M. Diogo, and J. M. S. Cabral, "Scaling up a chemically-defined aggregate-based suspension culture system for neural commitment of human pluripotent stem cells," *Biotechnology Journal*, vol. 11, no. 12, pp. 1628–1638, 2016.

[177] A. Rigamonti, G. G. Repetti, C. Sun et al., "Large-scale production of mature neurons from human pluripotent stem cells in a three-dimensional suspension culture system," *Stem Cell Reports*, vol. 6, no. 6, pp. 993–1008, 2016.

[178] H. Kempf, B. Andree, and R. Zweigerdt, "Large-scale production of human pluripotent stem cell derived cardiomyocytes," *Advanced Drug Delivery Reviews*, vol. 96, pp. 18–30, 2016.

[179] M. Vosough, E. Omidinia, M. Kadivar et al., "Generation of functional hepatocyte-like cells from human pluripotent stem cells in a scalable suspension culture," *Stem Cells and Development*, vol. 22, no. 20, pp. 2693–2705, 2013.

[180] P. Ovando-Roche, E. L. West, M. J. Branch et al., "Use of bioreactors for culturing human retinal organoids improves photoreceptor yields," *Stem Cell Research and Therapy*, vol. 9, no. 1, p. 156, 2018.

[181] X. Qian, H. N. Nguyen, M. M. Song et al., "Brain-region-specific organoids using mini-bioreactors for modeling ZIKV exposure," *Cell*, vol. 165, no. 5, pp. 1238–1254, 2016.

[182] A. Przepiorski, V. Sander, T. Tran et al., "A simple bioreactor-based method to generate kidney organoids from pluripotent stem cells," *Stem Cell Reports*, vol. 11, no. 2, pp. 470–484, 2018.

[183] Y.-C. Lu, D.-J. Fu, D. An et al., "Scalable production and cryostorage of organoids using core-shell decoupled hydrogel capsules," *Advanced Biosystems*, vol. 1, no. 12, 2017.

[184] D. Zhu, K. V. Larin, Q. Luo, and V. V. Tuchin, "Recent progress in tissue optical clearing," *Laser and Photonics Reviews*, vol. 7, no. 5, pp. 732–757, 2013.

[185] B.-C. Chen, W. R. Legant, K. Wang et al., "Lattice light-sheet microscopy: imaging molecules to embryos at high spatiotemporal resolution," *Science*, vol. 346, no. 6208, article 1257998, 2014.

[186] A. M. Paşca, S. A. Sloan, L. E. Clarke et al., "Functional cortical neurons and astrocytes from human pluripotent stem cells in 3D culture," *Nature Methods*, vol. 12, no. 7, pp. 671–678, 2015.

[187] J. A. Davies and M. L. Lawrence, "Four challenges for organoid engineers," in *Organs and Organoids*, pp. 255–259, Elsevier, 2018.

[188] T. Billiet, M. Vandenhaute, J. Schelfhout, S. Van Vlierberghe, and P. Dubruel, "A review of trends and limitations in hydrogel-rapid prototyping for tissue engineering," *Biomaterials*, vol. 33, no. 26, pp. 6020–6041, 2012.

[189] J. Li, M. Chen, X. Fan, and H. Zhou, "Recent advances in bioprinting techniques: approaches, applications and future prospects," *Journal of Translational Medicine*, vol. 14, no. 1, p. 271, 2016.

Hindawi
Stem Cells International
Volume 2019, Article ID 9831853, 18 pages
https://doi.org/10.1155/2019/9831853

Review Article

Stimuli-Responsive Graphene Nanohybrids for Biomedical Applications

Dinesh K. Patel,[1] Yu-Ri Seo,[2] and Ki-Taek Lim [1,2]

[1]*The Institute of Forest Science, Kangwon National University, Chuncheon 24341, Republic of Korea*
[2]*Department of Biosystems Engineering, College of Agriculture and Life Sciences, Kangwon National University, Chuncheon 24341, Republic of Korea*

Correspondence should be addressed to Ki-Taek Lim; ktlim@kangwon.ac.kr

Received 24 October 2018; Revised 14 December 2018; Accepted 17 January 2019; Published 2 April 2019

Guest Editor: Tiago Fernandes

Stimuli-responsive materials, also known as smart materials, can change their structure and, consequently, original behavior in response to external or internal stimuli. This is due to the change in the interactions between the various functional groups. Graphene, which is a single layer of carbon atoms with a hexagonal morphology and has excellent physiochemical properties with a high surface area, is frequently used in materials science for various applications. Numerous surface functionalizations are possible for the graphene structure with different functional groups, which can be used to alter the properties of native materials. Graphene-based hybrids exhibit significant improvements in their native properties. Since functionalized graphene contains several reactive groups, the behavior of such hybrid materials can be easily tuned by changing the external conditions, which is very useful in biomedical applications. Enhanced cell proliferation and differentiation of stem cells was reported on the surfaces of graphene-based hybrids with negligible cytotoxicity. In addition, pH or light-induced drug delivery with a controlled release rate was observed for such nanohybrids. Besides, notable improvements in antimicrobial activity were observed for nanohybrids, which demonstrated their potential for biomedical applications. This review describes the physiochemical properties of graphene and graphene-based hybrid materials for stimuli-responsive drug delivery, tissue engineering, and antimicrobial applications.

1. Introduction

Nowadays, on-demand release of active materials in desired areas has drawn tremendous attention in the rapidly developing field of materials science. For this purpose, stimuli-responsive materials (SRMs), which are also known as smart materials, are frequently used. They can change their shapes or dimensions in the presence of external stimuli such as electric field [1, 2], magnetic field [3, 4], temperature [5–7], pH [8], light [9–12], pressure [13], solvent [14], and moisture [15]. Stimuli-responsive polymers can be used in electrochemical devices [16], biomimetic devices [17], actuators and sensors [18], active sound-absorbing materials, smart textiles and apparel [19], intelligent medical instruments and auxiliaries [20, 21], and flexible devices [19]. Multiple cooperative interactions such as loss of hydrogen bonding and progressive ionization in polymer units are the key factors for such effects when the smart materials are exposed to external stimuli. Several polymers such as poly(ethylene oxide) (PEO), poly(propylene oxide) (PPO), poly(*N*-vinylcaprolactam), poly(*N*-isopropylacrylamide), poly(*N*,*N*″-diethylacrylamide), and other copolymers are frequently used as a smart material for various biomedical applications [22]. For biomedical applications, materials should be biocompatible and biodegradable and should not show any immune response in biological conditions. In addition, the materials should have adequate mechanical strength to support the proper growth of cells [23]. The properties of smart materials can be easily tuned by changing their structures or incorporating suitable fillers in their matrices. Metal and their oxides, clay with different modifications, nanocellulose, zeolites, and carbon in different forms such as fullerenes, carbon nanotubes, and graphite are frequently used to enhance the properties of native polymers

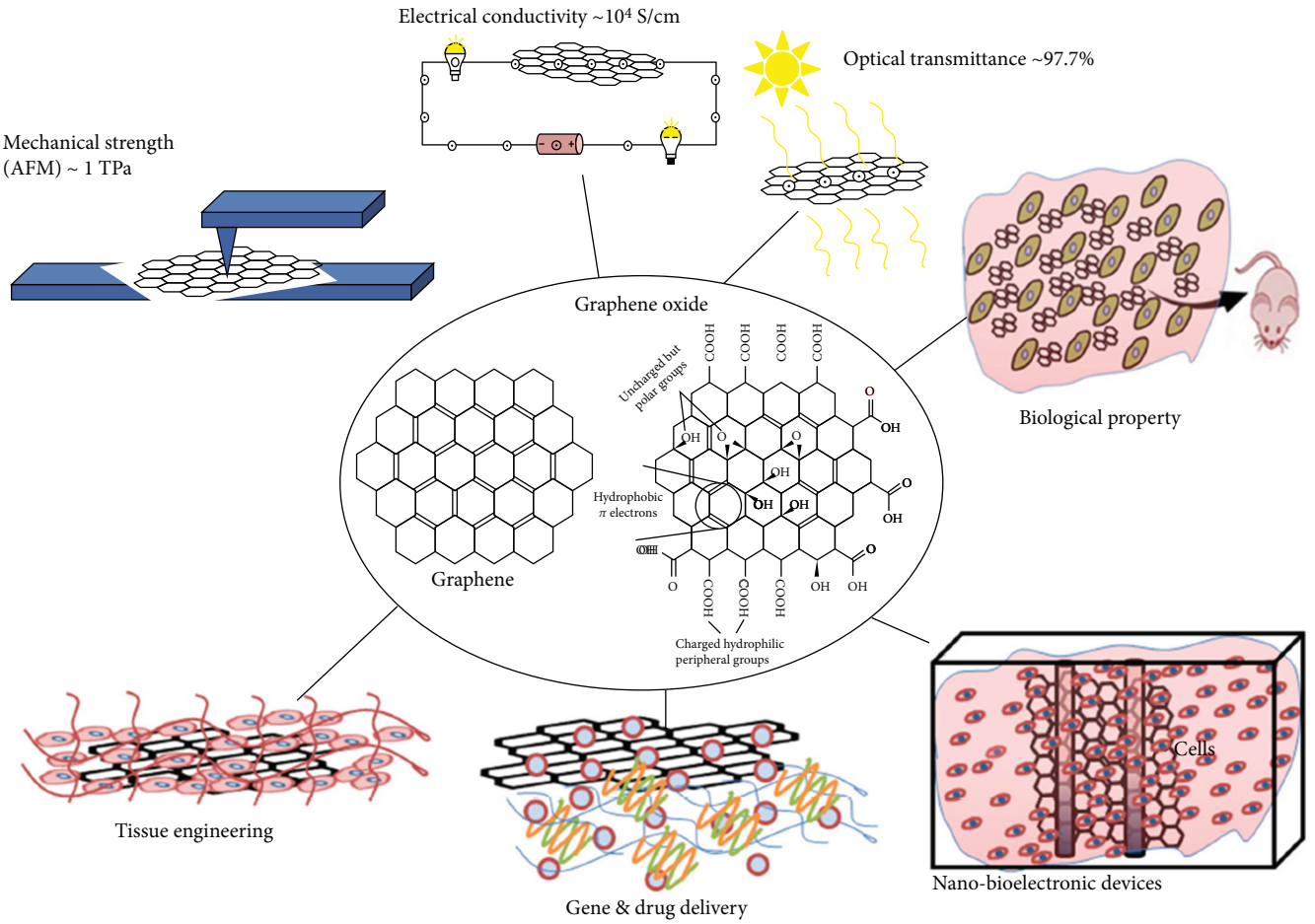

FIGURE 1: Schematic overview of various applications of graphene. Graphene-based nanomaterials have been explored for various nonmedical and biomedical applications due to their excellent mechanical, electrical, and optical properties [41].

[24–29]. According to the requirements, these fillers can be used to alter the properties of the matrix materials. Among these, graphite has drawn significant attention in the field of materials science as a reinforcing agent owing to its unique structural, thermal, mechanical, electrical, and biological properties [30–32]. Graphene is a single layer of sp^2-bonded carbon atoms with a honeycomb morphology. The higher surface area of graphene facilitates effective binding with several drugs through various interactions and is frequently used in targeted and controlled drug delivery applications [33, 34]. The hydrophobic nature of graphene restricts its use in polar environments. This problem can be overcome by rendering graphene hydrophilic by inserting different polar groups such as hydroxyl, epoxy, and carboxyl groups through surface functionalization. The presence of different functional groups in graphene oxide (GO) provides a platform for surface functionalization that can be used for various applications. Moreover, structural defects are created by oxidation, which lead to a decrease in their electrical property [35]. The structural defect is very useful in energy band gap applications. However, the electrical property can be restored by the reduction of GO, which is carried out through heating at higher temperatures in inert conditions or using various reducing agents such as hydrazine and alkaline media [36]. Extraordinary physiochemical properties of graphene make it a suitable material to develop the sensors, transparent and flexible electrodes, electronic circuits, and thermally and electrically conducting reinforced hybrids, which is not possible in the presence of other conventional fillers [37]. Graphene or functionalized graphene is extensively used to improve the various properties of native polymers. Nanohybrids show better mechanical, thermal, electrical, and biological properties than pure polymers do. This can be attributed to the high aspect ratio of the filler, which provides a better platform for interactions with the polymer matrix [38]. Enhancement in gas barrier property was observed for graphene-based nanohybrids owing to its two-dimensional (2D) sheet structure, which restricts the flow of gases [39]. Moreover, nanohybrids have shown more sustained or targeted drug delivery compared to pure polymers [40]. Figure 1 shows some possible applications of unique graphene or its derivatives [41].

This review describes the salient features of graphene and its biomedical applications such as stimuli-responsive drug delivery, tissue engineering, and antibacterial materials in the presence of different polymer matrices. Different

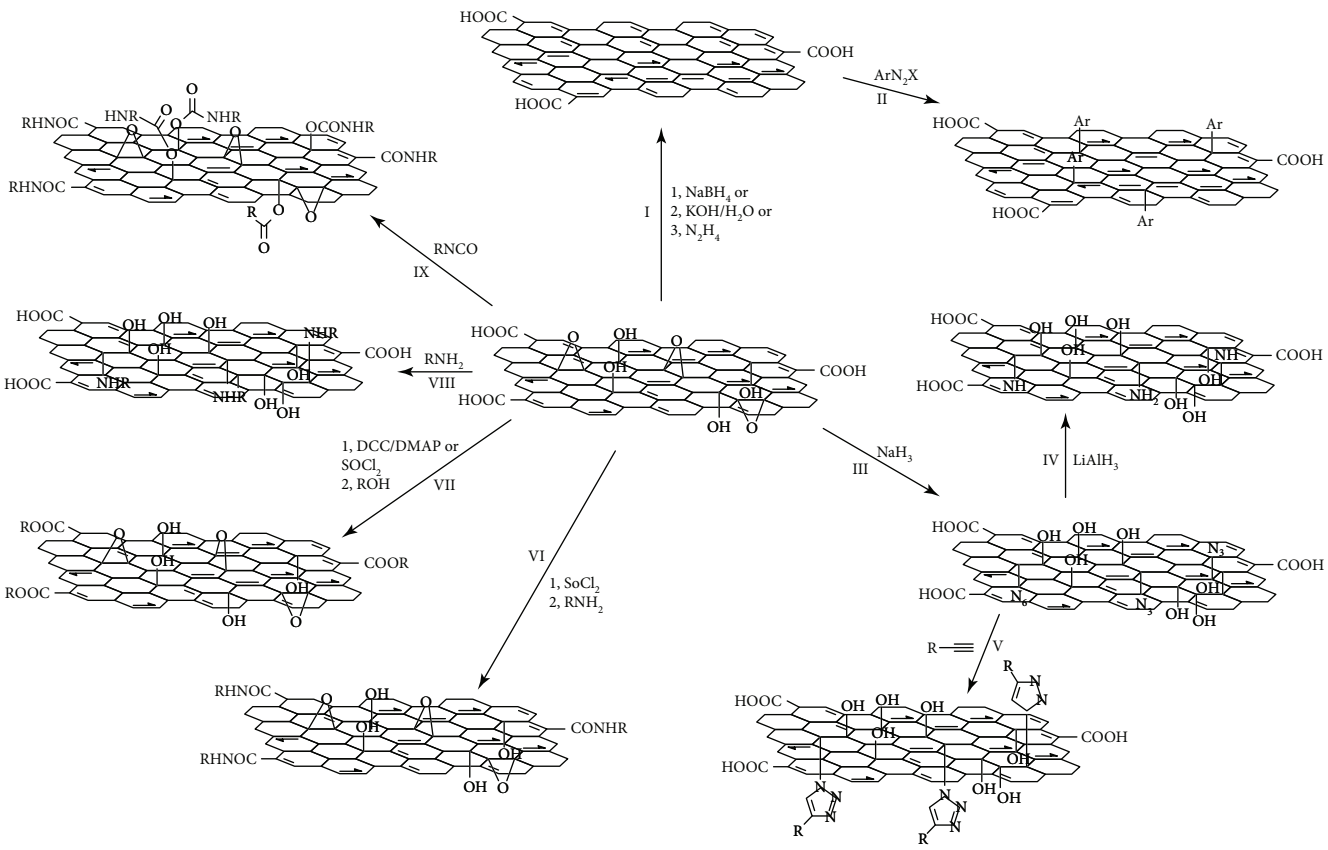

Figure 2: Schematic showing various covalent functionalization chemistries of graphene or GO. I: reduction of GO into graphene by various approaches ((1) $NaBH_4$, (2) KOH/H_2O, and (3) N_2H_4). II: covalent surface functionalization of reduced graphene via diazonium reaction (ArN2X). III: functionalization of GO by the reaction between GO and sodium azide. IV: reduction of azide functionalized GO (azide–GO) with $LiAlH_4$ resulting in the amino-functionalized GO. V: functionalization of azide–GO through click chemistry (R–ChCH/$CuSO_4$). VI: modification of GO with long alkyl chains ((1) $SOCl_2$ and (2) RNH_2) by the acylation reaction between the carboxyl acid groups of GO and alkylamine (after $SOCl_2$ activation of the COOH groups). VII: esterification of GO by DCC chemistry or the acylation reaction between the carboxyl acid groups of GO and ROH alkylamine (after $SOCl_2$ activation of the COOH groups) ((1) DCC/DMAP or $SOCl_2$ and (2) ROH). VIII: nucleophilic ring-opening reaction between the epoxy groups of GO and the amine groups of an amine-terminated organic molecular (RNH_2). IX: the treatment of GO with organic isocyanates leading to the derivatization of both the edge carboxyl and surface hydroxyl functional groups via formation of amides or carbamate esters (RNCO) [44].

techniques such as in situ polymerization, solution casting, and extrusion were used to fabricate graphene-based nanohybrids for desired applications.

2. Salient Features of Graphene

Among various nanomaterials, graphene has a variety of advantages and gained tremendous attention from the scientific community. Graphene is a 2D single atomic layer of graphite with sp^2-hybridized carbon atoms arranged in a honeycomb structure. It was initially described by Boehm et al. in 1986 followed by identification and isolation by Geim and Novoselov in 2004 [42, 43]. In graphene, each carbon atom is connected by σ bonds with a delocalized π electron network. These delocalized π electrons provide a high electron density above and below the 2D planar structure of graphene. Because of the planar structure and delocalized π electrons, graphene undergoes various reactions such as cycloadditions, click reactions, and carbine insertions [44]. Pure graphene is hydrophobic in nature and requires stabilizing agents or surfactants to disperse in water [45]. In addition to graphene, GO and reduced graphene oxide (RGO) are used to improve material properties. Since GO contains several functional groups in its structure, there is a high possibility of surface modification. Figure 2 shows a few chemical functionalizations of the GO structure [44]. Some salient features of graphene are given in the next sections.

3. Mechanical Properties

Several techniques such as force displacement, force volume, nanoindentation atomic force microscopy (AFM) [46–48], and numerical simulation [49–51] are used to determine the mechanical strength of the wonder graphene material. It is observed that defect-free single layer graphene is a much stronger than steel [52]. The Young's modulus, fracture strength, and Poisson's ratio of a defect-free single layer graphene are 1 TPa, 130 GPa, and 0.149 GPa, respectively [52]. On the other hand, GO has several defects and thus

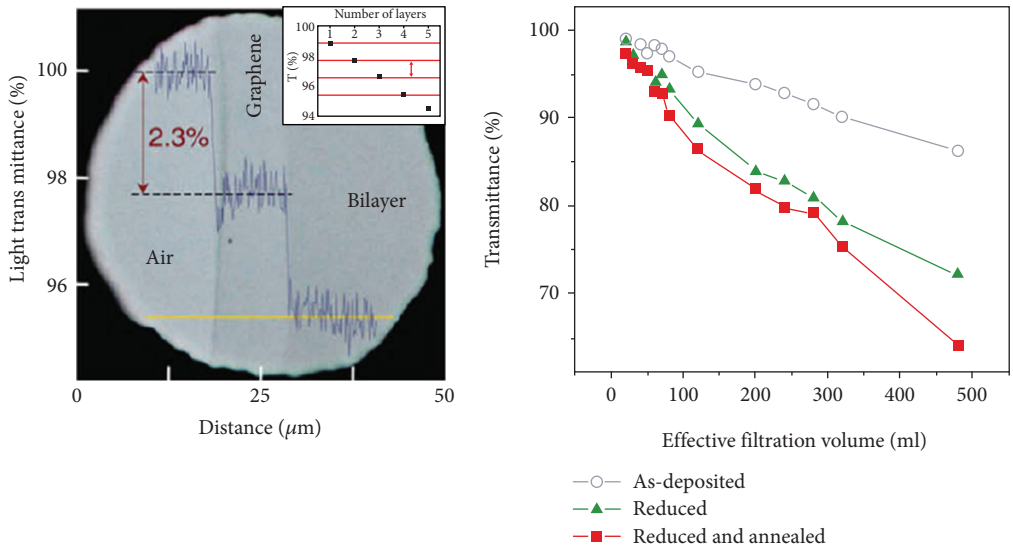

Figure 3: Optical transparency. (a) Optical micrograph of one- and two-atom-thick graphene crystals. The optical transmittance at 550 nm as a function of the lateral coordinate shows clear steps, the height of which is proportional to the hyperfine constant. In the inset, the linear variation of the transparency as function of number of layers is observed up to six layers. (b) Transmittance at λ~550 nm as a function of the thickness of reduced GO thin films, assessed indirectly by the total volume of filtered suspension. Plots are shown for thin films with different reduction steps [66].

shows significantly lower mechanical strength than that of a defect-free graphene with a Young's modulus of 0.15–0.35 TPa [53, 54], elastic modulus of 32 GPa, and fracture strength of 120 MPa [54]. The mechanical strength of defective GO films can be improved by the reduction process or using cross-linking agents [55]. Since graphene has exceptional mechanical strength, it is widely used to enhance the mechanical strength of polymeric materials for various applications. Besides, it was observed that graphene with other nanomaterials such as carbon nanotubes cause greater improvement in the mechanical strength of polymeric materials with individual nanomaterials due to the synergistic effect of both the nanomaterials [56].

4. Thermal and Electrical Properties

The presence of strong σ bonding and delocalized π electrons makes graphene a unique electrically and thermally conductive material with a low thermal expansion coefficient. The thermal conductivity of defect-free graphene is much higher than that of other carbon nanomaterials. Its thermal conductivity is approximately in the order of $4.5 - 5.5 \times 10^3$ W/mK, whereas it is approximately 2×10^3, 3×10^3, and 3.5×10^3 W/mK for graphene oxide, multiwalled carbon nanotubes, and single-walled carbon nanotubes, respectively [52, 57, 58]. The thermal conductivity of GO is lower than that of graphene due to the presence of defects in its structure that hinders the conductivity. This property is greatly influenced by several factors such as doping or defect edge scattering, which cause localization of phonons [59–61]. The electrical mobility of defect-free graphene is higher than that of defective GO and is in the order of 10^4 S/cm. The electrical mobility of GO is 10^{-1} S/cm [62]. With its excellent inherent thermal and electrical properties, graphene is extensively used in the fabrication of low-cost and highly efficient electronic devices. In addition, it is used in tissue engineering, biosensors, and other biomedical devices to measure the cell potential [63, 64].

5. Optical Properties

In addition to exceptional mechanical strength and thermal and electrical properties, graphene has an excellent optical property. Single layer defect-free graphene has shown 97.7% incident light transmission over a wide range of wavelengths [65]. This property is highly affected by the presence of impurities as well as the number of graphene layers. Figure 3 shows the optical transparency of one- and two-layer graphene sheets [66]. The excellent optical properties, as well as the superior conductivity of graphene-based materials, open a new dimension to replace the expensive ITO films. High optical transparency, superior conductivity, excellent mechanical strength, and chemical stability make graphene suitable for use as transparent electrodes in solar cells or liquid crystals as well as processable flexible transparent electrodes [67–69]. Photocurrent can be generated by applying an external or internal field during light absorption by the graphene surface. It has been observed that nanosized graphene such as quantum dots have an excellent photoluminescence property. The photoluminescence behavior is highly influenced by the electron-hole pair density in graphene. Higher transmittance and photoluminescence behaviors make graphene the most promising and appealing nanomaterial for application in magnetic resonance imaging (MRI) and biomedical imaging [41].

6. Biomedical Applications of Graphene-Based Nanohybrids

6.1. Stimuli-Responsive Drug Delivery. On-demand or targeted drug release from biomedical devices has attracted great attention in the field of medical science. It has been noted that targeted drug release from carrier molecules exhibits high efficiency with a controllable release and minimum side effects. Several factors such as light, heat, pH of the medium, ultrasound waves, and electric or magnetic fields are responsible for the controlled release of drugs [70–72]. For this purpose, graphene-based nanocarriers are frequently used owing to their large surface areas that facilitate easy loading of drugs and the presence of functional groups provides additional multiple modification routes for targeted and controlled drug release [33, 34]. Nevertheless, care should be taken so that no toxic materials are released from the nanocarriers during stimulation. An electrically responsive drug release material was synthesized by Weaver et al. using conducting pyrrole and GO through electropolymerization on glassy carbon electrodes. They loaded dexamethasone drug in this hybrid and evaluated its release behavior under an external electrical field. A linear drug release was observed from the nanohybrids, which could be changed by varying the magnitude of the external electric field. Interestingly, no passive release of loaded drug occurred from the nanohybrids in the absence of an electric field. The drug-release behavior of the nanohybrids can also be optimized by changing the size and thickness of GO. On the other hand, the released drug maintains its bioactivity without the leaching of additional toxic products during electrical stimulation. Since GO nanoparticles are larger than the loaded drug molecules, only small molecules are released from the nanohybrid film during stimulation, while larger materials are intact within the polymer matrix. Figure 4 shows the controlled release of dexamethasone drug from a GO/poly pyrrole nanohybrid film [73]. Photothermally induced drug release from nanomaterials has gained significant attention in the treatment of cancer to achieve controllable release with high efficiency and minimum side effects during the treatment [74]. Cancer treatment through chemotherapy has many limitations such as low efficacy, side effects, and drug resistance [75]. Xu et al. synthesized photothermally mediated nanocarriers using nano-GO and gold nanorods with the conjugation of folic acid-modified hyaluronic acid. A schematic representation of the synthesis of nano-GO-based hybrids and the possible mechanism in targeted chemophotothermal therapy are shown in Figure 5(a). The pH-dependent loading of anticancerous doxorubicin hydrochloride drug into the hybrids and its release profiles under different pH media are shown in Figure 5(b). It was observed that the loading capacity is higher in an alkaline medium than in a neutral or acidic medium due to the greater hydrophobic interactions between the nano-GO and the anticancer drug. However, a faster drug release behavior was observed in the acidic condition due to protonation of the loaded drug and, consequently, an increase in the water-soluble tendency. This property is very useful in the treatment of cancer cells because both the extracellular environment of a tumor and the intracellular lysosome and endosomes are acidic in nature, which facilitate greater release of the drug. The release profile was also influenced by light, and it was observed that irradiation with a near-infrared (NIR) laser for 30 min in 24 h caused a 3.5-fold increase in drug release than that in the absence of light irradiation. This can be attributed to dissociation of π-π stacking interactions between the drug and the polymer matrix [76]. In another study, Song et al. fabricated hyaluronic acid/GO hybrids as nanocarriers for targeted and pH-responsive release of the anticancer doxorubicin drug through π-π stacking and hydrogen bonding interactions. A faster drug release from the nanohybrids was observed at pH 5.3 than at pH 7.4, which indicated its potential as a targeted and pH-mediated anticancer drug delivery vehicle [77]. Kurapati and Raichur synthesized NIR light-responsive GO/poly (allylamine hydrochloride) (PAH) multilayered capsules for remote-controlled drug delivery. The capsule templates were prepared by dextran sulfate- (DS-) doped calcium carbonate. Scheme 1 shows the remote opening of GO-based hybrid capsules using NIR-laser light [78]. Further, pH-induced site-specific drug delivery through poly(2-(diethylamino) ethyl methacrylate) (PDEA)/GO hybrids was studied by Kavitha et al. The fabricated films exhibited good solubility and stability in physiological solutions. The anticancer drug camptothecin (CPT) was loaded through π-π stacking and hydrophobic interactions between the drug and the nanohybrids. However, drug release was observed only in an acidic medium but not in basic and neutral media, which are found in a tumor environment; this suggests the formation of a suitable site-specific drug carrier [79]. Hydrogel scaffolds with 2D and three-dimensional (3D) structures have been extensively used in drug delivery and other tissue engineering applications owing to their unique physiological properties. Li et al. synthesized NIR light-mediated on-demand release and reversible cell capture scaffolds using GO/poly(N-isopropylacrylamide) (pNIPAAm) via an in situ atom-transfer radical polymerization technique. They observed that the release profile was highly influenced by the laser light intensity and the presence of GO [80]. In another study, Chen et al. fabricated a self-healing, pH, and light-induced hydrogel using GO and ureidopyrimidinone and *N*-isopropylacrylamide (pNIPAAm) polymer matrices. They noted that a faster drug (doxorubicin hydrochloride) release from the hydrogel occurred in the acidic medium than in the neutral and alkaline media due to the protonation of polar groups. Furthermore, the developed hydrogels exhibited temperature-mediated drug release, which was more controlled at higher temperatures due to dehydration of the hydrogel leading to a more compact structure that hinders the diffusion of the drug. Figure 6 shows the pH and temperature-induced drug release from graphene-based hydrogels [81].

6.2. Tissue Engineering Applications. For tissue engineering applications, materials should be biocompatible, nontoxic, and biodegradable in nature. In addition, materials should not show any negative response in biological conditions [82–84]. Tissue engineering techniques overcome the

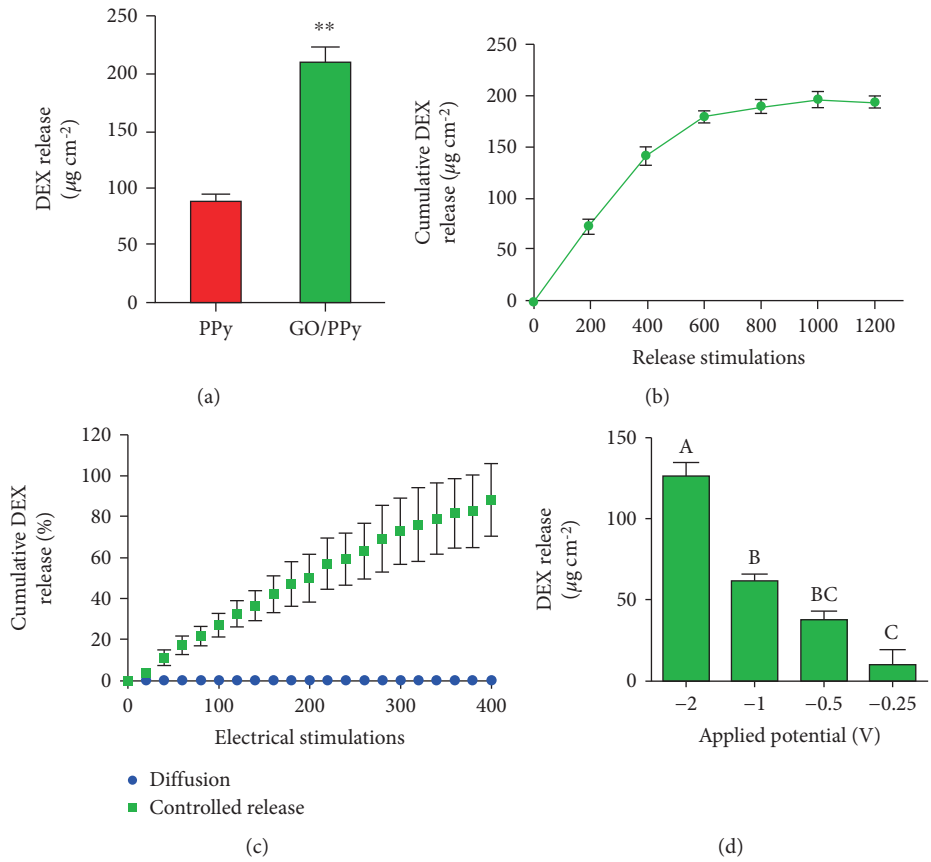

Figure 4: Electrically controlled DEX release from the GO/PPy nanocomposite film. (a) Total DEX release from PPy films with or without GO as a codopant in response to an aggressive square-wave, biphasic voltage stimulation (-2.0 V for 5 s, followed by 0 V for 5 s) repeated for 1000 stimulations. The GO/PPy-DEX nanocomposite released a significantly larger quantity of DEX ($p < 0.01$; $n = 3$). (b) Cumulative release profile of the GO/PPy-DEX nanocomposite in response to aggressive repeated square-wave, biphasic voltage stimulation (-2.0 V for 5 s, followed by 0 V for 5 s) for 1200 stimulations ($n = 6$). The release profile reaches a plateau at 600-voltage pulses under this aggressive stimulation paradigm, indicating that all available drugs have been released at this point. (c) Cumulative release profile of the GO/PPy-DEX nanocomposite in response to milder release stimulation (-0.5 V for 5 s, followed by 0.5 V for 5 s) and in the absence of electrical stimulation (passive diffusion) ($n = 3$). Electrical stimulation elicited a linear release for up to 400 pulses, while no drug passively diffused from the film when no voltage stimulation was applied. (d) Effect of voltage stimulus modulation on the amount of DEX released from nanocomposite films. GO/PPy-DEX nanocomposite films were submitted to 100 square-wave, biphasic stimulation pulses where the negative phase was varied from -2 to -0.25 V, the positive phase was 0.5 V, and the stimulus lingered at each phase for 5 s. Bars labeled with nonmatching letters indicate a significant difference between groups ($p < 0.01$, $n = 3$) [73].

limitation of traditional medical procedures, wherein repair or replacement of tissues is required. Nowadays, stem cells are most widely studied and used in cell lines for tissue engineering applications owing to their ability to differentiate into various other cells such as osteoblasts and chondrocytes, cardiac muscle cells, neural cells adipocytes, and endotheliocytes in the presence or absence of external stimuli on various surfaces [85–88]. Guo et al. synthesized graphene/poly(3,4-ethylenedioxythiophene) hybrid microfibers and observed its cellular response in the presence of mesenchymal stem cells (MSCs). They noted that neural differentiation of MSCs was dramatically improved by electrical stimulation due to greater interfacial interactions of the electroactive neural cells and the bioelectronic surface, which led to more differentiation of MSCs. Figure 7 shows the electric-induced cell differentiation of MSCs into neural cells [89]. Similarly, Weaver and Cui demonstrated direct neural stem cell (NSC) differentiation in the presence of a conducting polymer poly(3,4-ethylenedioxythiophene) and GO. They noted that when the surface had interferon-γ (INF γ) biomolecules, a larger population of neuron cells occurred, while in the presence of a platelet-derived growth factor (PDGF), a larger population of oligodendrocytes occurred, suggesting its potential for controlling the NSC differentiation tendency for therapeutic applications [90]. In another study, Luo et al. fabricated nanofibrous GO/poly(lactic-co-glycolic-acid) hybrids through the electrospinning technique and evaluated its biological responses in the presence of MSCs. A higher cell viability (on the 7th day) and adhesion behavior were observed for the nanohybrid mat compared to the pure polymer due to the strong adsorption of protein onto the nanohybrid surface. In addition, osteogenic differentiation of MSCs occurred on the nanohybrid surface, which was accelerated by GO [91]. Chemical functionalization of

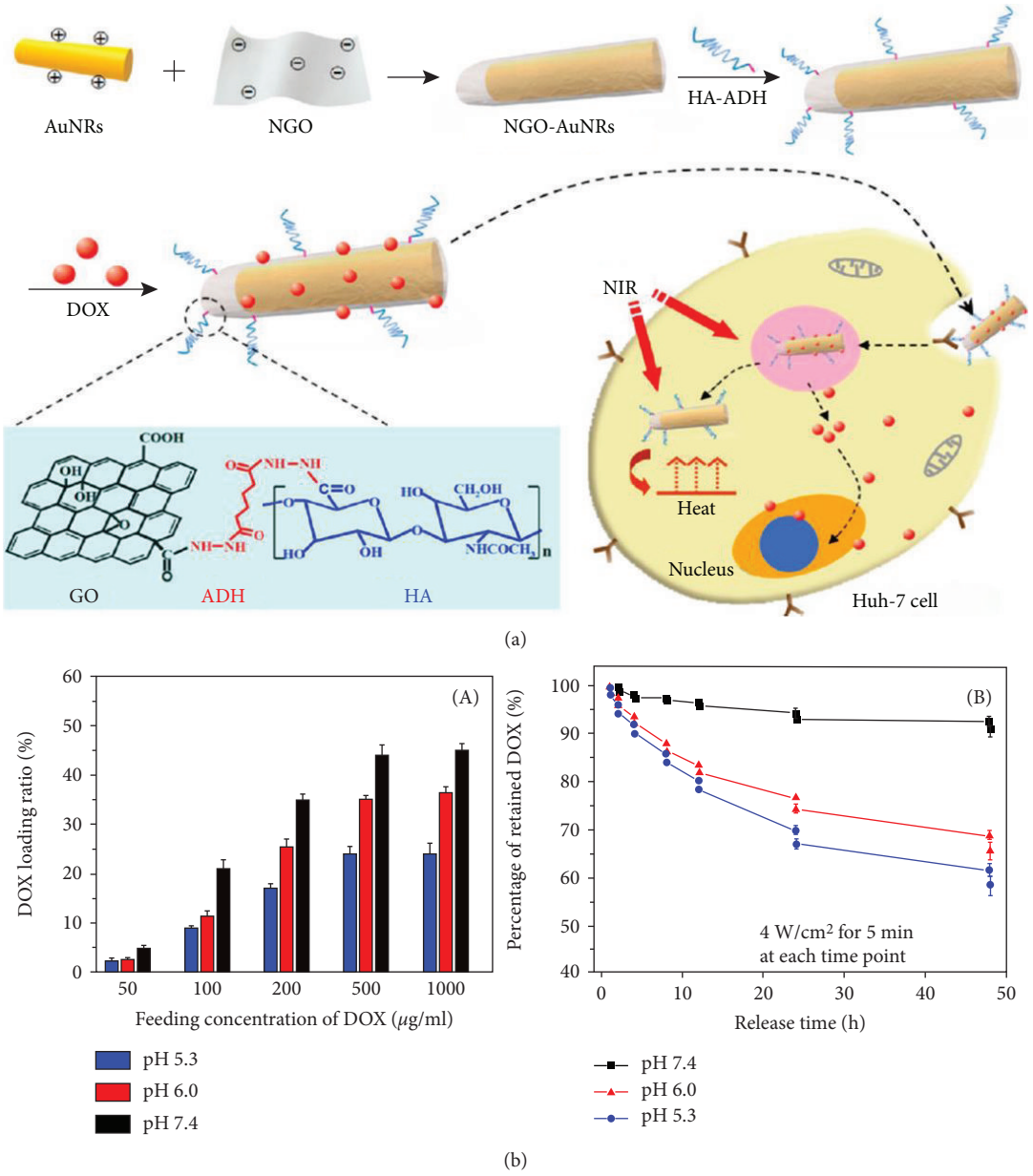

Figure 5: (a) Schematic illustration for the synthesis of NGOHA-AuNRs-DOX and the possible mechanism in targeted chemophotothermal therapy to hepatoma Huh-7 cells. (b, A) pH-dependent DOX loading efficiency of NGOHA-AuNRs at different DOX feeding concentrations. (B) Cumulative release profiles of DOX from NGOHA-AuNRs-DOX at different pH values with 4 W/cm^2 NIR light irradiation at each time point for 5 min. Data represent mean values for $n = 3$, and the bars are standard deviations for the means [76].

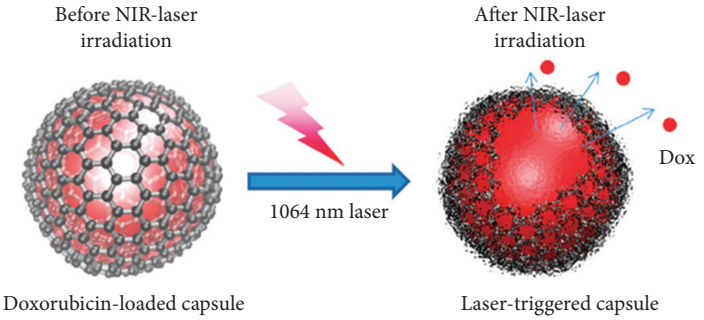

Scheme 1: Illustration of the remote opening of GO–polymer composite capsules using NIR-laser light [78].

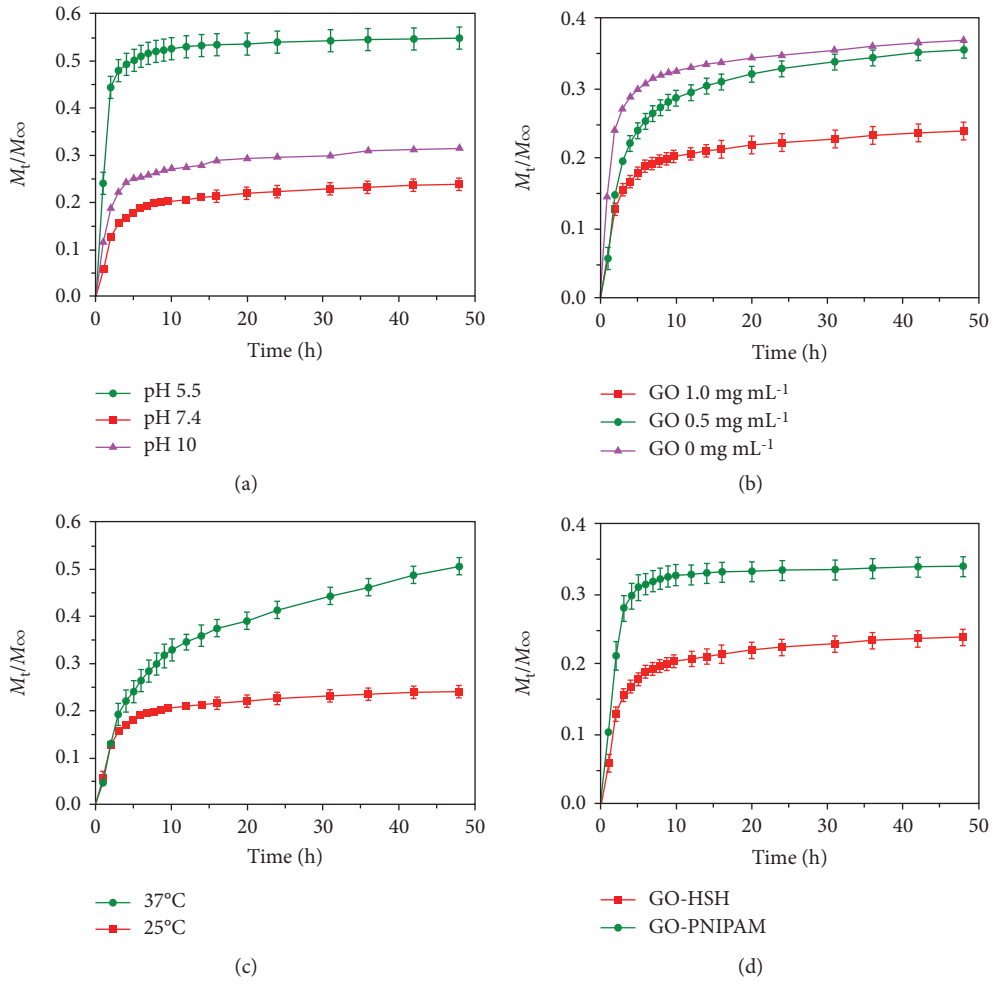

Figure 6: Stimuli-responsive release behavior of DOX from the GO-HSH hydrogel. (a) pH 5.5, pH 7.4, and pH 10 medium at 37°C; (b) varied concentrations of GO nanosheets at 37°C and (c) at 25 and 37°C; (d) DOX release curves of the GO-HSH and GO–PNIPAM hydrogels at 37°C [81].

graphene plays a crucial role in cellular behavior because it changes the electronic moiety surrounding the graphene sheet that influences the interactions. A comparative study was conducted by Kumar et al. using the GO, RGO, and diamine-modified GO in a poly(ε-caprolactone) (PCL) matrix to evaluate the cellular response toward stem cells. They observed that the composite with diamine-modified GO showed a higher proliferation and differentiation of human MSCs (hMSCs) followed by the GO composite. This was due to better interactions between the amine moiety and the cells [92]. Zhang and coworkers also synthesized a pH-sensitive GO conjugate purpurin-18 methyl ester nanocomplex for photodynamic therapy application. A significant decrease in cell viability (HepG-2 cells) was observed in the GO-Pu18 nanohybrids when it was irradiated with light, suggesting that the developed materials have excellent photocytotoxicity and negligible dark response. In vitro photocytotoxicity of the developed material toward HepG-2 cells is shown in Figure 8 [93]. Notably, myoblast differentiation of human cord blood-derived MSCs (CB-hMSCs) into skeletal muscle cells (hSkMCs) were observed on the electrospun fibers of the GO/PCL composite. A high rate of cell proliferation, differentiation, and orientation on the fibrous surface indicated its better biocompatibility. This was due to better interconnections with the fibers and the enhanced conductivity and dielectric properties provided by GO. This property plays a significant role in cell adhesion followed by higher proliferation and myotube orientation. Myoblast differentiation of CB-hMSCs via an early expression of myogenin-positive nuclei is shown in Figure 9 [94]. Further, it was reported that the conjugation of GO with low-molecular-weight polyethylenimine (PEI) enhanced the proliferation and differentiation of hMSCs. Kumar and coworkers synthesized GO/PEI-based composites using poly(acrylic acid) (PAA) as a spacer in a PCL matrix. A significant increase in cell proliferation and differentiation was observed in the composite fibers than in the pure PCL and GO/PEI conjugate. This was attributed to the higher number of amine and oxygen functional groups in the composite that led to better interactions between the cells and the fibrous surface [95]. Sayyar et al. synthesized a conducting graphene/chitosan hydrogel and observed its

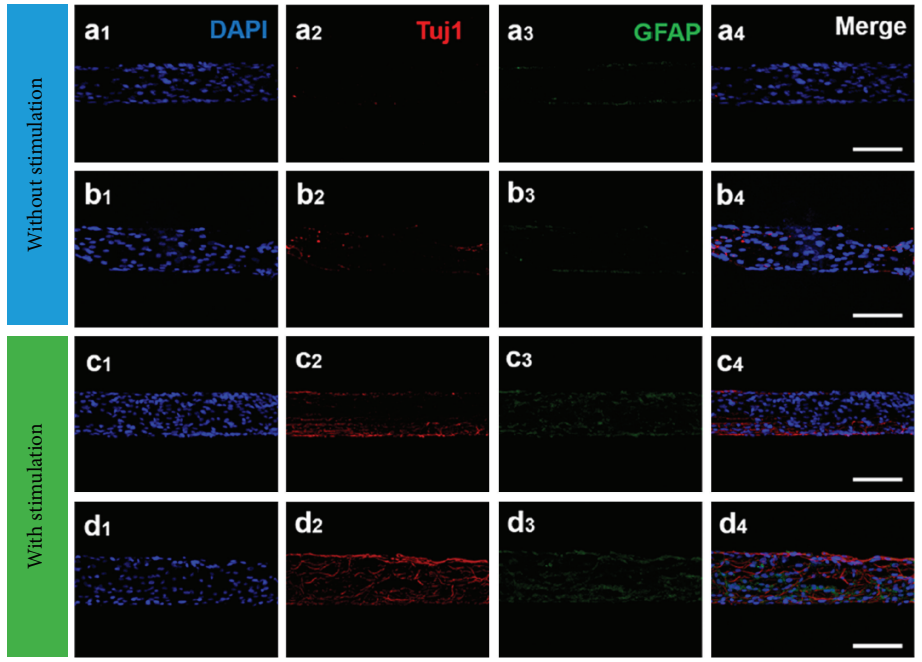

Figure 7: Cells were immunostained with (1) DAPI (blue) for the nucleus and neural-specific antibodies (2) Tuj1 (red, cy3) and (3) GFAP (green, FITC) after being cultured under stimulation culturing conditions without TENG electrical stimulation (a, b) or with human-motion-driven TENG electrical stimulation (c, d) for 21 days on an rGO microfiber (a, c) and 15% rGO-PEDOT hybrid microfiber (b, d). (Right) Merged fluorescence images (scale bar = 100 μm) [89].

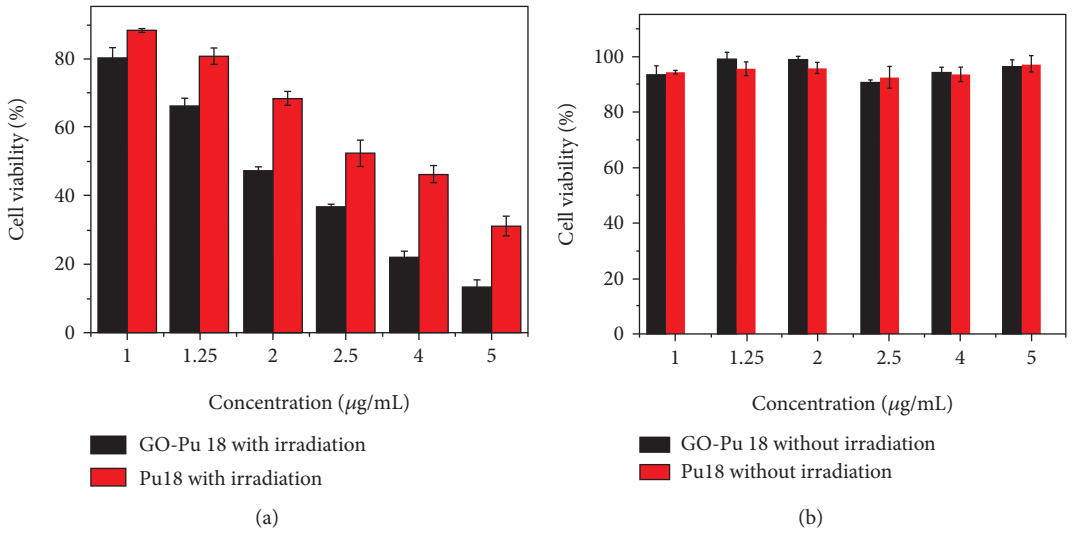

Figure 8: (a) In vitro PDT phototoxicity of GO-Pu18 and free Pu18 to HepG-2 cells and (b) GO-Pu18 composite and free Pu18 to HepG-2 cells without irradiation [93].

cellular response. They noted that fibroblast cells on the developed scaffold were healthy, which indicated the biocompatibility of the composite [96]. Hydroxyapatite (HA) is frequently used in bone tissue engineering applications; however, its poor mechanical strength restricts its application in long-term functional materials under load-bearing conditions [97, 98]. The properties of HA can be improved by incorporating reinforcing agents. Liu and coworkers prepared hydroxyapatite/RGO nanocomposites and examined their mechanical and biological activities. An enhanced mechanical behavior with improved proliferation and ALP activity of the human osteoblast cells on the nanohybrid surface suggests its potential for use as a biomaterial [99]. A similar observation was made by Li et al. using nanohydroxyapatite and chitosan-functionalized GO [100]. In another study, enhanced osteogenesis and neurogenesis were observed for hMSCs on chitosan/graphene composite surfaces. This can be attributed to the enhance cell-cell and cell-material interactions that promote the functions of hMSCs [101]. Degradation is also an important parameter

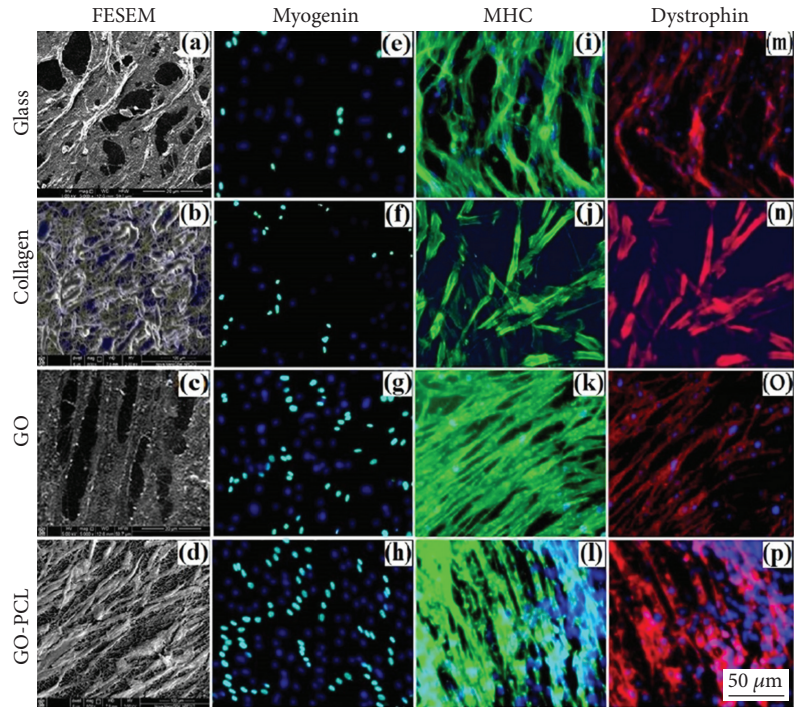

Figure 9: FESEM micrographs showing formation of myotubes on glass and collagen controls (a and b), GO sheets (c), and GO-PCL meshes (d). Expression of the early myogenic differentiation marker myogenin-positive nuclei (green) on controls (e and f), GO sheets (g), and GO-PCL meshes (h). Immunostaining of MHC (green), respectively, on controls (i and j), GO sheets (k), and GO-PCL meshes (l) and dystrophin (red) similarly on controls (m and n), GO sheets (o), and GO-PCL meshes (p). Nuclei were counterstained with DAPI [94].

that indicates whether the materials are useful or not for specific requirements in biological conditions. Natarajan and coworkers synthesized biodegradable composites using GO and galactitol and studied their biocompatibility. They observed that the developed materials were biocompatible with a stimulated osteogenesis property [102]. In addition, some other promising graphene-based scaffolds applications in the tissue engineering field are represented in Table 1.

7. Antibacterial Activities

Nowadays, several antibiotics and antimicrobial agents have been developed for the treatment of various infectious diseases. However, lethal microorganisms remain a challenge for public health, causing several infectious diseases annually [103]. Antibiotics are frequently used to minimize the effect of these pathogens. Moreover, due to the excess use of antibiotics, these pathogens are becoming multidrug resistant [104]. Recently, nanomaterials have gained tremendous attention in this area owing to their unique physical and antibacterial properties that are absent in their macroscopic forms [105]. Various nanomaterials such as graphene, gold, silver, copper, zinc oxide, and magnesium are frequently used for this purpose [106–110]. As mentioned earlier, graphene has drawn wide attention in materials science research owing to its excellent physiochemical and biocompatible properties. Some research works demonstrated that pure GO does not have any antibacterial, bacteriostatic, or cytotoxic properties toward bacteria or mammalian cells [111]. Zhao and coworkers synthesized poly(ethylene glycol)- (PEG-) conjugated GO/silver nanoparticle-loaded composites and evaluated their stability and antibacterial activity. They noted that the composites of PEG-conjugated GO with silver nanoparticles were more stable (over 1 month) than the GO/silver nanoparticle composite was. In addition, they observed that GO-PEG-Ag composites showed more antibacterial activity compared to GO-Ag composites toward Gram-negative/positive bacteria such as *E. coli* and *S. aureus* (~100% of *E. coli* and ~95.3% of *S. aureus*) by 10 μg/mL for 2.5 h. The higher antibacterial activity of GO-PEG-Ag composites was due to the damage of the bacterial structure and the production of reactive oxygen species, which led to cytoplasm leakage and decrease in metabolism [112]. Some et al. synthesized GO-based poly($_L$-lysine) (PLL) composites through electrostatic interactions and covalent bonding between the graphene derivatives and PLL and evaluated their cytotoxicity and antibacterial behavior. They observed that the composites showed a strong antibacterial nature and biocompatibility toward human adipose-derived stem cells and non-small-cell lung carcinoma cells (A549), which indicated its dual functionality that can be used to inhibit bacterial growth as well as enhance human cell growth [113]. In another study, Shao and coworkers synthesized silver nanoparticle-embedded graphene oxide nanocomposites and observed its antibacterial property toward Gram-negative *E. coli* (ATCC 25922) and Gram-positive *S. aureus* (ATCC 6538) by the plate count method and disk diffusion method.

Table 1: Graphene-based scaffolds for tissue engineering application.

Graphene-based scaffolds	Tissue engineering applications	Observations	References
Antibody coated Au-nanoparticles on pyrolytic graphite Graphene oxide-based silk fibroin (SF) nanoparticles	Immunosensor for stem and carcinoma cell through Nanog detection Stem cell differentiation	Good sensitivity (0.1-160 pg/mL) in human embryonic stem cell lysates Accelerated early cell adhesion and induced osteogenic differentiation of hMSCs	[102, 131]
Graphene-coated surfaces, e.g., polydimethylsiloxane (PDMS), glass, and Si/SiO_2 substrates	Stem cell differentiation	Controlled and accelerated differentiation of hMSCs Accelerated adherence of human osteoblasts and mesenchymal stromal cells	[132–134]
Graphene oxide/graphene oxide-coated surfaces	Culture and differentiation of stem cells	Induced pluripotent stem cell culture and differentiation Improved stem cell adhesion and differentiation	[135, 136]
Graphene foam	Stem cell differentiation	Promotion of osteogenic differentiation of hMSCs Promotion of neural stem cell (NSCs) differentiation into astrocytes and neurons Promotion of in vivo mimicking conditions as well as effective cell adhesion, proliferation, and differentiation towards any desired tissue regeneration Increased cell adhesion, proliferation, and differentiation of neural stem cells (NSCs) Promotion of mouse mesenchymal stem cell (MSC) differentiation toward dopaminergic neurons	[137–141]
Activated charcoal	Stem cell differentiation	Promotion of human embryonic stem cell differentiation toward neuronal lineage	[142]
Fluorinated graphene	Stem cell differentiation	Promotion of human stem cells into neuronal lineage	[143]
Graphene microfiber	Stem cells differentiation	Promotion of adhesion, proliferation, and differentiation of neural stem cells (NSCs)	[144]

Significant antibacterial activity was observed for the nanocomposites, which suggested its potential use in biomedical applications [114]. Microbial contamination such as waterborne pathogens including bacteria, protozoans, helminthes, fungi, and viruses cause several severe diseases to human beings [115]. Several techniques such as ultraviolet (UV) treatment and chemical and thermal treatments are frequently used for water purification processes [116]. Nanofiltration (NF), one of the most studied membrane technologies for a wide range of applications such as water purification/desalination, textile dyes/heavy metals/natural organic removal, and oil/water separation, uses membranes with pore sizes of 0.5–2 nm [117–121]. Zhu et al. prepared a nanofiltration membrane based on RGO and copper nanoparticles through an in situ reduction process on a polydopamine (PDA) surface and evaluated its dye purification or desalination behavior with antibacterial performance. Figure 10 shows the schematic of the synthesis routes to the nanocomposite and its deposition on a PDA surface. A PDA-rGOC-modified membrane exhibited strong antibacterial property toward *E. coli* (~97.9% reduction) after 3 h of contact, indicating its multidynamics applications with strong antibacterial and separation performances. The antibacterial activity of the PDA-rGOC-modified membrane is shown in Figure 11 [122]. Musico et al. modified the commercially available cellulose nitrate membrane filter papers with poly(*N*-vinylcarbazole) (PVK) and graphene/GO. The PVK-GO-modified membrane exhibited a strong antibacterial activity toward *B. subtilis* and *E. coli.* This was due to the production of reactive oxygen species by the nanoparticles, which influenced the metabolic activity of the microorganisms [123]. Liu et al. studied the antibacterial activity of a polylactic acid-GO-silver nanoparticles hybrid toward *S. aureus* [124]. It is well known that graphene has a high tendency to absorb NIR light and reflect it in the form of heat. This property of graphene has a wide range of applications in materials science. A light- (NIR-) induced antibacterial surface was prepared using PEI and RGO on a quartz surface through the layer-by-layer assembly technique. It was observed that >90% airborne bacteria were killed by the developed surface on exposure to light. Figure 12 shows the light-induced antibacterial activity of a PEI-rGO thin film synthesized by the layer-by-layer technique [125]. A similar study was carried out by Xie and coworkers in the presence of GO/Ag nanoparticles wrapped with a thin layer of type I collagen under 660 nm visible light irradiation. Approximately 96.3% and 99.4% of *E. coli* and *S. aureus* bacteria, respectively, were killed by the developed hybrids under irradiation of 660 nm light due to the formation of radical oxygen species; this indicated the strong photocatalytic activity of the hybrid toward microorganisms [126]. Konwar et al. fabricated graphene- (GIO-) based hydrogels using chitosan as a polymer matrix via a gel-casting technique and evaluated its antimicrobial activity against *S. aureus*, *E. coli*, and *C. albicans.* A significant improvement in antimicrobial activity was observed for the GIO-based hydrogel film compared to chitosan-GO and chitosan-iron oxide films [127]. Antibacterial and photocatalytic activities were also observed for a

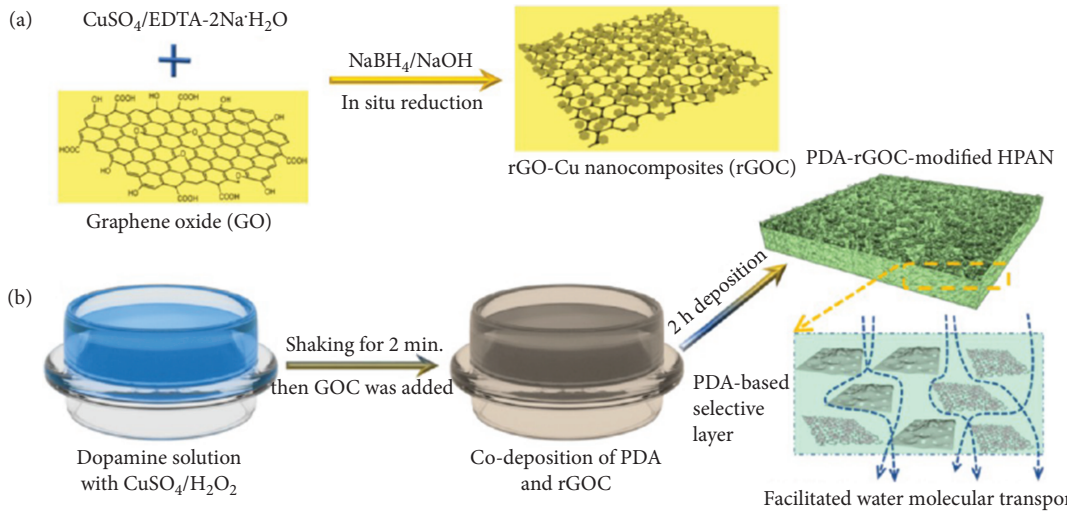

Figure 10: Schematic routes of (a) in situ growth of Cu NPs onto the surface of rGO nanosheets to make rGOC nanocomposites and (b) fast codeposition of PDA and rGOC nanocomposites triggered by $CuSO_4$ and H_2O_2 [122].

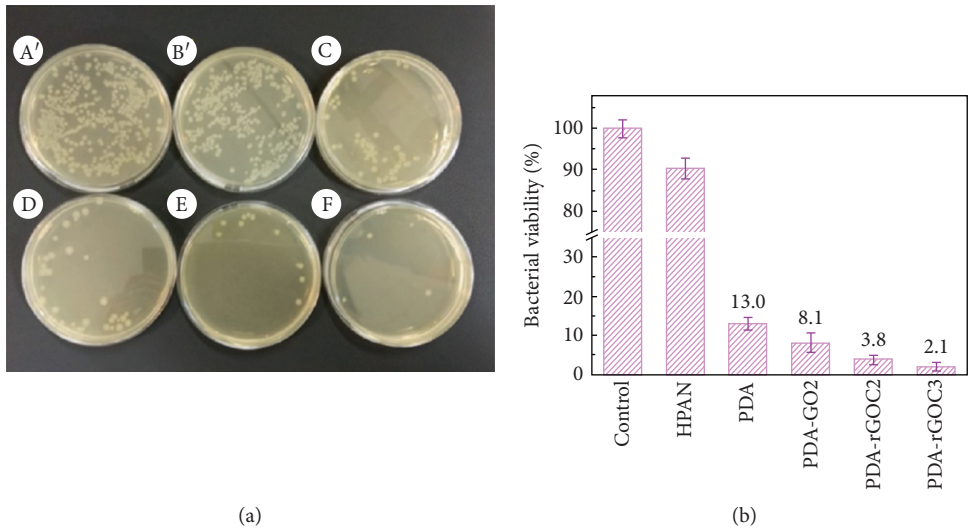

Figure 11: (a) Demonstrated antibacterial properties of the membranes based on the plate counting method: (A′) control without membrane, (B′) HPAN membrane, (C) PDA membrane, (D) PDA-GO2 membrane, (E) PDA-rGOC2 membrane, and (F) PDA-rGOC3 membrane. (b) Quantified antimicrobial ability of the HPAN, PDA-modified, and codeposition-modified membranes [122].

three-phase TiO_2/Ag_3PO_4/graphene composite synthesized by an ion-exchange method and a hydrothermal approach [128]. Materials with antimicrobial activity have drawn wide attention in wound healing applications owing to their ability to kill pathogens at a wound site. Dubey and Gopinath fabricated multicomponent composites based on silver nanoparticles, GO, chitosan, and curcumin. They noted that the fabricated nanofibers have good biocompatibility and better antibacterial activity, which indicated their potential for biomedical applications [129]. Further, a considerable enhancement in antibacterial activity toward *E. coli* and *S. aureus* with negligible cytotoxicity was observed for silver-incorporated ZnO-chemically converted graphene nanocomposites synthesized by a low-temperature technique using zinc acetate dehydrate, silver nitrate, and GO [130].

8. Conclusions

Nanomaterials with unique intrinsic physiochemical and biological properties, which are absent in their macro forms, have drawn significant attention in materials science for various applications. Several nanomaterials such as a graphene, carbon nanotubes, fullerenes, zeolite, and metals in different forms are frequently used to improve the native properties of materials for desired applications. Nowadays, graphene, an allotrope of carbon with excellent thermal, electrical, optical, mechanical, and biological properties and a higher surface area, is intensively used to enhance material properties. Moreover, properties of graphene can be tuned by surface functionalization with various groups. The higher surface area of graphene and the high charge density on the graphene

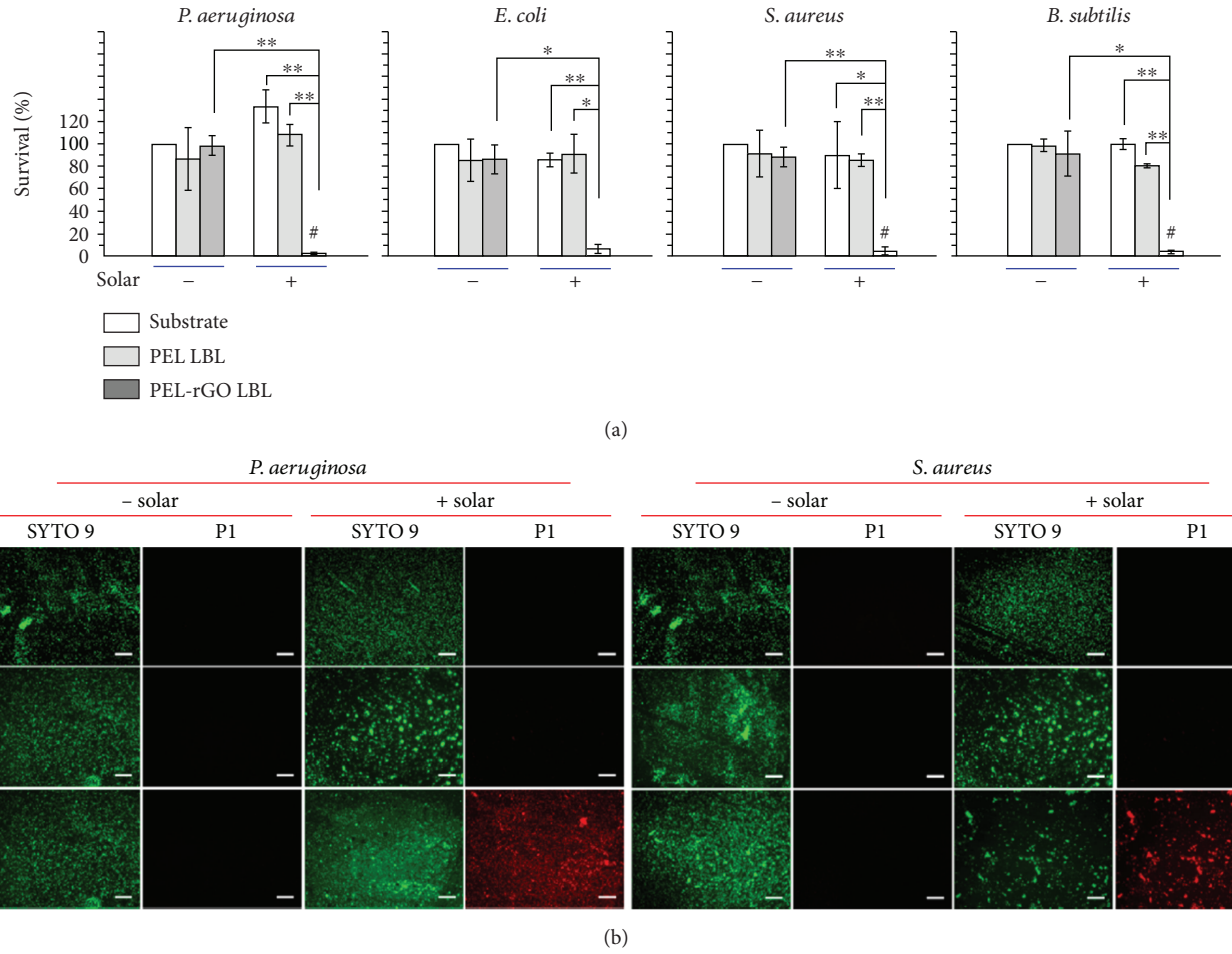

Figure 12: (a) CFU-counting antibacterial assays against four wild-type (wt) bacterial strains consistently reveal that the PEL-rGO LBL thin film, though barely bactericidal when in the dark, killed >90% airborne bacteria on contact within 10 min upon solar irradiation (AM 1.5 G, at one sun). In contrast, the PEL LBL multilayer barely affected bacterial survival no matter whether solar irradiation was applied or not, similar to the behavior of the bare quartz substrate. Data points are reported as mean ± standard deviation. ∗ and ∗∗ indicate $p < 0.05$ and $p < 0.01$, respectively. (b) Bacterial dead/live viability assays under fluorescence microscopy show that *P. aeruginosa* and *S. aureus* cells on a PEL-rGO LBL thin film after 10 min irradiation with a solar simulator (AM 1.5 G) stained intensely red, indicative of dead cells with compromised membranes, whereas those treated similarly but without solar irradiation remained dark in the red channel, indicative of live cells with intact membranes. In striking contrast, cells on a PEL LBL thin film or a quartz substrate remained dark in the red channel in similar assays, no matter whether solar irradiation was applied or not. Scale bar = 100 μm [125].

surface facilitate the loading of several drug molecules, and they consequently act as a nanocarrier with tune rate in the biological medium. In addition, the excellent physical property of the graphene surface facilitates the proliferation and differentiation of cells. Moreover, its light-absorbing behavior plays an essential role in light-triggered drug delivery or cellular response. A significant improvement in antibacterial activity without cytotoxicity was observed for various graphene-based hybrids, suggesting its potential as a biomaterial for various applications. Hence, a discovery of wonder graphene nanomaterial has opened a new area of research to produce lightweight, high-performance hybrid materials for various biomedical applications.

Conflicts of Interest

The authors declare no competing financial interest.

Acknowledgments

This research was supported by the Basic Science Research Program through the National Research Foundation of Korea (NRF) funded by the Ministry of Education (No. 2018R1A6A1A03025582) and the National Research Foundation of Korea (NRF-2016R1D1 A3B03932921).

References

[1] X. Xie, L. Qu, C. Zhou et al., "An asymmetrically surface-modified graphene film electrochemical actuator," *ACS Nano*, vol. 4, no. 10, pp. 6050–6054, 2010.

[2] Y. Osada, H. Okuzaki, and H. Hori, "A polymer gel with electrically driven motility," *Nature*, vol. 355, no. 6357, pp. 242–244, 1992.

[3] Z. He, N. Satarkar, T. Xie, Y. T. Cheng, and J. Z. Hilt, "Remote controlled multishape polymer nanocomposites

with selective radiofrequency actuations," *Advanced Materials*, vol. 23, no. 28, pp. 3192–3196, 2011.

[4] U. N. Kumar, K. Kratz, W. Wagermaier, M. Behl, and A. Lendlein, "Non-contact actuation of triple-shape effect in multiphase polymer network nanocomposites in alternating magnetic field," *Journal of Materials Chemistry*, vol. 20, no. 17, pp. 3404–3415, 2010.

[5] X. Zhang, C. L. Pint, M. H. Lee et al., "Optically and thermally responsive programmable materials based on carbon nanotube hydrogel polymer composites," *Nano Letters*, vol. 11, no. 8, pp. 3239–3244, 2011.

[6] P. Miaudet, A. Derre, M. Maugey et al., "Shape and temperature memory of nanocomposites with broadened glass transition," *Science*, vol. 318, no. 5854, pp. 1294–1296, 2007.

[7] X. Liu, R. Wei, P. T. Hoang, X. Wang, T. Liu, and P. Keller, "Reversible and rapid laser actuation of liquid crystalline elastomer micropillars with inclusion of gold nanoparticles," *Advanced Functional Materials*, vol. 25, no. 20, pp. 3022–3032, 2015.

[8] K. D. Harris, C. W. M. Bastiaansen, J. Lub, and D. J. Broer, "Self-assembled polymer films for controlled agent-driven motion," *Nano Letters*, vol. 5, no. 9, pp. 1857–1860, 2005.

[9] H. Yu and T. Ikeda, "Photocontrollable liquid-crystalline actuators," *Advanced Materials*, vol. 23, no. 19, pp. 2149–2180, 2011.

[10] T. Seki, "Meso- and Microscopic motions in photoresponsive liquid crystalline polymer films," *Macromolecular Rapid Communications*, vol. 35, no. 3, pp. 271–290, 2013.

[11] H. Yu, "Recent advances in photoresponsive liquid-crystalline polymers containing azobenzene chromophores," *Journal of Materials Chemistry C*, vol. 2, no. 17, pp. 3047–3054, 2014.

[12] A. Priimagi, C. J. Barrett, and A. Shishido, "Recent twists in photoactuation and photoalignment control," *Journal of Materials Chemistry C*, vol. 2, no. 35, pp. 7155–7162, 2014.

[13] F. Ilievski, A. D. Mazzeo, R. F. Shepherd, X. Chen, and G. M. Whitesides, "Soft robotics for chemists," *Angewandte Chemie*, vol. 123, no. 8, pp. 1930–1935, 2011.

[14] W.-E. Lee, Y.-J. Jin, L.-S. Park, and G. Kwak, "Fluorescent actuator based on microporous conjugated polymer with intramolecular stack structure," *Advanced Materials*, vol. 24, no. 41, pp. 5604–5609, 2012.

[15] S. Zakharchenko, N. Puretskiy, G. Stoychev, M. Stamm, and L. Ionov, "Temperature controlled encapsulation and release using partially biodegradable thermo-magneto-sensitive self-rolling tubes," *Soft Matter*, vol. 6, no. 12, pp. 2633–2636, 2010.

[16] B. Scrosati, *Applications of Electroactive Polymers*, Chapman & Hall, London, 1993.

[17] T. Xie and X. Xiao, "Self-peeling reversible dry adhesive system," *Chemistry of Materials*, vol. 20, no. 9, pp. 2866–2868, 2008.

[18] Y. Bar-Cohen and Q. Zhang, "Electroactive polymer actuators and sensors," *MRS Bulletin*, vol. 33, no. 3, pp. 173–181, 2008.

[19] J. Hu, H. Meng, G. Li, and S. I. Ibekwe, "A review of stimuli-responsive polymers for smart textile applications," *Smart Materials and Structures*, vol. 21, no. 5, article 053001, 2012.

[20] A. Lendlein and R. Langer, "Biodegradable, elastic shape-memory polymers for potential biomedical applications," *Science*, vol. 296, no. 5573, pp. 1673–1676, 2002.

[21] Y. Zhu, J. Hu, and K. Yeung, "Effect of soft segment crystallization and hard segment physical crosslink on shape memory function in antibacterial segmented polyurethane ionomers," *Acta Biomaterialia*, vol. 5, no. 9, pp. 3346–3357, 2009.

[22] C. de las Heras Alarcon, S. Pennadam, and C. Alexander, "Stimuli responsive polymers for biomedical applications," *Chemical Society Reviews*, vol. 36, no. 26, pp. 276–285, 2005.

[23] E. Oliveira, R. C. Assunção-Silva, O. Ziv-Polat et al., "Influence of different ECM-like hydrogels on neurite outgrowth induced by adipose tissue-derived stem cells," *Stem Cells International*, vol. 2017, Article ID 6319129, 10 pages, 2017.

[24] D. M. Bigg, "Mechanical thermal and electrical properties of metal fiber-filled polymer composites," *Polymer Engineering and Science*, vol. 19, no. 16, pp. 1188–1192, 1979.

[25] H.-T. Lee and L.-H. Lin, "Waterborne polyurethane/clay nanocomposites: novel effects of the clay and its interlayer ions on the morphology and physical and electrical properties," *Macromolecules*, vol. 39, no. 18, pp. 6133–6141, 2006.

[26] Q. Ding, X. Xu, Y. Yue et al., "Nanocellulose mediated electroconductive self-healing hydrogels with high strength, plasticity, viscoelasticity, stretchability, and biocompatibility toward multifunctional applications," *ACS Applied Materials & Interfaces*, vol. 10, no. 33, pp. 27987–28002, 2018.

[27] Q. Wang and D. O'Hare, "Recent advances in the synthesis and application of layered double hydroxide (LDH) nanosheets," *Chemical Reviews*, vol. 112, no. 7, pp. 4124–4155, 2012.

[28] F. Li, L. Qi, J. Yang, M. Xu, X. Luo, and D. Ma, "Polyurethane/conducting carbon black composites: structure, electric conductivity, strain recovery behavior, and their relationships," *Journal of Applied Polymer Science*, vol. 75, no. 1, pp. 68–77, 2000.

[29] X. Wang, Y. Hu, L. Song, H. Yang, W. Xing, and H. Lu, "In situ polymerization of graphene nanosheets and polyurethane with enhanced mechanical and thermal properties," *Journal of Materials Chemistry*, vol. 21, no. 12, pp. 4222–4227, 2011.

[30] A. A. Balandin, S. Ghosh, W. Bao et al., "Superior thermal conductivity of single-layer graphene," *Nano Letters*, vol. 8, no. 3, pp. 902–907, 2008.

[31] S. Latil and L. Henrard, "Charge carriers in few-layer graphene films," *Physical Review Letters*, vol. 97, no. 3, 2006.

[32] R.-M. Amărandi, D. F. Becheru, G. M. Vlăsceanu, M. Ioniță, and J. S. Burns, "Advantages of graphene biosensors for human stem cell therapy potency assays," *BioMed Research International*, vol. 2018, Article ID 1676851, 12 pages, 2018.

[33] A. Bianco, K. Kostarelos, and M. Prato, "Applications of carbon nanotubes in drug delivery," *Current Opinion in Chemical Biology*, vol. 9, no. 6, pp. 674–679, 2005.

[34] K. Yang, L. Feng, X. Shi, and Z. Liu, "Nano-graphene in biomedicine: theranostic applications," *Chemical Society Reviews*, vol. 42, no. 2, pp. 530–547, 2013.

[35] S. Park and R. S. Ruoff, "Erratum: chemical methods for the production of graphenes," *Nature Nanotechnology*, vol. 5, no. 4, pp. 309–309, 2010.

[36] D. He, Z. Kou, Y. Xiong et al., "Simultaneous sulfonation and reduction of graphene oxide as highly efficient supports for metal nanocatalysts," *Carbon*, vol. 66, pp. 312–319, 2014.

[37] T. Kuilla, S. Bhadra, D. Yao, N. H. Kim, S. Bose, and J. H. Lee, "Recent advances in graphene based polymer

composites," *Progress in Polymer Science*, vol. 35, no. 11, pp. 1350–1375, 2010.

[38] D. K. Patel, R. K. Singh, S. K. Singh et al., "Graphene as a chain extender of polyurethanes for biomedical applications," *RSC Advances*, vol. 6, no. 63, pp. 58628–58640, 2016.

[39] H. Kim, Y. Miura, and C. W. Macosko, "Graphene/polyurethane nanocomposites for improved gas barrier and electrical conductivity," *Chemistry of Materials*, vol. 22, no. 11, pp. 3441–3450, 2010.

[40] D. K. Patel, S. Senapati, P. Mourya et al., "Functionalized graphene tagged polyurethanes for corrosion inhibitor and sustained drug delivery," *ACS Biomaterials Science & Engineering*, vol. 3, no. 12, pp. 3351–3363, 2017.

[41] S. Goenka, V. Sant, and S. Sant, "Graphene-based nanomaterials for drug delivery and tissue engineering," *Journal of Controlled Release*, vol. 173, pp. 75–88, 2014.

[42] H. P. Boehm, R. Setton, and E. Stumpp, "Nomenclature and terminology of graphite intercalation compounds," *Carbon*, vol. 24, no. 2, pp. 241–245, 1986.

[43] K. S. Novoselov, A. K. Geim, S. V. Morozov et al., "Electric field effect in atomically thin carbon films," *Science*, vol. 306, no. 5696, pp. 666–669, 2004.

[44] K. P. Loh, Q. Bao, P. K. Ang, and J. Yang, "The chemistry of graphene," *Journal of Materials Chemistry*, vol. 20, no. 12, pp. 2277–2289, 2010.

[45] F. Taherian, V. Marcon, N. F. A. van der Vegt, and F. Leroy, "What is the contact angle of water on graphene?," *Langmuir*, vol. 29, no. 5, pp. 1457–1465, 2013.

[46] I. W. Frank, D. M. Tanenbaum, A. M. van der Zande, and P. L. McEuen, "Mechanical properties of suspended graphene sheets," *Journal of Vacuum Science & Technology B: Microelectronics and Nanometer Structures*, vol. 25, no. 6, p. 2558, 2007.

[47] M. Poot and H. S. J. van der Zant, "Nanomechanical properties of few-layer graphene membranes," *Applied Physics Letters*, vol. 92, no. 6, pp. 63111–63113, 2008.

[48] C. Lee, X. Wei, J. W. Kysar, and J. Hone, "Measurement of the elastic properties and intrinsic strength of monolayer graphene," *Science*, vol. 321, no. 5887, pp. 385–388, 2008.

[49] G. van Lier, C. van Alsenoy, V. van Doren, and P. Geerlings, "Ab initio study of the elastic properties of single-walled carbon nanotubes and graphene," *Chemical Physics Letters*, vol. 326, no. 1-2, pp. 181–185, 2000.

[50] C. D. Reddy, S. Rajendran, and K. M. Liew, "Equilibrium configuration and continuum elastic properties of finite sized graphene," *Nanotechnology*, vol. 17, no. 3, pp. 864–870, 2006.

[51] K. N. Kudin, G. E. Scuseria, and B. I. Yakobson, "C2F,BN, and C nano shell elasticity from *ab initio* computations," *Physical Review B*, vol. 64, no. 23, pp. 235406–235415, 2001.

[52] T. Kuila, S. Bose, A. K. Mishra, P. Khanra, N. H. Kim, and J. H. Lee, "Chemical functionalization of graphene and its applications," *Progress in Materials Science*, vol. 57, no. 7, pp. 1061–1105, 2012.

[53] J. W. Suk, R. D. Piner, J. An, and R. S. Ruoff, "Mechanical properties of monolayer graphene oxide," *ACS Nano*, vol. 4, no. 11, pp. 6557–6564, 2010.

[54] C. Gómez-Navarro, M. Burghard, and K. Kern, "Elastic properties of chemically derived single graphene sheets," *Nano Letters*, vol. 8, no. 7, pp. 2045–2049, 2008.

[55] S. Park, K. S. Lee, G. Bozoklu, W. Cai, S. B. T. Nguyen, and R. S. Ruoff, "Graphene oxide papers modified by divalent ions-enhancing mechanical properties via chemical cross-linking," *ACS Nano*, vol. 2, no. 3, pp. 572–578, 2008.

[56] K. E. Prasad, B. Das, U. Maitra, U. Ramamurty, and C. N. R. Rao, "Extraordinary synergy in the mechanical properties of polymer matrix composites reinforced with 2 nanocarbons," *Proceedings of the National Academy of Sciences*, vol. 106, no. 32, pp. 13186–13189, 2009.

[57] N. Mahanta and A. Abramson, "Thermal conductivity of graphene and graphene oxide nanoplatelets," in *13th InterSociety Conference on Thermal and Thermomechanical Phenomena in Electronic Systems*, pp. 1–6, San Diego, CA, USA, May 2012.

[58] I. M. Afanasov, V. A. Morozov, A. V. Kepman et al., "Preparation, electrical and thermal properties of new exfoliated graphite-based composites," *Carbon*, vol. 47, no. 1, pp. 263–270, 2009.

[59] J.-W. Jiang, J. Lan, J.-S. Wang, and B. Li, "Isotopic effects on the thermal conductivity of graphene nanoribbons: Localization mechanism," *Journal of Applied Physics*, vol. 107, no. 5, article 054314, 2010.

[60] D. L. Nika, E. P. Pokatilov, A. S. Askerov, and A. A. Balandin, "Phonon thermal conduction in graphene: role of Umklapp and edge roughness scattering," *Physical Review B*, vol. 79, no. 15, 2009.

[61] K. I. Bolotin, K. J. Sikes, Z. Jiang et al., "Ultrahigh electron mobility in suspended graphene," *Solid State Communications*, vol. 146, no. 9-10, pp. 351–355, 2008.

[62] W. Gao, L. B. Alemany, L. Ci, and P. M. Ajayan, "New insights into the structure and reduction of graphite oxide," *Nature Chemistry*, vol. 1, no. 5, pp. 403–408, 2009.

[63] T. Cohen-Karni, Q. Qing, Q. Li, Y. Fang, and C. M. Lieber, "Graphene and nanowire transistors for cellular interfaces and electrical recording," *Nano Letters*, vol. 10, no. 3, pp. 1098–1102, 2010.

[64] M. S. Artiles, C. S. Rout, and T. S. Fisher, "Graphene-based hybrid materials and devices for bio-sensing," *Advanced Drug Delivery Reviews*, vol. 63, no. 14-15, pp. 1352–1360, 2011.

[65] R. R. Nair, P. Blake, A. N. Grigorenko et al., "Fine structure constant defines visual transparency of graphene," *Science*, vol. 320, no. 5881, pp. 1308–1308, 2008.

[66] C. Soldano, A. Mahmood, and E. Dujardin, "Production, properties and potential of graphene," *Carbon*, vol. 48, no. 8, pp. 2127–2150, 2010.

[67] P. Blake, P. D. Brimicombe, R. R. Nair et al., "Graphene-based liquid crystal device," *Nano Letters*, vol. 8, no. 6, pp. 1704–1708, 2008.

[68] X. Wang, L. Zhi, and K. Müllen, "Transparent, conductive graphene electrodes for dye-sensitized solar cells," *Nano Letters*, vol. 8, no. 1, pp. 323–327, 2008.

[69] J.-H. Chen, M. Ishigami, C. Jang, D. . R. Hines, M. . S. Fuhrer, and E. . D. Williams, "Printed graphene circuits," *Advanced Materials*, vol. 19, no. 21, pp. 3623–3627, 2007.

[70] D. A. LaVan, T. McGuire, and R. Langer, "Small-scale systems for in vivo drug delivery," *Nature Biotechnology*, vol. 21, no. 10, pp. 1184–1191, 2003.

[71] S. Mura, J. Nicolas, and P. Couvreur, "Stimuli-responsive nanocarriers for drug delivery," *Nature Materials*, vol. 12, no. 11, pp. 991–1003, 2013.

[72] B. P. Timko, T. Dvir, and D. S. Kohane, "Remotely triggerable drug delivery systems," *Advanced Materials*, vol. 22, no. 44, pp. 4925–4943, 2010.

[73] C. L. Weaver, J. M. LaRosa, X. Luo, and X. T. Cui, "Electrically controlled drug delivery from graphene oxide nanocomposite films," *ACS Nano*, vol. 8, no. 2, pp. 1834–1843, 2014.

[74] Y. Wang, K. Wang, J. Zhao et al., "Multifunctional mesoporous silica-coated graphene nanosheet used for chemophotothermal synergistic targeted therapy of glioma," *Journal of the American Chemical Society*, vol. 135, no. 12, pp. 4799–4804, 2013.

[75] Z. Zhang, J. Wang, and C. Chen, "Near-infrared light-mediated nanoplatforms for cancer thermo-chemotherapy and optical imaging," *Advanced Materials*, vol. 25, no. 28, pp. 3869–3880, 2013.

[76] C. Xu, D. Yang, L. Mei, Q. Li, H. Zhu, and T. Wang, "Targeting chemophotothermal therapy of hepatoma by gold nanorods/graphene oxide core/shell nanocomposites," *ACS Applied Materials & Interfaces*, vol. 5, no. 24, pp. 12911–12920, 2013.

[77] E. Song, W. Han, C. Li et al., "Hyaluronic acid-decorated graphene oxide nanohybrids as nanocarriers for targeted and pH-responsive anticancer drug delivery," *ACS Applied Materials & Interfaces*, vol. 6, no. 15, pp. 11882–11890, 2014.

[78] R. Kurapati and A. M. Raichur, "Near-infrared light-responsive graphene oxide composite multilayer capsules: a novel route for remote controlled drug delivery," *Chemical Communications*, vol. 49, no. 7, pp. 734–736, 2013.

[79] T. Kavitha, S. I. Haider Abdi, and S.-Y. Park, "pH-Sensitive nanocargo based on smart polymer functionalized graphene oxide for site-specific drug delivery," *Physical Chemistry Chemical Physics*, vol. 15, no. 14, pp. 5176–5185, 2013.

[80] W. Li, J. Wang, J. Ren, and X. Qu, "3D graphene oxide-polymer hydrogel: near-infrared light-triggered active scaffold for reversible cell capture and on-demand release," *Advanced Materials*, vol. 25, no. 46, pp. 6737–6743, 2013.

[81] Y. Chen, W. Cheng, L. Teng et al., "Graphene oxide hybrid supramolecular hydrogels with self-healable, bioadhesive and stimuli-responsive properties and drug delivery application," *Macromolecular Materials and Engineering*, vol. 303, no. 8, 2018.

[82] S. Ebrahimi-Barough, A. Norouzi Javidan, H. Saberi et al., "Evaluation of motor neuron-like cell differentiation of hEnSCs on biodegradable PLGA nanofiber scaffolds," *Molecular Neurobiology*, vol. 52, no. 3, pp. 1704–1713, 2015.

[83] J. Wang, X. Cui, Y. Zhou, and Q. Xiang, "Core-shell PLGA/collagen nanofibers loaded with recombinant FN/CDHs as bone tissue engineering scaffolds," *Connective Tissue Research*, vol. 55, no. 4, pp. 292–298, 2014.

[84] Z. X. Meng, H. F. Li, Z. Z. Sun, W. Zheng, and Y. F. Zheng, "Fabrication of mineralized electrospun PLGA and PLGA/gelatin nanofibers and their potential in bone tissue engineering," *Materials Science and Engineering: C*, vol. 33, no. 2, pp. 699–706, 2013.

[85] P. Bianco and P. G. Robey, "Stem cells in tissue engineering," *Nature*, vol. 414, no. 6859, pp. 118–121, 2001.

[86] C. Toma, M. F. Pittenger, K. S. Cahill, B. J. Byrne, and P. D. Kessler, "Human mesenchymal stem cells differentiate to a cardiomyocyte phenotype in the adult murine heart," *Circulation*, vol. 105, no. 1, pp. 93–98, 2002.

[87] I. Aurich, L. P. Mueller, H. Aurich et al., "Functional integration of hepatocytes derived from human mesenchymal stem cells into mouse livers," *Gut*, vol. 56, no. 3, pp. 405–415, 2007.

[88] Y. Takashima, T. Era, K. Nakao et al., "Neuroepithelial cells supply an initial transient wave of MSC differentiation," *Cell*, vol. 129, no. 7, pp. 1377–1388, 2007.

[89] W. Guo, X. Zhang, X. Yu et al., "Self-powered electrical stimulation for enhancing neural differentiation of mesenchymal stem cells on graphene–poly(3,4-ethylenedioxythiophene) hybrid microfibers," *ACS Nano*, vol. 10, no. 5, pp. 5086–5095, 2016.

[90] C. L. Weaver and X. T. Cui, "Directed neural stem cell differentiation with a functionalized graphene oxide nanocomposite," *Advanced Healthcare Materials*, vol. 4, no. 9, pp. 1408–1416, 2015.

[91] Y. Luo, H. Shen, Y. Fang et al., "Enhanced proliferation and osteogenic differentiation of mesenchymal stem cells on graphene oxide-incorporated electrospun poly(lactic-co-glycolic acid) nanofibrous mats," *ACS Applied Materials & Interfaces*, vol. 7, no. 11, pp. 6331–6339, 2015.

[92] S. Kumar, S. Raj, E. Kolanthai, A. K. Sood, S. Sampath, and K. Chatterjee, "Chemical functionalization of graphene to augment stem cell osteogenesis and inhibit biofilm formation on polymer composites for orthopedic applications," *ACS Applied Materials & Interfaces*, vol. 7, no. 5, pp. 3237–3252, 2015.

[93] Y. Zhang, H. Zhang, Z. Wang, and Y. Jin, "pH-sensitive graphene oxide conjugate purpurin-18 methyl ester photosensitizer nanocomplex in photodynamic therapy," *New Journal of Chemistry*, vol. 42, no. 16, pp. 13272–13284, 2018.

[94] B. Chaudhuri, D. Bhadra, L. Moroni, and K. Pramanik, "Myoblast differentiation of human mesenchymal stem cells on graphene oxide and electrospun graphene oxide–polymer composite fibrous meshes: importance of graphene oxide conductivity and dielectric constant on their biocompatibility," *Biofabrication*, vol. 7, no. 1, pp. 15009–15021, 2015.

[95] S. Kumar, S. Raj, K. Sarkar, and K. Chatterjee, "Engineering a multi-biofunctional composite using poly(ethylenimine) decorated graphene oxide for bone tissue regeneration," *Nanoscale*, vol. 8, no. 12, pp. 6820–6836, 2016.

[96] S. Sayyar, E. Murray, B. C. Thompson et al., "Processable conducting graphene/chitosan hydrogels for tissue engineering," *Journal of Materials Chemistry B*, vol. 3, no. 3, pp. 481–490, 2015.

[97] L.-G. Yu, K. A. Khor, H. Li, and P. Cheang, "Effect of spark plasma sintering on the microstructure and in vitro behavior of plasma sprayed HA coatings," *Biomaterials*, vol. 24, no. 16, pp. 2695–2705, 2003.

[98] A. A. White, S. M. Best, and I. A. Kinloch, "Hydroxyapatite carbon nanotube composites for biomedical applications: a review," *International Journal of Applied Ceramic Technology*, vol. 4, no. 1, pp. 1–13, 2007.

[99] Y. Liu, J. Huang, and H. Li, "Synthesis of hydroxyapatite–reduced graphite oxide nanocomposites for biomedical applications: oriented nucleation and epitaxial growth of hydroxyapatite," *Journal of Materials Chemistry B*, vol. 1, no. 13, p. 1826, 2013.

[100] M. Li, Y. Wang, Q. Liu et al., "In situ synthesis and biocompatibility of nano hydroxyapatite on pristine and chitosan functionalized graphene oxide," *Journal of Materials Chemistry B*, vol. 1, no. 4, pp. 475–484, 2013.

[101] J. Kim, Y.-R. Kim, Y. Kim et al., "Graphene-incorporated chitosan substrata for adhesion and differentiation of human mesenchymal stem cells," *Journal of Materials Chemistry B*, vol. 1, no. 7, pp. 933–938, 2013.

[102] J. Natarajan, G. Madras, and K. Chatterjee, "Development of graphene oxide-/galactitol polyester-based biodegradable composites for biomedical applications," *ACS Omega*, vol. 2, no. 9, pp. 5545–5556, 2017.

[103] H. Ji, H. Sun, and X. Qu, "Antibacterial applications of graphene-based nanomaterials: recent achievements and challenges," *Advanced Drug Delivery Reviews*, vol. 105, Part B, pp. 176–189, 2016.

[104] M. Yu, Z. Wang, M. Lv et al., "Antisuperbug cotton fabric with excellent laundering durability," *ACS Applied Materials & Interfaces*, vol. 8, no. 31, pp. 19866–19871, 2016.

[105] S. Liu, T. H. Zeng, M. Hofmann et al., "Antibacterial activity of graphite, graphite oxide, graphene oxide, and reduced graphene oxide: membrane and oxidative stress," *ACS Nano*, vol. 5, no. 9, pp. 6971–6980, 2011.

[106] W. Hu, C. Peng, W. Luo et al., "Graphene-based antibacterial paper," *ACS Nano*, vol. 4, no. 7, pp. 4317–4323, 2010.

[107] W.-R. Li, X.-B. Xie, Q.-S. Shi, H.-Y. Zeng, Y.-S. OU-Yang, and Y.-B. Chen, "Antibacterial activity and mechanism of silver nanoparticles on *Escherichia coli*," *Applied Microbiology and Biotechnology*, vol. 85, no. 4, pp. 1115–1122, 2010.

[108] S. L. Smitha and K. G. Gopchandran, "Surface enhanced Raman scattering, antibacterial and antifungal active triangular gold nanoparticles," *Spectrochimica Acta Part A: Molecular and Biomolecular Spectroscopy*, vol. 102, pp. 114–119, 2013.

[109] L. Esteban-Tejeda, F. Malpartida, A. Esteban-Cubillo, C. Pecharromán, and J. S. Moya, "Antibacterial and antifungal activity of a soda-lime glass containing copper nanoparticles," *Nanotechnology*, vol. 20, no. 50, pp. 505701–505707, 2009.

[110] F. Cheng, J. W. Betts, S. M. Kelly et al., "Whiter, brighter, and more stable cellulose paper coated with antibacterial carboxymethyl starch stabilized ZnO nanoparticles," *Journal of Material Chemistry B*, vol. 2, no. 20, pp. 3057–3064, 2014.

[111] O. N. Ruiz, K. A. S. Fernando, B. Wang et al., "Graphene oxide: a nonspecific enhancer of cellular growth," *ACS Nano*, vol. 5, no. 10, pp. 8100–8107, 2011.

[112] R. Zhao, M. Lv, Y. Li et al., "Stable nanocomposite based on PEGylated and silver nanoparticles loaded graphene oxide for long-term antibacterial activity," *ACS Applied Materials & Interfaces*, vol. 9, no. 18, pp. 15328–15341, 2017.

[113] S. Some, S.-M. Ho, P. Dua et al., "Dual functions of highly potent graphene derivative–poly-l-lysine composites to inhibit bacteria and support human cells," *ACS Nano*, vol. 6, no. 8, pp. 7151–7161, 2012.

[114] W. Shao, X. Liu, H. Min, G. Dong, Q. Feng, and S. Zuo, "Preparation, characterization, and antibacterial activity of silver nanoparticle-decorated graphene oxide nanocomposite," *ACS Applied Materials & Interfaces*, vol. 7, no. 12, pp. 6966–6973, 2015.

[115] Y. I. Seo, K. H. Hong, S. H. Kim, D. Chang, K. Hwan Lee, and Y. Do Kim, "Removal of bacterial pathogen from wastewater using Al filter with Ag-containing nanocomposite film by in situ dispersion involving polyol process," *Journal of Hazardous Materials*, vol. 227-228, pp. 469–473, 2012.

[116] C. N. Haas and N. J. Hutzler, "Wastewater disinfection and infectious disease risks," *Critical Reviews in Environmental Control*, vol. 17, no. 1, pp. 1–20, 1986.

[117] X.-H. Ma, Z. Yang, Z.-K. Yao, Z.-L. Xu, and C. Y. Tang, "A facile preparation of novel positively charged MOF/chitosan nanofiltration membranes," *Journal of Membrane Science*, vol. 525, pp. 269–276, 2017.

[118] J. Gao, S.-P. Sun, W.-P. Zhu, and T.-S. Chung, "Chelating polymer modified P84 nanofiltration (NF) hollow fiber membranes for high efficient heavy metal removal," *Water Research*, vol. 63, pp. 252–261, 2014.

[119] L. Shen, C. Cheng, X. Yu et al., "Low pressure UV-cured CS–PEO–PTEGDMA/PAN thin film nanofibrous composite nanofiltration membranes for anionic dye separation," *Journal of Materials Chemistry A*, vol. 4, no. 40, pp. 15575–15588, 2016.

[120] S. Xia, L. Yao, Y. Zhao, N. Li, and Y. Zheng, "Preparation of graphene oxide modified polyamide thin film composite membranes with improved hydrophilicity for natural organic matter removal," *Chemical Engineering Journal*, vol. 280, pp. 720–727, 2015.

[121] X. Zhu, A. Dudchenko, X. Gu, and D. Jassby, "Surfactant-stabilized oil separation from water using ultrafiltration and nanofiltration," *Journal of Membrane Science*, vol. 529, pp. 159–169, 2017.

[122] J. Zhu, J. Wang, A. A. Uliana et al., "Mussel-inspired architecture of high-flux loose nanofiltration membrane functionalized with antibacterial reduced graphene oxide–copper nanocomposites," *ACS Applied Materials & Interfaces*, vol. 9, no. 34, pp. 28990–29001, 2017.

[123] Y. L. F. Musico, C. M. Santos, M. L. P. Dalida, and D. F. Rodrigues, "Surface modification of membrane filters using graphene and graphene oxide-based nanomaterials for bacterial inactivation and removal," *ACS Sustainable Chemistry & Engineering*, vol. 2, no. 7, pp. 1559–1565, 2014.

[124] C. Liu, J. Shen, K. W. K. Yeung, and S. C. Tjong, "Development and antibacterial performance of novel polylactic acid-graphene oxide-silver nanoparticle hybrid nanocomposite mats prepared by electrospinning," *ACS Biomaterials Science & Engineering*, vol. 3, no. 3, pp. 471–486, 2017.

[125] L. Hui, J. T. Auletta, Z. Huang et al., "Surface disinfection enabled by a layer-by-layer thin film of polyelectrolyte-stabilized reduced graphene oxide upon solar near-infrared irradiation," *ACS Applied Materials & Interfaces*, vol. 7, no. 19, pp. 10511–10517, 2015.

[126] X. Xie, C. Mao, X. Liu et al., "Synergistic bacteria killing through photodynamic and physical actions of graphene oxide/Ag/collagen coating," *ACS Applied Materials & Interfaces*, vol. 9, no. 31, pp. 26417–26428, 2017.

[127] A. Konwar, S. Kalita, J. Kotoky, and D. Chowdhury, "Chitosan–iron oxide coated graphene oxide nanocomposite hydrogel: a robust and soft antimicrobial biofilm," *ACS Applied Materials & Interfaces*, vol. 8, no. 32, pp. 20625–20634, 2016.

[128] X. Yang, J. Qin, Y. Jiang, R. Li, Y. Li, and H. Tang, "Bifunctional TiO_2/Ag_3PO_4/graphene composites with superior visible light photocatalytic performance and synergistic inactivation of bacteria," *RSC Advances*, vol. 4, no. 36, pp. 18627–18636, 2014.

[129] P. Dubey and P. Gopinath, "PEGylated graphene oxide-based nanocomposite-grafted chitosan/polyvinyl alcohol nanofiber as an advanced antibacterial wound dressing," *RSC Advances*, vol. 6, no. 73, pp. 69103–69116, 2016.

[130] A. Naskar, S. Bera, R. Bhattacharya et al., "Synthesis, characterization and antibacterial activity of Ag incorporated ZnO–graphene nanocomposites," *RSC Advances*, vol. 6, no. 91, pp. 88751–88761, 2016.

[131] B. V. Chikkaveeraiah, A. Soldà, D. Choudhary, F. Maran, and J. F. Rusling, "Ultrasensitive nanostructured immunosensor for stem and carcinoma cell pluripotency gatekeeper protein NANOG," *Nanomedicine*, vol. 7, no. 7, pp. 957–965, 2012.

[132] Y. Shuai, C. Mao, and M. Yang, "Protein nanofibril assemblies templated by graphene oxide nanosheets accelerate early cell adhesion and induce osteogenic differentiation of human mesenchymal stem cells," *ACS Applied Materials & Interfaces*, vol. 10, no. 38, pp. 31988–31997, 2018.

[133] T. R. Nayak, H. Andersen, V. S. Makam et al., "Graphene for controlled and accelerated osteogenic differentiation of human mesenchymal stem cells," *ACS Nano*, vol. 5, no. 6, pp. 4670–4678, 2011.

[134] W. C. Lee, C. H. Y. X. Lim, H. Shi et al., "Origin of enhanced stem cell growth and differentiation on graphene and graphene oxide," *ACS Nano*, vol. 5, no. 9, pp. 7334–7341, 2011.

[135] M. Kalbacova, A. Broz, J. Kong, and M. Kalbac, "Graphene substrates promote adherence of human osteoblasts and mesenchymal stromal cells," *Carbon*, vol. 48, no. 15, pp. 4323–4329, 2010.

[136] G.-Y. Chen, D. W.-P. Pang, S.-M. Hwang, H.-Y. Tuan, and Y.-C. Hu, "A graphene-based platform for induced pluripotent stem cells culture and differentiation," *Biomaterials*, vol. 33, no. 2, pp. 418–427, 2012.

[137] J. Kim, K. S. Choi, Y. Kim et al., "Bioactive effects of graphene oxide cell culture substratum on structure and function of human adipose-derived stem cells," *Journal of Biomedical Materials Research Part A*, vol. 101, no. 12, pp. 3520–3530, 2013.

[138] S. W. Crowder, D. Prasai, R. Rath et al., "Three-dimensional graphene foams promote osteogenic differentiation of human mesenchymal stem cells," *Nanoscale*, vol. 5, no. 10, pp. 4171–4176, 2013.

[139] Q. Ma, L. Yang, Z. Jiang et al., "Three-dimensional stiff graphene scaffold on neural stem cells behavior," *ACS Applied Materials & Interfaces*, vol. 8, no. 50, pp. 34227–34233, 2016.

[140] N. Li, Q. Zhang, S. Gao et al., "Three-dimensional graphene foam as a biocompatible and conductive scaffold for neural stem cells," *Scientific Reports*, vol. 3, no. 1, 2013.

[141] H. Amani, E. Mostafavi, H. Arzaghi et al., "Three-dimensional graphene foams: synthesis, properties, biocompatibility, biodegradability, and applications in tissue engineering," *ACS Biomaterials Science & Engineering*, vol. 5, no. 1, pp. 193–214, 2018.

[142] N. Tasnim, V. Thakur, M. Chattopadhyay, and B. Joddar, "The efficacy of graphene foams for culturing mesenchymal stem cells and their differentiation into dopaminergic neurons," *Stem Cells International*, vol. 2018, Article ID 3410168, 12 pages, 2018.

[143] E. Y. T. Chen, Y.-C. Wang, A. Mintz et al., "Activated charcoal composite biomaterial promotes human embryonic stem cell differentiation toward neuronal lineage," *Journal of Biomedical Materials Research Part A*, vol. 100A, no. 8, pp. 2006–2017, 2012.

[144] Y. Wang, W. C. Lee, K. K. Manga et al., "Tissue engineering: fluorinated graphene for promoting neuro-induction of stem cells," *Advanced Materials*, vol. 24, no. 31, pp. 4284–4284, 2012.

Hindawi
Stem Cells International
Volume 2019, Article ID 7867613, 17 pages
https://doi.org/10.1155/2019/7867613

Research Article

In Vitro Cultivation of Limbal Epithelial Stem Cells on Surface-Modified Crosslinked Collagen Scaffolds

Michel Haagdorens,[1,2] **Vytautas Cėpla**,[3,4] **Eline Melsbach**,[2,5] **Laura Koivusalo**,[6] **Heli Skottman**,[6] **May Griffith**,[7] **Ramūnas Valiokas**,[3,4] **Nadia Zakaria**,[1,2,5] **Isabel Pintelon**,[8] **and Marie-José Tassignon**[1,2]

[1]*Faculty of Medicine and Health Sciences, Department of Ophthalmology, Visual Optics and Visual Rehabilitation, University of Antwerp, Campus Drie Eiken, T building, T4-Ophthalmology, Universiteitsplein 1, 2610 Antwerp, Belgium*
[2]*Department of Ophthalmology, Antwerp University Hospital, Wilrijkstraat 10, 2650 Antwerp, Belgium*
[3]*Department of Nanoengineering, Center for Physical Sciences and Technology, Savanorių 231, 02300 Vilnius, Lithuania*
[4]*Ferentis UAB, Savanorių 235, 02300 Vilnius, Lithuania*
[5]*Center for Cell Therapy and Regenerative Medicine, Antwerp University Hospital, CCRG-Oogheelkunde, Wilrijkstraat 10, 2650 Edegem, Belgium*
[6]*Faculty of Medicine and Health Technology, Tampere University, Arvo Ylpön katu 34, 33014, Finland*
[7]*Maisonneuve-Rosemont Hospital Research Centre and Department of Ophthalmology, University of Montreal, Montreal, QC, Canada H1T 4B3*
[8]*Laboratory of Cell Biology and Histology, Antwerp University, Campus Drie Eiken, T building, T1-Veterinary Sciences, Universiteitsplein 1, 2610 Antwerp, Belgium*

Correspondence should be addressed to Michel Haagdorens; michelhaagdorens@gmail.com

Received 8 October 2018; Accepted 31 December 2018; Published 1 April 2019

Guest Editor: Howard Kim

Purpose. To investigate the efficacy of recombinant human collagen type I (RHC I) and collagen-like peptide (CLP) hydrogels as alternative carrier substrates for the cultivation of limbal epithelial stem cells (LESC) under xeno-free culture conditions. *Methods*. Human LESC were cultivated on seven different collagen-derived hydrogels: (1) unmodified RHC I, (2) fibronectin-patterned RHC I, (3) carbodiimide-crosslinked CLP (CLP-12 EDC), (4) DMTMM-(4-(4,6-dimethoxy-1,3,5-triazin-2-yl)-4-methyl-morpholinium-) crosslinked CLP (CLP-12), (5) fibronectin-patterned CLP-12, (6) "3D limbal niche-mimicking" CLP-12, and (7) DMTMM-crosslinked CLP made from higher CLP concentration solution. Cell proliferation, cell morphology, and expression of LESC markers were analyzed. All data were compared to cultures on human amniotic membrane (HAM). *Results*. Human LESC were successfully cultivated on six out of seven hydrogel formulations, with primary cell cultures on CLP-12 EDC being deemed unsuccessful since the area of outgrowth did not meet quality standards (i.e., inconsistence in outgrowth and confluence) after 14 days of culture. Upon confluence, primary LESC showed high expression of the stem cell marker ΔNp63, proliferation marker cytokeratin (KRT) 14, adhesion markers integrin-β4 and E-cadherin, and LESC-specific extracellular matrix proteins laminin-α1, and collagen type IV. Cells showed low expression of differentiation markers KRT3 and desmoglein 3 (DSG3). Significantly higher gene expression of KRT3 was observed for cells cultured on CLP hydrogels compared to RHC I and HAM. Surface patterning of hydrogels influenced the pattern of proliferation but had no significant effect on the phenotype or genotype of cultures. Overall, the performance of RHC I and DMTMM-crosslinked CLP hydrogels was equivalent to that of HAM. *Conclusion*. RHC I and DMTMM-crosslinked CLP hydrogels, irrespective of surface modification, support successful cultivation of primary human LESC using a xeno-free cultivation protocol. The regenerated epithelium maintained similar characteristics to HAM-based cultures.

1. Introduction

Located at the corneoscleral limbus, limbal epithelial stem cells (LESC) play a pivotal role in rejuvenating the corneal epithelium and keeping the cornea healthy, transparent, and avascular [1, 2]. Damage to the LESC or their stem cell niche may lead to limbal stem cell deficiency (LSCD). This condition is characterized by conjunctivalization and cicatrization of the cornea and may result in reduced vision, pain, and photophobia [3]. Historically, surgical treatment of patients suffering from LSCD includes conjunctival limbal grafting or keratolimbal allografting.

Since its introduction in 1997 [4], cultivated limbal epithelial transplantation (CLET) has shown to be an effective therapy for LSCD, with clinical trials reporting an average success rate of 70% [5]. In CLET, a small limbal biopsy is cultivated ex vivo on a stem cell carrier, after which cultured cells are grafted into the patient's diseased eye. The stem cell carrier most frequently used in these trials is the human amniotic membrane (HAM). Harvested by caesarian section, HAM has been used for many years in ocular surgery [6, 7]. It has the advantage of having anti-inflammatory, antimicrobial, and antiangiogenic properties [7, 8]. However, being a biological membrane, procurement of HAM requires costly donor screening for potential infectious pathogens [9]. In addition, standardization of HAM procedures is difficult due to inter- and intradonor variabilities in membrane thickness, mechanical properties, optical characteristics, and growth factor release [10–13]. Furthermore, *in vitro* processing remains labor intensive, costly, and challenging [9]. These limitations hamper the application of HAM in ocular tissue engineering. Other stem cell carriers such as fibrin and siloxane hydrogel contact lenses have been used in human clinical trials [5]. In 2015, Holoclar® (Chiesi, Italy), a technique in which limbal cells are expanded on fibrin scaffolds, was conditionally approved for release in Europe as the first commercially available stem cell therapy for LSCD. Nevertheless, use of this medicinal product is restricted to autologous stem cell transplantation in unilateral cases after chemical or thermal burn. Furthermore, fibrin hydrogels require the application of xenogenic culture protocols that involve murine 3T3 feeder layers, which brings into question safety of the end-product. Therefore, a safe and standardized therapy that targets all LSCD patients has yet to be developed.

Various biomaterials have been proposed as alternative carriers to the use of HAM and fibrin in corneal tissue engineering [5, 14]. A promising approach is the application of collagen hydrogels, as these are characterized by inherent biocompatibility and cost effectiveness [15, 16]. In 2009, the group of Fagerholm et al. were the first to report the successful implantation of acellular recombinant human collagen type III (RHC III) hydrogels, crosslinked by 1-ethyl-3-(3-dimethyl aminopropyl) carbodiimide/N-hydroxysuccinimide (EDC/NHS), as corneal stromal substitutes in humans [17]. In subsequent reports, RHC III-based hydrogels were implanted in 20 patients, with collagen being sourced from yeast in each of these cases [18–20]. After surgery, implants supported full epithelial regeneration, though slow reepithelialization rates could be noted, with full epithelial regeneration taking up to one year [20]. Additional exploration of RHC III-based hydrogels showed that surface modification, by means of fibronectin microcontact printing (F-μCP), improved reepithelialization rates *in vitro* [21]. Even though F-μCP of RHC III implants has yet to be validated *in vivo*, these results indicate the potential of surface modification in collagen-based corneal regeneration.

In recent years, alternative collagen sources have shown great promise in tissue engineering, including fully synthetic collagen-like peptide (CLP) and plant-derived RHC type I (RHC I) [22–25]. CLP [26] was introduced as a shorter and fully customizable alternative to RHC III peptide. As a synthetic peptide, CLP makes room for ready and scaled-up production. When tested as a corneal construct in an animal model, CLP proved to be functionally equivalent to RHC III, except for mechanical strength for which CLP underperformed [27, 28]. These reports provide a proof-of-principle and indicate that it is worthwhile exploring the versatility of CLP hydrogels as a scaffold for LESC cultivation.

Another type of collagen that recently became available is tobacco plant-derived RHC I [25]. Even though plant-derived RHC I has shown promise in experimental skin engineering and drug delivery [22, 29, 30], its application in ocular tissue engineering remains to be validated. Previous research compared the *in vitro* and *in vivo* performance of yeast-extracted RHC I and RHC III corneal constructs and concluded that both materials perform fairly similarly, though RHC III displayed marginally superior mechanical properties [31, 32]. These results, in combination with collagen type I being the most abundant protein of the native corneal stroma [33], suggest that plant-derived RHC I might offer greater potential in ocular tissue engineering. Our previous research demonstrated that plant-derived RHC I hydrogels are mechanically stable, transparent, and nongenotoxic and show good biocompatibility *in vitro* and *in vivo*. Even though plant-derived RHC I and CLP hydrogels appear promising substrates, both materials remain to be validated as carrier membranes for LESC cultivation.

Therefore, the aim of this study was to investigate *in vitro* performance of 4-(4,6-dimethoxy-1,3,5-triazin-2-yl)-4--methyl-morpholinium chloride- (DMTMM-) crosslinked CLP hydrogels, EDC/NHS-crosslinked CLP hydrogels, and EDC/NHS-crosslinked plant-derived RHC I hydrogels with regard to immortalized human corneal epithelial cell (iHCEC) and primary human limbal epithelial cell cultivation. The effect of surface topography and patterning was investigated for both hydrogels. All data were compared to HAM, the current gold standard in CLET.

2. Materials and Methods

The study followed the tenets of the Declaration of Helsinki and was approved by the Antwerp University Hospital-Ethical Committee (EC: 14/30/319).

2.1. Materials. Plant-derived RHC I and PEGylated CLP were provided by Collplant (Ness Ziona, Israel) and Ferentis (Vilnius, Lithuania), respectively. Laboratory

plastic was purchased from VWR (Radnor, PA, USA), Greiner Bio-One (Kremsmünster, Austria), or PerkinElmer (Waltham, MA, USA). Unless stated otherwise, all inorganic salts, enzymes, basic chemicals, Triton X, 4′,6-diamidino-2-fenylindool (DAPI), N-hydroxysuccinimide (NHS), N-(3-dimethylaminopropyl)-N′-ethylcarbodiimide hydrochloride (EDC), 4-(4,6-dimethoxy-1,3,5-triazin-2-yl)-4--methylmorpholinium chloride (DMTMM), and CellCrown inserts were purchased from Sigma-Aldrich (St. Louis, MO, USA). Materials obtained from Thermo Fisher Scientific (Waltham) include phosphate-buffered saline (PBS), PrestoBlue, Dulbecco's modified Eagle's medium (DMEM), keratinocyte serum-free medium, Live/Dead staining kit, Alexa Fluor® 568 hydrazide sodium salt, antibiotics, glycerol, and UltraPure distilled water (DW). Optimum cutting temperature (OCT) formulation was purchased from Sakura Finetek Europe (Zoeterwoude, the Netherlands); nitrocellulose paper and filter sterilizers were from Merck Millipore (Darmstadt, Germany); polydimethylsiloxane (PDMS) was from Dow Corning (Midland, MI, USA); balanced salt solution (BSS) was from Alcon (Fort Worth, TX, USA); CnT-prime medium (CnT-PR) was from CELLnTEC (Bern, Switzerland); PBS/glycerol Citifluor was from Citifluor Ltd. (London, UK); and RNeasy Mini Kit was from QIAGEN (Hilden, Germany). Human blood fibronectin was obtained through YO Proteins AB (Huddinge, Sweden) whereas bovine fibronectin was delivered by Cytoskeleton Inc. (Denver, CO, USA). iScript™ Advanced cDNA Synthesis kit, SsoAdvanced™ Universal SYBR® Green Supermix, and oligonucleotide primers were obtained from Bio-Rad (Hercules, CA, USA), unless stated otherwise. ΔNp63α primer was purchased from Eurogentec (Liege, Belgium) (Table 1). Antibodies used for immunohistochemistry and its dilutions are listed in supplementary Table S1.

2.2. Cell Carrier Preparation

2.2.1. Human Amniotic Membrane. With ethical approval from the UZA ethical committee (EC: EC: 14/30/319) and signed written informed consent from donors, amniotic membranes were obtained from women undergoing scheduled caesarean sections. HAM was cryopreserved and processed using previously described methods [34]. In brief, the HAM was peeled away from the chorion and washed in BSS containing penicillin/streptomycin and amphotericin B. It was then flattened onto a sterilized nitrocellulose filter paper and cryopreserved at −80°C in 1 : 1 solution containing DMEM and glycerol. The HAM was thawed 48 hrs before use and washed three times in saline, after which it was treated with 50 mL Thermolysin solution (0.12 mg/mL) for 8 min to remove amniotic epithelium. After enzymatic digestion, the membrane was washed in 0.01 M PBS after which orientation of the membrane was tested with the previously described 'cotton swab technique' [34]. When the de-epetheliazed surface was identified to be superior, the membrane was fixed in an interlockable ring [34]. Prior to primary cell cultivation, the HAM was immersed in the respective culture medium containing 5% human AB serum (hAB) for at least 24 hrs.

2.2.2. Recombinant Human Collagen Hydrogels. Plant-derived RHC I was obtained as a solution in 10 mM HCl. A 3 : 7 solution of pure (100%) ethanol/collagen was stirred for 30 min at 25°C, after which fibrillogenesis buffer (160 mM Na_2HPO_4 and 100 mM NaOH at pH 7.5) was added at a ratio of 1 : 10 *v*/*v* to the original collagen-HCl volume and stirred for 2 more hours. Water-diluted EDC and NHS were added for a final concentration of 50 mM EDC and 100 mM NHS and stirred for 24 hrs at 4°C. All stirring was performed using a magnetic stirrer at 200 rpm. After 24 hrs, excess EDC/NHS was washed out with DW in 6 cycles. One cycle consists of centrifugation at full speed (10 min, 5.000 rpm), discarding the supernatant and resuspending the collagen in 40 mL DW. At cycle 6, the collagen suspension was transferred to a Teflon mold and left air drying under a sterile hood. When fully dried, collagen gels were collected and stored in 100% ethanol until further use. Rehydration of gels was performed by 5 individual washes in PBS, each lasting 2 hrs. For cell cultivation, the hydrogels were soaked thrice for 2 hrs in the respective culture medium and immobilized with a CellCrown or interlockable ring.

2.2.3. Collagen-Like Peptide Hydrogels. CLP peptide synthesis, conjugation with PEG maleimide, and CLP-PEG hydrogel fabrication were described in the study of Islam et al. [21]. Briefly, 500 mg of aqueous solution of 18% or 12% (*w*/*w*) CLP-PEG was dispensed in a 2 mL glass syringe, and either EDC/NHS or DMTMM was added to the syringe mixing system. The molar equivalents of CLP-PEG-NH_2 : EDC were 1 : 2 and the molar ratio of EDC : NHS was 1 : 1. For CLP-PEG-NH_2 : DMTMM, the molar ratio was 1 : 2. All reagents were thoroughly mixed prior to casting the hydrogel into thin flat sheets. Alternatively, the hydrogel was molded in a PDMS mold with a surface topography of 50 μm wide and 20 μm deep grooves. All CLP-PEG hydrogel sheets were cut into 15 mm diameter disks using a trephine and kept in a PBS buffer. Hydrogel sheet thickness and the groove topography were measured using an Olympus BX51 upright microscope equipped with a Peltier-cooled Fview II CCD camera (Olympus, Tokyo, Japan).

Prior to cell cultivation, CLP hydrogels were soaked in respective culture medium for 96 hrs (4 days). CLP hydrogels did not require fixation to allow cell cultivation.

2.2.4. Surface Micropatterning. RCH I hydrogels were rehydrated in PBS and cut into approximately 20 × 25 mm^2 sized pieces. Microcontact printing (μCP) onto RHC I and CLP hydrogel surfaces was carried out as described previously [21]. Briefly, native surface carboxyl groups of RHC I and CLP-PEG hydrogels were activated by applying 10 mM EDC and 2.5 mM NHS in 0.1 M PBS (pH 5.7) for 15 min. The hydrogels were then washed with fresh PBS (pH 5.7). The surface of each sample was dried in a N_2 stream, keeping the material bulk hydrated. Stamps were made of PDMS, with rectangular stamps (~16 × 23 mm) used for RHC I and 12 mm diameter disks for CLP-PEG printing. The stamps contained surface topography of protruding 30 μm wide stripes with 60 μm spaces in between. They were inked by applying 0.1 mg/mL human blood fibronectin solution for

Table 1: Oligonucleotide primers and primers used for reverse transcriptase PCR.

Gene name	Gene symbol	Assay ID
Glyceraldehyde-3-phosphate dehydrogenase	GAPDH	qHsaCED0042632
β-2-Microglobulin	B2M	qHsaCED0015347
ΔNp63α [37]	ΔNp63α	Fw: GCATTGTCAGTTTCTTAGCGAG Rev: CCATGGAGTAATGCTCAATCTG
Cytokeratin 3	KRT3	qHsaCID0005917
Desmoglein 3	DSG3	qHsaCID0015226
Integrin-β1	INTB1	qHsaCED0005248
Integrin-α6	INTA6	qHsaCED0042632

5 min. For pattern visualization, ink contained 0.01 mg/mL of HiLyte488 dye-marked fibronectin. After inking, the PDMS stamp was brought into contact with the activated and dried hydrogel surface for 5 min. Subsequently, the remaining unreacted hydrogel surface was passivated by applying 10 mM PEG_3NH_2 (Molecular Biosciences, Boulder, CO, USA). The samples were washed with fresh PBS (pH 8.0) buffer and stored at 4°C until further use.

To investigate reproducibility of F-μCP patterning, the patterned hydrogels were imaged using an Olympus BX51 upright microscope. Fluorescence images of fibronectin-HiLyte488 patterns were acquired and analyzed using the Stream Motion software (Olympus). Fibronectin pattern quality was assessed manually, using stitched fluorescence microscopy images taken over the entire printed hydrogel surface area. Then the actual printed surface area was calculated by subtracting any defects from the total area occupied by the surface topographic features on the PDMS stamp.

An overview of hydrogel composition and their respective abbreviation is provided in Table 2. HAM serves as a control. Hydrogels are (1) unmodified RHC I, (2) RHC I that was F-μCP (RHC I F-μCP), (3) EDC/NHS-crosslinked CLP (CLP-12 EDC), (4) DMTMM-crosslinked CLP (CLP-12), (5) CLP-12 with surface F-μCP (CLP-12F-μCP), (6) CLP-12 with 3D-grooved surface topography (CLP-12 3D), (7) and DMTMM-crosslinked CLP at a CLP stock concentration of 18% (CLP-18).

2.3. Cell Cultivation

2.3.1. Immortalized Corneal Epithelial Cell Cultivation. For *in vitro* biocompatibility testing, immortalized human corneal epithelial cells (iHCECs) [35] were seeded onto the membranes and cultivated in keratinocyte serum-free medium. Cells were cultured in a humidified 37°C (5% CO_2) incubator. To perform live cell imaging, green fluorescence protein- (GFP-) transduced iHCECs (GFP-iHCECs) [21] were cultured using the same cultivation protocol.

2.3.2. Primary Limbal Epithelial Cell Cultivation. Cadaveric donor eyes were collected from the cornea tissue bank of the Antwerp University Hospital. The donor age ranged from 49 to 90 years with an average of 74 years. All donor eyes were processed within 32 hrs postmortem. In brief, the eyes were enucleated, transferred in 0.9% NaCl, and stored at 4°C. The eyes were disinfected for 1 min in povidone iodine 0.5%, after which they were rinsed 4 times in PBS. Biopsies of $\leq 2\,mm^2$ were taken from the superior and inferior keratolimbal regions and washed 6×10 min in CnT-PR (CELLnTEC) at 4°C. Biopsies were then placed epithelial side down on the tested carrier materials (Table 2) and cultivated for 14 days at 37°C, 5% CO_2, and 95% humidity. For cultivations on HAM and RHC I, 1% hAB was added to culture medium. Culture medium was changed every other day. The first 3 days, cells were cultivated at an air-liquid interface to allow biopsy attachment. Onwards, volume of the medium was increased to submerge cultures. At day 14 (or earlier if confluent), cells were characterized through immunohistochemistry and reverse transcriptase PCR (RT-PCR) analyses.

2.4. In Vitro Biocompatibility Testing. To assess *in vitro* biocompatibility of collagen-based hydrogels, samples of 6 mm diameter were punched out of the membranes and placed into 96-well plates. iHCECs were seeded onto the materials at a density of 5000 cells per membrane ($n = 3$) and cultured up to 4 days (96 hrs). Cell cultures on HAM served as a control. At 24 hrs, 48 hrs, 72 hrs, and 96 hrs of cultivation, a PrestoBlue cell metabolic activity assay was performed according to the manufacturer's protocol. In brief, PrestoBlue was added (1 : 10 *v*/*v*) to the cultures and incubated for 35 minutes. The supernatant was transferred to an opaque 96-well plate, and fluorescence was read at 590 nm with VICTOR^3. Supplementary Live/Dead staining was performed at 48 hrs of cultivation, where cells were double stained with calcein acetoxymethyl (Calcein AM) and ethidium homodimer-1 (EthD-1). Cells cultured on tissue culture plastic (TCP) and treated with 0.1% saponin for 20 min at 37°C were used as positive controls for EthD-1. For PrestoBlue analysis, independent nonparametric *t*-testing was performed using the SPSS 24 Kruskal-Wallis test (IBM Corp., NY, USA) and Prism 5 (GraphPad Software, CA, USA). $p < 0.05$ was considered significant.

To evaluate the pattern of proliferation, live cell imaging of GFP-iHCECs [21] was performed. Hydrogel samples of 15 mm diameter were placed into 12-well plates. RHC I hydrogels were fixated with CellCrown inserts. GFP-iHCECs were seeded onto the materials at a density of 10.000 cells per membrane. Live cell imaging was performed in an incubator that was mounted on a confocal

Table 2: Tested carrier material.

Abbreviation	Material	Crosslinker	Surface patterning	Collagen concentration*
HAM	Denuded HAM	—	—	—
RHC I	RHC I	EDC/NHS	—	~3 mg/cm^2
RHC I F-μCP	RHC I	EDC/NHS	Fibronectin microcontact printing	~3 mg/cm^2
CLP-12 EDC	CLP-PEG	EDC/NHS	—	12%
CLP-12	CLP-PEG	DMTMM	—	12%
CLP-12F-μCP	CLP-PEG	DMTMM	Fibronectin microcontact printing	12%
CLP-12 3D	CLP-PEG	DMTMM	3D topography	12%
CLP-18	CLP-PEG	DMTMM	—	18%

*Concentration of RHC I is expressed as net weight at collagen casting (mg/cm^2). Concentration of CLP is expressed as percentage of stock solute (%). —: not applicable; HAM: human amniotic membrane; RHC I: recombinant human collagen type I; CLP-PEG: PEGylated collagen-like peptide; EDC: 1-ethyl-3-(3-dimethyl aminopropyl) carbodiimide; NHS: N-hydroxysuccinimide; DMTMM: 4-(4,6-dimethoxy-1,3,5-triazin-2-yl)-4-methyl-morpholinium chloride.

laser scanning microscope (Eclipse Ti microscope, Nikon, Tokyo, Japan; UltraVIEW VoX, PerkinElmer). The microscope recorded images at 90-minute intervals for 3 days (72 hrs). Images obtained at 72 hrs of culture were analyzed with ImageJ (National Institutes of Health, Bethesda, MD, USA) to calculate the percentage area of confluence. Of each culture condition, images of 6 different sites were analyzed. To detect statistical significance, independent nonparametric t-testing was performed using the Mann-Whitney U test in Prism 5 (GraphPad Software, CA, USA). Live cell imaging was not performed for HAM as the composite graft was not compatible with the microscope setup.

After 72 hrs of imaging, cells were kept in culture until day 4, when samples were fixed in 2.5% glutaraldehyde solution in 0.1 M sodium cacodylate buffer (pH 7.4), and processed for scanning electron microscopy (SEM) and transmission electron microscopy (TEM).

2.5. Electron Microscopy

2.5.1. Scanning Electron Microscopy. For SEM, fixed samples were rinsed in 7.5% saccharose in 0.1 M cacodylate buffer, pH 7.4, and then dehydrated through an ascending ethanol gradient (50% ethanol 10 min; 70% - 90% - 95% ethanol 15 min each; 100% ethanol 3×30 min). After critical point drying, samples were mounted on a SEM grid and shutter coated with 20 nm gold. Images were recorded with a SEM 515 Microscope (Philips, Eindhoven, the Netherlands).

2.5.2. Transmission Electron Microscopy. Samples were post-fixed in 1% OsO_4 solution and dehydrated in an ethanol gradient (50% - 70% - 90% - 95% ethanol for 15 min each, 100% ethanol for 4×20 min). Samples were embedded in EMbed 812 (Electron Microscopy Sciences, Hatfield, Pennsylvania), sectioned, and stained with lead citrate. Slides were examined using a Tecnai G2 Spirit BioTWIN Microscope (FEI, Eindhoven, the Netherlands) at 120 kV.

2.6. Characterization of Primary LESC Cultures

2.6.1. Immunohistochemistry. For immunohistochemistry, cultures were fixed in 100% ethanol for 10 min at -20°C and rinsed thrice in PBS for 10 min each. Samples were embedded in OCT compound and stored at -80°C. Five cryostat sections (13 μm thick) of each sample were mounted on poly-L-lysine-coated microscope slides, dried at 37°C for 2 hrs, and processed for fluorescence immunolabeling. Sections were then permeabilized with Triton X 1% for 25 min. Primary antibodies were incubated overnight at 4°C. Anti-ΔNp63, anti-cytokeratin 3 (KRT3), anti-laminin, anti-KRT14, anti-collagen type IV (Coll-IV), anti-integrin-β4 (INTB4), anti-desmoglein 3 (DSG3), and anti-E-cadherin (E-cad) served as primary antibodies (supplementary Table S1). Fluorescent secondary and tertiary antibody labeling was incubated for 2 hrs at 4°C. Nuclei were counterstained using DAPI, and sections were mounted with Citifluor. Images were recorded with confocal microscopy.

2.6.2. RNA Extraction, Reverse Transcription, and Polymerase Chain Reaction. Prior to RNA extraction, cultures were rinsed once with 0.1 M PBS, preheated at 37°C. Cells were incubated with RNA lysis buffer, and total cell RNA was extracted, following RNeasy Mini Kit-enclosed guidelines. Total RNA was diluted in 14 μL water, and purity was evaluated from the 260/280 ratio of absorbance (1.80–2.00) using the NanoDrop™ spectrophotometer (Thermo Fischer Scientific). cDNA was synthesized from 10 μL of total RNA using iScript™ Advanced cDNA Synthesis kit and CFX96™ thermocycler (Bio-Rad), according to the manufacturer's protocol. cDNA was diluted to a 10 ng/μL concentration and frozen down (-20°C) until further use. PCR assays were performed from 10 ng of cDNA in SsoAdvanced Universal SYBR Green Supermix on the CFX96™ thermocycler with the following settings: an activation step of 30 seconds at 95°C and 40 amplification cycles of denaturation (95°C for 5 sec) and annealing/extension (60°C for 30 sec). Oligonucleotide primers that were used are listed in Table 1. All samples were run in duplicate. To confirm their amplification specificity, the PCR products were subjected to a melting curve analysis. A nontemplate control was included in all experiments, and the GAPDH gene was used as endogenous control for normalization. The comparative cycle threshold (Ct) method, where the target fold = $2^{-\Delta\Delta Ct}$, was used to analyze the results [36]. Primary LESC cultured on TCP in

12-well plates served as the calibrator controls and had an assigned value of 1. The results were reported as a fold upregulation or fold downregulation when the fold change was greater or less than 1, respectively. Cultures from four different donor corneas were analyzed for each type of hydrogel. As cultures on hydrogels had a donor-matched culture on HAM, 6 donors were included for HAM analysis.

For statistical analysis, a linear mixed model was fitted to account for the nonindependence between observations within the same hydrogel (i.e., interdonor variation). Within this model, gene expression served as a dependent variable, the hydrogel group as an independent variable, and the donor cornea as a random intercept. The significance of the fixed effect, testing the null hypothesis that the mean outcome is the same across different culture substrates within one donor, was tested using an F-test with Kenward-Roger correction for the degrees of freedom. When significance of the fixed effect was observed, a post hoc analysis was carried out with a Tukey correction for multiple comparison.

3. Results

3.1. Hydrogel Production and Surface Modification. All hydrogel manufacturing protocols resulted in the successful production of hydrogels that were mechanically robust. Thickness values of collagen hydrogels which varied between groups were as follows: $133 \pm 28\,\mu$m for RHC I, $500 \pm 50\,\mu$m for CLP-12 EDC, $241 \pm 98\,\mu$m for CLP-12 (including CLP-12 F-μCP), $303 \pm 91\,\mu$m for CLP-12 3D, and $244 \pm 90\,\mu$m for CLP-18 hydrogels. We can now confirm that thin RHC I and CLP-12 membranes can successfully undergo F-μCP (Figure S1), with the quality of surface patterns being higher for CLP (75%±6) than RHC I (40%±28) hydrogels. Surface topography on CLP hydrogels was deemed successful as hydrogels remained intact and displayed a groove width close to $49 \pm 2\,\mu$m on bright field microscopy.

Physical characterization (Table 3; supplementary data "physical characterization of carrier membranes—Fig. S2") shows that water content (%) of collagen hydrogels varied between 88% and 93%, indicating that the type of collagen, type of crosslinker, and percentage of CLP did not make much of a difference. Light transmittance of collagen hydrogels was much higher than that of HAM, with values being comparable to those of native corneas. Transparency of CLP hydrogels (≥91%) was higher than that of RHC I hydrogels (84.8 ± 1.45). The refractive index of collagen hydrogels (1.34 – 1.35) was closer to that of the human cornea (1.37-1.38) compared to HAM (1.33). Permeability of the hydrogels was comparable to that of HAM, the currently used gold standard.

3.2. In Vitro Biocompatibility Testing of Hydrogels. In the first set of experiments, iHCECs were cultured on different substrates and cell metabolic activity was monitored. PrestoBlue assay (Figure 1) revealed that cell metabolic activity was comparable for each of the substrates. Supplementary Live/Dead staining performed at 48 hrs postculture confirmed the biocompatibility of collagen hydrogels as cells exhibit minimal cell death on the hydrogels and comparable or lower cell death than HAM (Figure S3).

Live cell imaging confirmed that both RHC I and CLP hydrogels, regardless of surface modification, supported attachment and proliferation of cells (Figure 2). Cells were found to attach to the respective hydrogel 3 hrs after seeding, which was comparable between hydrogel groups. F-μCP appeared to influence cell proliferation on CLP hydrogels, unlike on RHC I hydrogels, as cells seemingly first attached to fibronectin stripes before populating the rest of the CLP hydrogel (Figure 2(b)). For CLP-12 3D, cells showed to preferentially grow first in the grooves, prior to spreading over the hydrogel's ridges (Figure 2(b)). At 72 hrs of culture, cells cultivated on CLP DMTMM hydrogels showed cell a confluence of ≥80% with an average confluence of 91.0%±1.3 for CLP-12, 85.0%±3.3 for CLP-12 F-μCP, 90.0%±2.7 for CLP-12 3D, and 89.6%±1.2 for CLP-18 (Figure 2(c)). The average confluence of RHC I and RHC I F-μCP was 71.4%±4.1 and 66.27%±8.3, respectively, with RHC I showing significantly less confluence compared to any of CLP DMTMM hydrogels and RHC I F-μCP being less confluent then CLP-12, CLP-12 3D, and CLP-18 (Figure 2(c)). The lowest average confluence was observed for CLP-12 EDC (65.1%±18.3), with 2 sites showing a confluence of <10% (data not shown).

After 4 days of cultivation, SEM imaging (Figure 3) was performed at regions that had reached full confluence. Cultured cells displayed the typical cobblestone appearance; however, at RHC I hydrogels, some isolated cells displayed an elongated morphology. In a region where cells had not reached full confluence on CLP-12 3D hydrogels, cells were mainly observed in the grooves and not on the ridges of the hydrogel. TEM imaging (Figure 4) of cultures confirmed that a monolayer of cells had formed on all substrates and that cells displayed apical microvilli. Furthermore, it was noted that cells cultivated on collagen hydrogels had not initiated differentiation, whereas cells cultivated on HAM expressed gap junctions in the absence of stratification, indicating early differentiation.

3.3. Cultivation and Characterization of Primary LESC Cultures. A total of 41 eyes of 22 donors, with an average donor age of 73.7 ± 11.3 years (range 49-90 years), were used for this study. Cultured epithelial cells were analyzed every 2 days with phase contrast microscopy (Figure 5). By day 3 of culture, epithelial cells had emerged from 83% of limbal biopsies. Explants that did not prove successful by day 3 did not display cell outgrowth later. No significant difference for successful initiation of explant cultivation was observed between different substrates (data not shown). During the first week of cultivation, cells that were cultivated on the surface of the modified CLP hydrogels displayed a distinctive proliferation pattern (Figure 5(a)). In accordance with the observations made at live cell imaging, pioneer cells followed fibronectin patterns, colonizing the intermediate area in the following hours and days. Similarly, cells on 3D hydrogels grew first in the grooves before expanding over the ridges. On day 14 of culture (Figure 5(b)), outgrowth on all substrates contained small and cuboidal epithelial-like cells of varying cell

Table 3: Properties of RHC I, CLP-12 EDC, and CLP DMTMM hydrogels, with HAM and the human cornea serving as control.

Properties	HAM	RHC I	CLP-12 EDC	CLP-12	CLP-18	Human cornea
Water content (%)	87.68 ± 0.02	89.21 ± 0.01	91.65 ± 1.10 [28]	90.31 ± 0.02	88.42 ± 0.01	78 [39]
Refractive index	1.33	1.35	1.34 [27]	1.35	1.35	1.37-1.38 [40]
Transmission at 490 nm (%)	60.0 ± 2.2	84.8 ± 1.5	92.4 ± 1.0 [28]	91.0 ± 0.8	91.0 ± 0.5	87.1 ± 2.0 [41]
Apparent permeability (P_{app}) (cm/sec)	0.039 ± 0.007	0.057 ± 0.03	0.061 ± 0.003	0.056 ± 0.006	0.047 ± 0.006	NA

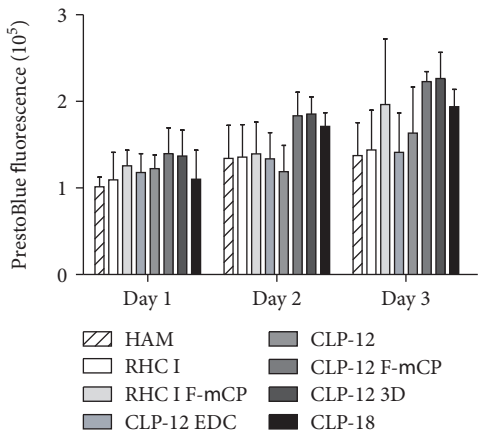

Figure 1: *In vitro* biocompatibility of collagen hydrogels. PrestoBlue viability assay showed that for all substrates, cumulative cell viability of iHCECs was similar at days 1, 2, and 3 of culture.

size. Cells cultured on HAM maintained a smaller round shape compared to cells cultivated on hydrogels. In contrast, cells cultured on RHC I and RHC I F-μCP displayed a more heterogeneous morphology with singular elongated cells being observed in between simple squamous epithelial cell growth. By day 14, all cultures on CLP DMTMM hydrogels had reached near confluence on the 15 mm diameter gel. In contrast, none of the CLP-12 EDC hydrogels reached confluence; moreover, 3 out of 9 cultures generated too low cell yield for further characterization and 5 out of 9 cultures did not meet the minimum 8 mm diameter outgrowth, which is deemed a quality standard at our center. At day 14, RHC I and RHC I F-μCP cultures displayed an average cellular outgrowth of >15 mm, whereas HAM cultures had reached subconfluence in a 14-15 mm diameter.

3.3.1. Immunohistochemical Characterization

(1) Expression of Stem Cell Markers. The stemness of cultivated cells was verified with ΔNp63 and KRT14 (Figure 6). Both markers have been attributed to progenitor epithelial cells in the basal and suprabasal layers of the limbus [38–40]. Cells cultivated on any of the substrates showed nuclear staining of ΔNp63 and cytoplasmic staining of KRT14. No immediate difference in the pattern of expression was observed between different substrates.

(2) Expression of Differentiation Markers. KRT3 and DSG3 were used as differentiation markers for corneal epithelial cells. KRT3 is a cytoplasmic keratin that has been shown to be specific for corneal epithelium [41], and DSG3 is a glycoprotein component of desmosomes [42, 43]; both markers display differentiation-related expression. Cultivated cells showed low expression of both markers, with only few isolated cells that were KRT3 or DSG3 positive. Double staining with ΔNp63 confirmed that DSG3-positive cells lacked expression of the stem cell marker (Figure 6—HAM). Pattern of expression was comparable between tested scaffolds.

(3) Expression of Extracellular Matrix Proteins and Cell Adhesion Markers. Laminin and Coll-IV have been described as extracellular matrix and basement membrane components of the human cornea and limbus [42, 44]. Extracellular expression of both markers was noted, indicating deposition of laminin and Coll-IV by cultivated cells on the respective substrate (Figure 6). Coll-IV also is a key component of HAM [45], which is shown by the Coll-IV-positive staining of HAM stroma (Figure 6). INTB4 and E-cad have been proposed to mediate cell anchorage of basal epithelial cells, with INTB4 expression being confined to LESC [43, 46] and E-cadherin expression being more specific for basal and suprabasal corneal epithelial cells [47]. Both markers show positive membrane expression in cultivated cells. INTB4 expression appears to be confined to the basal side, whereas E-cad expression is more diffuse and is expressed in the cytoplasm and at the basal and apical sides. No apparent difference in the pattern of expression was noted between the tested substrates.

3.3.2. Gene Expression of Limbal Epithelial and Corneal Epithelial Cell Makers. With the house keeping gene, GAPDH, as an internal control and cell cultures on TCP as a calibrator, RT-qPCR showed positive expression for ΔNp63α, KRT3, DSG3, INTB1, and INTA6 (Figure 7). Integrin-β1 and integrin-α6 are known to be progenitor cell-specific adhesion proteins [43]. A statistically significant difference between groups was only observed for KRT3 expression (Figure 7), with RHC I, RHC I F-μCP, and HAM showing significantly lower expression levels compared to CLP hydrogels. More specifically, significantly lower KRT3 expression was noted for RHC I when compared to any of the CLP hydrogels, whereas lower expression was noted for RHC I F-μCP when compared to CLP-12 F-μCP, CLP-12 3D, and CLP-18 and for HAM when compared to CLP-18. Furthermore, a trend ($p \leq 0.1$) was observed for lower KRT3 expression in HAM than in CLP-12 F-μCP and CLP-12 3D and in RHC I F-μCP than in CLP-12. The relative fold change in gene expression is listed as supplementary data (Table S2).

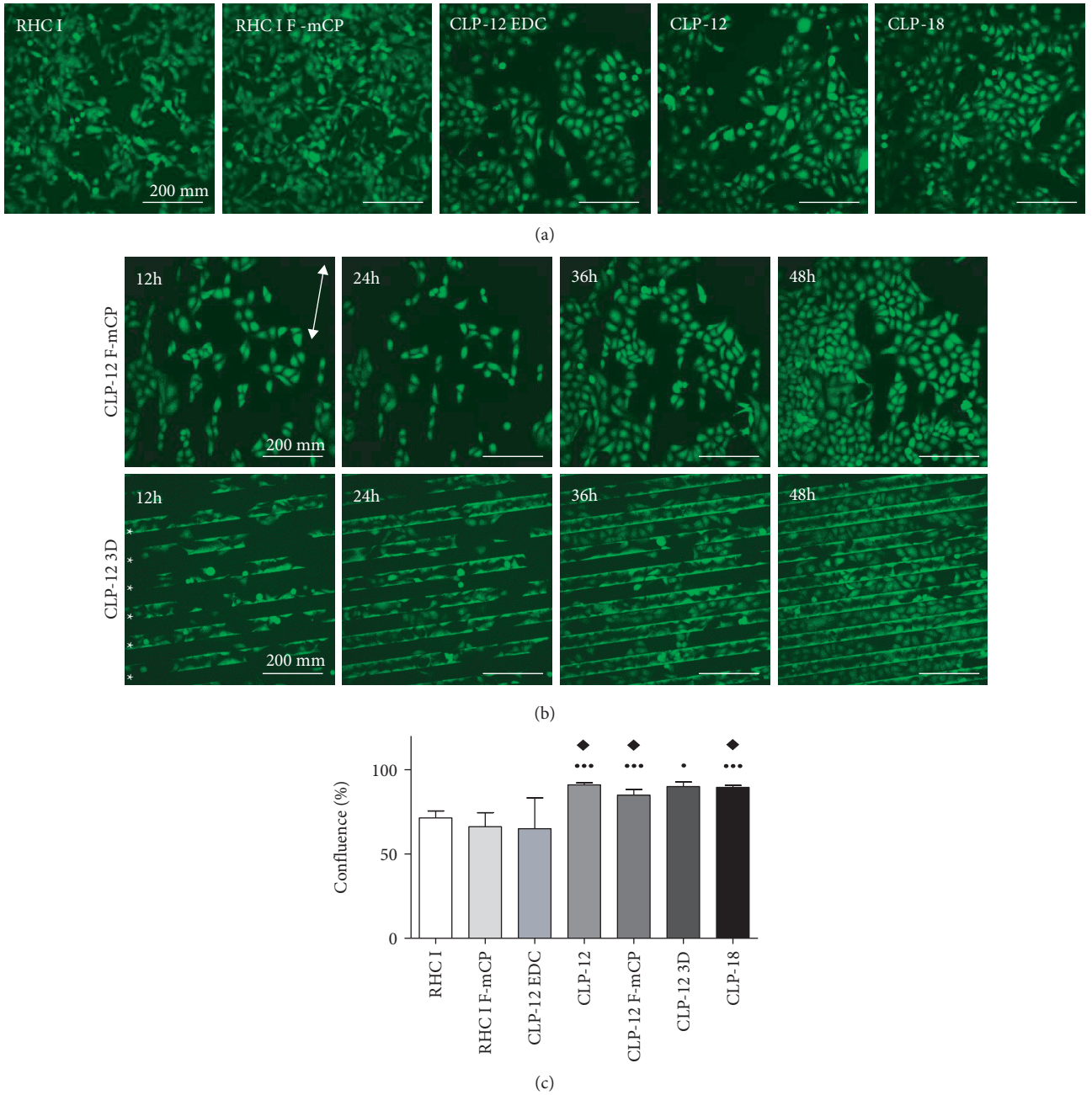

Figure 2: Cell growth of GFP-iHCECs on collagen hydrogels. (a) Representative images of cells cultivated for 36 hrs on RHC I, RHC I F-μCP, CLP-12 EDC, CLP-12, and CLP-18 demonstrate that cells proliferate in a random pattern. (b) Micrographs of cultures on surface-modified CLP-12 F-μCP and CLP-12 3D at 12 hrs, 24 hrs, 36 hrs, and 48 hrs. Cells cultured on surface-modified CLP hydrogels display a proliferation pattern that is being influenced by the fibronectin striping and 3D grooving. Orientation of F-μCP stripes is shown with a double white arrow. Grooves of CLP-12 3D hydrogels are marked by white asterisk (*). (c) The area of confluence at 72 hrs of culture. RHC I hydrogels displayed less confluence when compared to any of the CLP DMTMM hydrogels. RHC I F-μCP showed less confluence when compared to CLP-12, CLP18%, and CLP-12 3D. ● and ●●● indicate $p < 0.05$ and $p < 0.005$, respectively, as compared to RHC I. ◆$p < 0.05$ as compared to RHC I F-μCP.

4. Discussion

CLET has been a major breakthrough for the treatment of patients suffering from LSCD [4, 5, 14]. However, protocols for LESC cultivation need further optimization and standardization as they commonly involve animal-derived supplements, such as growth factors, serum, and/or fibroblast feeder layers [48], all of which could induce zoonosis, allergy, and other side effects [49]. In the context of GMP regulations, both stem cell carrier and culture protocol should meet strict guidelines in quality. Attempts have been made to remove xenogeneic products from culture protocols [5, 50, 51] in order to achieve standardization. Standardizing HAM, the carrier material most frequently used in CLET, remains

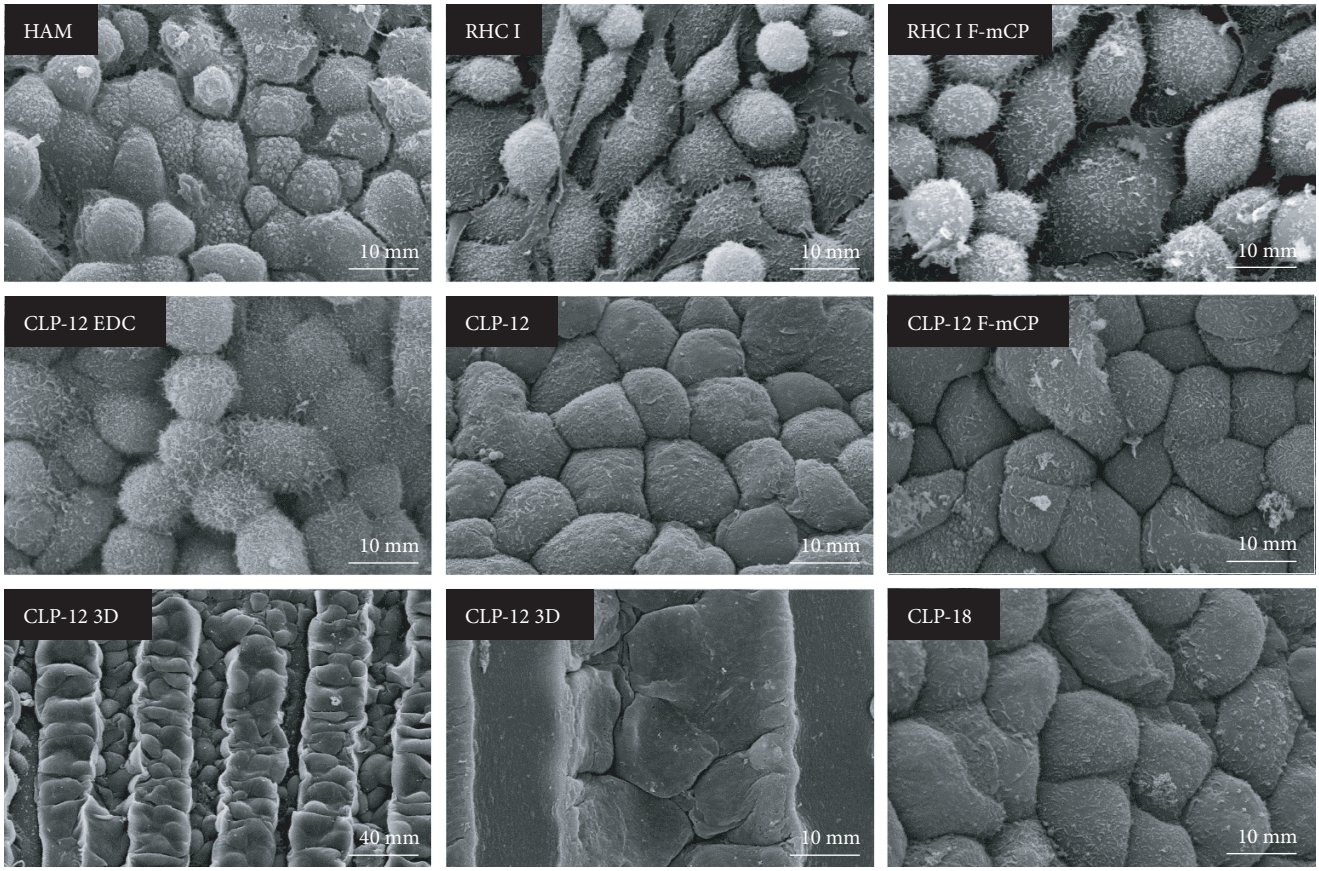

Figure 3: SEM imaging of iHCECs cultivated on HAM and collagen hydrogels for 4 days. Cells had formed a confluent monolayer. In general, cells exhibited a typical cobblestone appearance. At a region where cells had not reached full confluence on CLP-12 3D (lower middle), cells were mainly present in the grooves.

challenging as it is characterized by considerable variation in physicochemical properties [10–13].

CLP and RHC I both originate from xeno-free sources and are optically transparent, mechanically stable, and biocompatible *in vivo* [27, 28]. CLP-12 EDC hydrogels have shown great promise as an acellular corneal construct *in vivo* [27, 28]. However, EDC/NHS crosslinking is too fast to allow successful casting and production of thin hydrogels (<300 μm thick) [52]. To generate a flexible and thin scaffold, we used DMTMM as an alternative crosslinker. Other groups have demonstrated the efficiency of DMTMM over EDC/NHS for crosslinking of peptides and glycosaminoglycans as DMTMM resulted in slower crosslinking time and hence more homogenous hydrogels [53]. Similar to EDC/NHS, DMTMM is a zero-length crosslinker, implying that it is not incorporated into the scaffold. DMTMM has the advantage of not requiring pH control or cause pH shift during the reaction over EDC/NHS, ensuring good reaction yields and biocompatibility [53, 54]. In this study, we used DMTMM to crosslink collagen derivatives [55] and tested its *in vitro* performance. RHC I was not crosslinked with DMTMM since our previous research demonstrated that EDC/NHS-crosslinked RHC I gels were of desired thickness (<150 μm thick) and flexibility.

Our data demonstrate that RHC I and CLP hydrogels, irrespective of type of crosslinker, support cultivation of iHCECs and primary limbal epithelial cells. CLP-12 EDC, however, was the only tested carrier material for which primary limbal epithelial cultures did not meet quality standards due to low cell yield. Interestingly, our previous data indicate that CLP-12 EDC might be a suitable acellular alternative to conventional corneal transplantion [27]. In the work of Jangamreddy et al., we noted that suboptimal growth of iHCECs at days 1 and 2 on CLP-12 EDC hydrogels does not necessarily translate into inferior *in vivo* performance [27]. After all, acellular CLP-12 EDC corneas supported functional reepithelialization when implanted in pigs. Moreover, CLP implants performed equally with RHC III-based hydrogels, of which the latter have successfully been implanted in humans [18, 20]. Nonetheless, we have now shown that CLP-12 EDC is less suitable for standardized *in vitro* cultivation of primary limbal epithelium. Conversely, RHC I hydrogels did meet quality standards of cell outgrowth for primary limbal cultures, although significant lower confluence was observed for iHCEC cultures compared to CLP DMTMM hydrogels after 3 days of cultivation. This discrepancy might be explained by the fact that iHCECs display a significantly altered genomic profile to primary limbal epithelium [56]. This must be carefully considered when drawing conclusions on data obtained through their use.

In our experiments, surface modification of RHC I did not influence pattern of cell proliferation, which

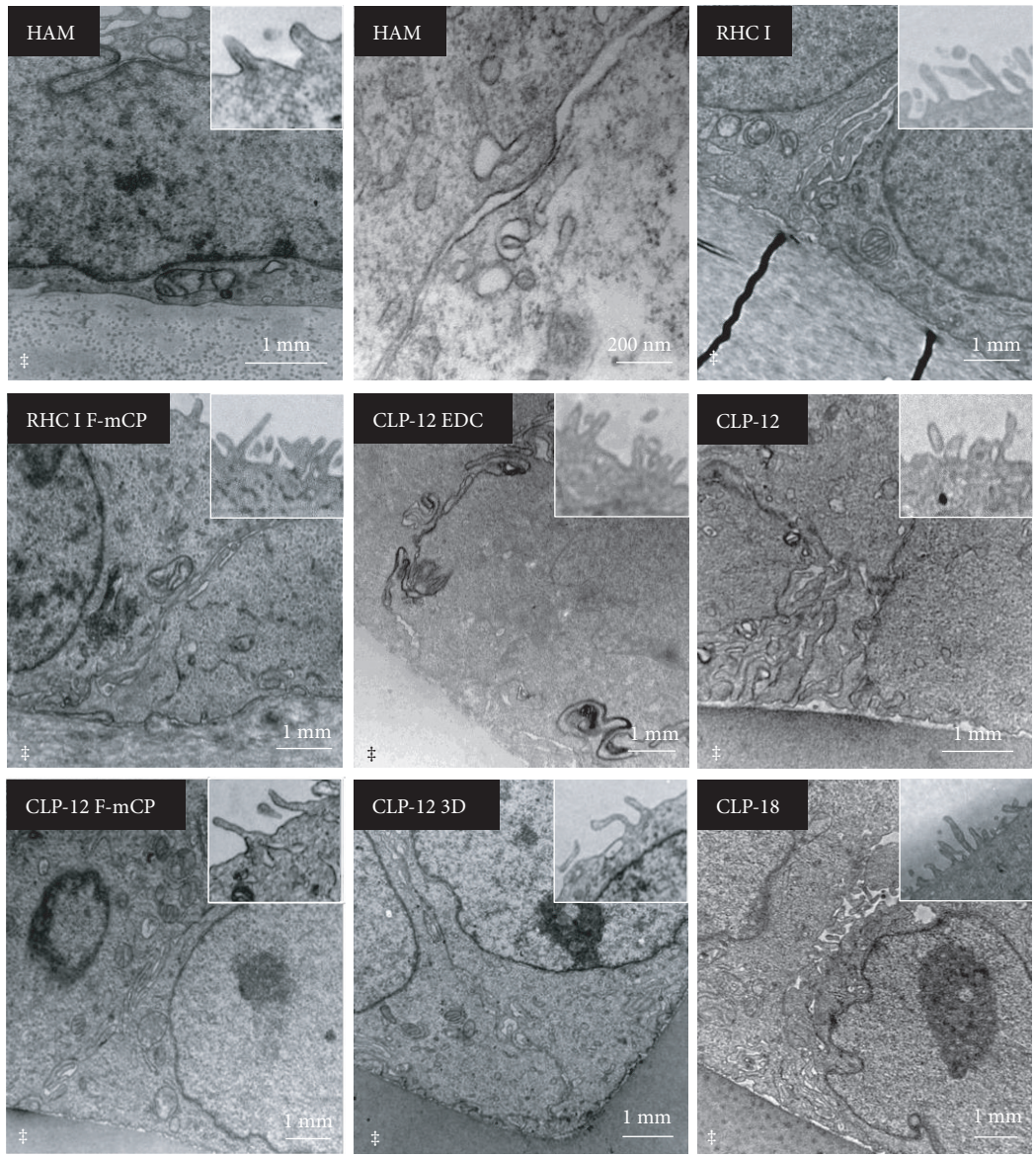

Figure 4: TEM micrographs of iHCECs on different substrates after 4 days of cultivation. A confluent monolayer had formed, in which cells displayed multiple interdigitations and apical microvilli (inset). Cells cultivated on HAM displayed expression of gap junctions (middle top), whereas cells cultivated on collagen hydrogels had not initiated differentiation as desmosomes, hemidesmosomes, and gap junctions could not be observed. ‡ denotes the carrier material.

might be attributed to the inherent biocompatibility of RHC [18–21, 27, 31, 32, 57, 58]. Even though surface modification of CLP DMTMM hydrogels influenced the pattern of cell proliferation, the rate of outgrowth and the genotype and phenotype of cultured cells were not significantly altered. It can therefore be assumed that surface patterning of RHC I and CLP DMTMM hydrogels may be unnecessary to attain successful LESC-enriched cultures *in vitro*. Our results confirm the findings of Hogerheyde et al. [59], in which fibronectin coating of silk fibroin membranes did not significantly improve cell outgrowth of iHCECs or of primary LESC. Conversely, our results are in contradiction to previous research that showed the benefit of fibronectin patterning of carrier membranes on cell proliferation of iHCECs [21, 60]. In the study of Islam et al., a similar fibronectin patterning protocol was used as that in our study; however, the membrane of interest was RHC III-MPC and anti-Ki67, anti-focal adhesion kinase, and anti-integrin-β1 were used as antibodies in immunohistochemical characterization [21].

In 2013, the group of Levis et al. introduced RAFT (Real Architecture for 3D Tissue) hydrogels, a collagen construct produced through plastic compression of bovine type I collagen, as an *in vitro* model of the human cornea [61]. To mimic limbal crypts, 3D grooves were created in the hydrogel's surface (RAFT TE). RAFT TE successfully support limbal epithelium cultivation; however, clinical impact is limited since RAFT lacks chemical crosslinking and thus results in heterogeneous hydrogels with suboptimal optical and mechanical properties [61–63]. Furthermore, biocompatibility of RAFT gels has yet to be validated *in vivo*.

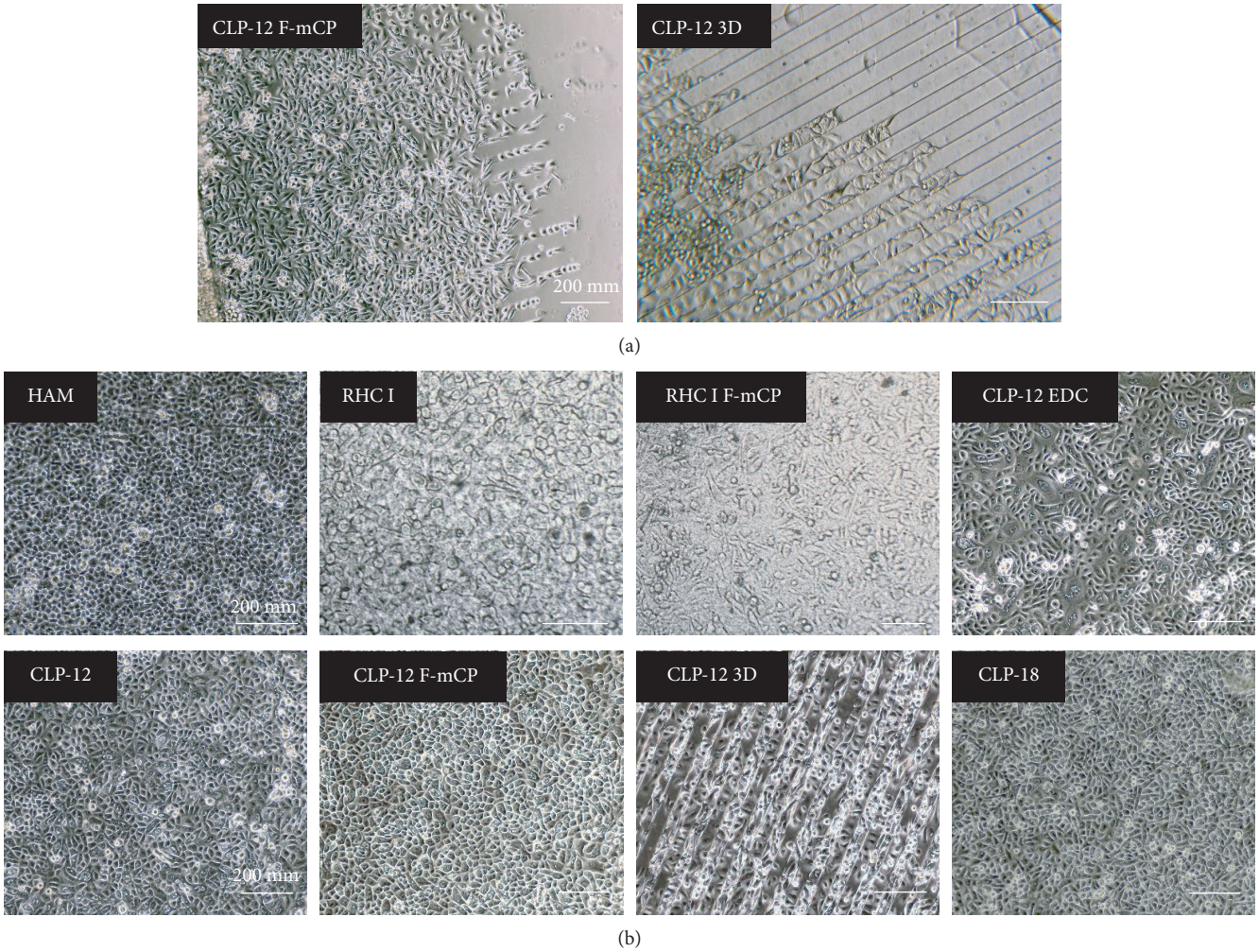

Figure 5: Representative images of primary limbal epithelial cell cultures at day 4 (a) and day 14 (b) on various carrier materials. At day 4, it is evident that surface modification of CLP hydrogels influences limbal epithelial cell outgrowth, as cell first grew on fibronectin stripes or in grooves, before spreading over the rest of the hydrogel growth. By day 14, cell confluence was reached in a 15 mm diameter outgrowth on both types of RHC I gel, all types of CLP DMTMM gel, and HAM. After 14 days, cells on CLP-12 EDC had not reached full confluence.

When compared to our study, aforementioned reports [21, 59–62] lacked (i) extensive phenotyping and genotyping of cultured primary cells, (ii) comparison to HAM, the carrier of choice in CLET, and/or (iii) implementation of a xeno-free, standardized cultivation protocol; all of which indicate further need of optimization-described techniques.

To the best of our knowledge, we are the first to cultivate primary human limbal epithelium on collagen hydrogels using a xeno-free and fully standardized culture protocol. The CnT-PR medium is a GMP-grade culture medium that has been selectively developed to target progenitor cells of epithelial lineage and to inhibit proliferation of cells from mesenchymal lineage [50, 64]. By using a GMP-grade culture medium, the proposed cultivation protocol could be translated into a clinical setting with relative ease. In our setup, primary cells grew to confluence within 14 days of culture, except for CLP-12 EDC, without the addition of 3T3 feeder layers or xenobiotics. RHC I hydrogels could only successfully support primary cells when 1% hAB was added to the culture medium. For CLP hydrogels, a serum-free culture medium was attained but hydrogels had to be soaked for at least 4 days in culture medium to consistently demonstrate explant outgrowth (data not shown).

Immunostaining revealed that cultured cells show low expression of differentiation markers KRT3 and DSG3 and high expression of progenitor marker ΔNp63, proliferation marker KRT14, and adhesion markers INTB4 and E-cad. Furthermore, cells deposited extracellular matrix and basement membrane proteins laminin and Coll-IV. This pattern of protein expression strongly suggests that cells cultured on any of the carriers can be identified as LESC [38–43, 46, 65]. E-cad expression remained largely cytoplasmic, with cell membrane localization to a certain extent. This pattern of staining shows that E-cad expression had not reached a maximum, indicating that cells were in a relatively undifferentiated state. *In vitro* supplementation with $CaCl_2$ (Figure S4) shows that E-cad expression is located mainly at the cell membrane when cells are initiating differentiation. Even though a nonspecific ΔNp63 antibody was used for

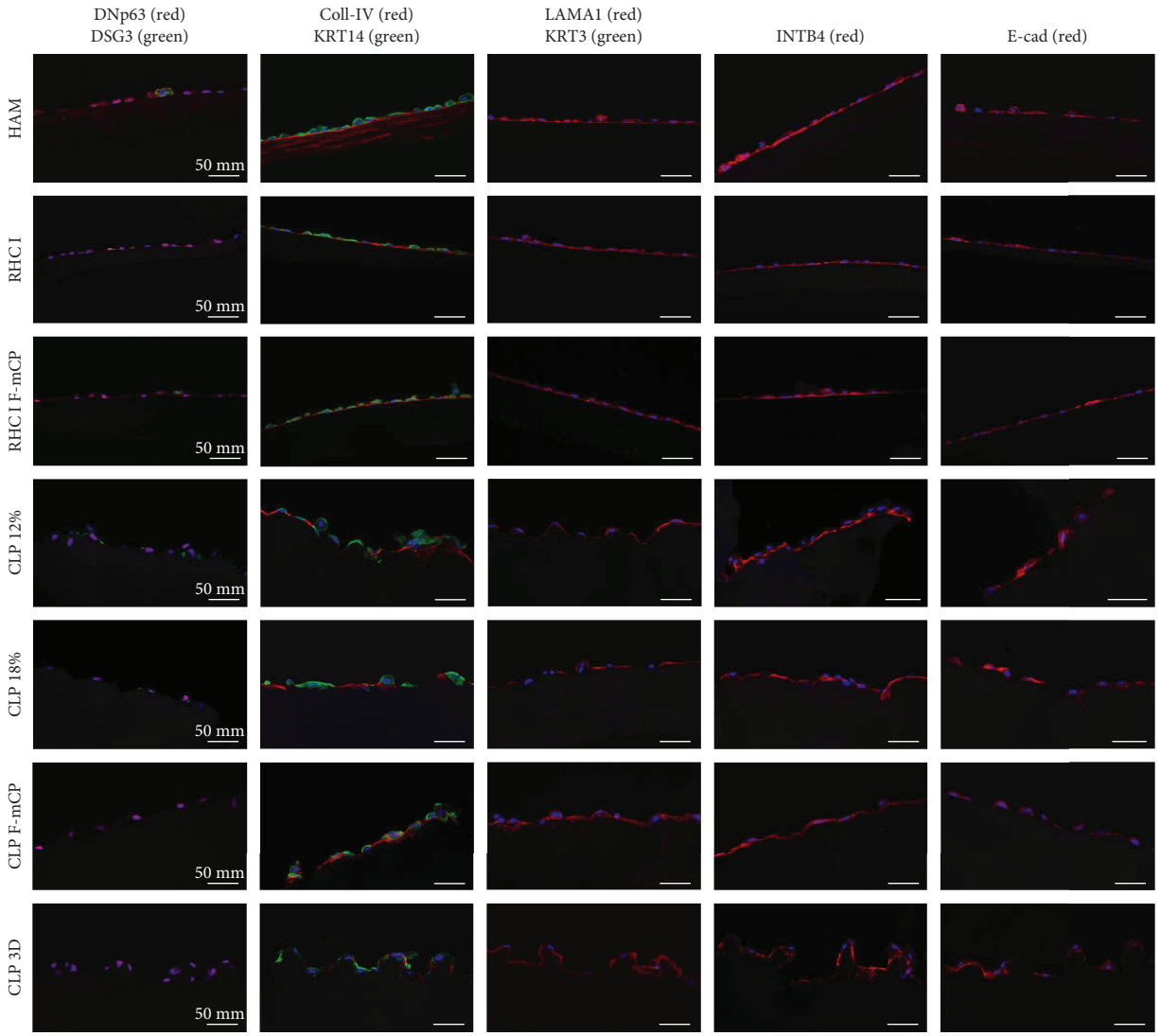

Figure 6: Immunohistochemistry of primary limbal epithelial cells cultured on different carrier materials. Representative images of double immunostaining for detection of ΔNp63-DSG3, laminin-KRT3, and Coll-IV-KRT14 and monostaining for detection of INTB4 and E-cad. Overall, cultivated cells show high expression of (i) ΔNp63, a nuclear stem cell marker, (ii) KRT14, a cytoplasmic proliferation marker, and (iii) laminin, Coll-IV, INTB4, and E-cad, markers of corneolimbal basal cell adhesion molecules and LESC niche-related extracellular matrix. Low expression of proliferation markers DSG3 and KRT3 indicates that cultivated primary cells exhibit a LESC phenotype. All stains were negative in hydrogel-only (no cell) control samples (data not shown).

immunohistochemistry that targeted all three ΔNp63 isoforms (α, β, and γ), previous work from Di Iorio et al. [39] indicated that LESC strictly contain the α-isoform and not β- or γ-isoforms. Differentiated corneal epithelium on the other hand does not contain any of the isoforms. In PCR analysis, a specific ΔNp63α primer was used.

Apart from KRT3, other markers that were targeted with RT-PCR have shown comparable expression between different groups. In general, a significant difference in relative expression of KRT3 between CLP and RHC I hydrogels was observed, with the RHC group showing lower expression. KRT3 expression levels for CLP hydrogels are well below levels observed for corneal epithelium (>2500; data not shown) or *in vitro*-differentiated limbal epithelial cells (Figure S4). Placing gene expression patterns into the perspective of differentiated cells indicates that all hydrogels perform extremely well, with RHC I slightly outperforming CLP DMTMM. It is not clear whether lower KRT3 expression is inherent to RHC I hydrogels or must be attributed to the adjusted culture protocol that involves 1% hAB supplementation. Both our results and the data from González et al. indicate that the concentration of hAB, more than the carrier material, might influence the level of differentiation [51]. Finally, it should be noted that KRT3 mRNA expression is relatively low (Cq value: 27-38) compared to the other investigated markers (Cq: 21-27). Therefore, mRNA expression might not be present in sufficient quantities to promote protein expression, hence, KRT3-negative IHC staining in LESC cultures. Data obtained through *in vitro* differentiation confirm this

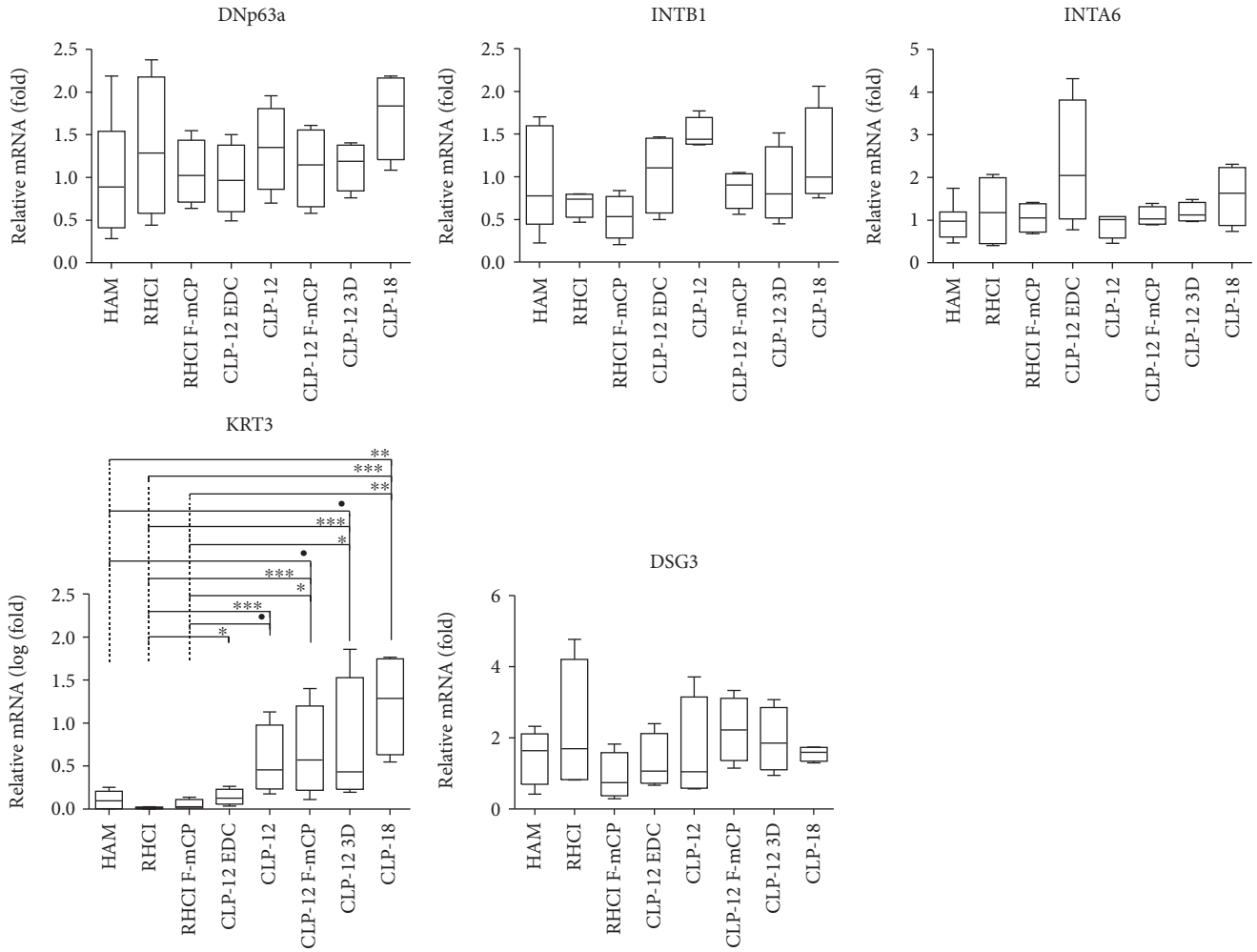

Figure 7: Relative gene expression of stem cell markers (ΔNp63α), adhesion markers (INTB1, INTA6), and differentiation markers (KRT3, DSG3) of primary limbal epithelial cells cultured on different carrier materials. Statistical significance ($p \leq 0.05$) and statistical trends ($p \leq 0.1$) were noted only for KRT3 expression. •$p \leq 0.1$; $^{*}p \leq 0.05$; $^{**}p \leq 0.01$; $^{***}p \leq 0.001$.

theory, as mRNA expression of KRT3 resulted in KRT3 protein detection (Figure S4).

Both primary cells and iHCECs were cultured in the absence of airlifting and $CaCl_2$ supplementation and therefore did not initiate differentiation nor stratification [66–68]. This may be regarded as a limitation of our study since most methods used to establish limbal epithelial cultures favor terminal differentiation over preservation of stemness [69–71]. However, for long-term restoration of the damaged ocular surface, preservation of LESC population may be required during the culture process and postgrafting [4, 39, 51, 66–68, 72–74]. Previous research using an *in vitro* RAFT TE model concluded that airlifting was not required to maintain a functional epithelium on collagen hydrogels and that a higher yield of ΔNp63α-positive cells was obtained in nonairlifted cultures [74]. In our study, we provide evidence that cells cultivated in CnT-PR successfully sustained their undifferentiated LESC state, not only on HAM [51] but also on collagen-based hydrogels. Furthermore, cells cultivated in CnT-PR maintain their ability to initiate differentiation, simply by adding 1.1 mM $CaCl_2$ to the culture medium (Figure S4).

Finally, it should be stressed that collagen-based hydrogels are highly tunable, creating opportunities previously unseen in CLET. Firstly, the thickness of collagen hydrogels can be adjusted to tackle deeper corneal disease and thus reduce the need for secondary corneal transplantation post-CLET. This would be a considerable advantage over other carrier materials such as HAM, silk fibroin, siloxane hydrogels, and fibrin-coated contact lenses [4, 5, 75, 76]. Secondly, supporting niche cells such as limbal MSCs and melanocytes could be incorporated into collagen hydrogels to allow coculture of niche-related cells. Cocultures could play an important role in the maintenance of a vast LESC side population through improved mimicry of the native stem cell niche [74, 77]. However, long-term survival of supporting niche cells and possible clinical benefit remain to be validated *in vivo*. Thirdly, collagen hydrogels offer additional opportunities of surface patterning, which is a fully customizable process. Even though our results did not indicate a short-term benefit for *in vitro* cultivation of LESC, surface patterning might potentially result in an ideal microenvironment for long-term LESC proliferation and preservation. In addition to F-μCP and 3D fabrication, other groups have suggested

surface tethering and bulk incorporation of laminin, collagen type III, Coll-IV, IKVAV, YIGSR, RGD, and vitronectin [46, 59, 78, 79]. All of these possibilities support the promise of collagen hydrogels in tissue engineering, not only in ophthalmology but also in other disciplines such orthopedics [80], dermatology [81], and cardiology [82].

5. Conclusion

Based on our findings, we conclude that RHC I and CLP hydrogels successfully support *in vitro* cultivation of iHCECs and primary LESC. When compared to HAM, primary cell cultivation on RHC I and CLP DMTMM hydrogels showed comparable (i) cell outgrowth and (ii) ΔNp63α-positive cell yield. We provide evidence that surface patterning, through 3D molding or F-μCP, influences cell attachment and cell proliferation for CLP DMTMM hydrogels but not for RHC I hydrogels. Our results indicate that surface patterning does not impact the cell phenotype or genotype, but it could be that the clinical significance of surface patterning may only become apparent in an *in vivo* setting. Finally, for reasons unknown to us, CLP-12 EDC hydrogels resulted in suboptimal primary cell cultivation and underperformed when compared to the other tested carriers. In conclusion, RHC I and CLP DMTMM show promise in the cultivation of LESC and contribute to the development of a culture protocol in which both the carrier material and culturing technique are xeno-free and fully standardized.

Data Availability

The data used to support the findings of this study are available from the corresponding author upon request.

Conflicts of Interest

RV and MG are co-founders, majority and minority shareholders of UAB Ferentis, respectively. The CLP-PEG hydrogel technology is patented by UAB Ferentis, WO2016/165788A1.

Authors' Contributions

Nadia Zakaria, Isabel Pintelon, and Marie-José Tassignon equally contributed to this work.

Acknowledgments

We gratefully acknowledge funding from the Research Foundation Flanders (FWO - 11ZB315N), EuroNanoMed2 (REGENERATE), European Cooperation in Science and Technology (EU-COST BM1302), Tekes (Finnish funding agency of innovation), University of Tampere Graduate School for Medicine and Life Sciences, Funds for Research in Ophthalmology, and Research Council of Lithuania (grant EuroNanoMed2—01/2015). The authors thank Nezahat Bostan and Sara Van Acker for the procurement of amniotic membranes and cadaveric donor eyes. We thank Sofie Thys, Elien Theuns, and Carine Moers for their contribution in electron microscopy and Peter Verstraelen and Dominique De Rijck for their assistance in confocal microscopy. Erik Fransen is acknowledged for performing statistical analysis of qPCR data. Agnė Vailionytė and Gintarė Garbenčiūtė from Ferentis are thanked for the production of CLP hydrogels and performing F-μCP, respectively. Tsvika Shtein and Amit Yaari from Hebrew University in Rehovot are acknowledged for producing RHC I hydrogels.

Supplementary Materials

Supplementary 1. Figure S1: surface modification of RHC I and DMTMM-crosslinked CLP-12 hydrogels. Fluorescence micrograph of RHC I (a) and CLP (b) hydrogel that have been surface modified with 488 nm fluorescent fibronectin. SEM image (c) of CLP-12 3D hydrogels with grooves that are 50 μm wide and 20 μm deep.

Supplementary 2. "Physical characterization of carrier membranes—Fig. S2": methodology and results of physical characterization of tested carrier materials. Figure S2 is an illustration of the cumulative permeability of the tested collagen hydrogels and HAM.

Supplementary 3. Figure S3: Live/Dead staining of iHCECs cultured on various carrier membranes.

Supplementary 4. Figure S4: characterization of in vitro differentiation of primary limbal epithelial cells.

Supplementary 5. Table S1: antibodies used in immunohistochemical analyses.

Supplementary 6. Table S2: relative fold change in gene expression of limbal epithelium cultivated on different carrier materials.

References

[1] J. W. McTigue, "The human cornea: a light and electron microscopic study of the normal cornea and its alterations in various dystrophies," *Transactions of the American Ophthalmological Society*, vol. 65, pp. 591–660, 1967.

[2] G. Cotsarelis, S.-Z. Cheng, G. Dong, T.-T. Sun, and R. M. Lavker, "Existence of slow-cycling limbal epithelial basal cells that can be preferentially stimulated to proliferate: implications on epithelial stem cells," *Cell*, vol. 57, no. 2, pp. 201–209, 1989.

[3] M. S. Shapiro, J. Friend, and R. A. Thoft, "Corneal re-epithelialization from the conjunctiva," *Investigative Ophthalmology & Visual Science*, vol. 21, no. 1, pp. 135–142, 1981.

[4] G. Pellegrini, C. E. Traverso, A. T. Franzi, M. Zingirian, R. Cancedda, and M. De Luca, "Long-term restoration of damaged corneal surfaces with autologous cultivated corneal epithelium," *The Lancet*, vol. 349, no. 9057, pp. 990–993, 1997.

[5] M. Haagdorens, S. I. Van Acker, V. Van Gerwen et al., "Limbal stem cell deficiency: current treatment options and emerging therapies," *Stem Cells International*, vol. 2016, Article ID 9798374, 22 pages, 2016.

[6] A. Rotth, "Plastic repair of conjunctival defects with fetal membrane," *Archives of Ophthalmology*, vol. 23, no. 3, pp. 522–525, 1940.

[7] J. C. Kim and S. C. Tseng, "Transplantation of preserved human amniotic membrane for surface reconstruction in

severely damaged rabbit corneas," *Cornea*, vol. 14, no. 5, pp. 473–484, 1995.

[8] H. Niknejad, H. Peirovi, M. Jorjani, A. Ahmadiani, J. Ghanavi, and A. M. Seifalian, "Properties of the amniotic membrane for potential use in tissue engineering," *European Cells & Materials*, vol. 7, pp. 88–99, 2008.

[9] I. Mariappan, S. Maddileti, S. Savy et al., "In vitro culture and expansion of human limbal epithelial cells," *Nature Protocols*, vol. 5, no. 8, pp. 1470–1479, 2010.

[10] C. J. Connon, J. Doutch, B. Chen et al., "The variation in transparency of amniotic membrane used in ocular surface regeneration," *The British Journal of Ophthalmology*, vol. 94, no. 8, pp. 1057–1061, 2010.

[11] J.-J. Gicquel, H. S. Dua, A. Brodie et al., "Epidermal growth factor variations in amniotic membrane used for ex vivo tissue constructs," *Tissue Engineering Part A*, vol. 15, no. 8, pp. 1919–1927, 2009.

[12] M. J. López-Valladares, M. Teresa Rodríguez-Ares, R. Touriño, F. Gude, M. Teresa Silva, and J. Couceiro, "Donor age and gestational age influence on growth factor levels in human amniotic membrane," *Acta Ophthalmologica*, vol. 88, no. 6, pp. e211–e216, 2010.

[13] I. Massie, A. K. Kureshi, S. Schrader, A. J. Shortt, and J. T. Daniels, "Optimization of optical and mechanical properties of real architecture for 3-dimensional tissue equivalents: towards treatment of limbal epithelial stem cell deficiency," *Acta Biomaterialia*, vol. 24, pp. 241–250, 2015.

[14] K. N. Nguyen, S. Bobba, A. Richardson et al., "Native and synthetic scaffolds for limbal epithelial stem cell transplantation," *Acta Biomaterialia*, vol. 65, pp. 21–35, 2018.

[15] H. S. Geggel, J. Friend, and R. A. Thoft, "Collagen gel for ocular surface," *Investigative Ophthalmology & Visual Science*, vol. 26, no. 6, pp. 901–905, 1985.

[16] J. Glowacki and S. Mizuno, "Collagen scaffolds for tissue engineering," *Biopolymers*, vol. 89, no. 5, pp. 338–344, 2008.

[17] P. Fagerholm, N. S. Lagali, D. J. Carlsson, K. Merrett, and M. Griffith, "Corneal regeneration following implantation of a biomimetic tissue-engineered substitute," *Clinical and Translational Science*, vol. 2, no. 2, pp. 162–164, 2009.

[18] O. Buznyk, N. Pasyechnikova, M. M. Islam, S. Iakymenko, P. Fagerholm, and M. Griffith, "Bioengineered corneas grafted as alternatives to human donor corneas in three high-risk patients," *Clin Transl Sci*, vol. 8, no. 5, pp. 558–562, 2015.

[19] P. Fagerholm, N. S. Lagali, J. A. Ong et al., "Stable corneal regeneration four years after implantation of a cell-free recombinant human collagen scaffold," *Biomaterials*, vol. 35, no. 8, pp. 2420–2427, 2014.

[20] M. M. Islam, O. Buznyk, J. C. Reddy et al., "Biomaterials-enabled cornea regeneration in patients at high risk for rejection of donor tissue transplantation," *NPJ Regenerative Medicine*, vol. 3, no. 1, p. 2, 2018.

[21] M. Mirazul Islam, V. Cėpla, C. He et al., "Functional fabrication of recombinant human collagen–phosphorylcholine hydrogels for regenerative medicine applications," *Acta Biomaterialia*, vol. 12, pp. 70–80, 2015.

[22] J. J. Willard, J. W. Drexler, A. Das et al., "Plant-derived human collagen scaffolds for skin tissue engineering," *Tissue Engineering Part A*, vol. 19, no. 13-14, pp. 1507–1518, 2013.

[23] C. M. Rubert Pérez, N. Stephanopoulos, S. Sur, S. S. Lee, C. Newcomb, and S. I. Stupp, "The powerful functions of peptide-based bioactive matrices for regenerative medicine," *Annals of Biomedical Engineering*, vol. 43, no. 3, pp. 501–514, 2015.

[24] R. M. Capito, H. S. Azevedo, Y. S. Velichko, A. Mata, and S. I. Stupp, "Self-assembly of large and small molecules into hierarchically ordered Sacs and membranes," *Science*, vol. 10, no. 5871, pp. 369–385, 2008.

[25] H. Stein, M. Wilensky, Y. Tsafrir et al., "Production of bioactive, post-translationally modified, heterotrimeric, human recombinant type-I collagen in transgenic tobacco," *Biomacromolecules*, vol. 10, no. 9, pp. 2640–2645, 2009.

[26] L. E. R. O'Leary, J. A. Fallas, E. L. Bakota, M. K. Kang, and J. D. Hartgerink, "Multi-hierarchical self-assembly of a collagen mimetic peptide from triple helix to nanofibre and hydrogel," *Nature Chemistry*, vol. 3, no. 10, pp. 821–828, 2011.

[27] J. R. Jangamreddy, M. K. C. Haagdorens, M. Mirazul Islam et al., "Corrigendum to "short peptide analogs as alternatives to collagen in pro-regenerative corneal implants" [Acta Biomaterialia 69 (2018) 120–130]," *Acta Biomaterialia*, vol. 81, pp. 330-331, 2018.

[28] M. Islam, R. Ravichandran, D. Olsen et al., "Self-assembled collagen-like-peptide implants as alternatives to human donor corneal transplantation," *RSC Advances*, vol. 6, no. 61, pp. 55745–55749, 2016.

[29] S. Shilo, S. Roth, T. Amzel et al., "Cutaneous wound healing after treatment with plant-derived human recombinant collagen flowable gel," *Tissue Engineering Part A*, vol. 19, no. 13-14, pp. 1519–1526, 2013.

[30] D. Olsen, C. Yang, M. Bodo et al., "Recombinant collagen and gelatin for drug delivery," *Advanced Drug Delivery Reviews*, vol. 55, no. 12, pp. 1547–1567, 2003.

[31] N. Lagali, M. Griffith, P. Fagerholm, K. Merrett, M. Huynh, and R. Munger, "Innervation of tissue-engineered recombinant human collagen-based corneal substitutes: a comparative in vivo confocal microscopy study," *Investigative Ophthalmology & Visual Science*, vol. 49, no. 9, pp. 3895–3902, 2008.

[32] K. Merrett, P. Fagerholm, C. R. McLaughlin et al., "Tissue-engineered recombinant human collagen-based corneal substitutes for implantation: performance of type I versus type III collagen," *Investigative Ophthalmology & Visual Science*, vol. 49, no. 9, pp. 3887–3894, 2008.

[33] T. Ihanamäki, L. J. Pelliniemi, and E. Vuorio, "Collagens and collagen-related matrix components in the human and mouse eye," *Progress in Retinal and Eye Research*, vol. 23, no. 4, pp. 403–434, 2004.

[34] N. Zakaria, C. Koppen, V. Van Tendeloo, Z. Berneman, A. Hopkinson, and M.-J. Tassignon, "Standardized Limbal epithelial stem cell graft generation and transplantation," *Tissue Engineering. Part C, Methods*, vol. 16, no. 5, pp. 921–927, 2010.

[35] K. Araki-Sasaki, Y. Ohashi, T. Sasabe et al., "An SV40-immortalized human corneal epithelial cell line and its characterization," *Investigative Ophthalmology & Visual Science*, vol. 36, no. 3, pp. 614–621, 1995.

[36] T. D. Schmittgen and K. J. Livak, "Analyzing real-time PCR data by the comparative C(T) method," *Nature Protocols*, vol. 3, no. 6, pp. 1101–1108, 2008.

[37] V. Barbaro, A. A. Nasti, P. Raffa et al., "Personalized stem cell therapy to correct corneal defects due to a unique homozygous-heterozygous mosaicism of ectrodactyly-ectodermal dysplasia-clefting syndrome," *Stem Cells Translational Medicine*, vol. 5, no. 8, pp. 1098–1105, 2016.

[38] E. C. Figueira, N. Di Girolamo, M. T. Coroneo, and D. Wakefield, "The phenotype of Limbal epithelial stem cells," *Investigative Opthalmology & Visual Science*, vol. 48, no. 1, pp. 144–156, 2007.

[39] E. Di Iorio, V. Barbaro, A. Ruzza, D. Ponzin, G. Pellegrini, and M. De Luca, "Isoforms of ΔNp63 and the migration of ocular limbal cells in human corneal regeneration," *Proceedings of the National Academy of Sciences of the United States of America*, vol. 102, no. 27, pp. 9523–9528, 2005.

[40] M. A. Kurpakus, M. T. Maniaci, and M. Esco, "Expression of keratins K12, K4 and K14 during development of ocular surface epithelium," *Current Eye Research*, vol. 13, no. 11, pp. 805–814, 1994.

[41] A. Schermer, S. Galvin, and T. T. Sun, "Differentiation-related expression of a major 64K corneal keratin in vivo and in culture suggests limbal location of corneal epithelial stem cells," *The Journal of Cell Biology*, vol. 103, no. 1, pp. 49–62, 1986.

[42] U. Schlötzer-Schrehardt, T. Dietrich, K. Saito et al., "Characterization of extracellular matrix components in the limbal epithelial stem cell compartment," *Experimental Eye Research*, vol. 85, no. 6, pp. 845–860, 2007.

[43] N. Polisetti, M. Zenkel, J. Menzel-Severing, F. E. Kruse, and U. Schlötzer-Schrehardt, "Cell adhesion molecules and stem cell-niche-interactions in the limbal stem cell niche," *Stem Cells*, vol. 34, no. 1, pp. 203–219, 2016.

[44] A. V. Ljubimov, R. E. Burgeson, R. J. Butkowski, A. F. Michael, T. T. Sun, and M. C. Kenney, "Human corneal basement membrane heterogeneity: topographical differences in the expression of type IV collagen and laminin isoforms," *Laboratory Investigation*, vol. 72, no. 4, pp. 461–473, 1995.

[45] A. Modesti, S. Scarpa, G. D'Orazi, L. Simonelli, and F. G. Caramia, "Localization of type IV and V collagens in the stroma of human amnion," *Progress in Clinical and Biological Research*, vol. 296, pp. 459–463, 1989.

[46] N. Polisetti, L. Sorokin, N. Okumura et al., "Laminin-511 and -521-based matrices for efficient ex vivo-expansion of human limbal epithelial progenitor cells," *Scientific Reports*, vol. 7, no. 1, p. 5152, 2017.

[47] D. H.-K. Ma, H.-C. Chen, K. S.-K. Ma et al., "Preservation of human limbal epithelial progenitor cells on carbodiimide cross-linked amniotic membrane via integrin-linked kinase-mediated Wnt activation," *Acta Biomaterialia*, vol. 31, pp. 144–155, 2016.

[48] B. E. Ramírez, A. Sánchez, J. M. Herreras et al., "Stem cell therapy for corneal epithelium regeneration following good manufacturing and clinical procedures," *BioMed Research International*, vol. 2015, 19 pages, 2015.

[49] I. R. Schwab, N. T. Johnson, and D. G. Harkin, "Inherent risks associated with manufacture of bioengineered ocular surface tissue," *Archives of Ophthalmology*, vol. 124, no. 12, pp. 1734–1740, 2006.

[50] Z. Lužnik, C. Breda, V. Barbaro et al., "Towards xeno-free cultures of human limbal stem cells for ocular surface reconstruction," *Cell and Tissue Banking*, vol. 18, no. 4, pp. 461–474, 2017.

[51] S. González, L. Chen, and S. X. Deng, "Comparative study of xenobiotic-free media for the cultivation of human limbal epithelial stem/progenitor cells," *Tissue Engineering. Part C, Methods*, vol. 23, no. 4, pp. 219–227, 2017.

[52] Y. Liu, L. Gan, D. J. Carlsson et al., "A simple, cross-linked collagen tissue substitute for corneal implantation," *Investigative Ophthalmology & Visual Science*, vol. 47, no. 5, pp. 1869–1875, 2006.

[53] M. D'Este, D. Eglin, and M. Alini, "A systematic analysis of DMTMM vs EDC/NHS for ligation of amines to hyaluronan in water," *Carbohydrate Polymers*, vol. 108, pp. 239–246, 2014.

[54] A. Leitner, L. A. Joachimiak, P. Unverdorben et al., "Chemical cross-linking/mass spectrometry targeting acidic residues in proteins and protein complexes," *Proceedings of the National Academy of Sciences of the United States of America*, vol. 111, no. 26, pp. 9455–9460, 2014.

[55] C. Samarawickrama, A. Samanta, A. Liszka et al., "Collagen--based fillers as alternatives to cyanoacrylate glue for the sealing of large corneal perforations," *Cornea*, vol. 37, no. 5, pp. 609–616, 2018.

[56] K. Yamasaki, S. Kawasaki, R. D. Young et al., "Genomic aberrations and cellular heterogeneity in SV40-immortalized human corneal epithelial cells," *Investigative Ophthalmology & Visual Science*, vol. 50, no. 2, p. 604, 2009.

[57] W. Liu, K. Merrett, M. Griffith et al., "Recombinant human collagen for tissue engineered corneal substitutes," *Biomaterials*, vol. 29, no. 9, pp. 1147–1158, 2008.

[58] S. Dravida, S. Gaddipati, M. Griffith et al., "A biomimetic scaffold for culturing limbal stem cells: a promising alternative for clinical transplantation," *Journal of Tissue Engineering and Regenerative Medicine*, vol. 2, no. 5, pp. 263–271, 2008.

[59] T. A. Hogerheyde, S. Suzuki, J. Walshe et al., "Optimization of corneal epithelial progenitor cell growth on *Bombyx mori* silk fibroin membranes," *Stem Cells International*, vol. 2016, Article ID 8310127, 11 pages, 2016.

[60] J. T. Jacob, J. R. Rochefort, J. Bi, and B. M. Gebhardt, "Corneal epithelial cell growth over tethered-protein/peptide surface-modified hydrogels," *Journal of Biomedical Materials Research Part B, Applied Biomaterials*, vol. 72B, no. 1, pp. 198–205, 2005.

[61] H. J. Levis, I. Massie, M. A. Dziasko, A. Kaasi, and J. T. Daniels, "Rapid tissue engineering of biomimetic human corneal limbal crypts with 3D niche architecture," *Biomaterials*, vol. 34, no. 35, pp. 8860–8868, 2013.

[62] H. J. Levis and J. T. Daniels, "Recreating the human limbal epithelial stem cell niche with bioengineered limbal crypts," *Current Eye Research*, vol. 41, no. 9, pp. 1153–1160, 2016.

[63] T. Alekseeva, E. Hadjipanayi, E. A. Abou Neel, and R. A. Brown, "Engineering stable topography in dense bio-mimetic 3D collagen scaffolds," *European Cells and Materials*, vol. 23, pp. 28–40, 2012.

[64] Z.-H. Zhang, H.-Y. Liu, K. Liu, and X. Xu, "Comparison of explant and enzyme digestion methods for *ex vivo* isolation of limbal epithelial progenitor cells," *Current Eye Research*, vol. 41, no. 3, pp. 318–325, 2015.

[65] T. Nieto-Miguel, M. Calonge, A. de la Mata et al., "A comparison of stem cell-related gene expression in the progenitor-rich limbal epithelium and the differentiating central corneal epithelium," *Molecular Vision*, vol. 17, pp. 2102–2117, 2011.

[66] K. Lekhanont, L. Choubtum, R. S. Chuck, T. Sa-ngiampornpanit, V. Chuckpaiwong, and A. Vongthongsri, "A serum- and feeder-free technique of culturing human corneal epithelial stem cells on amniotic membrane," *Molecular Vision*, vol. 15, pp. 1294–1302, 2009.

[67] Y. Minami, H. Sugihara, and S. Oono, "Reconstruction of cornea in three-dimensional collagen gel matrix culture,"

Investigative Ophthalmology & Visual Science, vol. 34, no. 7, pp. 2316–2324, 1993.

[68] B. Chen, S. Mi, B. Wright, and C. J. Connon, "Differentiation status of limbal epithelial cells cultured on intact and denuded amniotic membrane before and after air-lifting," *Tissue Engineering. Part A*, vol. 16, no. 9, pp. 2721–2729, 2010.

[69] M. K. Kim, J. L. Lee, J. Y. Oh et al., "Efficient cultivation conditions for human limbal epithelial cells," *Journal of Korean Medical Science*, vol. 23, no. 5, pp. 864–869, 2008.

[70] M. S. Lehrer, T. T. Sun, and R. M. Lavker, "Strategies of epithelial repair: modulation of stem cell and transit amplifying cell proliferation," *Journal of Cell Science*, vol. 177, no. 19, pp. 63–67, 1998.

[71] T. T. Sun and H. Green, "Cultured epithelial cells of cornea, conjunctiva and skin: absence of marked intrinsic divergence of their differentiated states," *Nature*, vol. 269, no. 5628, pp. 489–493, 1977.

[72] R. R. Loureiro, P. C. Cristovam, C. M. Martins et al., "Comparison of culture media for ex vivo cultivation of limbal epithelial progenitor cells," pp. 69–77, 2013.

[73] G. Pellegrini, O. Golisano, P. Paterna et al., "Location and clonal analysis of stem cells and their differentiated progeny in the human ocular surface," *The Journal of Cell Biology*, vol. 145, no. 4, pp. 769–782, 1999.

[74] I. Massie, H. J. Levis, and J. T. Daniels, "Response of human limbal epithelial cells to wounding on 3D RAFT tissue equivalents: effect of airlifting and human limbal fibroblasts," *Experimental Eye Research*, vol. 127, pp. 196–205, 2014.

[75] Y. Li, Y. Yang, L. Yang, Y. Zeng, X. Gao, and H. Xu, "Poly(ethylene glycol)-modified silk fibroin membrane as a carrier for limbal epithelial stem cell transplantation in a rabbit LSCD model," *Stem Cell Research & Therapy*, vol. 8, no. 1, p. 256, 2017.

[76] N. Di Girolamo, M. Bosch, K. Zamora, M. T. Coroneo, D. Wakefield, and S. L. Watson, "A contact lens-based technique for expansion and transplantation of autologous epithelial progenitors for ocular surface reconstruction," *Transplantation*, vol. 87, no. 10, pp. 1571–1578, 2009.

[77] A. K. Kureshi, M. Dziasko, J. L. Funderburgh, and J. T. Daniels, "Human corneal stromal stem cells support limbal epithelial cells cultured on RAFT tissue equivalents," *Scientific Reports*, vol. 5, no. 1, p. 16186, 2015.

[78] E. A. Gosselin, T. Torregrosa, C. E. Ghezzi et al., "Multilayered silk film coculture system for human corneal epithelial and stromal stem cells," *Journal of Tissue Engineering and Regenerative Medicine*, vol. 12, no. 1, pp. 285–295, 2017.

[79] S. Mi, V. V. Khutoryanskiy, R. R. Jones, X. Zhu, I. W. Hamley, and C. J. Connon, "Photochemical cross-linking of plastically compressed collagen gel produces an optimal scaffold for corneal tissue engineering," *Biomedical Materials Research Part A*, vol. 367, no. 1, pp. 365–374, 2011.

[80] D. Docheva, S. A. Müller, M. Majewski, and C. H. Evans, "Biologics for tendon repair," *Advanced Drug Delivery Reviews*, vol. 84, pp. 222–239, 2015.

[81] S. Shahrokhi, A. Arno, and M. G. Jeschke, "The use of dermal substitutes in burn surgery: acute phase," *Wound Repair and Regeneration*, vol. 22, no. 1, pp. 14–22, 2014.

[82] A. Kochegarov and L. F. Lemanski, "New trends in heart regeneration: a review," *Journal of stem cells & Regenerative medicine*, vol. 12, no. 2, pp. 61–68, 2016.

Hindawi
Stem Cells International
Volume 2019, Article ID 8203950, 20 pages
https://doi.org/10.1155/2019/8203950

Review Article

Unchain My Heart: Integrins at the Basis of iPSC Cardiomyocyte Differentiation

Rosaria Santoro,[1] **Gianluca Lorenzo Perrucci**,[1] **Aoife Gowran**,[1] **and Giulio Pompilio**[1,2]

[1]*Unità di Biologia Vascolare e Medicina Rigenerativa, Centro Cardiologico Monzino IRCCS, via Carlo Parea 4, Milan, Italy*
[2]*Dipartimento di Scienze Cliniche e di Comunità, Università degli Studi di Milano, via Festa del Perdono 7, Milan, Italy*

Correspondence should be addressed to Rosaria Santoro; rosaria.santoro@ccfm.it
and Gianluca Lorenzo Perrucci; gianluca.perrucci@ccfm.it

Received 31 October 2018; Revised 20 December 2018; Accepted 10 January 2019; Published 13 February 2019

Guest Editor: Tiago Fernandes

The cellular response to the extracellular matrix (ECM) microenvironment mediated by integrin adhesion is of fundamental importance, in both developmental and pathological processes. In particular, mechanotransduction is of growing importance in groundbreaking cellular models such as induced pluripotent stem cells (iPSC), since this process may strongly influence cell fate and, thus, augment the precision of differentiation into specific cell types, e.g., cardiomyocytes. The decryption of the cellular machinery starting from ECM sensing to iPSC differentiation calls for new *in vitro* methods. Conveniently, engineered biomaterials activating controlled integrin-mediated responses through chemical, physical, and geometrical designs are key to resolving this issue and could foster clinical translation of optimized iPSC-based technology. This review introduces the main integrin-dependent mechanisms and signalling pathways involved in mechanotransduction. Special consideration is given to the integrin-iPSC linkage signalling chain in the cardiovascular field, focusing on biomaterial-based *in vitro* models to evaluate the relevance of this process in iPSC differentiation into cardiomyocytes.

1. Introduction

The integrin protein family is a large group of transmembrane receptors, particularly involved in cell-extracellular matrix (ECM) proteins and cell-cell adhesion. Moreover, integrins constitute an important and functional bridge between the ECM and the cytoskeleton and are able to activate several intracellular signalling pathways. After the first report of their identification [1, 2], in the last 30 years, how the integrin protein family assumed a key role in mechanotransduction biology, particularly as mediators of a bidirectional signalling mode, has been extensively reported. Integrins are able to read and transmit signals from the extracellular microenvironment to the internal cellular *milieu*, including the cytoplasm and nucleus (outside-in), leading to a cellular reaction that may alter cell behaviour and/or also the composition of the ECM (inside-out). Several downstream mechanisms of integrins activate biochemical signalling cascades which have impact on different cell functions by regulating crucial molecular pathways involved in cell survival, proliferation, motility, and differentiation, both in physiological and pathological scenarios [3–6].

In 2007, the groundbreaking discovery of a universal protocol to reprogram mammalian somatic cells into induced pluripotent stem cells (iPSC) [7], made by Takahashi and colleagues, brought immense potential to the fields of regenerative and personalized medicine. In fact, these cells can differentiate into cell types from all the three developmental germ layers: ectoderm, mesoderm, and endoderm. iPSC-derived cells have modelled, previously unreproducible, human diseases, e.g., long QT (LQT) syndrome [8], and have already been used in two clinical trials for age-related macular degeneration [9] and advanced heart failure [10].

The efficacy of iPSC as a model system for the study of the molecular mechanisms guiding pathological development is tightly linked to the success of *in vitro* simulation of the environmental cues responsible for cell fate *in vivo*. Mechanosensing-mediated pathways are relevant not only

for enhancing iPSC reprogramming efficiency [11] but also for supporting iPSC-derived cardiomyocyte (iPSC-d-CM) maturation [12]. Thus, several techniques have been proposed for the design of substrates regulating integrin activation by tuning chemical, geometrical, or mechanical parameters. The last part of this review is dedicated to the discussion of these methods and their relevance to spearheading the clinical translation of the iPSC technology.

2. Integrin Structure, Extracellular Ligands, and Focal Adhesion (FA) Complexes

The integrin family was firstly identified by using antibodies against integrin β subunits which unveiled several coimmunoprecipitating proteins. Integrin heterodimers are composed of noncovalently associated α and β subunits [3]. The heterodimeric structure and functionality of these receptors were made clear only after the use of specific peptides, e.g., arginine-glycine-aspartic acid (Arg-Gly-Asp; RGD tripeptide) and integrin α subunit-recognizing antibodies. To date, it is well known that the integrin family is constituted by 18 α subunits and 8 β subunits, possibly assembled in 24 different heterodimers [13]. Depending on integrin subunit composition, these molecules show specific extracellular ligand properties and can be classified into 4 main subgroups [14] listed in Table 1. This feature implies that the expression pattern of integrins is tissue specific [3]. In addition to a large extracellular domain, each heterodimer also has a transmembrane domain and a short cytoplasmic domain, which forms a fundamental functional link with the cytoskeleton [14].

As shown in Table 1, cells expressing β1 integrin are generally outbound to collagen when associated with α1, α2, α10, and α11 subunits. Otherwise, when β1 integrin is bound to laminin, it is complexed with α3, α6, and α7 subunits. Depending on which specific α subunit it heterodimerizes with, β1 integrin recognizes the RGD motif ($\alpha v\beta$1, α5β1, or α8β1) or leukocyte-specific receptors (α9β1, α4β1). All integrin heterodimers containing αv subunits are specifically associated with substrates with the RGD sequence. Similarly, all integrins expressing β2 subunit are members of the leukocyte-specific receptor-binding integrin subgroup. Lastly, α6β4 integrin belongs to the previously mentioned laminin receptor binding group [15].

It has been reported that β1 subunit-containing integrins, such as α5β1, are predominantly recruited to the leading edge of cells moving on a 2D surface [16], whereas β3 subunit-containing integrins are responsible for the increase in the number of focal adhesions (FA) and cell spreading area because of its role in structural reinforcement of adhesion [17, 18].

Since integrins work as receptors of several ECM components, they strongly contribute individually to FA-mediated signalling and rigidity sensing by mechanically changing their structural conformation. In external force mechanosensing, this integrin function can be considered as a primary step, followed by a series of secondary mechanosensor activities, which respond intracellularly to force-dependent alterations. Thus, extracellular tension transmitted through integrins elicits the binding of several intracellular elements, which in turn activate themselves and strengthen the integrin connection to actin (Figure 1(a)). Among these intracellular factors, the main ones involved in mechanotransduction are talin, vinculin, kindlin, α-actinin, zyxin, filamin, and p130Cas. The interaction of integrin cytoplasmic tails with one of these adaptor proteins, such as talin, is the main mechanism leading to full integrin activation. For example, talin, together with vinculin, plays a crucial role in the force-dependent stabilization of FA by changing its conformation after tension. Talin binds through its FERM (four-point-one protein/ezrin/radixin/moesin) domain to the NPxY amino acid motifs on integrin tails, inducing their activation [19–21]. Vinculin presents a self-inhibited state, exerted by its head and tail domain interaction [22], and becomes activated after its tail domain binds to α-actinin alone or together with actin and phosphatidyl-inositol-4,5-bisphosphate (PIP2) [23–26]. An increase in cellular tension, which is strictly related to ECM stiffness and cytoskeletal recruitment, stabilizes vinculin in the activated conformation, and leads to its FA recruitment [27, 28]. Another cooperating adaptor protein is kindlin which contributes to integrin activation [29, 30]. Until this link of the mechanotransduction chain, talin and vinculin act as direct mechanical sensors, able to feel ECM properties, while α-actinin, a spectrin superfamily component important for the structural organization of the cell, also provides a scaffold to connect the mechanotransduction chain with the previously mentioned downstream effectors [31]. Thus, α-actinin is an indirect link in the mechanotransduction chain. For this reason, cell stretching could result in the dissociation of several proteins that are weakly bound to α-actinin at multiple sites [32]. Among these weakly bound proteins, zyxin binds a central region of α-actinin [33]; when a certain type of mechanical stimulus occurs, this molecule translocates from FA to stress fibres [34]. Other connecting proteins between integrins and actin such as filamins [35] play a mechanoprotective role by stabilizing the actin cytoskeleton through linkage to the cytoplasmatic membrane. In fact, under mechanical stress, filamin domains change their conformational status considerably [36]. This event leads to extension and reversible unfolding [37], which allows filamin stretching and subsequent protection of the linkage between F-actin and the cytoplasmatic membrane [38]. Interestingly, force applied through clustered β1 integrins leads to the transcriptional upregulation of filamin A [39].

Lastly, Src family kinase p130Cas (Cas: Crk-associated substrate) contains a N-terminal SH3 domain, which binds the polyproline motifs of the tyrosine kinases, FA kinase (FAK) [40, 41], and other proteins such as vinculin [42]. The SH3 domain is followed by a large substrate domain with 15 repetitions of the YxxP motif (where x is any amino acid), which is a main site of tyrosine phosphorylation on the Cas molecule [43]. Once phosphorylated, the p130Cas SH3 domain serves as a docking site for the SH2 domains of Crk or Nck adaptor proteins [44, 45]. In nonadherent cells, p130Cas is localized in the cytoplasm and, after integrin receptor activation, translocates to FA where the phosphorylation of substrate domain tyrosine residues takes place [46]. p130Cas activation after integrin engagement

Table 1: Integrin heterodimers, extracellular ligands and downstream signalling pathways.

	Integrin heterodimers	Ligands	Pathway	Ref.
Collagen receptor	$\alpha1\beta1$	Collagen (IV, I, and IX)	(i) RhoA/ROCK	[51]
	$\alpha2\beta1$	Collagen (I, IV, and IX)	(i) RhoA/ROCK (ii) YAP/TAZ	[52]
	$\alpha10\beta1$	Collagen (IV, VI, II, and IX)	(i) RhoA/ROCK	[51]
	$\alpha11\beta1$	Collagen (I, IV, and IX)	(i) RhoA/ROCK	
Laminin receptor	$\alpha3\beta1$	Laminin (LN-511, LN-332, and LN-211)	(i) RhoA/ROCK	[51]
	$\alpha7\beta1$	Laminin (LN-511, LN-211, LN-411, and LN-111)	(i) RhoA/ROCK	
	$\alpha6\beta1$	Laminin (LN-511, LN-332, LN-111, and LN-411)	(i) RhoA/ROCK	
	$\alpha6\beta4$	Laminin (LN-332, LN-511)	/	
RGD receptor	$\alpha v\beta1$	Fibronectin, vitronectin (RGD)	(i) RhoA/mDia	[17, 18, 50, 53]
	$\alpha v\beta3$	Vitronectin, fibronectin, and fibrinogen (RGD)	(i) RhoA/mDia (ii) MKL-1/SRF (Responsible for the increase in the number of FA and cell spreading areas)	
	$\alpha v\beta5$	Vitronectin (RGD)	(i) RhoA/mDia (Responsible for the increase in the number of FA and cell spreading areas)	[17, 53]
	$\alpha v\beta6$	Fibronectin, TGF-β-LAP (RGD)	/	
	$\alpha v\beta8$	Vitronectin, TGF-β-LAP (RGD)	/	
	$\alpha5\beta1$	Fibronectin (RGD)	In the leading edge of moving cells in the 2D surface	[16]
	$\alpha8\beta1$	Fibronectin, vitronectin, and nephronectin (RGD)	/	
	αIIb$\beta3$	Fibrinogen, fibronectin (RGD)	/	
Leucocyte-specific receptor	$\alpha9\beta1$	Tenascin-C, VEGF-C, and VEGF-D	/	
	$\alpha4\beta1$	Fibronectin, VCAM-1 (LDV)	/	
	$\alpha4\beta7$	MadCAM-1 (LDV), fibronectin, and VCAM-1	/	
	αD$\beta2$	ICAM-3, VCAM-1	/	
	αE$\beta2$	E-cadherin	/	
	αL$\beta2$	ICAM-1, ICAM-2, ICAM-3, and ICAM-5	/	
	αM$\beta2$	iC3b, fibrinogen	/	
	αX$\beta2$	iC3b, fibrinogen	/	

regulates the reorganization of the actin cytoskeleton and cell processes, such as spreading and migration [47]. Moreover, this tyrosine phosphorylation triggers signalling pathways leading to the regulation of cell survival and proliferation [48, 49]. Recently, investigators highlighted how p130Cas is able to influence actin remodelling and concomitant muscle-specific gene expression [42, 50].

2.1. Mechanical Stress-Reactive Nuclear Complexes. Based on the previous discussion, it can be said that cells perceive, adapt themselves to, and modify the ECM microenvironment physical features by using specific protein structures including the mechanosensing machinery of cell-ECM and cell-cell interactions, secondary mechanosensors, and different mechanotransduction pathways. Interestingly, this mechanism is mediated by a direct effect of mechanical linkage which is specific and sufficient to transmit the extracellular stimuli into the nuclei [42, 54, 55].

The strong and intimate relationship between integrins, FA, actin cytoskeleton, and nuclear structures has been well documented in the last years. Several lines of evidence report that actin fibres communicate the mechanical properties of the internal cellular environment to the nucleus and consequently strongly affecting gene regulation and expression [56, 57]. The nucleus contains a stratified network of mediators, linking the nuclear envelope to the nucleoskeleton and chromatin (Figure 1(b)). Structural alterations of nuclei are responsible for gene modulation of multiple mediators such

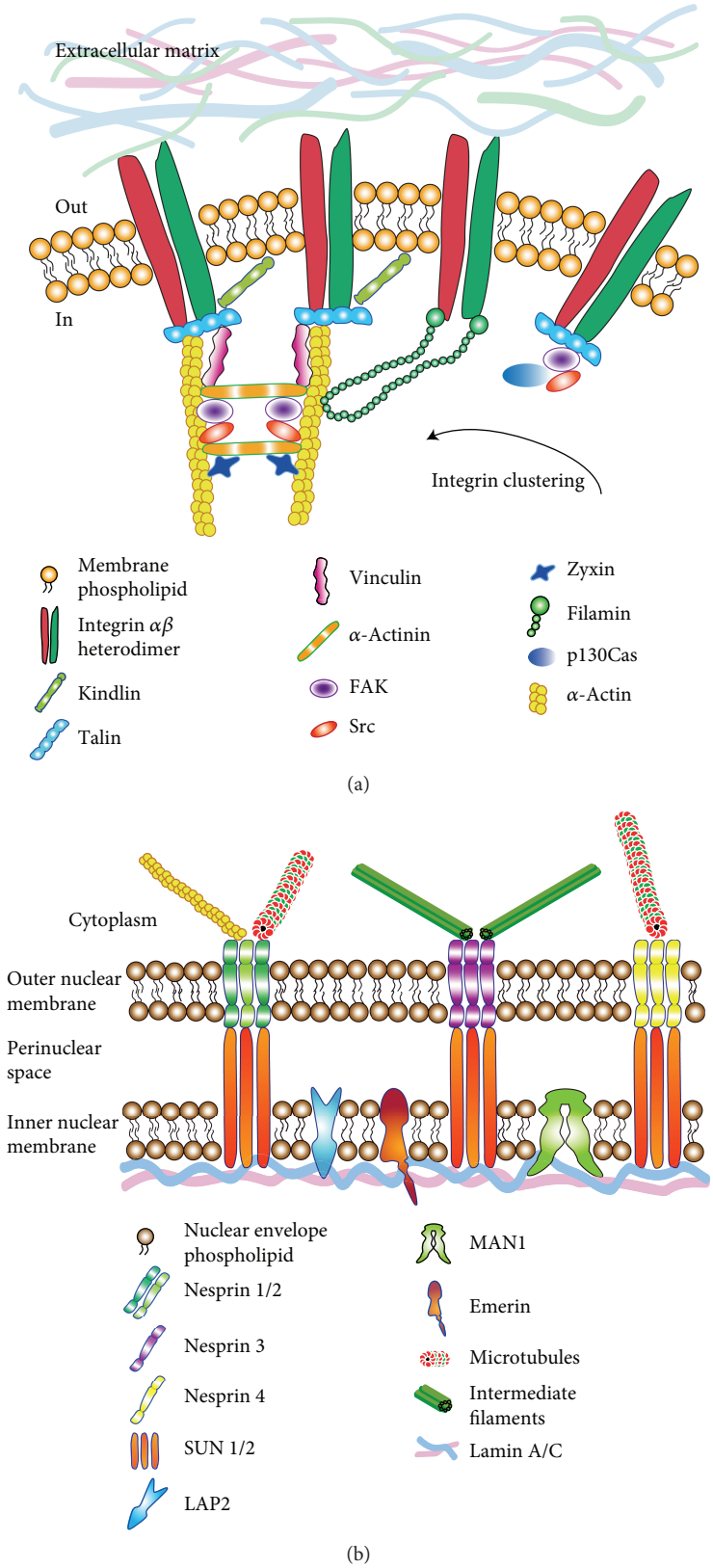

Figure 1: Cytoplasmatic membrane and nuclear envelope mechanotransduction protein complexes. (a) The image depicts the main mediators involved in the mechanotransduction chain, starting from the integrin subunits, specifically binding ECM compounds, to cytoskeleton polymerization, through the activity of focal adhesion effectors. (b) The figure summarizes the link between cytoskeleton and nuclear lamin A/C, through the nuclear envelope complexes, responsible for the gene expression modulation downstream to mechanotransduction.

as those related to mechanotransduction and differentiation [58]. The nuclear lamina consists in filamentous lamin proteins (lamins A, B, and C) that form the mechanical support of the inner nuclear membrane. Several other membrane proteins, including LAP2, emerin, and MAN1, are essential nuclear constituents [59]. To date, it is well known that the cytoskeleton is strongly linked with the nuclear lamina [60]; nevertheless, most of the current information is derived from studies on isolated nuclei [61]. Two distinct protein families, the SYNE/nesprin family and the SUN family [62] colocalize in the nuclear membrane and are connected both with cytoskeleton and nuclear lamina. Studies on *C. elegans* revealed that homologues of nesprin 2 and SUN1/2 were associated with actin, at their N- and C-terminals, respectively. For this reason, the term LINC was coined, indicating that these protein structures were linkers of nucleoskeleton and cytoskeleton [63, 64]. Every molecular component of this important complex shows distinct binding peculiarity; while nesprins 1 and 2 are specialized in actin, microtubule, and kinesin binding, on the other hand, nesprins 3 and 4 are able to bind intermediate filaments and microtubules, respectively [65–67]. Concerning the SUN protein family, the oligomerization as a trimer of these molecules is strongly required for nesprin binding [68]. These molecular events, which were experimentally observed on isolated nuclei, suggested their effectiveness in whole cell systems, thus supporting their contribution to mechanical cues. Thus, isolated nuclei react to the physical forces in a similar manner to complete cells, because of the presence of LINC complex, by which nuclei display adhesion ability acting as force-sensitive signalling hubs for cytoplasmic proteins and tuning nuclear responses to various mechanosensory inputs [61]. Finally, among LINC complex members, emerin plays a strategic role on the inner nuclear membrane, since it can be phosphorylated by Src kinases after a tension stimulus applied on isolated nuclei through nesprin 1 [61]. This event overlaps lamin A/C accumulation, which leads to the strengthening of the nuclear membrane. It is important to point out that Emery-Dreifuss muscular dystrophy is predominantly due to emerin gene mutations [69]; moreover, cells derived from emerin knockout transgenic mice show mechanotransduction impairments [62, 70].

2.2. Mechanosensing Signalling Pathways. The major chemical signals elicited by mechanical stress at the cell surface are as follows: (i) calcium influx through cation channels activated by stretch stimuli, (ii) activation of nuclear factor kappa-B (NF-κB), (iii) stimulation of mitogen-activated protein kinases (MAPKs), and (iv) changes in the activity of small GTPases, e.g., Ras, Rac1, and RhoA [71–79].

Peculiar mechanisms have been unveiled, e.g., the adaptor protein p130Cas which is physically stretched in response to applied force both *in vivo* and *in vitro*. This stimulus exposes the previously masked phosphorylatable sites of p130Cas [80], that are substrates for Src family kinases which trigger further downstream responses [81].

Among the previously mentioned signalling pathways, there are two cascades which are strongly involved in the context of integrin-mediated mechanotransduction, namely, Rac1 and RhoA. In fact, these two members of the small Rho family GTPases regulate actin assembly and contraction [82, 83]. While active Rac1 controls actin polymerization at the leading edges of motile cells and is involved in lamellipodia focal complex formation, active RhoA is necessary for stress fibre formation. Notably, the two main RhoA downstream effectors are the diaphanous-related formin protein mDia1, a formin family member that serves as an actin nucleating factor and so facilitates actin polymerization and assembly [42, 84–86] and the protein kinases ROCK-1 and ROCK-2, which promote actin contraction mediated by nonmuscle myosin-II [82, 83].

One important feature of Rac1 and RhoA is that each of these two mediators negatively regulates the other, leading to a discrimination of the activity in certain cell subareas [82], as depicted in Figure 2. Indeed, while some cell regions show higher Rac1 activity responsible for moving and protrusion, other subareas of the same cell with higher RhoA activity are more concentrated on adhesion and contraction. Several studies addressed the strong relationship between the integrin-dependent mechanical stress and the sustained modulation in Rac1 and RhoA activity [87–91]. As previously mentioned, several information on different features of small GTPase response to integrin-derived mechanical stimulation are, to date, still missing, e.g., the exact signalling time course and the types of cells and stresses involved. However, it is well established that mechanical stimulation leads to small GTPase activity driving the cell to undergo a strong and complex actin cytoskeleton remodelling which also influences the adhesion features [92].

The main molecular events leading to the activation of these numerous pathways are considerably distinct and depend on the signal being activated. Activation of tyrosine kinases and protein tyrosine phosphorylation play crucial roles in the assembly and turnover of FA, as well as in mechanotransduction. FAK and members of the Src family are key tyrosine kinases, controlling FA functions and complex stability [93]. After integrin engagement, FAK is recruited to adhesion areas to provide both scaffolding and kinase activity. The autophosphorylation of FAK defines a docking site for Src kinase, which subsequently phosphorylates FAK on multiple tyrosine residues. All these events are helpful for full FAK activation [94]. Following this, the FAK-Src complex recruits the p130Cas protein and several other adaptor proteins, phosphorylating multiple residues on their sequence. After FAK autophosphorylation and the generation of docking substrates for the SH2 domains of the adaptor protein Crk (also known as p38), this interaction leads to the activation of downstream signalling cascades, such as Rac1 GTPase, previously reported as the pathway involved in actin polymerization and the formation of new focal complexes at the leading edge of the cell [95, 96]. It has been demonstrated that inhibitors of actomyosin contractility lead to a loss of tension due to a rapid dismantling of FA [23, 27]. Mechanical tension activates guanine nucleotide exchange factors (GEFs) for Rho, such as Vav2, GEF-H1, or LARG, which subsequently induce GTP loading of Rho. This leads, in turn, to the activation of downstream effectors

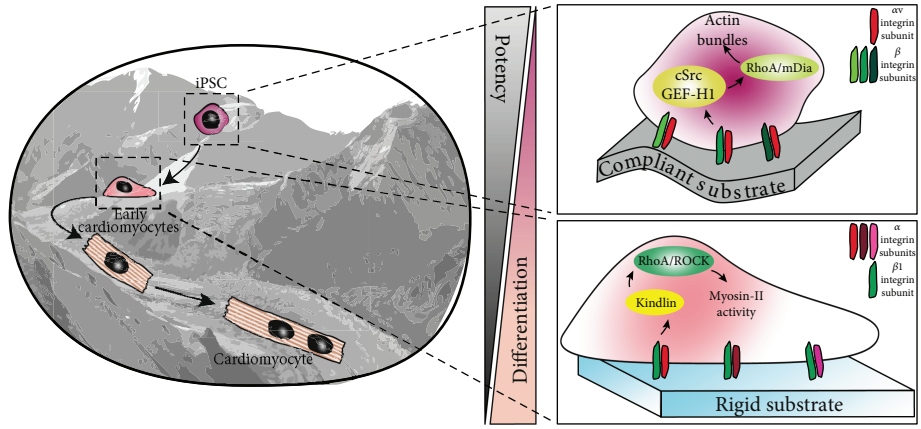

Figure 2: Integrin expression in iPSC at different stages of differentiation. The picture on (a), inspired by the Waddington diagram and John Piper's original artwork [103], represents iPSC undergoing cardiomyocyte differentiation. During these early stages, cells lose their potency, acquiring, in parallel, cardiomyocyte features. This process is linked to a specific integrin expression, further exacerbated by the growing substrates. As displayed in (b), cells with a higher potency and a lower degree of differentiation express, on compliant substrates, a higher amount of integrin heterodimers, preferentially containing αv integrin subunits. On the other hand, iPSC on rigid substrates lose potency in favour of differentiation and express integrins with $\beta 1$ integrin subunits.

ROCK and mDia. Furthermore, several integrins containing $\beta 1$ subunits (e.g., $\alpha 5\beta 1$) activate the pathway mediated by Rho-ROCK-myosin-II to induce forces mediated by actomyosin (Figure 2), whereas αv subunit-containing integrins, e.g., $\alpha v\beta 3$ and $\alpha v\beta 5$, are more involved in external force adaptation and regulate both the stress fibre synthesis and FA area expansion through the pathway mediated by Rho-mDia [97]. ROCK-mediated activation of myosin light chain, together with inhibition of myosin light chain phosphatase, rapidly increases myosin-II activity and actomyosin contractility (Figure 2). Overall, ROCK activity leads to actin stress fibre stabilization.

3. Integrins and iPSC

Human embryonic stem cells (ESC) and iPSC, obtained by somatic cell reprogramming, are promising pluripotent stem cells, with the potential for recapitulating monogenic diseases and producing cell-based therapies [98]. In order to maximize the full potential of these cells, it is mandatory to enhance investigation and knowledge on the best culture conditions able to maintain plasticity, self-renewal, and external stimuli responsiveness as well as attenuate cell death events. Despite the lack of knowledge, there is increasing evidence regarding the contribution of integrins on pluripotent cell-ECM interaction [98–101].

The intricate and incompletely understood nature of cell fate and potency routes was succinctly represented in the self-acknowledged oversimplified [102] Waddington diagram [103] which is based on original artwork created by John Piper [104]. We have reimagined this iconic diagram to better summarize integrin engagement for cell-cell and cell-ECM binding and how these interactions affect cell fate (Figure 2). Mechanisms governing the transition from a somatic cell to an iPSC, which is initiated by the expression of exogenously acquired transcription factors, are continuously evolving, and much effort is directed to optimize the stochastic process of cell fate rewinding, in order to achieve a fully predictable process [105]. Reprogramming involves three sequential steps: initiation, stabilization, and maturation [106]. Indeed, molecular mediators, e.g., microRNA, or biophysical cues, e.g., nanotopography, can supplement or replace some of the classical reprogramming factors commonly used to enhance reprogramming efficiency [107–113].

In this context, the activation of the transforming growth factor-β (TGF-β) pathway and the expression of E-cadherin are of interest. While the former is a potent inhibitor of mesenchymal-to-epithelial transition, which is essential for a successful reprogramming [114], the latter is not only important for the maintenance of pluripotency and proper colony morphology but is also an absolute requirement for iPSC generation as well as the primary gatekeeper to the differentiation progression [115]. Moreover, iPSC kinome-wide functional analysis during reprogramming found a critical role in the cytoskeletal remodelling process. Specifically, the key serine/threonine kinases, testicular protein kinase-1 and LIM kinase-2, phosphorylate the actin-binding protein cofilin to modulate the cell reprogramming process.

Attempts have been made to transfer from the traditional 2D culture of iPSC to 3D culture in large-scale bioreactors, a step which would facilitate iPSC culture on industrially and clinically relevant scales [116, 117]. Since iPSC normally exist in tightly packed colonies, their dissociation into single cells, which is needed to ensure uniform cell distribution and diffusion of treatments, is a major stressor and initially caused high rates of cell death before the routine use of ROCK inhibitors during passaging [118]. Indeed, approaches that prevent actin-myosin contraction, such as downregulation of myosin heavy or light chains and ROCK inhibition [119], protect cells from cell death processes. Moreover, it has been demonstrated that a direct inhibition of Rho-ROCK-myosin-II activation involving E-cadherin

leads to a uniform differentiation of pluripotent stem cell colonies [115].

To date, the generation of iPSC in two parallel states of pluripotency has been described: naïve and primed [120]. Naïve iPSC are considered closer to a ground state, similar to preimplantation epiblasts, while primed iPSC correspond to cells found in the postimplantation epiblasts which are ready or "primed" to differentiate [121–123]. The importance of the pluripotency state is crucial to understand and to harness in research field, as it is currently appreciated that naïve and primed states have differing biological functions, e.g., developmental potency and chimeric contribution ability [124]. However, most of human iPSC are cultured in a primed state; therefore, much attention focuses on defining the factors (frequently soluble factors) that can revert primed cells to a naïve state [125–129]. A major driver to appreciate the role of culture substrates in pluripotency *continuum* came from the clearly recognizable morphological differences in naïve and primed colonies: naïve cells form dome-shaped 3D colonies, while colonies consisting of primed cells possess a flattened appearance. Despite the lack of information on the effect of growth substrates on the pluripotency status, suppression of ECM-integrin signalling has been linked to the maintenance of naïve human iPSC [130, 131].

Much of the information concerning ESC- and iPSC-integrin interaction stems from the gradual transition of feeder layer-cultured cell lines to more defined matrices such as Matrigel®, Cultrex BME®, Geltrex®, fibronectin, collagen IV, laminins, and vitronectin. A comparison of ESC and iPSC mRNA microarray data revealed that the expression profiles of integrins are similar in both types of pluripotent stem cells. Specifically, $\alpha 5$, $\alpha 6$, αv, $\beta 1$, and $\beta 5$ are all abundantly expressed on iPSC; however, not all iPSC lines displayed identical integrin profiles [132, 133]. Similarly, the integrin $\alpha 3$, $\alpha 5$, $\alpha 6$, $\alpha 9$, αv, and $\beta 1$ subunits, but not the $\alpha 1$, $\alpha 2$, $\alpha 4$, $\alpha 7$, and $\alpha 8$ subunits, were identified as markers of undifferentiated porcine-primed ESC, with a subsequent significant increase in their adhesion features on fibronectin, tenascin C, and vitronectin coatings. The blockade of integrin heterodimers $\alpha 5\beta 1$, $\alpha 9\beta 1$, and $\alpha v\beta 1$ lead to a strong inhibition in cell-ECM adhesion [134]. Moreover, $\alpha v\beta 3$, $\alpha 6\beta 1$, and $\alpha 2\beta 1$ play a significant role in the initial adhesion of the human ESC to Matrigel [135]. Interestingly, human but not porcine ESC display the active integrin heterodimer $\alpha 6\beta 1$ [136] suggesting species-dependent differences in the mechanotransduction signalling context. Concerning iPSC features, the parental cell-type origin impacts integrin expression, with enhanced levels of certain integrins observed in iPSC derived from adherent cell types, e.g., foreskin fibroblasts. Interestingly, Rowland and colleagues uncovered important differences between human ESC and iPSC in terms of the essential integrins necessary for initial adhesion and subsequent proliferation on different matrices. Specifically, they showed that $\beta 1$ is necessary for both functions when each cell type was grown on Matrigel® whereas $\alpha v\beta 5$ and $\beta 1$ are important for iPSC attachment and proliferation when cultured on vitronectin as described in Section 2. Lastly, integrins and integrin-mediated signalling are important in maintaining iPSC self-renewal and pluripotency as indicated by reduced Nanog, Oct-4, and Sox2 levels in $\alpha 6$-silenced iPSC lines, localization of the FAK N-terminal domain in nuclei, and AKT signalling activation [136, 137]. Similarly, murine ESC interaction with the RGD peptide plays a role in the expression of core transcription factors, i.e., Oct-4, Sox2, and Nanog. Cyclic RGD synthetic compound supplementation was sufficient to mimic the effect of a mechanical stimulus, in terms of pluripotent gene expression. Specifically, this molecule or mechanical stimulus significantly influenced ESC pluripotency by downregulating core transcription factors. Moreover, RGD peptide, by inhibiting integrin binding and, in turn, integrin expression [6], upregulated early lineage markers (mesoderm and ectoderm) by leukaemia inhibitory factor (LIF) signalling [138]. Interestingly, human ESC, expressing integrin $\alpha 6\beta 1$, preferentially bind human recombinant laminin-111, laminin-332, and laminin-511, which are good substrates able to maintain undifferentiated pluripotent human ESC cultures [139].

The ultimate destination of iPSC is differentiation along specific cell lineages culminating in the generation of functional terminally differentiated cells. Tailored protocols now exist to generate most cell types from each of the three germ layers, e.g., neurons, pancreatic islet β-cells, and, of specific relevance to this review, cardiomyocytes. Subsequently, these iPSC-derived cells can be used to model various diseases and screen novel drugs. Early cardiomyocyte differentiation protocols relied on the appearance of beating clusters within stochastically formed embryoid bodies (EB). The inefficient nature of producing cardiomyocytes from EB leads to the discovery of more efficient methods for cardiogenesis. One option considered here is the employment of small molecules modulating the key stages of embryonic cardiac development, i.e., early mesoderm formation by molecules targeting bone morphogenetic proteins, the wingless/INT (Wnt) proteins, and fibroblast growth factors, followed by activation of the conserved cardiac transcriptional program, i.e., Nkx2.5, Tbx5, Isl1, GATA4, and SRP. This program ultimately leads to the expression of the structural proteins essential for the function of cardiomyocytes, e.g., actin, myosin light/heavy chains, desmin, and the troponins (elegantly reviewed in [140]). Zeng et al. demonstrated that EB growth and cardiac differentiation of EB rely on collagen/integrin $\beta 1$ interaction [141]. Specifically, they observed a synergistic upregulation of collagen and integrin $\beta 1$ which peaked on the third post differentiation induction day [141]. Interestingly, the size and shape of EB as well as the confluence of iPSC are strongly linked to cardiogenic capacity [142–146]. The Wnt pathway is a pivotal pathway strongly linked to iPSC self-renewal and differentiation which is exploited by cardiomyocyte differentiation protocols relying on its temporal activation and inhibition in order to achieve highly efficient cardiomyogenesis [145, 147]. The noncanonical Wnt-planar cell polarity (PCP) pathway is able to induce actin cytoskeleton change promotion through Rac1, RhoA, and small GTPase signalling, which controls cell movement and tissue geometrical features. Good examples are the RhoA signalling cascade activated by DAAM1 and DAAM2 formin homology proteins or the JNK signalling cascade,

which is activated by MAPKKK and MAPKK 4/7 [148, 149]. Critically, following prolonged Wnt/β-catenin activation, the E-cadherin suppressors, SLUG and SNAIL, act as watershed factors that turn the iPSC fate from self-renewal to committed differentiation [150]. Lastly and more interestingly, for the clinical relevance, is the observation of Zhao and colleagues [151] who showed that the ROCK inhibitor, Y-27632, enhanced the transplantation success (in terms of engraftment) of human iPSC in a murine myocardial infarction model. The same compound revealed positive effects also on human ESC, e.g., increasing migration and supporting differentiation into EB. In the same study, integrin β1 blockade abolished the adhesion of ESC which decreased their survival and pluripotent status [152].

3.1. Mechanotransduction and Cell Differentiation. The genes under the direct control of the signalling pathways described in Section 3 are multiple. In this section, we will focus on the genes and pathways involved in pluripotent stem cell differentiation into cardiomyocytes.

An interesting 2013 study highlighted how integrin-mediated response to strain can be modulated by cell geometry more than by the cell area. Indeed, given the relevance of cell geometrical cues in mechanotransduction, in several cell types, efficient RhoA activation leads to megakaryocytic leukaemia-1 (MKL-1) protein translocation into the nucleus, in a cell shape-independent manner [153]. MKL-1 is a member of the so-called myocardin-related transcription factor family and physically interacts with the serum response factor (SRF) which activates SRF-dependent downstream gene transcription [154], e.g., actin cytoskeletal/-FA-related proteins [155, 156].

In a previous study, it was shown that the skeletal α-actin promoter activation, which is downstream of RhoA, was strongly potentiated by β1 integrin expression and function. These events were demonstrated to be specifically displayed by cardiomyocytes, but not by NIH 3T3 fibroblasts. This observation further supported RhoA/SRF-dependent cardiomyocyte gene expression by the β1 integrin signalling pathway [157]. Concerning the role of SRF in stem cells, the study of murine SRF$^{-/-}$ ESC showed that SRF deficiency causes impairments in cell spreading, adhesion, and migration, due to cytoskeletal structure modifications in terms of actin stress fibres and FA. Moreover, stem cells lacking SRF displayed downregulated FA, FAK, β1 integrin, talin, zyxin, and vinculin [158]. Furthermore, depletion of the adhesion molecule integrin β3, a key regulator of myogenic differentiation and actin organization, attenuated p130Cas phosphorylation and MKL nuclear localization during myoblast *in vitro* differentiation [50].

The MKL-1/SRF pathway is firmly linked to another important signalling pathway, strongly involved in mechanosensing in cardiovascular cells, namely, yes-associated protein (YAP) and transcriptional coactivator with PDZ-binding motif (TAZ) [159, 160]. Tuning YAP transcriptional activity leads to the modification of cell mechanics, force, and adhesion and determines cell shape, migration, and differentiation [161]. In the last years, this signalling pathway, deeply related to the HIPPO pathway, which is strongly related to developmental biology, is a hot topic in mechanotransduction studies. Indeed, there are numerous papers describing the involvement of YAP/TAZ in osteogenesis [159, 162].

Several studies underlined the indirect role of small GTPase Rho in YAP/TAZ nuclear localization control, exerted by promoting the actin bundles and stress fibre formation in response to cell spreading on the ECM [163–165]. Nardone et al. in 2017 demonstrated that YAP nuclear localization is controlled through Rho/ROCK activation and YAP transcriptionally controls FA formation and cytoskeleton stability which, in turn, determines cell adhesion to the ECM [161].

Experiments on conditional mouse YAP$^{-/-}$ and TAZ$^{-/-}$ in the skin resemble the profibrotic phenotype of skin-specific loss of integrin β1, highlighting the strong linkage and interplay of all these molecules *in vivo* [166].

Recently, β1 integrin-dependent cell adhesion was seen as a critical element in mesenchymal cell proliferation, both *in vivo* and *in vitro*. In fact, it was demonstrated that β1 integrin-dependent activation of the small GTPase Rac1 leads to YAP dephosphorylation and its nuclear shuttling, confirming that β1 integrin-dependent Rac1 function plays a key role in YAP regulation, triggered by cell adhesion [167]. Another recent paper identified a pathway involving both activation of integrin α3 and a FAK cascade-controlling YAP phosphorylation and thus its nuclear localization in transit-amplifying stem cells. In this work, the authors highlighted that this specific signalling pathway potentiates mTOR signalling, driving cell proliferation, and that the YAP/TAZ signalling mechanism coordinates stem cell expansion and differentiation during organ self-renewal [51].

4. Integrin Relevance in iPSC-Derived Cells: In Vitro Biomimetic Approaches

As discussed in the first section, mechanosensing, in general and specifically integrin activation, can be used to guide lineage-specific cell fate by activating mechanotransduction pathways. In order to better elucidate the fundamental mechanisms driving pathophysiological mechanisms, several *in vitro* models, based on biomimetic approaches, have been proposed and discussed. This section provides an overview of the *in vitro* models (Figure 3), focusing on the potential of biomimetic approaches to direct iPSC cardiomyocyte differentiation and maturation, possibly supporting their use in the field of cardiovascular regenerative medicine and tissue engineering.

4.1. Surface Chemistry. Substrate chemical composition and the motifs decorating a given surface have a strong effect on selective integrin engagement. Here, we will discuss two different approaches to engineering substrates: the first employing ECM obtained by decellularization of biological tissues and the second relying on the functionalization of synthetic biomaterials.

*4.1.1. Decellularized ECM. In vivo*ECM, thanks to its chemical composition and mechanical/topographic properties, establishes the bases to support cell proliferation and differentiation

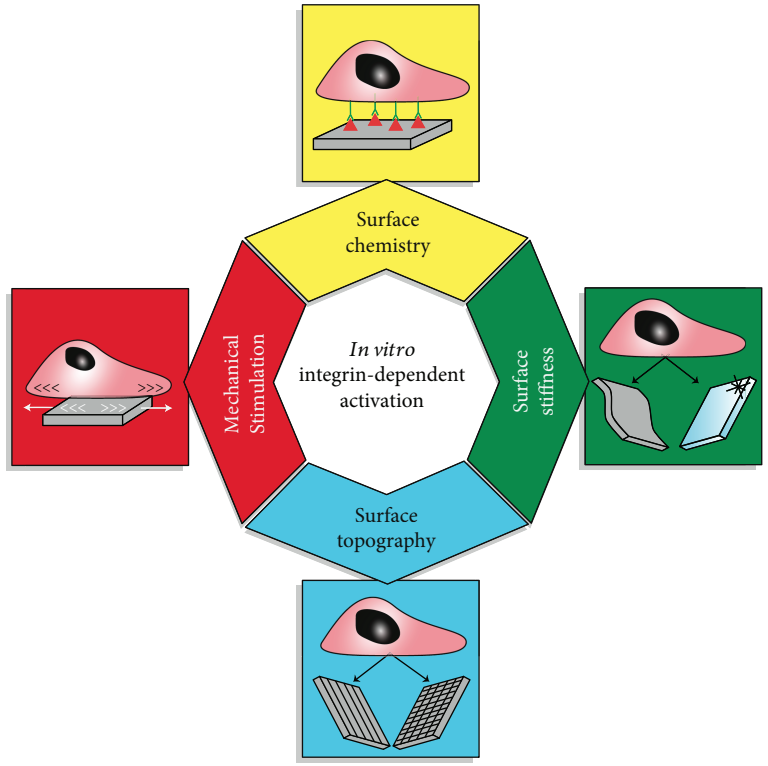

Figure 3: Engineered materials supporting *in vitro* modelling. Integrin-mediated pathways relevant for iPSC cardiac differentiation can be enhanced *in vitro* by the use of ad hoc-designed biomaterials. Toward this aim, chemical, geometrical, mechanical, and physical properties of the substrates are relevant.

[168, 169]. Indeed, the ECM surface does not only mediate cell attachment by exhibiting anchorage sites for different cell surface receptors and coreceptors but also regulates the diffusion of soluble factors secreted by the neighbouring cells, e.g., ECM composition modifies chemical diffusion coefficient and, as a product of its own remodelling, releases functional fragments constituting additional soluble factors.

For this reason, the use of decellularized tissues, maintaining composition, architecture, mechanical properties, and, interestingly, cell-binding domains, has been widely proposed as a suitable scaffold for *in vitro* cell seeding, expansion, and differentiation [170–174]. In parallel, its specific capacity to guide stem cell differentiation has been also shown [168, 175–177]. In particular, the ability to selectively increase the expression of integrins [171] has been demonstrated, underlining the relevance of ECM protein composition, e.g., the ratio of collagen, fibronectin, laminin, vitronectin [178], and their topology, supporting cell adhesion and subsequently stimulating controlled cell differentiation [171]. The potentiality of scaffolds realized by tissue decellularization is maximized by the use of dynamic culture methods, i.e., perfusion bioreactors supporting homogeneous repopulation of the whole scaffold volume [179–181] and recreating a controlled and reproducible 3D environment.

Nevertheless, although experiments are performed under highly controlled culture conditions, the coexistence of multiple parameters limits the understanding of the impact of specific factors. Therefore, decellularized ECM scaffolds are good multifactorial model systems, comprehensive of the complexities of the *in vivo* scenarios, and are suitable for translational studies. On the other hand, biomaterials have been designed and functionalized ad hoc, by means of either coating with ECM components or generating specific cell-binding domains, in order to interpret different mechanisms.

The intermediate link in this chain is constituted by 3D bioprinting technologies. The technological advances in the field have allowed the use of liquefied decellularized tissues for high-resolution precise simulation of native tissue structures, with encapsulated cells [182, 183], thus providing the chance to observe the biological effects induced by fine tuning of local chemical/architectural matrix modifications.

4.1.2. Engineered Biomaterials. Polymers, both synthetic and natural, have been widely used for the manufacture of substrates and scaffolds intended for in vitro cell culture and cardiovascular tissue engineering [184]. The most used synthetic polymers in the field are poly(ethylene-glycol) (PEG), poly(lactic-acid) (PLA), poly(glycolic-acid) (PGA), poly(ε-caprolactone) (PCL), and their copolymers such as poly(lactide-co-glycolide) (PLGA) and polyurethanes (PU) [185–190]. In contrast, natural materials include ECM constituents, i.e., collagen, fibrin, and silk [178, 191, 192]. The advantages of using engineered biomaterials rely on their amenability to fine-tune parameters, such as biocompatibility, local rigidity, micro/nanoarchitecture, and

functionalization with ECM proteins, integrin-binding peptides, or growth factors [186, 193].

By coating synthetic materials, e.g., PU, with fibronectin (REDV, PHSRN, RGD, and GRGDSP), laminin (IKLLI, IKVAV, LRE, PDSGR, RGD, and YIGSR), and collagen (DGEA) sequences [194–196] together with supplementing cell culture media with selective integrin inhibitors [197], the effect of integrin expression on cell attachment and proliferation has been highlighted. In addition, polymer functionalization with ECM peptides has been proposed to actively promote cell differentiation. An example, performed with an elegant and innovative approach, has been proposed by Ovadia and colleagues [198]. Matrigel®, a commercial solubilized basement membrane preparation extracted from the Engelbreth-Holm-Swarm mouse sarcoma cells, consisting of laminin, collagen IV, proteoglycans, and a number of growth factors, is widely recommended as an iPSC culture support. However, the specific reasons behind its success have not been elucidated. In their work, Ovadia et al. proposed iPSC single-cell encapsulation within 3D photopolymerized with UV light (365 nm for 2 minutes) PEG-peptide-based synthetic gels conveniently functionalized by a range of motifs inspired by Matrigel and known to bind a variety of integrins (including $\alpha 6$, αv, and $\beta 1$), which generally promotes cell adhesion. Knowing that ROCK inhibition increases the expression of αv, $\alpha 6$, and $\beta 1$ integrins during iPSC culture on Matrigel®, in the proposed 3D culture system, the authors showed that iPSC viability, growth, and differentiation were enhanced in response to the environment, in particular to $\beta 1$ integrin activation.

Another parameter that needs to be taken into account when modelling cell adhesion *in vitro* is the coupling strength between integrin ligand and substrate. Human mesenchymal stem cells exhibit enhanced osteogenesis in response to high-strength binding which results from the activation of a YAP-mediated pathway [199]. This result suggests that traditional covalent biological coatings could generate a bias in data interpretation, which implies the need for novel coating methods, such as noncovalent coatings [200]. Based on these findings, it is clear that the study of integrin recruitment can not omit the consideration of forces acting on the whole chain, from the substrate, e.g., substrate rigidity to the engaged cytoskeleton filaments. Combinatorial approaches have been implemented for the production of copolymers able to tune cell-substrate interaction. An example of this approach is provided by Cheng et al. [201], who demonstrated that novel supramolecular PCL-containing self-complementary sextuple hydrogen-bonded uracil-diamidopyridine moieties can positively support cell attachment and proliferation. Moreover, as demonstrated by Chun et al. in 2015 [202], the copolymer generated by polymerization of monomeric ε-caprolactone with methoxy-PEG, in the ratio of 4% PEG-96% PCL, was able to enhance iPSC-d-CM contractility, upregulating the expression of mature cardiomyocyte markers such as myosin light chain-2v and cardiac troponin I. The authors demonstrated that these effects are linked to the engagement of a subset of integrins which activate a mechanosensory transduction pathway regulated by the polymerization of intermediate filaments.

4.2. Surface Topography. *In vivo* cardiac tissue functionality is aided by the anisotropic tissue structure which results from ECM protein organization, cell orientation, and cell-ECM/-cell-cell junctions. *In vitro*, the relevance of ECM architecture in iPSC maturation has been demonstrated by means of micro- and nanostructured substrates. Results demonstrated how geometrical cues could support iPSC pluripotency and differentiation [203, 204] by the formation of cell-cell junctions, not only leading to the generation of more functional grafts, increased beating rate, and enhancing tissue-specific protein arrangement, e.g., sarcomeric-actinin, connexin 43, and troponins, but also allowing better stratification of the pathology, e.g., muscular dystrophy [203, 205–207].

At the aim of understanding the involvement of integrins in geometrical feature-driven cell differentiation, substrates controlling either cell shape and size or cell alignment or spacing of adhesion ligands have been designed.

4.2.1. Cell Alignment. *In vivo*, physiological cardiac functionality is supported by coordinated muscular contraction, which is allowed by highly organized cell alignment, guaranteeing controlled anisotropic conduction of the electrical stimuli. *In vitro* iPSC-d-CM assemble in heterogeneous randomly organized clusters, missing accurate reproduction of the *in vivo* scenario. This limits their level of maturation and excludes from the *in vitro* model the effects of possibly relevant mechanotransduction-guided mechanisms. The introduction of nanotopographical features into culture substrates, i.e., grooves in the 700–1000 nm range [11], has been demonstrated to improve cardiomyocyte development by acting on one hand through a reorganization of the integrin activation of the single iPSC (i.e., enhancing integrin expression and formation of FA and increasing F-actin polymerization) and, on the other, geometrically organizing the colony polarization. Culturing on grooved substrates finally impacts on iPSC-d-CM intrinsic molecular machinery, i.e., through the activation of the YAP-dependent pathway [208, 209], resulting in more physiological behaviours, showing a reduction of arrhythmias and inducing more mature Ca^{2+} spark patterns [210, 211]. The maturity level not only would benefit from cell alignment but could permit a more significant stratification of the pathology, as demonstrated by the limited capacity of iPSC-d-CM from patients affected by Duchenne muscular dystrophy versus healthy donors in their ability to reorient when cultured on grooved substrates [212].

More recently, the introduction of polymeric nanowires offers the chance to couple cell alignment with electrical conductivity and stimulation, reproducing preferential routes for geometrical organization and electrical signal timing. The application of this technology resulted in a significantly more advanced cellular structure, i.e., showed by cell-cell junction formation, and contractile function efficiency [213–215], enhancing *in vitro* iPSC-d-CM maturation and functionality and leading towards the design of a better model system for the evaluation of the *in vivo* pathophysiological mechanisms.

4.2.2. Cell Shape and Size. In between, the geometrical features able to guide *in vitro* stem cell differentiation, shape,

and size have been widely studied [216]. Indeed, several screening platforms, also commercial platforms, e.g., BioSurface Structure Array, Nano-TopoChip [217], have been used to demonstrate that by regulating the width/length ratio, in the presence or absence of soluble factors, cell fate can be moved from osteogenic to adipogenic commitment.

Regarding iPSC, they are often cultured as aggregates and not as single cells; therefore, the mechanotransduction-driven effects of whole-colony size and shape should be taken into account. Indeed, by controlling colony size, density, shape, and spacing, Myers et al. [218] improved homogeneity in the expression of pluripotency markers (SSEA4 and Nanog). Moreover, the proposed micropatterning technique, through the standardization of cell density, increased the percentage of spontaneous beating cells. In particular, the generation of circular patterns leads to the formation of connecting rings of cardiomyocytes, supporting *in vitro* physiological electrical behaviour, i.e., supporting the propagation of contractile waves throughout the ring. Another example of how cell shape, coupled with the supracellular structure, can be used to promote *in vitro* cardiomyocyte maturation is provided by the work of Xu et al. [211]. Here, by imposing single-cell elongation by culturing on silicon-patterned substrates, FA can be regulated to support alignment and cell-cell contacts leading to increased cardiac differentiation efficiency. Moreover, in their recent work, Grespan and colleagues [203] cultured iPSC onto microstructured (square micropillars) silicon substrates and observed that, while not affecting pluripotency, nuclear deformability is sensibly regulated during germ layer specification, happening during iPSC differentiation.

These observations, taken together, finally call for the design of more complex *in vitro* substrates, taking into account mechanosensing mechanisms for better iPSC differentiation.

4.2.3. Integrin Clustering Methods. The methods described in the previous paragraphs are based either on functionalization of substrates by random decoration with integrin-binding domains or by induction of adhesion sites by geometrical constraint and do not encompass the relevance of integrin geometrical distribution. It has been made possible to involve this aspect thanks to the development of novel nanotechnologies, which can be divided in three different approaches [219]: (i) blending of polymers with different degrees of ligand incorporation [220, 221], (ii) nanoprinting lithography of nanoparticle arrays [222–224], and (iii) transfection of proteins by chimera constructs [225]. Results demonstrated that not only identity, abundance, and density of adhesion sites but also their spatial confinement, including global and local density, regulate cell adhesion [226], migration, proliferation, and differentiation acting on both cell-substrate and cell-cell contact [224]. Furthermore, the capacity of nanoscale spatially organized cell-adhesive ligands to direct stem cell fate was also demonstrated [210, 227].

4.3. Surface Elasticity. Substrate stiffness has been shown to be a very strong mechanotransduction stimulus, regulating physiopathological cell behaviour and cell reprogramming and subsequently guiding the development of mature cell phenotypes [164, 228–233]. In particular, regarding the *in vitro* application of iPSC technology in the cardiac field, matrix rigidity can guide iPSC-d-CM differentiation: the use of a substrate with compliance similar to that of native cardiac tissue [234–236] supports cardiac commitment and enhances metabolic maturity, sarcomeric protein subtype, cardiac troponin T expression, and force generation [230, 235, 237, 238]. The molecular events transferring the force from the substrate to the nuclei, through cytoskeleton engagement, have been described by Zhou et al. [239], and other reviews discussed this topic at length [240, 241]. Here, we will underline some specific aspects about the involvement of integrins in this phenomenon. Indeed, the selective switching from the activation of $\beta 3$ to $\beta 1$ integrins in response to reduced substrate stiffness has been demonstrated [197, 242, 243]. From a technological point of view, it is interesting to underline the sensitivity of the whole traction chain to integrin-substrate binding force. Indeed, a modification in the substrate-anchoring strength of integrin-binding ligands, i.e., choosing covalent binding to obtain stable substrate coating, could lead to a misinterpretation of *in vitro* cell behaviour [15, 199, 244, 245], thus highlighting the importance of considering mechanical stimuli, i.e., surface elasticity, with the feeling of cells, recognizing the role of all the nanoscale players.

4.4. Mechanical Stimulation. Mechanical stimulation has been demonstrated to regulate FA assembly, modulating the downstream pathways affecting cardiomyogenesis [246–249]. Based on this assumption, several methods have been described for the application of controlled mechanical stimulation (i.e., temporal, spatial, and amplitude), some of them aiming to verify the positive impact of integrin-mediated adhesion pathways on iPSC reprogramming [113] and differentiation [250, 251]. Although far from being exhaustively described, the pathways seem to be regulated by the change in FA density and local conformation [252], followed by impacting cytoskeleton rearrangement [56], finally regulating cardiomyocyte maturity, e.g., cell-cell contact, sarcomeric structure, and electrical activity. As an example, the interconnection between the mechanical stimulation, in particular shear stress, and the modulation of cellular electrical activity was demonstrated by Roy and Mathew [253], who underlined how the gene encoding the α-subunit of human ether-a-go-go-related gene (hERG) potassium ion channel could be modulated by integrins via a mechanoelectric feedback pathway. Not only that mechanical stimulation enhances cell electrical behaviour but that a positive effect on maturation of cardiomyocytes *in vitro* has been demonstrated by coupling pacing with mechanical stimulation [254]. Finally, the *in vitro* implementation of mechanical stimulation has been shown of benefit in the model for the pathology stratification. Chun and colleagues proposed [249] that the application of cyclic or static strain modulated the gene expression of a cell-cell connection-related protein (connexin-43) in iPSC-d-CM which was more pronounced in iPSC-d-CM from patients affected by primary dilated cardiomyopathy.

5. Conclusions

Each integrin type is coupled to a different combination of signalling cascades which drive specific cellular processes, e.g., stem cell differentiation [255, 256]. Integrins are involved not only in the recognition of substrate composition but also in sensing ECM rigidity and adapting cell morphology, motility, and fate to the mechanical properties of the matrix, through the activation of mechanotransduction pathways.

However, the high specificity in the link between integrin-mediated cell response to tissue-specific microenvironment is far from being completely decrypted, both in general [15] and more specifically in pluripotent stem cells [98]. A detailed understanding of the cellular machinery linking mechanosensing to mechanotransduction would be beneficial for effective *in vitro* modelling and the future clinical translation of tissue-specific differentiated iPSC.

As discussed in this review, the implementation of *in vitro* novel biomaterials, taking into account integrin-mediated mechanotransduction signalling, coupled with controlled systems, i.e., microfluidic bioreactors, could be relevant to improving the study of iPSC-d-CM differentiation and supporting maturation [12, 257], inspired by an "organ/lab-on-chip" approach [227]. The design of such models would benefit (i) *in vitro* modelling of the molecular basis of the pathologies, (ii) *in vitro* evaluation of possible mechanisms and specific molecular targets for personalized pharmacological approaches, and (iii) development of a mature cell source available for future transplantation perspectives. Indeed, the high risk of teratoma formation intrinsic to transplantation of iPSC-derived cells is well acknowledged. Moreover, the maturity of the implanted cells, especially thinking about cardiac applications of iPSC-d-CM, should guarantee their survival and functionality shortly after the procedure.

In conclusion, these aspects would raise the level of iPSC-d-CM quality and provide an effective model system for the study of different cardiac pathologies. Moreover, in an optimal scenario, the use of bioactive scaffolds in controlled culture systems could permit the utilization of read-out parameters that provide a culture quality feedback signal.

Conflicts of Interest

The authors declare that they have no conflicts of interest.

Authors' Contributions

R. Santoro and G.L. Perrucci contributed equally to this work.

Acknowledgments

This work was supported by the Italian Ministry of Health Ricerca Corrente to Centro Cardiologico Monzino IRCCS (RC 2017/18).

References

[1] J. W. Tamkun, D. W. DeSimone, D. Fonda et al., "Structure of integrin, a glycoprotein involved in the transmembrane linkage between fibronectin and actin," *Cell*, vol. 46, no. 2, pp. 271–282, 1986.

[2] R. O. Hynes, "Integrins: a family of cell surface receptors," *Cell*, vol. 48, no. 4, pp. 549–554, 1987.

[3] R. O. Hynes, "Integrins: bidirectional, allosteric signaling machines," *Cell*, vol. 110, no. 6, pp. 673–687, 2002.

[4] G. L. Perrucci, E. Rurali, and G. Pompilio, "Cardiac fibrosis in regenerative medicine: destroy to rebuild," *Journal of Thoracic Disease*, vol. 10, Supplement 20, pp. S2376–S2389, 2018.

[5] G. L. Perrucci, M. Zanobini, P. Gripari et al., "Pathophysiology of aortic stenosis and mitral regurgitation," *Comprehensive Physiology*, vol. 7, no. 3, pp. 799–818, 2017.

[6] G. L. Perrucci, V. A. Barbagallo, M. Corlianò et al., "Integrin $\alpha v\beta 5$ in vitro inhibition limits pro-fibrotic response in cardiac fibroblasts of spontaneously hypertensive rats," *Journal of Translational Medicine*, vol. 16, no. 1, p. 352, 2018.

[7] K. Takahashi, K. Tanabe, M. Ohnuki et al., "Induction of pluripotent stem cells from adult human fibroblasts by defined factors," *Cell*, vol. 131, no. 5, pp. 861–872, 2007.

[8] I. Itzhaki, L. Maizels, I. Huber et al., "Modelling the long QT syndrome with induced pluripotent stem cells," *Nature*, vol. 471, no. 7337, pp. 225–229, 2011.

[9] M. Mandai, A. Watanabe, Y. Kurimoto et al., "Autologous induced stem-cell-derived retinal cells for macular degeneration," *The New England Journal of Medicine*, vol. 376, no. 11, pp. 1038–1046, 2017.

[10] S. Miyagawa, K. Domae, Y. Yoshikawa et al., "Phase I clinical trial of autologous stem cell-sheet transplantation therapy for treating cardiomyopathy," *Journal of the American Heart Association*, vol. 6, no. 4, 2017.

[11] D. Carson, M. Hnilova, X. Yang et al., "Nanotopography-induced structural anisotropy and sarcomere development in human cardiomyocytes derived from induced pluripotent stem cells," *ACS Applied Materials & Interfaces*, vol. 8, no. 34, pp. 21923–21932, 2016.

[12] Y. Li, L. Li, Z. N. Chen, G. Gao, R. Yao, and W. Sun, "Engineering-derived approaches for iPSC preparation, expansion, differentiation and applications," *Biofabrication*, vol. 9, no. 3, article 032001, 2017.

[13] Y. Takada, X. Ye, and S. Simon, "The integrins," *Genome Biology*, vol. 8, no. 5, p. 215, 2007.

[14] M. Barczyk, S. Carracedo, and D. Gullberg, "Integrins," *Cell and Tissue Research*, vol. 339, no. 1, pp. 269–280, 2010.

[15] S. Seetharaman and S. Etienne-Manneville, "Integrin diversity brings specificity in mechanotransduction," *Biology of the Cell*, vol. 110, no. 3, pp. 49–64, 2018.

[16] C. G. Galbraith, K. M. Yamada, and J. A. Galbraith, "Polymerizing actin fibers position integrins primed to probe for adhesion sites," *Science*, vol. 315, no. 5814, pp. 992–995, 2007.

[17] P. Costa, T. M. E. Scales, J. Ivaska, and M. Parsons, "Integrin-specific control of focal adhesion kinase and RhoA regulates membrane protrusion and invasion," *PLoS One*, vol. 8, no. 9, article e74659, 2013.

[18] H. B. Schiller and R. Fassler, "Mechanosensitivity and compositional dynamics of cell-matrix adhesions," *EMBO Reports*, vol. 14, no. 6, pp. 509–519, 2013.

[19] D. A. Calderwood, B. Yan, J. M. de Pereda et al., "The phosphotyrosine binding-like domain of Talin activates integrins," *The Journal of Biological Chemistry*, vol. 277, no. 24, pp. 21749–21758, 2002.

[20] C. Kim, F. Ye, X. Hu, and M. H. Ginsberg, "Talin activates integrins by altering the topology of the β transmembrane domain," *The Journal of Cell Biology*, vol. 197, no. 5, pp. 605–611, 2012.

[21] J. H. Wang, "Pull and push: talin activation for integrin signaling," *Cell Research*, vol. 22, no. 11, pp. 1512–1514, 2012.

[22] W. H. Ziegler, R. C. Liddington, and D. R. Critchley, "The structure and regulation of vinculin," *Trends in Cell Biology*, vol. 16, no. 9, pp. 453–460, 2006.

[23] A. Carisey and C. Ballestrem, "Vinculin, an adapter protein in control of cell adhesion signalling," *European Journal of Cell Biology*, vol. 90, no. 2-3, pp. 157–163, 2011.

[24] R. Zaidel-Bar and B. Geiger, "The switchable integrin adhesome," *Journal of Cell Science*, vol. 123, no. 9, pp. 1385–1388, 2010.

[25] K. R. Legate, S. Takahashi, N. Bonakdar et al., "Integrin adhesion and force coupling are independently regulated by localized PtdIns(4,5)$_2$ synthesis," *The EMBO Journal*, vol. 30, no. 22, pp. 4539–4553, 2011.

[26] V. Martel, C. Racaud-Sultan, S. Dupe et al., "Conformation, localization, and integrin binding of talin depend on its interaction with phosphoinositides," *The Journal of Biological Chemistry*, vol. 276, no. 24, pp. 21217–21227, 2001.

[27] A. M. Pasapera, I. C. Schneider, E. Rericha, D. D. Schlaepfer, and C. M. Waterman, "Myosin II activity regulates vinculin recruitment to focal adhesions through FAK-mediated paxillin phosphorylation," *The Journal of Cell Biology*, vol. 188, no. 6, pp. 877–890, 2010.

[28] C. Möhl, N. Kirchgeßner, C. Schäfer et al., "Becoming stable and strong: the interplay between vinculin exchange dynamics and adhesion strength during adhesion site maturation," *Cell Motility and the Cytoskeleton*, vol. 66, no. 6, pp. 350–364, 2009.

[29] C. Margadant, M. Kreft, G. Zambruno, and A. Sonnenberg, "Kindlin-1 regulates integrin dynamics and adhesion turnover," *PLoS One*, vol. 8, no. 6, article e65341, 2013.

[30] M. Régent, E. Planus, A. P. Bouin et al., "Specificities of β1 integrin signaling in the control of cell adhesion and adhesive strength," *European Journal of Cell Biology*, vol. 90, no. 2-3, pp. 261–269, 2011.

[31] P. Bubeck, S. Pistor, J. Wehland, and B. M. Jockusch, "Ligand recruitment by vinculin domains in transfected cells," *Journal of Cell Science*, vol. 110, Part 12, pp. 1361–1371, 1997.

[32] C. M. Hampton, D. W. Taylor, and K. A. Taylor, "Novel structures for α-actinin:F-actin interactions and their implications for actin-membrane attachment and tension sensing in the cytoskeleton," *Journal of Molecular Biology*, vol. 368, no. 1, pp. 92–104, 2007.

[33] B. Li and B. Trueb, "Analysis of the α-actinin/zyxin interaction," *Journal of Biological Chemistry*, vol. 276, no. 36, pp. 33328–33335, 2001.

[34] M. Yoshigi, L. M. Hoffman, C. C. Jensen, H. J. Yost, and M. C. Beckerle, "Mechanical force mobilizes zyxin from focal adhesions to actin filaments and regulates cytoskeletal reinforcement," *The Journal of Cell Biology*, vol. 171, no. 2, pp. 209–215, 2005.

[35] A. X. Zhou, J. H. Hartwig, and L. M. Akyurek, "Filamins in cell signaling, transcription and organ development," *Trends in Cell Biology*, vol. 20, no. 2, pp. 113–123, 2010.

[36] Z. Razinia, T. Mäkelä, J. Ylänne, and D. A. Calderwood, "Filamins in mechanosensing and signaling," *Annual Review of Biophysics*, vol. 41, no. 1, pp. 227–246, 2012.

[37] S. Furuike, T. Ito, and M. Yamazaki, "Mechanical unfolding of single filamin A (ABP-280) molecules detected by atomic force microscopy," *FEBS Letters*, vol. 498, no. 1, pp. 72–75, 2001.

[38] M. Yamazaki, S. Furuike, and T. Ito, "Mechanical response of single filamin A (ABP-280) molecules and its role in the actin cytoskeleton," *Journal of Muscle Research and Cell Motility*, vol. 23, no. 5/6, pp. 525–534, 2002.

[39] M. D'Addario, P. D. Arora, R. P. Ellen, and C. A. G. McCulloch, "Interaction of p38 and Sp1 in a mechanical force-induced, β_1 integrin-mediated transcriptional circuit that regulates the actin-binding protein filamin-A," *Journal of Biological Chemistry*, vol. 277, no. 49, pp. 47541–47550, 2002.

[40] X. Li and H. S. Earp, "Paxillin is tyrosine-phosphorylated by and preferentially associates with the calcium-dependent tyrosine kinase in rat liver epithelial cells," *The Journal of Biological Chemistry*, vol. 272, no. 22, pp. 14341–14348, 1997.

[41] T. R. Polte and S. K. Hanks, "Interaction between focal adhesion kinase and Crk-associated tyrosine kinase substrate p130Cas," *Proceedings of the National Academy of Sciences of the United States of America*, vol. 92, no. 23, pp. 10678–10682, 1995.

[42] R. Janoštiak, A. C. Pataki, J. Brábek, and D. Rösel, "Mechanosensors in integrin signaling: the emerging role of p130Cas," *European Journal of Cell Biology*, vol. 93, no. 10-12, pp. 445–454, 2014.

[43] B. J. Mayer, H. Hirai, and R. Sakai, "Evidence that SH2 domains promote processive phosphorylation by protein-tyrosine kinases," *Current Biology*, vol. 5, no. 3, pp. 296–305, 1995.

[44] R. Sakai, A. Iwamatsu, N. Hirano et al., "A novel signaling molecule, p130, forms stable complexes in vivo with v-Crk and v-Src in a tyrosine phosphorylation-dependent manner," *The EMBO Journal*, vol. 13, no. 16, pp. 3748–3756, 1994.

[45] D. D. Schlaepfer, M. A. Broome, and T. Hunter, "Fibronectin-stimulated signaling from a focal adhesion kinase-c-Src complex: involvement of the Grb2, p130cas, and Nck adaptor proteins," *Molecular and Cellular Biology*, vol. 17, no. 3, pp. 1702–1713, 1997.

[46] P. M. Fonseca, N. Y. Shin, J. Brábek, L. Ryzhova, J. Wu, and S. K. Hanks, "Regulation and localization of CAS substrate domain tyrosine phosphorylation," *Cellular Signalling*, vol. 16, no. 5, pp. 621–629, 2004.

[47] H. Honda, T. Nakamoto, R. Sakai, and H. Hirai, "p130(Cas), an assembling molecule of actin filaments, promotes cell movement, cell migration, and cell spreading in fibroblasts," *Biochemical and Biophysical Research Communications*, vol. 262, no. 1, pp. 25–30, 1999.

[48] E. A. C. Almeida, D. Ilić, Q. Han et al., "Matrix survival signaling: from fibronectin via focal adhesion kinase to c-Jun NH_2-terminal kinase," *The Journal of Cell Biology*, vol. 149, no. 3, pp. 741–754, 2000.

[49] M. Oktay, K. K. Wary, M. Dans, R. B. Birge, and F. G. Giancotti, "Integrin-mediated activation of focal adhesion

kinase is required for signaling to Jun NH_2-terminal kinase and progression through the G1 phase of the cell cycle," *Journal of Cell Biology*, vol. 145, no. 7, pp. 1461–1470, 1999.

[50] K. Kawauchi, W. W. Tan, K. Araki et al., "p130Cas-dependent actin remodelling regulates myogenic differentiation," *The Biochemical Journal*, vol. 445, no. 3, pp. 323–332, 2012.

[51] J. K.-H. Hu, W. Du, S. J. Shelton, M. C. Oldham, C. M. DiPersio, and O. D. Klein, "An FAK-YAP-mTOR signaling axis regulates stem cell-based tissue renewal in mice," *Cell Stem Cell*, vol. 21, no. 1, pp. 91–106.e6, 2017.

[52] E. Rozengurt, J. Sinnett-Smith, and G. Eibl, "Yes-associated protein (YAP) in pancreatic cancer: at the epicenter of a targetable signaling network associated with patient survival," *Signal Transduction and Targeted Therapy*, vol. 3, no. 1, p. 11, 2018.

[53] B. Xiang, Y. Liu, W. Zhao, H. Zhao, and H. Yu, "Extracellular calcium regulates the adhesion and migration of osteoclast via integrin $\alpha v\beta 3$/ Rho A/cytoskeleton signaling," *Cell Biology International*, 2018.

[54] A. del Rio, R. Perez-Jimenez, R. Liu, P. Roca-Cusachs, J. M. Fernandez, and M. P. Sheetz, "Stretching single talin rod molecules activates vinculin binding," *Science*, vol. 323, no. 5914, pp. 638–641, 2009.

[55] F. Kong, Z. Li, W. M. Parks et al., "Cyclic mechanical reinforcement of integrin-ligand interactions," *Molecular Cell*, vol. 49, no. 6, pp. 1060–1068, 2013.

[56] D. H. Kim, S. B. Khatau, Y. Feng et al., "Actin cap associated focal adhesions and their distinct role in cellular mechanosensing," *Scientific Reports*, vol. 2, no. 1, p. 555, 2012.

[57] R. P. Martins, J. D. Finan, G. Farshid, and D. A. Lee, "Mechanical regulation of nuclear structure and function," *Annual Review of Biomedical Engineering*, vol. 14, no. 1, pp. 431–455, 2012.

[58] I. Solovei, A. S. Wang, K. Thanisch et al., "LBR and lamin A/C sequentially tether peripheral heterochromatin and inversely regulate differentiation," *Cell*, vol. 152, no. 3, pp. 584–598, 2013.

[59] L. J. Barton, A. A. Soshnev, and P. K. Geyer, "Networking in the nucleus: a spotlight on LEM-domain proteins," *Current Opinion in Cell Biology*, vol. 34, pp. 1–8, 2015.

[60] V. P. Lehto, I. Virtanen, and P. Kurki, "Intermediate filaments anchor the nuclei in nuclear monolayers of cultured human fibroblasts," *Nature*, vol. 272, no. 5649, pp. 175–177, 1978.

[61] C. Guilluy, L. D. Osborne, L. van Landeghem et al., "Isolated nuclei adapt to force and reveal a mechanotransduction pathway in the nucleus," *Nature Cell Biology*, vol. 16, no. 4, pp. 376–381, 2014.

[62] D. M. Graham and K. Burridge, "Mechanotransduction and nuclear function," *Current Opinion in Cell Biology*, vol. 40, pp. 98–105, 2016.

[63] D. A. Starr and M. Han, "Role of ANC-1 in tethering nuclei to the actin cytoskeleton," *Science*, vol. 298, no. 5592, pp. 406–409, 2002.

[64] M. Crisp, Q. Liu, K. Roux et al., "Coupling of the nucleus and cytoplasm: role of the LINC complex," *The Journal of Cell Biology*, vol. 172, no. 1, pp. 41–53, 2006.

[65] X. Zhang, K. Lei, X. Yuan et al., "SUN1/2 and Syne/-nesprin-1/2 complexes connect centrosome to the nucleus during neurogenesis and neuronal migration in mice," *Neuron*, vol. 64, no. 2, pp. 173–187, 2009.

[66] K. Wilhelmsen, S. H. M. Litjens, I. Kuikman et al., "Nesprin-3, a novel outer nuclear membrane protein, associates with the cytoskeletal linker protein plectin," *The Journal of Cell Biology*, vol. 171, no. 5, pp. 799–810, 2005.

[67] K. J. Roux, M. L. Crisp, Q. Liu et al., "Nesprin 4 is an outer nuclear membrane protein that can induce kinesin-mediated cell polarization," *Proceedings of the National Academy of Sciences of the United States of America*, vol. 106, no. 7, pp. 2194–2199, 2009.

[68] N. E. Cain, E. C. Tapley, K. L. McDonald, B. M. Cain, and D. A. Starr, "The SUN protein UNC-84 is required only in force-bearing cells to maintain nuclear envelope architecture," *The Journal of Cell Biology*, vol. 206, no. 2, pp. 163–172, 2014.

[69] S. Blone, K. Small, V. M. A. Aksmanovic et al., "Identification of new mutations in the Emery-Dreifuss muscular dystrophy gene and evidence for genetic heterogeneity of the disease," *Human Molecular Genetics*, vol. 4, no. 10, pp. 1859–1863, 1995.

[70] J. Lammerding, J. Hsiao, P. C. Schulze, S. Kozlov, C. L. Stewart, and R. T. Lee, "Abnormal nuclear shape and impaired mechanotransduction in emerin-deficient cells," *The Journal of Cell Biology*, vol. 170, no. 5, pp. 781–791, 2005.

[71] B. D. Matthews, D. R. Overby, R. Mannix, and D. E. Ingber, "Cellular adaptation to mechanical stress: role of integrins, Rho, cytoskeletal tension and mechanosensitive ion channels," *Journal of Cell Science*, vol. 119, no. 3, pp. 508–518, 2006.

[72] K. Hayakawa, H. Tatsumi, and M. Sokabe, "Actin stress fibers transmit and focus force to activate mechanosensitive channels," *Journal of Cell Science*, vol. 121, no. 4, pp. 496–503, 2008.

[73] K. A. DeMali, K. Wennerberg, and K. Burridge, "Integrin signaling to the actin cytoskeleton," *Current Opinion in Cell Biology*, vol. 15, no. 5, pp. 572–582, 2003.

[74] A. J. Putnam, J. J. Cunningham, B. B. L. Pillemer, and D. J. Mooney, "External mechanical strain regulates membrane targeting of Rho GTPases by controlling microtubule assembly," *American Journal of Physiology. Cell Physiology*, vol. 284, no. 3, pp. C627–C639, 2003.

[75] T. Ishida, M. Takahashi, M. A. Corson, and B. C. Berk, "Fluid shear stress-mediated signal transduction: how do endothelial cells transduce mechanical force into biological responses?," *Annals of the New York Academy of Sciences*, vol. 811, pp. 12–24, 1997.

[76] S. Lehoux, Y. Castier, and A. Tedgui, "Molecular mechanisms of the vascular responses to haemodynamic forces," *Journal of Internal Medicine*, vol. 259, no. 4, pp. 381–392, 2006.

[77] T. Ishida, T. E. Peterson, N. L. Kovach, and B. C. Berk, "MAP kinase activation by flow in endothelial cells. Role of $\beta 1$ integrins and tyrosine kinases," *Circulation Research*, vol. 79, no. 2, pp. 310–316, 1996.

[78] C. Schmidt, H. Pommerenke, F. Dürr, B. Nebe, and J. Rychly, "Mechanical stressing of integrin receptors induces enhanced tyrosine phosphorylation of cytoskeletally anchored proteins," *Journal of Biological Chemistry*, vol. 273, no. 9, pp. 5081–5085, 1998.

[79] J. L. Schwachtgen, P. Houston, C. Campbell, V. Sukhatme, and M. Braddock, "Fluid shear stress activation of egr-1 transcription in cultured human endothelial and epithelial cells is mediated via the extracellular signal-related kinase 1/2

mitogen-activated protein kinase pathway," *The Journal of Clinical Investigation*, vol. 101, no. 11, pp. 2540–2549, 1998.

[80] Y. Sawada, M. Tamada, B. J. Dubin-Thaler et al., "Force sensing by mechanical extension of the Src family kinase substrate p130Cas," *Cell*, vol. 127, no. 5, pp. 1015–1026, 2006.

[81] M. Tamada, M. P. Sheetz, and Y. Sawada, "Activation of a signaling cascade by cytoskeleton stretch," *Developmental Cell*, vol. 7, no. 5, pp. 709–718, 2004.

[82] K. Burridge and K. Wennerberg, "Rho and Rac take center stage," *Cell*, vol. 116, no. 2, pp. 167–179, 2004.

[83] A. B. Jaffe and A. Hall, "Rho GTPases: biochemistry and biology," *Annual Review of Cell and Developmental Biology*, vol. 21, no. 1, pp. 247–269, 2005.

[84] E. C. Lessey, C. Guilluy, and K. Burridge, "From mechanical force to RhoA activation," *Biochemistry*, vol. 51, no. 38, pp. 7420–7432, 2012.

[85] V. Vogel and M. Sheetz, "Local force and geometry sensing regulate cell functions," *Nature Reviews Molecular Cell Biology*, vol. 7, no. 4, pp. 265–275, 2006.

[86] K. G. Young and J. W. Copeland, "Formins in cell signaling," *Biochimica et Biophysica Acta (BBA) - Molecular Cell Research*, vol. 1803, no. 2, pp. 183–190, 2010.

[87] G. Civelekoglu-Scholey, A. Wayne Orr, I. Novak, J. J. Meister, M. A. Schwartz, and A. Mogilner, "Model of coupled transient changes of Rac, Rho, adhesions and stress fibers alignment in endothelial cells responding to shear stress," *Journal of Theoretical Biology*, vol. 232, no. 4, pp. 569–585, 2005.

[88] D. Zhou, D. J. Herrick, J. Rosenbloom, and B. Chaqour, "Cyr61 mediates the expression of VEGF, α_v-integrin, and α-actin genes through cytoskeletally based mechanotransduction mechanisms in bladder smooth muscle cells," *Journal of Applied Physiology*, vol. 98, no. 6, pp. 2344–2354, 2005.

[89] A. Sarasa-Renedo, V. Tunc-Civelek, and M. Chiquet, "Role of RhoA/ROCK-dependent actin contractility in the induction of tenascin-C by cyclic tensile strain," *Experimental Cell Research*, vol. 312, no. 8, pp. 1361–1370, 2006.

[90] E. Tzima, W. B. Kiosses, M. A. del Pozo, and M. A. Schwartz, "Localized cdc42 activation, detected using a novel assay, mediates microtubule organizing center positioning in endothelial cells in response to fluid shear stress," *Journal of Biological Chemistry*, vol. 278, no. 33, pp. 31020–31023, 2003.

[91] X. H. Zhao, C. Laschinger, P. Arora, K. Szaszi, A. Kapus, and C. A. McCulloch, "Force activates smooth muscle α-actin promoter activity through the Rho signaling pathway," *Journal of Cell Science*, vol. 120, no. 10, pp. 1801–1809, 2007.

[92] M. B. Asparuhova, L. Gelman, and M. Chiquet, "Role of the actin cytoskeleton in tuning cellular responses to external mechanical stress," *Scandinavian Journal of Medicine & Science in Sports*, vol. 19, no. 4, pp. 490–499, 2009.

[93] R. Zaidel-Bar, C. Ballestrem, Z. Kam, and B. Geiger, "Early molecular events in the assembly of matrix adhesions at the leading edge of migrating cells," *Journal of Cell Science*, vol. 116, no. 22, pp. 4605–4613, 2003.

[94] S. K. Hanks, L. Ryzhova, N. Y. Shin, and J. Brábek, "Focal adhesion kinase signaling activities and their implications in the control of cell survival and motility," *Frontiers in Bioscience*, vol. 8, no. 4, pp. d982–d996, 2003.

[95] Y. Nojima, N. Morino, T. Mimura et al., "Integrin-mediated cell adhesion promotes tyrosine phosphorylation of p130*Cas*, a Src homology 3-containing molecule having multiple Src homology 2-binding motifs," *Journal of Biological Chemistry*, vol. 270, no. 25, pp. 15398–15402, 1995.

[96] T. S. Panetti, "Tyrosine phosphorylation of paxillin, FAK, and p130CAS: effects on cell spreading and migration," *Frontiers in Bioscience*, vol. 7, pp. d143–d150, 2002.

[97] H. B. Schiller, M. R. Hermann, J. Polleux et al., "β1- and αv-class integrins cooperate to regulate myosin II during rigidity sensing of fibronectin-based microenvironments," *Nature Cell Biology*, vol. 15, no. 6, pp. 625–636, 2013.

[98] L. Vitillo and S. J. Kimber, "Integrin and FAK regulation of human pluripotent stem cells," *Current Stem Cell Reports*, vol. 3, no. 4, pp. 358–365, 2017.

[99] M. Ohgushi, M. Matsumura, M. Eiraku et al., "Molecular pathway and cell state responsible for dissociation-induced apoptosis in human pluripotent stem cells," *Cell Stem Cell*, vol. 7, no. 2, pp. 225–239, 2010.

[100] M. A. Baxter, M. V. Camarasa, N. Bates et al., "Analysis of the distinct functions of growth factors and tissue culture substrates necessary for the long-term self-renewal of human embryonic stem cell lines," *Stem Cell Research*, vol. 3, no. 1, pp. 28–38, 2009.

[101] D. Soteriou, B. Iskender, A. Byron et al., "Comparative proteomic analysis of supportive and unsupportive extracellular matrix substrates for human embryonic stem cell maintenance," *The Journal of Biological Chemistry*, vol. 288, no. 26, pp. 18716–18731, 2013.

[102] J. Rajagopal and B. Z. Stanger, "Plasticity in the adult: how should the Waddington diagram be applied to regenerating tissues?," *Developmental Cell*, vol. 36, no. 2, pp. 133–137, 2016.

[103] C. H. Waddington, *The Strategy of the Genes: A Discussion of some Aspects of Theoretical Biology*, George Allen & Unwin Ltd, London, 1957.

[104] J. M. W. Slack, "Conrad Hal Waddington: the last renaissance biologist?," *Nature Reviews Genetics*, vol. 3, no. 11, pp. 889–895, 2002.

[105] B. Ebrahimi, "Reprogramming barriers and enhancers: strategies to enhance the efficiency and kinetics of induced pluripotency," *Cell Regeneration*, vol. 4, no. 1, p. 10, 2015.

[106] P. Samavarchi-Tehrani, A. Golipour, L. David et al., "Functional genomics reveals a BMP-driven mesenchymal-to-epithelial transition in the initiation of somatic cell reprogramming," *Cell Stem Cell*, vol. 7, no. 1, pp. 64–77, 2010.

[107] L. Warren, P. D. Manos, T. Ahfeldt et al., "Highly efficient reprogramming to pluripotency and directed differentiation of human cells with synthetic modified mRNA," *Cell Stem Cell*, vol. 7, no. 5, pp. 618–630, 2010.

[108] Z. Li and T. M. Rana, "A kinase inhibitor screen identifies small-molecule enhancers of reprogramming and iPS cell generation," *Nature Communications*, vol. 3, no. 1, p. 1085, 2012.

[109] B. Feng, J. H. Ng, J. C. D. Heng, and H. H. Ng, "Molecules that promote or enhance reprogramming of somatic cells to induced pluripotent stem cells," *Cell Stem Cell*, vol. 4, no. 4, pp. 301–312, 2009.

[110] N. Miyoshi, H. Ishii, H. Nagano et al., "Reprogramming of mouse and human cells to pluripotency using mature microRNAs," *Cell Stem Cell*, vol. 8, no. 6, pp. 633–638, 2011.

[111] M. J. Dalby, N. Gadegaard, and R. O. C. Oreffo, "Harnessing nanotopography and integrin-matrix interactions to

influence stem cell fate," *Nature Materials*, vol. 13, no. 6, pp. 558–569, 2014.

[112] T. L. Downing, J. Soto, C. Morez et al., "Biophysical regulation of epigenetic state and cell reprogramming," *Nature Materials*, vol. 12, no. 12, pp. 1154–1162, 2013.

[113] Y. M. Kim, Y. G. Kang, S. H. Park et al., "Effects of mechanical stimulation on the reprogramming of somatic cells into human-induced pluripotent stem cells," *Stem Cell Research & Therapy*, vol. 8, no. 1, p. 139, 2017.

[114] D. Li, J. Zhou, L. Wang et al., "Integrated biochemical and mechanical signals regulate multifaceted human embryonic stem cell functions," *The Journal of Cell Biology*, vol. 191, no. 3, pp. 631–644, 2010.

[115] Y. C. Toh, J. Xing, and H. Yu, "Modulation of integrin and E-cadherin-mediated adhesions to spatially control heterogeneity in human pluripotent stem cell differentiation," *Biomaterials*, vol. 50, pp. 87–97, 2015.

[116] S. Abbasalizadeh, M. R. Larijani, A. Samadian, and H. Baharvand, "Bioprocess development for mass production of size-controlled human pluripotent stem cell aggregates in stirred suspension bioreactor," *Tissue Engineering Part C: Methods*, vol. 18, no. 11, pp. 831–851, 2012.

[117] C. Kropp, H. Kempf, C. Halloin et al., "Impact of feeding strategies on the scalable expansion of human pluripotent stem cells in single-use stirred tank bioreactors," *Stem Cells Translational Medicine*, vol. 5, no. 10, pp. 1289–1301, 2016.

[118] J. Beers, D. R. Gulbranson, N. George et al., "Passaging and colony expansion of human pluripotent stem cells by enzyme-free dissociation in chemically defined culture conditions," *Nature Protocols*, vol. 7, no. 11, pp. 2029–2040, 2012.

[119] G. Chen, Z. Hou, D. R. Gulbranson, and J. A. Thomson, "Actin-myosin contractility is responsible for the reduced viability of dissociated human embryonic stem cells," *Cell Stem Cell*, vol. 7, no. 2, pp. 240–248, 2010.

[120] S. Kilens, D. Meistermann, D. Moreno et al., "Parallel derivation of isogenic human primed and naive induced pluripotent stem cells," *Nature Communications*, vol. 9, no. 1, p. 360, 2018.

[121] J. Nichols and A. Smith, "Naive and primed pluripotent states," *Cell Stem Cell*, vol. 4, no. 6, pp. 487–492, 2009.

[122] I. G. M. Brons, L. E. Smithers, M. W. B. Trotter et al., "Derivation of pluripotent epiblast stem cells from mammalian embryos," *Nature*, vol. 448, no. 7150, pp. 191–195, 2007.

[123] P. J. Tesar, J. G. Chenoweth, F. A. Brook et al., "New cell lines from mouse epiblast share defining features with human embryonic stem cells," *Nature*, vol. 448, no. 7150, pp. 196–199, 2007.

[124] Y. Yang, B. Liu, J. Xu et al., "Derivation of pluripotent stem cells with in vivo embryonic and extraembryonic potency," *Cell*, vol. 169, no. 2, pp. 243–257.e25, 2017.

[125] H. Chen, I. Aksoy, F. Gonnot et al., "Reinforcement of STAT3 activity reprogrammes human embryonic stem cells to naive-like pluripotency," *Nature Communications*, vol. 6, no. 1, p. 7095, 2015.

[126] Y. S. Chan, J. Göke, J. H. Ng et al., "Induction of a human pluripotent state with distinct regulatory circuitry that resembles preimplantation epiblast," *Cell Stem Cell*, vol. 13, no. 6, pp. 663–675, 2013.

[127] O. Gafni, L. Weinberger, A. A. Mansour et al., "Derivation of novel human ground state naive pluripotent stem cells," *Nature*, vol. 504, no. 7479, pp. 282–286, 2013.

[128] Y. Takashima, G. Guo, R. Loos et al., "Resetting transcription factor control circuitry toward ground-state pluripotency in human," *Cell*, vol. 158, no. 6, pp. 1254–1269, 2014.

[129] T. W. Theunissen, B. E. Powell, H. Wang et al., "Systematic identification of culture conditions for induction and maintenance of naive human pluripotency," *Cell Stem Cell*, vol. 15, no. 4, pp. 471–487, 2014.

[130] Y. Hayashi and M. K. Furue, "Biological effects of culture substrates on human pluripotent stem cells," *Stem Cells International*, vol. 2016, Article ID 5380560, 11 pages, 2016.

[131] Y. Hayashi, M. K. Furue, T. Okamoto et al., "Integrins regulate mouse embryonic stem cell self-renewal," *Stem Cells*, vol. 25, no. 12, pp. 3005–3015, 2007.

[132] T. J. Rowland, L. M. Miller, A. J. Blaschke et al., "Roles of integrins in human induced pluripotent stem cell growth on Matrigel and vitronectin," *Stem Cells and Development*, vol. 19, no. 8, pp. 1231–1240, 2010.

[133] T. Yu, S. Miyagawa, K. Miki et al., "In vivo differentiation of induced pluripotent stem cell-derived cardiomyocytes," *Circulation Journal*, vol. 77, no. 5, pp. 1297–1306, 2013.

[134] H. Y. Kim, S. Baek, N. R. Han, E. Lee, C. K. Park, and S. T. Lee, "Identification of integrin heterodimers functioning on the surface of undifferentiated porcine primed embryonic stem cells," *Cell Biology International*, vol. 42, no. 9, pp. 1221–1227, 2018.

[135] Y. Meng, S. Eshghi, Y. J. Li, R. Schmidt, D. V. Schaffer, and K. E. Healy, "Characterization of integrin engagement during defined human embryonic stem cell culture," *The FASEB Journal*, vol. 24, no. 4, pp. 1056–1065, 2010.

[136] S. T. Lee, J. I. Yun, Y. S. Jo et al., "Engineering integrin signaling for promoting embryonic stem cell self-renewal in a precisely defined niche," *Biomaterials*, vol. 31, no. 6, pp. 1219–1226, 2010.

[137] L. G. Villa-Diaz, J. K. Kim, A. Laperle, S. P. Palecek, and P. H. Krebsbach, "Inhibition of focal adhesion kinase signaling by integrin $\alpha 6\beta 1$ supports human pluripotent stem cell self-renewal," *Stem Cells*, vol. 34, no. 7, pp. 1753–1764, 2016.

[138] O. Hazenbiller, N. A. Duncan, and R. J. Krawetz, "Reduction of pluripotent gene expression in murine embryonic stem cells exposed to mechanical loading or Cyclo RGD peptide," *BMC Cell Biology*, vol. 18, no. 1, p. 32, 2017.

[139] T. Miyazaki, S. Futaki, K. Hasegawa et al., "Recombinant human laminin isoforms can support the undifferentiated growth of human embryonic stem cells," *Biochemical and Biophysical Research Communications*, vol. 375, no. 1, pp. 27–32, 2008.

[140] C. L. Mummery, J. Zhang, E. S. Ng, D. A. Elliott, A. G. Elefanty, and T. J. Kamp, "Differentiation of human embryonic stem cells and induced pluripotent stem cells to cardiomyocytes: a methods overview," *Circulation Research*, vol. 111, no. 3, pp. 344–358, 2012.

[141] D. Zeng, D. B. Ou, T. Wei et al., "Collagen/β_1 integrin interaction is required for embryoid body formation during cardiogenesis from murine induced pluripotent stem cells," *BMC Cell Biology*, vol. 14, no. 1, p. 5, 2013.

[142] H. C. Moeller, M. K. Mian, S. Shrivastava, B. G. Chung, and A. Khademhosseini, "A microwell array system for stem cell culture," *Biomaterials*, vol. 29, no. 6, pp. 752–763, 2008.

[143] B. Valamehr, S. J. Jonas, J. Polleux et al., "Hydrophobic surfaces for enhanced differentiation of embryonic stem cell-derived embryoid bodies," *Proceedings of the National Academy of Sciences of the United States of America*, vol. 105, no. 38, pp. 14459–14464, 2008.

[144] Y. S. Hwang, B. G. Chung, D. Ortmann, N. Hattori, H. C. Moeller, and A. Khademhosseini, "Microwell-mediated control of embryoid body size regulates embryonic stem cell fate via differential expression of WNT5a and WNT11," *Proceedings of the National Academy of Sciences of the United States of America*, vol. 106, no. 40, pp. 16978–16983, 2009.

[145] X. Lian, J. Zhang, S. M. Azarin et al., "Directed cardiomyocyte differentiation from human pluripotent stem cells by modulating Wnt/β-catenin signaling under fully defined conditions," *Nature Protocols*, vol. 8, no. 1, pp. 162–175, 2013.

[146] S. Bhattacharya, P. W. Burridge, E. M. Kropp et al., "High efficiency differentiation of human pluripotent stem cells to cardiomyocytes and characterization by flow cytometry," *Journal of Visualized Experiments*, vol. 91, no. 91, article 52010, 2014.

[147] P. W. Burridge, S. Thompson, M. A. Millrod et al., "A universal system for highly efficient cardiac differentiation of human induced pluripotent stem cells that eliminates interline variability," *PLoS One*, vol. 6, no. 4, article e18293, 2011.

[148] R. G. James, W. H. Conrad, and R. T. Moon, "β-Catenin-independent Wnt pathways: signals, core proteins, and effectors," *Methods in Molecular Biology*, vol. 468, pp. 131–144, 2008.

[149] D. Kumar, S. Sharma, S. Verma, P. Kumar, and R. K. Ambasta, "Role of Wnt-p53-Nox signaling pathway in cancer development and progression," *British Journal of Medicine and Medical Research*, vol. 8, no. 8, pp. 651–676, 2015.

[150] T. S. Huang, L. Li, L. Moalim-Nour et al., "A regulatory network involving β-catenin, e-cadherin, PI3k/Akt, and SLUG balances self-renewal and differentiation of human pluripotent stem cells in response to Wnt signaling," *Stem Cells*, vol. 33, no. 5, pp. 1419–1433, 2015.

[151] M. Zhao, C. Fan, P. J. Ernst et al., "Y-27632 preconditioning enhances transplantation of human-induced pluripotent stem cell-derived cardiomyocytes in myocardial infarction mice," *Cardiovascular Research*, vol. 115, no. 2, pp. 343–356, 2019.

[152] A. Kallas-Kivi, A. Trei, A. Stepanjuk et al., "The role of integrin β1 in the heterogeneity of human embryonic stem cells culture," *Biology Open*, vol. 7, no. 11, article bio034355, 2018.

[153] N. Gadhari, M. Charnley, M. Marelli, J. Brugger, and M. Chiquet, "Cell shape-dependent early responses of fibroblasts to cyclic strain," *Biochimica et Biophysica Acta (BBA) - Molecular Cell Research*, vol. 1833, no. 12, pp. 3415–3425, 2013.

[154] G. Posern and R. Treisman, "Actin' together: serum response factor, its cofactors and the link to signal transduction," *Trends in Cell Biology*, vol. 16, no. 11, pp. 588–596, 2006.

[155] T. Kishi, T. Mayanagi, S. Iwabuchi, T. Akasaka, and K. Sobue, "Myocardin-related transcription factor A (MRTF-A) activity-dependent cell adhesion is correlated to focal adhesion kinase (FAK) activity," *Oncotarget*, vol. 7, no. 44, pp. 72113–72130, 2016.

[156] G. Galmiche, C. Labat, M. Mericskay et al., "Inactivation of serum response factor contributes to decrease vascular muscular tone and arterial stiffness in mice," *Circulation Research*, vol. 112, no. 7, pp. 1035–1045, 2013.

[157] L. Wei, L. Wang, J. A. Carson, J. E. Agan, K. Imanaka-Yoshida, and R. J. Schwartz, "β1 integrin and organized actin filaments facilitate cardiomyocyte-specific RhoA-dependent activation of the skeletal α-actin promoter," *The FASEB Journal*, vol. 15, no. 3, pp. 785–796, 2001.

[158] G. Schratt, U. Philippar, J. Berger, H. Schwarz, O. Heidenreich, and A. Nordheim, "Serum response factor is crucial for actin cytoskeletal organization and focal adhesion assembly in embryonic stem cells," *The Journal of Cell Biology*, vol. 156, no. 4, pp. 737–750, 2002.

[159] S. Dupont, L. Morsut, M. Aragona et al., "Role of YAP/TAZ in mechanotransduction," *Nature*, vol. 474, no. 7350, pp. 179–183, 2011.

[160] M. Pesce and R. Santoro, "Feeling the right force: how to contextualize the cell mechanical behavior in physiologic turnover and pathologic evolution of the cardiovascular system," *Pharmacology & Therapeutics*, vol. 171, pp. 75–82, 2017.

[161] G. Nardone, J. Oliver-de la Cruz, J. Vrbsky et al., "YAP regulates cell mechanics by controlling focal adhesion assembly," *Nature Communications*, vol. 8, article 15321, 2017.

[162] S. Dupont, "Role of YAP/TAZ in cell-matrix adhesion-mediated signalling and mechanotransduction," *Experimental Cell Research*, vol. 343, no. 1, pp. 42–53, 2016.

[163] J. S. Mo, F. X. Yu, R. Gong, J. H. Brown, and K. L. Guan, "Regulation of the Hippo-YAP pathway by protease-activated receptors (PARs)," *Genes & Development*, vol. 26, no. 19, pp. 2138–2143, 2012.

[164] R. Santoro, D. Scaini, L. U. Severino et al., "Activation of human aortic valve interstitial cells by local stiffness involves YAP-dependent transcriptional signaling," *Biomaterials*, vol. 181, pp. 268–279, 2018.

[165] R. McBeath, D. M. Pirone, C. M. Nelson, K. Bhadriraju, and C. S. Chen, "Cell shape, cytoskeletal tension, and RhoA regulate stem cell lineage commitment," *Developmental Cell*, vol. 6, no. 4, pp. 483–495, 2004.

[166] A. Elbediwy and B. J. Thompson, "Evolution of mechanotransduction via YAP/TAZ in animal epithelia," *Current Opinion in Cell Biology*, vol. 51, pp. 117–123, 2018.

[167] H. Sabra, M. Brunner, V. Mandati et al., "β1 integrin-dependent Rac/group I PAK signaling mediates YAP activation of Yes-associated protein 1 (YAP1) via NF2/merlin," *The Journal of Biological Chemistry*, vol. 292, no. 47, pp. 19179–19197, 2017.

[168] F. Gattazzo, A. Urciuolo, and P. Bonaldo, "Extracellular matrix: a dynamic microenvironment for stem cell niche," *Biochimica et Biophysica Acta (BBA) - General Subjects*, vol. 1840, no. 8, pp. 2506–2519, 2014.

[169] T. Rozario and D. W. DeSimone, "The extracellular matrix in development and morphogenesis: a dynamic view," *Developmental Biology*, vol. 341, no. 1, pp. 126–140, 2010.

[170] R. Santoro, F. Consolo, M. Spiccia et al., "Feasibility of pig and human-derived aortic valve interstitial cells seeding on fixative-free decellularized animal pericardium," *Journal of Biomedical Materials Research Part B: Applied Biomaterials*, vol. 104, no. 2, pp. 345–356, 2016.

[171] K. Narayanan, V. Y. Lim, J. Shen et al., "Extracellular matrix-mediated differentiation of human embryonic stem

cells: differentiation to insulin-secreting beta cells," *Tissue Engineering Part A*, vol. 20, no. 1-2, pp. 424–433, 2014.

[172] B. Liau, N. Christoforou, K. W. Leong, and N. Bursac, "Pluripotent stem cell-derived cardiac tissue patch with advanced structure and function," *Biomaterials*, vol. 32, no. 35, pp. 9180–9187, 2011.

[173] F. Moroni and T. Mirabella, "Decellularized matrices for cardiovascular tissue engineering," *American Journal of Stem Cells*, vol. 3, no. 1, pp. 1–20, 2014.

[174] K. P. Robb, A. Shridhar, and L. E. Flynn, "Decellularized matrices as cell-instructive scaffolds to guide tissue-specific regeneration," *ACS Biomaterials Science & Engineering*, vol. 4, no. 11, pp. 3627–3643, 2018.

[175] E. Garreta, L. de Oñate, M. E. Fernández-Santos et al., "Myocardial commitment from human pluripotent stem cells: rapid production of human heart grafts," *Biomaterials*, vol. 98, pp. 64–78, 2016.

[176] P. L. Sánchez, M. E. Fernández-Santos, S. Costanza et al., "Acellular human heart matrix: a critical step toward whole heart grafts," *Biomaterials*, vol. 61, pp. 279–289, 2015.

[177] J. P. Guyette, J. M. Charest, R. W. Mills et al., "Bioengineering human myocardium on native extracellular matrix," *Circulation Research*, vol. 118, no. 1, pp. 56–72, 2016.

[178] W. L. Stoppel, A. E. Gao, A. M. Greaney et al., "Elastic, silk-cardiac extracellular matrix hydrogels exhibit time-dependent stiffening that modulates cardiac fibroblast response," *Journal of Biomedical Materials Research Part A*, vol. 104, no. 12, pp. 3058–3072, 2016.

[179] F. Amadeo, F. Boschetti, G. Polvani, C. Banfi, M. Pesce, and R. Santoro, "Aortic valve cell seeding into decellularized animal pericardium by perfusion-assisted bioreactor," *Journal of Tissue Engineering and Regenerative Medicine*, vol. 12, no. 6, pp. 1481–1493, 2018.

[180] D. A. Taylor, O. H. Frazier, A. Elgalad, C. Hochman-Mendez, and L. C. Sampaio, "Building a total bioartificial heart: harnessing nature to overcome the current hurdles," *Artif Organs*, vol. 42, no. 10, pp. 970–982, 2018.

[181] S. Yesmin, M. B. Paget, H. E. Murray, and R. Downing, "Bio-scaffolds in organ-regeneration: clinical potential and current challenges," *Current Research in Translational Medicine*, vol. 65, no. 3, pp. 103–113, 2017.

[182] F. Pati, J. Jang, D. H. Ha et al., "Printing three-dimensional tissue analogues with decellularized extracellular matrix bioink," *Nature Communications*, vol. 5, no. 1, article 3935, 2014.

[183] X. Ma, C. Yu, P. Wang et al., "Rapid 3D bioprinting of decellularized extracellular matrix with regionally varied mechanical properties and biomimetic microarchitecture," *Biomaterials*, vol. 185, pp. 310–321, 2018.

[184] A. Moorthi, Y. C. Tyan, and T. W. Chung, "Surface-modified polymers for cardiac tissue engineering," *Biomaterials Science*, vol. 5, no. 10, pp. 1976–1987, 2017.

[185] H. Kasahara and I. Hayashi, "Polyglycolic acid sheet with fibrin glue potentiates the effect of a fibrin-based haemostat in cardiac surgery," *Journal of Cardiothoracic Surgery*, vol. 9, no. 1, p. 121, 2014.

[186] V. Chiono, P. Mozetic, M. Boffito et al., "Polyurethane-based scaffolds for myocardial tissue engineering," *Interface Focus*, vol. 4, no. 1, article 20130045, 2014.

[187] M. Boffito, F. di Meglio, P. Mozetic et al., "Surface functionalization of polyurethane scaffolds mimicking the myocardial microenvironment to support cardiac primitive cells," *PLoS One*, vol. 13, no. 7, article e0199896, 2018.

[188] M. H. Yang, S. B. Jong, C. Y. Lu et al., "Assessing the responses of cellular proteins induced by hyaluronic acid-modified surfaces utilizing a mass spectrometry-based profiling system: over-expression of CD36, CD44, CDK9, and PP2A," *Analyst*, vol. 137, no. 21, pp. 4921–4933, 2012.

[189] F. Vozzi, F. Logrand, M. Cabiati et al., "Biomimetic engineering of the cardiac tissue through processing, functionalization, and biological characterization of polyester urethanes," *Biomedical Materials*, vol. 13, no. 5, p. 055006, 2018.

[190] J. Yang, Y. Mei, A. L. Hook et al., "Polymer surface functionalities that control human embryoid body cell adhesion revealed by high throughput surface characterization of combinatorial material microarrays," *Biomaterials*, vol. 31, no. 34, pp. 8827–8838, 2010.

[191] W. H. Zimmermann, I. Melnychenko, and T. Eschenhagen, "Engineered heart tissue for regeneration of diseased hearts," *Biomaterials*, vol. 25, no. 9, pp. 1639–1647, 2004.

[192] C. Castaldo, F. di Meglio, R. Miraglia et al., "Cardiac fibroblast-derived extracellular matrix (biomatrix) as a model for the studies of cardiac primitive cell biological properties in normal and pathological adult human heart," *BioMed Research International*, vol. 2013, Article ID 352370, 7 pages, 2013.

[193] R. V. Nair, A. Farrukh, and A. Del Campo, "A photoactivatable $\alpha 5\beta 1$-specific integrin ligand," *Chembiochem*, vol. 19, no. 12, pp. 1280–1287, 2018.

[194] S. Y. Boateng, S. S. Lateef, W. Mosley, T. J. Hartman, L. Hanley, and B. Russell, "RGD and YIGSR synthetic peptides facilitate cellular adhesion identical to that of laminin and fibronectin but alter the physiology of neonatal cardiac myocytes," *American Journal of Physiology Cell Physiology*, vol. 288, no. 1, pp. C30–C38, 2005.

[195] S. Mukherjee, J. Reddy Venugopal, R. Ravichandran, S. Ramakrishna, and M. Raghunath, "Evaluation of the biocompatibility of PLACL/collagen nanostructured matrices with cardiomyocytes as a model for the regeneration of infarcted myocardium," *Advanced Functional Materials*, vol. 21, no. 12, pp. 2291–2300, 2011.

[196] D. A. Wang, J. Ji, Y. H. Sun, J. C. Shen, L. X. Feng, and J. H. Elisseeff, "In situ immobilization of proteins and RGD peptide on polyurethane surfaces via poly(ethylene oxide) coupling polymers for human endothelial cell growth," *Biomacromolecules*, vol. 3, no. 6, pp. 1286–1295, 2002.

[197] M. Riaz, M. Versaevel, D. Mohammed, K. Glinel, and S. Gabriele, "Persistence of fan-shaped keratocytes is a matrix-rigidity-dependent mechanism that requires $\alpha_5\beta_1$ integrin engagement," *Scientific Reports*, vol. 6, no. 1, p. 34141, 2016.

[198] E. M. Ovadia, D. W. Colby, and A. M. Kloxin, "Designing well-defined photopolymerized synthetic matrices for three-dimensional culture and differentiation of induced pluripotent stem cells," *Biomaterials Science*, vol. 6, no. 6, pp. 1358–1370, 2018.

[199] C. K. K. Choi, Y. J. Xu, B. Wang, M. Zhu, L. Zhang, and L. Bian, "Substrate coupling strength of integrin-binding ligands modulates adhesion, spreading, and differentiation of human mesenchymal stem cells," *Nano Letters*, vol. 15, no. 10, pp. 6592–6600, 2015.

[200] W. S. Chen, L. Y. Guo, A. M. Masroujeh et al., "A single-step surface modification of electrospun silica nanofibers using a

silica binding protein fused with an RGD motif for enhanced PC12 cell growth and differentiation," *Materials*, vol. 11, no. 6, 2018.

[201] C. C. Cheng, D. J. Lee, and J. K. Chen, "Self-assembled supramolecular polymers with tailorable properties that enhance cell attachment and proliferation," *Acta Biomaterialia*, vol. 50, pp. 476–483, 2017.

[202] Y. W. Chun, D. A. Balikov, T. K. Feaster et al., "Combinatorial polymer matrices enhance in vitro maturation of human induced pluripotent stem cell-derived cardiomyocytes," *Biomaterials*, vol. 67, pp. 52–64, 2015.

[203] E. Grespan, G. G. Giobbe, F. Badique, K. Anselme, J. Rühe, and N. Elvassore, "Effect of geometrical constraints on human pluripotent stem cell nuclei in pluripotency and differentiation," *Integrative Biology*, vol. 10, no. 5, pp. 278–289, 2018.

[204] H. R. Seo, H. J. Joo, D. H. Kim et al., "Nanopillar surface topology promotes cardiomyocyte differentiation through cofilin-mediated cytoskeleton rearrangement," *ACS Applied Materials & Interfaces*, vol. 9, no. 20, pp. 16803–16812, 2017.

[205] E. Cimetta, S. Pizzato, S. Bollini, E. Serena, P. de Coppi, and N. Elvassore, "Production of arrays of cardiac and skeletal muscle myofibers by micropatterning techniques on a soft substrate," *Biomedical Microdevices*, vol. 11, no. 2, pp. 389–400, 2009.

[206] A. Tijore, S. A. Irvine, U. Sarig, P. Mhaisalkar, V. Baisane, and S. Venkatraman, "Contact guidance for cardiac tissue engineering using 3D bioprinted gelatin patterned hydrogel," *Biofabrication*, vol. 10, no. 2, article 025003, 2018.

[207] B. Xu, A. Magli, Y. Anugrah, S. J. Koester, R. C. R. Perlingeiro, and W. Shen, "Nanotopography-responsive myotube alignment and orientation as a sensitive phenotypic biomarker for Duchenne muscular dystrophy," *Biomaterials*, vol. 183, pp. 54–66, 2018.

[208] G. Abagnale, A. Sechi, M. Steger et al., "Surface topography guides morphology and spatial patterning of induced pluripotent stem cell colonies," *Stem Cell Reports*, vol. 9, no. 2, pp. 654–666, 2017.

[209] Y. Chen, L. Ju, M. Rushdi, C. Ge, and C. Zhu, "Receptor-mediated cell mechanosensing," *Molecular Biology of the Cell*, vol. 28, no. 23, pp. 3134–3155, 2017.

[210] J. Wang, A. Chen, D. K. Lieu et al., "Effect of engineered anisotropy on the susceptibility of human pluripotent stem cell-derived ventricular cardiomyocytes to arrhythmias," *Biomaterials*, vol. 34, no. 35, pp. 8878–8886, 2013.

[211] C. Xu, L. Wang, Y. Yu et al., "Bioinspired onion epithelium-like structure promotes the maturation of cardiomyocytes derived from human pluripotent stem cells," *Biomaterials Science*, vol. 5, no. 9, pp. 1810–1819, 2017.

[212] G. K. Xu, X. Q. Feng, and H. Gao, "Orientations of cells on compliant substrates under biaxial stretches: a theoretical study," *Biophysical Journal*, vol. 114, no. 3, pp. 701–710, 2018.

[213] Y. Tan, D. Richards, R. Xu et al., "Silicon nanowire-induced maturation of cardiomyocytes derived from human induced pluripotent stem cells," *Nano Letters*, vol. 15, no. 5, pp. 2765–2772, 2015.

[214] D. J. Richards, Y. Tan, R. Coyle et al., "Nanowires and electrical stimulation synergistically improve functions of hiPSC cardiac spheroids," *Nano Letters*, vol. 16, no. 7, pp. 4670–4678, 2016.

[215] E. Huethorst, M. Hortigon, V. Zamora-Rodriguez et al., "Enhanced human-induced pluripotent stem cell derived cardiomyocyte maturation using a dual microgradient substrate," *ACS Biomaterials Science & Engineering*, vol. 2, no. 12, pp. 2231–2239, 2016.

[216] K. A. Kilian, B. Bugarija, B. T. Lahn, and M. Mrksich, "Geometric cues for directing the differentiation of mesenchymal stem cells," *Proceedings of the National Academy of Sciences of the United States of America*, vol. 107, no. 11, pp. 4872–4877, 2010.

[217] F. F. B. Hulshof, Y. Zhao, A. Vasilevich et al., "NanoTopoChip: high-throughput nanotopographical cell instruction," *Acta Biomaterialia*, vol. 62, pp. 188–198, 2017.

[218] F. B. Myers, J. S. Silver, Y. Zhuge et al., "Robust pluripotent stem cell expansion and cardiomyocyte differentiation via geometric patterning," *Integrative Biology*, vol. 5, no. 12, pp. 1495–1506, 2013.

[219] F. Karimi, A. J. O'Connor, G. G. Qiao, and D. E. Heath, "Integrin clustering matters: a review of biomaterials functionalized with multivalent integrin-binding ligands to improve cell adhesion, migration, differentiation, angiogenesis, and biomedical device integration," *Advanced Healthcare Materials*, vol. 7, no. 12, article e1701324, 2018.

[220] D. J. Irvine, A. M. Mayes, and L. G. Griffith, "Nanoscale clustering of RGD peptides at surfaces using comb polymers. 1. Synthesis and characterization of Comb thin films," *Biomacromolecules*, vol. 2, no. 1, pp. 85–94, 2001.

[221] D. J. Irvine, A. V. G. Ruzette, A. M. Mayes, and L. G. Griffith, "Nanoscale clustering of RGD peptides at surfaces using comb polymers. 2. Surface segregation of comb polymers in polylactide," *Biomacromolecules*, vol. 2, no. 2, pp. 545–556, 2001.

[222] E. Altrock, C. A. Muth, G. Klein, J. P. Spatz, and C. Lee-Thedieck, "The significance of integrin ligand nanopatterning on lipid raft clustering in hematopoietic stem cells," *Biomaterials*, vol. 33, no. 11, pp. 3107–3118, 2012.

[223] M. Schvartzman, M. Palma, J. Sable et al., "Nanolithographic control of the spatial organization of cellular adhesion receptors at the single-molecule level," *Nano Letters*, vol. 11, no. 3, pp. 1306–1312, 2011.

[224] V. Schaufler, H. Czichos-Medda, V. Hirschfeld-Warnecken et al., "Selective binding and lateral clustering of $\alpha 5\beta 1$ and $\alpha v\beta 3$ integrins: unraveling the spatial requirements for cell spreading and focal adhesion assembly," *Cell Adhesion & Migration*, vol. 10, no. 5, pp. 505–515, 2016.

[225] P. L. Benitez, S. Mascharak, A. C. Proctor, and S. C. Heilshorn, "Use of protein-engineered fabrics to identify design rules for integrin ligand clustering in biomaterials," *Integrative Biology*, vol. 8, no. 1, pp. 50–61, 2016.

[226] S. R. Coyer, A. Singh, D. W. Dumbauld et al., "Nanopatterning reveals an ECM area threshold for focal adhesion assembly and force transmission that is regulated by integrin activation and cytoskeleton tension," *Journal of Cell Science*, vol. 125, no. 21, pp. 5110–5123, 2012.

[227] L. Ye, X. Ni, Z. A. Zhao, W. Lei, and S. Hu, "The application of induced pluripotent stem cells in cardiac disease modeling and drug testing," *Journal of Cardiovascular Translational Research*, vol. 11, no. 5, pp. 366–374, 2018.

[228] A. J. Engler, S. Sen, H. L. Sweeney, and D. E. Discher, "Matrix elasticity directs stem cell lineage specification," *Cell*, vol. 126, no. 4, pp. 677–689, 2006.

[229] G. Pennarossa, R. Santoro, E. F. M. Manzoni, M. Pesce, F. Gandolfi, and T. A. L. Brevini, "Epigenetic erasing and pancreatic differentiation of dermal fibroblasts into insulin-producing cells are boosted by the use of low-stiffness substrate," *Stem Cell Reviews*, vol. 14, no. 3, pp. 398–411, 2018.

[230] A. Arshi, Y. Nakashima, H. Nakano et al., "Rigid microenvironments promote cardiac differentiation of mouse and human embryonic stem cells," *Science and Technology of Advanced Materials*, vol. 14, no. 2, article 025003, 2013.

[231] S. Acevedo-Acevedo and W. C. Crone, "Substrate stiffness effect and chromosome missegregation in hIPS cells," *Journal of Negative Results in Biomedicine*, vol. 14, no. 1, p. 22, 2015.

[232] I. G. Kim, C. H. Gil, J. Seo et al., "Mechanotransduction of human pluripotent stem cells cultivated on tunable cell-derived extracellular matrix," *Biomaterials*, vol. 150, pp. 100–111, 2018.

[233] Y. Zhu, X. Li, R. R. R. Janairo et al., "Matrix stiffness modulates the differentiation of neural crest stem cells in vivo," *Journal of Cellular Physiology*, vol. 234, no. 5, pp. 7569–7578, 2019.

[234] A. J. Engler, C. Carag-Krieger, C. P. Johnson et al., "Embryonic cardiomyocytes beat best on a matrix with heart-like elasticity: scar-like rigidity inhibits beating," *Journal of Cell Science*, vol. 121, no. 22, pp. 3794–3802, 2008.

[235] S. Lee, V. Serpooshan, X. Tong et al., "Contractile force generation by 3D hiPSC-derived cardiac tissues is enhanced by rapid establishment of cellular interconnection in matrix with muscle-mimicking stiffness," *Biomaterials*, vol. 131, pp. 111–120, 2017.

[236] L. Macri-Pellizzeri, E. M. De-Juan-Pardo, F. Prosper, and B. Pelacho, "Role of substrate biomechanics in controlling (stem) cell fate: implications in regenerative medicine," *Journal of Tissue Engineering and Regenerative Medicine*, vol. 12, no. 4, pp. 1012–1019, 2018.

[237] M. Wheelwright, Z. Win, J. L. Mikkila, K. Y. Amen, P. W. Alford, and J. M. Metzger, "Investigation of human iPSC-derived cardiac myocyte functional maturation by single cell traction force microscopy," *PLoS One*, vol. 13, no. 4, article e0194909, 2018.

[238] A. J. S. Ribeiro, Y. S. Ang, J. D. Fu et al., "Contractility of single cardiomyocytes differentiated from pluripotent stem cells depends on physiological shape and substrate stiffness," *Proceedings of the National Academy of Sciences of the United States of America*, vol. 112, no. 41, pp. 12705–12710, 2015.

[239] D. W. Zhou, T. T. Lee, S. Weng, J. Fu, and A. J. García, "Effects of substrate stiffness and actomyosin contractility on coupling between force transmission and vinculin-paxillin recruitment at single focal adhesions," *Molecular Biology of the Cell*, vol. 28, no. 14, pp. 1901–1911, 2017.

[240] X. Yang, L. Pabon, and C. E. Murry, "Engineering adolescence: maturation of human pluripotent stem cell-derived cardiomyocytes," *Circulation Research*, vol. 114, no. 3, pp. 511–523, 2014.

[241] M. Jafarkhani, Z. Salehi, R. Kowsari-Esfahan et al., "Strategies for directing cells into building functional hearts and parts," *Biomaterials Science*, vol. 6, no. 7, pp. 1664–1690, 2018.

[242] H. Yu, Y. S. Lui, S. Xiong et al., "Insights into the role of focal adhesion modulation in myogenic differentiation of human mesenchymal stem cells," *Stem Cells and Development*, vol. 22, no. 1, pp. 136–147, 2013.

[243] J. Du, X. Chen, X. Liang et al., "Integrin activation and internalization on soft ECM as a mechanism of induction of stem cell differentiation by ECM elasticity," *Proceedings of the National Academy of Sciences of the United States of America*, vol. 108, no. 23, pp. 9466–9471, 2011.

[244] D. Missirlis and J. P. Spatz, "Combined effects of PEG hydrogel elasticity and cell-adhesive coating on fibroblast adhesion and persistent migration," *Biomacromolecules*, vol. 15, no. 1, pp. 195–205, 2014.

[245] Z. Wu, S. V. Plotnikov, A. Y. Moalim, C. M. Waterman, and J. Liu, "Two distinct actin networks mediate traction oscillations to confer focal adhesion mechanosensing," *Biophysical Journal*, vol. 112, no. 4, pp. 780–794, 2017.

[246] W. W. Sharp, D. G. Simpson, T. K. Borg, A. M. Samarel, and L. Terracio, "Mechanical forces regulate focal adhesion and costamere assembly in cardiac myocytes," *American Journal of Physiology-Heart and Circulatory Physiology*, vol. 273, no. 2, pp. H546–H556, 1997.

[247] S. Hirth, A. Bühler, J. B. Bührdel et al., "Paxillin and focal adhesion kinase (FAK) regulate cardiac contractility in the zebrafish heart," *PLoS One*, vol. 11, no. 3, article e0150323, 2016.

[248] P. M. Tan, K. S. Buchholz, J. H. Omens, A. D. McCulloch, and J. J. Saucerman, "Predictive model identifies key network regulators of cardiomyocyte mechano-signaling," *PLoS Computational Biology*, vol. 13, no. 11, article e1005854, 2017.

[249] Y. W. Chun, D. E. Voyles, R. Rath et al., "Differential responses of induced pluripotent stem cell-derived cardiomyocytes to anisotropic strain depends on disease status," *Journal of Biomechanics*, vol. 48, no. 14, pp. 3890–3896, 2015.

[250] K. Kroll, M. Chabria, K. Wang, F. Häusermann, F. Schuler, and L. Polonchuk, "Electro-mechanical conditioning of human iPSC-derived cardiomyocytes for translational research," *Progress in Biophysics and Molecular Biology*, vol. 130, Part B, pp. 212–222, 2017.

[251] O. J. Abilez, E. Tzatzalos, H. Yang et al., "Passive stretch induces structural and functional maturation of engineered heart muscle as predicted by computational modeling," *Stem Cells*, vol. 36, no. 2, pp. 265–277, 2018.

[252] L. F. Kadem, K. G. Suana, M. Holz et al., "High-frequency mechanostimulation of cell adhesion," *Angewandte Chemie*, vol. 56, no. 1, pp. 225–229, 2017.

[253] S. Roy and M. K. Mathew, "Fluid flow modulates electrical activity in cardiac hERG potassium channels," *The Journal of Biological Chemistry*, vol. 293, no. 12, pp. 4289–4303, 2018.

[254] J. L. Ruan, N. L. Tulloch, M. V. Razumova et al., "Mechanical stress conditioning and electrical stimulation promote contractility and force maturation of induced pluripotent stem cell-derived human cardiac tissue," *Circulation*, vol. 134, no. 20, pp. 1557–1567, 2016.

[255] C. M. Borza, Y. Su, X. Chen et al., "Inhibition of integrin $\alpha 2\beta 1$ ameliorates glomerular injury," *Journal of the American Society of Nephrology*, vol. 23, no. 6, pp. 1027–1038, 2012.

[256] C. A. Lowell and T. N. Mayadas, "Overview: studying integrins in vivo," in *Integrin and Cell Adhesion Molecules. Methods in Molecular Biology (Methods and Protocols), vol 757*, M. Shimaoka, Ed., pp. 369–397, Humana Press, Totowa, NJ, USA, 2012.

[257] E. Cimetta and G. Vunjak-Novakovic, "Microscale technologies for regulating human stem cell differentiation," *Experimental Biology and Medicine*, vol. 239, no. 9, pp. 1255–1263, 2014.

Hindawi
Stem Cells International
Volume 2019, Article ID 8347595, 7 pages
https://doi.org/10.1155/2019/8347595

Research Article

Scalable Culture Strategies for the Expansion of Patient-Derived Cancer Stem Cell Lines

Ana Teresa Serra,[1,2] **Margarida Serra**,[1,2] **Ana Carina Silva**,[1,2] **Tamara Brckalo**,[3,4] **Anita Seshire**,[3,4] **Catarina Brito**,[1,2] **Michael Wolf**,[3] **and Paula M. Alves**[1,2]

[1]*Instituto de Tecnologia Química e Biológica António Xavier, Universidade Nova de Lisboa, Av. da República, 2780-157 Oeiras, Portugal*
[2]*Instituto de Biologia Experimental e Tecnológica (iBET), Apartado 12, 2780-901 Oeiras, Portugal*
[3]*Merck KGaA, Merck Serono, ImmunoOncology, Emerging Immunotherapies, Frankfurter Str. 250, 64293 Darmstadt, Germany*
[4]*Merck KGaA, Biopharma, Global R&D, Translational Innovation Platform Oncology, Cellular Pharmacology, Frankfurter Str. 250, 64293 Darmstadt, Germany*

Correspondence should be addressed to Paula M. Alves; marques@ibet.pt

Received 6 June 2018; Accepted 15 November 2018; Published 6 February 2019

Guest Editor: Ricardo Baptista

Cancer stem cells (CSCs) have recently raised great interest as a promising biological system for designing effective cancer therapies. The scarcity of CSCs *in vivo* and the consequent low numbers obtained from biopsies represent a major hurdle to the development of such strategies. It is therefore necessary to design robust scalable methods to enable efficient expansion of bona fide CSCs *in vitro*. Here, we evaluated the applicability of computer-controlled bioreactors combined with 3D aggregate culture and microcarrier technology, widely used in stem cell bioprocessing, for the expansion and enrichment of CSCs isolated from different types of solid tumors—colorectal cancer (CRC) and non-small-cell lung cancer (NSCLC) from two patients. Results show that these culture strategies improved cell expansion and CSC enrichment. Both patient-derived CSC lines were able to grow on microcarriers, the best results being achieved for PPlus 102-L, Pro-F 102-L, Fact 102-L, and CGEN 102-L beads (5-fold and 40-fold increase in total cell concentration for CRC and NSCLC cells, respectively, in 6 days). As for 3D aggregate culture strategy, the cell proliferation profile was donor dependent. NSCLC cells were the only cells able to form aggregates and proliferate, and the flat-bottom bioreactor vessel equipped with a trapezoid-shaped paddle impeller was the most efficient configuration for cell growth (21-fold increase in cell concentration achieved in 8 days). Serum-free medium promotes CSC enrichment in both 3D aggregate and microcarrier cultures. The protocols developed herein for CSC expansion have the potential to be transferred to clinical and industrial settings, providing key insights to guide bioprocess design towards the production of enriched CSC cultures in higher quantity and improved quality.

1. Introduction

Cancer stem cells (CSCs) represent a promising target for effective anticancer therapies [1, 2] as these immortal tumor-initiating cells have the capacity to self-renew and differentiate into the spectrum of cell types observed in tumors [3–5]. Due to their characteristics (enhanced motility, invasion, tumor-initiating ability, and resistance to chemotherapy), CSCs are thought to be the basis for tumor initiation, development, metastasis, and recurrence, thus contributing to the failure of conventional cancer treatments [6, 7].

It has been reported that CSCs exist within almost every solid tumor [5, 6] at a very small number (<0.04%) [4]. Difficulties in identifying these cells, their reduced number, and the lack of protocols for efficient CSC expansion and enrichment have hindered the development of effective CSC-targeted therapies. The use of stirred culture systems, previously applied to the (i) expansion and differentiation

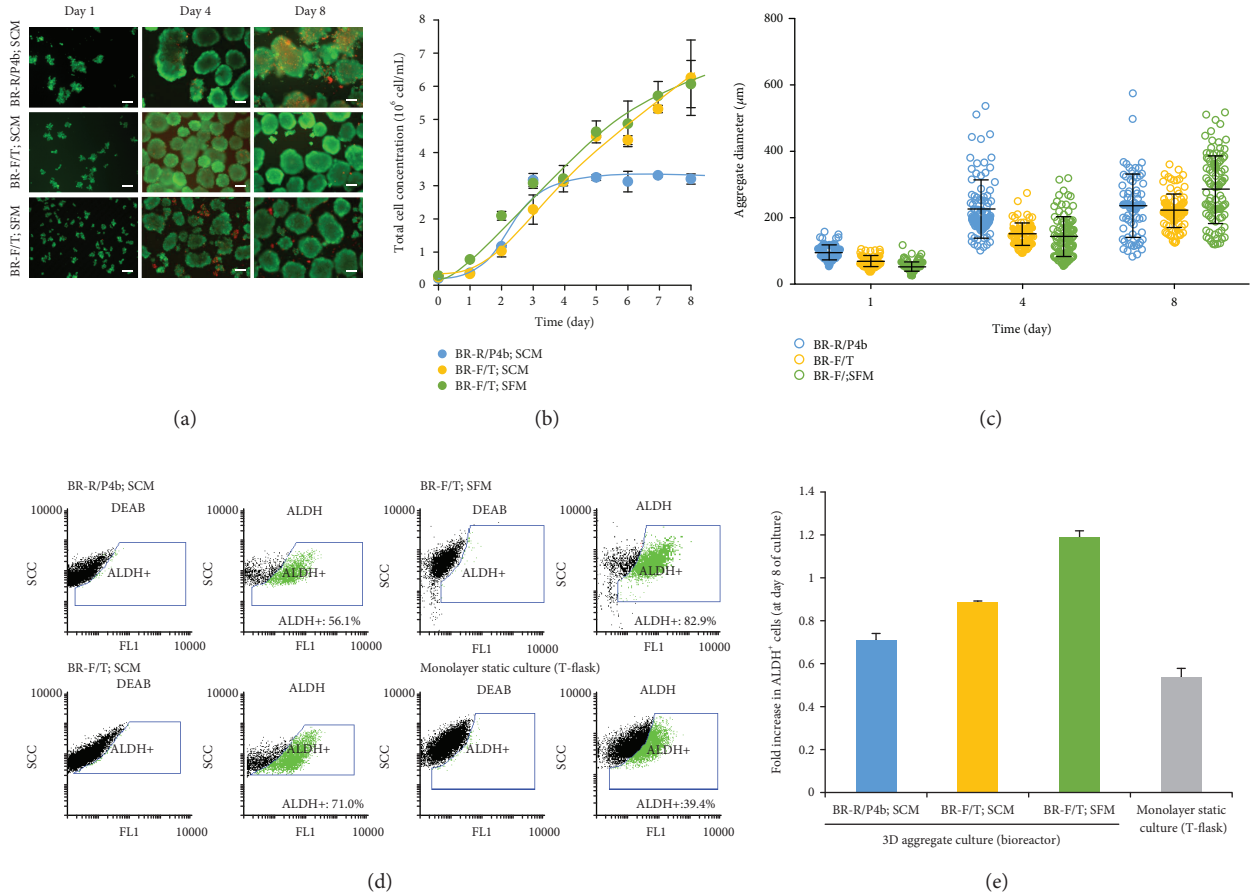

Figure 1: Effect of bioreactor configuration and culture medium composition on the expansion of NSCLC cells. Cells were inoculated at 0.25×10^6 cells/mL and cultured in a round-bottom bioreactor vessel equipped with a pitched 4-bladde impeller (BR-R/P4b) or in a flat-bottom bioreactor vessel equipped with a trapezoid-shaped paddle impeller (BR-F/T) using serum-containing medium (SCM) and serum-free medium (SFM). (a) Fluorescence microscopy images of NSCLC cultures at days 1, 4, and 8 of the three bioreactor experiments. Viability analysis of cultures stained with fluorescein diacetate (FDA—live cells, green) and propidium iodide (PI—dead cells, red). Scale bars: 100 μm. (b) Growth curve expressed in terms of cell number per volume of medium (determined by crystal violet nuclei stain assay; error bars denote SD of 3 measurements). (c) Aggregate size (average diameters of aggregates were determined by ImageJ software; error bars denote SD of measurements from 100 aggregates). (d) Flow cytometry analysis of NSCLC culture in bioreactors and in monolayer static systems: percentage of $ALDH^+$ cells at day 8 of culture. The left panel shows the dot blot of ALDEFLUOR™ assay with an inhibitor (DEAB), and the right panel shows the dot blot without an inhibitor. The $ALDH^+$ cell population is identified in green. (e) Fold increase in $ALDH^+$ cells obtained at day 8 of culture in bioreactors and monolayer static culture systems in relation to the inoculum population.

of human stem cells [8–11] and ii) cultivation of (primary) cancer cells [12–14], can offer great advantages for CSC expansion over static culture systems [15–18], including higher cell production yields, reproducibility, scalability, and easy transfer to clinic and industry [19].

In this work, computer-controlled stirred tank bioreactors combined with 3D cell aggregate cultures as well as microcarrier technology were applied for the first time to expand and enrich CSCs from two different patient-derived cell lines—non-small-cell lung cancer (NSCLC) and colorectal cancer (CRC). The findings reported herein provide novel knowledge to guide cell bioprocess design towards the production of CSC in higher quantity and improved quality, which are key requisites for their application in drug discovery and in the development of new cancer therapeutics.

2. Material and Methods

2.1. Cell Source. CSC lines were established in Merck Biopharma, ImmunoOncology, following a proprietary protocol. Tumor cells were derived from lung and colorectal cancer patients and purchased from Indivumed (Hamburg, Germany). Classification of the tumors was large-cell carcinoma, NOS, and colorectal carcinoma. CSC lines (CRC and NSCLC) were routinely propagated in collagen I-coated T-flasks as described in supplemental online data.

2.2. Culture of CSC Lines as Aggregates in Stirred Tank Bioreactors. CSC lines were inoculated as single cells in computer-controlled stirred tank bioreactors at a concentration of 0.25×10^6 cell/mL and cultured during 8 days in two different bioreactor configurations—round-bottom

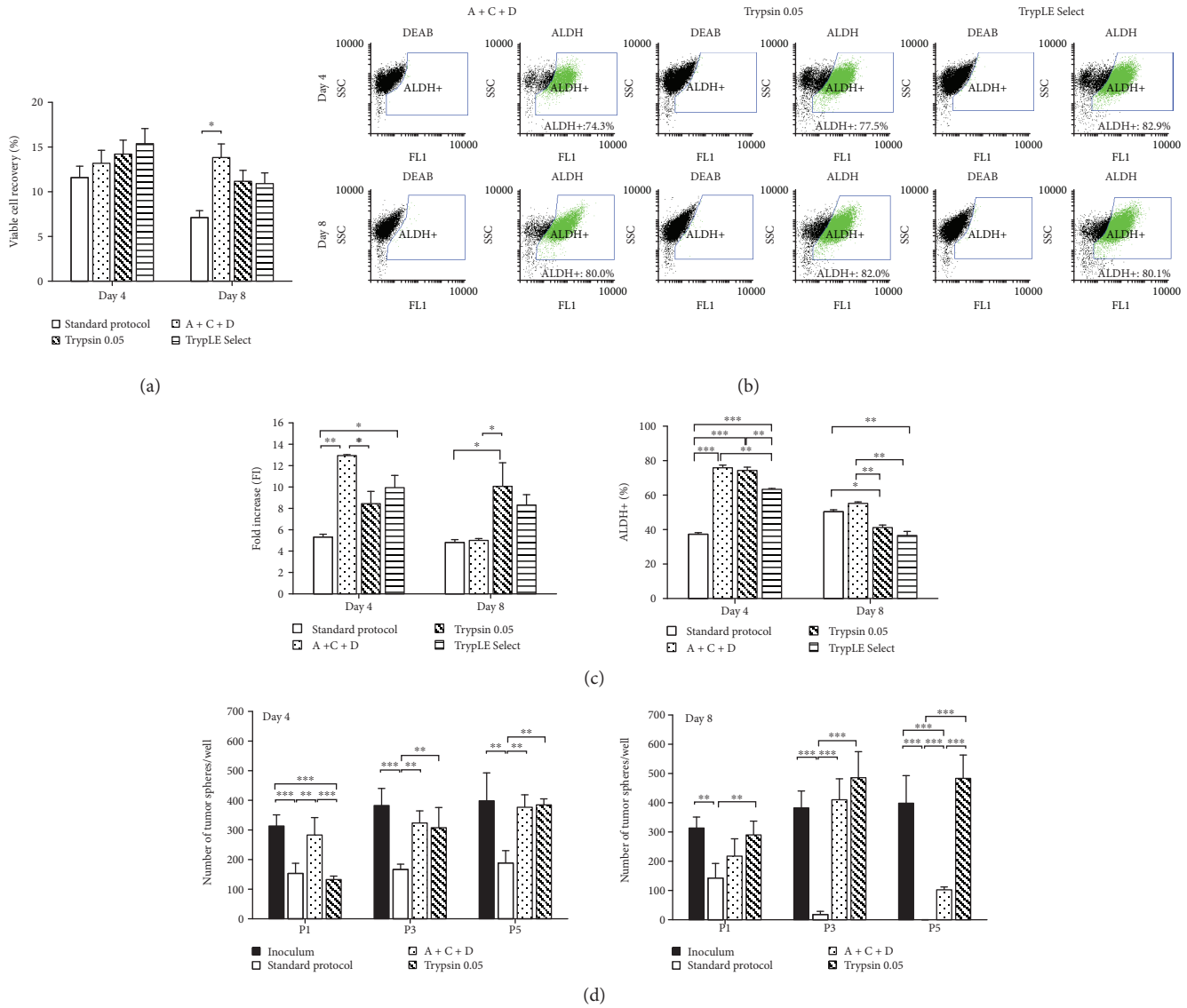

FIGURE 2: Results from harvesting studies of NSCLC cell aggregates cultured in stirred tank bioreactors. Cells were cultured in BR-F/T using serum-free medium (SFM) and harvested at days 4 and 8 of culture using different cell dissociation protocols, namely, Standard protocol, Accutase+Collagenase III+DNase I (A+C+D), Trypsin 0.05%, and TrypLE Select. (a) Percentage of viable cells recovered after each dissociation protocol. Values were estimated by the X_t/X_{ti} ratio, where X_t is the number of total cells recovered after dissociation protocol (determined by trypan blue exclusion assay) and X_{ti} is the number of total cells harvested from the bioreactor (determined by crystal violet nucleic stain assay) (error bars denote SD of 2 measurements). (b) Flow cytometry analysis of NSCLC culture after cell aggregate dissociation by A+C+D, trypsin 0.05, and TrypLE Select protocols: percentage of $ALDH^+$ cells recovered at days 4 and 8 of culture. The left panel shows the dot blot of ALDEFLUOR™ assay with an inhibitor (DEAB), and the right panel shows the dot blot without an inhibitor. The $ALDH^+$ cell population is identified in green. (c) Readhesion and expansion capacity of NSCLC cells harvested at days 4 and 8 using different dissociation protocols. Cells were dissociated and plated in collagen I-coated flasks and cultured for 4 days in static culture conditions using serum-containing medium. Left panel: fold increase in total cell concentration (estimated by crystal violet nucleic stain assay; error bars denote SD of 2 measurements). Right panel: percentage of $ALDH^+$ cells determined after 4 days of culture (error bars denote SD of 2 measurements). (d) Number of tumor spheres per well generated by NSCLC cells derived from the inoculum and harvested from bioreactor culture at days 4 (left panel) and 8 (right panel) using different dissociation protocols. The number of tumor spheres was estimated up to five passages. Error bars denote SD of measurements from 4 wells. Statistical significance is indicated as follows: $^*p < 0.05$, $^{**}p < 0.01$, and $^{***}p < 0.001$.

bioreactor vessel equipped with a pitched 4-bladde impeller (BR-R/P4b) and flat-bottom bioreactor vessel equipped with a trapezoid-shaped paddle impeller (BR-F/T) (DASGIP CellFerm-Pro bioreactor system, Eppendorf AG). Two culture medium formulations (serum-containing medium (SCM) and serum-free medium (SFM)) and four cell aggregate dissociation protocols were tested (more information available in the supplemental online data).

2.3. Culture of CSCs on Microcarriers. CSC lines were inoculated as single cells with empty microcarriers (2.0×10^4 cell/cm^2) in ultra-low-attachment plates and cultured for 6

Table 1: Effect of the microcarrier type on CRC (colorectal cancer) and NSCLC (non-small-cell lung cancer) cell growth using serum-containing medium.

Microcarrier type	Cytodex1™	PPlus 102-L	Fact 102-L	Cytodex3™	CGEN 102-L	Pro-F 102-L	Cytopore2™	CultiSpher®-S
CSC line	CRC							
X_{inoc} ($\times 10^4$ cell/cm^2)	2.0							
X_{6d} ($\times 10^4$ cell/cm^2)	2.9 ± 0.5	6.6 ± 0.3	6.0 ± 0.1	2.9 ± 0.4	7.3 ± 1.5	8.8 ± 0.2	1.9 ± 0.1	1.5 ± 0.2
Expansion ratio*	**1.4 ± 0.3**	**3.3 ± 0.1**	**3.0 ± 0.1**	**1.5 ± 0.2**	**3.6 ± 0.8**	**4.4 ± 0.1**	**1.0 ± 0.1**	**0.8 ± 0.1**
CSC line	NSCLC							
X_{inoc} ($\times 10^4$ cell/cm^2)	2.0							
X_{6d} ($\times 10^4$ cell/cm^2)	95.8 ± 19.2	66.7 ± 1.4	89.6 ± 5.9	62.0 ± 18.4	85.4 ± 8.8	77.1 ± 3.0	31.8 ± 0.7	66.1 ± 0.7
Expansion ratio*	**47.9 ± 9.6**	**33.3 ± 0.7**	**44.8 ± 2.9**	**31.0 ± 9.2**	**42.7 ± 4.4**	**38.5 ± 1.5**	**15.9 ± 0.4**	**33.1 ± 0.4**

*Fold increase in total cell concentration attained at day 6 of culture determined by the ratio between cell concentration achieved at day 6 (X_{6d}) and cell concentration used at inoculum (X_{inoc}), respectively.

days at 37°C in a humidified atmosphere of 5% CO_2 using SCM or SFM. Eight commercially available microcarriers were tested: Cytodex1™, Cytodex3™, PPlus 102-L, Pro-F 102-L, Fact 102-L, CGEN 102-L, Cytopore2™, and CultiSpher®-S as described in the supplemental online data.

2.4. Analytical Methods. Protocols for CSC characterization are included in the supplemental online data.

3. Results and Discussion

Primary CSC lines generated from colorectal cancer (CRC) and non-small-cell lung cancer (NSCLC) from two patients, when routinely cultured in static adherent culture systems, show percentage of ALDH$^+$ cells higher than 50% and have the capacity to generate tumor spheres (SFUs) (data not shown). For their expansion, different bioreactor configurations and aggregate dissociation protocols were evaluated. In addition, microcarrier-based cultures were investigated; eight different microcarriers (selection made based on previous works performed with human stem cells [10, 11], supplemental online Table S1) were screened for CRC and NSCLC cell expansion. The impact of culture medium composition (serum-containing medium (SCM) and serum-free medium (SFM)) on the cell expansion ratio and CSC enrichment was also evaluated.

NSCLC cells were able to grow as aggregates in computer-controlled stirred tank bioreactors independently of the medium used (SCM or SFM) (Figures 1(a) and 1(b)). Importantly, cell growth kinetics (Figure 1(b)) and aggregate size (Figure 1(c)) seem to be driven by hydrodynamics, evaluated through the use of different vessel designs and impeller geometries (see Material and Methods). BR-F/T was the most efficient configuration as it allowed (i) cell growth as spherical aggregates of uniform size (Figures 1(a) and 1(c)) and (ii) a 21-fold increase in cell concentration after day 8 (Figure 1(b)). The maximum cell concentration (Figure 1(b)) and cell expansion factors achieved in our study are within the range of values reported by our group [10] and others [20–22] for the expansion of human pluripotent stem cells as 3D aggregates in bioreactors. The small variations observed in the cell growth profile may reflect the distinct cell types and the different culture conditions used in those studies, such as the culture medium formulation and feeding strategy. Lower cell concentrations were obtained in BR-R/P4b configuration; the cell growth arrest observed for this bioreactor at day 4 might be related to oxygen diffusion limitations within the aggregate as suggested by the high heterogeneity and size of aggregates analyzed (Figure 1(c)), and the values reported to exhibit hypoxia regions (diameter > 400 μm) [23]. Noteworthy, aggregates cultured in BR-F/T presented the highest percentage of ALDH$^+$ cells (>70%) (Figure 1(d)). Culture medium composition impacts on CSC enrichment. Indeed, a 1.2-fold increase in ALDH$^+$ cells relative to inoculum was observed in SFM (BR-F/T; SFM), contrasting to SCM cultures where no increase was attained (BR-F/T; SCM) (Figure 1(e)).

Aggregates were harvested at two time points, days 4 and 8, and the impact of different aggregate dissociation protocols on the ability of NSCLC cells to readhere to collagen I-coated flasks and to form tumor spheres was investigated (Figure 2). Results indicate that recovery yields of viable cells (7-15%) (Figure 2(a)) and ALDH$^+$ subpopulations (74-83%) (Figures 1(d) and 2(b)) are independent of the protocol used. Nonetheless, A+C+D and Trypsin 0.05 were the enzymatic solutions best suited for dissociation of NSCLC cell aggregates. Both protocols improved cell readhesion and expansion capacity (up to 2-fold) and enhanced cells' ability to generate tumor spheres when compared to the standard protocol for the two harvesting days (Figures 2(c) and 2(d)). In contrast, TrypLE Select showed lower percentage of ALDH$^+$ subpopulation than A+C+D and Trypsin 0.05 (Figure 2(c)), and the ability to generate tumor spheres was negligible (data not shown). The evaluation of other digestion reagents such as those recently reported for the isolation of human glioma stem cells [24] may be considered in the future to improve cell recovery yields from NSCLC cell aggregates.

When NSCLC cells were cultured in microcarriers, higher expansion ratios (up to 48) were obtained in less culture time (6 days) when compared to aggregate culture in bioreactors, the exception being Cytopore2™ beads (Table 1). In addition, cells efficiently attach and grow on microcarriers using both SCM and SFM (Figures 3(a) and

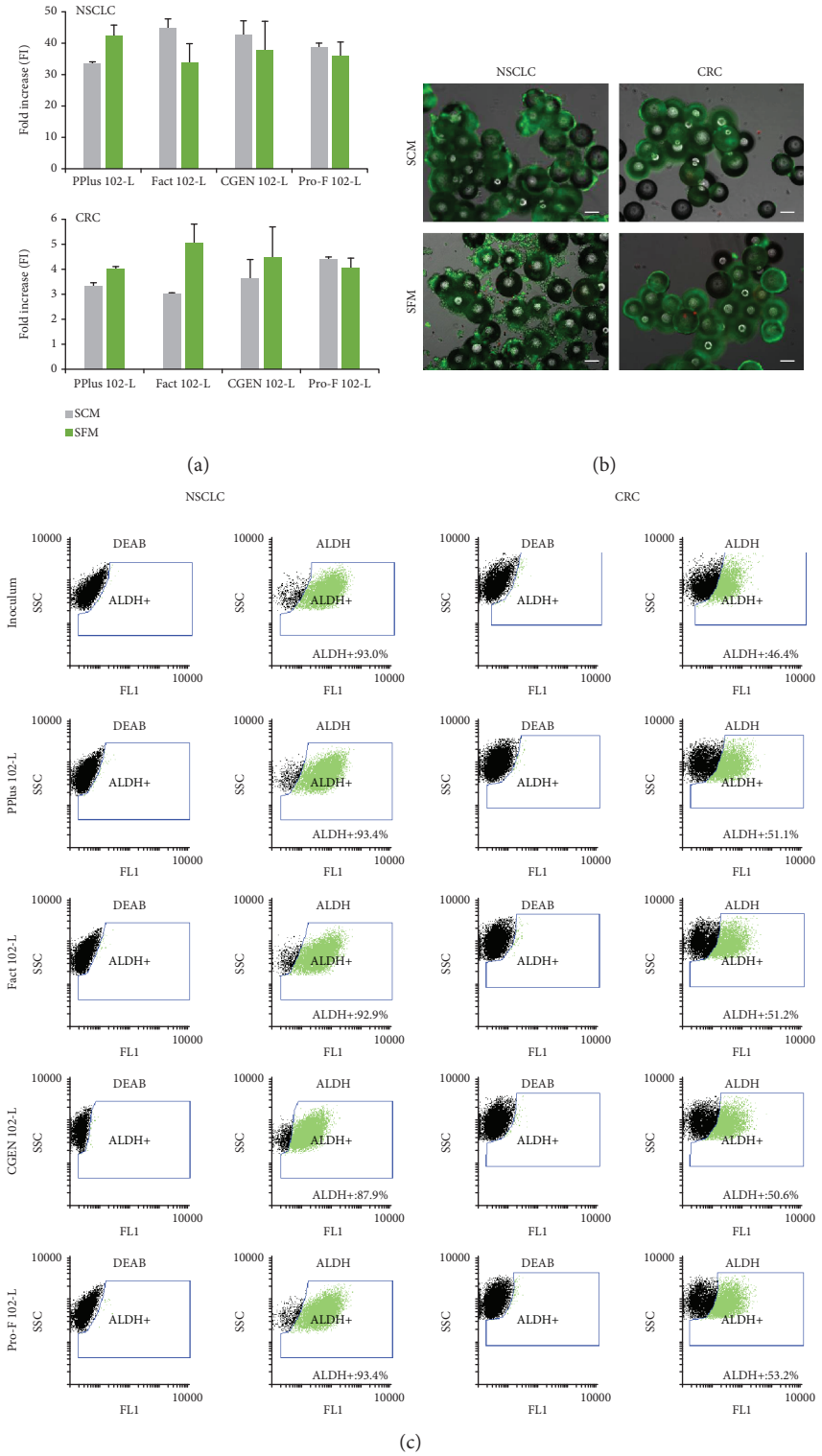

Figure 3: NSCLC and CRC cell culture in four different microcarriers: PPlus 102-L, Pro-F 102-L, Fact 102-L, and CGEN 102-L. Cells were inoculated at 0.2×10^4 cell/cm^2 and cultured for 6 days under static culture systems using two different culture media: serum-containing medium (SCM) and serum-free medium (SFM). (a) Fold increase in NSCLC (upper panel) and CRC (lower panel) cell concentration at day 6 of culture on microcarriers using both culture media. Total cell concentration was determined by crystal violet nucleic stain assay. (b) Phase-contrast and fluorescence microscopy images of NSCLC and CRC cells cultured on PPlus 102-L microcarriers. Viability analysis of cultures stained with fluorescein diacetate (FDA—live cells, green) and propidium iodide (PI—dead cells, red). Scale bars: 100 μm. (c) Flow cytometry analysis of NSCLC and CRC cell population at inoculum and after 6 days of culture in microcarriers using serum-free medium. The left panel shows the dot blot of ALDEFLUOR™ assay with an inhibitor (DEAB), and the right panel shows the dot blot without an inhibitor. The ALDH$^+$ cell population is identified in green.

3(b)). The use of SFM did not compromise ALDH activity of NSCLC cells (percentage of $ALDH^+$ cells obtained at day 6 is similar to that of the inoculum) (Figure 3(c)).

Microcarrier-based culture was also suitable for the expansion of CRC cells, and the highest increase in cell concentration (>3-fold) was observed for PPlus 102-L, Fact 102-L, CGEN 102, and Pro-F 102-L beads (Table 1). The culture medium seems to have a negligible impact on the expansion ratio and microcarrier colonization (Figures 3(a) and 3(b)). In particular, higher percentages of $ALDH^+$ subpopulations in relation to the inoculum were observed for cultures using SFM (Figure 3(c)). The two macroporous microcarriers evaluated (CultiSpher®-S and Cytopore2™) did not support CRC cell expansion. Although initial cell attachment to the bead surface was observed, cell proliferation inside microcarriers did not occur (supplemental online Figure S1, Table 1). In addition, these patient-derived CSC lines did not proliferate when cultured as aggregates in computer-controlled stirred tank bioreactors, showing low aggregation and expansion capacity regardless of the different media and inoculum concentrations (0.1, 0.25, and 0.4×10^6 cells/mL) tested (supplemental online Figure S2). The differences in aggregation and growth observed between NSCLC and CRC cells may be related to the distinct sources (tissues and patients) from which the cells were derived. Alternative/complementary approaches (e.g., cell microencapsulation in hydrogels as reported for human cancer cell lines [13, 14]) might be considered in the future for the scalable expansion of CRC cells.

4. Conclusion

This work describes, for the first time, the successful application of computer-controlled stirred tank bioreactors combined with 3D aggregate cultures as well as microcarrier technology to expand and enrich human CSCs. Despite the fact that there is no universal culture strategy capable of embracing different types/patient-derived CSCs, the protocols developed herein for CSC expansion can be easily screened prior to their transfer to clinical and industrial settings. This study also provides key insights to guide bioprocess design towards scalable production of patient-derived CSCs with improved quality. This will potentiate their application in drug discovery and for the development of new cancer therapeutics.

Data Availability

No data were used to support this study.

Conflicts of Interest

The authors indicated no potential conflicts of interest. Anita Seshire and Tamara Brckalo are employees of Merck KGaA. This does not alter the authors' adherence to all the policies of the journal on sharing data and materials.

Acknowledgments

The authors acknowledge Eng. Marcos Sousa (iBET) for the technical support on bioreactor experiments. The authors acknowledge iNOVA4Health-UID/Multi/04462/2013, a program financially supported by FCT/Ministério da Educação e Ciência, through national funds, and cofunded by FEDER under the PT2020 Partnership Agreement.

Supplementary Materials

Figure S1: Phase-contrast and fluorescence microscopy images of CRC cells cultured on macroporous microcarriers, Cytopore2™ and CultiSpher®-S, at days 1, 4, and 6. Viability analysis of cultures stained with fluorescein diacetate (FDA—live cells, green) and propidium iodide (PI—dead cells, red). Scale bars: 100 μm. Figure S2: Fluorescence microscopy images of CRC cultures at day 4 on BR-F/T using culture medium with serum (a) and serum-free medium (b). Viability analysis of cultures stained with fluorescein diacetate (FDA—live cells, green) and propidium iodide (PI—dead cells, red). Scale bars: 100 μm. Figure S3: Representative image of the ImageJ mask for aggregate size distribution analysis. Table S1: Main characteristics of microcarriers tested. Classification of microcarrier type was indicated according to Chen et al. [11]. ECM: extracellular matrix. *(Supplementary Materials)*

References

[1] J. C. Chang, "Cancer stem cells: role in tumor growth, recurrence, metastasis, and treatment resistance," *Medicine*, vol. 95, no. 1S, pp. S20–S25, 2016.

[2] D. L. Dragu, L. G. Necula, C. Bleotu et al., "Therapies targeting cancer stem cells : current trends and future challenges," *World Journal of Stem Cells*, vol. 7, no. 9, pp. 1185–1201, 2015.

[3] T. Reya, S. J. Morrison, M. F. Clarke, and I. L. Weissman, "Stem cells, cancer, and cancer stem cells," *Nature*, vol. 414, no. 6859, pp. 105–111, 2001.

[4] J. E. Visvader and G. J. Lindeman, "Cancer stem cells in solid tumours: accumulating evidence and unresolved questions," *Nature Reviews. Cancer*, vol. 8, no. 10, pp. 755–768, 2008.

[5] C. A. O. Brien, A. Kreso, and C. H. M. Jamieson, "Cancer stem cells and self-renewal," *Clinical Cancer Research*, vol. 16, no. 12, pp. 3113–3120, 2010.

[6] T. Yang, K. Rycaj, Z. M. Liu, and D. G. Tang, "Cancer stem cells: constantly evolving and functionally heterogeneous therapeutic targets," *Cancer Research*, vol. 74, no. 11, pp. 2922–2927, 2014.

[7] K. Chen, Y. Huang, and J. Chen, "Understanding and targeting cancer stem cells: therapeutic implications and challenges," *Acta Pharmacologica Sinica*, vol. 34, no. 6, pp. 732–740, 2013.

[8] M. Serra, C. Brito, E. M. Costa, M. F. Q. Sousa, and P. M. Alves, "Integrating human stem cell expansion and neuronal differentiation in bioreactors," *BMC Biotechnology*, vol. 9, no. 1, p. 82, 2009.

[9] M. Serra, C. Brito, M. F. Q. Sousa et al., "Improving expansion of pluripotent human embryonic stem cells in perfused bioreactors through oxygen control," *Journal of Biotechnology*, vol. 148, no. 4, pp. 208–215, 2010.

[10] B. Abecasis, T. Aguiar, É. Arnault et al., "Expansion of 3D human induced pluripotent stem cell aggregates in bioreactors: bioprocess intensification and scaling-up approaches," *Journal of Biotechnology*, vol. 246, pp. 81–93, 2017.

[11] A. K. Chen, S. Reuveny, S. Kah, and W. Oh, "Application of human mesenchymal and pluripotent stem cell microcarrier cultures in cellular therapy: achievements and future direction," *Biotechnology Advances*, vol. 31, no. 7, pp. 1032–1046, 2013.

[12] K. M. Panchalingam, W. J. Paramchuk, C. Y. Chiang et al., "Bioprocessing of human glioblastoma brain cancer tissue," *Tissue Engineering Part A*, vol. 16, no. 4, pp. 1169–1177, 2010.

[13] V. E. Santo, M. F. Estrada, S. P. Rebelo et al., "Adaptable stirred-tank culture strategies for large scale production of multicellular spheroid-based tumor cell models," *Journal of Biotechnology*, vol. 221, pp. 118–129, 2016.

[14] M. F. Estrada, P. Rebelo, E. J. Davies et al., "Modelling the tumour microenvironment in long-term microencapsulated 3D co-cultures recapitulates phenotypic features of disease progression," *Biomaterials*, vol. 78, pp. 50–61, 2016.

[15] a. Eramo, F. Lotti, G. Sette et al., "Identification and expansion of the tumorigenic lung cancer stem cell population," *Cell Death & Differentiation*, vol. 15, no. 3, pp. 504–514, 2008.

[16] L. Ricci-Vitiani, D. G. Lombardi, E. Pilozzi et al., "Identification and expansion of human colon-cancer-initiating cells," *Nature*, vol. 445, no. 7123, pp. 111–115, 2007.

[17] G. Dontu, W. M. Abdallah, J. M. Foley et al., "In vitro propagation and transcriptional profiling of human mammary stem/progenitor cells," *Genes & Development*, vol. 17, no. 10, pp. 1253–1270, 2003.

[18] D. Ponti, A. Costa, N. Zaffaroni et al., "Isolation and in vitro propagation of tumorigenic breast cancer cells with stem/progenitor cell properties," *Cancer Research*, vol. 65, no. 13, pp. 5506–5511, 2005.

[19] M. Serra, C. Brito, C. Correia, and P. M. Alves, "Process engineering of human pluripotent stem cells for clinical application," *Trends in Biotechnology*, vol. 30, no. 6, pp. 350–359, 2012.

[20] C. Kropp, H. Kempf, C. Halloin et al., "Impact of feeding strategies on the scalable expansion of human pluripotent stem cells in single-use stirred tank bioreactors," *Stem Cells Translational Medicine*, vol. 5, no. 10, pp. 1289–1301, 2016.

[21] C. K. Kwok, K. Günther, S. Ergün, A. Heron, F. Edenhofer, and M. Rook, "Scalable stirred suspension culture for the generation of billions of human induced pluripotent stem cells using single-use bioreactors," *Journal of Tissue Engineering and Regenerative Medicine*, vol. 12, no. 2, pp. e1076–e1087, 2018.

[22] R. Olmer, A. Lange, S. Selzer et al., "Suspension culture of human pluripotent stem cells in controlled, stirred bioreactors," *Tissue Engineering Part C: Methods*, vol. 18, no. 10, pp. 772–784, 2012.

[23] J. Wu, M. R. Rostami, D. P. Cadavid Olaya, and E. S. Tzanakakis, "Oxygen transport and stem cell aggregation in stirred-suspension bioreactor cultures," *PLoS One*, vol. 9, no. 7, article e102486, 2014.

[24] D. Lv, Q. Ma, J. Duan et al., "Optimized dissociation protocol for isolating human glioma stem cells from tumorspheres via fluorescence-activated cell sorting," *Cancer Letters*, vol. 377, no. 1, pp. 105–115, 2016.

Hindawi
Stem Cells International
Volume 2019, Article ID 9704945, 9 pages
https://doi.org/10.1155/2019/9704945

Research Article

Laminin as a Potent Substrate for Large-Scale Expansion of Human Induced Pluripotent Stem Cells in a Closed Cell Expansion System

Fernanda C. Paccola Mesquita, Camila Hochman-Mendez, Jacquelynn Morrissey, Luiz C. Sampaio, and Doris A. Taylor

Regenerative Medicine Research, Texas Heart Institute, Houston, TX 77225, USA

Correspondence should be addressed to Doris A. Taylor; dtaylor@texasheart.org

Received 28 July 2018; Revised 28 September 2018; Accepted 31 October 2018; Published 22 January 2019

Guest Editor: Tiago Fernandes

The number of high-quality cells required for engineering an adult human-sized bioartificial organ is greater than one billion. Until the emergence of induced pluripotent stem cells (iPSCs), autologous cell sources of this magnitude and with the required complexity were not available. Growing this number of cells in a traditional 2D cell culture system requires extensive time, resources, and effort and does not always meet clinical requirements. The use of a closed cell culture system is an efficient and clinically applicable method that can be used to expand cells under controlled conditions. We aimed to use the Quantum Cell Expansion System (QES) as an iPSC monolayer-based expansion system. Human iPSCs were expanded (up to 14-fold) using the QES on two different coatings (laminin 521 (LN521) and vitronectin (VN)), and a karyotype analysis was performed. The cells were characterized for spontaneous differentiation and pluripotency by RT-PCR and flow cytometry. Our results demonstrated that the QES provides the necessary environment for exponential iPSC growth, reaching $689.75 \times 10^6 \pm 86.88 \times 10^6$ in less than 7 days using the LN521 coating with a population doubling level of 3.80 ± 0.19. The same result was not observed when VN was used as a coating. The cells maintained normal karyotype (46-XX), expressed pluripotency markers (OCT4, NANOG, LIN28, SOX2, REX1, DPPA4, NODAL, TDGFb, TERT3, and GDF), and expressed high levels of OCT4, SOX2, NANOG, SSEA4, TRA1-60, and TRA1-81. Spontaneous differentiation into ectoderm (NESTIN, TUBB3, and NEFH), mesoderm (MSX1, BMP4, and T), and endoderm (GATA6, AFP, and SOX17) lineages was detected by RT-PCR with both coating systems. We conclude that the QES maintains the stemness of iPSCs and is a promising platform to provide the number of cells necessary to recellularize small human-sized organ scaffolds for clinical purposes.

1. Introduction

Bioengineering a whole human-sized organ requires billions of cells, which can be difficult to obtain in a laboratory setting [1]. The traditional two-dimensional (2D) cell culture system, adherent cells in flask-based culture or in a multilayer cell factory, requires intensive time, resources, personnel, and effort. Furthermore, it uses open processing steps that increase the risk of microbial contamination and preclude clinical use.

Standard cultivation of pluripotent stem cells (PSCs) occurs on 2D feeder-dependent or feeder-free systems. Multiple groups have cultured human PSCs in suspension to scale-up their production [2–5]. Various bioreactor systems have been developed that cultivate cells on microcarriers [6], hydrogels [7], or within three-dimensional (3D) aggregates [8]. These technologies present benefits, such as increased surface areas for cell adhesion and growth, and minimize the heterogeneity of the cell culture environment [9, 10]. Currently, there are several types of microcarriers available with variable cell attachment properties for PSC culture [11]. Under these culture conditions, after multiple passages, cells maintain pluripotency and a normal karyotype [12, 13], can be easily frozen and thawed

[14], and proliferate more than 10-fold in 6 days [11, 13]. However, the medium must be manually exchanged, which increases the risk of contamination.

Large-scale expansion of PSCs in a robust, well-defined, and monitored process is essential for therapeutic and industrial applications [3]. The Quantum Cell Expansion System (QES) (Terumo BCT) provides an automated, functionally closed cell culture system with customizable settings to coat, seed, feed, and harvest adherent and suspended cells. QES is an integrated system that provides incubation, gas provision, and fluid handling for the management of the cells in hollow-fiber bioreactors.

In the past, cell-derived feeder layer systems were used to expand PSCs while maintaining their pluripotency [15–17]. To replace feeder-dependent culture systems, several matrices have been tested for coating plates and microcarriers during PSC expansion. This feeder-free condition is pivotal in maintaining the phenotype of the cells. Matrigel™, the most common coating solution described in the literature, usually polymerizes at room temperature (RT) [11, 18–20], but various substrates such as vitronectin (VN) [21], laminin (LN) [22, 23], and synthetic polymers or conjugated peptides [24–27] have also been reported for cultivating PSCs in 2D or 3D systems. However, since the coating in the QES occurs in a range of 34°–40°C, Matrigel™ is not a preferred substrate as it will likely polymerize during the process, forming gels and thereby invalidating the complete use of the hollow-fiber bioreactor. More importantly, Matrigel is derived from Engelbreth-Holm-Swarm (EHS) mouse sarcoma cells [28], which precludes its use clinically. In the present study, we evaluated two substrates (LN and VN) under xeno-free condition cultivating cells to develop a method that supports the clinical use of the expanded cells.

We established a closed functional system that provides the necessary environment to scale-up production of human induced pluripotent stem cells (hiPSCs) while maintaining their stemness. We also demonstrated that laminin 521 (LN521) is a more efficient coating than VN in the QES hollow-fiber system, resulting in a greater yield of viable hiPSCs. All parameters were compared to the standard PSC culture conditions (Matrigel™).

2. Materials and Methods

2.1. Culture and Maintenance of hiPSCs in Culture Dishes. The hiPSCs (SCVI273) used in this study were kindly donated by the Joseph Wu Lab (Stanford Medicine, Department of Medicine and Radiology, Stanford CVI Biobank). Briefly, peripheral blood mononuclear cells were collected from a healthy donor, and the hiPSCs were generated by using the nonintegrative Sendai virus system.

Cells were cultured and maintained in a feeder-free system—hESC-qualified Matrigel™ (Corning) and TeSR1™ E8™ (STEMCELL Technologies Inc., Cambridge, MA) under standard culture conditions (37°C at 5% CO_2). Briefly, we coated 100 mm Petri dishes with Matrigel™ for at least 1 hour at 37°C and plated 1×10^5 cells in TeSR™ E8™ media supplemented with ROCK Inhibitor Y-27632 (10 μM, ATCC) for 24 hours. The ROCK inhibitor was used to increase the cell survival by preventing dissociation-induced apoptosis (anoikis). The media was changed every day, and the cells were passaged using the cell dissociation recombinant enzymatic solution TrypLE™ Express (Gibco). Viable cells were determined by staining with trypan blue and counting in a hemocytometer.

2.2. Quantum System Cell Expansion Set. The Quantum System is a disposable, sterile cell expansion set, consisting of a functionally closed network made of a hollow-fiber bioreactor; gas transfer module; intracapillary circulation loop; extracapillary circulation loop; four pressure pods; five inlet lines; and a harvest line. Each QES has 11,500 hollow fibers (200 μm diameter per fiber) and a total surface area of 21,000 cm^2. The hollow fibers are composed of 3 polymers (PAES, PVP, and PA) and have pores to distribute solutions homogenously throughout the bioreactor's interior. Pore size filters incoming reagents by molecular weight, allowing small molecules to enter the bioreactor easily compared to higher molecular weight molecules. Each cell expansion set is housed in a console that allows controlling of the intracapillary circulation, extracapillary circulation, and gas exchange. Cells are routinely loaded onto the hollow fiber after it is coated with a suitable substrate.

2.3. Culture of hiPSCs in Quantum Expansion System. Before loading the hiPSCs, the culture surface area of the intracapillary hollow fibers of the bioreactor was coated using one of the following xeno-free coating matrices: human recombinant LN521 (5 μg/ml, BioLamina, Stockholm, Sweden) and VN (Vitronectin XF™ by Primorigen, 10 μg/ml, STEMCELL Technologies Inc.). The hollow-fiber surfaces were coated for at least 4 hours. Cells were loaded into the bioreactors at a density of $40–60 \times 10^6$ cells in 100 ml of TeSR™ E8™ media and Y-27632 (10 μM). The bioreactor was rotated to create uniform suspension and homogenous distribution of the cells before attachment under static conditions (Figure 1). This cell density was comparable to our initial seeding density in a 100 mm Petri dish (~20,000 cells/cm^2). After 24 hours, we began media perfusion at 0.1 ml/min, gradually increasing the rate in response to lactate levels according to the manufacturer's recommendation. For that, the lactate level was measured daily (Lactate Plus, Nova Biomedical). Human iPSCs cultivated in a 100 mm Petri dish in the incubator (37°C, 5% CO_2) were used as a control.

2.4. Harvest of hiPSCs in Quantum Expansion System. Cells were harvested when the predicted number of cells reached a plateau. The plateau was evaluated using a manufacturer's QES template, which calculates the predicted number of cells based on lactate production over time, according to the following formula: $PNC = (A/\Delta t) \div RPR$, where PNC is the predicted number of cells; A is the amount of lactate production (mmol); Δt is the variation of time (days); and RPR is the reference production rate (mmol/day/cell). The RPR was determined using a plate-based experiment, correlating the number of cells and the lactate level.

The harvest process was performed with 200 ml of TrypLE™ Express for 8 min followed by two washes with

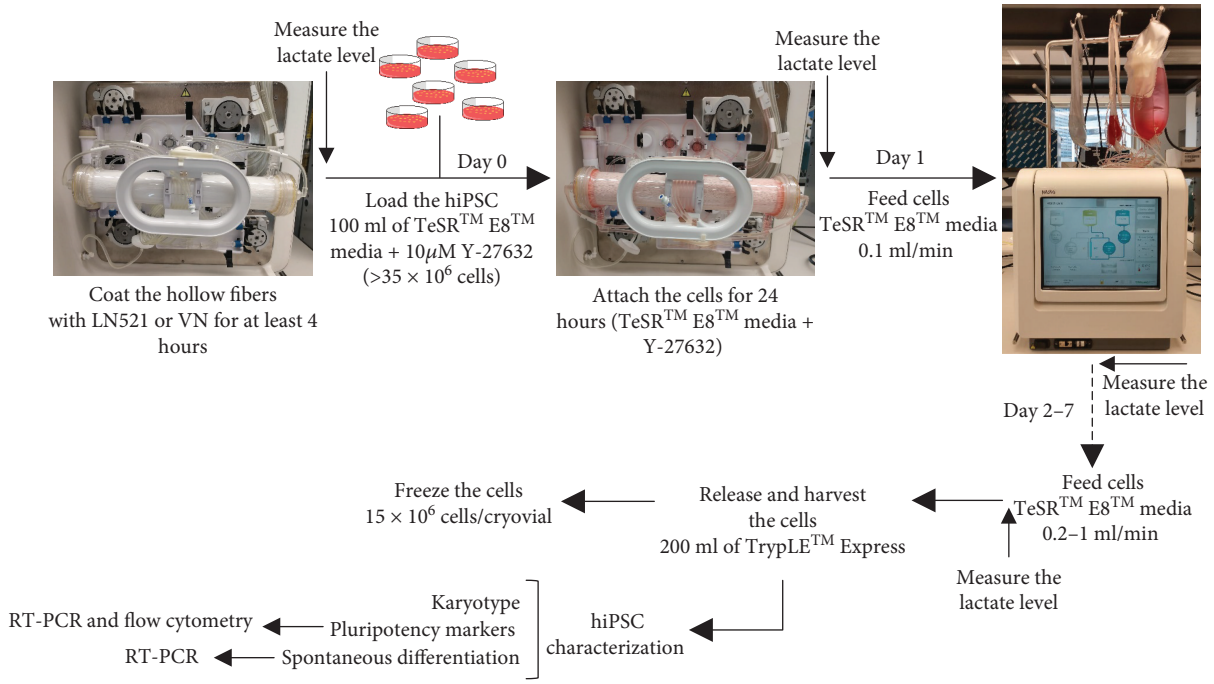

Figure 1: Experimental design of hiPSC expansion. The QES hollow fibers were coated with LN521 or VN for at least 4 hours. Human iPSCs were loaded in the QES on day 0 in a density of $>35 \times 10^6$ cells in 100 ml of TeSR™ E8™ media with 10 μM Y-27632. Cells were fed via the media inlet line from days 1–6/7, at which time the cells were harvested, frozen, and/or characterized for pluripotency and differentiation markers.

phosphate-buffered saline (PBS) (Figure 1). All cells were collected into the harvest bag and transferred to a 500 ml tube, and samples were stained with trypan blue and counted in a hemocytometer.

Cells were centrifuged at 300 × g for 5 minutes and frozen with 10% dimethyl sulfoxide (DMSO, Sigma) and fetal bovine serum in 3 ml cryovials (15×10^6 cells/vial).

2.5. Karyotyping. Human iPSCs were karyotyped by standard cytogenetic procedures using the GTG-banding method. Cells were treated with 0.05 μg/ml of KaryoMAX® Colcemid™ solution (Life Technologies) in TeSR™ E8™ media for 3 hours and then dissociated, placed in a hypotonic treatment with 0.057 M potassium chloride, and fixed in methanol and acetic acid. GTG-banding was performed by the Molecular Cytogenetics Facility, MD Anderson Cancer Center, Houston, TX, according to ISCN [29].

2.6. Differentiation Potential of hiPSC. For spontaneous differentiation into the three embryonic germ layers, the hiPSCs were harvested from the QES and cultured in ultra-low attachment 6-well plates (Corning) to form embryoid bodies (EBs). The EBs were cultured in suspension for 7 days at 37°C and 5% CO_2 with the basal medium containing DMEM/F12, 20% KnockOut™ Serum Replacement, 4 mM glutamine, 1% MEM Non-Essential Amino Acids, and 55 mM 2-mercaptoethanol (Gibco). After this, the EBs were transferred back to adherent plates and cultured for another 7 days with the basal media [30]. Differentiated cells were analyzed by RT-PCR.

2.7. RT-PCR. RNA was extracted using the RNeasy Mini kit (QIAGEN), and total RNA was quantified with a NanoDrop Spectrophotometer. Reverse transcription was performed using the High-Capacity cDNA Reverse Transcription Kit (Applied Biosystems™) according to the manufacturer's instructions. For PCR amplification, Platinum™ Green Hot Start PCR Master Mix kit (Invitrogen™) was used. PCR products were analyzed by electrophoresis in agarose gels.

The list of primers used is presented in Table 1.

2.8. Flow Cytometry. Cells harvested from QES were fixed and permeabilized using the BD Cytofix/Cytoperm™ kit, according to the manufacturer's instructions. Briefly, cells were resuspended and incubated in 250 μl of BD Cytofix/Cytoperm solution for 20 min at 4°C, and after centrifugation (300 × g for 5 min), the cells were resuspended in BD Perm/Wash buffer for 30 min at 4°C. Cells were stained with Alexa Fluor® 488 mouse anti-Oct3/4, PE mouse anti-human Nanog, Alexa Fluor® 647 mouse anti-Sox2, PE mouse anti-SSEA-4, FITC mouse anti-human TRA-1-60, and Alexa Fluor® 647 mouse anti-human TRA-1-81 (BD). Isotypes were used as negative controls. Samples were analyzed using BD LSRFortessa and FlowJo v10 software.

2.9. Population Doubling. Population doubling level (PDL) was calculated using the following formula: PDL = (log N – log N_0)/log 2, where N is the number of harvested cells and N_0 is the number of seeded cells [31]. We used the PDL to denote the total number of times that the hiPSC population had doubled during expansion in the QES.

Table 1: List of primers for pluripotency and germ layer differentiation.

	Primer	Forward	Reverse
Pluripotency	OCT4	CCATGCATTCAAACTGAGGTG	CCTTTGTGTTCCCAATTCCTTC
	NANOG	CTCCAGGATTTTAACGTTCTGC	TGGGATAAAGTGAGTTGCCTG
	LIN28	AAGAAATCCACAGCCCTACC	CCCCCCTAACCCATCACCTCCACCACCTAA
	SOX2	GAGAAGTTTGAGCCCCAGG	AGAGGCAAACTGGAATCAGG
	REX1	CAGATCCTAAACAGCTCGCAGAAT	GCGTACGCAAATTAAAGTCCAGA
	DPPA4	CAGCTCTGCTCATGACTGTTG	ATAGTAGCTAGCTTTGATGGCA
	NODAL	GGGCAAGAGGCACCGTCGACATCA	GGGACTCGGTGGGGCTGGTAACGTTTC
	TDGFb	CTGCTGCCTGAATGGGGGAACCTGC	GCCACGAGGTGCTCATCCATCACAAGG
	TERT3	CCTGCTCAAGCTGACTCGACACCGTG	GGAAAAGCTGGCCCTGGGGTGGAGC
	GDF3	GTGCCAACCCAGGTCCGGAAGTT	CTTATGCTACGTAAAGGAGCTGGG
Ectoderm	NESTIN	CACCTCAAGATGTCCCTCAG	AGCAAAGATCCAAGACGCC
	TUBB3	GCTCAGGGGCCTTTGGACATCTCTT	TTTTCACACTCCTTCCGCACCACATC
	NEFH	ACCTATACCCGAATGCCTTCTT	AGAAGCACTTGGTTTTATTGCAC
Mesoderm	MSX1	CGAGAGGACCCCGTGGATGCAGAG	GGCGGCCATCTTCAGCTTCTCCAG
	BMP4	GCACTGGTCTTGAGTATCCTG	TGCTGAGGTTAAAGAGGAAACG
	Brachyury (T)	GCCCTCTCCCTCCCCTCCACGCACAG	CGGCGCCGTTGCTCACAGACCACAGG
Endoderm	GATA6	CCAACTGTCACACCACAAC	TGGGGGAAGTATTTTTGCTG
	AFP	GAATGCTGCAAACTGACCACGCTGGAAC	TGGCATTCAAGAGGGTTTTCAGTCTGGA
	SOX17	GACGACCAGAGCCAGACC	CGCCTCGCCCTTCACC
	GAPDH	AATCCCATCACCATCTTCCAG	AAATGAGCCCCAGCCTTC

2.10. Statistical Analyses. Data are shown as the mean ± standard deviation. Comparison between LN521 and VN was performed using Student's *t*-test or two-way ANOVA depending on the necessity, and $p < 0.05$ was considered significant. The GraphPad Prism® software, version 7.0 (GraphPad Software Inc., La Jolla, CA, USA), was used for statistical analyses. We performed 3 biological replicates for expansions using VN coating and 4 biological replicates for expansions on LN521 coating.

3. Results

To select the better substrate for our hollow-fiber QES in combination with TeSR™ E8™ media, we tested and compared two different coatings: LN521 and VN. A critical step for closed cell expansion systems is determining the appropriate time for harvesting cells, because it is impossible to see the morphology and confluency of the cells. To address this, we used two surrogates to define the optimal time for harvesting: (1) a control plate: cells cultivated in a conventional cell expansion system (cells on plates in the CO_2 incubator) and (2) the lactate level of the media in the QES. Before starting the QES expansion, we cultivated cells in a conventional cell expansion system, measured the lactate level, and quantified the number of cells obtained after 5 days. Using these numbers, we created a table with the total number of cells and the correlated lactate level. Based on this table, we could predict the number of cells inside the bioreactor by measuring the lactate level. This technique was successful, and the predicted number of cells was similar to our count after harvesting (Figure 2(a)).

After being expanded in the QES, the hiPSCs attached (Figure 2(b)) and maintained the typical PSC morphology, with rounded colonies, defined borders, and high nucleus-to-cytoplasm ratio on these two surfaces in tissue culture dishes (Figure 2(c)), based on the criteria reported by Yu et al. [16]. On the hollow-fiber QES coated with LN521, we observed an exponential growth of the hiPSCs, starting with $49.32 \times 10^6 \pm 5.75 \times 10^6$ cells and finishing with $689.75 \times 10^6 \pm 86.88 \times 10^6$ in 6/7 days ($n = 4$). This was not observed when we coated the hollow-fiber QES with VN (starting with $44.10 \times 10^6 \pm 4.84 \times 10^6$ cells and finishing with $59.7 \times 10^6 \pm 13.93 \times 10^6$ in 8/9 days, $n = 3$) (Figures 2(a) and 2(d)). A similar growth pattern was observed when we cultivated a second hiPSC line (ACS-1030, ATCC) on LN521 (5.17 times) compared to VN (1.4 times; see Supplementary Figure 1). Despite the cells receiving the same volume of medium (LN521 4.76 ± 0.67 l vs. VN 4.14 ± 1.17 l) (Figure 2(e)), the hiPSC on LN521 had significantly higher PDL (Figure 2(f)) compared to VN (3.80 ± 0.19 vs. 0.36 ± 0.46 $p < 0.001$). Even with an additional 3 days in the QES and increased media flow rate (day 7 0.43 ± 0.15 and day 10 0.80 ± 0.34 ml/min), cells on VN did not increase the PDL (Figures 2(d), 2(e), and 2(f)).

A sample of the cells was collected before and after each QES expansion for karyotyping and PCR analysis. After the QES expansion on both substrates, the cells maintained the normal karyotype (46-XX) (Figure 2(g)) and their pluripotency (Figure 3(a)), similar to the effect seen with the standard culturing system (tissue culture dish coated with Matrigel™), despite the difference in growth.

	Lactate prediction	Hemocytometer count
LN521 ($n = 4$)	$68.97 \times 10^7 \pm 8.68 \times 10^7$	$79.9 \times 10^7 \pm 22.35 \times 10^7$
VN ($n = 3$)	$5.97 \times 10^7 \pm 1.39 \times 10^7$	$3.03 \times 10^7 \pm 2.43 \times 10^7$

(a)

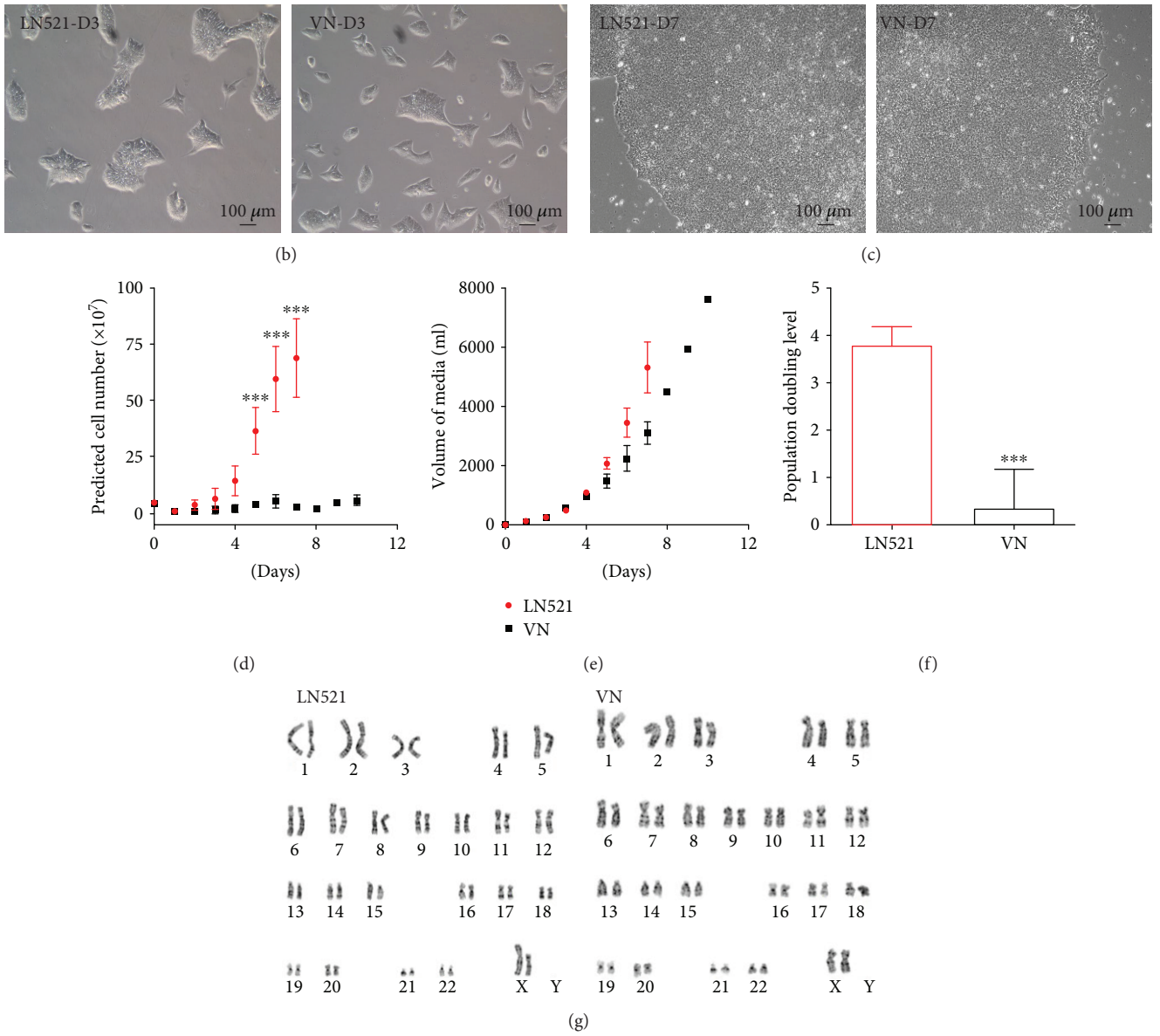

Figure 2: Human iPSC after expansion in the QES. (a) Comparison between predicted and counted cells harvested from the QES. (b, c) Bright field of iPSC cultivated in LN521 and VN 3 (b) and 7 (c) days after harvesting from the QES. (d) Lactate-predicted cell number during expansion in QES. (e) Media consumption during expansion in QES. (f) Population doubling level (PDL) of hiPSCs during QES expansion; red: LN521 coating ($n = 4$); black: vitronectin coating ($n = 3$). (g) Karyotyping of hiPSCs after expansion, $^{***}p < 0.0001$.

To validate these findings, after harvesting the hiPSCs in the QES, we performed immunophenotyping by flow cytometry for pluripotency markers. We observed high expression of OCT4 (LN521: 97.2%, VN: 97.9%, and CTRL: 94.3%), NANOG (LN521: 93.3%, VN: 99.1%, and CTRL: 75.8%), SOX2 (LN521: 97.6%, VN: 99.6%, and CTRL: 99.9%), SSEA4 (LN521: 100%, VN: 100%, and CTRL: 100%), TRA1-60 (LN521: 97.6%, VN: 98.6%, and CTRL: 97.1%), and TRA1-81 (LN521: 97.5%, VN: 99.7%, and CTRL: 99.3%) in the cells after the QES expansion on both substrates and in cells grown under the standard culturing system (Figure 3(b)).

Spontaneous differentiation was performed in a 14-day protocol. The hiPSCs harvested from the QES under LN521 and VN conditions were cultivated in suspension for 7 days. We observed the formation of cell aggregates, EBs, with circular shapes and defined borders (Figure 4(a)). After the 7th day, we plated and cultivated the cells for an additional

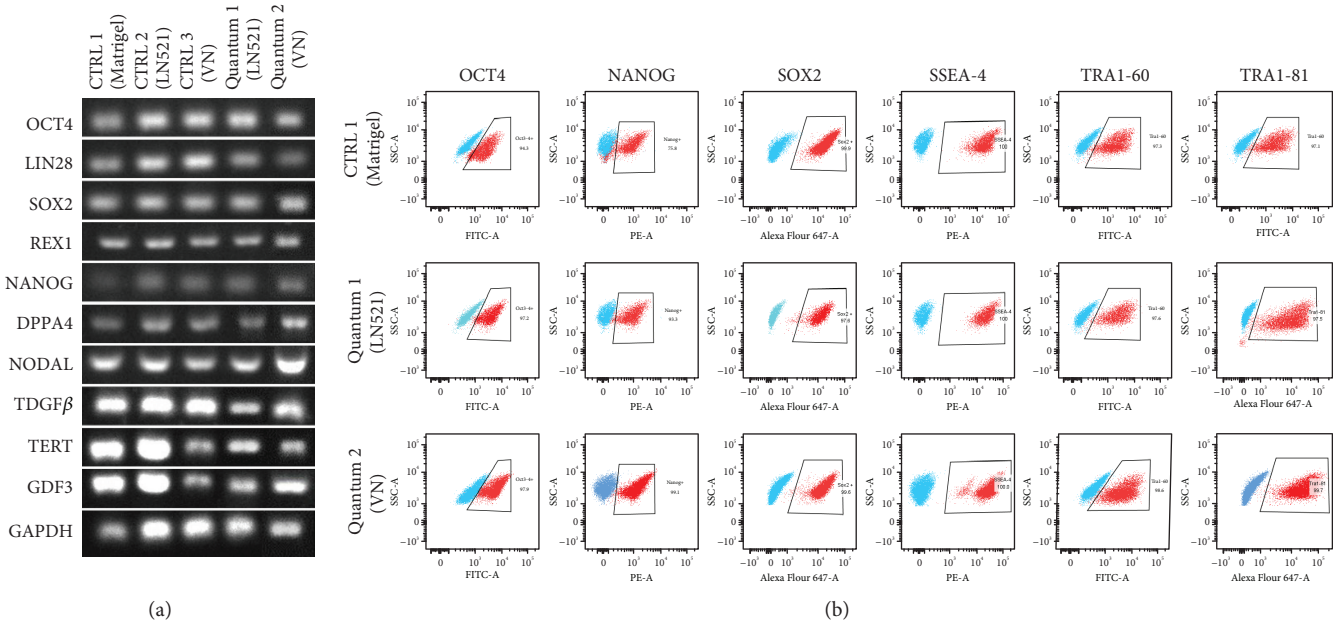

Figure 3: Pluripotency characterization after QES expansion: (a) RT-PCR for pluripotency transcripts of cells cultivated on Matrigel (CTRL1), LN521 (CTRL2), and VN (CTRL3) both in 2D culture and after the QES expansion (quantum 1—LN521 and quantum 2—VN). GAPDH was used as endogenous control. (b) Representative dot plots of pluripotency markers after QES expansion: OCT4 (CTRL 1: 94.3%, quantum 1: 97.2%, quantum 2: 97.9%), NANOG (CTRL 1: 75.8%, quantum 1: 93.3%, quantum 2: 99.1%), SOX2 (CTRL 1: 99.9.%, quantum 1: 97.6%, quantum 2: 99.6%), SSEA4 (CTRL 1: 100%, quantum 1: 100%, quantum 2: 100%), TRA1-60 (CTRL 1: 97.1%, quantum 1: 97.6%, quantum 2: 98.6%), and TRA1-81 (CTRL 1: 99.3%, quantum 1: 97.5%, quantum 2: 99.7%). Blue represents isotype controls.

7 days and observed cells migrating from the EBs to the tissue culture dish (Figure 4(b)). RT-PCR was performed, which demonstrated that cells of all three germ layers—ectoderm (NESTIN, TUBB3, and NEFH), mesoderm (MSX1, T, and BMP4), and endoderm (GATA6, AFP, and SOX17)—were present (Figure 4(c)), providing additional evidence of pluripotency in the cells after QES expansion.

4. Discussion

In this study, we report the use of a closed system for reproducible large-scale expansion of hiPSCs while maintaining stemness and viability, a major step forward in the hiPSC arena.

In the last few years, biologists have striven to establish and optimize more consistent and safe PSC culture systems that maintain cell phenotype while permitting exponential expansion, regardless of the source of the PSCs. In traditional 2D culture systems, only about 10 million cells can be obtained per 100 mm plate. Scaled-up production to generate the billions of cells needed for tissue engineering using this standard culture condition is both time- and resource-consuming, making it impractical. Thus, 3D cell culture conditions are often used to scale up PSC production [9, 10, 32, 33], including those that rely on suspension, hydrogel, or scaffold strategies in the presence of agitation or stirring [4, 7, 12, 34]. Although these approaches have attractive aspects, cultivating PSCs in these systems becomes challenging if the cells form agglomerates or intercalate in the 3D environment. The former generates a heterogeneous microenvironment with limited diffusion of soluble factors, gradients in nutrient delivery, and heterogeneous oxygenation and pH, whereas the latter makes viable harvest/recovery very difficult. This uncontrolled 3D environment can lead to differentiation and/or loss of the cells and, due to agitation, can compromise cell viability and limit cell expansion rates [35].

Microcarriers can be used in suspension bioreactor systems for PSC expansion [36–38]. Using an electrospun polycaprolactone fiber system, Leino et al. [36] expanded PSCs in a 3D environment. The authors observed a homogeneous culture environment and the cells maintained pluripotency. However, the cells failed to proliferate when low seeding density was used and could not be detached from the system without compromising cell viability due to the porosity of the fibers. Though these systems maintain the stemness of the cells, they exert the negative effect of bead agitation on cell yield, including increased risk of cell detachment [9, 32, 36]. However, lower agitation rates compromise nutrient exchange, resulting in larger aggregates that are difficult to dissociate.

A stirred-suspension bioreactor system is another option for expanding cells to large numbers. By using this, Krawetz et al. [19] were able to expand hPSCs 9–12-fold. However, the authors described the necessity of an extra passage (adaptation passage) to reach this growth pattern and reported a need for adding rapamycin to the media to guarantee cell survival and the undifferentiated phenotype. Using a similar system, Meng et al. [13] described a 12-fold expansion of hiPSCs, but they needed to optimize inoculation conditions,

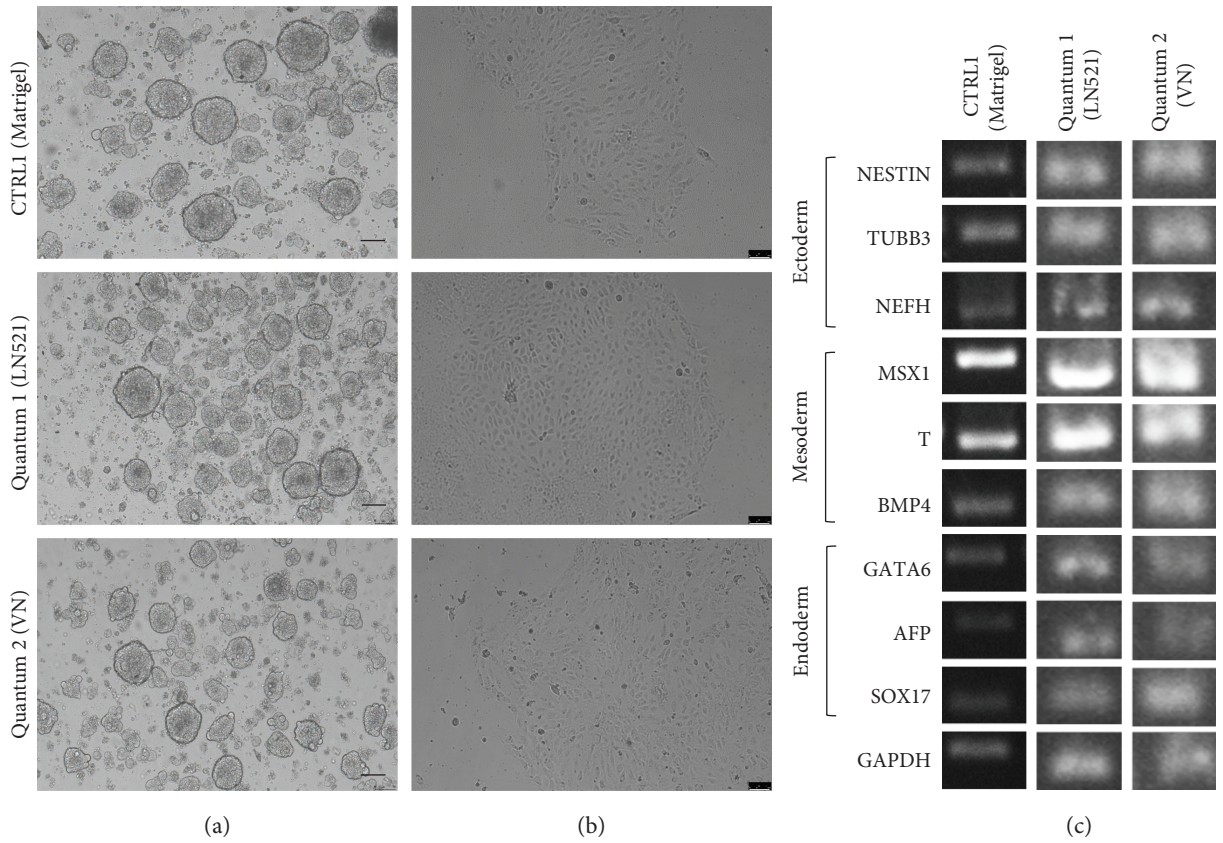

Figure 4: Spontaneous differentiation of iPSCs after expansion in QES. (a) Floating embryoid bodies (EB) 7 days after aggregation. (b) Colony morphology after attachment. (c) Expression of markers of three embryonic germ layers by RT-PCR when cultivated on Matrigel (CTRL1) or after QES expansion on LN521 and VN. Scale bars represent 100 μm.

seeding density, aggregate size, agitation rate, and cell passaging methodology for each cell line used in the study, limiting the reproducibility of the expansion.

Here, we used the QES as a 2D cell culture system to reproducibly expand hiPSCs while maintaining stemness. In this system, we reduced over 99% of opening events compared to other bioreactors and eliminated the need for multiple incubators since each QES has 11,500 hollow fibers (200 μm diameter per fiber) reaching a total surface area of 21,000 cm^2 (about 380,100 mm tissue culture dishes). After expansion in the QES, the cells expressed high levels of pluripotency markers, maintained the normal karyotype, and could be spontaneously differentiated into the three germ layers, suggesting that the QES environment did not change the pluripotency status of the hiPSC line.

In our study, we observed a significant increase in the proliferation of hiPSCs when the hollow fibers of the QES were coated with LN521 versus VN. When we treated the hollow fibers with VN, the cell yield was not as high after 10 days as when the system was coated with LN521 for just 7 days, even though media consumption was the same under both conditions. This indicated that the coating can alter the proliferation rate of the cells. It is possible that interactions between the QES fibers and VN are weak, leading to a small available area for cell attachment. Therefore, we suggest that LN521 is able to cover all of the hollow-fiber surface, providing a larger area for cell attachment, which maximizes hiPSC expansion.

Chemically defined media [21, 39] and feeder-free culture systems coated with various ECM proteins [11, 23, 32, 40] were developed to maintain the phenotype of PSCs in culture. Matrigel™ is the gold standard ECM for PSC feeder-free culture in the laboratory but consists of a tumor-derived complex mixture of ECM, proteoglycans, and growth factors that cannot be used for clinical cell production [28, 41]. Furthermore, even in a research setting, Matrigel™ is heterologous, chemically undefined, and has high variability, making it more difficult to use when developing a scalable and reproducible PSC culture system. To avoid the variability of Matrigel™ and to generate simplified but robust well-defined culture conditions, we used purified matrix proteins LN and VN. These coatings have previously been utilized to increase the reliability and reproducibility of cell expansion and differentiation protocols [22, 32, 40, 42, 43]. Both coatings (LN and VN) allowed cells to be expanded, to self-renew with a normal karyotype, and to maintain pluripotency markers; furthermore, they allowed the formation of teratomas containing cells from three germ layers [22, 32, 36, 40, 44]. Although VN could substitute for Matrigel™, Rowland et al. [45] demonstrated that Matrigel™ had a slightly better performance in the adhesion and proliferation of cells.

In conclusion, we have demonstrated that QES can be used for efficient, reproducible hiPSC expansion, while preserving the stem cell phenotype of the cells. Utilizing

the clinically approved QES in tandem with xeno-free reagents provided an optimized cell culture system to generate large quantities of hiPSCs. This provides a major step forward in the generation of the number of cells needed for human-sized whole organ bioengineering and subsequent therapeutic applications.

Data Availability

The data used to support the findings of this study are included within the article.

Conflicts of Interest

The authors declare that they have no conflicts of interest.

Supplementary Materials

Figure S1: Lactate-predicted cell number using ACS1030 hiPSC line during expansion in QES. Red: LN521 coating; black: VN coating (referenced in Results, second paragraph). *(Supplementary Materials)*

References

[1] R. Zweigerdt, "Large scale production of stem cells and their derivatives," *Advances in biochemical engineering/biotechnology*, vol. 114, pp. 201–235, 2009.

[2] L. T. Lock and E. S. Tzanakakis, "Expansion and differentiation of human embryonic stem cells to endoderm progeny in a microcarrier stirred-suspension culture," *Tissue engineering Part A*, vol. 15, no. 8, pp. 2051–2063, 2009.

[3] R. Olmer, A. Lange, S. Selzer et al., "Suspension culture of human pluripotent stem cells in controlled, stirred bioreactors," *Tissue engineering Part C, Methods*, vol. 18, no. 10, pp. 772–784, 2012.

[4] Y. Fan, M. Hsiung, C. Cheng, and E. S. Tzanakakis, "Facile engineering of xeno-free microcarriers for the scalable cultivation of human pluripotent stem cells in stirred suspension," *Tissue engineering Part A*, vol. 20, no. 3-4, pp. 588–599, 2014.

[5] J. C. Mohr, J. J. de Pablo, and S. P. Palecek, "3-D microwell culture of human embryonic stem cells," *Biomaterials*, vol. 27, no. 36, pp. 6032–6042, 2006.

[6] A. M. Fernandes, P. A. Marinho, R. C. Sartore et al., "Successful scale-up of human embryonic stem cell production in a stirred microcarrier culture system," *Brazilian journal of medical and biological research*, vol. 42, no. 6, pp. 515–522, 2009.

[7] M. Serra, C. Correia, R. Malpique et al., "Microencapsulation technology: a powerful tool for integrating expansion and cryopreservation of human embryonic stem cells," *PLoS One*, vol. 6, no. 8, article e23212, 2011.

[8] R. Olmer, A. Haase, S. Merkert et al., "Long term expansion of undifferentiated human iPS and ES cells in suspension culture using a defined medium," *Stem cell research*, vol. 5, no. 1, pp. 51–64, 2010.

[9] C. Kropp, H. Kempf, C. Halloin et al., "Impact of feeding strategies on the scalable expansion of human pluripotent stem cells in single-use stirred tank bioreactors," *Stem cells translational medicine*, vol. 5, no. 10, pp. 1289–1301, 2016.

[10] W. Almutawaa, L. Rohani, and D. E. Rancourt, "Expansion of human induced pluripotent stem cells in stirred suspension bioreactors," *Methods in molecular biology*, vol. 1502, pp. 53–61, 2016.

[11] L. G. Villa-Diaz, A. M. Ross, J. Lahann, and P. H. Krebsbach, "Concise review: the evolution of human pluripotent stem cell culture: from feeder cells to synthetic coatings," *Stem Cells*, vol. 31, no. 1, pp. 1–7, 2013.

[12] M. Amit, J. Chebath, V. Margulets et al., "Suspension culture of undifferentiated human embryonic and induced pluripotent stem cells," *Stem cell reviews*, vol. 6, no. 2, pp. 248–259, 2010.

[13] G. Meng, S. Liu, A. Poon, and D. E. Rancourt, "Optimizing human induced pluripotent stem cell expansion in stirred-suspension culture," *Stem cells and development*, vol. 26, no. 24, pp. 1804–1817, 2017.

[14] M. R. Larijani, A. Seifinejad, B. Pournasr et al., "Long-term maintenance of undifferentiated human embryonic and induced pluripotent stem cells in suspension," *Stem cells and development*, vol. 20, no. 11, pp. 1911–1923, 2011.

[15] J. A. Thomson, J. Itskovitz-Eldor, S. S. Shapiro et al., "Embryonic stem cell lines derived from human blastocysts," *Science*, vol. 282, no. 5391, pp. 1145–1147, 1998.

[16] J. Yu, M. A. Vodyanik, K. Smuga-Otto et al., "Induced pluripotent stem cell lines derived from human somatic cells," *Science*, vol. 318, no. 5858, pp. 1917–1920, 2007.

[17] K. Takahashi, K. Tanabe, M. Ohnuki et al., "Induction of pluripotent stem cells from adult human fibroblasts by defined factors," *Cell*, vol. 131, no. 5, pp. 861–872, 2007.

[18] Z. Tong, A. Solanki, A. Hamilos et al., "Application of biomaterials to advance induced pluripotent stem cell research and therapy," *The EMBO journal*, vol. 34, no. 8, pp. 987–1008, 2015.

[19] R. Krawetz, J. T. Taiani, S. Liu et al., "Large-scale expansion of pluripotent human embryonic stem cells in stirred-suspension bioreactors," *Tissue engineering Part C, Methods*, vol. 16, no. 4, pp. 573–582, 2010.

[20] A. Manzo, Y. Ootaki, C. Ootaki, K. Kamohara, and K. Fukamachi, "Comparative study of heart rate variability between healthy human subjects and healthy dogs, rabbits and calves," *Laboratory animals*, vol. 43, no. 1, pp. 41–45, 2009.

[21] G. Chen, D. R. Gulbranson, Z. Hou et al., "Chemically defined conditions for human iPSC derivation and culture," *Nature methods*, vol. 8, no. 5, pp. 424–429, 2011.

[22] S. Rodin, A. Domogatskaya, S. Strom et al., "Long-term self-renewal of human pluripotent stem cells on human recombinant laminin-511," *Nature biotechnology*, vol. 28, no. 6, pp. 611–615, 2010.

[23] H. Hongisto, S. Vuoristo, A. Mikhailova et al., "Laminin-511 expression is associated with the functionality of feeder cells in human embryonic stem cell culture," *Stem cell research*, vol. 8, no. 1, pp. 97–108, 2012.

[24] D. A. Brafman, C. W. Chang, A. Fernandez, K. Willert, S. Varghese, and S. Chien, "Long-term human pluripotent stem cell self-renewal on synthetic polymer surfaces," *Biomaterials*, vol. 31, no. 34, pp. 9135–9144, 2010.

[25] P. Zhou, F. Wu, T. Zhou et al., "Simple and versatile synthetic polydopamine-based surface supports reprogramming of human somatic cells and long-term self-renewal of human pluripotent stem cells under defined conditions," *Biomaterials*, vol. 87, pp. 1–17, 2016.

[26] L. G. Villa-Diaz, H. Nandivada, J. Ding et al., "Synthetic polymer coatings for long-term growth of human embryonic stem cells," *Nature biotechnology*, vol. 28, no. 6, pp. 581–583, 2010.

[27] Z. Melkoumian, J. L. Weber, D. M. Weber et al., "Synthetic peptide-acrylate surfaces for long-term self-renewal and cardiomyocyte differentiation of human embryonic stem cells," *Nature biotechnology*, vol. 28, no. 6, pp. 606–610, 2010.

[28] C. S. Hughes, L. M. Postovit, and G. A. Lajoie, "Matrigel: a complex protein mixture required for optimal growth of cell culture," *Proteomics*, vol. 10, no. 9, pp. 1886–1890, 2010.

[29] J. McGowan-Jordan, A. Simons, and M. Schmid, *ISCN 2016: An International System for Human Cytogenomic Nomenclature*, A. S. Jean McGowan-Jordan and M. Schmid, Eds., Karger, Switzerland, Basel, New York, 2016.

[30] I. Kehat, D. Kenyagin-Karsenti, M. Snir et al., "Human embryonic stem cells can differentiate into myocytes with structural and functional properties of cardiomyocytes," *The Journal of clinical investigation*, vol. 108, no. 3, pp. 407–414, 2001.

[31] M. Haack-Sorensen, B. Follin, M. Juhl et al., "Culture expansion of adipose derived stromal cells. A closed automated Quantum Cell Expansion System compared with manual flask-based culture," *Journal of Translational Medicine*, vol. 14, no. 1, p. 319, 2016.

[32] S. M. Badenes, T. G. Fernandes, C. S. Cordeiro et al., "Defined essential 8™ medium and vitronectin efficiently support scalable xeno-free expansion of human induced pluripotent stem cells in stirred microcarrier culture systems," *PLoS One*, vol. 11, no. 3, article e0151264, 2016.

[33] Y. Shao, J. Sang, and J. Fu, "On human pluripotent stem cell control: the rise of 3D bioengineering and mechanobiology," *Biomaterials*, vol. 52, pp. 26–43, 2015.

[34] R. Derda, L. Li, B. P. Orner, R. L. Lewis, J. A. Thomson, and L. L. Kiessling, "Defined substrates for human embryonic stem cell growth identified from surface arrays," *ACS chemical biology*, vol. 2, no. 5, pp. 347–355, 2007.

[35] Y. Lei and D. V. Schaffer, "A fully defined and scalable 3D culture system for human pluripotent stem cell expansion and differentiation," *Proceedings of the National Academy of Sciences of the United States of America*, vol. 110, no. 52, pp. E5039–E5048, 2013.

[36] M. Leino, C. Astrand, N. Hughes-Brittain, B. Robb, R. McKean, and V. Chotteau, "Human embryonic stem cell dispersion in electrospun PCL fiber scaffolds by coating with laminin-521 and E-cadherin-Fc," *Journal of biomedical materials research Part B, Applied biomaterials*, vol. 106, no. 3, pp. 1226–1236, 2018.

[37] Y. Fan, F. Zhang, and E. S. Tzanakakis, "Engineering xeno-free microcarriers with recombinant vitronectin, albumin and UV irradiation for human pluripotent stem cell bioprocessing," *ACS biomaterials science & engineering*, vol. 3, no. 8, pp. 1510–1518, 2017.

[38] Y. Li, L. Li, Z. N. Chen, G. Gao, R. Yao, and W. Sun, "Engineering-derived approaches for iPSC preparation, expansion, differentiation and applications," *Biofabrication*, vol. 9, no. 3, article 032001, 2017.

[39] T. E. Ludwig, M. E. Levenstein, J. M. Jones et al., "Derivation of human embryonic stem cells in defined conditions," *Nature biotechnology*, vol. 24, no. 2, pp. 185–187, 2006.

[40] A. B. Prowse, M. R. Doran, J. J. Cooper-White et al., "Long term culture of human embryonic stem cells on recombinant vitronectin in ascorbate free media," *Biomaterials*, vol. 31, no. 32, pp. 8281–8288, 2010.

[41] A. D. Celiz, J. G. Smith, R. Langer et al., "Materials for stem cell factories of the future," *Nature materials*, vol. 13, no. 6, pp. 570–579, 2014.

[42] S. M. Azarin and S. P. Palecek, "Matrix revolutions: a trinity of defined substrates for long-term expansion of human ESCs," *Cell Stem Cell*, vol. 7, no. 1, pp. 7-8, 2010.

[43] H. Albalushi, M. Kurek, L. Karlsson et al., "Laminin 521 stabilizes the pluripotency expression pattern of human embryonic stem cells initially derived on feeder cells," *Stem cells international*, vol. 2018, Article ID 7127042, 9 pages, 2018.

[44] S. Rodin, L. Antonsson, C. Niaudet et al., "Clonal culturing of human embryonic stem cells on laminin-521/E-cadherin matrix in defined and xeno-free environment," *Nature Communications*, vol. 5, no. 1, p. 3195, 2014.

[45] T. J. Rowland, L. M. Miller, A. J. Blaschke et al., "Roles of integrins in human induced pluripotent stem cell growth on Matrigel and vitronectin," *Stem cells and development*, vol. 19, no. 8, pp. 1231–1240, 2010.

Hindawi
Stem Cells International
Volume 2019, Article ID 9671206, 18 pages
https://doi.org/10.1155/2019/9671206

Review Article

Immunomodulatory Functions of Mesenchymal Stem Cells in Tissue Engineering

Haojiang Li,[1,2] Shi Shen,[1,3] Haitao Fu,[1,4] Zhenyong Wang,[1,5] Xu Li,[1] Xiang Sui,[1] Mei Yuan,[1] Shuyun Liu,[1] Guiqin Wang,[2] and Quanyi Guo[1]

[1]*Institute of Orthopedics, Chinese PLA General Hospital, Beijing Key Lab of Regenerative Medicine in Orthopedics, Key Laboratory of Musculoskeletal Trauma War Injuries, PLA, No. 28 Fuxing Road, Haidian District, Beijing 100853, China*
[2]*Department of Microbiology and Immunology, Shanxi Medical University, Taiyuan, China*
[3]*Department of Bone and Joint Surgery, The Affiliated Hospital of Southwest Medical University, No. 25 Taiping Road, Luzhou 646000, China*
[4]*School of Medicine, Nankai University, Tianjin 300071, China*
[5]*First Department of Orthopedics, First Affiliated Hospital of Jiamusi University, No. 348 Dexiang Road, Xiangyang District, Jiamusi 154002, China*

Correspondence should be addressed to Quanyi Guo; doctorguo_301@163.com

Received 8 July 2018; Revised 26 October 2018; Accepted 29 November 2018; Published 13 January 2019

Guest Editor: Tiago Fernandes

The inflammatory response to chronic injury affects tissue regeneration and has become an important factor influencing the prognosis of patients. In previous stem cell treatments, it was revealed that stem cells not only have the ability for direct differentiation or regeneration in chronic tissue damage but also have a regulatory effect on the immune microenvironment. Stem cells can regulate the immune microenvironment during tissue repair and provide a good "soil" for tissue regeneration. In the current study, the regulation of immune cells by mesenchymal stem cells (MSCs) in the local tissue microenvironment and the tissue damage repair mechanisms are revealed. The application of the concepts of "seed" and "soil" has opened up new research avenues for regenerative medicine. Tissue engineering (TE) technology has been used in multiple tissues and organs using its biomimetic and cellular cell abilities, and scaffolds are now seen as an important part of building seed cell microenvironments. The effect of tissue engineering techniques on stem cell immune regulation is related to the shape and structure of the scaffold, the preinflammatory microenvironment constructed by the implanted scaffold, and the material selection of the scaffold. In the application of scaffold, stem cell technology has important applications in cartilage, bone, heart, and liver and other research fields. In this review, we separately explore the mechanism of MSCs in different tissue and organs through immunoregulation for tissue regeneration and MSC combined with 3D scaffolds to promote MSC immunoregulation to repair damaged tissues.

1. Introduction

The combination of MSCs and TE can promote the immunoregulatory properties of MSCs than MSCs alone can. MSCs can regulate immune responses, especially adaptive immune response. The addition of tissue engineering techniques can affect this role of MSCs and is closely related to the material and shape of the cell carrier scaffolds. Through the introduction of the immunomodulatory capacity of MSCs and the application of tissue engineering scaffolds, the paper discusses the mechanism of MSC immune regulation in different organs (cartilage, bone, cardiovascular, and liver) and the effect of TE on the immune regulation of MSCs.

1.1. Immune Regulation of Mesenchymal Stem Cells in the Microenvironment. The interaction between mesenchymal stem cells (MSCs) and immune cells is complex. MSCs can regulate immune cells through cell contact and secretion

and can directly act on immune cells to inhibit their activity. Cells that express immunosuppressive properties on the cell surface, such as programmed death-ligand 1 (PD-L1) and Fas ligand (Fas-L) [1, 2], bind to receptors on the surface of immune cells, resulting in immune cell loss of function. Evidence has suggested that MSCs bind to activated immune cells, which may keep them in close proximity and thus enhance immunosuppressive effects [3]. In addition to their direct action on immune cells, MSCs can also inhibit immune cells by secreting cytokines, including transforming growth factor-β (TGF-β), hepatocyte growth factor (HGF), and prostaglandin E2 (PGE2), as well as other anti-inflammatory factors [4, 5]. For example, MSCs secrete TGF-β and other factors, which can promote the induction of regulatory T cells (Tregs) [6] and macrophages [7], and in this way transmit their immunosuppressive effects to other cells to activate different immunosuppressive mechanisms. MSCs express TNF-α-stimulated gene/protein 6 (TSG-6) which mediates the regulation of immune inflammation. It antagonizes the binding of CXCL8 to heparin by interacting with the GAG-binding site of CXCL8, thereby inhibiting CXCL8-mediated neutrophil chemotaxis [8]. Among them, TSG-6 can inhibit extravasation of leukocytes (mainly neutrophils and macrophages) at the site of inflammation [9]. TSG-6 is another key factor that plays an important role in tissue repair function in human MSCs and is demonstrated in mouse models of myocardial infarction, peritonitis, and acute corneal and lung injury [10–13].

Therefore, MSCs play a central role in maintaining immune homeostasis by interacting with cytokines, chemokines, and cell surface molecules. Previous studies on the immune regulation of MSCs have focused on the interaction between MSCs and B lymphocytes, natural killer cells, and dendritic cells. More recently, the use of MSCs in the repair of tissue damage and regulation of the inflammatory response has attracted increasing attention with respect to macrophage and T cell regulation.

MSCs have significant immunomodulatory capacity and play a role in both the innate and adaptive immune systems. In recent years, research has focused on the repair of tissue damage by stem cells, and there has been a great deal of interest in understanding the role of MSCs in the adaptive immune response. MSCs negatively regulate the activation and proliferation of T cells (including $CD4^+$ and $CD8^+$ cells) by cell contact and the secretion of inflammatory soluble factors [14]. The data indicate that MSCs inhibit proliferation by inducing G0 arrest in the T cell cycle [15, 16]. MSCs can also induce T cell apoptosis mediated by the Fas-L-dependent pathway [17]. Under normal conditions, MSCs can promote the survival of T lymphocytes [18] and stimulate their proliferation through interleukin- 6 (IL-6) dependent pathways [19]. However, with activation of the immune system following tissue damage, T cell-derived interferon- γ (IFN-γ) activates the immunoregulatory properties of MSCs, resulting in suppression of the activation and proliferation of immune cells [20]. Then, MSCs upregulate the expression of indamine 2 (IDO), HGF, PD-L1, PGE2, and cyclooxygenase-2 to regulate immune function [21, 22]. Experiments have shown that more than 30 soluble factors are involved in the immune regulation of MSCs during the activation and proliferation of T lymphocytes [23], including HGF, TGF-β [4], IDO [24], PGE2 [5, 25], nitric oxide (NO) [26], and IL-10 [25]. It was also found that adenosine produced by MSCs reduces T cell proliferation by binding to adenosine receptors on the surface of lymphocytes [27, 28]. The ability of MSCs to inhibit T cell activation and alter T cell polarization remains a major focus of many MSC immunomodulatory studies, and soluble signals and pathways that control the interaction between MSCs and T cells are compared to other leukocyte populations. However, the immune microenvironment composed of inflammatory cytokines plays a key role in stimulating the innate and adaptive immunomodulatory activities of MSCs. Inhibition of T cell proliferation and activation by MSCs was induced by the IFN-γ induced expression of indoleamine 2,3-dioxygenase (IDO). Although pretreatment with IFN-γ is commonly used for direct MSC immunomodulatory activity prior to transplantation, transient effects resulting from pretreatment may limit the regulation of immune response by MSCs. The addition of tissue engineering technology can precisely improve and continuously induce the immunomodulatory activity of MSC to a certain extent. In order to overcome these difficulties, local transplantation of MSCs aggregates can improve the local inflammatory environment of the cells at the injection site, while increasing the expression of immunoregulatory factors. The authors believe that MSCs can maintain the structural basis of cell-cell and cell-matrix contact by means of aggregate delivery, which can prevent cell loss due to apoptosis and better implant into host tissues [29]. In one experiment, it was found that by constructing mesenchymal stem cells in a three-dimensional state, the immunosuppressive effect of T cells can be enhanced by continuously presenting bioactive IFN-γ, compared with MSCs pretreated alone. Microparticle delivery of IFN-γ in MSC spheroids can maintain immunomodulatory activity [30]. Found in a study on bone regeneration, three-dimensional cultured clumps of a mesenchymal stem cell (MSC)/extracellular matrix (ECM) complex (C-MSC) consists of cells and self-produced ECM. C-MSCs can use ECM as a cell scaffold to regulate in vitro cell function and induce successful bone regeneration. IFN-γ pretreatment effectively enhanced the immunomodulatory capacity of C-MSCs. X-transplantation of C-MSCγ into the skull of immunocompetent mice induced bone regeneration, while C-MSC xenograft failed and induced T cell infiltration [31]. In addition to regulating secretion by MSCs, T cells can exert a similar effect through cell contact. The attraction of MSCs to T cells has been explained by the expression of high levels of the leukocyte chemokine ligands CXCL9, CXCL10, and CXCL11. Neutralization with CXCR3, a T cell chemokine, as well as CXCL9, CXCL10, and CXCL11 receptors, initiates the immunosuppressive effects of MSCs, revealing the role of chemokines in regulation of the stem cell-mediated immune environment [32]. In addition to CXCR3, other molecules, such as vascular cell adhesion molecule-1 (VCAM-1), intercellular adhesion molecule-1 (ICAM-1), and programmed cell death protein 1 (PD-1), are also involved in contact inhibition of T cells by MSCs [1, 33,

34]. The effective immunosuppression of mesenchymal stem cells (MSCs) is caused by IFN-γ and is accompanied by the simultaneous presence of three other proinflammatory cytokines, TNF-α, IL-1a, or IL-1b. These cytokine combinations stimulate several chemokines and inducible nitric oxide synthase (iNOS) expressed by MSCs. Chemokines cause T cells to migrate to the vicinity of MSCs, where nitric oxide (NO) inhibits T cell immune responses [32]. Pretreatment of MSC by proinflammatory cytokines is a key link in the production of immunosuppressive properties.

Some reports have suggested that MSCs can not only reduce M1 infiltration [35] but can also reprogram macrophages from the inflammatory M1 phenotype to the anti-inflammatory M2 phenotype [36, 37]. In recent years, the effect of MSCs on macrophages has become increasingly clear. MSCs within tissues can induce macrophage migration and turn it into a regulatory phenotype [7, 37]. Coculture with MSCs can induce macrophages to increase IL-10 expression, reduce the levels of tumor necrosis factor-α (TNF-α and IL-12, and lower the expression of the costimulatory molecules CD86 and HLA class II to reduce inflammation [7, 36]. Studies have shown that MSC-mediated M2 macrophage polarization depends on the secretion of soluble factors, including PGE2, TNF-inducible gene-6 (TSG-6, IL-6, IDO, and TGF-β1 [12, 37, 38]. PGE2 is considered an important factor in the initiation of macrophage phenotypic changes [5].

The role of MSCs and Tregs in suppressing T cell proliferation has triggered interest in the factors and media involved. The current view is that the key factors involved in MSC induction of classical $CD4^+$ $CD25^+$ $Foxp3^+$ Tregs are MSC-derived TGF-β and PGE2 [39–41]. A number of mediators and mechanisms have been proposed to participate in the role of MSCs in promoting this classical Treg phenotype. MSCs have been shown to induce Foxp3 and CD25 expression in $CD4^+$ T cells by direct cell contact, followed by production of MSC-derived TGF-β1 and PGE2 [40, 41]. MSCs excreting TGF-β1 can also directly induce the production of $CD4^+$ $CD25^+$ $Foxp3^+$ Tregs [42]. PGE2 regulates the expression of Foxp3 in human lymphocytes and induces the regulatory phenotype of $CD4^+$ $CD25^-$ T cells by modulating the expression of Foxp3, thus contributing to Treg function [43]. In one study, when MSCs were cocultured with allogeneic Tregs, MSCs enhanced the immunosuppressive capacity of Tregs, and this effect was accompanied by IL-10 production and upregulation of PD-1 receptors on Tregs [44].

1.2. Effects of Tissue Engineering Materials and Structure on the Immune Regulatory Ability of MSCs. Tissue engineering (TE) and regenerative medicine applications are aimed at improving or replacing damaged biological functions by stimulating the body's inherent regenerative capacity or by replacing damaged tissues. TE implants include biomaterials, which may be natural, synthetic, or derived from deassimilated (xenogeneic, allogeneic, or autologous) materials and/or cells derived from allogeneic or autologous sources. Given the biomaterials and antigens that exist, TE implants are usually immunostimulatory. As a foreign body, the TE implant triggers a foreign body reaction (FBR) when introduced into an organism. When the reaction occurs, monocytes are recruited to the site of implantation under signals from IL-4 and IL-1, for example, followed by differentiation into macrophages [45, 46]. By identifying surface molecules on the implanted material, macrophages phagocytose foreign bodies and form foreign body giant cells (FBGCs) [46]. The main function of FBGCs is to parcel foreign agents by secreting degradative agents (such as superoxide and free radicals) to the lesions followed by avascular collagen deposition [46]. However, there are also reports of tissue-engineered implants forming FBGCs. This process affects the rate of degradation of the scaffold and the subsequent immune response [47, 48]. Inflammatory cells have been shown to play an important role in regeneration, where the implant induces inflammation [49].

TE implant material properties are an important factor for maximizing cell recruitment and differentiation. The TE materials are selected according to the following characteristics: (i) ability to provide appropriate mechanical support to the tissue, (ii) ability to determine the digestibility of the scaffold [50], and (iii) ability to trigger the appropriate immune response to promote tissue regeneration and healing [48]. The choice of materials affects the likelihood of inflammation. Many naturally occurring biomaterials have intrinsic anti-inflammatory signals, including high molecular weight hyaluronic acid (HA) and chitosan [51], which can reduce reactive oxygen species [52, 53]. However, for most materials, the use of anti-inflammatory drugs has been more extensively studied in anti-inflammatory repair of tissue defects. In addition, with respect to the regulation of posttransplant inflammation by MSC composite scaffolds, in one study it was found that MSCs in TE can regulate macrophage activation and attenuate the FBR through continuous cross-talk with inflammatory cells [54]. Consequently, with a greater understanding of stem cell immune regulation, the use of TE materials constructed with stem cells will be increasingly important.

In addition to the choice of scaffold materials, the structure and shape of the scaffold in TE can affect inflammation. In a study on the effect of the geometry of the implanted material on its biocompatibility *in vivo*, it was found that the choice of stent had an effect on inflammation. Experimental studies have found that implanted spherical materials in various biomaterials (including hydrogels, ceramics, metals, and plastics) can significantly reduce FBRs and fibrosis depending on the diameter of the materials [55]. In a study of MSCs, construction of a three-dimensional (3D) structure in the scaffold microstructure affected the occurrence of posttransplant inflammation. Compared with conventional two-dimensional (2D) culture, 3D culture reduced macrophage recruitment and produced the anti-inflammatory proteins PGE2 and TSG-6 [56]. In recent years, the differences in MSC immunoregulation between 3D and 2D culture conditions have been studied (Table 1), including differential expression of 3D stem cell culture and conventional 2D culture in recent years. Current spheroidal culture of stem cells is most common in 3D culture [57–59], but there are also reports on polymer scaffolds [60] and 3D culture systems [61].

Table 1

Material	Scaffold structure	Stem cell source	Stem cell pretreatment	Function	Reference
MSC	3D spheroid	Human bone marrow-derived	Interleukin- (IL-) 1	The 3D MSC construct was reduced in LPS-induced TNF-a secretion and decreased IL-6 secretion	[58]
PLA/chitosan	Cylinders	Human bone marrow-derived	no	MSC interaction with macrophage within 3D scaffolds hampers fibroblast recruitment	[60]
MSC	3D spheroid	Human bone marrow-derived	IFN-g	MSCs express high levels of proliferating genes, lower levels of inflammation, apoptosis, and senescence genes in 3D	[59]
MSC	3D spheroid	Human adipose-derived	no	Increased angiogenic cytokine levels and immunosuppression against apoptosis in MSC spheroids	[57]
MSC	ALN bioreactor system	Rat bone marrow-derived	no	High function efficacy of MSC in the ALN-reactor system than the 2D culture	[61]

In the study by Emmanuel Pinteaux, MSCs increased the secretion of anti-inflammatory markers in the 3D environment, and 3D MSCs reduced the secretion of tumor necrosis factor TNF-α induced by LPS. These data highlight the importance of optimizing the initiation of therapeutic and culture conditions to maximize the therapeutic potential of MSC spheroids [58]. In the study by Catarina R. Almeida, macrophages in chitosan scaffolds promoted a significant increase in fibroblast recruitment rather than a significant increase in MSCs. However, macrophages that interact with MSCs in the scaffold are no longer able to recruit fibroblasts. This study demonstrates the potential of scaffolds to regulate regeneration through immune regulation [60]. In the Ren-He Xu study, the 3D construct was compared to monolayer-cultured BMSC (BMSCML). After IFN-γ treatment, a series of anti-inflammatory and proinflammatory genes including IDO, PD-L1, CCL2, and CXCL-10 were upregulated in the 3D group compared to untreated controls and expressed in all three IFN-γ-treated samples. The change of inflammatory cytokine IL-6 is small and IL-8 is decreased [59]. In a study by Sang Hun Lee, MSC spheroids showed an increase in IDO expression, as well as increased M2 macrophage ratio and reduced macrophage proliferation, compared to 2D cultured MSCs. Transplantation of MSC spheroids improved the survival rate of experimental mice and reduced the inflammatory response [57]. In the study by Christoph Giese, both TNF-α and IFN-γ were significantly inhibited in the scaffold construct. However, the production of other cytokines IL-1, IL-6, and IL-12 was also induced [61].

In many experiments, although stem cells have found to promote repair, the mechanism of repair has not been clearly explained. Does immunomodulation play a key role in this? There is no clear study on the fate and duration of stem cells during treatment and whether stem cells from different sources differ in immune regulation. In many experiments, the measurement of preinflammation factors should be used as a criterion for stimulating the immune regulation of MSCs. The effect of the material, the porosity, and the shape of the scaffold on MSCs still require further investigation. The spatial characteristics of the 3D scaffold structure also have certain limitations in culture. According to its structure, the diffusion of nutrients, oxygen, and waste through the stent is size-dependent, resulting in insufficient oxygen and nutrient supply [62–64]. In a harsh microenvironment, this can affect cell viability [64].

2. Effect of Stem Cell Immunomodulation on Tissue and Organ Injury Repair

2.1. Tissue of Regeneration. In the development of inflammation in effective tissue regeneration, the regenerative repair of tissue is a continuous process involving the interaction of stem cells with tissue-retained and recruited immune cells. The regression of the inflammatory phase and the transition to the regeneration phase are critical to the outcome of postinjury repair, which may aggravate the disease and impede repair. The application of stem cell combined tissue engineering technology has been widely used in liver, heart, and skeletal systems. In orthopedic systems, the application of stem cell tissue engineering technology in connective tissue such as cartilage and meniscus still has great development prospects.

2.2. Regulatory Effects of MSCs on Cartilage Macrophages. In clinical practice, cartilage injury is a multifactorial disease. At present, therapeutic interventions do not provide satisfactory therapeutic results and can lead to a decline in exercise capacity. Cartilage injury occurs primarily at the joint site, and the regenerative capacity of cartilage tissue is limited when the articular cartilage is damaged. If treatment is not effective, injury can lead to osteoarthritis (OA). Cartilage degeneration and inflammation are key features of OA, an inflammatory and degenerative joint disease that affects the entire joint and causing pain, deformity, and loss of function [65, 66]. In recent years, with the in-depth study of the immune microenvironment in tissue repair, we believe that creating a suitable microenvironment during cartilage regeneration can promote this process.

Mesoderm-derived MSCs are perivascularly derived pluripotent stem cells that have the ability to differentiate into multiple cell types, including cartilage, bone, and adipocytes

[67]. In previous experiments, MSCs have been used in preclinical studies of sepsis and acute respiratory syndrome treatment, suggesting that the paracrine effect of stem cells plays a role in the regulation of inflammation [68, 69]. Moreover, MSC regulation in the immune microenvironment promotes MSC chondrogenesis [70]. The induced polarization of macrophages and exosome secretion by stem cells also play a regulatory role in the immune microenvironment [70].

The immunomodulatory effects of stem cells are particularly important in TE development. The pathogenesis of arthritis is partly mediated by the action of proinflammatory cytokines, such as IL-1, which are elevated in the synovial fluid of joints in OA [71–73]. IL-1 induces the release of proinflammatory cytokines, such as matrix metalloproteinases (MMPs) and NO, and downregulates the expression of primary extracellular matrix (ECM) components to promote catabolism and antisynthesis in the metabolic signaling of articular chondrocytes [72, 73]. The MSC-based engineered cartilage can promote macrophage polarization to the M2 phenotype, enabling macrophages to exhibit anti-inflammatory properties, including upregulation of CD206, increased synthesis of IL-10, reduced secretion of IL-1β, and expression of genes indicative of the M1 to M2 transition. It has been suggested that MSC-based TE constructs may improve scaffold-induced inflammation and cartilage tissue regeneration through M2-polarized macrophages (Figure 1). The bone marrow stromal cell (BMSC) based engineered cartilage can inhibit inflammation *in vivo* by increasing the M2 polarization of macrophages, resulting in improved survival compared with the use of chondrocytes as seed cells [70]. However, with respect to the immunosuppressive properties of MSCs, conflicting results have been reported for cartilage-differentiated cells. Ren et al. showed that chondrogenic differentiation of MSCs can increase the anti-host immune response following allogeneic transplantation [33]. However, another study highlighting the differentiation of MSCs into chondrocytes found that MSCs exhibit similar properties in terms of suppressing T cell responses in allogeneic models [74]. Therefore, the relationship between the differentiation of stem cells and the change in immunosuppressive capacity during cell transplantation is particularly important for the immune regulation of stem cells. In one study of MSC-mediated repair of cartilage injury, MSC secretion of exosomes, to promote tissue repair, also involved regulation of the immune response. Secretion of exosomes can promote the enrichment of $CD163^+$ M2 cells, decrease the infiltration of $CD81^+$ M1 cells, and reduce the release of related inflammatory factors [75]. From the above observations, it has been suggested that effective cartilage regeneration can be achieved by coordinated mobilization and efficient activation of multiple cell types.

In the past experiment, the immunogenicity of MSCs was not fully explored. With the changes of MSCs after implantation, the immunogenicity of MSCs will affect the occurrence of inflammatory reaction. How to maximize the low immunogenicity of foreign implanted MSCs is worthy of further experimental research.

2.3. Regulatory Effects of MSCs on T Lymphocytes in Bone. In the event of a fracture, the early inflammatory response plays a crucial role in bone healing. However, when inflammation persists, it can inhibit fracture repair. Since the innate immune system is stimulated by a variety of cytokines, it activates and reaches the site of injury after fracture [76, 77]. The immunomodulatory capacity of MSCs plays a role in both the innate and the adaptive immune response. The adaptive immune response, which is mainly composed of lymphocytes, has important implications for the fracture healing process [78, 79]. With respect to the adaptive immune response, MSCs inhibit proliferation by inducing G0 arrest in the T cell cycle [15, 16]. Moreover, MSCs can induce apoptosis of T cells mediated by the Fas-L-dependent pathway [17]. MSCs induce Foxp3 and CD25 expression in $CD4^+$ T cells through direct cellular contact and secretion of TGF-β and PGE2 and induce classical $CD4^+$ $CD25^+$ $Foxp3^+$ Tregs [41, 42] (Figure 2). When MSCs are cocultured with Tregs, MSCs enhance the immunosuppressive capacity of Tregs, leading to the upregulation of PD-1 receptors on Tregs via production of IL-10 [44]. MSC production of heme oxygenase- 1 (HO-1) is also involved in the induction of Tregs [80]. Reinke et al. investigated the role of T cells in MSC-mediated osteogenesis in mouse skull defects and showed that proinflammatory T cells inhibit MSC-induced bone formation by releasing IFN-γ and TNF-α [81]. Conversely, $Foxp3^+$ Tregs significantly reduce TNF-α and IFN-γ levels and lead to MSC-mediated bone regeneration and skull defect repair [81]. Contrary to the view that T cells inhibit bone healing, Nam et al. reported that the proinflammatory cytokine IL-17, produced by Th17 lymphocytes, appears to mediate bone formation during fracture healing [82]. Through the regulation of immune cells, the use of MSC therapy is an attractive option for promoting bone fracture repair.

The effects of MSCs on T cells in bone damage and the effects in negative regulatory T cells were mentioned in the above experiments. However, it is still necessary to further explain the mechanism of MSCs negatively regulating T cells from the direct contact of cells and the secretion of cytokines.

2.4. MSCs Reduce Liver Fibrosis by Regulating Macrophage Differentiation during Liver Regeneration. The liver is a highly regenerative organ with a strong ability to self-regenerate. However, in chronic injury, the structure of normal hepatic lobules is destroyed or lost and is replaced by pseudo-lobules, which eventually result in regenerative failure. However, when acute or repetitive injury is caused by a toxin or viral infection, the liver can be effectively regenerated [83, 84]. This process benefits from the activation of immune cells immediately following injury, which can mobilize liver growth factors as well as initiate synergistic responses of immune cells [85, 86]. The treatment of MSCs in acute and chronic hepatic failure mainly improves immune function following hepatic injury through immunoregulatory factors released by MSCs [87, 88]. Regulation of the immune system may be a viable alternative in the treatment of liver failure. Fibrosis reflects a pathological change in liver failure. During the study of liver fibrosis, macrophages were found to perform dual functions in this process. Kupffer cells and

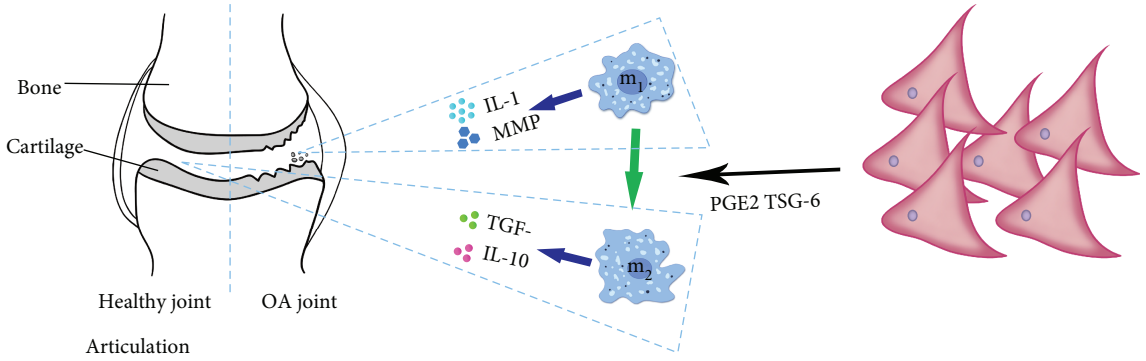

Figure 1: MSCs affect the development of arthritis through immunosuppression. MSCs promote the differentiation of macrophage to M1 by secreting PGE2 and TSG-6 and secrete anti-inflammation factors against soft inflammatory lesions. The blue arrow indicates the secretion of cellular cytokines, and the green arrow indicates the differentiation process.

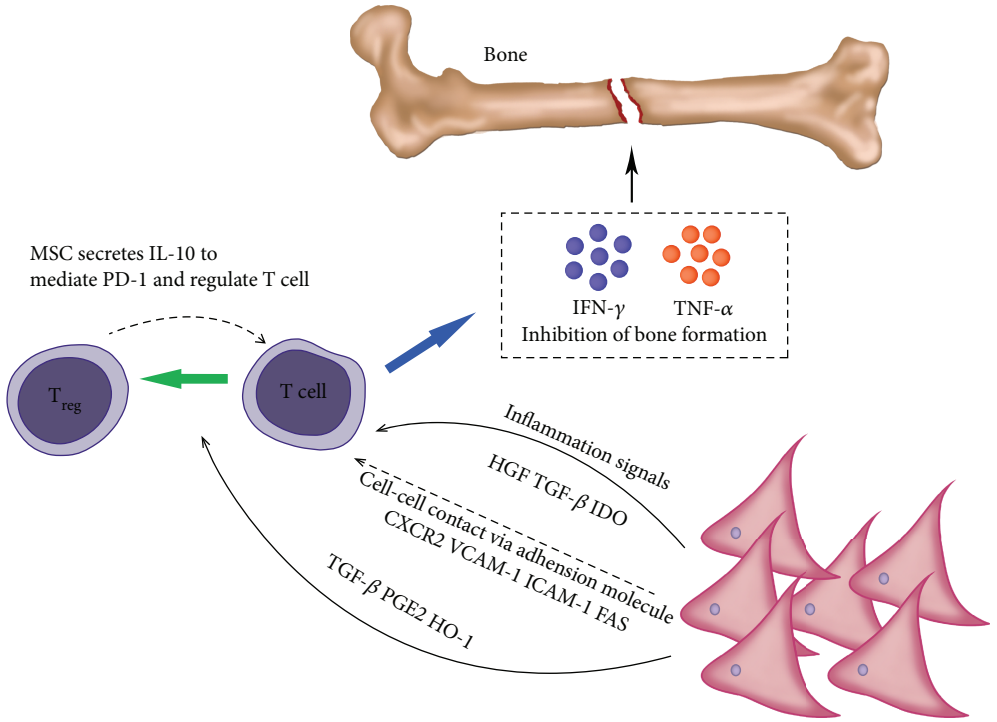

Figure 2: In addition to direct immunosuppressive inhibition, T cells can induce Treg cells under the regulation of MSCs and vice versa. Blue arrow: cytokine secretion, dotted arrow: inhibition of MSCs and Treg, black arrow: positive promotion, and green arrow: differentiation of T cells to Treg.

infiltrating mononuclear cells in scar tissue following liver injury induced and activated hepatic fibroblasts to participate in the occurrence and development of hepatic fibrosis [89]. However, different subpopulations of monocytes/macrophages exhibit antifibrotic properties because of their anti-inflammatory properties [90]. Animal studies have demonstrated that the expression of Ly-6C and Gr1 on macrophages provides a better indication of their role in fibrosis. Macrophages with high expression of Ly-6C or Gr1 are profibrotic [91, 92] and are a major source of TGF-β, platelet-derived growth factor, and insulin growth factor-1 (IGF-1), which is used to activate HSCs and initiate NF-κB-mediated fibroblast survival signals [93]. By contrast, low-Ly-6C-expressing macrophages [94, 95] exhibit antifibrotic properties [94, 96, 97]. They produce MMPs that directly degrade the ECM [94] and promote hepatic stellate cell (HSC) apoptosis through caspase-9 and TNF-related apoptosis-inducing ligand-dependent mechanisms. This duality of macrophage function has been demonstrated in a series of fibrotic mouse models (CCl_4, dimethylnitrosamine, and thioacetamide models) [97–99]. Mononuclear cells cause regression of fibrosis due to matrix degradation [94, 95] (Figure 3). In another study, different subpopulations of monocytes and differentiated macrophages were shown to exhibit different effects on hepatic fibrosis [100]. Thus, it has been suggested that the immunomodulatory capacity of

MSCs will be important in the treatment of hepatic fibrosis. In liver injury, MSCs mediate the antifibrotic effect of regulation of the conversion of macrophages to the anti-inflammatory M2 type, which is important in the treatment of hepatic fibrosis.

In the control of inflammatory response and correction of liver fibrosis in MSCs, the mechanism of action of MSCs against liver fibrosis is lacking, thus providing more insights for optimal treatment.

2.5. MSCs Regulate Angiogenesis through Regulation of Macrophages in the Damaged Myocardium. Cardiovascular disease is caused by damage to myocardial cells. Cardiomyocytes have long been considered to be highly differentiated cells and do not have the ability to regenerate following injury [101]. However, it has been shown that in the process of cardiac damage, myocardial cells and cardiac stem cells around the injured area can migrate under the promotion of inflammatory cells and quickly reenter the cell cycle, thereby promoting the recovery of cardiac function [102, 103]. Current stem cell-based therapies have provided new treatments for ischemic heart damage and heart failure; however, in the absence of nutrients and oxygen in the microenvironment, the regenerative repair of stem cells declines [104, 105]. Thus, the creation of a suitable microenvironment is also important. In the early stages of heart damage, activation of classical M1 macrophages will clear debris and produce proinflammatory cytokines such as IL-1β, TNF-α, and IFN-γ [106]. Different subpopulations [107, 108] were discovered in the late stage of cardiac injury, with similar phenotypes to those of anti-inflammatory M2 macrophages, showing that the presence of MSC promotes the differentiation of macrophages into M2 subtypes (Figure 4). Many molecules have been identified as being involved in this process, including IDO, PGE2, and MSC-derived IL-4 and IL-10 [7, 38, 109]. MSCs secrete TGF-β1 which together with PGE2 reduces macrophage-induced inflammatory factors such as IL-1β, IL-6, TNF-α, and IFN-γ [7, 109]. M2 macrophages promote angiogenesis by secreting anti-inflammatory and angiogenic cytokines, as well as promoting infarct healing and myocardial remodeling. M2 macrophages can also secrete growth factors, such as IGF-1 [110], to improve recovery following myocardial infarction [111]. M2 macrophages secrete vascular endothelial growth factor-A, which improves cardiac function following myocardial infarction by promoting angiogenesis. By studying the role of MSCs in an acute myocardial infarction mouse model [109], it was found that MSCs can reduce overall macrophage/monocyte counts (including M1 and M2 macrophages). However, the proportion of M2 macrophages increased significantly. Transplantation of MSCs significantly improved cardiac function and reduced myocardial fibrosis in the MSC-transplanted and nontransplanted groups following myocardial infarction [112]. In the MSC-transplanted group, capillary density increased around the infarct and M2 macrophages increased significantly at the site of transplantation. In another myocardial infarction study in mice, depletion of macrophages in the MSC-free group increased the incidence of myocardial infarction [113].

In the study of MSCs regulating the differentiation of M1 and M2 against myocardial injury, there is still no mechanism study on how MSCs regulate the regulation of inflammation into M2, thus providing a treatment for myocardial injury and fibrosis.

3. Application of TE Scaffold Composite MSCs

3.1. Immune Regulation of Cartilage Tissue Repair with MSC Seed Cells and 3D Scaffolds. The construction of cartilage TE takes into account the 3D microstructure of the selected material, as well as its biocompatibility and mechanical properties. Alternative materials, including the ECM, hydrogels, and polymers, have been used extensively in cartilage TE. For polymer scaffolds, cells should be contained within the internal structure of the polymer scaffold, such that they are retained in the body for a long period of time. Through appropriate manufacturing methods, porous scaffolds can help cells infiltrate the scaffold when implanted in the body [114, 115]. In a 3D hydrogel construct, coculture with autologous chondrocytes and MSCs may show a significantly higher rate of chondrogenesis [116]. Synthetic ECM must take into account several factors, including mechanical properties, which allow functional tissue growth and provide suitable cell-matrix interactions to stimulate tissue growth [117, 118]. Currently, the 3D behavior of specific cells (including MSCs) is considered to be different from the 2D behavior, suggesting that the cell generation environment can be imitated more closely in 3D *in vitro* culture systems compared with 2D culture [119, 120]. In the study of cartilage 3D scaffolds, scaffolds for tissue engineering (TE) are very similar to the physicochemical properties of natural extracellular matrices (ECM) and have been shown to facilitate cell attachment, proliferation, migration, and new tissue formation [121] (Table 2).

In the study of Corradetti et al., a biomimetic scaffold based on chondroitin sulfate was proposed, which can preserve the immunosuppressive potential of MSC in vitro, can respond to the immunomodulatory effects of proinflammatory cytokines, and can be immunosuppressive in the scaffold construct group. The production of molecules related to nitric oxide and prostaglandins and the expression of their inducible enzymes (iNos, PGEs, Cox-2, and TGF-β) are significantly increased [122]. In the Du et al. study, alginate/hyaluronic acid (Alg/HA) hydrogel scaffolds were used and bone marrow and adipose tissue-derived MSCs were induced into chondrocytes under three-dimensional conditions. MSCs before and after chondrocyte differentiation were treated with or without treatment of inflammatory conditions of IFN-γ and TNF-α, and the construct was found to have low immunogenicity and exert immunosuppressive effects on HLA-mismatched PBMC and undifferentiated MSCs [123]. Taken together, the activation of MSCs' immunoregulatory ability is related to scaffold material composition and mechanical properties. CS and HA have shown an effect in the immune regulation of MSCs. Moreover, it was found that the maintenance of the immunomodulatory ability of MSCs after differentiation was related to the microenvironment constructed by different materials, but there was

Table 2

Organ	MSC source	MSC pretreatment	Scaffold type	Immunomodulatory	Reference
Cartilage	Rabbit bone marrow-derive	IFN-g	Hydrogel scaffold	The hydrogel structure helps to reduce the immune response of MSCs after vaccination, even in the presence of inflammation cytokines.	[125]
	Human bone marrow-derived	IFN-g TNF-a	Alginate/hydrogel scaffold	MSCs under 3D hydrogel have low immunogenicity and can exert an immunosuppressive effect on HLA-mismatched PBMCs. And it has an inhibitory effect in NK cell-mediated cytolysis.	[123]
	Human bone marrow-derived	Overexpression of IL-1 receptor antagonist in MSCs induced by lentivirus	Woven PCL scaffold	Enhancement of collagen/GAG production in scaffolds expressing IL-1Ra under inflammatory conditions MMP was reduced in the construct compared to the untreated group, and the level of PGE2 was elevated.	[124]
	Rat bone marrow-derived	No	Hydrogel-sponge concentration	The production of NO, PGE2, HGF, and IDO increased gradually in 2D culture, and the immunoregulatory factor secreted by MSC in the 3D group reduced the activation ability of allogeneic lymphocytes.	[126]
	Pig bone marrow-derived	No	Cylindrical unwoven PGA fiber	The cytokines IL-10 and TGF-b were increased in the construction group, and the ability of FBGC recruitment was decreased.	[70]
	Human umbilical cord-derived	No	Decellularized pig ECM scaffold	Molecular IDO, PEG2, TGF-b1, IL-10, VEGF, and HGF increased in the scaffold concentration group.	[127]
	Rat bone marrow-derived	TNF-a	Freeze-dried collagen scaffolds	The scaffold construct group exhibited an immunosuppressive potential with a significant increase in iNos. And an upward trend was also observed for Cox and TGF-b.	[122]
Bone	mice bone marrow-derived	No	Transglutaminase glutathionase-crosslinked gelatin (TG-gel)	Cytokines and gene profiles of TNF-a and IL-10 in the scaffold construct showed elevated cincentractions in the test group.	[129]
	Human bone marrow-derived	No	3D instantaneously solidifying material (acBSP)	The scaffold construct synergizes with macrophage to promote cytokine expression of IL-11, IL-17, IL-4, and IL-6 and low expression of IL-1b and TNF-a.	[130]
	Human bone marrow-derived	No	MSC loaded on hydroxyapatite-tricalcium phosphate	After implantation of the scaffold construct, histologically, no lymphocytic infiltration occurred. And new bone was formed throughout the implant.	[131]
	Human bone marrow-derived	IFN-g	ECM	The scaffold construct can induce bone regeneration and inhibit xenografting of mouse T cells in the transplanted area.	[31]
liver	Mice bone marrow-derived	No	MSC transplantation	In the experiment group, TNF-a, IFN-g, IL-2, IL-17, IL-1b, and MPO secretion was decreased, and IL-10 was reversed. Expression of CXCL1, CCL2, CCL4, CCL7, and CXCL10 was inhibited.	[135]
	Rat bone marrow-derived	No	MSC transplantation	The expression of TNF-a, IL-1b, CXCL1, and CXCL2 was decreased, and the expression of the anti-inflammatory cytokine IL-10 was increased.	[136]
	Human umbilical cord-derived	No	3D spheroid	PGE2 secreted by the 3D group was significantly increased, and IFN-g was decreased.	[137]

Table 2: Continued.

Organ	MSC source	MSC pretreatment	Scaffold type	Immunomodulatory	Reference
Heart	Mice bone marrow-derived	No	Decellularized ECM	MSC vaccination results in positive immunomodulatory effect but a persistent chronic inflammatory response.	[149]
	Rat bone marrow-derived	No	3D hydrogel	Compared with the control group, the scaffold construct played a role in inhibiting leukocyte and promoting repair in the late stage of inflammation.	[150]
	Human bone marrow-derived	Simulated inflammatory environment	3D collagen scaffold	The immunosuppressive function of MSCs is retained in the 3D scaffold and promotes the activation of M2 macrophage. Single-layer cocultures with IL-10 levels lower than MSCs	[151]
	Rat bone marrow-derived	No	PCL	For the infiltration of CD68(+) macrophage in the absence of the scaffold construct, and the control group had a higher number of CD68(+)	[152]

no mechanism to study the immune regulation of MSCs by materials.

In the Butler et al. study, engineered cartilage with immunomodulatory properties was developed in conjunction with gene therapy and functional tissue engineering. Chondrogenesis was performed in the presence of IL-1 by inducing overexpression of an IL-1 receptor antagonist (IL-1Ra) in MSCs on the scaffold. A construct that painfully delivers a modulating anti-inflammatory cytokine enhances cartilage repair [124]. It was found that the treatment of proinflammatory factors inhibited the cartilage differentiation of MSCs to a large extent and maintained the immunoregulatory effect of MSCs, but the mechanism of tissue MSC differentiation was not explored in the article.

In the study of Zhang et al., the 3D structure affects the immunological properties of stem cells and the interaction between seed cells and the immune system of the host. Experimental results have shown that addition of the hydrogel structure helps to reduce the immune response generated following implantation of MSCs in the scaffold. Therefore, the supportive and isolating effects of 3D microstructured scaffolds (such as hydrogels prepared from higher collagen concentrations) can further reduce the immune response during transplantation, thus making them more suitable as candidates for cartilage TE [125]. In the Xingdong Zhang study, scaffold structures regulate the secretion of MSCs' immunoregulatory factors in allogeneic cartilage tissue engineering. The 3D groups (hydrogels and sponges) are more effective than under 2D monolayer culture conditions in promoting mRNA expression and protein production of soluble immune-related factors. The supernatant collected in the 3D group showed inhibition of allogeneic lymphocyte activation. The scaffold structure can regulate the secretion of MSCs. Research has allowed tissue regeneration scaffolds to control host immune rejection through immune regulation [126]. In the experiments, it was found that the 3D hydrogel was lower in expression of MHC-II on the MSCs than in the 2D culture, and the 3D scaffold produced a retraction effect under the action of MSCs, which in turn affected the immune regulation of MSCs. However, the interaction between the scaffold structure and MSCs need to be further experimentally analyzed from the mechanism.

In Ding et al.'s study, inflammation was inhibited by increasing M2 polarization of macrophages based on the engineered cartilage of BMSCs. This study indicated that the BMSC-based engineered cartilage inhibits inflammation *in vivo* through changes in the macrophage phenotype and that the tissue exhibits improved survival compared with the use of chondrocytes alone or in combination with BMSCs. BMSC-inoculated constructs improve stent-induced inflammation and promote cartilage tissue regeneration through M2 polarization of macrophages [70]. The 3D scaffold combined with MSCs promoted the recruitment and polarization of M2, but did not study the underlying mechanism of MSC-induced M2 cell recruitment and polarization.

In the study of Liu et al., the scaffold loaded with MSCs derived from human umbilical cord Wharton's jelly mesenchymal stem cells (hWJMSCs) reduced the immune response to subcutaneous implantation. hWJMSCs implanted on the back of rats did not induce an immune response in the subcutaneous environment during the observation period. The use of novel undifferentiated hWJMSCs as seed cells may be a better method for *in vivo* TE treatment of cartilage defects than differentiated hWJMSCs induced using TGF-β [127]. For ECM combined with MSCs, the former can promote the immune regulation of MSCs, but the xenograft of MSCs in the article is currently controversial. In the experiment, different anti-inflammatory factors were compared but lacked resistance of MSCs.

3.2. Immunoregulatory Effects of MSCs in Bone TE. The incorporation of MSCs into TE biomaterials is an extensively researched strategy aimed at accelerating bone formation and osteointegration during bone defect repair and regeneration. TE-related 3D delivery methods in MSC clinical application studies and the combination of porous scaffolds and MSCs have been reported for the treatment of critical-sized defects

[128]. The 3D delivery of MSCs has been explored as a new strategy to improve cell delivery, functional activation, and retention in the body, to improve treatment outcomes (Table 2).

He et al.'s study was the first to investigate how macrophages in TG-gel affect bone formation in bone marrow mesenchymal stem cells (BMMSCs). It was found that macrophages encapsulated in a low-stiffness matrix played an active role in the osteogenesis of cocultured BMMSCs [129]. It was found that under 3D culture conditions, the hardness of the scaffold could have a strong influence on the polarization of macrophages. The high-hardness gel material would differentiate macrophages into M1 and prevent osteogenic differentiation of MSCs, but in the experiment the mechanism by which MSCs interact with macrophages in this process was not further explored.

Niu et al.'s study designed an injectable, transient coagulation coating material (acBSP) based on the unique macrophage affinity of glucomannan polysaccharide and can effectively promote the adhesion and activation of macrophages and mesenchymal stem cell load. Hydrogels demonstrate potent macrophage activation. The osteogenesis is achieved by activating macrophages [130]. The regulation of T cells by MSCs plays a key role in bone repair. The experiment can further explore the interaction of scaffolds with MSCs on T cells and macrophages and study the mechanism of material influence.

In a study by Arinzeh et al., autologous MSCs were loaded into hollow cylinders of hydroxyapatite-tricalcium phosphate and implanted in femoral defects in dogs. Imaging assessment, histology, and serum antibody assessment were performed at 4, 8, and 16 weeks, respectively, and no severe inflammatory reaction was found [131]. This experiment was carried out earlier to study the role of MSCs in promoting the regeneration of bone by affecting inflammatory response. It was found that allogeneic bone transplantation was consistent with autologous bone graft in the presence of MSCs, but no more molecular and cellar levels were detected.

Three-dimensional cultures of MSC/ECM complexes (C-MSCs) have been shown to repair bone damage. C-MSCs can regulate cell function *in vitro* and use the ECM as a scaffold to induce successful bone regeneration and enhance the immunoregulatory capacity of C-MSCs. MSC xenotransplantation, which exerts immunoregulatory properties by upregulating IDO activity *in vitro*, can attenuate xenogeneic reactive host immune responses and thereby induce bone regeneration in mice [31]. After pretreatment of MSCs with IFN-g, the immunogenicity of MSCs should be further tested and the relationship with bone regeneration further explored, and the mechanism of modulating T cells with MSCs needs further experimental research.

3.3. Immunoregulatory Effects of MSCs in Liver TE. The construction of the functional TE liver has been increasingly favored by researchers, and the emerging concept of "organizational engineering" has been proposed. With the development of TE technology, scaffolds of collagen and polymer materials have been used to evaluate their support for cell growth, liver-specific functions, and regenerative capabilities [132, 133]. The whole organ decellularization technique can largely preserve natural tissue and the macroscopic 3D structure of the liver, ensuring biocompatibility and allowing extensive cell regeneration to occur [134]. Liver ECM composition, topography, and biomechanical properties influence cell-matrix interactions. Recent advances in stent fabrication techniques for complex cells have led to the evolution of decellularized hepatic tissue matrices from a simple 2D culture to a 3D porous scaffold (Table 2).

Tian et al.'s research reveals the protective effects of MSCs and elucidates the underlying mechanisms of immune regulation in liver transplantation models. And this work provides a promising and viable option for clinical application of MSC infusion to protect liver grafts and prolong survival after transplantation [135]. The regulation of the paracrine effects of MSCs on immune cells was found in the experiment, and the role of the apoptotic process in this process was elucidated. But this immune regulation involves more other mechanisms that still require further experimental research. And the lack of relevant clinical trials of MSCs transplantation demonstrated the survival of MSCs.

In the study of Zhao et al., MSC transplantation can effectively improve liver function and reduce the number and activity of peripheral blood and liver neutrophils in acute liver failure (ALF) rats [136]. Although the immune regulation of MSCs used together with antineutrophil serum was found in the experiment, the lack of inflammatory factors involved in ALF neutrophil mediated immune regulation.

One study showed that hepatic injury could be treated with decellularized liver tissue (DLS) as scaffold-derived composite human umbilical cord-derived mesenchymal stem cells (hUC-MSCs). hUC-MSCs in 2D culture express higher levels of human leukocyte antigen-DR and IFN-γ compared with 3D culture and reduce the prostaglandins that inhibit lymphocyte proliferation and PGE2 secretion. The 3D-DLS system has been shown to exhibit higher immunosuppressive capacity than the *in vitro* 2D culture [137]. MSCs exhibit low immunogenicity but are enhanced after differentiation into the liver. The mechanism is still unknown. The protection of ECM scaffolds on the low immunogenicity of MSCs was pointed out, but the mechanism was not further tested.

In tissue engineering treatment of liver injury, the current method is transplant MSC-based. In order to ensure the stable existence of MSC, MSC-combined scaffold construction is one of the future development directions of liver injury tissue engineering.

3.4. Immune Regulation of MSCs and the Effect of MSC Immunomodulation on Myocardial Regeneration in a 3D Structure. MSCs continue to be investigated for their potential application in the restoration of myocardial function following injury. However, conventional single-layer cell cultures on the surface of 2D scaffolds do not mimic the cell-generated microenvironment well. Thus, cell cultures that have developed various 3D scaffolds further mimic the cell-producing microenvironment in which cells naturally exist and have been used to provide a platform for cell growth and transportation (Table 2). As a substrate, 3D collagen is

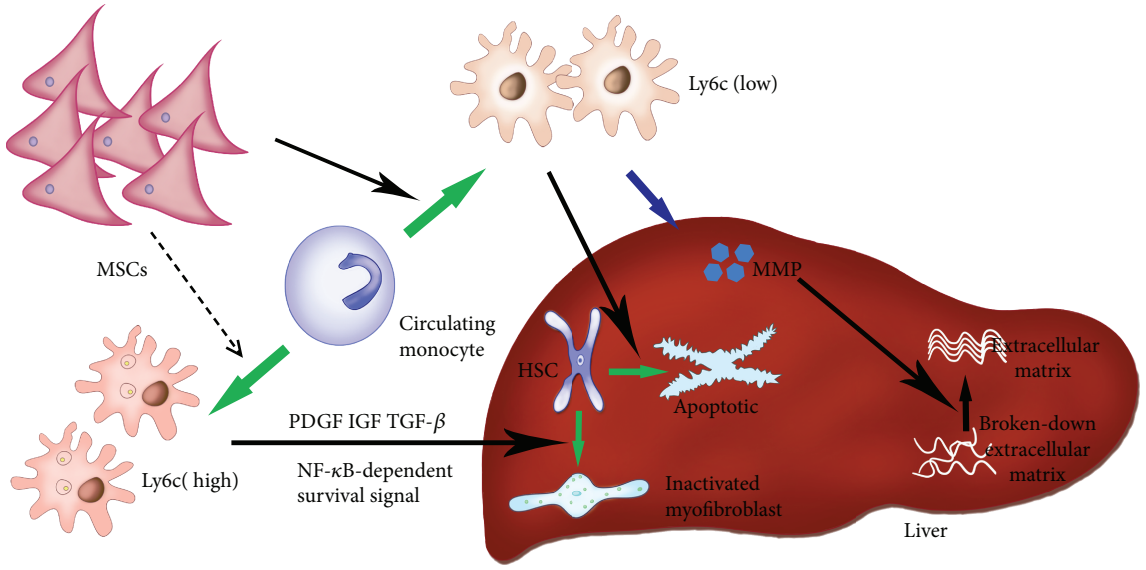

Figure 3: MSCs regulate the differentiation of monocytes and differentiated low-expression Ly6c macrophages in liver fibrosis through the apoptosis of HSC and the secretion of MMP against the inflammatory fibrosis of the liver. Blue arrow: cells secrete cytokines. Green arrow: differentiation and alteration of monocytes and HSC. Dotted arrow: MSCs inhibit differentiation to high expression of Ly6c macrophage. Black arrow: positive promotion of cells and cytokines.

an attractive bioengineering method for myocardial repair because collagen is a natural polymer and the primary component of the ECM of heart muscle [138, 139]. The 3D culture environment of cells also changes the biological characteristics of MSCs, including lineage differentiation [140–146], and further enhances its therapeutic efficacy [143, 147, 148]. However, the mechanism underlying this functional improvement is unknown to a large extent (Table 2).

In the study by Papalamprou et al., de-antigen scaffolds and murine MSCs were used as controls to assess MSCs to provide any additional benefit in terms of specific immune responses. Surprisingly, although mMSCs in the scaffold construct group exert immunomodulatory benefits compared to the scaffold group alone, the mMSCs vaccinated in the de-antigenic scaffolds are still immunostimulatory and can cause chronic inflammation [149]. It was found that the use of materials should retain the stem cell characteristics of MSCs as much as possible to maintain the immunomodulatory properties of MSCs to the greatest extent, but the interaction mechanism between ECM scaffolds and MSCs should be studied experimentally.

Shin et al.'s study identified a novel mechanism by which mesenchymal stromal cells (MSCs) and hydrogel scaffold constructs can reduce the recruitment of innate immune cells by locally producing adenosine. Mesenchymal stromal cells regulate excessive inflammation: implanted MSCs are found to increase the bioavailability of adenosine by the action of CD73 (ecto-50-nucleotidase). This is essential for reducing early innate immune cell infiltration and ROS formation, and mesenchymal stromal cells regulate excessive inflammation [150]. In the experiment, because of the small sample size, although the authors made a comparison between the MSCs and the carrier scaffold, but did not detect the difference between the hydrogel scaffold group and the blank group, further experimental proof is needed. And because of the importance of CD73, the necessity of further research on the implantation of MSCs is proposed.

The potential for cardiac repair has been shown to be limited in standard 2D cultures, and fiber characteristics develop as culture time increases. Three-dimensional collagen scaffolds can enhance the production of trophic factors, modify their immunomodulatory and fibrogenic phenotypes, and promote the cardioprotective effects of MSCs. MSCs have been shown to maintain an antiapoptotic effect and enhance the expression of cardiac trophic factors in 3D collagen scaffolds. Understanding the mechanism of MSC-mediated tissue repair will help to further improve the therapeutic efficacy of MSCs [151]. The effect of the scaffold on MSC is attributed to the biophysical properties of 3D, and the hardness of the ECM scaffold is a key influencing factor. However, biochemical effects were not excluded in this experiment and may both work at the same time; further experimental proof is needed.

MSC-seeded plasma-coated PCL grafts were beneficial for cardiac function in a rodent model of myocardial infarction. By examining the recruitment of macrophages, significantly fewer $CD68^+$ macrophages were found in the MSC composite scaffold group than in the control group, indicating significant anti-inflammatory effects [152]. The experimental results show that the chemical and structural characteristics of the scaffold can regulate the occurrence of immune response, and the early inflammation response of the scaffold during the delivery of MSC is regulated by MSC, which may play an important role in the late stage of inflammation. Further experiment is needed to investigate the balance of inflammation between myocardial repair and fibrosis.

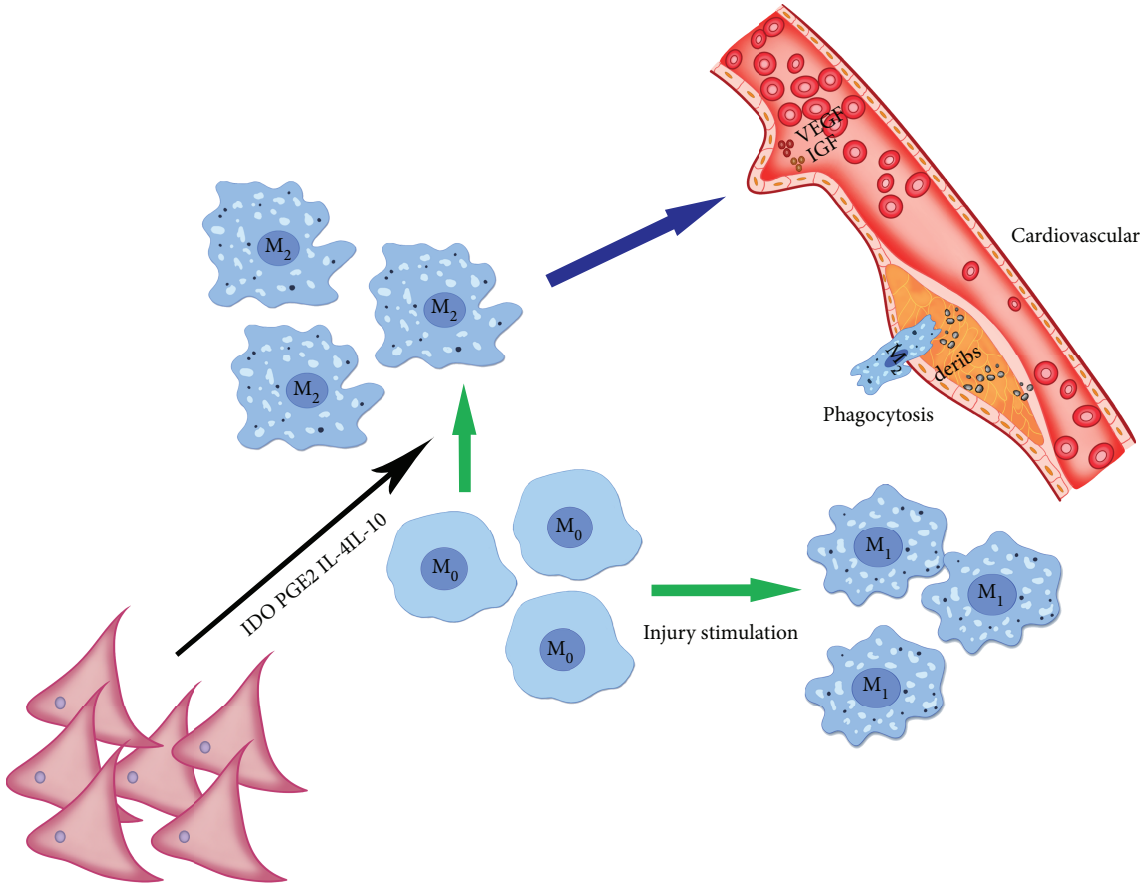

Figure 4: MSCs promote the differentiation of M0 to M2, which secretes VEGF, and IGF promotes recanalization of blood vessels. Green arrow: M0 differentiates into M1 and M2. Blue arrow: M2 secretes cytokines that promote recanalization of blood vessels. Black arrows: MSCs promote the differentiation of M0 to M2.

4. Perspectives and Conclusions

The rapid development of regenerative medicine has made it possible to repair damaged tissues with the help of stem cells. With increased research on stem cell repair, it is clear that the immune system plays a key role in stem cell repair-mediated tissue regeneration. According to regulation of the immune system by stem cells, paracrine production by the stimulation of immune cells in damaged tissue may be another promising therapeutic strategy. The use of stem cells and immune cells to regulate inflammation in areas of tissue damage can be used to reduce disease progression in cases with chronic tissue injury. In a series of tissue repairs, it is clear that the immune system plays an important role in tissue regeneration and repair. However, at the same time, the effects of stem cell differentiation on immunoregulatory activity still require further experimental investigation.

The role of stem cells in regulating the immune microenvironment is affected by the addition of TE technology. It is mentioned that MSCs under the influence of 3D scaffolds increase the secretion of anti-inflammatory cytokines and reduce the infiltration of inflammatory cells. The choice of 3D scaffolds in different tissues (cartilage, bone, liver, and myocardium) is particularly important in the scaffold structure as well as material properties and the preconstruction inflammatory microenvironment. In this review, 3D scaffolds of different organs are exemplified in the immune regulation of MSC. MSCs in the treatment of cartilage damage, tissue engineering scaffolds of 3D structure of different materials (hydrogel, cell-based ECM) affect MSC immune regulation and promote cartilage tissue repair. In the treatment of myocardial injury, 3D scaffold (collagen, polymer material) composite MSC for the treatment of anti-inflammatory fibrosis in myocardial injury. In the treatment of liver injury, 3D decellularization scaffold liver scaffold composite stem cells affect the secretion of inflammatory factors. In the treatment of bone injury, ECM and polymer material combined with MSCs to regulate the immune microenvironment promotes bone tissue regeneration.

Multidisciplinary research will be imperative to this end, and TE technology provides a vehicle for the transport of cells and paracrine factors. In some situations, TE can meet the mechanical requirements. Combined with the organizational engineering technology developed by medical personnel, TE now provides new ideas for organizational repair. However, the best means of constructing a reasonable immune microenvironment remains an important issue faced by TE technology. Combined with stem cell treatment of tissue defects, 3D scaffolds can provide a reasonable carrier for stem cells and enhance the immunosuppressive effect of

MSCs. However, at the same time, inhomogeneous oxygen and nutrient distribution in the 3D spatial structure also impact on stem cells. The stem cell microenvironment will be an important factor in stem cell TE.

To achieve greater clinical efficacy in the future, we should focus on the construction of the immune microenvironment of damaged tissues and the use of TE in the construction of a suitable microenvironment. In terms of regenerative therapy, multidisciplinary cooperation and a greater understanding of the microenvironment will be important for future developments.

Conflicts of Interest

The authors declare that they have no conflicts of interest.

Acknowledgments

The authors would like to thank the funding provided by National Key R&D (2018YFC1105901) and the financial support provided by Nation Nature (81772319). The authors would also like to thank Mei Yuan and Shunyun Liu for their support and help at work.

References

[1] A. Augello, R. Tasso, S. M. Negrini et al., "Bone marrow mesenchymal progenitor cells inhibit lymphocyte proliferation by activation of the programmed death 1 pathway," *European Journal of Immunology*, vol. 35, no. 5, pp. 1482–1490, 2005.

[2] Y. Z. Gu, Q. Xue, Y. J. Chen et al., "Different roles of PD-L1 and FasL in immunomodulation mediated by human placenta-derived mesenchymal stem cells," *Human Immunology*, vol. 74, no. 3, pp. 267–276, 2013.

[3] M. E. Quaedackers, C. C. Baan, W. Weimar, and M. J. Hoogduijn, "Cell contact interaction between adipose-derived stromal cells and allo-activated T lymphocytes," *European Journal of Immunology*, vol. 39, no. 12, pp. 3436–3446, 2009.

[4] M. Di Nicola, C. Carlo-Stella, M. Magni et al., "Human bone marrow stromal cells suppress T-lymphocyte proliferation induced by cellular or nonspecific mitogenic stimuli," *Blood*, vol. 99, no. 10, pp. 3838–3843, 2002.

[5] S. Aggarwal and M. F. Pittenger, "Human mesenchymal stem cells modulate allogeneic immune cell responses," *Blood*, vol. 105, no. 4, pp. 1815–1822, 2005.

[6] A. U. Engela, M. J. Hoogduijn, K. Boer et al., "Human adipose-tissue derived mesenchymal stem cells induce functional de-novo regulatory T cells with methylated *FOXP3* gene DNA," *Clinical & Experimental Immunology*, vol. 173, no. 2, pp. 343–354, 2013.

[7] J. Maggini, G. Mirkin, I. Bognanni et al., "Mouse bone marrow-derived mesenchymal stromal cells turn activated macrophages into a regulatory-like profile," *PLoS One*, vol. 5, no. 2, article e9252, 2010.

[8] D. P. Dyer, J. M. Thomson, A. Hermant et al., "TSG-6 inhibits neutrophil migration via direct interaction with the chemokine CXCL8," *The Journal of Immunology*, vol. 192, no. 5, pp. 2177–2185, 2014.

[9] J. Lesley, N. M. English, I. Gál, K. Mikecz, A. J. Day, and R. Hyman, "Hyaluronan binding properties of a CD44 chimera containing the link module of TSG-6," *The Journal of Biological Chemistry*, vol. 277, no. 29, pp. 26600–26608, 2002.

[10] R. H. Lee, A. A. Pulin, M. J. Seo et al., "Intravenous hMSCs improve myocardial infarction in mice because cells embolized in lung are activated to secrete the anti-inflammatory protein TSG-6," *Cell Stem Cell*, vol. 5, no. 1, pp. 54–63, 2009.

[11] J. Y. Oh, G. W. Roddy, H. Choi et al., "Anti-inflammatory protein TSG-6 reduces inflammatory damage to the cornea following chemical and mechanical injury," *Proceedings of the National Academy of Sciences of the United States of America*, vol. 107, no. 39, pp. 16875–16880, 2010.

[12] H. Choi, R. H. Lee, N. Bazhanov, J. Y. Oh, and D. J. Prockop, "Anti-inflammatory protein TSG-6 secreted by activated MSCs attenuates zymosan-induced mouse peritonitis by decreasing TLR2/NF-κB signaling in resident macrophages," *Blood*, vol. 118, no. 2, pp. 330–338, 2011.

[13] S. Danchuk, J. H. Ylostalo, F. Hossain et al., "Human multipotent stromal cells attenuate lipopolysaccharide-induced acute lung injury in mice via secretion of tumor necrosis factor-α-induced protein 6," *Stem Cell Research & Therapy*, vol. 2, no. 3, p. 27, 2011.

[14] E. Klyushnenkova, J. D. Mosca, V. Zernetkina et al., "T cell responses to allogeneic human mesenchymal stem cells: immunogenicity, tolerance, and suppression," *Journal of Biomedical Science*, vol. 12, no. 1, pp. 47–57, 2005.

[15] M. Krampera, S. Glennie, J. Dyson et al., "Bone marrow mesenchymal stem cells inhibit the response of naive and memory antigen-specific T cells to their cognate peptide," *Blood*, vol. 101, no. 9, pp. 3722–9, 2003.

[16] S. Glennie, I. Soeiro, P. J. Dyson, E. W. Lam, and F. Dazzi, "Bone marrow mesenchymal stem cells induce division arrest anergy of activated T cells," *Blood*, vol. 105, no. 7, pp. 2821–7, 2005.

[17] K. Akiyama, C. Chen, D. D. Wang et al., "Mesenchymal-stem-cell-induced immunoregulation involves FAS-ligand-/-FAS-mediated T cell apoptosis," *Cell Stem Cell*, vol. 10, no. 5, pp. 544–555, 2012.

[18] F. Benvenuto, S. Ferrari, E. Gerdoni et al., "Human mesenchymal stem cells promote survival of T cells in a quiescent state," *Stem Cells*, vol. 25, no. 7, pp. 1753–1760, 2007.

[19] M. J. Crop, C. C. Baan, S. S. Korevaar, J. N. M. Ijzermans, W. Weimar, and M. J. Hoogduijn, "Human adipose tissue-derived mesenchymal stem cells induce explosive T-cell proliferation," *Stem Cells and Development*, vol. 19, no. 12, pp. 1843–1853, 2010.

[20] M. Krampera, L. Cosmi, R. Angeli et al., "Role for interferon-γ in the immunomodulatory activity of human bone marrow mesenchymal stem cells," *Stem Cells*, vol. 24, no. 2, pp. 386–398, 2006.

[21] M. J. Crop, C. C. Baan, S. S. Korevaar et al., "Inflammatory conditions affect gene expression and function of human adipose tissue-derived mesenchymal stem cells," *Clinical & Experimental Immunology*, vol. 162, no. 3, pp. 474–486, 2010.

[22] D. J. Prockop, "Concise review: two negative feedback loops place mesenchymal stem/stromal cells at the center of early regulators of inflammation," *Stem Cells*, vol. 31, no. 10, pp. 2042–2046, 2013.

[23] R. Anzalone, M. Lo Iacono, T. Loria et al., "Wharton's jelly mesenchymal stem cells as candidates for beta cells

regeneration: extending the differentiative and immunomodulatory benefits of adult mesenchymal stem cells for the treatment of type 1 diabetes," *Stem Cell Reviews*, vol. 7, no. 2, pp. 342–363, 2011.

[24] R. Meisel, A. Zibert, M. Laryea, U. Göbel, W. Däubener, and D. Dilloo, "Human bone marrow stromal cells inhibit allogeneic T-cell responses by indoleamine 2,3-dioxygenase-mediated tryptophan degradation," *Blood*, vol. 103, no. 12, pp. 4619–4621, 2004.

[25] S. H. Yang, M. J. Park, I. H. Yoon et al., "Soluble mediators from mesenchymal stem cells suppress T cell proliferation by inducing IL-10," *Experimental & Molecular Medicine*, vol. 41, no. 5, pp. 315–324, 2009.

[26] K. Sato, K. Ozaki, I. Oh et al., "Nitric oxide plays a critical role in suppression of T-cell proliferation by mesenchymal stem cells," *Blood*, vol. 109, no. 1, pp. 228–234, 2007.

[27] F. Saldanha-Araujo, F. I. S. Ferreira, P. V. Palma et al., "Mesenchymal stromal cells up-regulate CD39 and increase adenosine production to suppress activated T-lymphocytes," *Stem Cell Research*, vol. 7, no. 1, pp. 66–74, 2011.

[28] C. Sattler, M. Steinsdoerfer, M. Offers et al., "Inhibition of T-cell proliferation by murine multipotent mesenchymal stromal cells is mediated by CD39 expression and adenosine generation," *Cell Transplantation*, vol. 20, no. 8, pp. 1221–1230, 2011.

[29] E. J. Lee, S. J. Park, S. K. Kang et al., "Spherical bullet formation via E-cadherin promotes therapeutic potency of mesenchymal stem cells derived from human umbilical cord blood for myocardial infarction," *Molecular Therapy*, vol. 20, no. 7, pp. 1424–1433, 2012.

[30] J. A. Zimmermann, M. H. Hettiaratchi, and T. C. McDevitt, "Enhanced immunosuppression of T cells by sustained presentation of bioactive interferon-γ within three-dimensional mesenchymal stem cell constructs," *Stem Cells Translational Medicine*, vol. 6, no. 1, pp. 223–237, 2017.

[31] K. Takeshita, S. Motoike, M. Kajiya et al., "Xenotransplantation of interferon-gamma-pretreated clumps of a human mesenchymal stem cell/extracellular matrix complex induces mouse calvarial bone regeneration," *Stem Cell Research & Therapy*, vol. 8, no. 1, p. 101, 2017.

[32] G. Ren, L. Zhang, X. Zhao et al., "Mesenchymal stem cell-mediated immunosuppression occurs via concerted action of chemokines and nitric oxide," *Cell Stem Cell*, vol. 2, no. 2, pp. 141–150, 2008.

[33] G. Ren, X. Zhao, L. Zhang et al., "Inflammatory cytokine-induced intercellular adhesion molecule-1 and vascular cell adhesion molecule-1 in mesenchymal stem cells are critical for immunosuppression," *The Journal of Immunology*, vol. 184, no. 5, pp. 2321–2328, 2010.

[34] R. Chinnadurai, I. B. Copland, S. R. Patel, and J. Galipeau, "IDO-independent suppression of T cell effector function by IFN-γ–licensed human mesenchymal stromal cells," *The Journal of Immunology*, vol. 192, no. 4, pp. 1491–1501, 2014.

[35] Y. H. Zheng, Y. Y. Deng, W. Lai et al., "Effect of bone marrow mesenchymal stem cells on the polarization of macrophages," *Molecular Medicine Reports*, vol. 17, no. 3, pp. 4449–4459, 2018.

[36] J. Kim and P. Hematti, "Mesenchymal stem cell-educated macrophages: a novel type of alternatively activated macrophages," *Experimental Hematology*, vol. 37, no. 12, pp. 1445–1453, 2009.

[37] K. Németh, A. Leelahavanichkul, P. S. T. Yuen et al., "Bone marrow stromal cells attenuate sepsis via prostaglandin E_2–dependent reprogramming of host macrophages to increase their interleukin-10 production," *Nature Medicine*, vol. 15, no. 1, pp. 42–49, 2009.

[38] M. François, R. Romieu-Mourez, M. Li, and J. Galipeau, "Human MSC suppression correlates with cytokine induction of indoleamine 2,3-dioxygenase and bystander M2 macrophage differentiation," *Molecular Therapy*, vol. 20, no. 1, pp. 187–195, 2012.

[39] C. Prevosto, M. Zancolli, P. Canevali, M. R. Zocchi, and A. Poggi, "Generation of $CD4^+$ or $CD8^+$ regulatory T cells upon mesenchymal stem cell-lymphocyte interaction," *Haematologica*, vol. 92, no. 7, pp. 881–888, 2007.

[40] K. English, J. M. Ryan, L. Tobin, M. J. Murphy, F. P. Barry, and B. P. Mahon, "Cell contact, prostaglandin E_2 and transforming growth factor beta 1 play non-redundant roles in human mesenchymal stem cell induction of $CD4^+$ $CD25^{High}$forkhead box $P3^+$ regulatory T cells," *Clinical & Experimental Immunology*, vol. 156, no. 1, pp. 149–160, 2009.

[41] K. English and K. J. Wood, "Mesenchymal stromal cells in transplantation rejection and tolerance," *Cold Spring Harbor Perspectives in Medicine*, vol. 3, no. 5, article a015560, 2013.

[42] S. M. Melief, E. Schrama, M. H. Brugman et al., "Multipotent stromal cells induce human regulatory T cells through a novel pathway involving skewing of monocytes toward anti-inflammatory macrophages," *Stem Cells*, vol. 31, no. 9, pp. 1980–1991, 2013.

[43] F. Baratelli, Y. Lin, L. Zhu et al., "Prostaglandin E_2 induces *FOXP3* gene expression and T regulatory cell function in human $CD4^+$ T cells," *The Journal of Immunology*, vol. 175, no. 3, pp. 1483–1490, 2005.

[44] Z. Yan, Y. Zhuansun, R. Chen, J. Li, and P. Ran, "Immunomodulation of mesenchymal stromal cells on regulatory T cells and its possible mechanism," *Experimental Cell Research*, vol. 324, no. 1, pp. 65–74, 2014.

[45] T. R. Kyriakides, M. J. Foster, G. E. Keeney et al., "The CC chemokine ligand, CCL2/MCP1, participates in macrophage fusion and foreign body giant cell formation," *The American Journal of Pathology*, vol. 165, no. 6, pp. 2157–2166, 2004.

[46] M. R. Major, V. W. Wong, E. R. Nelson, M. T. Longaker, and G. C. Gurtner, "The foreign body response: at the interface of surgery and bioengineering," *Plastic and Reconstructive Surgery*, vol. 135, no. 5, pp. 1489–1498, 2015.

[47] K. B. Chien, B. A. Aguado, P. J. Bryce, and R. N. Shah, "In vivo acute and humoral response to three-dimensional porous soy protein scaffolds," *Acta Biomaterialia*, vol. 9, no. 11, pp. 8983–8990, 2013.

[48] S. F. Badylak and T. W. Gilbert, "Immune response to biologic scaffold materials," *Seminars in Immunology*, vol. 20, no. 2, pp. 109–116, 2008.

[49] Y. H. Kim, H. Furuya, and Y. Tabata, "Enhancement of bone regeneration by dual release of a macrophage recruitment agent and platelet-rich plasma from gelatin hydrogels," *Biomaterials*, vol. 35, no. 1, pp. 214–224, 2014.

[50] D. Kosuge, W. S. Khan, B. Haddad, and D. Marsh, "Biomaterials and scaffolds in bone and musculoskeletal engineering," *Current Stem Cell Research & Therapy*, vol. 8, no. 3, pp. 185–191, 2013.

[51] J. Y. Je and S. K. Kim, "Reactive oxygen species scavenging activity of aminoderivatized chitosan with different degree of deacetylation," *Bioorganic & Medicinal Chemistry*, vol. 14, no. 17, pp. 5989–5994, 2006.

[52] K. Nakamura, S. Yokohama, M. Yoneda et al., "High, but not low, molecular weight hyaluronan prevents T-cell-mediated liver injury by reducing proinflammatory cytokines in mice," *Journal of Gastroenterology*, vol. 39, no. 4, pp. 346–354, 2004.

[53] S. Hirabara, T. Kojima, N. Takahashi, M. Hanabayashi, and N. Ishiguro, "Hyaluronan inhibits TLR-4 dependent cathepsin K and matrix metalloproteinase 1 expression in human fibroblasts," *Biochemical and Biophysical Research Communications*, vol. 430, no. 2, pp. 519–522, 2013.

[54] M. D. Swartzlander, A. K. Blakney, L. D. Amer, K. D. Hankenson, T. R. Kyriakides, and S. J. Bryant, "Immunomodulation by mesenchymal stem cells combats the foreign body response to cell-laden synthetic hydrogels," *Biomaterials*, vol. 41, pp. 79–88, 2015.

[55] O. Veiseh, J. C. Doloff, M. Ma et al., "Size- and shape-dependent foreign body immune response to materials implanted in rodents and non-human primates," *Nature Materials*, vol. 14, no. 6, pp. 643–651, 2015.

[56] G. Vallés, F. Bensiamar, L. Crespo, M. Arruebo, N. Vilaboa, and L. Saldaña, "Topographical cues regulate the crosstalk between MSCs and macrophages," *Biomaterials*, vol. 37, pp. 124–133, 2015.

[57] S. Kim, Y. S. Han, J. H. Lee, and S. H. Lee, "Combination of MSC spheroids wrapped within autologous composite sheet dually protects against immune rejection and enhances stem cell transplantation efficacy," *Tissue and Cell*, vol. 53, pp. 93–103, 2018.

[58] E. Redondo-Castro, C. J. Cunningham, J. Miller, H. Brown, S. M. Allan, and E. Pinteaux, "Changes in the secretome of tri-dimensional spheroid-cultured human mesenchymal stem cells in vitro by interleukin-1 priming," *Stem Cell Research & Therapy*, vol. 9, no. 1, p. 11, 2018.

[59] L. Yan, B. Jiang, E. Li et al., "Scalable generation of mesenchymal stem cells from human embryonic stem cells in 3D," *International Journal of Biological Sciences*, vol. 14, no. 10, pp. 1196–1210, 2018.

[60] H. R. Caires, P. Barros da Silva, M. A. Barbosa, and C. R. Almeida, "A co-culture system with three different primary human cell populations reveals that biomaterials and MSC modulate macrophage-driven fibroblast recruitment," *Journal of Tissue Engineering and Regenerative Medicine*, vol. 12, no. 3, pp. e1433–e1440, 2018.

[61] M. Seifert, A. Lubitz, J. Trommer et al., "Crosstalk between immune cells and mesenchymal stromal cells in a 3D bioreactor system," *The International Journal of Artificial Organs*, vol. 35, no. 11, pp. 986–995, 2018.

[62] W. Mueller-Klieser, "Multicellular spheroids. A review on cellular aggregates in cancer research," *Journal of Cancer Research and Clinical Oncology*, vol. 113, no. 2, pp. 101–122, 1987.

[63] W. Mueller-Klieser, "Three-dimensional cell cultures: from molecular mechanisms to clinical applications," *American Journal of Physiology-Cell Physiology*, vol. 273, no. 4, pp. C1109–C1123, 1997.

[64] A. C. Tsai, Y. Liu, X. Yuan, and T. Ma, "Compaction, fusion, and functional activation of three-dimensional human mesenchymal stem cell aggregate," *Tissue Engineering Part A*, vol. 21, no. 9-10, pp. 1705–1719, 2015.

[65] R. F. Loeser, S. R. Goldring, C. R. Scanzello, and M. B. Goldring, "Osteoarthritis: a disease of the joint as an organ," *Arthritis & Rheumatism*, vol. 64, no. 6, pp. 1697–1707, 2012.

[66] W. S. Toh, M. Brittberg, J. Farr et al., "Cellular senescence in aging and osteoarthritis," *Acta Orthopaedica*, vol. 87, Supplement 363, pp. 6–14, 2017.

[67] T. Wu, Y. Liu, B. Wang, and G. Li, "The roles of mesenchymal stem cells in tissue repair and disease modification," *Current Stem Cell Research & Therapy*, vol. 9, no. 5, pp. 424–431, 2014.

[68] A. Uccelli, L. Moretta, and V. Pistoia, "*Mesenchymal stem cells in health and disease*," *Nature Reviews Immunology*, vol. 8, no. 9, pp. 726–736, 2008.

[69] E. Lombardo, T. van der Poll, O. DelaRosa, and W. Dalemans, "Mesenchymal stem cells as a therapeutic tool to treat sepsis," *World Journal of Stem Cells*, vol. 7, no. 2, pp. 368–379, 2015.

[70] J. Ding, B. Chen, T. Lv et al., "Bone marrow mesenchymal stem cell-based engineered cartilage ameliorates polyglycolic acid/polylactic acid scaffold-induced inflammation through M2 polarization of macrophages in a pig model," *Stem Cells Translational Medicine*, vol. 5, no. 8, pp. 1079–1089, 2016.

[71] J. F. Schlaak, I. Pfers, K. H. Meyer Zum Büschenfelde, and E. Märker-Hermann, "Different cytokine profiles in the synovial fluid of patients with osteoarthritis, rheumatoid arthritis and seronegative spondylarthropathies," *Clinical and Experimental Rheumatology*, vol. 14, no. 2, pp. 155–162, 1996.

[72] C. Jacques, M. Gosset, F. Berenbaum, and C. Gabay, "The role of IL-1 and IL-1Ra in joint inflammation and cartilage degradation," *Vitamins & Hormones*, vol. 74, pp. 371–403, 2006.

[73] M. Kapoor, J. Martel-Pelletier, D. Lajeunesse, J. P. Pelletier, and H. Fahmi, "Role of proinflammatory cytokines in the pathophysiology of osteoarthritis," *Nature Reviews Rheumatology*, vol. 7, no. 1, pp. 33–42, 2011.

[74] Z. H. Zheng, X. Y. Li, J. Ding, J. F. Jia, and P. Zhu, "Allogeneic mesenchymal stem cell and mesenchymal stem cell-differentiated chondrocyte suppress the responses of type II collagen-reactive T cells in rheumatoid arthritis," *Rheumatology*, vol. 47, no. 1, pp. 22–30, 2008.

[75] S. Zhang, S. J. Chuah, R. C. Lai, J. H. P. Hui, S. K. Lim, and W. S. Toh, "MSC exosomes mediate cartilage repair by enhancing proliferation, attenuating apoptosis and modulating immune reactivity," *Biomaterials*, vol. 156, pp. 16–27, 2018.

[76] E. Canalis, "Effect of growth factors on bone cell replication and differentiation," *Clinical Orthopaedics and Related Research*, vol. 193, pp. 246–263, 1985.

[77] H. M. Frost, "The biology of fracture healing. An overview for clinicians. Part I," *Clinical Orthopaedics and Related Research*, vol. 248, pp. 283–293, 1989.

[78] P. Kolar, K. Schmidt-Bleek, H. Schell et al., "The early fracture hematoma and its potential role in fracture healing," *Tissue Engineering Part B: Reviews*, vol. 16, no. 4, pp. 427–434, 2010.

[79] L. Claes, S. Recknagel, and A. Ignatius, "Fracture healing under healthy and inflammatory conditions," *Nature Reviews Rheumatology*, vol. 8, no. 3, pp. 133–143, 2012.

[80] D. Mougiakakos, R. Jitschin, C. C. Johansson, R. Okita, R. Kiessling, and K. le Blanc, "The impact of inflammatory licensing on heme oxygenase-1-mediated induction of

regulatory T cells by human mesenchymal stem cells," *Blood*, vol. 117, no. 18, pp. 4826–4835, 2011.

[81] S. Reinke, S. Geissler, W. R. Taylor et al., "Terminally differentiated $CD8^+$ T cells negatively affect bone regeneration in humans," *Science Translational Medicine*, vol. 5, no. 177, article 177ra36, 2013.

[82] D. Nam, E. Mau, Y. Wang et al., "T-lymphocytes enable osteoblast maturation via IL-17F during the early phase of fracture repair," *PLoS One*, vol. 7, no. 6, article e40044, 2012.

[83] S. A. Mao, J. M. Glorioso, and S. L. Nyberg, "Liver regeneration," *Translational Research*, vol. 163, no. 4, pp. 352–362, 2014.

[84] T. G. Bird, S. Lorenzini, and S. J. Forbes, "Activation of stem cells in hepatic diseases," *Cell and Tissue Research*, vol. 331, no. 1, pp. 283–300, 2008.

[85] R. A. Boulton, M. R. Alison, M. Golding, C. Selden, and H. J. F. Hodgson, "Augmentation of the early phase of liver regeneration after 70% partial hepatectomy in rats following selective Kupffer cell depletion," *Journal of Hepatology*, vol. 29, no. 2, pp. 271–280, 1998.

[86] C. Meijer, M. J. Wiezer, A. M. Diehl et al., "Kupffer cell depletion by CI_2MDP-liposomes alters hepatic cytokine expression and delays liver regeneration after partial hepatectomy," *Liver*, vol. 20, no. 1, pp. 66–77, 2000.

[87] B. Parekkadan, D. van Poll, K. Suganuma et al., "Mesenchymal stem cell-derived molecules reverse fulminant hepatic failure," *PLoS One*, vol. 2, no. 9, article e941, 2007.

[88] Y. O. Jang, Y. J. Kim, S. K. Baik et al., "Histological improvement following administration of autologous bone marrow-derived mesenchymal stem cells for alcoholic cirrhosis: a pilot study," *Liver International*, vol. 34, no. 1, pp. 33–41, 2014.

[89] F. Heymann, C. Trautwein, and F. Tacke, "Monocytes and macrophages as cellular targets in liver fibrosis," *Inflammation & Allergy Drug Targets*, vol. 8, no. 4, pp. 307–318, 2009.

[90] E. Morán-Salvador, E. Titos, B. Rius et al., "Cell-specific PPARγ deficiency establishes anti-inflammatory and anti-fibrogenic properties for this nuclear receptor in non-parenchymal liver cells," *Journal of Hepatology*, vol. 59, no. 5, pp. 1045–1053, 2013.

[91] K. R. Karlmark, R. Weiskirchen, H. W. Zimmermann et al., "Hepatic recruitment of the inflammatory $Gr1^+$ monocyte subset upon liver injury promotes hepatic fibrosis," *Hepatology*, vol. 50, no. 1, pp. 261–274, 2009.

[92] C. Baeck, X. Wei, M. Bartneck et al., "Pharmacological inhibition of the chemokine C-C motif chemokine ligand 2 (monocyte chemoattractant protein 1) accelerates liver fibrosis regression by suppressing Ly-$6C^+$ macrophage infiltration in mice," *Hepatology*, vol. 59, no. 3, pp. 1060–1072, 2014.

[93] J. P. Pradere, J. Kluwe, S. De Minicis et al., "Hepatic macrophages but not dendritic cells contribute to liver fibrosis by promoting the survival of activated hepatic stellate cells in mice," *Hepatology*, vol. 58, no. 4, pp. 1461–1473, 2013.

[94] J. A. Fallowfield, M. Mizuno, T. J. Kendall et al., "Scar-associated macrophages are a major source of hepatic matrix metalloproteinase-13 and facilitate the resolution of murine hepatic fibrosis," *The Journal of Immunology*, vol. 178, no. 8, pp. 5288–5295, 2007.

[95] P. Ramachandran and J. P. Iredale, "Liver fibrosis: a bidirectional model of fibrogenesis and resolution," *QJM*, vol. 105, no. 9, pp. 813–817, 2012.

[96] J. A. Thomas, C. Pope, D. Wojtacha et al., "Macrophage therapy for murine liver fibrosis recruits host effector cells improving fibrosis, regeneration, and function," *Hepatology*, vol. 53, no. 6, pp. 2003–2015, 2011.

[97] J. S. Duffield, S. J. Forbes, C. M. Constandinou et al., "Selective depletion of macrophages reveals distinct, opposing roles during liver injury and repair," *The Journal of Clinical Investigation*, vol. 115, no. 1, pp. 56–65, 2005.

[98] M. Ide, M. Kuwamura, T. Kotani, O. Sawamoto, and J. Yamate, "Effects of gadolinium chloride ($GdCl_3$) on the appearance of macrophage populations and fibrogenesis in thioacetamide-induced rat hepatic lesions," *Journal of Comparative Pathology*, vol. 133, no. 2-3, pp. 92–102, 2005.

[99] M. Imamura, T. Ogawa, Y. Sasaguri, K. Chayama, and H. Ueno, "Suppression of macrophage infiltration inhibits activation of hepatic stellate cells and liver fibrogenesis in rats," *Gastroenterology*, vol. 128, no. 1, pp. 138–146, 2005.

[100] E. Liaskou, H. W. Zimmermann, K. K. Li et al., "Monocyte subsets in human liver disease show distinct phenotypic and functional characteristics," *Hepatology*, vol. 57, no. 1, pp. 385–398, 2013.

[101] T. Hosoda, J. Kajstura, A. Leri, and P. Anversa, "Mechanisms of myocardial regeneration," *Circulation Journal*, vol. 74, no. 1, pp. 13–17, 2010.

[102] C. Jopling, E. Sleep, M. Raya, M. Martí, A. Raya, and J. C. I. Belmonte, "Zebrafish heart regeneration occurs by cardiomyocyte dedifferentiation and proliferation," *Nature*, vol. 464, no. 7288, pp. 606–609, 2010.

[103] F. K. Swirski and M. Nahrendorf, "Leukocyte behavior in atherosclerosis, myocardial infarction, and heart failure," *Science*, vol. 339, no. 6116, pp. 161–166, 2013.

[104] C. C. Wang, C. H. Chen, W. W. Lin et al., "Direct intramyocardial injection of mesenchymal stem cell sheet fragments improves cardiac functions after infarction," *Cardiovascular Research*, vol. 77, no. 3, pp. 515–524, 2008.

[105] S. T. Lee, A. J. White, S. Matsushita et al., "Intramyocardial injection of autologous cardiospheres or cardiosphere-derived cells preserves function and minimizes adverse ventricular remodeling in pigs with heart failure post-myocardial infarction," *Journal of the American College of Cardiology*, vol. 57, no. 4, pp. 455–465, 2011.

[106] J. M. Lambert, E. F. Lopez, and M. L. Lindsey, "Macrophage roles following myocardial infarction," *International Journal of Cardiology*, vol. 130, no. 2, pp. 147–158, 2008.

[107] A. R. Pinto, R. Paolicelli, E. Salimova et al., "An abundant tissue macrophage population in the adult murine heart with a distinct alternatively-activated macrophage profile," *PLoS One*, vol. 7, no. 5, article e36814, 2012.

[108] S. Epelman, K. J. Lavine, A. E. Beaudin et al., "Embryonic and adult-derived resident cardiac macrophages are maintained through distinct mechanisms at steady state and during inflammation," *Immunity*, vol. 40, no. 1, pp. 91–104, 2014.

[109] V. Dayan, G. Yannarelli, F. Billia et al., "Mesenchymal stromal cells mediate a switch to alternatively activated monocytes/macrophages after acute myocardial infarction," *Basic Research in Cardiology*, vol. 106, no. 6, pp. 1299–1310, 2011.

[110] D. J. Gow, D. P. Sester, and D. A. Hume, "CSF-1, IGF-1, and the control of postnatal growth and development," *Journal of Leukocyte Biology*, vol. 88, no. 3, pp. 475–481, 2010.

[111] M. P. Santini, L. Tsao, L. Monassier et al., "Enhancing repair of the mammalian heart," *Circulation Research*, vol. 100, no. 12, pp. 1732–1740, 2007.

[112] S. Ishikane, H. Hosoda, K. Yamahara et al., "Allogeneic transplantation of fetal membrane-derived mesenchymal stem cell sheets increases neovascularization and improves cardiac function after myocardial infarction in rats," *Transplantation*, vol. 96, no. 8, pp. 697–706, 2013.

[113] T. Ben-Mordechai, R. Holbova, N. Landa-Rouben et al., "Macrophage subpopulations are essential for infarct repair with and without stem cell therapy," *Journal of the American College of Cardiology*, vol. 62, no. 20, pp. 1890–1901, 2013.

[114] N. S. Hwang, S. Varghese, Z. Zhang, and J. Elisseeff, "Chondrogenic differentiation of human embryonic stem cell-derived cells in arginine-glycine-aspartate-modified hydrogels," *Tissue Engineering*, vol. 12, no. 9, pp. 2695–2706, 2006.

[115] J. S. Park, D. G. Woo, B. K. Sun et al., "In vitro and in vivo test of PEG/PCL-based hydrogel scaffold for cell delivery application," *Journal of Controlled Release*, vol. 124, no. 1-2, pp. 51–59, 2007.

[116] L. Bian, D. Y. Zhai, R. L. Mauck, and J. A. Burdick, "Coculture of human mesenchymal stem cells and articular chondrocytes reduces hypertrophy and enhances functional properties of engineered cartilage," *Tissue Engineering Part A*, vol. 17, no. 7-8, pp. 1137–1145, 2011.

[117] D. L. Butler, S. A. Goldstein, and F. Guilak, "Functional tissue engineering: the role of biomechanics," *Journal of Biomechanical Engineering*, vol. 122, no. 6, pp. 570–575, 2000.

[118] F. Guilak, D. L. Butler, and S. A. Goldstein, "Functional tissue engineering: the role of biomechanics in articular cartilage repair," *Clinical Orthopaedics and Related Research*, vol. 391, pp. S295–S305, 2001.

[119] M. Jäger, F. Urselmann, F. Witte et al., "Osteoblast differentiation onto different biometals with an endoprosthetic surface topography in vitro," *Journal of Biomedical Materials Research Part A*, vol. 86A, no. 1, pp. 61–75, 2008.

[120] M. T. Valarmathi, M. J. Yost, R. L. Goodwin, and J. D. Potts, "The influence of proepicardial cells on the osteogenic potential of marrow stromal cells in a three-dimensional tubular scaffold," *Biomaterials*, vol. 29, no. 14, pp. 2203–2216, 2008.

[121] Y. Zhou, H. L. Gao, L. L. Shen et al., "Chitosan microspheres with an extracellular matrix-mimicking nanofibrous structure as cell-carrier building blocks for bottom-up cartilage tissue engineering," *Nanoscale*, vol. 8, no. 1, pp. 309–317, 2016.

[122] B. Corradetti, F. Taraballi, S. Minardi et al., "Chondroitin sulfate immobilized on a biomimetic scaffold modulates inflammation while driving chondrogenesis," *Stem Cells Translational Medicine*, vol. 5, no. 5, pp. 670–682, 2016.

[123] W. J. Du, L. Reppel, L. Leger et al., "Mesenchymal stem cells derived from human bone marrow and adipose tissue maintain their immunosuppressive properties after chondrogenic differentiation: role of HLA-G," *Stem Cells and Development*, vol. 25, no. 19, pp. 1454–1469, 2016.

[124] K. A. Glass, J. M. Link, J. M. Brunger, F. T. Moutos, C. A. Gersbach, and F. Guilak, "Tissue-engineered cartilage with inducible and tunable immunomodulatory properties," *Biomaterials*, vol. 35, no. 22, pp. 5921–5931, 2014.

[125] T. Yuan, K. Li, L. Guo, H. Fan, and X. Zhang, "Modulation of immunological properties of allogeneic mesenchymal stem cells by collagen scaffolds in cartilage tissue engineering," *Journal of Biomedical Materials Research Part A*, vol. 98, no. 3, pp. 332–341, 2011.

[126] J. Yang, X. Chen, T. Yuan, X. Yang, Y. Fan, and X. Zhang, "Regulation of the secretion of immunoregulatory factors of mesenchymal stem cells (MSCs) by collagen-based scaffolds during chondrogenesis," *Materials Science and Engineering: C*, vol. 70, Part 2, pp. 983–991, 2017.

[127] S. Liu, M. Yuan, K. Hou et al., "Immune characterization of mesenchymal stem cells in human umbilical cord Wharton's jelly and derived cartilage cells," *Cellular Immunology*, vol. 278, no. 1-2, pp. 35–44, 2012.

[128] G. El-Adl, M. F. Mostafa, A. Enan, and M. Ashraf, "Biphasic ceramic bone substitute mixed with autogenous bone marrow in the treatment of cavitary benign bone lesions," *Acta Orthopaedica Belgica*, vol. 75, no. 1, pp. 110–118, 2009.

[129] X. T. He, R. X. Wu, X. Y. Xu, J. Wang, Y. Yin, and F. M. Chen, "Macrophage involvement affects matrix stiffness-related influences on cell osteogenesis under three-dimensional culture conditions," *Acta Biomaterialia*, vol. 71, pp. 132–147, 2018.

[130] Y. Niu, Q. Li, R. Xie et al., "Modulating the phenotype of host macrophages to enhance osteogenesis in MSC-laden hydrogels: design of a glucomannan coating material," *Biomaterials*, vol. 139, pp. 39–55, 2017.

[131] T. L. Arinzeh, S. J. Peter, M. P. Archambault et al., "Allogeneic mesenchymal stem cells regenerate bone in a critical-sized canine segmental defect," *The Journal of Bone and Joint Surgery-American Volume*, vol. 85, no. 10, pp. 1927–1935, 2003.

[132] K. A. Faraj, T. H. van Kuppevelt, and W. F. Daamen, "Construction of collagen scaffolds that mimic the three-dimensional architecture of specific tissues," *Tissue Engineering*, vol. 13, no. 10, pp. 2387–2394, 2007.

[133] Y. S. Li, H. J. Harn, D. K. Hsieh et al., "Cells and materials for liver tissue engineering," *Cell Transplantation*, vol. 22, no. 4, pp. 685–700, 2013.

[134] Y. Wang, C. B. Cui, M. Yamauchi et al., "Lineage restriction of human hepatic stem cells to mature fates is made efficient by tissue-specific biomatrix scaffolds," *Hepatology*, vol. 53, no. 1, pp. 293–305, 2011.

[135] Y. Tian, J. Wang, W. Wang et al., "Mesenchymal stem cells improve mouse non-heart-beating liver graft survival by inhibiting Kupffer cell apoptosis via TLR4-ERK1/2-Fas/-FasL-caspase3 pathway regulation," *Stem Cell Research & Therapy*, vol. 7, no. 1, p. 157, 2016.

[136] X. Zhao, X. Shi, Z. Zhang, H. Ma, X. Yuan, and Y. Ding, "Combined treatment with MSC transplantation and neutrophil depletion ameliorates D-GalN/LPS-induced acute liver failure in rats," *Clinics and Research in Hepatology and Gastroenterology*, vol. 40, no. 6, pp. 730–738, 2016.

[137] Y. Li, Q. Wu, Y. Wang et al., "Immunogenicity of hepatic differentiated human umbilical cord mesenchymal stem cells promoted by porcine decellularized liver scaffolds," *Xenotransplantation*, vol. 24, no. 1, article e12287, 2017.

[138] P. Maureira, P. Y. Marie, F. Yu et al., "Repairing chronic myocardial infarction with autologous mesenchymal stem cells engineered tissue in rat promotes angiogenesis and limits ventricular remodeling," *Journal of Biomedical Science*, vol. 19, no. 1, p. 93, 2012.

[139] A. Shafy, T. Fink, V. Zachar, N. Lila, A. Carpentier, and J. C. Chachques, "Development of cardiac support bioprostheses for ventricular restoration and myocardial regeneration," *European Journal of Cardio-Thoracic Surgery*, vol. 43, no. 6, pp. 1211–1219, 2013.

[140] S. Duggal, K. B. Frønsdal, K. Szöke, A. Shahdadfar, J. E. Melvik, and J. E. Brinchmann, "Phenotype and gene expression of human mesenchymal stem cells in alginate scaffolds," *Tissue Engineering Part A*, vol. 15, no. 7, pp. 1763–1773, 2009.

[141] D. H. Kim, S. H. Kim, S. J. Heo et al., "Enhanced differentiation of mesenchymal stem cells into NP-like cells via 3D co-culturing with mechanical stimulation," *Journal of Bioscience and Bioengineering*, vol. 108, no. 1, pp. 63–67, 2009.

[142] W. Wang, K. Itaka, S. Ohba et al., "3D spheroid culture system on micropatterned substrates for improved differentiation efficiency of multipotent mesenchymal stem cells," *Biomaterials*, vol. 30, no. 14, pp. 2705–2715, 2009.

[143] T. J. Bartosh, J. H. Ylostalo, A. Mohammadipoor et al., "Aggregation of human mesenchymal stromal cells (MSCs) into 3D spheroids enhances their antiinflammatory properties," *Proceedings of the National Academy of Sciences of the United States of America*, vol. 107, no. 31, pp. 13724–13729, 2010.

[144] L. T. Nguyen, S. Liao, C. K. Chan, and S. Ramakrishna, "Enhanced osteogenic differentiation with 3D electrospun nanofibrous scaffolds," *Nanomedicine*, vol. 7, no. 10, pp. 1561–1575, 2012.

[145] J. H. Ylöstalo, T. J. Bartosh, K. Coble, and D. J. Prockop, "Human mesenchymal stem/stromal cells cultured as spheroids are self-activated to produce prostaglandin E2 that directs stimulated macrophages into an anti-inflammatory phenotype," *Stem Cells*, vol. 30, no. 10, pp. 2283–2296, 2012.

[146] B. Follin, M. Juhl, S. Cohen, A. E. Pedersen, J. Kastrup, and A. Ekblond, "Increased paracrine immunomodulatory potential of mesenchymal stromal cells in three-dimensional culture," *Tissue Engineering Part B: Reviews*, vol. 22, no. 4, pp. 322–329, 2016.

[147] J. E. Frith, B. Thomson, and P. G. Genever, "Dynamic three-dimensional culture methods enhance mesenchymal stem cell properties and increase therapeutic potential," *Tissue Engineering Part C: Methods*, vol. 16, no. 4, pp. 735–749, 2010.

[148] L. Guo, J. Ge, Y. Zhou, S. Wang, R. C. H. Zhao, and Y. Wu, "Three-dimensional spheroid-cultured mesenchymal stem cells devoid of embolism attenuate brain stroke injury after intra-arterial injection," *Stem Cells and Development*, vol. 23, no. 9, pp. 978–989, 2014.

[149] A. Papalamprou, C. W. Chang, N. Vapniarsky, A. Clark, N. Walker, and L. G. Griffiths, "Xenogeneic cardiac extracellular matrix scaffolds with or without seeded mesenchymal stem cells exhibit distinct in vivo immunosuppressive and regenerative properties," *Acta Biomaterialia*, vol. 45, pp. 155–168, 2016.

[150] E. Y. Shin, L. Wang, M. Zemskova et al., "Adenosine production by biomaterial-supported mesenchymal stromal cells reduces the innate inflammatory response in myocardial ischemia/reperfusion injury," *Journal of the American Heart Association*, vol. 7, no. 2, article e006949, 2018.

[151] I. Rashedi, N. Talele, X. H. Wang, B. Hinz, M. Radisic, and A. Keating, "Collagen scaffold enhances the regenerative properties of mesenchymal stromal cells," *PLoS One*, vol. 12, no. 10, article e0187348, 2017.

[152] A. G. Guex, A. Frobert, J. Valentin et al., "Plasma-functionalized electrospun matrix for biograft development and cardiac function stabilization," *Acta Biomaterialia*, vol. 10, no. 7, pp. 2996–3006, 2014.

Hindawi
Stem Cells International
Volume 2018, Article ID 7173481, 10 pages
https://doi.org/10.1155/2018/7173481

Research Article

Novel Calcium Phosphate Cement with Metformin-Loaded Chitosan for Odontogenic Differentiation of Human Dental Pulp Cells

Wei Qin,[1,2] **Jia-Yao Chen**,[1] **Jia Guo**,[1] **Tao Ma**,[3] **Michael D. Weir**,[2] **Dong Guo**,[4] **Yan Shu**,[4] **Zheng-Mei Lin**,[1] **Abraham Schneider**,[3] **and Hockin H. K. Xu**[2,5,6]

[1]*Department of Operative Dentistry and Endodontics, Guanghua School of Stomatology, Sun Yat-sen University, Guangdong Provincial Key Laboratory of Stomatology, Guangzhou, China*
[2]*Department of Advanced Oral Sciences and Therapeutics, University of Maryland School of Dentistry, Baltimore, USA*
[3]*Department of Oncology and Diagnostic Sciences, University of Maryland School of Dentistry, Baltimore, USA*
[4]*Department of Pharmaceutical Sciences, School of Pharmacy, University of Maryland, Baltimore, USA*
[5]*Center for Stem Cell Biology & Regenerative Medicine, University of Maryland School of Medicine, Baltimore, USA*
[6]*Department of Mechanical Engineering, University of Maryland Baltimore County, Baltimore County, USA*

Correspondence should be addressed to Zheng-Mei Lin; linzhm@mail.sysu.edu.cn, Abraham Schneider; schneider66@umaryland.edu, and Hockin H. K. Xu; hxu@umaryland.edu

Received 20 May 2018; Accepted 13 September 2018; Published 27 November 2018

Guest Editor: Howard Kim

Metformin is an old and widely accepted first-line drug for treating type 2 diabetes. Our previous studies demonstrate that metformin can stimulate the osteo/odontogenic differentiation of human-induced pluripotent stem cell-derived mesenchymal stem cells and human dental pulp cells (DPCs). Due to the rapid dilution of metformin from the defect area, the aim of this study was to develop a drug delivery system with controlled release of metformin to promote cell viability and odontogenic differentiation of DPCs favoring dentin regeneration. Calcium phosphate cement (CPC) containing chitosan and metformin as a scaffold was synthesized. DPCs were seeded onto the scaffold, and the viability and proliferation were evaluated at several time points. For osteogenic differentiation analysis, alkaline phosphatase (ALP) activity was tested, cells were stained with Alizarin Red, and the expression of odontogenic markers was evaluated by real-time polymerase chain reaction. DPCs remained viable and attached well to the CPC-chitosan composite scaffold. Moreover, the addition of metformin to the CPC-chitosan composite did not adversely affect cell proliferation, compared to that of CPC control. Our data further revealed that the novel CPC-chitosan-metformin composite enhanced the odontogenic differentiation of DPCs, as evidenced by higher ALP activity, elevated expression of odontoblastic markers, and strong mineral deposition. These results suggest that the new CPC-chitosan-metformin composite is a highly promising scaffold with the potential for tissue engineering applications including dentin regeneration.

1. Introduction

Dental pulp is often damaged by cariogenic infection, mechanical trauma, and clinical operative procedures. A conventional endodontic treatment for infected pulp tissues is root canal therapy, which involves the extirpation of the inflammatory pulp, but will decrease the fracture toughness and infection-resistance of the residual tooth because of malnutrition [1]. Dental pulp regeneration is one of the most promising therapeutic strategies, which would promote the repair of the pulp-dentin complex and improve the patient's life quality [2]. Notably, as biotechnology has progressed, there have been several attempts to establish new methods to better control the parameters of regenerative

endodontic treatment procedures using tissue engineering strategies [3].

Tissue engineering is fundamentally based on the interaction among progenitor cells, biochemical molecules, and three-dimensional scaffold materials [4]. Human dental pulp cells (DPCs) as progenitor cells are an excellent cell source for dentin regeneration. DPCs are easy to harvest from donors including children losing their primary teeth and teenagers having their wisdom teeth removed, which are otherwise discarded as medical waste [5, 6]. In addition, DPCs are capable of odontogenic differentiation to form the dentin-pulp complex in dental pulp tissues [7, 8]. Biochemical factors are critical signalling molecules that instruct the DPCs to achieve pulp regeneration. Our previous studies demonstrated that the small molecule compound metformin has osteo/odontogenic effects by promoting the differentiation of human-induced pluripotent stem cell- (hiPSC-) derived mesenchymal stem cells (MSCs) and DPCs [9, 10]. Although metformin is important for the differentiation of DPCs with its ability to enhance odontogenic differentiation, the application of metformin was limited in dentin regeneration because of its rapid dilution from the defect area leading to inefficient tissue formation [11]. Therefore, it is important to achieve sustained local release of metformin to the dental pulp exposure site.

Several studies have incorporated growth factors into calcium phosphate cement (CPC) [12–14]. However, the strength of the protein-releasing CPC was significantly lower than that without proteins [15]. Our previous studies have shown that a reinforced CPC composite containing chitosan is an effective carrier and delivery vehicle for proteins [13] because chitosan can provide good mechanical strength and toughness to the scaffold [16]. However, to date, there has been no report of developing a CPC-chitosan-metformin composite. Therefore, the aim of this study was to develop a novel CPC-chitosan-metformin composite and investigate its effect on cell viability, proliferation, the expression of odontogenic genes, and mineral matrix deposition. The results of our study will provide a foundation for the future use of CPC-chitosan-metformin composite for cell-based dentin and other tissue regeneration therapies.

2. Materials and Methods

2.1. Fabrication of CPC-Chitosan-Metformin Scaffold. CPC powder consisted of tetracalcium phosphate [TTCP: $Ca_4(PO_4)_2O$] and dicalcium phosphate anhydrous (DCPA: $CaHPO_4$). Briefly, TTCP powder was formed via the solid-state reaction of DCPA and $CaCO_3$ (both from J. T. Baker, Phillipsburg, NJ), which were mixed and heated in a furnace (Lindberg, Watertown, WI) at 1500°C for 6 hours. The heated mixture was quenched to room temperature in a desiccator and then ground in a ball mill (Retsch PM4, Brinkman, NY) to obtain particles with a 5 μm median particle size. DCPA was ground in ball mill with 95% ethanol to obtain a powder with a median particle size of 1 μm. TTCP and DCPA were mixed at 1 : 3 molar ratio to form the CPC powder. The CPC liquid contained water and chitosan. Chitosan is a natural polymer and is often used as scaffold in bone tissue engineering because of its biocompatibility, low toxicity, and degradability by enzymes [17]. First, 10, 30, and 50 μg of metformin were, respectively, dissolved in water. Second, chitosan lactate was mixed with water containing various doses of metformin and dissolved in water at chitosan/(chitosan + metformin + water) mass fraction of 15% to form the CPC liquid. The 15% mass fraction was used because it yielded a good strength for CPC in a previous study [13]. Third, CPC paste was formed by mixing the sterile CPC powder with the CPC liquid at a CPC powder to liquid ratio of 3 to 1 by mass. The paste was placed in a mold with a diameter of 10 mm and a thickness of 1 mm and incubated in a humidor for 24 hours at 37°C. Five groups of specimens were thus fabricated:

(1) CPC + 0% chitosan (CPC control)

(2) CPC + the 15% chitosan liquid without metformin (CPC + CN control)

(3) CPC + the 15% chitosan liquid + 10 μg metformin in each specimen (CPC + CN + 10Met)

(4) CPC + the 15% chitosan liquid + 30 μg metformin in each specimen (CPC + CN + 30Met)

(5) CPC + the 15% chitosan liquid + 50 μg metformin in each specimen (CPC + CN + 50Met)

2.2. Metformin Release from CPC Scaffold. Carbon 14 [^{14}C]-labeled compounds are often used to determine drug release amounts. The release of metformin was assessed following our previous method [18, 19]. Briefly, 10, 30, and 50 μg of metformin (containing 1/10 [^{14}C]-metformin) were dissolved in 15% chitosan to form the metformin + chitosan liquid. The powder and liquid portions were mixed under sterile conditions by hand spatulation. [^{14}C] metformin-loaded scaffold was placed in 24-well plates containing 1 mL of PBS in an incubator at 37°C. At each time period, the microsphere suspension was centrifuged, and the PBS without microspheres was collected for [^{14}C]-metformin concentration analysis. 100 μL PBS was transferred to the scintillation tube containing 3 mL Biodegradable Counting Cocktail buffer (Fisher Scientific Inc., Pittsburgh, PA). Radioactivity was counted by a multipurpose scintillation counter (Beckman LS6500 Counter, Brea, CA).

2.3. Cell Culture. DPCs were isolated and characterized as described previously [20]. Dental pulp tissues were obtained from explants of clinically healthy dental pulps from human adult third molars that were removed from individuals undergoing tooth extraction for orthodontic treatment. The procedure was approved by the Institutional Review Board of the University of Maryland Baltimore. Briefly, pulp tissues were minced and digested in a solution of 3 mg/mL of collagenase type I and 4 mg/mL dispase for 30–60 min at 37°C. Cell suspension was obtained by passing the digested tissue through a 70 μm cell strainer. The cells were pelleted and seeded in culture dishes and incubated in α-MEM supplemented with 20% FBS, 100 units/mL penicillin G, 100 mg/mL streptomycin, and 50 mg/mL ascorbic acid (Sigma-Aldrich, St. Louis, MO)

Table 1: The sequences of specific primers for real-time PCR operation.

Gene	Forward	Reverse
DSPP	GCCACTTTCAGTCTTCAAAGAGA	GCCCAAATGCAAAAATATGTAA
DMP-1	AAAATTCTTTGTGAACTACGGAGG	GAGCACAGGATAATCCCCAA
Runx2	GACTGTGGTTACCGTCATGGC	ACTTGGTTTTTCATAACAGCGGA
OCN	CTCACACTCCTCGCCCTATT	TTGGACACAAAGGCTGCAC
GAPDH	TCAACGACCCCTTCATTGAC	ATGCAGGGATGATGTTCTGG

at 37°C in 5% CO_2. Nonadherent cells were removed 48 h after the initial plating. The medium was replaced every 3 days. When primary culture became subconfluent after approximately 1–2 weeks, cells were collected by trypsinization and subcultured at 5000 cells per cm^2 in growth medium.

2.4. Flow Cytometry Analysis. To analyze the cell surface antigen expressions, the cells from the second passage were harvested by trypsin/EDTA treatment for 4 min at 37°C then washed twice with PBS. 1×10^5 cells/tube were incubated with the conjugated antibody for 20 min on ice in the dark. The cell suspensions were washed twice, resuspended in 2% FBS/PBS, and analyzed using a flow cytometry cell sorting Vantage cell sorter (BD Biosciences, San Jose, CA). Data were analyzed using the FACS software (FlowJo LLC, Ashland, OR). The following conjugated antibodies were used: STRO-1-PE (Santa Cruz Biotech, sc-47733, Santa Cruz, CA), CD-29-PE (BD Biosciences, Cat. No. 557332, San Jose, CA), CD-90-PE (BD Biosciences, Cat. No. 555596), CD105-FITC (BD Biosciences, Cat. No. 561443), CD-34-PE (BD Biosciences, Cat. No. 560941), CD-45-PE (Santa Cruz Biotech, sc-28369), FITC-conjugated IgG control antibody (BD Biosciences, Cat. No. 555748), and PE-conjugated IgG control antibody (BD Biosciences, Cat. No. 555749). Isotype control antibodies were used as negative controls.

2.5. Cell Viability Assays. DPCs were seeded on a disk with a diameter of 10 mm and a thickness of 1 mm in 24-well plates at a cell seeding density of 1.5×10^5 cells/well. At 1 and 7 days, cells were stained by live/dead viability assay kit (Invitrogen, Carlsbad, CA) as previously described [21]. Cells were washed with PBS, followed by incubation with the dye. Live cells were stained green with 2 mM calcein AM and dead cells were marked red with 4 mM ethidium homodimer-1 (EthD-1), and they were examined using epifluorescence microscopy (Eclipse TE2000-S, Nikon, Melville, NY). The percentage of live cells and the live cell density were calculated as previously described [21].

2.6. Cell Proliferation Assays. Cell proliferation was measured by the Cell Counting Kit-8 assay (CCK-8, Dojindo, Tokyo, Japan). DPCs were seeded on disks with a diameter of 10 mm and a thickness of 1 mm in 24-well plates at a density of 1.5×10^5 cells/well, and cells were incubated for 1, 3, 5, and 7 d at 37°C and 5% CO_2. The culture medium was replaced with fresh medium every 2 days. At each time point, a total of 450 μL of DMEM and 50 μL of CCK-8 solution were added to each well and incubated for 2 h. After this incubation, 100 μL of the supernatant was transferred into a 96-well plate and read at 450 nm using a SpectraMax M5 plate reader (Molecular Devices, Sunnyvale, CA) according to the manufacturer's protocol. At least three independent experiments were performed, each of which was performed in triplicate.

2.7. ALP Assay. Cells were seeded at a density of 1.5×10^5 cells/well with CPC scaffold in 24-well plates. ALP activity was measured at 1, 7, and 14 d using an ALP kit (Wako, Tokyo, Japan) following the manufacturer's instructions. Samples were washed twice in PBS before adding 0.5 mL cell lysis buffer containing 0.2% Triton X-100 (Sigma-Aldrich) with 10 mM Tris (pH 7.0) and 1 mM EDTA (Sigma-Aldrich) onto the CPC disks. They were incubated for 20 minutes and transferred to −80°C freezer for 30 minutes and thawed at room temperature for 30 minutes. The freeze-thawing procedure was performed twice to lyse cells and collect all the ALP samples. Finally, the test sample was transferred to a 96-well plate, and its activity was measured at 520 nm concurrently with standard samples. The ALP activity was calculated against the total cellular protein concentrations to obtain [pNpp (μM/min)]/[Protein (mg)]. The amount of protein in each sample was measured by a BCA protein assay kit (Thermo Scientific, Waltham, MA). For the ALP activity assays, each sample was performed in triplicate and the results were repeated in at least three independent tests.

2.8. Reverse Transcriptase PCR (RT-PCR) and Real-Time Quantitative PCR (qPCR). The expression levels of dentin sialophosphoprotein (DSPP), dentin matrix protein-1 (DMP-1), runt-related transcription factor-2 (Runx2), and osteocalcin (OCN) mRNA were determined by SYBR green real-time reverse transcription-PCR (RT-PCR) as previously described [22–24]. Total RNA was extracted using Trizol reagent. Quantitative determination of RNA levels was performed in triplicate in three independent experiments. Real-time PCR and data collection were performed with an ABI PRISM 7500 sequence detection system. The housekeeping gene GAPDH was used as an internal control to normalize the expression levels of different genes. For each primer set, the melting curves were performed to ensure that a single peak was produced. The data for gene expression were analyzed using the $\triangle\triangle$Ct method. The primers used for the amplification of the indicated genes are listed in Table 1.

2.9. Alizarin Red Staining (ARS) of Mineral Synthesis by DPCs. ARS was performed to evaluate the mineralization by DPCs [25]. At days 1 and 21, disks were fixed using 10%

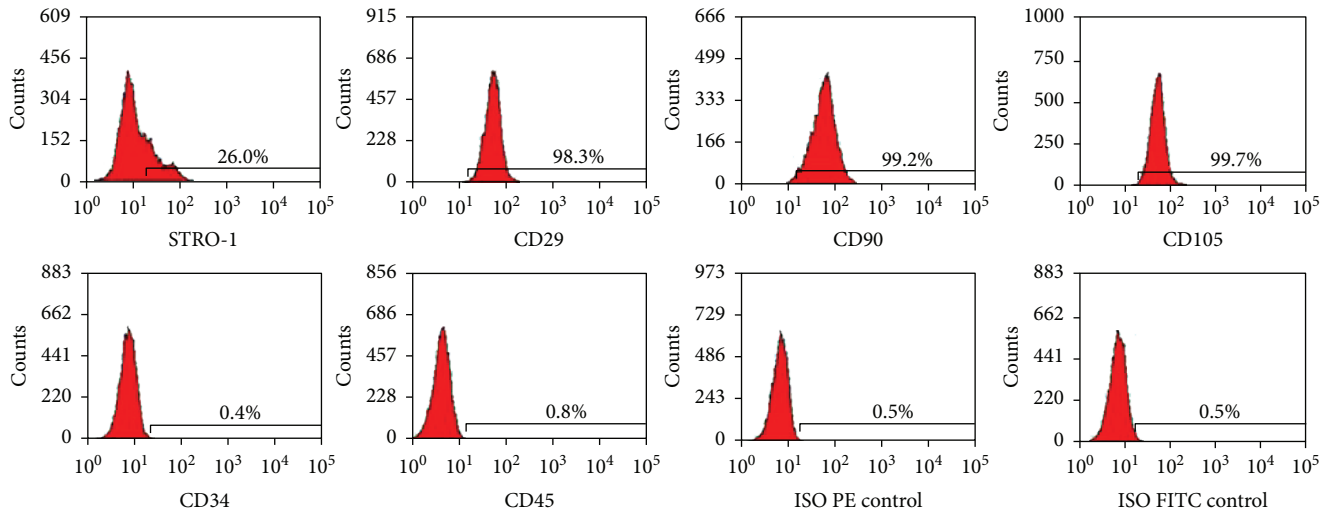

Figure 1: DPC phenotype by flow cytometry. The expression of a series of cell surface markers associated with the MSC phenotype was investigated using flow cytometry. Analysis of molecular surface antigen markers in DPCs by flow cytometry indicated that the cells were negative for CD34 and CD45, whereas they were positive for STRO-1, CD29, CD90, and CD105.

formaldehyde for 30 minutes, washed by PBS, and stained with 2% Alizarin Red S (Millipore, Billerica, MA) for 45 minutes. To quantify the mineral deposition, the stained minerals were dissolved by 10% cetylpyridinium chloride-monohydrate, then the extracted stain was transferred to a 96-well plate. The absorbance at 562 nm was measured using a microplate reader, as previously described [26, 27].

2.10. Statistical Analyses. Statistical analysis was performed with one-way analysis of variance (ANOVA), followed by post hoc LSD (least significant difference) tests using the Statistical Package for the Social Sciences (SPSS 20.0). All data were expressed as mean ± standard deviation (SD). Kolmogorov–Smirnov test and Levene's test were first performed to confirm the normality and equal variance of the data. A $P < 0.05$ was considered statistically significant.

3. Results

3.1. Identification of Stem Cell Phenotypic Markers in Primary DPCs. STRO-1$^+$, CD29$^+$, CD90$^+$, and CD105$^+$ have been shown to exhibit mesenchymal stem cell (MSC) properties, and these markers have been used to identify DPCs [28]. The surface markers of DPCs were analyzed by flow cytometry. Consistent with other MSCs, the majority of DPCs were negative for CD34 and CD45. The culture population contained 26.0% STRO-1-positive cells, 98.3% CD29-positive cells, 99.2% CD90-positive cells, and 99.7% CD105-positive cells (Figure 1). These results indicate that the DPCs were mesenchymal progenitors.

3.2. Metformin Release from Metformin-Loaded CPC Scaffold. The drug release of metformin-CPC scaffold was analyzed using [^{14}C] label. The release profile showed a typical fast release initially, reaching an accumulative release of about 29.9, 199.4, and 505.1 ng/mL in the first 12 h for samples containing 10, 30, and 50 μg of metformin, respectively.

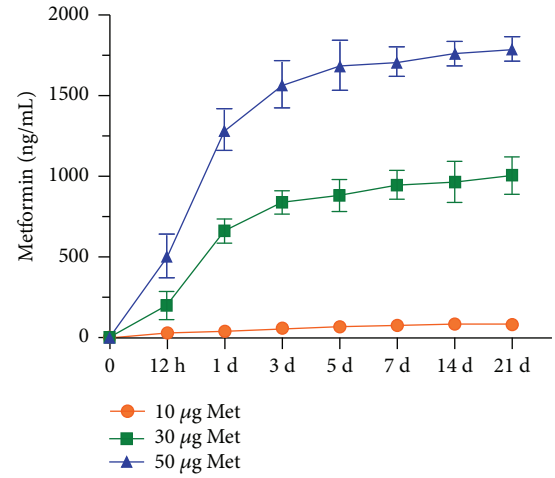

Figure 2: Metformin release from CPC-chitosan scaffold. CPC + CN + 50Met composite exhibited greater release in the first 12 h as compared to CPC + CN + 10Met and CPC + CN + 30Met. Metformin from CPC-chitosan scaffolds had sustained release over 21 days. CPC: calcium phosphate cement.

Then, the CPC continued to release metformin at a sustained rate during the next 21 days (Figure 2). The release amount was related to the initial loading concentrations of metformin. Based on the initial burst release of metformin and followed by continuous release, the 50 μg metformin was selected in all further experiments. These results showed that metformin release from CPC-chitosan scaffold was sustained and relatively long lasting, to meet the requirement of a drug carrier to last for 2–3 weeks in order to stimulate the odontogenic differentiation of DPCs.

3.3. Viability and Cell Proliferation of DPCs on CPC Scaffold. Representative live/dead staining images are shown in

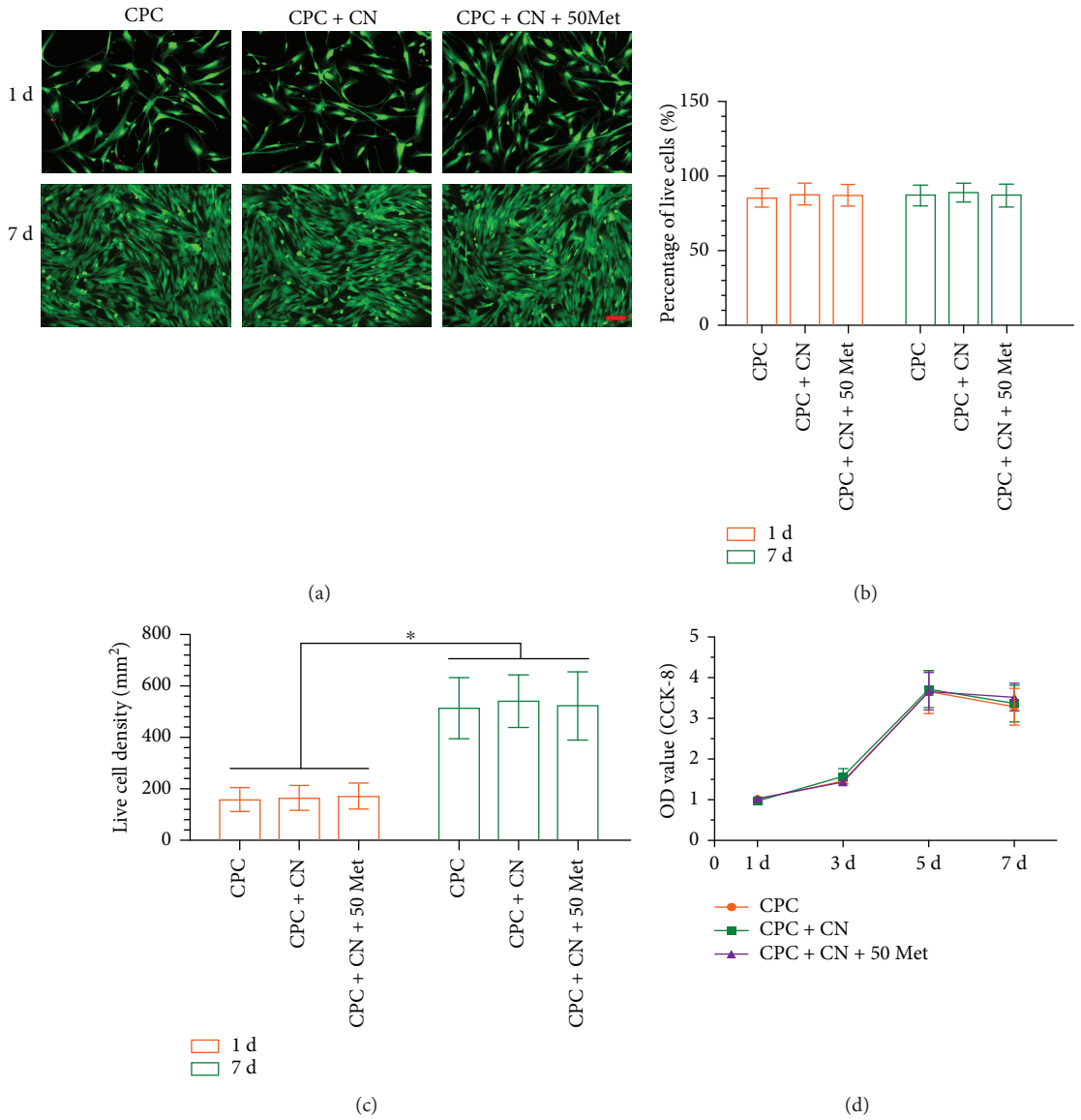

Figure 3: Viability and proliferation of DPCs attached on CPC scaffold surface. (a) Representative live/dead images of metformin-treated DPCs at days 1 and 7, with live cells stained green and dead cells shown in red. In all three groups, live cells were abundant, and dead cells were few (scale bar = 50 μm). (b) The percentage of live cells of DPCs was around 89%. (c) All groups exhibited an increasing live cell density; $^*P < 0.05$. (d) CPC + CN + 50Met had no effect on cell proliferation. Data represent mean ± SD of three independent experiments with triplicates.

Figure 3(a). There were numerous live cells (stained green) and a few dead cells (stained red). The cell number increased from day 1 to day 7 due to proliferation. In Figure 3(b), the percentages of live cells on CPC control, CPC + CN control, and CPC + CN + 50Met groups were greater than 89% and were not significantly different from each other ($P > 0.05$). As shown in Figure 3(c), the live cell density increased with time due to proliferation, with no significant difference among the three groups ($P > 0.05$). The OD value suggests that there were no significant differences in the cell proliferation for the three groups ($P > 0.05$) (Figure 3(d)). Overall, no noticeable difference was observed among the three groups, indicating that the metformin in the CPC scaffold was not cytotoxic to DPCs.

3.4. Alkaline Phosphatase (ALP) Activity. The ALP activity of DPCs is plotted in Figure 4. The addition of metformin to CPC resulted in a significant increase in ALP activity compared to CPC control and CPC + CN control. The ALP activity of CPC containing no chitosan was similar to that of CPC + CN control ($P > 0.05$), indicating that the addition of chitosan to CPC had no effect on ALP activity. These results demonstrate the great potential of DPCs + CPC + metformin construct as an ideal "stem cell-scaffold-small molecule" system for dentin regeneration.

3.5. Odontogenic Differentiation. To further investigate the effects of CPC containing metformin on odontogenic differentiation of DPCs, the DPC odontogenic differentiation in

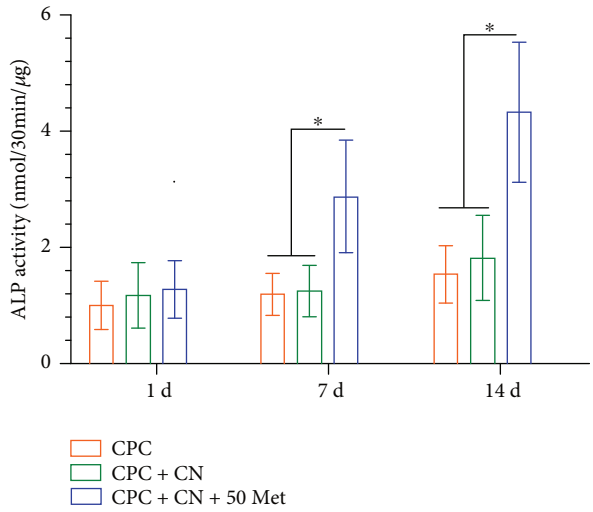

Figure 4: Alkaline phosphatase (ALP) assay. ALP activity was measured at days 1, 7, and 14. A significant increase in ALP activity was observed in the CPC + CN + 50Met group compared with the CPC control and CPC + CN control ($^*P < 0.05$). Data represent mean ± SD of three independent experiments with triplicates.

the three groups was evaluated. Metformin significantly increased the mRNA expression of odontoblastic gene markers, including DSPP, DMP-1, Runx2, and OCN mRNA (Figure 5).

3.6. Mineralization by DPCs. Next, we investigated the formation of mineralized nodules, an index of terminal odontoblastic differentiation, in DPCs after 21 days of incubation with metformin. The mineralized extracellular deposits produced by DPCs on scaffold surfaces are shown in Figure 6(a). The staining of the synthesized bone mineral matrix became denser and darker, reflecting that the mineral synthesis was increased significantly from day 1 to 21. Data from the cetylpyridinium chloride monohydrate are plotted in Figure 6(b). For each group, the mineral amount synthesized by the cells increased dramatically from day 1 to 21 ($P < 0.05$). These results indicate that CPC + CN + 50Met had the greatest bone mineral synthesis by the cells than other groups ($P < 0.05$).

4. Discussion

DPCs were selected as suitable MSCs for dentin regeneration, mainly for the treatment of pulp exposures [29]. Although bone marrow MSCs have become the main cell source for bone tissue engineering [30], bone marrow donation is an invasive surgical procedure. Previous studies demonstrated the high capacity of DPCs for odontogenic differentiation and potential to form dentin-pulp complexes when transplanted into immunocompromised mice [31]. These cells exhibited high proliferation rate, great differentiation potential, and expression of mesenchymal and embryonic stem cell markers. In the present study, DPCs strongly expressed MSC markers, indicating that DPCs maintained the stem cell characteristics and may have a high capacity for differentiation.

Currently, the application of tissue engineering concepts for the development of biodegradable scaffolds capable of driving dental pulp cell migration and differentiation has been the focus of dentin regeneration [32]. Loading scaffolds with small molecule compounds to facilitate tissue regeneration has already been studied and reported in the tissue engineering literature. CPC has been increasingly used in dental, craniofacial, and orthopaedic repairs as bone graft substitutes [33]. However, its use is limited by the relatively poor strength properties. It has been reported that chitosan-based scaffolds showed no cytotoxicity toward various cell types [34]. Chitosan incorporation into CPC could improve the load-bearing capability of the scaffold. For example, in a previous study, the CPC-chitosan scaffold had a flexural strength of (19.5 ± 1.4) MPa, higher than the (8.0 ± 1.4) MPa of CPC control without chitosan [35]. In addition, several studies indicated that metformin has osteogenic effects by promoting the differentiation of MSCs and preosteoblasts [36, 37]. Therefore, in our current study, metformin was added to the chitosan solution, which was then mixed with CPC powder to form the CPC paste. The release profile from CPC in 10, 30, and 50 μg concentration of metformin per specimen displayed a sustained manner up to 21 days. Nevertheless, there was a significantly smaller amount of metformin released from 10 μg and 30 μg specimens, compared to the 50 μg specimens. The sustained release of metformin from these specimens was likely due to the distribution of metformin into chitosan, whereas the initial burst release was likely due to the binding of metformin to the CPC surface. Furthermore, the bioactivity of the released metformin is very important; our results showed that the cell viability at 1 day and 7 days was similar for all CPC-based materials. Live cell density for all CPC-based materials was also similar. Therefore, CPC + CN and CPC + CN + 50Met did not adversely affect the cell proliferation when compared with CPC control, which was approved by the FDA for craniofacial repairs. Hence, by comparing with the results of previous studies [16], our current study showed an acceptable biocompatibility for CPC-metformin.

After confirmation of the effects of metformin on DPC viability and cell proliferation, we examined the odontogenic differentiation ability of cells seeded on CPC-chitosan scaffolds with and without metformin. ALP activity is most often used as an early marker of odontoblastic differentiation [38] and plays an important role in cell mineralization. In the current study, the CPC + CN + 50Met construct yielded a significantly higher ALP activity than the CPC control and CPC + CN control. Consistent with this finding, more mineralized nodules were also observed in DPCs cultured with CPC + CN + 50Met group at the late stage of odontogenic differentiation.

Moreover, the gene expression levels of the related odontogenic gene markers such as DSPP, DMP-1, Runx2, and OCN were measured to elucidate the effects of the CPC + CN + 50Met composite on the odontogenic differentiation in vitro. DSPP was originally thought to be a dentin-specific marker. Although several studies have also indicated its expression in bone [39, 40], DSPP remains to be an important marker for odontogenic differentiation. In addition,

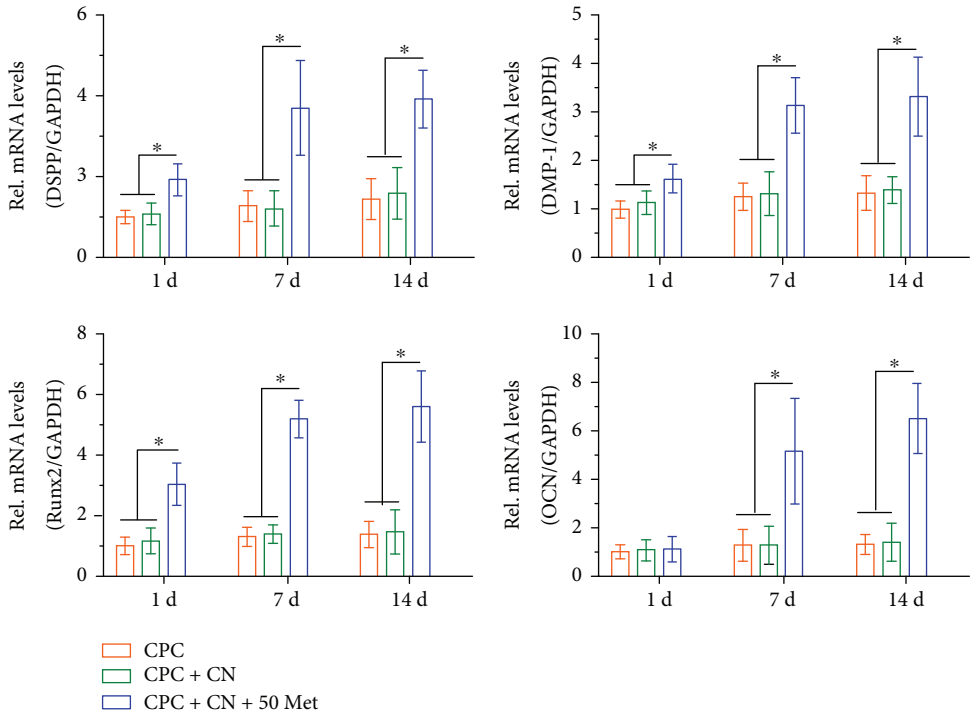

Figure 5: DPC odontogenic differentiation on CPC control, CPC + CN control, and CPC + CN + 50Met. The mRNA expression levels of DSPP, DMP-1, Runx2, and OCN were determined using qRT-PCR. The mRNA expression levels of DSPP, DMP-1, Runx2, and OCN significantly increased in the CPC + CN + 50Met compared with the CPC control and CPC + CN control ($^*P < 0.05$). GAPDH was used as an internal control. Data represent mean ± SD of three independent experiments with triplicates.

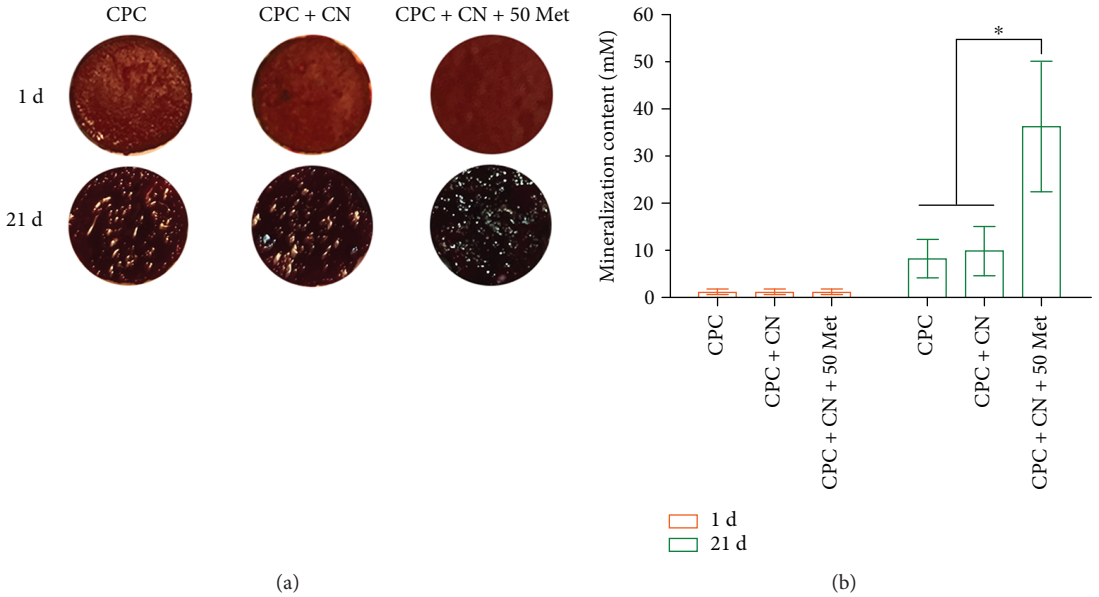

Figure 6: Mineralization by DPCs analyzed by Alizarin Red S staining. (a) After the cells were cultured for 21 days in osteogenic differentiation media, the mineral matrix exhibited a denser and darker red staining with increasing culture time. (b) Quantification of Alizarin Red S staining. The graph shows that the amount of calcium was significantly greater in the CPC + CN + 50Met than in the CPC control and CPC + CN control ($^*P < 0.05$). Data represent mean ± SD of three independent experiments with triplicates.

DMP-1 is a key regulator of odontogenic differentiation and the formation of mineralization and the dentin tubular system [41]. Furthermore, Runx2, of the runt domain gene family, is a key transcription factor that controls bone and tooth formation by regulating the osteo/odontogenic differentiation [42, 43]. Moreover, OCN can be released by

odontoblasts and is present in the dentin matrix, and it is also used as a reparative molecule within the dental pulp [44–46]. In the present study, DSPP, DMP-1, Runx2, and OCN mRNA levels were all upregulated in DPCs cultured with the CPC + CN + 50Met group. However, no effect was observed by metformin on the mRNA level of OCN during the early stages of treatment. These results may be attributed to the fact that OCN was expressed at the later stage of cell mineralization [47]. These results suggest that metformin can be considered to be a potential biochemical factor for odontogenic differentiation of DPCs when cultured in CPC-chitosan scaffold.

However, the present work possesses several limitations. The accurate and quantitative control of metformin release from scaffolds is difficult. There are controversies surrounding even well-investigated small molecules, and studies based on different models often yield different results [48, 49]. Thus, a further in-depth investigation should be performed to identify the mechanism of metformin on odontogenesis stimulation at the molecular level. In addition, further in vivo experiments should also be performed using an animal model to demonstrate dentin and other tissue regeneration for future clinical applications.

5. Conclusions

The present study showed for the first time that the incorporation of metformin into CPC-chitosan composite significantly enhanced odontogenic differentiation of DPCs, without negatively altering the cell viability and proliferation. CPC-chitosan composite scaffold is promising to be a moderate load-bearing matrix for cell delivery [35] and dentin regeneration, with the potential to serve as a delivery vehicle for metformin to promote the regeneration of dentin as well as other types of tissues. These findings will provide critical insights towards the future use of DPCs/chitosan/metformin combinations in dentin pulp and other tissue engineering applications.

Data Availability

The data used to support the findings of this study are available from the corresponding author upon request.

Conflicts of Interest

The authors declare that they have no competing interests.

Authors' Contributions

Wei Qin and Jia-Yao Chen contributed equally to this work.

Acknowledgments

This study was supported by the National Institutes of Health/National Institute of Dental and Craniofacial Research Grant R01 DE023578 (to AS).

References

[1] U. Sjogren, B. Hagglund, G. Sundqvist, and K. Wing, "Factors affecting the long-term results of endodontic treatment," *Journal of Endodontics*, vol. 16, no. 10, pp. 498–504, 1990.

[2] S. R. J. Simon, A. Berdal, P. R. Cooper, P. J. Lumley, P. L. Tomson, and A. J. Smith, "Dentin-pulp complex regeneration: from lab to clinic," *Advances in Dental Research*, vol. 23, no. 3, pp. 340–345, 2011.

[3] T. Gong, B. C. Heng, E. C. M. Lo, and C. Zhang, "Current advance and future prospects of tissue engineering approach to dentin/pulp regenerative therapy," *Stem Cells International*, vol. 2016, Article ID 9204574, 13 pages, 2016.

[4] R. Langer and J. Vacanti, "Tissue engineering," *Science*, vol. 260, no. 5110, pp. 920–926, 1993.

[5] M. Atari, C. Gil-Recio, M. Fabregat et al., "Dental pulp of the third molar: a new source of pluripotent-like stem cells," *Journal of Cell Science*, vol. 125, no. 14, pp. 3343–3356, 2012.

[6] A. H.-C. Huang, Y.-K. Chen, A. W.-S. Chan, T.-Y. Shieh, and L.-M. Lin, "Isolation and characterization of human dental pulp stem/stromal cells from nonextracted crown-fractured teeth requiring root canal therapy," *Journal of Endodontics*, vol. 35, no. 5, pp. 673–681, 2009.

[7] R. Kuang, Z. Zhang, X. Jin et al., "Nanofibrous spongy microspheres for the delivery of hypoxia-primed human dental pulp stem cells to regenerate vascularized dental pulp," *Acta Biomaterialia*, vol. 33, pp. 225–234, 2016.

[8] V. Rosa, N. Dubey, I. Islam, K. S. Min, and J. E. Nör, "Pluripotency of stem cells from human exfoliated deciduous teeth for tissue engineering," *Stem Cells International*, vol. 2016, Article ID 5957806, 6 pages, 2016.

[9] P. Wang, T. Ma, D. Guo et al., "Metformin induces osteoblastic differentiation of human induced pluripotent stem cell-derived mesenchymal stem cells," *Journal of Tissue Engineering and Regenerative Medicine*, vol. 12, no. 2, pp. 437–446, 2018.

[10] W. Qin, X. Gao, T. Ma et al., "Metformin enhances the differentiation of dental pulp cells into odontoblasts by activating AMPK signaling," *Journal of Endodontics*, vol. 44, no. 4, pp. 576–584, 2018.

[11] F. Kajbaf, Y. Bennis, A. S. Hurtel-Lemaire, M. Andrejak, and J. D. Lalau, "Unexpectedly long half-life of metformin elimination in cases of metformin accumulation," *Diabetic Medicine*, vol. 33, no. 1, pp. 105–110, 2016.

[12] P. Q. Ruhé, H. C. Kroese-Deutman, J. G. C. Wolke, P. H. M. Spauwen, and J. A. Jansen, "Bone inductive properties of rhBMP-2 loaded porous calcium phosphate cement implants in cranial defects in rabbits," *Biomaterials*, vol. 25, no. 11, pp. 2123–2132, 2004.

[13] M. D. Weir and H. H. Xu, "Osteoblastic induction on calcium phosphate cement-chitosan constructs for bone tissue engineering," *Journal of Biomedical Materials Research Part A*, vol. 94A, no. 1, pp. 223–233, 2010.

[14] E. J. Blom, J. Klein-Nulend, J. G. C. Wolke, K. Kurashina, M. A. J. van Waas, and E. H. Burger, "Transforming growth factor-β1 incorporation in an α-tricalcium phosphate/dicalcium phosphate dihydrate/tetracalcium phosphate monoxide cement: release characteristics and physicochemical properties," *Biomaterials*, vol. 23, no. 4, pp. 1261–1268, 2002.

[15] Q. P. Ruhe, E. L. Hedberg, N. T. Padron, P. H. M. Spauwen, J. A. Jansen, and A. G. Mikos, "rhBMP-2 release from injectable poly(DL-lactic-co-glycolic acid)/calcium-phosphate

cement composites," *The Journal of Bone and Joint Surgery-American Volume*, vol. 85, no. 3, pp. 75–81, 2003.

[16] H. H. K. Xu and C. G. Simon Jr., "Fast setting calcium phosphate–chitosan scaffold: mechanical properties and biocompatibility," *Biomaterials*, vol. 26, no. 12, pp. 1337–1348, 2005.

[17] A. R. Costa-Pinto, R. L. Reis, and N. M. Neves, "Scaffolds based bone tissue engineering: the role of chitosan," *Tissue Engineering Part B: Reviews*, vol. 17, no. 5, pp. 331–347, 2011.

[18] Q. Li, D. Guo, Z. Dong et al., "Ondansetron can enhance cisplatin-induced nephrotoxicity via inhibition of multiple toxin and extrusion proteins (MATEs)," *Toxicology and Applied Pharmacology*, vol. 273, no. 1, pp. 100–109, 2013.

[19] F. E. al Jofi, T. Ma, D. Guo et al., "Functional organic cation transporters mediate osteogenic response to metformin in human umbilical cord mesenchymal stromal cells," *Cytotherapy*, vol. 20, no. 5, pp. 650–659, 2018.

[20] W. Qin, Q.-T. Huang, M. D. Weir et al., "Alcohol inhibits odontogenic differentiation of human dental pulp cells by activating mTOR signaling," *Stem Cells International*, vol. 2017, Article ID 8717454, 10 pages, 2017.

[21] L. Zhao, M. D. Weir, and H. H. K. Xu, "An injectable calcium phosphate-alginate hydrogel-umbilical cord mesenchymal stem cell paste for bone tissue engineering," *Biomaterials*, vol. 31, no. 25, pp. 6502–6510, 2010.

[22] P. Wang, X. Liu, L. Zhao et al., "Bone tissue engineering via human induced pluripotent, umbilical cord and bone marrow mesenchymal stem cells in rat cranium," *Acta Biomaterialia*, vol. 18, pp. 236–248, 2015.

[23] J. Guo, W. Qin, Q. Xing et al., "TRIM33 is essential for osteoblast proliferation and differentiation via BMP pathway," *Journal of Cellular Physiology*, vol. 232, no. 11, pp. 3158–3169, 2017.

[24] X. Yang, Y. Li, X. Liu, R. Zhang, and Q. Feng, "In vitro uptake of hydroxyapatite nanoparticles and their effect on osteogenic differentiation of human mesenchymal stem cells," *Stem Cells International*, vol. 2018, Article ID 2036176, 10 pages, 2018.

[25] X. Liu, W. Chen, C. Zhang et al., "Co-seeding human endothelial cells with human-induced pluripotent stem cell-derived mesenchymal stem cells on calcium phosphate scaffold enhances osteogenesis and vascularization in rats," *Tissue Engineering Part A*, vol. 23, no. 11-12, pp. 546–555, 2017.

[26] W. Chen, H. Zhou, M. D. Weir, C. Bao, and H. H. K. Xu, "Umbilical cord stem cells released from alginate–fibrin microbeads inside macroporous and biofunctionalized calcium phosphate cement for bone regeneration," *Acta Biomaterialia*, vol. 8, no. 6, pp. 2297–2306, 2012.

[27] P. S. P. Poh, C. Seeliger, M. Unger, K. Falldorf, E. R. Balmayor, and M. van Griensven, "Osteogenic effect and cell signaling activation of extremely low-frequency pulsed electromagnetic fields in adipose-derived mesenchymal stromal cells," *Stem Cells International*, vol. 2018, Article ID 5402853, 11 pages, 2018.

[28] F.-J. Lv, R. S. Tuan, K. M. C. Cheung, and V. Y. L. Leung, "Concise review: the surface markers and identity of human mesenchymal stem cells," *Stem Cells*, vol. 32, no. 6, pp. 1408–1419, 2014.

[29] I. S. Yang, D. S. Lee, J. T. Park, H. J. Kim, H. H. Son, and J. C. Park, "Tertiary dentin formation after direct pulp capping with odontogenic ameloblast-associated protein in rat teeth," *Journal of Endodontics*, vol. 36, no. 12, pp. 1956–1962, 2010.

[30] D. G. Phinney and D. J. Prockop, "Concise review: mesenchymal stem/multipotent stromal cells: the state of transdifferentiation and modes of tissue repair-current views," *Stem Cells*, vol. 25, no. 11, pp. 2896–2902, 2007.

[31] S. Gronthos, M. Mankani, J. Brahim, P. G. Robey, and S. Shi, "Postnatal human dental pulp stem cells (DPSCs) in vitro and in vivo," *Proceedings of the National Academy of Sciences of the United States of America*, vol. 97, no. 25, pp. 13625–13630, 2000.

[32] E. Piva, A. F. Silva, and J. E. Nör, "Functionalized scaffolds to control dental pulp stem cell fate," *Journal of Endodontics*, vol. 40, no. 4, pp. S33–S40, 2014.

[33] P. Wang, L. Zhao, W. Chen, X. Liu, M. D. Weir, and H. H. K. Xu, "Stem cells and calcium phosphate cement scaffolds for bone regeneration," *Journal of Dental Research*, vol. 93, no. 7, pp. 618–625, 2014.

[34] W. Chen, H. Zhou, M. D. Weir, M. Tang, C. Bao, and H. H. K. Xu, "Human embryonic stem cell-derived mesenchymal stem cell seeding on calcium phosphate cement-chitosan-RGD scaffold for bone repair," *Tissue Engineering Part A*, vol. 19, no. 7-8, pp. 915–927, 2013.

[35] M. D. Weir and H. H. K. Xu, "Culture human mesenchymal stem cells with calcium phosphate cement scaffolds for bone repair," *Journal of Biomedical Materials Research Part B: Applied Biomaterials*, vol. 93, no. 1, pp. 93–105, 2010.

[36] W. G. Jang, E. J. Kim, I. H. Bae et al., "Metformin induces osteoblast differentiation via orphan nuclear receptor SHP-mediated transactivation of Runx2," *Bone*, vol. 48, no. 4, pp. 885–893, 2011.

[37] Y. Gao, Y. Li, J. Xue, Y. Jia, and J. Hu, "Effect of the anti-diabetic drug metformin on bone mass in ovariectomized rats," *European Journal of Pharmacology*, vol. 635, no. 1–3, pp. 231–236, 2010.

[38] K. S. Min, Y. M. Lee, S. O. Hong, and E. C. Kim, "Simvastatin promotes odontoblastic differentiation and expression of angiogenic factors via heme oxygenase-1 in primary cultured human dental pulp cells," *Journal of Endodontics*, vol. 36, no. 3, pp. 447–452, 2010.

[39] J. K. Kim, R. Shukla, L. Casagrande et al., "Differentiating dental pulp cells via RGD-dendrimer conjugates," *Journal of Dental Research*, vol. 89, no. 12, pp. 1433–1438, 2010.

[40] I. S. Kim, Y. M. Song, and S. J. Hwang, "Osteogenic responses of human mesenchymal stromal cells to static stretch," *Journal of Dental Research*, vol. 89, no. 10, pp. 1129–1134, 2010.

[41] Y. Lu, L. Ye, S. Yu et al., "Rescue of odontogenesis in *Dmp1*-deficient mice by targeted re-expression of DMP1 reveals roles for DMP1 in early odontogenesis and dentin apposition in vivo," *Developmental Biology*, vol. 303, no. 1, pp. 191–201, 2007.

[42] F. Posa, A. di Benedetto, G. Colaianni et al., "Vitamin D effects on osteoblastic differentiation of mesenchymal stem cells from dental tissues," *Stem Cells International*, vol. 2016, Article ID 9150819, 9 pages, 2016.

[43] B. Jin and P. H. Choung, "Recombinant human plasminogen activator inhibitor-1 accelerates odontoblastic differentiation of human stem cells from apical papilla," *Tissue Engineering Part A*, vol. 22, no. 9-10, pp. 721–732, 2016.

[44] H. Zou, G. Wang, F. Song, and X. Shi, "Investigation of human dental pulp cells on a potential injectable poly(lactic-co-glycolic acid) microsphere scaffold," *Journal of Endodontics*, vol. 43, no. 5, pp. 745–750, 2017.

[45] O. Egbuniwe, B. D. Idowu, J. M. Funes, A. D. Grant, T. Renton, and L. Di Silvio, "P16/p53 expression and telomerase activity in immortalized human dental pulp cells," *Cell Cycle*, vol. 10, no. 22, pp. 3912–3919, 2011.

[46] N. Goto, K. Fujimoto, S. Fujii et al., "Role of MSX1 in osteogenic differentiation of human dental pulp stem cells," *Stem Cells International*, vol. 2016, Article ID 8035759, 13 pages, 2016.

[47] A. Linde and M. Goldberg, "Dentinogenesis," *Critical Reviews in Oral Biology and Medicine*, vol. 4, no. 5, pp. 679–728, 1993.

[48] Q. Q. Han, Y. Du, and P. S. Yang, "The role of small molecules in bone regeneration," *Future Medicinal Chemistry*, vol. 5, no. 14, pp. 1671–1684, 2013.

[49] C. E. Segar, M. E. Ogle, and E. A. Botchwey, "Regulation of angiogenesis and bone regeneration with natural and synthetic small molecules," *Current Pharmaceutical Design*, vol. 19, no. 19, pp. 3403–3419, 2013.

Hindawi
Stem Cells International
Volume 2018, Article ID 7396905, 17 pages
https://doi.org/10.1155/2018/7396905

Review Article

Human Pluripotent Stem Cell Culture: Current Status, Challenges, and Advancement

Sushrut Dakhore,[1] Bhavana Nayer,[1] and Kouichi Hasegawa[1,2]

[1]*Institute for Stem Cell Biology and Regenerative Medicine (inStem), National Centre for Biological Sciences (NCBS), Bangalore, India*
[2]*Institute for Integrated Cell-Material Sciences (iCeMS), Institute for Advanced Study, Kyoto University, Japan*

Correspondence should be addressed to Kouichi Hasegawa; khasegawa@icems.kyoto-u.ac.jp

Received 27 July 2018; Revised 23 October 2018; Accepted 24 October 2018; Published 22 November 2018

Guest Editor: Tiago Fernandes

Over the past two decades, human embryonic stem cells (hESCs) have gained attention due to their pluripotent and proliferative ability which enables production of almost all cell types in the human body *in vitro* and makes them an excellent tool to study human embryogenesis and disease, as well as for drug discovery and cell transplantation therapies. Discovery of human-induced pluripotent stem cells (hiPSCs) further expanded therapeutic applications of human pluripotent stem cells (PSCs). hPSCs provide a stable and unlimited original cell source for producing suitable cells and tissues for downstream applications. Therefore, engineering the environment in which these cells are grown, for stable and quality-controlled hPSC maintenance and production, is one of the key factors governing the success of these applications. hPSCs are maintained in a particular niche using specific cell culture components. Ideally, the culture should be free of xenobiotic components to render hPSCs suitable for therapeutic applications. Substantial efforts have been put to identify effective components, and develop culture conditions and protocols, for their large-scale expansion without compromising on quality. In this review, we discuss different media, their components and functions, including specific requirements to maintain the pluripotent and proliferative ability of hPSCs. Understanding the role of culture components would enable the development of appropriate conditions to promote large-scale, quality-controlled expansion of hPSCs thereby increasing their potential applications.

1. Introduction

The quest to understand early embryonic development and the differentiation into mature cell types dates back to the early twentieth century when important experiments described the development of testicular teratocarcinomas in mice [1]. The observation that they were composed of undifferentiated cells of germ cell origin and could give rise to various types of differentiated cells sparked growing interest in the subject. This was followed by the derivation of embryonal carcinoma cells (ECC) from murine teratocarcinomas, which were cultured as embryoid bodies (EBs) and were multipotent [2]. The observation that even single ECCs obtained from a teratocarcinoma had the capacity to grow indefinitely and give rise to multiple cell types gave proof of the existence of individual pluripotent stem cells and opened a unique window into the study of early mammalian development [3]. This discovery that ECCs could be derived from teratocarcinomas, which are tumors induced by the transplantation of implantation-stage mouse embryos to extrauterine sites in histocompatible hosts, inspired researchers to isolate pluripotent cells directly from embryos itself, thus circumventing the need for generating/obtaining teratocarcinomas for pluripotent stem cell isolation. Subsequently, the *in vitro* culture of pluripotent cells was established by successfully isolating the cells from the inner cell mass (ICM) of normal preimplantation mouse blastocysts, and the term "embryonic stem cell" (ESC) was coined [4, 5], thus distinguishing it from teratocarcinoma-derived pluripotent ECCs. These pioneering experiments determined the optimal time point of isolation of pluripotent ESCs from embryos and allowed the development of appropriate culture conditions to maintain

ESC lines in their undifferentiated state with indefinite proliferation capacity [4, 6]. Further advances allowing development of nonhuman primate ESC lines [7] eventually led to the breakthrough establishment of hESC lines.

hESCs are derived from the ICM of preimplantation blastocysts and can propagate and retain their pluripotency when grown in proper culture conditions [4, 6]. These cells show undifferentiated morphology, expression of pluripotency markers, unlimited proliferation, and the potential to differentiate into all three embryonic germ layers, even after prolonged culture, while maintaining a normal karyotype. These features have since then become the defining characteristics of PSCs. Following hESCs, an important discovery was the development of induced pluripotent stem cells (iPSCs) by forced expression of transcription factors necessary for reprogramming adult somatic cells into pluripotent cells. This approach bypassed the need of embryos for obtaining pluripotent stem cells, thereby resolving the ethical concerns posed by hESC research [8].

The unique potential of hPSCs to self-renew in culture and give rise to all somatic cell types in the embryo makes them an exciting candidate for cell replacement therapy (CRT) in various diseases such as degenerative disorders and cancer, as well as offers limitless possibilities for understanding early development and establishing *in vitro* disease models. Studies have demonstrated the capability of hPSCs to differentiate into various cell types derived from ectoderm, endoderm, and mesoderm, such as cardiomyocytes, neurons, glia, hepatocytes, pancreatic islet cells, chondrocytes, skeletal myocytes, adipocytes, and endothelial cells. Thus, an unprecedented level of research is directed towards elucidating the factors involved in regulating pluripotency and differentiation. Knowledge of the same can be applied towards recapitulating developmental stages and understanding the mechanisms underlying normal and diseased states. It therefore has wide-ranging applications in advancing drug discovery, regenerative medicine, and gene therapy.

Furthermore, the use of hiPSCs opened up the possibility of autologous CRT, moving us one step closer to the hope of bringing stem cell therapies from the bench to bedside. It is worth noting that hiPSCs share similar characteristics with hESCs in terms of signaling mechanisms, and the culture systems for hiPSCs are similar to those used for hESCs as well.

Recent studies have shown that "pluripotency" exists in different states, depending on the culture condition of hPSCs. Amongst them, two functionally distinct stem cell states have been identified, namely, "naïve" and "primed," which are similar to mouse ICM cells in preimplantation blastocyst and epiblast layer cells in postimplantation blastocyst, respectively [9–12]. Conventionally, hESC lines have been derived and maintained in a pluripotent state resembling the primed state in a mouse, represented by mouse epiblast stem cells (mEpiSCs) [9, 11]. The same holds true for hiPSC lines that have been reprogrammed using the method first described by Takahashi et al. [8]. Since the discovery of the two pluripotency states, it has been established that mouse hESCs, which are in a "naïve" state, represent an earlier time point than primed EpiSCs, in mouse embryonic development [9–11]. Consequently, a huge body of research has been aimed at optimizing culture conditions for each stage, and recently, "naïve" hESCs have also been generated by toggling conventional hESCs back from the "primed" state [13–15] or by deriving new hESC lines from human six-cell to eight-cell stage embryos, using naïve-state growth conditions from the beginning of derivation itself [15]. Although hPSCs in the naïve-state growth conditions are more unstable than primed-state condition, these led to an increased understanding of the pathways that are active/inactive *in vitro* and how they can be manipulated by growth factor and small molecule supplementation of media, thus underscoring the importance of hPSC culture media all the more.

The use of hPSCs in all downstream applications requires the establishment of protocols that will allow large-scale, cost-effective cultivation of cells, without compromising on their quality. It is now well known that culture conditions can affect several parameters, which are important to evaluate for stem cell engineering applications, such as gene correction or selection of genetically stable and highly pluripotent populations. Studies have shown how prolonged culture of hPSCs can introduce spontaneous mutations or genomic abnormalities, which invariably affect the purity, consistency, potency, and functional capacity of hPSCs, as they can bias or prime the cells away from their truly pluripotent state [16–21]. Suboptimal hPSC culture conditions can therefore alter their identity and their compatibility with downstream differentiation protocols. This can skew results in research for disease modeling and drug-based studies and also affect the final product that is to be used for transplantation therapy. The possibility of such alterations in hPSC quality and stability, introduced by culture media itself, raises important concerns regarding the safety and risks associated with using these cells for engineering and therapeutic applications (Figure 1).

Since hPSCs are the most powerful and promising raw material for cell engineering applications, understanding and controlling the behavior of hPSCs by optimizing the culture media, small molecules, growth factors, and microenvironment, will allow the identification of appropriate culture conditions for downstream applications such as deriving specific cell types in CRT, drug discovery, and study of human embryogenesis and disease mechanisms. This review describes different media used to maintain hPSCs in their pluripotent state, their components and functions, and advancements in the development of appropriate conditions to promote large-scale, quality-controlled expansion of hPSCs thereby increasing their potential applications.

2. Evolution of an Adherent Culture System for hPSCs

2.1. Traditional Culture System. The ICM cells, once isolated, need to be placed on suitable appropriate extracellular matrices (ECMs) and cultured in media that can support their pluripotency and maintain self-renewal. Traditionally, the blastocyst-derived cells were plated and serially propagated on mouse embryonic fibroblasts (MEFs) that are mitotically inactivated by mitomycin C treatment or gamma irradiation

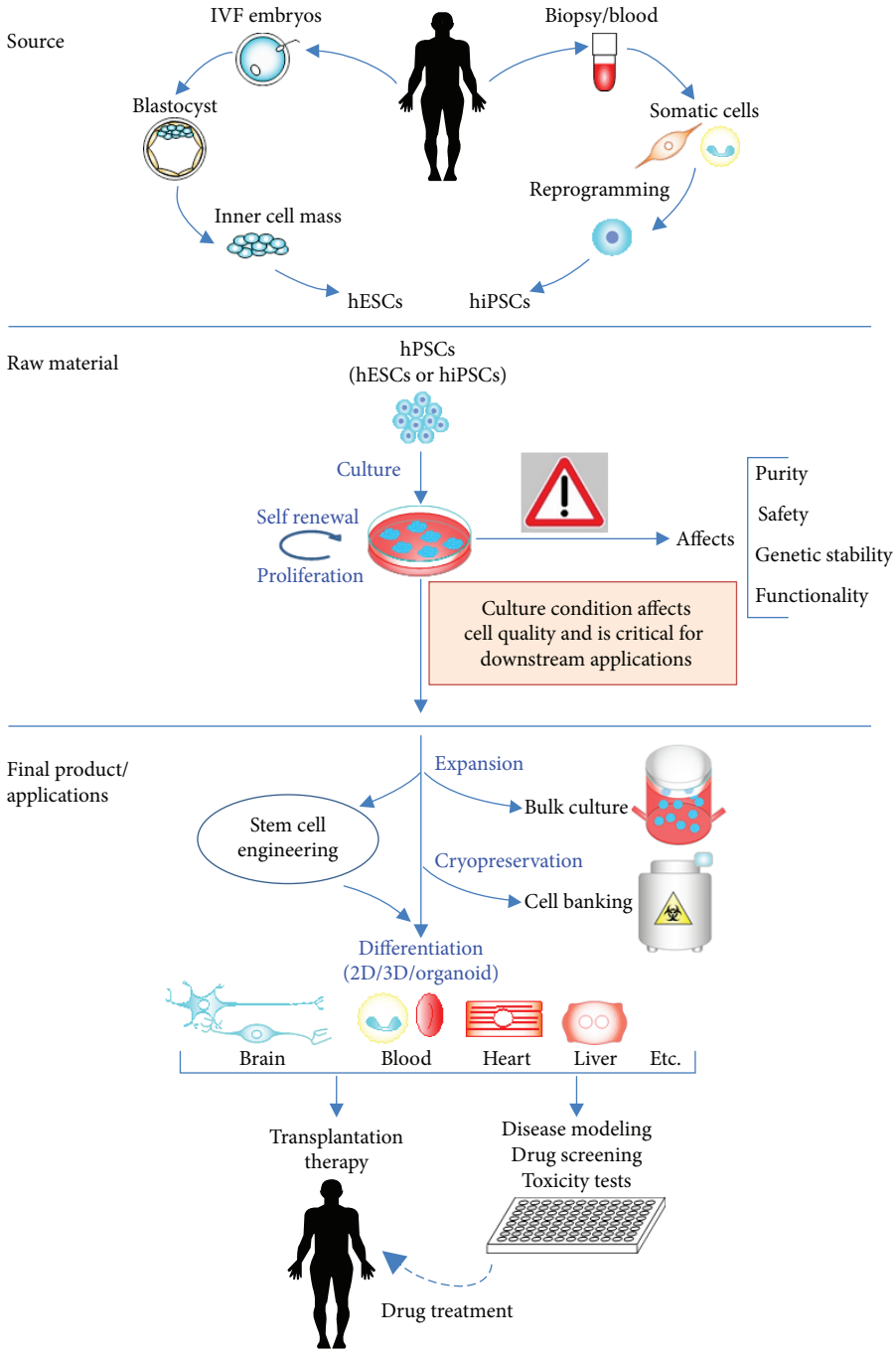

Figure 1: Importance of culture media optimization for stem cell engineering.

[6]. Studies that have analyzed fibroblast conditioned media and decellularized matrices with mass spectrometry have revealed that these feeder cells secrete essential growth factors, ECM components, and cytokines into the culture media, which support hESC growth and proliferation, such as fibroblast growth factors (FGFs), transforming growth factor-β (TGFβ), bone morphogenetic proteins (BMPs), Activin A, laminin-511, laminin-binding integrins, vitronectin, heparan sulphate proteoglycans, fibronectin, and collagen [22, 23].

However, several factors can affect the performance of feeder layers, thereby affecting the secretion of factors and deposition of ECM components, which can negatively impact the consistency of feeder-based culture. This would also limit the ability to interpret differences in the biology of hPSCs due to undefined determinants contributed by the feeder microenvironment. Moreover, feeder cells can also be a source of animal pathogens and mycoplasma contamination. In this regard, Martin et al. showed that most animal-derived products were a source of the nonhuman sialic acid Neu5Gc, which get incorporated into hESCs under standard culture conditions, and the transplantation of the same would thus induce an immune response [24]. The use

Table 1: Commonly used commercial media for feeder-free culture of hPSCs.

Medium	Components	Extracellular matrix	XF/CD	Company
mTeSR™1	DMEM/F12, BSA bFGF, TGFβ, insulin, transferrin, cholesterol, lipids, pipecolic acid, GABA, β-mercaptoethanol	Corning® Matrigel®, vitronectin	NA	STEMCELL Technologies
TeSR™2	DMEM/F12, with recombinant HSA, bFGF, TGFβ, insulin, transferrin, cholesterol, lipids, pipecolic acid, GABA, β-mercaptoethanol	Corning® Matrigel®, vitronectin	XF, CD	STEMCELL Technologies
Essential 8™	DMEM/F12 bFGF, TGFβ, insulin, transferrin, selenium, ascorbic acid	Corning® Matrigel®, vitronectin	XF, CD	Thermo Fisher Scientific
TeSR™-E8™	Based on E8 formulation	Corning® Matrigel®, vitronectin	XF, CD	STEMCELL Technologies
StemPro®	DMEM/F12, BSA bFGF, TGFβ, Activin, transferrin, LR3-IGF1, HRG1β	Geltrex®	NA	Thermo Fisher Scientific
PluriSTEM™	DMEM/F12, HSA Activin A, TGFβ1, bFGF, lipids, insulin, transferrin, selenium	Not defined	XF	Millipore

XF: xeno-free; CD: chemically defined medium; NA: not available (neither XF nor CD).

of human feeders was therefore proposed as an alternative to MEFs, in order to prevent the use of nonhuman components. While feeders from fetal human tissue seem to be the most supportive, such as feeders from human fetal muscle and skin [25], fetal foreskin [26], and fetal liver stromal cells [27], the use of aborted embryos for fetal fibroblast extraction poses ethical implications. Therefore, several other human cell types have been tested for their ability to maintain hPSC pluripotency in culture, including human adult fallopian tubal fibroblasts, bone marrow cells [28], umbilical cord [29], placental cells [30, 31], and endometrial cells [32]. Autogenic feeder layers derived from differentiated fibroblasts from the hESCs itself were another approach taken to circumvent the use of donor feeder cells altogether thereby completely eliminating the risk of allogenic pathogen contamination [33, 34]. Despite these innovative advances, it is important to realize the limitation of feeder cell-dependent culture systems, mainly owing to their lot-to-lot variability and inconsistencies between different culture batches, ultimately making them unsuitable for therapeutic applications.

2.2. Feeder-Free Culture System. The studies done using different types of feeders, the analysis of the components they produce in culture, and the comparison between different feeder types have enabled us to understand the mechanisms and pathways that are fundamental in maintaining pluripotency. To fully harness the potential of these cells, it is imperative to establish defined culture systems, which can support large-scale generation of hPSCs and their therapeutic derivatives. Since the derivation of hPSCs, several animal-derived products have been employed to provide conditions suitable for maintaining pluripotency and directing them towards differentiation. Traditionally, hPSCs have been cultured on a layer of MEFs in media supplemented with fetal bovine/calf serum (FBS or FCS) and animal-derived growth factors. The use of animal-derived components, however, raises the possibility of xeno-contamination and immune rejection. Hence, these culture systems render hPSCs unsuitable for clinical transplantation. In order to satisfy clinical-grade standards, culture systems that are completely xeno-free need to be developed without compromising on hPSC quality and quantity. Therefore, significant research has been dedicated to understanding the mechanisms that regulate pluripotency. This has led to the development of chemically synthesized xeno-free products and small molecules that allow replacement of all animal-derived components *in vitro*, while maintaining suitable culture conditions for pluripotent stem cells.

Approaches to develop feeder-free systems consisted of identifying a suitable basal medium, as well as a synthetic substrate/coating which would substitute for the defined and undefined soluble factors provided by feeders in culture. For example, Chin et al. identified nearly 30 proteins secreted by feeders derived from different sources, out of which they demonstrated the capability of six proteins in supporting hESC culture [35]. The use of MEF-conditioned media and animal-derived ECM proteins, specifically Matrigel™ (Corning), which was produced by Engelbreth-Holm-Swarm mouse sarcoma cells, or laminin, was reported to stably maintain hESCs for several passages [36]. Since then, several approaches have aimed at replacing both MEF-conditioned media with supplements or small molecules and Matrigel with purified recombinant ECM proteins [22, 37–40]. In the following sections, we discuss the key components of feeder-free media and their roles, an understanding of which is required for the development of chemically defined media.

Attempts to generate defined media for hPSCs, ensuring batch-to-batch consistency, have yielded several commercially available options for feeder-free culture, some of which are xeno-free and some that also comply with cGMP (Current Good Manufacturing Practices) (Table 1). Commonly used commercial media include mTeSR1, TeSR2, TeSR-E8, RSeT and NaïveCult (STEMCELL Technologies), StemPro, Essential 8 and StemFlex (Thermo Fisher Scientific), Pluripro (Cell Guidance Systems), PluriSTEM (Millipore), StemFit (Ajinomoto), and Nutristem (Corning). Some of these media such as TeSR2 contain human serum albumin (HSA),

whereas the more recent and widely used Essential 8 medium, which is derived from TeSR2, does not contain either HSA or bovine serum albumin (BSA) and was amongst the first to be considered truly defined media. However, most commercially available and in-house media contain expensive recombinant growth factor proteins, such as FGF2 and TGFβ/Activin A/Nodal, at varying concentrations, the functions of which will be discussed in upcoming sections.

3. Basic hPSC Culture Media Components

3.1. Basal Media. DMEM/F12 is the standard basal media used in hPSC culture, and a comparative analysis of 12 different base media did not lead to the identification of any other basal medium which performed better than DMEM/F12 even in serum-free conditions [41]. Apart from glucose, amino acids, and vitamins, which are components of DMEM/F12 itself, cholesterol, lipids, insulin, transferrin, selenium, ascorbic acid, g-aminobutyric acid (GABA), lithium chloride (LiCl), pipecolic acid, and β-mercaptoethanol (BME) are other components often included in serum-free culture media. Another component of serum-free media is L-ascorbic acid-2-phosphate, which has been included in media compositions as it enhances hPSC survival and proliferation, along with FGF2, as was shown by Furue et al. and Chen et al. [38, 41]. Cholesterol, another additive, is the precursor of a steroid hormone and a component of signaling proteins, due to which it is also included in media compositions [42]. BME which is often added in media to prevent toxicity from oxygen radicals is itself toxic to cells, and the presence of BSA in media offsets any detrimental effects from BME. Chen et al. showed that in the absence of BME, BSA was no longer necessary for hPSC media [41]. They also reported the need for selenium in media to support sustained expansion and transferrin to improve survival and cloning efficiency [41]. Selenium is also important in culture media as it has been shown to protect cells against oxidative damage by optimizing the activity of glutathione peroxidase and thioredoxin reductase, in addition to stimulating cell growth and proliferation [43].

3.2. Microenvironment of hPSC Culture. In general, hPSCs are cultured in normal atmospheric oxygen (21%), although mammalian preimplantation embryos develop in relatively hypoxic conditions in vivo, characterized by 1.5-8% oxygen tension [44]. While hESCs can be maintained reproducibly at 21% oxygen tension, several studies have provided evidence that mimicking physiological oxygen levels (~4%) is beneficial to hESCs by reducing spontaneous differentiation [45, 46] and by upregulation of genes that are known to support pluripotency of hPSCs, suggesting that some transcriptional programs in hPSCs are oxygen-sensitive [47]. In contrast, Chen et al. reported no clear benefit of culturing hESCs in 5% oxygen tension, with respect to morphology, survival, and gene expression, as long as a 7-day splitting interval was maintained [48]. However, others have also reported that low oxygen tension (2%) enhanced hESC clonal recovery and decreased the frequency of spontaneous chromosomal aberrations, without any significant changes in pluripotent marker expression [49]. Furthermore, it has also been shown that 2-5% oxygen tension increases hESC proliferation rate as well as expression of NANOG and POU5F1, the key pluripotency genes [39, 50]. A recent study interestingly reported that hypoxia could indeed influence cell fate decisions in culture, as 2% oxygen alone could reactivate expression of hESC markers in hPSC-derived differentiated cells [51]. These studies show that while hPSCs can be maintained at atmospheric oxygen tension, it may be more beneficial to lower the same to 2–5%; however, the impact is still controversial, and the effects may vary with differences in culture media, splitting intervals, and may be cell line-dependent too.

A study of the physiochemical environment of culture media showed that hESCs were better maintained when the basal media had high D-glucose concentration (4.5 g/l) and an osmolarity that mimicked the natural environment of embryonic tissue, with optimal performance obtained with 320 mOsm [52]. However, the use of 340–350 mOsm has also been reported in the development of TeSR1, mTeSR1, and E8 media [39, 41, 53].

Given the influence that pH has on every biological process and in maintaining homeostasis in vivo and *in vitro*, variations in pH affect several mechanisms within the cells and their microenvironment. The pH of the culture media is an important factor involved in maintenance of hESCs, in the successful reprogramming of somatic cells to hiPSCs, and in the induction of differentiation of hPSCs. Several cellular traits can be affected actively or passively by the pH, such as the motility, enzymatic activity, cell cycle, and apoptosis. It also affects cell motility through changes in the cytoskeletal components [54]. It has also been shown that upon reprogramming, the colonies obtained when the culture media was within pH 7.0 to 7.4 showed a compact morphology with strong alkaline phosphatase activity, whereas a slight change in pH to 7.6–7.8 made the colony morphology dispersed and flat. Similarly, when hPSCs were cultured at different pH values, morphological differences were observed at each pH, with colonies being more compact at a pH of 6.8, and as pH increased to 7.8, the cells were more dispersed and could be observed as single cells.

3.3. Serum Alternatives for hPSC Media. As the use of FBS/FCS in hESC cultures was a risk factor, other studies used human serum- (HS-) containing medium and demonstrated the ability of HS to efficiently maintain hESC pluripotency, self-renewal, and a stable karyotype for at least over 30 passages [25, 55]. Although this provided an animal-free alternative, it did not address the issue of undefined serum compositions and lot-to-lot variation, which could lead to variability in hPSC culture with respect to their ability to maintain pluripotency, self-renewal, differential potential, and a stable karyotype. These made them unsuitable for downstream therapeutic applications. One of the earliest attempts to generate a substitute for serum led to the development of the proprietary Knockout Serum Replacement (KSR) [56], now commercially available and used as a standard in media for hPSCs grown on MEFs. Amit et al.

showed that the cloning efficiency of hESCs increased by several folds in the presence of 20% KSR as compared to serum-containing medium and that hPSCs derived by serum-containing media could easily be transitioned to KSR-containing media without any compromise on self-renewal capacity or pluripotency [26]. The expression profiles of pluripotency-associated genes were observed to be similar under FBS-containing and KSR-containing media formulations [57]. It was also shown that hPSCs exhibited an increased growth rate when grown in KSR-containing medium compared to FBS-containing medium [58]. Rajala et al. tested several combinations of culture media and showed that KSR-containing medium was superior to HS containing one [59]. Other publications reported the ability of KSR to efficiently derive hPSC lines thus confirming the efficacy of KSR and its compatibility with hPSC media [30, 60].

Further, enormous efforts have been invested in finding essential factors in the serum or serum replacement to come up with a simple and defined culture condition. Supplementation of DMEM/F12 with N2 and/or B-27, in the presence of growth factors like bFGF, was shown to support prolonged self-renewal of hESCs [22, 61]. Replacement of serum and KSR with albumin, specifically HSA and BSA, in TeSR1 [39] and mTeSR1 [53], respectively, has also been widely used for hPSC cultivation. Interestingly, the addition of 0.1% HSA reportedly rescued the loss in hPSC viability caused by insulin depletion in suspension-grown hPSCs, thus demonstrating the diverse ways in which albumin can support hPSC pluripotency and viability in culture [62]. Another serum replacement product, lipid-rich BSA, known as AlbuMAX, was identified as the active ingredient and predominant lipid source in KSR [63]. It is a mixture of albumin with lipids (such as cholesterol, phospholipids, and triacylglycerides) and free fatty acids (alpha-linolenic acid, linoleic acid, oleic acid, stearic acid, and palmitic acid) [64]. It was shown that hESCs could be stably maintained in KSR-deficient media supplemented with 1% AlbuMAX and N2/B27, thus achieving a more defined media composition [63]. Another study showed how supplementation of chemically defined media (CDM) such as E8, with AlbuMAX, reduced the alterations in metabolic flux that are usually induced upon culture in CDM such as E8 [65]. Indeed, most serum replacements include albumin (such as BSA/HSA), as it is the most abundant protein in serum. The addition of albumin helps in protecting the cellular surface and stabilizing other proteins in the culture media, making it a beneficial additive in serum-free media. However, it is not an absolute requirement in hPSC media, as the commercially available media E8 does not include any albumin [41]. In this regard, Chen et al. and Yasuda et al. reported that in the absence of any serum replacement, insulin and transferrin are the two minimum required proteins in addition to growth factors and chemical compounds [41, 66]. Moreover, the purification of albumin from serum or culture supernatants (in the case of recombinant protein expression) can introduce contaminants, owing to albumin's high capacity of binding proteins, ions, chemicals, and pathogens, which are difficult to get rid of upon purification. Further studies are required to elucidate the precise roles and mechanisms by which these proteins in serum replacements maintain pluripotency and self-renewal, so that they can be replaced by defined and cost-effective chemical compounds, which could possibly make serum replacements obsolete in the future.

4. Growth Factors for hPSC Culture

4.1. Fibroblast Growth Factors (FGFs). Along with KSR, the earliest identified component that was found to contribute to stem cell pluripotency and self-renewal was basic fibroblast growth factor (bFGF or FGF2), which was shown to be endogenously produced by human feeder layers in hESC cultures [27, 43]. It was found that FGF2 was indispensable for maintaining undifferentiated proliferation of ES cells in KSR-based media [26]. Xu et al. also reported that FGF2 was essential to support undifferentiated hESC growth in serum replacement media, alone or in combination with other growth factors in the absence of feeders or conditioned media, while maintaining comparable morphology, surface marker and transcription factor expressions, karyotype, telomerase activity, and differentiation potential [67]. In feeder-free systems, it has been shown that FGF2 at a range of concentrations (4 to 100 ng/ml) was required to sustain the pluripotency of hPSCs over several passages, equivalent to conditioned media from MEFs [68]. FGF2 was found to stimulate the secretion of supportive factors from MEFs which reduced differentiation-inducing activity, and it regulated the expression of TGFβ family members, enabling them to act on hPSCs in an autocrine way to promote self-renewal [69]. cDNA microarray analyses of hESCs compared to mESCs and differentiated human cells showed the enrichment of FGF2/13 and FGFR1, 2, and 4 in PSCs [70–72]. Another group validated this with real-time PCR results confirming that FGFR1-4 were indeed expressed in hESCs with FGFR1 being the most abundant [73], while Eiselleova et al. reported that FGF2 dominantly signaled via FGFR2 [74]. Furthermore, addition of the FGFR inhibitor SU5402 led to rapid cell differentiation by suppressing the activation of downstream protein kinases and downregulating OCT3/4, thus suggesting the existence of autocrine FGF signaling in hPSC cultures [73]. Consistent with this, another report showed that the knockdown of FGF2 led to rapid differentiation in hPSCs, and the undifferentiated phenotype could not be rescued by the addition of exogenous FGF2 either. Instead, exogenous FGF2 functioned to reinforce the pluripotency maintenance program of intracrine FGF2 signaling [74]. Altogether, FGF2 promotes hPSC self-renewal and proliferation in the undifferentiated state in several ways. It binds to FGFR and activates the cascade of the mitogen-activated protein kinase (MAPK) pathway, as well as the phosphatidylinositide 3-kinases (PI3-kinase)/AKT pathway, leading to high basal levels of extracellular signal-regulated kinases (ERK) 1/2 and protein kinase B (PKB)/AKT, respectively, in hPSCs, both of which are implicated in the expression of stem cell genes and suppression of cell death and apoptosis genes [73–75]. This was confirmed by Li et al. who also showed that both mitogen-activated protein kinase (MEK)/ERK and PI3K/AKT signalings were downstream targets of

the FGF pathway, as shown by high levels of phosphorylated MEKs, ERKs, and PKB/AKT, upon FGF2 treatment of hESCs [75]. Interestingly, while the inhibition of MEK/ERK and PI3K/AKT alone or together led to the rapid loss of self-renewal capacity in hPSCs, the inhibition of only PI3K/AKT led to a significant decrease in cell proliferation and a marked increase in apoptosis, thus suggesting both common and distinct roles of these two pathways downstream of FGF signaling in hPSCs [75]. In another study, it was also shown that neurotrophins (brain-derived neurotrophic factor, neurotrophin 3, and neurotrophin 4) improve hESC survival significantly, and this effect is mediated by the PI3K pathway but not the MEK/ERK pathway [76].

As mentioned above, the MEK/ERK pathway is known as one of FGF target pathways in hPSCs. Kang et al. were amongst the first to report that FGF signaling in hESCs induced the activation of ERK (extracellular signal-regulated kinase), which in turn induced expression of c-fos, an early downstream target of the MEK/ERK1/2 pathway [77]. It was shown that MEK/ERK inhibition in hESCs by specific MEK inhibitors PD98059 and U0126, or by RNA interference, rapidly caused the loss of the undifferentiated state; however, it did not affect cell proliferation or survival, while PI3K/AKT inhibition by LY294002 induced a significant decrease in cell proliferation and increase in apoptosis [75]. These data suggest that in response to FGF, the MEK/ERK pathway supports hPSC self-renewal in cooperation with other pathways such as the PI3K/AKT pathway. The physiological role and targets of MEK/ERK in hPSCs have not yet been clarified and need to be determined. However, as a common effector downstream of both platelet-derived growth factor (PDGF) and FGF, MEK/ERK seems to be crucial for supporting pluripotency-related processes regulated by receptor tyrosine kinases (RTKs).

Heparin and heparan sulfate proteoglycans form high-affinity binding complexes with FGFs and are therefore included in media to control the activity and stability of FGFs [78]. Furue et al. showed that the addition of heparin also promoted hESC proliferation in the absence of FGF2 in a dose-dependent manner [38]. Heparin induced expression of cyclin D1, a cell cycle regulator, and also rapid phosphorylation of the FGF receptors in hESCs, in the absence of exogenous FGF2, suggesting that it helps hPSCs in stabilizing endogenously produced FGF [38]. In addition, heparin has also been found to enhance the activity of Wnt and FGF signalings in hESCs [79].

4.2. Other Ligands of Receptor Tyrosine Kinases (RTKs). A proteomic screen of MEF-conditioned media aimed at identifying candidate growth factors that support hESCs in culture showed that insulin-like growth factor (IGF), specifically IGFII, was the most abundant [80]. It has been shown previously that autologous feeder layers derived from spontaneous differentiation of hESCs into fibroblasts supported the growth of pluripotent hESCs, and these fibroblast-like differentiated hESCs expressed a higher level of FGF receptors than the undifferentiated hESCs in the same culture dish [34]. Under such culture conditions, treatment with FGF2 led to the release of IGFII and TGFβ factors from the autologous feeder cells which then acted upon the undifferentiated hESCs in a paracrine manner to promote self-renewal and pluripotency [80]. They reported that undifferentiated hESCs expressed IGF1 receptor RTK (IGF1R) which, when blocked, reduced survival and clonogenicity of hESCs, while the surrounding feeder cells expressed FGFR1 which, when blocked, led to differentiation. Their results suggested that IGFII alone could sustain hPSC growth and expansion in long-term culture, and its IGF signaling was mediated via activation of the PI3K/AKT pathway [80]. The importance of insulin in hPSC media was also confirmed by Wang et al. who showed that the IGF1R blocking antibody reduced hESC proliferation and induced differentiation, and moreover, IGF1R-specific shRNA transduced in hESCs was incapable of self-renewal in culture [81]. Other studies aimed at identifying specific factors in serum that promote the growth of hESCs showed that the lysophospholipid sphingosine 1-phosphate (S1P), together with PDGF, needs to be present to maintain hESCs in their undifferentiated state in feeder-free culture and that S1P and PDGF have an antiapoptotic effect in hESCs [82, 83]. Phosphoproteomic analysis of hESCs also revealed that the PDGF receptor RTK (PDGFR) inhibitor led to differentiation of hESCs and a decrease in expression of pluripotency markers. PDGF-AA cooperated with bFGF to stably maintain undifferentiated hESCs in culture, and it helped preserve their undifferentiated state even under suboptimal concentrations of FGF2 [84].

Furthermore, the role of RTK signaling was demonstrated in another study that investigated the contribution of epidermal growth factor receptor (EGFR) family members, in hESC culture. They found that the ERBB2/3 was expressed on hESC cells thus implying a role for its ligand neuregulin 1 (NRG1) [81]. Furthermore, inhibition of ERBB2 significantly reduced hESC proliferation and induced apoptosis in feeder-free cultures [81]. Taking into account the roles of these identified growth factors, Wang et al. assembled a simple feeder-, serum-, and KSR-free defined medium (DC-HAIF), designed to stimulate IGF1R and ERBB2/3 signalings, by incorporating neuregulin 1 (or heregulin-1β), FGF2, LR3-IGF1 (a GMP-grade recombinant human IGF1), and Activin A [81]. They showed that hESCs could be successfully and stably propagated in this media for several months with minimal spontaneous differentiation.

4.3. TGFβ Superfamily. The TGFβ superfamily consists of over 100 proteins, including the TGFβ proteins, Activin, Nodal, bone morphogenetic proteins (BMPs), and growth and differentiation factors (GDFs), all of which mediate several biological effects through receptor serine/threonine kinases, to maintain stem cell fate. Once activated by binding of TGFβ family ligands, these receptors phosphorylate and activate Smad proteins, which translocate to the nucleus, and function as transcriptional cofactors to activate target genes. Type I receptors (TGFRI), also termed Activin-like kinases (ALKs), play a central role in pluripotency, as BMP ligands and Activin/Nodal/TGFβ ligands exert their effects through receptor ALK 2/3/6 (activating SMAD 1/5/8) and ALK 4/5/7 (activating SMAD 2/3), respectively [85].

The effect of eight different growth factors on the differentiation of hESCs was evaluated by Schuldiner et al. wherein TGFβ1 did not lead to the production of transcripts in differentiated cells, thus suggesting its role in the repression of hPSC differentiation. Amit et al. showed that TGFβ1 contributed to a cocktail of growth factors that also included FGF2, to maintain the undifferentiated state of hESCs in feeder-free culture [37, 86]. It was reported that in undifferentiated cells, the TGFβ/Activin/Nodal branch was activated through the signal transducer SMAD2/3 which was achieved by addition of Activin A (25 ng/ml), and this was shown to be required downstream of canonical Wnt activation, which was necessary to maintain hPSCs [87–89]. This dependence was further confirmed by studies which showed that TGFβ/Activin/Nodal-responsive SMAD2/3 directly binds to the Nanog proximal promoter and activates its expression [90]. The requirement of Activin/Nodal signaling through SMAD2/3 activation for maintaining pluripotency was confirmed by another study as well [88], wherein inhibitors of this signaling pathway led to hPSC differentiation. However, according to this study, neither Nodal nor Activin alone was capable of sustaining long-term hPSC growth, but either of these, when combined with FGF2, helped achieve the optimal conditions for maintaining long-term hPSC pluripotency and self-renewal [88]. This was in agreement with Xu et al. who also showed that either FGF or TGFβ alone was incapable of maintaining long-term pluripotency of hESCs [91].

While Nodal and Activin A act on the same receptors and activate the same signaling mechanisms to suppress hPSC differentiation [87–89], the latter is used more often *in vitro* for cell culture due to its wider availability as a recombinant protein and comparatively lower cost. Beattie et al. also showed that Activin A was secreted by MEF feeders and enriching the culture medium with a combination of exogenous Activin A (optimum concentration determined to be 50 ng/ml), along with FGF7 (keratinocyte growth factor, 50 ng/ml) and nicotinamide (10 mM), maintained hESCs in an undifferentiated state for over 20 passages without MEF feeders or conditioned medium [92]. Removal of Activin A on the contrary led to rapid differentiation of hPSCs thereby confirming the inevitability of this growth factor in hPSC culture media [92]. A detailed study by Xiao et al. provided evidence for the first time that low concentrations of Activin A (5 ng/ml) was necessary and sufficient to support undifferentiated hESC growth on feeder-free culture (Matrigel) [40]. They also showed that Activin A induced the expression of OCT4, Nanog, Nodal, Wnt3, and FGF2 and suppressed the BMP signal, thereby reflecting its central role in maintenance of hPSC pluripotency and self-renewal [40]. Interestingly, however, Activin A has paradoxical effects on hPSCs in both maintenance of pluripotency and induction of differentiation, as Activin A-induced differentiation of hPSCs into mesoendodermal cells is well documented, wherein studies suggest that higher concentrations induce differentiation while lower concentrations are necessary for pluripotency [86, 93].

Another member of the TGFβ superfamily, BMP4, which is known to synergize with leukemia inhibitory factor (LIF) to maintain pluripotency in mESCs, has an opposite role in hPSCs. While BMP signaling maintains self-renewal in mESCs, it induces differentiation in hPSCs [94]. This was revealed through reports which showed that hESCs, grown in serum-free media supplemented with FGF2, were induced by BMP4 to differentiate into a different extraembryonic lineage, the trophoblast [95], or spontaneously differentiate into extraembryonic endoderm-like cells due to BMP2 [96]. This was confirmed by other studies in which the addition of BMP4 in the medium induced a rapid loss of pluripotency in hESCs [92], and the BMP4 antagonist Noggin (500 ng/ml) had a synergistic effect with FGF2 (40 ng/ml) in maintaining the undifferentiated state of hESCs [67, 97]. The latter group showed that BMP2 and BMP4 proteins were detected at higher levels in serum replacement-based hESC cultures, as compared to MEF-conditioned media-based cultures, which could be repressed by either a combination of Noggin and FGF2 or a high dose of FGF2 (100 ng/ml), both of which sustained long-term undifferentiated proliferation of hPSCs in feeder-free culture condition [67]. Xu et al. also showed that both TGFβ and FGF signalings synergize to antagonize BMP signaling, thereby sustaining expression of genes associated with pluripotency, such as NANOG, OCT4, and SOX2 [91]. Dorsomorphin, another small molecule included in some xeno-free media compositions, acts by inhibiting BMP signaling thereby promoting hPSC self-renewal and preventing BMP-induced differentiation in hPSCs [98, 99].

4.4. Wnt Family. Wnt signaling has been implicated in numerous functions in stem cells, and in general, they act to maintain stem cells in their undifferentiated state. Sato et al. showed that the activation of the canonical Wnt pathway was sufficient to maintain the self-renewal capacity of hESCs [71]. They reported that Wnt activation by inhibition of glycogen synthase kinase-3 (GSK-3) or addition of recombinant Wnt3a in the media promoted the growth of compact, undifferentiated hESC colonies, compared to nontreated cells. Furthermore, withdrawal of the GSK-3 inhibitor led to reversal of the pluripotent state and induced differentiation [71]. Dravid et al. on the other hand, reported that Wnt activation was not sufficient to maintain the pluripotent state of hESCs, but Wnt3a application stimulated hESC proliferation instead [100]. Cai et al. also showed that if FGF2 or MEF-conditioned media- (MEF-CM-) derived factors were absent, addition of Wnt3a or Wnt1 stimulated hESC proliferation and also differentiation [101]. In the presence of FGF2 and MEF-CM, however, Wnt can stimulate proliferation of the undifferentiated hESCs [101]. A meta-analysis of microarray data identified the Wnt receptor FZD7 to be a hESC-specific antigen, which upon knockdown led to a rapid change in morphology of cells and loss of expression of pluripotency markers, thereby suggesting the contribution of Wnt signaling to the pluripotency and self-renewal capacity of hPSCs [102]. Wnt activation in media can be achieved by using chemical GSK-3 inhibitors, which are, in increasing order of specificity, lithium chloride, 6-bromoindirubin-3′-oxime (BIO), and CHIR99021, thus eliminating the need for any xenogenic compounds for modulating Wnt signaling [103, 104]. In another study, Hasegawa et al. identified a small molecule Wnt signaling modulator,

ID-8, which along with Wnt3a completely prevented Wnt-induced differentiation without affecting proliferation and while maintaining stable hPSC survival as well [105]. Therefore, although the role of Wnt/β-catenin signaling in hPSCs is unclear and there is no consensus regarding its effect on self-renewal or differentiation, the above studies highlight how FGF2, Wnt, and TGFβ signalings collaborate to maintain hPSC self-renewal, pluripotency, and proliferation *in vitro*. In another study, it was reported that Wnt3a and FGF alone were not capable of supporting hPSC growth on feeder-free systems, but with the addition of insulin, transferrin, albumin, chemically defined cholesterol, and a proliferation-inducing ligand (April)/B cell-activating factor belonging to TNF (BAFF), a modified medium named HESCO was developed which was able to support hESC proliferation and self-renewal for over three passages [42]. Interestingly, Tsutsui et al. developed a defined culture system wherein a unique combination of molecules including bFGF, along with inhibitors against GSK, MEK, and Rho-associated kinases (ROCK), allowed long-term maintenance of hESCs through single cell passaging [106].

Recent studies have shown that Wnt/β-catenin signaling is active in the naïve state of pluripotency in hPSCs, while it is reduced or absent in the primed state. Naïve hPSCs secrete Wnts that activate Wnt/β-catenin signaling in an autocrine or paracrine manner, which promote efficient self-renewal and inhibit their transition to a primed state [107]. Inhibition of Wnt/b-catenin signaling in naïve hPSCs does not lead to differentiation, and the cells continue to express stem cell markers. Also, it induces transition towards primed like hPSC state [107].

5. Chemical Compounds

Over the past two decades, majority of hPSCs have been maintained in culture including xenobiotic components which carry a risk of contamination of immunogens or pathogens rendering those cells incompetent for regenerative medicine applications. Hence, the development of chemically defined or xeno-free systems for the hPSC culture system is necessary. To circumvent these challenges researchers have been putting efforts to develop defined conditions for hPSCs by using chemically synthesized molecules which regulate a biological process. Chemical compounds such as MEK inhibitors (PD98059 and PD0325901), GSK-3 inhibitors (Wnt signal activator) (BIO and CHIR99021), Rho-associated kinase (ROCK) inhibitor (Y-27632), FGF/RTK inhibitor (PD173074), and TGFβ/ALK inhibitor (SB431542) are commercially available and most widely used for the maintenance, proliferation, and differentiation of hPSCs. Since FGFs/RTKs, TGFβs/ALKs, and Wnts/GSK-3 signaling have been described in previous chapters, compounds widely used for regulating other signaling in hPSCs will be reviewed in this chapter.

5.1. ROCK Inhibitor. Rho-associated protein kinase (ROCK), a downstream effector of Ras homolog gene family member A (RhoA), is a kinase belonging to the family of serine/threonine kinases and is involved mainly in regulating the shape and movement of cells by acting on the cytoskeleton [108]. Poor viability of hPSCs during passage caused by apoptosis, due to actomyosin hyperactivation called blebbing [109], is an obstacle to researchers, hampering daily routine culture such as dissociation/expansion. ROCK inhibitors such as Y-27632 reduce this blebbing and minimize apoptosis, thereby enhancing the cloning efficiency after cell dissociation [110]. Studies have also shown that the ROCK inhibitor enhances the efficiency and survivability of hPSCs after freeze-thaw cycles [111, 112]. It also helps to keep hPSCs in an undifferentiated state in feeder as well as feeder-free conditions [113]. In the absence of ROCK inhibition, apoptosis can be reduced by dissociating hPSCs as cell clumps instead of single cells, while ROCK inhibitor addition at the time of passage can partially reduce the apoptosis induced during single cell dissociation. Therefore, further studies highlighting methods for reducing stress induced by dissociation into single cells even further are required for achieving maximum viability.

5.2. Compounds Used for Naïve Culture Condition. Initial attempts to derive or maintain naïve hESCs relied on the continuous ectopic expression of pluripotency genes in addition to hPSC media containing leukemia inhibitory factor (LIF) and inhibitors of both MEK and GSK-3 (termed 2i) [114–116]. However, recently, Gafni et al. developed a chemically defined media called naïve human stem cell medium (NHSM), which contained a basal media of DMEM + KSR, N2, AlbuMAX and insulin, and growth factors FGF2 and TGFβ, supplemented with 2i/LIF (described above), p38/MAPK inhibitor (SB203580), and the noncanonical Wnt/c-Jun-N-terminal kinase (JNK) inhibitor (SP600125), which was further optimized to improve cell viability by addition of the ROCK inhibitor (Y-27632) and protein kinase C (PKC) inhibitor (Gö6983) [13]. Other studies have shown, however, that minimal media consisting of bFGF, with MEK and GSK inhibitors [15], or additionally with the ROCK inhibitor and LIF [117] can support naïve pluripotency. Interestingly, [118] showed that a different cocktail of 5 inhibitors (5i) including inhibitors of MEK (PD98059), GSK (IM12), ROCK (Y-27632), BRAF (SB590885), and LCK/SRC (WH-4-023) along with LIF, bFGF, and Activin A (5i/L/F/A) was the most efficient for derivation and maintenance of naïve hPSCs. They also showed that inclusion of 20% KSR was detrimental to induction of naïve pluripotency, compared with culture in N2/B27 media, as well as supplementation with the GSK inhibitor (CHIR99021) was tricky because lower concentrations improved the maintenance of naïve pluripotency, while higher concentrations led to the opposite. The reduction in CHIR99021 concentration to 1 μM also cooperated well with MEK and PKC inhibitions, in the presence of LIF (termed t2iL + Go) for maintaining naïve pluripotency [119]. Interestingly, a recent report has shown that Wnt5A is a crucial component which, together with 2i/LIF and bFGF, promotes induction of naïve pluripotency in established hESC lines [120].

6. Extracellular Matrices

The knowledge of feeders and an understanding of the cross-talk between ECM components, cells, and media have been exploited to develop feeder-free extracellular matrices (ECMs) which mimic the conditions that feeders provided, for hPSCs while reducing the dependency on xenogeneic components. As mentioned earlier, one of the first substrates used as a feeder-free alternative was Matrigel, which is mainly composed of attachment proteins like laminin, entactin, collagen IV, and heparan sulfate proteoglycans, in addition to growth factors, and each of these individual components show varying levels of efficiency in supporting hPSC culture [36]. However, since Matrigel is derived from an animal source, it can introduce unwanted xenogeneic contaminants too, thus making this unsuitable for clinical therapies. Significant progress has been made in identifying individual ECM components such as laminin-511, fibronectin, and vitronectin in the hope of developing chemically defined and synthetic substrates. Laminin-coated surfaces are very efficient in supporting the pluripotency and proliferation of hPSCs, while collagen IV and fibronectin are not [36]. Furthermore, specific laminin isoforms show different effects as ECM substrate with isoforms -111, -332, and -511, but not -211 and -411, being able to support the attachment and proliferation of undifferentiated hPSCs. In addition, it has been shown that supportive feeder cells and hPSCs produce laminin isoforms -511/-521 and express the integrin $\alpha 6\beta 1$ receptor, the primary receptor for these laminin isoforms [121]. Since integrins are the principal molecules that mediate cell-ECM interactions, other substrates such as vitronectin, which has been shown to support hPSC self-renewal via integrin $\alpha V\beta 519$, have been developed [122]. Recombinant human laminin-511 and -521, vitronectin and E-cadherin, and their short fragments were amongst the first defined ECM substrates to be described, and they have now been routinely employed in feeder-free culture. Their use therefore represents an important milestone in hPSC culture. These led to the development of polymers, modified with synthetic peptides, such as SyntheMax [123]. However, the exact mechanisms of cell-ECM and cell-cell adhesion in hPSCs are still not clear and need to be addressed.

7. hPSC Bulk Culture Systems

For applications in engineering and medicine, hPSCs need to be generated in quantities of 10^{10} cells or more, while also adhering to cGMP guidelines and the requirements of regulations governing hPSC-based therapeutics [124, 125]. 2D adherent feeder-free culture can be "scaled-out" by multiplying the culture volume through the use of multilayered flasks, and some robotic platforms that can automate the process have been shown to provide large-scale quality-controlled manufacture of hPSCs [126, 127]. However, this method of bulk culture is still limited for commercial use by requirements of considerable space, time, cost, and operators, while also restricting online monitoring of culture parameters. This can considerably affect the reproducibility and stability of the cells in culture. Three dimensional (3D) or suspension culture in spinner flasks or Erlenmeyer flasks has been reported for bulk expansion of hPSCs [128–131], while their volume, control of culture parameters, and monitoring system may not be sufficient for hPSC applications that require large-scale production of hPSCs. Thus, bioreactors providing control over the culture environment and real-time monitoring of the system parameters need to be developed for industrial level expansion of hPSCs. In these 3D suspension culture systems, cells are cultured in the form of matrix-free hPSC clumps as aggregates or as hPSCs immobilized on microcarriers or by microencapsulation of the hPSCs. Importantly, the media used for such large-scale 3D expansion of hPSCs are based on the culture media used in 2D feeder-free systems itself, such as KSR-based media, mTeSR1, StemPro hESC SFM, and Essential 8. Defined protocols for hPSC suspension culture in mTeSR1 medium have been published and have been widely used [132, 133]. However, hPSCs cultured successfully in 2D systems in certain media may not continue to behave in the same way when cultured in the same media, in 3D suspension. This could be because certain media components may not remain stable in suspension, as shown by a recent study, where insulin was found to precipitate from commercial hPSC media (E8, TeSR-E8, mTeSR1, and StemMAXs iPS-Brew XF), only when used in a peristaltic pump circuit suspension system [62]. Interestingly, the depletion of insulin from culture media led to excessive disintegration of hPSC aggregates with subsequent loss of viability in the applied culture system, while the omission of bFGF, TGFβ1, or transferrin did not significantly hamper the morphology and viability of hPSCs. This showed how insulin was an absolute necessity for hPSC maintenance [62]. Studies such as these highlight how necessary it is to closely monitor media components while establishing automated bulk culture systems. In an interesting report by Lipsitz et al., it has been shown that the conversion of hPSCs from a primed to an alternative naïve-like state is advantageous for suspension-grown hPSCs and shifts them to a high-yield state [134]. They reported that for dynamic suspension cultures, the use of media supplemented with LIF, TGFβ1, and FGF2, including inhibitors of GSK-3 (CHIR99021), JNK (SP600125), p38/MAPK (BIRB796), and PKC (Gö6983), was the most efficient in supporting a faster growth rate and higher densities, compared to conventional hPSC media. Furthermore, they showed that the conversion of primed hPSCs to this alternative "high-suspension-yield" state in adherent culture required the MEK inhibitor (PD0325901) in addition to the above 4 inhibitors, following which when cells were transferred to suspension culture, it was essential to withdraw MEK/ERK inhibition, in order to maintain pluripotency. This shows how our understanding of the role of media components at each stage of the process can enable more efficient and cost-effective manufacturing of hPSCs for therapeutic applications. Overall, this system demonstrated how cell-state conversion induced by specific media components provided a strategy for long-term, high-density expansion of hPSCs, in scalable suspension cultures. This emphasizes the importance of culture media optimization to overcome the challenge of the low yield of hPSCs in suspension bioreactors [134].

These 3D culture systems usually consist of biomaterials to mimic the *in vivo* microenvironment and 3D niche much better than 2D systems. These biomaterials contribute to signaling within the culture and improve cellular crosstalk, thereby simulating the biophysical and biochemical properties of the native cellular niche. Therefore, such culture systems can be used to study embryogenesis and organogenesis as well as for drug toxicity and screening assays. It is worth noting that such scalable hPSC suspension cultures can also be used as a convenient starting point for inducing them to differentiate by changing hPSC expansion media to lineage-specific media [135–137]. Thus, 3D cultivation of hPSCs in bioreactors allows mass and automated production of hPSCs and their differentiated cells. Indeed, recent developments in stem cell research have led to the establishment of protocols using which hPSCs can be differentiated in suspension to various cell types and hence grown into miniorgans, termed "organoids." Organoid cultures are structures composed of thousands of cells, often coming from different lineages (that make up an organ *in vivo*), which self-assemble themselves into 3D structures, in the presence or absence of exogenous ECM substrates. This creates a dynamic microenvironment between the self-renewing and differentiating cells, providing the closest *in vitro* equivalent of the architecture of real organs. They exhibit increased functionality compared to 2D-differentiated cells and thus have wide-ranging applications in research and the clinic [138].

Various vessels and bioreactors are available for the hPSC scale-up culture system, such as the stirred tank, airlift, spinner flasks, wave-rocking, rotating wall, hollow fiber, multiplate, magnetic microcarrier, and 3D scaffold bioreactor. They consist of a glass or plastic vessel equipped with or without an impeller that ensures a homogenous growth environment by efficient mixing of the cells, nutrients, and gases, while maintaining an uplift against gravity, to keep cell aggregates or microcarriers in suspension [139, 140]. hPSCs can be inoculated as single cells or aggregates, with single cell inoculation, using the ROCK inhibitor, being better at preventing extensively large-sized aggregates that can limit nutrient diffusion [141]. Nutrient feeding can be carried out in batches or by perfusion, although the latter is reported to result in a more uniform environment enabling superior cell densities and yields [142]. The key parameters such as pH, dissolved oxygen (DO) levels, fluid shear stress, growth factors, nutrients, and metabolite concentrations in hPSC scale-up culture are precisely and carefully controlled to ensure a uniform environment with adequate nutrient levels and oxygenation [129].

Using coated microcarrier beads in bioreactors can be considered as a practical option. Several studies have demonstrated that using microcarriers such as polystyrene coated with laminin and vitronectin, vitronectin and HSA further treated with UV, or those that are positively charged with cellulose achieve high attachment efficiencies and viability even at the high confluency, while also reducing consumption of media and growth factors owing to their adjustable growth surface area [143–146]. Beads with multiple pores give a much larger surface area for cell adhesion and gas diffusion, than flat 2D culture, while the adherent hPSCs on/in the beads may be very similar to what is obtained in traditional 2D culture [147]. Lastly, microencapsulation of hPSCs in hydrogels, such as calcium alginate capsules, has been developed as a technique to minimize excessive clumping in suspension culture, as well as improve cell recovery rates after cryopreservation [148]. Although this method offers increased cell protection, it is limited by reduced diffusion of gases and nutrients through the capsule, plus the requirement of decapsulation for cell harvest. Thus, 3D cell culture systems can offer substantial benefits for hPSC culture and are an attractive platform for manufacture of cellular products, due to their scalability, ease of monitoring, and convenient cell feeding and harvesting options. However, certain important issues, such as controlling growth rate, aggregate size, differentiation pressure, and ensuring genomic stability, need to be addressed before they can be approved for clinical applications [149].

8. Conclusion

The growth and advancement in the applications of hESC/hiPSC technology have been accompanied by a huge body of work dedicated to optimizing and standardizing hPSC culture. Optimization of culture systems is not only limited to defining culture media components but also the extracellular matrices, environmental cues, and modes of passaging. As discussed above, this has led to the development of simple and defined culture conditions and also facilitated the development of 3D and bulk cell culture systems. Chemically defined media are ideal for minimizing lot-to-lot variation and ensure consistency, for both research-based and clinical applications, while xeno-free and cGMP-compliant culture systems are preferred for cellular transplantation. Efforts in this direction have largely focused on understanding the signaling molecules required, replacing nonhuman components of media and developing synthetic substrates, which have an immediate application in disease modelling and can eventually be used to engineer cells and their substrates for therapeutic applications.

The recent findings about the isolation and maintenance of naïve hPSCs have given immense insight into early human development, but it is yet to be determined how relevant these different states of pluripotency are, with respect to downstream engineering applications in research and therapy. As such, future platforms should ideally attempt to be adaptable for the bioprocessing of both naïve and primed hPSCs.

With stem cell therapies becoming a reality, through the approval of human trials, preventing any alterations in the cellular state and identity is of paramount importance. As new therapies emerge, questions about the safety and efficacy of the cellular products will also rise. Studies have revealed the heterogeneity of hPSCs in culture, and some procedures to isolate and propagate homogenous hPSC clones have been described. Nevertheless, clearer and more stringent regulations need to define how to maintain cellular homogeneity in scalable culture systems. It is important to note that one of the obstacles in the implantation of hPSC-based therapies is the risk of tumorigenicity, owing to the intrinsic properties of unlimited self-renewal and expansion of hPSCs. However,

in addition to the in vivo effects, prolonged periods of *in vitro* expansion required for cell therapy itself can lead to stochastic generation of chromosomal aberrations which can then accumulate rapidly through positive selection pressure. Such culture adaptations by cells precede the highly undesirable build-up of gross genomic abnormalities, characteristic of certain high passage number hPSC lines. Therefore, along with the establishment of bulk culture systems, the validation of assays that can efficiently and reproducibly monitor growth conditions, cellular stress, spontaneous differentiation signals, gene expression profiles, and chromosomal integrity during production, processing, and storage of hPSCs is absolutely vital to the success of all downstream applications. Future research should address these challenges by establishing protocols for providing robust, stable, and homogenous cell populations as raw material.

Another potential challenge lies in determining the long-term effects of major media used for propagation of hPSCs in large-scale culture systems and addressing the costs associated with maintenance of these systems. The economics of hPSC processing are as important to address, as are the concerns with their safety and functionality in patients. Costs associated with media components have been largely reduced with an improved understanding of their functions and the subsequent discovery of small molecules which can substitute for the expensive growth factors and cytokines, as discussed above. Apart from making media cost-effective, it has also led to the media being more defined, hence increasing their reproducibility.

There are now multidisciplinary approaches available for the derivation and culture of different stages of pluripotency, development of xeno-free culture conditions as well as the generation of GMP-compatible protocols, which would help standardize and streamline the process on a commercial scale. The amalgamation of 3D culture systems, chemically defined media, and synthetic biomaterials mimicking ECMs shows enormous potential in improving propagation, safety, and functionality of stem cells for various applications.

The derivation and maintenance of the raw material, hPSCs, including both hESCs and hiPSCs, have to be done in a manner that recapitulates their equivalent niche in vivo; therefore, the media in which these cells are cultured in are central to the success of all downstream applications. Therefore, as a starting point, it is necessary to understand the media components and their roles in regulating the self-renewal, proliferation, survival, stability, and functionality of hPSCs as this is a critical step in ensuring large-scale, safe, reproducible, and quality-controlled expansion of hPSCs for use in stem cell engineering.

Conflicts of Interest

The authors declare that they have no conflicts of interest.

References

[1] L. C. Stevens and C. C. Little, "Spontaneous testicular teratomas in an inbred strain of mice," *Proceedings of the National Academy of Sciences*, vol. 40, no. 11, pp. 1080–1087, 1954.

[2] P. GB Jr, D. FJ Jr, and V. EL, "Teratocarcinogenic and tissue-forming potentials of the cell types comprising neoplastic embryoid bodies," *Laboratory Investigation*, vol. 9, pp. 583–602, 1960.

[3] G. B. Pierce and T. F. Beals, "The ultrastructure of primordial germinal cells of the fetal testes and of embryonal carcinoma cells of mice," *Cancer Research*, vol. 24, 1964.

[4] G. R. Martin, "Isolation of a pluripotent cell line from early mouse embryos cultured in medium conditioned by teratocarcinoma stem cells," *Proceedings of the National Academy of Sciences*, vol. 78, no. 12, pp. 7634–7638, 1981.

[5] M. J. Evans and M. H. Kaufman, "Establishment in culture of pluripotential cells from mouse embryos," *Nature*, vol. 292, no. 5819, pp. 154–156, 1981.

[6] G. R. Martin and M. J. Evans, "Differentiation of clonal lines of teratocarcinoma cells: formation of embryoid bodies in vitro," *Proceedings of the National Academy of Sciences*, vol. 72, no. 4, pp. 1441–1445, 1975.

[7] J. A. Thomson, J. Kalishman, T. G. Golos et al., "Isolation of a primate embryonic stem cell line," *Proceedings of the National Academy of Sciences*, vol. 92, no. 17, pp. 7844–7848, 1995.

[8] K. Takahashi, K. Tanabe, M. Ohnuki et al., "Induction of pluripotent stem cells from adult human fibroblasts by defined factors," *Cell*, vol. 131, no. 5, pp. 861–872, 2007.

[9] I. G. M. Brons, L. E. Smithers, M. W. B. Trotter et al., "Derivation of pluripotent epiblast stem cells from mammalian embryos," *Nature*, vol. 448, no. 7150, pp. 191–195, 2007.

[10] J. Nichols and A. Smith, "Naive and primed pluripotent states," *Cell Stem Cell*, vol. 4, no. 6, pp. 487–492, 2009.

[11] P. J. Tesar, J. G. Chenoweth, F. A. Brook et al., "New cell lines from mouse epiblast share defining features with human embryonic stem cells," *Nature*, vol. 448, no. 7150, pp. 196–199, 2007.

[12] S. Warrier, M. van der Jeught, G. Duggal et al., "Direct comparison of distinct naive pluripotent states in human embryonic stem cells," *Nature Communications*, vol. 8, p. 15055, 2017.

[13] O. Gafni, L. Weinberger, A. A. F. Mansour et al., "Derivation of novel human ground state naive pluripotent stem cells," *Nature*, vol. 504, no. 7479, pp. 282–286, 2013.

[14] H. Sperber, J. Mathieu, Y. Wang et al., "The metabolome regulates the epigenetic landscape during naive-to-primed human embryonic stem cell transition," *Nature Cell Biology*, vol. 17, no. 12, pp. 1523–1535, 2015.

[15] C. B. Ware, A. M. Nelson, B. Mecham et al., "Derivation of naive human embryonic stem cells," *Proceedings of the National Academy of Sciences*, vol. 111, no. 12, pp. 4484–4489, 2014.

[16] N. Hyka-Nouspikel, J. Desmarais, P. J. Gokhale et al., "Deficient DNA damage response and cell cycle checkpoints lead to accumulation of point mutations in human embryonic stem cells," *Stem Cells*, vol. 30, no. 9, pp. 1901–1910, 2012.

[17] Y. Mayshar, U. Ben-David, N. Lavon et al., "Identification and classification of chromosomal aberrations in human induced pluripotent stem cells," *Cell Stem Cell*, vol. 7, no. 4, pp. 521–531, 2010.

[18] C. Spits, I. Mateizel, M. Geens et al., "Recurrent chromosomal abnormalities in human embryonic stem cells," *Nature Biotechnology*, vol. 26, no. 12, pp. 1361–1363, 2008.

[19] M. H. Stewart, M. Bossé, K. Chadwick, P. Menendez, S. C. Bendall, and M. Bhatia, "Clonal isolation of hESCs reveals

heterogeneity within the pluripotent stem cell compartment," *Nature Methods*, vol. 3, no. 10, pp. 807–815, 2006.

[20] E. Vanneste, T. Voet, C. le Caignec et al., "Chromosome instability is common in human cleavage-stage embryos," *Nature Medicine*, vol. 15, no. 5, pp. 577–583, 2009.

[21] T. E. Werbowetski-Ogilvie, M. Bossé, M. Stewart et al., "Characterization of human embryonic stem cells with features of neoplastic progression," *Nature Biotechnology*, vol. 27, no. 1, pp. 91–97, 2009.

[22] S. Yao, S. Chen, J. Clark et al., "Long-term self-renewal and directed differentiation of human embryonic stem cells in chemically defined conditions," *Proceedings of the National Academy of Sciences*, vol. 103, no. 18, pp. 6907–6912, 2006.

[23] P. B. Yu, D. Y. Deng, C. S. Lai et al., "BMP type I receptor inhibition reduces heterotopic ossification," *Nature Medicine*, vol. 14, no. 12, pp. 1363–1369, 2008.

[24] M. J. Martin, A. Muotri, F. Gage, and A. Varki, "Human embryonic stem cells express an immunogenic nonhuman sialic acid," *Nature Medicine*, vol. 11, no. 2, pp. 228–232, 2005.

[25] M. Richards, C.-Y. Fong, W.-K. Chan, P.-C. Wong, and A. Bongso, "Human feeders support prolonged undifferentiated growth of human inner cell masses and embryonic stem cells," *Nature Biotechnology*, vol. 20, no. 9, pp. 933–936, 2002.

[26] M. Amit, M. K. Carpenter, M. S. Inokuma et al., "Clonally derived human embryonic stem cell lines maintain pluripotency and proliferative potential for prolonged periods of culture," *Developmental Biology*, vol. 227, no. 2, pp. 271–278, 2000.

[27] J. Xi, Y. Wang, P. Zhang et al., "Human fetal liver stromal cells that overexpress bFGF support growth and maintenance of human embryonic stem cells," *PLoS One*, vol. 5, no. 12, article e14457, 2010.

[28] L. Cheng, H. Hammond, Z. Ye, X. Zhan, and G. Dravid, "Human adult marrow cells support prolonged expansion of human embryonic stem cells in culture," *Stem Cells*, vol. 21, no. 2, pp. 131–142, 2003.

[29] M. Cho, E. J. Lee, H. Nam et al., "Human feeder layer system derived from umbilical cord stromal cells for human embryonic stem cells," *Fertility and Sterility*, vol. 93, no. 8, pp. 2525–2531, 2010.

[30] O. Genbacev, A. Krtolica, T. Zdravkovic et al., "Serum-free derivation of human embryonic stem cell lines on human placental fibroblast feeders," *Fertility and Sterility*, vol. 83, no. 5, pp. 1517–1529, 2005.

[31] K. Miyamoto, K. Hayashi, T. Suzuki et al., "Human placenta feeder layers support undifferentiated growth of primate embryonic stem cells," *Stem Cells*, vol. 22, no. 4, pp. 433–440, 2004.

[32] Y. Gao, S. Li, and Q. Li, "Uterine epithelial cell proliferation and endometrial hyperplasia: evidence from a mouse model," *Molecular Human Reproduction*, vol. 20, no. 8, pp. 776–786, 2014.

[33] A. Choo, A. S. Ngo, V. Ding, S. Oh, and L. S. Kiang, "Autogeneic feeders for the culture of undifferentiated human embryonic stem cells in feeder and feeder-free conditions," in *Methods in Cell Biology*, vol. 86, pp. 15–28, Elsevier, 2008.

[34] P. Stojkovic, M. Lako, R. Stewart et al., "An autogeneic feeder cell system that efficiently supports growth of undifferentiated human embryonic stem cells," *Stem Cells*, vol. 23, no. 3, pp. 306–314, 2005.

[35] A. C. P. Chin, W. J. Fong, L.-T. Goh, R. Philp, S. K. W. Oh, and A. B. H. Choo, "Identification of proteins from feeder conditioned medium that support human embryonic stem cells," *Journal of Biotechnology*, vol. 130, no. 3, pp. 320–328, 2007.

[36] C. Xu, M. S. Inokuma, J. Denham et al., "Feeder-free growth of undifferentiated human embryonic stem cells," *Nature Biotechnology*, vol. 19, no. 10, pp. 971–974, 2001.

[37] M. Amit, C. Shariki, V. Margulets, and J. Itskovitz-Eldor, "Feeder layer- and serum-free culture of human embryonic stem cells," *Biology of Reproduction*, vol. 70, no. 3, pp. 837–845, 2004.

[38] M. K. Furue, J. Na, J. P. Jackson et al., "Heparin promotes the growth of human embryonic stem cells in a defined serum-free medium," *Proceedings of the National Academy of Sciences*, vol. 105, no. 36, pp. 13409–13414, 2008.

[39] T. E. Ludwig, M. E. Levenstein, J. M. Jones et al., "Derivation of human embryonic stem cells in defined conditions," *Nature Biotechnology*, vol. 24, no. 2, pp. 185–187, 2006.

[40] L. Xiao, X. Yuan, and S. J. Sharkis, "Activin A maintains self-renewal and regulates fibroblast growth factor, Wnt, and bone morphogenic protein pathways in human embryonic stem cells," *Stem Cells*, vol. 24, no. 6, pp. 1476–1486, 2006.

[41] G. Chen, D. R. Gulbranson, Z. Hou et al., "Chemically defined conditions for human iPSC derivation and culture," *Nature Methods*, vol. 8, no. 5, pp. 424–429, 2011.

[42] J. Lu, R. Hou, C. J. Booth, S.-H. Yang, and M. Snyder, "Defined culture conditions of human embryonic stem cells," *Proceedings of the National Academy of Sciences*, vol. 103, no. 15, pp. 5688–5693, 2006.

[43] Y.-G. Park, S. E. Lee, E. Y. Kim et al., "Effects of feeder cell types on culture of mouse embryonic stem cell *in vitro*," *Development & Reproduction*, vol. 19, no. 3, pp. 119–126, 2015.

[44] B. Fischer and B. D. Bavister, "Oxygen tension in the oviduct and uterus of rhesus monkeys, hamsters and rabbits," *Reproduction*, vol. 99, no. 2, pp. 673–679, 1993.

[45] T. Ezashi, P. Das, and R. M. Roberts, "Low O2 tensions and the prevention of differentiation of hES cells," *Proceedings of the National Academy of Sciences*, vol. 102, no. 13, pp. 4783–4788, 2005.

[46] V. Zachar, S. M. Prasad, S. C. Weli et al., "The effect of human embryonic stem cells (hESCs) long-term normoxic and hypoxic cultures on the maintenance of pluripotency," *In Vitro Cellular & Developmental Biology - Animal*, vol. 46, no. 3-4, pp. 276–283, 2010.

[47] S. D. Westfall, S. Sachdev, P. Das et al., "Identification of oxygen-sensitive transcriptional programs in human embryonic stem cells," *Stem Cells and Development*, vol. 17, no. 5, pp. 869–882, 2008.

[48] H.-F. Chen, H.-C. Kuo, W. Chen, F.-C. Wu, Y.-S. Yang, and H.-N. Ho, "A reduced oxygen tension (5%) is not beneficial for maintaining human embryonic stem cells in the undifferentiated state with short splitting intervals," *Human Reproduction*, vol. 24, no. 1, pp. 71–80, 2008.

[49] N. R. Forsyth, A. Musio, P. Vezzoni, A. H. R. W. Simpson, B. S. Noble, and J. McWhir, "Physiologic oxygen enhances human embryonic stem cell clonal recovery and reduces chromosomal abnormalities," *Cloning and Stem Cells*, vol. 8, no. 1, pp. 16–23, 2006.

[50] C. E. Forristal, K. L. Wright, N. A. Hanley, R. O. C. Oreffo, and F. D. Houghton, "Hypoxia inducible factors regulate pluripotency and proliferation in human embryonic stem cells cultured at reduced oxygen tensions," *Reproduction*, vol. 139, no. 1, pp. 85–97, 2010.

[51] J. Mathieu, Z. Zhang, A. Nelson et al., "Hypoxia induces re-entry of committed cells into pluripotency: hypoxia controls cell fate decision," *Stem Cells*, vol. 31, no. 9, pp. 1737–1748, 2013.

[52] K. Rajala, H. Vaajasaari, R. Suuronen, O. Hovatta, and H. Skottman, "Effects of the physiochemical culture environment on the stemness and pluripotency of human embryonic stem cells," *Stem Cell Studies*, vol. 1, no. 1, p. 3, 2011.

[53] T. E. Ludwig, V. Bergendahl, M. E. Levenstein, J. Yu, M. D. Probasco, and J. A. Thomson, "Feeder-independent culture of human embryonic stem cells," *Nature Methods*, vol. 3, no. 8, pp. 637–646, 2006.

[54] N. Kim, N. Minami, M. Yamada, and H. Imai, "Immobilized pH in culture reveals an optimal condition for somatic cell reprogramming and differentiation of pluripotent stem cells," *Reproductive Medicine and Biology*, vol. 16, no. 1, pp. 58–66, 2017.

[55] C. Ellerström, R. Strehl, K. Moya et al., "Derivation of a xeno-free human embryonic stem cell line," *Stem Cells*, vol. 24, no. 10, pp. 2170–2176, 2006.

[56] P. J. Price, M. D. Goldsborough, and M. L. Tilkins, "Embryonic stem cell serum replacement," 1998, Patent CA2277278A1.

[57] H. Skottman, M. S. Dilber, and O. Hovatta, "The derivation of clinical-grade human embryonic stem cell lines," *FEBS Letters*, vol. 580, no. 12, pp. 2875–2878, 2006.

[58] H. Koivisto, M. Hyvärinen, A. M. Strömberg et al., "Cultures of human embryonic stem cells: serum replacement medium or serum-containing media and the effect of basic fibroblast growth factor," *Reproductive Biomedicine Online*, vol. 9, no. 3, pp. 330–337, 2004.

[59] K. Rajala, H. Hakala, S. Panula et al., "Testing of nine different xeno-free culture media for human embryonic stem cell cultures," *Human Reproduction*, vol. 22, no. 5, pp. 1231–1238, 2007.

[60] J. Inzunza, S. Sahlén, K. Holmberg et al., "Comparative genomic hybridization and karyotyping of human embryonic stem cells reveals the occurrence of an isodicentric X chromosome after long-term cultivation," *Molecular Human Reproduction*, vol. 10, no. 6, pp. 461–466, 2004.

[61] Y. Liu, Z. Song, Y. Zhao et al., "A novel chemical-defined medium with bFGF and N2B27 supplements supports undifferentiated growth in human embryonic stem cells," *Biochemical and Biophysical Research Communications*, vol. 346, no. 1, pp. 131–139, 2006.

[62] D. Massai, E. Bolesani, D. R. Diaz et al., "Sensitivity of human pluripotent stem cells to insulin precipitation induced by peristaltic pump-based medium circulation: considerations on process development," *Scientific Reports*, vol. 7, no. 1, p. 3950, 2017.

[63] F. R. Garcia-Gonzalo and J. C. Izpisúa Belmonte, "Albumin-associated lipids regulate human embryonic stem cell self-renewal," *PLoS One*, vol. 3, no. 1, article e1384, 2008.

[64] Thermo Fisher Scientific Inc., "AlbuMAX® I and AlbuMAX® II," Thermo Fisher Scientific Inc. https://assets.thermofisher.com/TFS-Assets/LSG/manuals/3117.pdf.

[65] H. Zhang, M. G. Badur, A. S. Divakaruni et al., "Distinct metabolic states can support self-renewal and lipogenesis in human pluripotent stem cells under different culture conditions," *Cell Reports*, vol. 16, no. 6, pp. 1536–1547, 2016.

[66] S. Yasuda, T. Ikeda, H. Shahsavarani et al., "Chemically defined and growth-factor-free culture system for the expansion and derivation of human pluripotent stem cells," *Nature Biomedical Engineering*, vol. 2, no. 3, pp. 173–182, 2018.

[67] C. Xu, E. Rosler, J. Jiang et al., "Basic fibroblast growth factor supports undifferentiated human embryonic stem cell growth without conditioned medium," *Stem Cells*, vol. 23, no. 3, pp. 315–323, 2005.

[68] M. E. Levenstein, T. E. Ludwig, R. H. Xu et al., "Basic fibroblast growth factor support of human embryonic stem cell self-renewal," *Stem Cells*, vol. 24, no. 3, pp. 568–574, 2006.

[69] B. Greber, H. Lehrach, and J. Adjaye, "Fibroblast growth factor 2 modulates transforming growth factor β signaling in mouse embryonic fibroblasts and human ESCs (hESCs) to support hESC self-renewal," *Stem Cells*, vol. 25, no. 2, pp. 455–464, 2007.

[70] I. Ginis, Y. Luo, T. Miura et al., "Differences between human and mouse embryonic stem cells," *Developmental Biology*, vol. 269, no. 2, pp. 360–380, 2004.

[71] N. Sato, I. M. Sanjuan, M. Heke, M. Uchida, F. Naef, and A. H. Brivanlou, "Molecular signature of human embryonic stem cells and its comparison with the mouse," *Developmental Biology*, vol. 260, no. 2, pp. 404–413, 2003.

[72] J. M. Sperger, X. Chen, J. S. Draper et al., "Gene expression patterns in human embryonic stem cells and human pluripotent germ cell tumors," *Proceedings of the National Academy of Sciences*, vol. 100, no. 23, pp. 13350–13355, 2003.

[73] P. Dvorak, D. Dvorakova, S. Koskova et al., "Expression and potential role of fibroblast growth factor 2 and its receptors in human embryonic stem cells," *Stem Cells*, vol. 23, no. 8, pp. 1200–1211, 2005.

[74] L. Eiselleova, K. Matulka, V. Kriz et al., "A complex role for FGF-2 in self-renewal, survival, and adhesion of human embryonic stem cells," *Stem Cells*, vol. 27, no. 8, pp. 1847–1857, 2009.

[75] J. Li, G. Wang, C. Wang et al., "MEK/ERK signaling contributes to the maintenance of human embryonic stem cell self-renewal," *Differentiation*, vol. 75, no. 4, pp. 299–307, 2007.

[76] A. D. Pyle, L. F. Lock, and P. J. Donovan, "Neurotrophins mediate human embryonic stem cell survival," *Nature Biotechnology*, vol. 24, no. 3, pp. 344–350, 2006.

[77] H. B. Kang, J. S. Kim, H. J. Kwon et al., "Basic fibroblast growth factor activates ERK and induces c-Fos in human embryonic stem cell line MizhES1," *Stem Cells and Development*, vol. 14, no. 4, pp. 395–401, 2005.

[78] M. W. Pantoliano, R. A. Horlick, B. A. Springer et al., "Multivalent ligand-receptor binding interactions in the fibroblast growth factor system produce a cooperative growth factor and heparin mechanism for receptor dimerization," *Biochemistry*, vol. 33, no. 34, pp. 10229–10248, 1994.

[79] N. Sasaki, K. Okishio, K. Ui-Tei et al., "Heparan sulfate regulates self-renewal and pluripotency of embryonic stem cells," *The Journal of Biological Chemistry*, vol. 283, no. 6, pp. 3594–3606, 2008.

[80] S. C. Bendall, M. H. Stewart, P. Menendez et al., "IGF and FGF cooperatively establish the regulatory stem cell niche of pluripotent human cells in vitro," *Nature*, vol. 448, no. 7157, pp. 1015–1021, 2007.

[81] L. Wang, T. C. Schulz, E. S. Sherrer et al., "Self-renewal of human embryonic stem cells requires insulin-like growth factor-1 receptor and ERBB2 receptor signaling," *Blood*, vol. 110, no. 12, pp. 4111–4119, 2007.

[82] A. Pébay, R. C. B. Wong, S. M. Pitson et al., "Essential roles of sphingosine-1-phosphate and platelet-derived growth factor in the maintenance of human embryonic stem cells," *Stem Cells*, vol. 23, no. 10, pp. 1541–1548, 2005.

[83] R. C. B. Wong, I. Tellis, P. Jamshidi, M. Pera, and A. Pébay, "Anti-apoptotic effect of sphingosine-1-phosphate and platelet-derived growth factor in human embryonic stem cells," *Stem Cells and Development*, vol. 16, no. 6, pp. 989–1002, 2007.

[84] L. M. Brill, W. Xiong, K. B. Lee et al., "Phosphoproteomic analysis of human embryonic stem cells," *Cell Stem Cell*, vol. 5, no. 2, pp. 204–213, 2009.

[85] K.-S. Park, "TGF-beta family signaling in embryonic stem cells," *International Journal of Stem Cells*, vol. 4, no. 1, pp. 18–23, 2011.

[86] M. Schuldiner, O. Yanuka, J. Itskovitz-Eldor, D. A. Melton, and N. Benvenisty, "Effects of eight growth factors on the differentiation of cells derived from human embryonic stem cells," *Proceedings of the National Academy of Sciences*, vol. 97, no. 21, pp. 11307–11312, 2000.

[87] D. James, A. J. Levine, D. Besser, and A. Hemmati-Brivanlou, "TGFβ/activin/nodal signaling is necessary for the maintenance of pluripotency in human embryonic stem cells," *Development*, vol. 132, no. 6, pp. 1273–1282, 2005.

[88] L. Vallier, "Activin/Nodal and FGF pathways cooperate to maintain pluripotency of human embryonic stem cells," *Journal of Cell Science*, vol. 118, no. 19, pp. 4495–4509, 2005.

[89] L. Vallier, D. Reynolds, and R. A. Pedersen, "Nodal inhibits differentiation of human embryonic stem cells along the neuroectodermal default pathway," *Developmental Biology*, vol. 275, no. 2, pp. 403–421, 2004.

[90] L. Vallier, S. Mendjan, S. Brown et al., "Activin/Nodal signalling maintains pluripotency by controlling Nanog expression," *Development*, vol. 136, no. 8, pp. 1339–1349, 2009.

[91] R.-H. Xu, T. L. Sampsell-Barron, F. Gu et al., "NANOG is a direct target of TGFβ/Activin-mediated SMAD signaling in human ESCs," *Cell Stem Cell*, vol. 3, no. 2, pp. 196–206, 2008.

[92] G. M. Beattie, A. D. Lopez, N. Bucay et al., "Activin A maintains pluripotency of human embryonic stem cells in the absence of feeder layers," *Stem Cells*, vol. 23, no. 4, pp. 489–495, 2005.

[93] T. Watabe and K. Miyazono, "Roles of TGF-β family signaling in stem cell renewal and differentiation," *Cell Research*, vol. 19, no. 1, pp. 103–115, 2009.

[94] Z. Li and Y.-G. Chen, "Functions of BMP signaling in embryonic stem cell fate determination," *Experimental Cell Research*, vol. 319, no. 2, pp. 113–119, 2013.

[95] R.-H. Xu, X. Chen, D. S. Li et al., "BMP4 initiates human embryonic stem cell differentiation to trophoblast," *Nature Biotechnology*, vol. 20, no. 12, pp. 1261–1264, 2002.

[96] M. F. Pera, "Regulation of human embryonic stem cell differentiation by BMP-2 and its antagonist noggin," *Journal of Cell Science*, vol. 117, no. 7, pp. 1269–1280, 2004.

[97] G. Wang, H. Zhang, Y. Zhao et al., "Noggin and bFGF cooperate to maintain the pluripotency of human embryonic stem cells in the absence of feeder layers," *Biochemical and Biophysical Research Communications*, vol. 330, no. 3, pp. 934–942, 2005.

[98] R. Gonzalez, J. W. Lee, E. Y. Snyder, and P. G. Schultz, "Dorsomorphin promotes human embryonic stem cell self-renewal," *Angewandte Chemie*, vol. 123, no. 15, pp. 3501–3503, 2011.

[99] P. B. Yu, C. C. Hong, C. Sachidanandan et al., "Dorsomorphin inhibits BMP signals required for embryogenesis and iron metabolism," *Nature Chemical Biology*, vol. 4, no. 1, pp. 33–41, 2008.

[100] G. Dravid, Z. Ye, H. Hammond et al., "Defining the role of Wnt/β-catenin signaling in the survival, proliferation, and self-renewal of human embryonic stem cells," *Stem Cells*, vol. 23, no. 10, pp. 1489–1501, 2005.

[101] L. Cai, Z. Ye, B. Y. Zhou, P. Mali, C. Zhou, and L. Cheng, "Promoting human embryonic stem cell renewal or differentiation by modulating Wnt signal and culture conditions," *Cell Research*, vol. 17, no. 1, pp. 62–72, 2007.

[102] K. Melchior, J. Weiß, H. Zaehres et al., "The WNT receptor FZD7 contributes to self-renewal signaling of human embryonic stem cells," *Biological Chemistry*, vol. 389, no. 7, pp. 897–903, 2008.

[103] O. Naujok, J. Lentes, U. Diekmann, C. Davenport, and S. Lenzen, "Cytotoxicity and activation of the Wnt/beta-catenin pathway in mouse embryonic stem cells treated with four GSK3 inhibitors," *BMC Research Notes*, vol. 7, no. 1, p. 273, 2014.

[104] Y. Wu, Z. Ai, K. Yao et al., "CHIR99021 promotes self-renewal of mouse embryonic stem cells by modulation of protein-encoding gene and long intergenic non-coding RNA expression," *Experimental Cell Research*, vol. 319, no. 17, pp. 2684–2699, 2013.

[105] K. Hasegawa, S. Y. Yasuda, J. L. Teo et al., "Wnt signaling orchestration with a small molecule DYRK inhibitor provides long-term xeno-free human pluripotent cell expansion," *Stem Cells Translational Medicine*, vol. 1, no. 1, pp. 18–28, 2012.

[106] H. Tsutsui, B. Valamehr, A. Hindoyan et al., "An optimized small molecule inhibitor cocktail supports long-term maintenance of human embryonic stem cells," *Nature Communications*, vol. 2, no. 1, p. 167, 2011.

[107] Z. Xu, A. M. Robitaille, J. D. Berndt et al., "Wnt/β-catenin signaling promotes self-renewal and inhibits the primed state transition in naïve human embryonic stem cells," *Proceedings of the National Academy of Sciences*, vol. 113, no. 42, pp. E6382–E6390, 2016.

[108] T. Ishizaki, M. Uehata, I. Tamechika et al., "Pharmacological properties of Y-27632, a specific inhibitor of rho-associated kinases," *Molecular Pharmacology*, vol. 57, no. 5, pp. 976–983, 2000.

[109] M. Ohgushi, M. Matsumura, M. Eiraku et al., "Molecular pathway and cell state responsible for dissociation-induced apoptosis in human pluripotent stem cells," *Cell Stem Cell*, vol. 7, no. 2, pp. 225–239, 2010.

[110] K. Watanabe, M. Ueno, D. Kamiya et al., "A ROCK inhibitor permits survival of dissociated human embryonic stem cells," *Nature Biotechnology*, vol. 25, no. 6, pp. 681–686, 2007.

[111] X. Li, R. Krawetz, S. Liu, G. Meng, and D. E. Rancourt, "ROCK inhibitor improves survival of cryopreserved serum/feeder-free single human embryonic stem cells," *Human Reproduction*, vol. 24, no. 3, pp. 580–589, 2008.

[112] R. Martin-Ibanez, C. Unger, A. Stromberg, D. Baker, J. M. Canals, and O. Hovatta, "Novel cryopreservation method for dissociated human embryonic stem cells in the presence of a ROCK inhibitor," *Human Reproduction*, vol. 23, no. 12, pp. 2744–2754, 2008.

[113] M. Pakzad, M. Totonchi, A. Taei, A. Seifinejad, S. N. Hassani, and H. Baharvand, "Presence of a ROCK inhibitor in extracellular matrix supports more undifferentiated growth of feeder-free human embryonic and induced pluripotent stem cells upon passaging," *Stem Cell Reviews and Reports*, vol. 6, no. 1, pp. 96–107, 2010.

[114] J. Hanna, A. W. Cheng, K. Saha et al., "Human embryonic stem cells with biological and epigenetic characteristics similar to those of mouse ESCs," *Proceedings of the National Academy of Sciences*, vol. 107, no. 20, pp. 9222–9227, 2010.

[115] W. Wang, J. Yang, H. Liu et al., "Rapid and efficient reprogramming of somatic cells to induced pluripotent stem cells by retinoic acid receptor gamma and liver receptor homolog 1," *Proceedings of the National Academy of Sciences*, vol. 108, no. 45, pp. 18283–18288, 2011.

[116] C. Buecker, R. Srinivasan, Z. Wu et al., "Reorganization of enhancer patterns in transition from naive to primed pluripotency," *Cell Stem Cell*, vol. 14, no. 6, pp. 838–853, 2014.

[117] B. Valamehr, M. Robinson, R. Abujarour et al., "Platform for induction and maintenance of transgene-free hiPSCs resembling ground state pluripotent stem cells," *Stem Cell Reports*, vol. 2, no. 3, pp. 366–381, 2014.

[118] T. W. Theunissen, B. E. Powell, H. Wang et al., "Systematic identification of culture conditions for induction and maintenance of naive human pluripotency," *Cell Stem Cell*, vol. 15, no. 4, pp. 471–487, 2014.

[119] Y. Takashima, G. Guo, R. Loos et al., "Resetting transcription factor control circuitry toward ground-state pluripotency in human," *Cell*, vol. 158, no. 6, pp. 1254–1269, 2014.

[120] M. Van der Jeught, J. Taelman, G. Duggal et al., "Application of small molecules favoring naïve pluripotency during human embryonic stem cell derivation," *Cellular Reprogramming*, vol. 17, no. 3, pp. 170–180, 2015.

[121] T. Miyazaki, S. Futaki, K. Hasegawa et al., "Recombinant human laminin isoforms can support the undifferentiated growth of human embryonic stem cells," *Biochemical and Biophysical Research Communications*, vol. 375, no. 1, pp. 27–32, 2008.

[122] S. R. Braam, L. Zeinstra, S. Litjens et al., "Recombinant vitronectin is a functionally defined substrate that supports human embryonic stem cell self-renewal via $\alpha V\beta 5$ integrin," *Stem Cells*, vol. 26, no. 9, pp. 2257–2265, 2008.

[123] Z. Melkoumian, J. L. Weber, D. M. Weber et al., "Synthetic peptide-acrylate surfaces for long-term self-renewal and cardiomyocyte differentiation of human embryonic stem cells," *Nature Biotechnology*, vol. 28, no. 6, pp. 606–610, 2010.

[124] A. Trounson and N. D. DeWitt, "Pluripotent stem cells progressing to the clinic," *Nature Reviews. Molecular Cell Biology*, vol. 17, no. 3, pp. 194–200, 2016.

[125] Y. Wang, L. Cheng, and S. Gerecht, "Efficient and scalable expansion of human pluripotent stem cells under clinically compliant settings: a view in 2013," *Annals of Biomedical Engineering*, vol. 42, no. 7, pp. 1357–1372, 2014.

[126] S. Terstegge, I. Laufenberg, J. Pochert et al., "Automated maintenance of embryonic stem cell cultures," *Biotechnology and Bioengineering*, vol. 96, no. 1, pp. 195–201, 2007.

[127] R. J. Thomas, D. Anderson, A. Chandra et al., "Automated, scalable culture of human embryonic stem cells in feeder-free conditions," *Biotechnology and Bioengineering*, vol. 102, no. 6, pp. 1636–1644, 2009.

[128] J. A. King and W. M. Miller, "Bioreactor development for stem cell expansion and controlled differentiation," *Current Opinion in Chemical Biology*, vol. 11, no. 4, pp. 394–398, 2007.

[129] C. Kropp, D. Massai, and R. Zweigerdt, "Progress and challenges in large-scale expansion of human pluripotent stem cells," *Process Biochemistry*, vol. 59, pp. 244–254, 2017.

[130] F. F. dos Santos, P. Z. Andrade, C. L. da Silva, and J. M. S. Cabral, "Bioreactor design for clinical-grade expansion of stem cells," *Biotechnology Journal*, vol. 8, no. 6, pp. 644–654, 2013.

[131] A. J. Want, A. W. Nienow, C. J. Hewitt, and K. Coopman, "Large-scale expansion and exploitation of pluripotent stem cells for regenerative medicine purposes: beyond the T flask," *Regenerative Medicine*, vol. 7, no. 1, pp. 71–84, 2012.

[132] H. Singh, P. Mok, T. Balakrishnan, S. N. B. Rahmat, and R. Zweigerdt, "Up-scaling single cell-inoculated suspension culture of human embryonic stem cells," *Stem Cell Research*, vol. 4, no. 3, pp. 165–179, 2010.

[133] R. Zweigerdt, R. Olmer, H. Singh, A. Haverich, and U. Martin, "Scalable expansion of human pluripotent stem cells in suspension culture," *Nature Protocols*, vol. 6, no. 5, pp. 689–700, 2011.

[134] Y. Y. Lipsitz, C. Woodford, T. Yin, J. H. Hanna, and P. W. Zandstra, "Modulating cell state to enhance suspension expansion of human pluripotent stem cells," *Proceedings of the National Academy of Sciences*, vol. 115, no. 25, pp. 6369–6374, 2018.

[135] V. C. Chen, J. Ye, P. Shukla et al., "Development of a scalable suspension culture for cardiac differentiation from human pluripotent stem cells," *Stem Cell Research*, vol. 15, no. 2, pp. 365–375, 2015.

[136] H. Fonoudi, H. Ansari, S. Abbasalizadeh et al., "A universal and robust integrated platform for the scalable production of human cardiomyocytes from pluripotent stem cells: scalable production of hPSC-derived cardiomyocytes," *Stem Cells Translational Medicine*, vol. 4, no. 12, pp. 1482–1494, 2015.

[137] H. Kempf, C. Kropp, R. Olmer, U. Martin, and R. Zweigerdt, "Cardiac differentiation of human pluripotent stem cells in scalable suspension culture," *Nature Protocols*, vol. 10, no. 9, pp. 1345–1361, 2015.

[138] S. N. Boers, J. J. van Delden, H. Clevers, and A. L. Bredenoord, "Organoid biobanking: identifying the ethics: organoids revive old and raise new ethical challenges for basic research and therapeutic use," *EMBO Reports*, vol. 17, no. 7, pp. 938–941, 2016.

[139] Y. Fan, J. Wu, P. Ashok, M. Hsiung, and E. S. Tzanakakis, "Production of human pluripotent stem cell therapeutics under defined xeno-free conditions: progress and challenges," *Stem Cell Reviews and Reports*, vol. 11, no. 1, pp. 96–109, 2015.

[140] M. Serra, C. Brito, C. Correia, and P. M. Alves, "Process engineering of human pluripotent stem cells for clinical application," *Trends in Biotechnology*, vol. 30, no. 6, pp. 350–359, 2012.

[141] M. A. Kinney, C. Y. Sargent, and T. C. McDevitt, "The multiparametric effects of hydrodynamic environments on stem cell culture," *Tissue Engineering Part B, Reviews*, vol. 17, no. 4, pp. 249–262, 2011.

[142] C. Kropp, H. Kempf, C. Halloin et al., "Impact of feeding strategies on the scalable expansion of human pluripotent stem cells in single-use stirred tank bioreactors: hPSC expansion in perfused single-use bioreactors," *Stem Cells Translational Medicine*, vol. 5, no. 10, pp. 1289–1301, 2016.

[143] A. K. Chen, X. Chen, A. B. H. Choo, S. Reuveny, and S. K. W. Oh, "Expansion of human embryonic stem cells on cellulose microcarriers," *Current Protocols in Stem Cell Biology*, vol. 14, 2010.

[144] A. M. Fernandes, P. A. N. Marinho, R. C. Sartore et al., "Successful scale-up of human embryonic stem cell production in a stirred microcarrier culture system," *Brazilian Journal of Medical and Biological Research*, vol. 42, no. 6, pp. 515–522, 2009.

[145] B. C. Heng, J. Li, A. K. L. Chen et al., "Translating human embryonic stem cells from 2-dimensional to 3-dimensional cultures in a defined medium on laminin- and vitronectin-coated surfaces," *Stem Cells and Development*, vol. 21, no. 10, pp. 1701–1715, 2012.

[146] Y. Fan, F. Zhang, and E. S. Tzanakakis, "Engineering xeno-free microcarriers with recombinant vitronectin, albumin and UV irradiation for human pluripotent stem cell bioprocessing," *ACS Biomaterials Science & Engineering*, vol. 3, no. 8, pp. 1510–1518, 2016.

[147] A. K.-L. Chen, X. Chen, A. B. H. Choo, S. Reuveny, and S. K. W. Oh, "Critical microcarrier properties affecting the expansion of undifferentiated human embryonic stem cells," *Stem Cell Research*, vol. 7, no. 2, pp. 97–111, 2011.

[148] N. Siti-Ismail, A. E. Bishop, J. M. Polak, and A. Mantalaris, "The benefit of human embryonic stem cell encapsulation for prolonged feeder-free maintenance," *Biomaterials*, vol. 29, no. 29, pp. 3946–3952, 2008.

[149] V. C. Chen and L. A. Couture, "The suspension culture of undifferentiated human pluripotent stem cells using spinner flasks," in *Stem Cells and Good Manufacturing Practices*, K. Turksen, Ed., vol. 1283, pp. 13–21, Springer New York, New York, NY, USA, 2014.

Hindawi
Stem Cells International
Volume 2018, Article ID 7315218, 9 pages
https://doi.org/10.1155/2018/7315218

Review Article

New Strategies and In Vivo Monitoring Methods for Stem Cell-Based Anticancer Therapies

Ping Wang[1] **and Aitor Aguirre**[2,3]

[1]*Precision Health Program, Department of Radiology, College of Human Medicine, Michigan State University, East Lansing, MI 48823, USA*
[2]*Division of Developmental and Stem Cell Biology, Institute for Quantitative Health Science and Engineering, Michigan State University, East Lansing, MI 48823, USA*
[3]*Department of Biomedical Engineering, College of Engineering, Michigan State University, East Lansing, MI 48823, USA*

Correspondence should be addressed to Aitor Aguirre; aaguirre@msu.edu

Received 4 September 2018; Accepted 22 October 2018; Published 15 November 2018

Guest Editor: Tiago Fernandes

Cancer is a devastating disease and the second cause of death in the developed world. Despite significant advances in recent years, such as the introduction of targeted therapies such as receptor tyrosine kinase inhibitors and immunotherapy, current approaches are insufficient to stop the advance of the disease and many cancer types remain largely intractable. In this review, we describe the latest and most revolutionary stem cell-based approaches for the treatment of cancer. We also summarize the emerging imaging modalities being applied for monitoring anticancer stem cell therapy success and discuss the implications of these novel technologies for precision medicine.

1. Introduction

Cancer is the second cause of death of men and women in the United States and a major health problem worldwide [1]. Mortality data for 2018 predicts 1.7 million new cancer cases and 0.6 million cancer-related deaths only in the US [2]. There is however room for hope. Among the top 10 causes of death, cancer is the only one steadily declining (about 26% for men and women in the US in the last 25 years), reflecting continuous improvements in diagnosis, care, and treatment [2]. Therapeutic intervention has significantly advanced in the last two decades, particularly with the introduction of targeted therapeutics such as receptor tyrosine kinase inhibitors (e.g., erlotinib in 2003) [3, 4] and immunotherapy (e.g., pembrolizumab in 2014) [5, 6]. These compounds exhibit much higher selectivity for cancer cells over conventional treatments and minimize side effects. Unfortunately, despite the extensive efforts invested in clinical development of cancer therapeutics, many cancers remain difficult or impossible to treat by traditional approaches. Furthermore, tumors evolve under treatment, and cells become widely chemoresistant and highly invasive, reducing treatment options as the disease progresses [7, 8]. An innovative approach for cancer treatment in recent years is the use of stem cell-based therapies [9, 10]. In this context, rather than regenerating, repairing, or replenishing tissues, stem cells are carriers that infiltrate tumors to deliver lethal payloads and tell us about the mechanisms of cancer cell survival and immune evasion. Stem cells possess at least two unique biological characteristics that make them ideally suited to fight cancer. For starters, embryos and tumors share many characteristics, including surface antigens, production of growth factors, and the capacity to evade, at least partially, the immune system [9]. In 1838, these similarities led Muller to formulate what could be considered the first stem cell theory of cancer origin (still highly controversial) [11]. In 1906 Schone would show that vaccination of animals with fetal tissues could render them partially resistant to cancer, demonstrating the close connection existing between cancer cells and stem cells [11]. More recent efforts have established

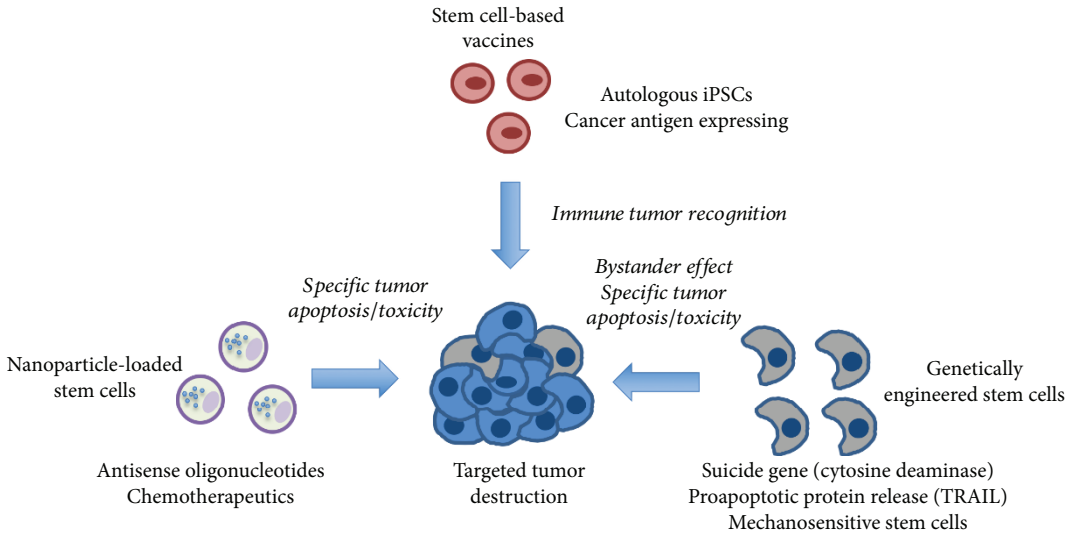

Figure 1: Stem cell-based strategies for anticancer therapy. Tumors can be specifically targeted with stem cells to make them vulnerable to therapy. Top: stem cell-based vaccines leverage the similarities between cancer cells and stem cells to promote immune tumor recognition; left: nanoparticle-loaded stem cells exhibit efficient homing to tumors, where they deliver their payload in the form of chemotherapies or apoptosis-inducing oligonucleotides; right: genetically engineered stem cells can express and release proapoptotic proteins or ligands in the tumor microenvironment or contain enzymes metabolizing prodrugs to their cytotoxic form (e.g., cytosine deaminase). Stem cells can also be engineered to recognize biophysical features of the tumor microenvironment before activating their engineered cytotoxic program.

beyond any doubt that stem cells and cancer cells share many common features at the molecular level, including the activation of developmental signaling pathways promoting cell survival, proliferation, self-renewal, and tissue invasion (e.g., Wnt, Notch, Hippo, and epithelial to mesenchymal transition) [12, 13]. It might be due to these similarities that stem cells also exhibit strong tropism towards tumors, which in turn makes them attractive candidates for targeted delivery of drugs or other compounds with minimal side effects. Strategies for fighting cancer with stem cell-based therapies fall into two broad categories: (1) stem cell vaccines, using the identity property, and (2) stem cell carriers, exploiting their tumortropic behavior. The different strategies and examples of their use can be found in Figure 1. Additionally, Table 1 includes a number of ongoing clinical trials in the US using stem cell-based therapies for anticancer treatment to highlight the relevance of this growing field for translational applications.

2. Stem Cell-Based Antitumor Vaccines

The idea of generating immunity against cancer cells (immunotherapy) is not new and has been pursued for many decades. In the 19th century, scientists noticed the similarity between embryonic cells and cancer cells. It was observed that when mice had been exposed to fetal tissue from another mouse, the recipient would reject transplanted tumors (for a detailed review on this topic, see [11]). These ideas were explored in-depth during the following decades, particularly during the 60s and 70s. Stem cells and cancer cells share significant cellular and molecular properties. Immunization with embryonal material was enough to prevent tumor growth and to suppress tumor formation by administration of carcinogens [11]. However, due to technical and ethical limitations at the time (inoculation of human fetal tissue would not be feasible in humans), these approaches were progressively abandoned. This changed at the turn of the century, with the enormous expansion in the stem cell biology in the last two decades, the establishment of numerous human embryonic stem cell lines and the introduction of induced pluripotent stem cells [14, 15]. These advances render the previous ethical and social concerns associated with fetal immunization obsolete, leading to a resurging interest in human anticancer stem cell-based vaccines.

In a breakthrough study published very recently, Kooreman et al. reported using irradiated induced pluripotent stem cells in conjunction with adjuvant therapy to vaccinate mice against a wide number of cancer types, including breast cancer, mesothelioma, and melanoma with great success [16]. Using RNA-seq, the authors found that iPSCs and cancer cells possessed a similar signature in several potential cancer antigens, suggesting that iPSCs could be used to prime the host's immune system. This approach has several advantages, including use of autologous cells minimizing host rejection and exposure to known and unknown cancer-associated antigens simultaneously to promote a more solid immune response against the tumor. As a proof of concept, the authors injected mouse iPSCs in mice and then transplanted cancer cells (breast, melanoma) in subcutaneous and orthotopic models. In all cases, a spectacular regression of the tumors was observed when compared with nonvaccinated control mice [16]. It was possible to determine that B and T lymphocytes were primarily responsible for this activity. Although iPSC vaccination was successful in preventing or reducing tumor growth, it was insufficient as a therapy to prevent the growth of established tumors, suggesting tumor immunosuppressive mechanisms

Table 1: Current clinical trials using stem cell-based therapies for anticancer treatment in the US.

Title	NCT number	Status	Sponsors	Enrollment	Funding	Start	Location
Generation of Cancer Antigen-Specific T-cells From Human Induced Pluripotent Stem Cells (iPSC) for Research and Potential Future Therapy	NCT03407040	Enrolling by invitation	National Cancer Institute (NCI), National Institutes of Health Clinical Center (CC)	7000	NIH	30 Jan. 18	National Institutes of Health Clinical Center, Bethesda
Stem Cells in NF1 Patients with Tumors of the Central Nervous System	NCT03332030	Recruiting	Children's Research Institute	20	Other	27 Nov. 15	Children's National Medical Center, Washington
Neural Stem Cell Based Virotherapy of Newly Diagnosed Malignant Glioma	NCT03072134	Recruiting	Northwestern University	36	Other	24 Apr. 17	Northwestern Memorial Hospital, Chicago
Umbilical & Cord Blood (CB) Derived CAR-Engineered NK Cells for B Lymphoid Malignancies	NCT03056339	Recruiting	MD Anderson Cancer Center	36	Other	21 Jun. 17	University of Texas MD Anderson Cancer Center, Houston
Mesenchymal Stem Cells (MSC) for Ovarian Cancer	NCT02530047	Active, not recruiting	MD Anderson Cancer Center	5	Other	16 May 16	University of Texas MD Anderson Cancer Center, Houston
MV-NIS Infected Mesenchymal Stem Cells in Treating Patients with Recurrent Ovarian Cancer	NCT02068794	Recruiting	Mayo Clinic, National Cancer Institute (NCI)	54	Other, NIH	Mar. 14	Mayo Clinic, Rochester
Genetically Modified Neural Stem Cells, Flucytosine, and Leucovorin for Treating Patients with Recurrent High-Grade Gliomas	NCT02015819	Active, not recruiting	City of Hope Medical Center, National Cancer Institute (NCI)	18	Other, NIH	7 Oct. 14	City of Hope Medical Center, Duarte
Allogeneic Human Bone Marrow Derived Mesenchymal Stem Cells in Localized Prostate Cancer	NCT01983709	Terminated	Sidney Kimmel Comprehensive Cancer Center at Johns Hopkins	7	Other	Oct. 13	Johns Hopkins Hospital, Baltimore
Stem Cell Transplantation as Immunotherapy for Hematologic Malignancies	NCT00143559	Completed	St. Jude Children's Research Hospital	17	Other	Aug. 05	St. Jude Children's Research Hospital, Memphis

Data was obtained from NIH clinicaltrials.gov by performing searches for cancer-related clinical trials using the following terms: stem cell-based anticancer vaccine, engineered stem cells, targeted stem cell therapy, stem cell virus carrier, stem cell nanoparticle carrier, and stem cell immunotherapy.

might be still too strong [16]. Combination of iPSC-based vaccines with targeted immunotherapy might be an interesting avenue for treatment in the future. Of note, the authors did not detect any negative effects derived from iPSC vaccination, such as autoimmunity or teratoma formation, making this approach more attractive for translation into the clinic.

An alternative approach at stem cell-based anticancer vaccination is the use of iPSCs to derive dendritic cells (DCs), which play an essential role in T cell activation, engineered to express tumor-specific antigens. Kitadani et al. applied this concept to the treatment of gastrointestinal cancer [17]. After generating iPSC-derived DCs (iPSDCs) with typical DC markers and cytokine secretion, iPSDCs were engineered to express carcinoembryonic antigen (CEA) employing adenoviral transduction. T cells from healthy human donors were exposed to the CEA-iPSDCs in vitro and then c-cultured with a panel of gastrointestinal cancer cell lines. Human T cells responded with strong cytotoxic activity to cancer cells expressing CEA, but not others [17]. Transplantation of mouse iPSDCs into a mouse subcutaneous model of gastrointestinal cancer resulted in remarkable cytotoxicity and tumor growth inhibition (~4-fold smaller tumor volume compared to controls) [17]. More studies will be necessary to determine the safety and efficacy of stem cell-based vaccines for controlling or eradicating human tumors; however, present advances support their feasibility and guarantee further research.

3. Targeted Suicide Stem Cells to Destroy Tumors

Stem cells have a significant capacity to home to tumors due to shared chemotactic and signaling pathways with cancer cells [9]. This property can be exploited for targeted therapies by placing specific stem cell types into the tumor mass. Protocols for growing and maintaining many different types of tissue-specific stem cells are now available and have significantly improved over the last decade [18, 19]. Introducing genetic modifications in stem cells is now easier than ever before since the implementation of CRISPR technologies [20]. These technical advances facilitate the making of engineered stem cell types for targeting tumors based on their origin and characteristics with minimal side effects in other tissues or organs. Successful attempts following this strategy can be found for the treatment of aggressive brain tumors, which are among the most deadly and challenging cancers to treat. Survival for patients with glioblastoma multiforme (GBM) ranges from 12 to 15 months, and treatment options are very limited and consist on aggressive chemo and radiotherapy [21]. Attempts to efficiently target glioblastoma have traditionally been insufficient for sustained therapeutic benefit [21]. Using a transdifferentiation approach, Bagó et al. generated autologous neural stem cells from skin fibroblasts for theranostic applications (iNSCs) [22]. The authors determined that iNSCs exhibited strong tumor-homing activity towards GBM cell lines due to CXCR4 chemotaxis [22]. The authors decided to genetically engineer iNSCs to express a secreted variant of the proapoptotic molecule TRAIL (TNF-related apoptosis-inducing ligand) and transplanted cells intravenously into mice carrying human glioblastoma xenografts. Over a period of 3 weeks, iNSCs lead to a 250-fold tumor mass reduction and a median increase in survival from 22 to 49 days. Other genetic modifications of iNSCs, such as ganciclovir prodrug therapy, were also successful. To mimic the postoperative setting in humans, mice with xenografted GBM were subjected to surgical resection and iNSC therapy. The treatment delayed the regrowth of GBMs 3-fold and extended survival from 46 to 60 days [22]. Taken together, these results suggest that tumor-homing stem cells are a powerful option for therapy, particularly in inaccessible tumors. Locally residing stem cells are present in almost every tissue in the body, potentially making this approach applicable to other tumor types.

4. Targeting the Metastatic Niche with Mechanosensitive Stem Cells

Another aspect of cancer that can be tackled with stem cell therapy is metastasis. Cancer metastases are responsible for 90% of cancer deaths [23, 24]. Treatments to directly target metastatic tumors are sorely lacking, and surgical resection is not always a feasible option, particularly when multiple metastatic sites are present. Interestingly, metastases frequently differ from their tissues of origin by possessing largely altered extracellular microenvironments, which leads to altered matrix stiffness, particularly in tumors with strong lysyl oxidase (LOX) expression (e.g., breast cancer metastases have 15-fold increased stiffness versus normal breast tissue) [25, 26]. Taking these properties into consideration, Liu et al. hypothesized that a mechanosensitive mesenchymal stem cell-based system, named mechanoresponsive cell system (MRCS), could be created to target cancer metastases [27]. Systemically infused MSCs target tumor sites due to naturally occurring combinations of tumor tropic molecules (growth factors, cytokines), and matrix stiffness is an important contributor to their behavior, including chemotaxis and differentiation, indicating that a fine-tuned mechanoresponsive machinery is already present in this cell type [27, 28]. Autologous MSCs can be easily obtained from a patient's adipose tissue or differentiated from iPSCs and expanded *in vitro* [29]. MSCs sense and transduce extracellular mechanical cues through the Hippo pathway effector YAP. In soft substrates, YAP remains in the cytoplasm in its inactive form, while hard substrates promote YAP nuclear translocation and associated transcriptional programs [30]. Taking advantage of this property, the authors genetically engineered MSCs to express the suicide gene cytosine deaminase (CD) under the control of the YAP promoter (referred to as CD-MCRS) [27]. In this system conditions, systemically infused CD-MCRS cells are attracted to metastatic sites and, once exposed to the matrix stiffness present at those locations, start expressing CD. Administration of 5-fluorocytosine at this point specifically kills metastatic cells by the bystander effect. To provide proof of concept on this approach, Liu et al. used mice transplanted with MDA-MB-231 breast cancer cells into the lung to mimic metastatic spread [27]. As expected, infused CD-MCRS

homed to the lungs and activated CD expression. When administered in conjunction with 5-fluorocytosine, metastatic tumors shrank 2- to 3-fold and treated animals experienced significantly improved survival [27]. Overall, these results show great promise for the treatment of metastatic cancer and highlight the importance of using the biophysical properties of the tumor environment for targeted therapies.

5. Stem Cells as a Nanoparticle Delivery System

The tumor homing characteristics of stem cells can be leveraged to specifically deliver particles to tumor sites [31]. In a similar approach to the one described before for metastatic mechanosensing, MSCs can be induced to take up drug-loaded nanoparticles. Zhao et al. attempted this approach by loading MSCs with doxorubicin-containing poly-lactic-coglycolic acid nanoparticles (PLGA-DOX) [32]. MSCs readily took up PLGA-DOX and, due to low bioavailability of the drug in this composition, received low cytotoxicity. When transplanted into mice bearing lung metastases, MSCs homed to the tumor sites and locally released DOX, resulting in a significantly reduced number of tumor nodules (~3-fold reduction) [32]. An interesting recent variation of this approach involves the use of a physical phenomenon known as magnetic hyperthermia. Magnetic hyperthermia consists on the heating of tissues by means of magnetic nanoparticles and alternating magnetic fields (AMF). MSCs can be loaded with superparamagnetic iron oxide nanoparticles (SPIONs), which have minimal toxicity [33]. Once MSCs have homed into the tumor, SPIONs are delivered to the surrounding cells by exosome delivery. At this point, application of a high-frequency AMF will produce a localized hyperthermic effect reaching temperatures of 42–45 Celsius at intervals of 20 minutes. This localized effect exerts extensive damage to tumor cells in vitro, with up to 80% growth inhibition [33]. Although very promising, stem cell-mediated-magnetic hyperthermia therapeutic effects have not been explored *in vivo* in enough detail yet.

6. Stem Cells as Oncolytic Virus Carriers

Oncolytic viruses are an emerging class of cancer therapeutics. In 2017, the FDA approved the first immunogenic oncolytic virus (OV) for therapy in advanced melanoma [34]. However, the systemic administration of OV can lead to serious side effects. To circumvent this problem, Du et al. designed a strategy in which MSCs could act as oncolytic herpes simplex virus (oHSV) carriers into the tumor mass [34]. Using a mouse model that closely recapitulates melanoma progression, the authors demonstrated the therapeutic efficacy of oHSV-loaded MSCs. The cells, which were delivered via carotid artery, efficiently homed to the tumor metastases and reduced tumor size and foci number by ~2- to 4-fold [34]. Furthermore, treatment also extended survival by approximately 20 days. The authors have also demonstrated the efficacy of this approach in other tumor types before [35]. Overall, oncolytic virus therapies remain a strong option for therapy in the close future and this study demonstrates that further refinement using stem cells as carriers can improve therapeutic outcomes and minimize side effects.

7. Stem Cell Reprogramming Technologies for Cancer Immunotherapy

The field of cancer immunotherapy has seen important advances in recent years, including several clinical trials and approval of pembrolizumab. Transfer of T cell receptor (TCR) genes into patients' peripheral T cells has achieved good clinical outcomes [36], indicating that targeting a single antigen can be effective for some types of cancer. In addition, T cell expressing chimeric antigen receptor (CAR), an engineered receptor molecule, which combines an antibody recognition domain and cytoplasmic signaling domains, has demonstrated therapeutic effect in a certain type of leukemia [37]. In both TCR and CAR engineering, peripheral T cells are transduced by a retrovirus, bringing about the risk of tumorigenicity due to the random integration of a transfected gene into the genome. Moreover, in the autologous setting, it would be costly to produce T cells. To address this issue, a strategy has been proposed to regenerate T cells utilizing iPSC technology. Themeli et al. reported that CAR-expressing T cells were regenerated from iPSCs transduced with a CAR gene. iPSCs were generated by retrovirus reprogramming T cells isolated from peripheral blood of healthy donors. The CAR sequence specific for CD19 was inserted into iPSCs using CRISPR/Cas9. iPSC-derived CAR specific-T cells were phenotypically similar to innate T$\gamma\delta$ cells and showed ability to inhibit tumor growth in a xenograft animal model [38–40]. This strategy brings hope that CAR-T therapy may also work for other types of cancer beside hematologic malignancies. Certain obstacles associated with CAR-T including further customization of the technology to recognize specific/other tumor types and predicting and limiting cross-reactivity need to be resolved. CRISPR/Cas9 technologies will be useful to target CAR-T gene constructs to genomic safe harbor sites, reducing the risk of undesired effects. However, challenges related to the use of this cutting-edge technology for human therapy remain. Two recently published studies reported that stem cells whose genomes were successfully edited by CRISPR-Cas9 had the potential to be tumorigenic themselves due to p53 mutations. These results indicated that p53 and related genes should be monitored when developing stem cell-based therapies utilizing CRISPR-Cas9 [41, 42].

8. New Imaging Modalities for Stem Cell Theranostics in Cancer

Stem cell-based therapies have enormous potential for cancer treatment. For maximal efficacy, these promising therapies require targeted cell delivery to specific sites followed by successful cell engraftment. Various imaging methods have been applied for in vivo tracing of stem cells, including optimal imaging, nuclear imaging, and magnetic resonance imaging. Each imaging modality has its advantages and limitations in terms of sensitivity, tissue penetration, spatial

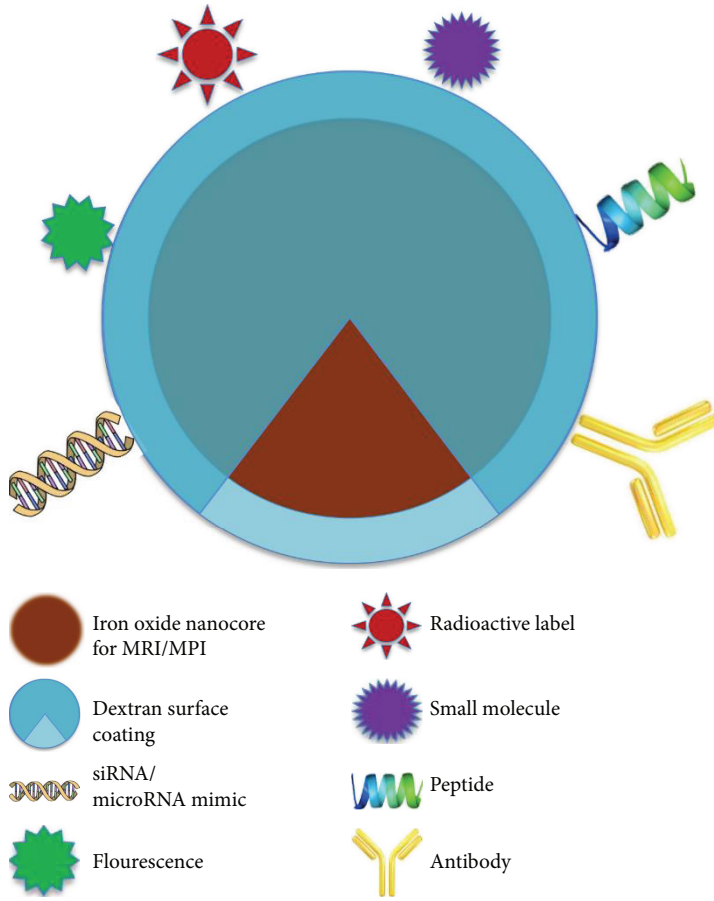

Figure 2: Theranostic magnetic nanoparticles for stem cell anticancer therapy. Iron oxide nanoparticles can be functionalized by applying a dextran coating. Different biologically active substances (antibodies, RNA/DNA, and drugs) intended to target or damage the tumor, or labeling probes for tracing and diagnostics, can be then tethered to the nanoparticle for theranostic applications.

resolution, and clinical potential [43, 44]. Optical imaging is a group of technologies that produce the image formed by the light rays from a self-luminous or an illuminated object that traverse an optical system. So far, this method is mainly restricted in tracking transplanted cells in animal models. In addition, low spatial resolution and limited tissue penetration are some disadvantages related to this method [45]. Nuclear imaging is based on the use of radiolabeled ligands targeting cell-specific antigens, receptors, metabolites, or pharmacologic agents. Many isotopes and labeling strategies have been investigated for stem cell labeling for nuclear imaging [46]. Lack of available isotopes, low spatial resolution, poor cellular uptake, and potential negative affect in cellular proliferation are some weaknesses of this modality. Magnetic resonance imaging (MRI) has some advantages over other modalities used for in vivo cellular imaging. It is clinically applicable and does not use radiation; it has high spatial resolution and unlimited tissue penetration, which can provide anatomical information of localizing transplanted cells. For MRI detection, stem cells usually need to be labeled with imaging contrast agents before transplantation. Superparamagnetic iron oxide (SPIO) nanoparticles, which result in signal-intensity voids or hypointense regions in T2-weighted or T2*-weighted MR images [43], are the most common imaging probes used for tracking transplanted stem cells using MRI. However, signal voids in MR images produced by iron-labeled cells/cell clusters were difficult to distinguish from other low MR signals produced by tissue including intestine and blood vessel structures or artifacts [47]. Magnetic particle imaging (MPI) is an emerging imaging technique introduced in 2005 that directly identifies the intense magnetization of SPIOs rather than indirectly detecting SPIOs via signal dropouts, which could potentially overcome the disadvantages of cell tracking with MRI. MPI unambiguously detects superparamagnetic iron oxide nanoparticles with high specificity and sensitivity and other advantages over previous methods, such as the absence of background signal, linear quantitative ability, and high potential for clinic translation. MPI's great specificity results from its high image contrast, since magnetic particles serve as the only source for signal [48]. MPI's high sensitivity derives from the direct detection of the electronic magnetization of SPIO nanoparticles, which is 10^8 times larger than the nuclear magnetization of protons seen in MRI [49], translating to a sensitivity to detect hundreds of magnetic nanoparticle-labeled cells with current hardware. MPI's safety is driven using clinically approved iron oxide nanoparticles, which have been proven safe for patients with

compromised renal function. This new imaging modality has been tested for in vivo monitoring of transplanted stem cells. Zheng et al. firstly utilized MPI to monitor SPIO-labeled human embryonic stem cell- (hESC-) derived neural progenitor cells (NPCs) in vivo in a rat model. The results showed a 200-cell detection limit in vitro and in vivo, allowing them to monitor graft clearance over 87 days in the animal's brain using MPI [50]. In a more recent study, Zheng and colleagues imaged intravenously transplanted mesenchymal stem cells (MSCs) using MPI. Their studies demonstrated that labeled MSCs immediately entrapped in the lung tissue posttransplantation and then relocated to the liver within one day. Longitudinal MPI demonstrated a clearance half-life of MSC iron- oxide labels in the liver at 4.6 days [51]. These first in vivo MPI results indicate that MPI offers strong utility for quantitating transplanted stem cells labeled using SPIO. These results demonstrate that MPI's quantitative capacity arises from the linear signal change with nanoparticle concentration, which occurs independent of tissue depth. For clinical translation, a whole-body human MPI system for high-speed imaging is currently being developed and the first one has already delivered initial images. In terms of SPIO probe availability for MPI, there are several FDA-approved iron oxide nanoparticles under several brand names including ferucarbotran (Resovist®, Schering AG, Germany), ferumoxtran-10 (Sinerem®, Guerbet, France; Combidex® Advanced Magnetics Inc., MA, USA), and ferumoxytol (Feraheme®, AMAG Pharmaceuticals, Cambridge, MA) [52]. In addition, VivoTrax™ is provided for preclinical use by Magnetic Insight, CA, USA. Iron oxide nanoparticles used for cell labeling in MRI/MPI serve not only as imaging probes but also as nanocarriers for therapies. Various functional moieties could be attached to the coating of nanoparticle that serve as targeting macromolecules, therapeutic payloads, or additional imaging tags for multimodality in vivo imaging [53, 54]. These multifunctional nanodrugs could be carried by stem cells towards cancer cells for theranostic cancer treatment (Figure 2).

9. Perspectives and Conclusions

In conclusion, stem cell-based anticancer therapies offer great promise for the treatment of cancer. Although stem cells might be useful as cancer therapies of their own, they might also serve as powerful adjuvants in combination with traditional chemoradiotherapy treatment, or after surgery. Furthermore, cancer patient-derived iPSCs can be used to draw association between genotype and treatment responses and to identify biomarkers to inform patient selection for precision oncology [55, 56]. Emerging technologies such as CRISPR/Cas9 genome engineering and novel theranostic tools will be important factors in the successful implementation and continued improvement of stem cell-based anticancer therapies [57]. Many challenges remain, particularly regarding safety of stem cell transplants and CRISPR/Cas9 genomic manipulations. These issues are the focus of intense research and will be progressively clarified in the near future.

Conflicts of Interest

The authors declare no conflicts of interest.

Acknowledgments

The work in the Aguirre Laboratory is supported by the National Heart, Lung, and Blood Institute of the National Institutes of Health under award number K01HL135464.

References

[1] R. L. Siegel, K. D. Miller, and A. Jemal, "Cancer statistics, 2017," *CA: a Cancer Journal for Clinicians*, vol. 67, no. 1, pp. 7–30, 2017.

[2] R. L. Siegel, K. D. Miller, and A. Jemal, "Cancer statistics, 2015," *CA: a Cancer Journal for Clinicians*, vol. 65, no. 1, pp. 5–29, 2015.

[3] F. A. Shepherd, J. Rodrigues Pereira, T. Ciuleanu et al., "Erlotinib in previously treated non-small-cell lung cancer," *The New England Journal of Medicine*, vol. 353, no. 2, pp. 123–132, 2005.

[4] M. Hojjat-Farsangi, "Small-molecule inhibitors of the receptor tyrosine kinases: promising tools for targeted cancer therapies," *International Journal of Molecular Sciences*, vol. 15, no. 8, pp. 13768–13801, 2014.

[5] N. L. Syn, M. W. L. Teng, T. S. K. Mok, and R. A. Soo, "De-novo and acquired resistance to immune checkpoint targeting," *The Lancet Oncology*, vol. 18, no. 12, pp. e731–e741, 2017.

[6] R. H. Vonderheide and K. L. Nathanson, "Immunotherapy at large: the road to personalized cancer vaccines," *Nature Medicine*, vol. 19, no. 9, pp. 1098–1100, 2013.

[7] L. N. Abdullah and E. K.-H. Chow, "Mechanisms of chemoresistance in cancer stem cells," *Clinical and Translational Medicine*, vol. 2, no. 1, p. 3, 2013.

[8] H. C. Zheng, "The molecular mechanisms of chemoresistance in cancers," *Oncotarget*, vol. 8, no. 35, pp. 59950–59964, 2017.

[9] D. W. Stuckey and K. Shah, "Stem cell-based therapies for cancer treatment: separating hope from hype," *Nature Reviews. Cancer*, vol. 14, no. 10, pp. 683–691, 2014.

[10] C. L. Zhang, T. Huang, B. L. Wu, W. X. He, and D. Liu, "Stem cells in cancer therapy: opportunities and challenges," *Oncotarget*, vol. 8, no. 43, pp. 75756–75766, 2017.

[11] B. G. Brewer, R. A. Mitchell, A. Harandi, and J. W. Eaton, "Embryonic vaccines against cancer: an early history," *Experimental and Molecular Pathology*, vol. 86, no. 3, pp. 192–197, 2009.

[12] E. Batlle and H. Clevers, "Cancer stem cells revisited," *Nature Medicine*, vol. 23, no. 10, pp. 1124–1134, 2017.

[13] D. Nassar and C. Blanpain, "Cancer stem cells: basic concepts and therapeutic implications," *Annual Review of Pathology*, vol. 11, no. 1, pp. 47–76, 2016.

[14] K. Takahashi, K. Tanabe, M. Ohnuki et al., "Induction of pluripotent stem cells from adult human fibroblasts by defined factors," *Cell*, vol. 131, no. 5, pp. 861–872, 2007.

[15] J. A. Thomson, J. Itskovitz-Eldor, S. S. Shapiro et al., "Embryonic stem cell lines derived from human blastocysts," *Science*, vol. 282, no. 5391, pp. 1145–1147, 1998.

[16] N. G. Kooreman, Y. Kim, P. E. de Almeida et al., "Autologous iPSC-based vaccines elicit anti-tumor responses *in vivo*," *Cell Stem Cell*, vol. 22, no. 4, pp. 501–513.e7, 2018.

[17] J. Kitadani, T. Ojima, H. Iwamoto et al., "Cancer vaccine therapy using carcinoembryonic antigen - expressing dendritic cells generated from induced pluripotent stem cells," *Scientific Reports*, vol. 8, no. 1, p. 4569, 2018.

[18] J. Wu and J. C. Izpisua Belmonte, "Stem cells: a renaissance in human biology research," *Cell*, vol. 165, no. 7, pp. 1572–1585, 2016.

[19] C. E. Murry and G. Keller, "Differentiation of embryonic stem cells to clinically relevant populations: lessons from embryonic development," *Cell*, vol. 132, no. 4, pp. 661–680, 2008.

[20] W. T. Hendriks, C. R. Warren, and C. A. Cowan, "Genome editing in human pluripotent stem cells: approaches, pitfalls, and solutions," *Cell Stem Cell*, vol. 18, no. 1, pp. 53–65, 2016.

[21] M. Davis, "Glioblastoma: overview of disease and treatment," *Clinical Journal of Oncology Nursing*, vol. 20, no. 5, pp. S2–S8, 2016.

[22] J. R. Bagó, O. Okolie, R. Dumitru et al., "Tumor-homing cytotoxic human induced neural stem cells for cancer therapy," *Science Translational Medicine*, vol. 9, no. 375, article eaah6510, 2017.

[23] A. W. Lambert, D. R. Pattabiraman, and R. A. Weinberg, "Emerging biological principles of metastasis," *Cell*, vol. 168, no. 4, pp. 670–691, 2017.

[24] S. Valastyan and R. A. Weinberg, "Tumor metastasis: molecular insights and evolving paradigms," *Cell*, vol. 147, no. 2, pp. 275–292, 2011.

[25] D. A. Kirschmann, E. A. Seftor, S. F. Fong et al., "A molecular role for lysyl oxidase in breast cancer invasion," *Cancer Research*, vol. 62, no. 15, pp. 4478–4483, 2002.

[26] T. H. Wang, S. M. Hsia, and T. M. Shieh, "Lysyl oxidase and the tumor microenvironment," *International Journal of Molecular Sciences*, vol. 18, no. 1, 2017.

[27] L. Liu, S. X. Zhang, W. Liao et al., "Mechanoresponsive stem cells to target cancer metastases through biophysical cues," *Science Translational Medicine*, vol. 9, no. 400, article eaan2966, 2017.

[28] A. J. Engler, S. Sen, H. L. Sweeney, and D. E. Discher, "Matrix elasticity directs stem cell lineage specification," *Cell*, vol. 126, no. 4, pp. 677–689, 2006.

[29] P. A. Zuk, M. Zhu, P. Ashjian et al., "Human adipose tissue is a source of multipotent stem cells," *Molecular Biology of the Cell*, vol. 13, no. 12, pp. 4279–4295, 2002.

[30] F. X. Yu and K. L. Guan, "The hippo pathway: regulators and regulations," *Genes & Development*, vol. 27, no. 4, pp. 355–371, 2013.

[31] M. R. Reagan and D. L. Kaplan, "Concise review: mesenchymal stem cell tumor-homing: detection methods in disease model systems," *Stem Cells*, vol. 29, no. 6, pp. 920–927, 2011.

[32] Y. Zhao, S. Tang, J. Guo et al., "Targeted delivery of doxorubicin by nano-loaded mesenchymal stem cells for lung melanoma metastases therapy," *Scientific Reports*, vol. 7, no. 1, 2017.

[33] U. Altanerova, M. Babincova, P. Babinec et al., "Human mesenchymal stem cell-derived iron oxide exosomes allow targeted ablation of tumor cells via magnetic hyperthermia," *International Journal of Nanomedicine*, vol. 12, pp. 7923–7936, 2017.

[34] W. du, I. Seah, O. Bougazzoul et al., "Stem cell-released oncolytic herpes simplex virus has therapeutic efficacy in brain metastatic melanomas," *Proceedings of the National Academy of Sciences of the United States of America*, vol. 114, no. 30, pp. E6157–E6165, 2017.

[35] M. Duebgen, J. Martinez-Quintanilla, K. Tamura et al., "Stem cells loaded with multimechanistic oncolytic herpes simplex virus variants for brain tumor therapy," *JNCI: Journal of the National Cancer Institute*, vol. 106, no. 6, article dju090, 2014.

[36] P. F. Robbins, R. A. Morgan, S. A. Feldman et al., "Tumor regression in patients with metastatic synovial cell sarcoma and melanoma using genetically engineered lymphocytes reactive with NY-ESO-1," *Journal of Clinical Oncology*, vol. 29, no. 7, pp. 917–924, 2011.

[37] S. S. Neelapu, S. Tummala, P. Kebriaei et al., "Chimeric antigen receptor T-cell therapy - assessment and management of toxicities," *Nature Reviews. Clinical Oncology*, vol. 15, no. 1, pp. 47–62, 2018.

[38] M. Themeli, C. C. Kloss, G. Ciriello et al., "Generation of tumor-targeted human T lymphocytes from induced pluripotent stem cells for cancer therapy," *Nature Biotechnology*, vol. 31, no. 10, pp. 928–933, 2013.

[39] H. Kawamoto, K. Masuda, S. Nagano, and T. Maeda, "Cloning and expansion of antigen-specific T cells using iPS cell technology: development of "off-the-shelf" T cells for the use in allogeneic transfusion settings," *International Journal of Hematology*, vol. 107, no. 3, pp. 271–277, 2018.

[40] F. Rami, H. Mollainezhad, and M. Salehi, "Induced pluripotent stem cell as a new source for cancer immunotherapy," *Genetics Research International*, vol. 2016, Article ID 3451807, 9 pages, 2016.

[41] R. J. Ihry, K. A. Worringer, M. R. Salick et al., "p53 inhibits CRISPR-Cas9 engineering in human pluripotent stem cells," *Nature Medicine*, vol. 24, no. 7, pp. 939–946, 2018.

[42] E. Haapaniemi, S. Botla, J. Persson, B. Schmierer, and J. Taipale, "CRISPR-Cas9 genome editing induces a p53-mediated DNA damage response," *Nature Medicine*, vol. 24, no. 7, pp. 927–930, 2018.

[43] P. Wang and A. Moore, "Molecular imaging of stem cell transplantation for neurodegenerative diseases," *Current Pharmaceutical Design*, vol. 18, no. 28, pp. 4426–4440, 2012.

[44] P. Wang, F. Petrella, L. Nicosia, M. Bellomi, and S. Rizzo, "Molecular imaging of stem cell transplantation for liver diseases: monitoring, clinical translation, and theranostics," *Stem Cells International*, vol. 2016, Article ID 4058656, 8 pages, 2016.

[45] M. Mangoni, L. Livi, G. Biti et al., "Stem cell tracking: toward clinical application in oncology?," *Tumori*, vol. 98, no. 5, pp. 535–542, 2012.

[46] C. Wu, G. Ma, J. Li et al., "In vivo cell tracking via ^{18}F-fluorodeoxyglucose labeling: a review of the preclinical and clinical applications in cell-based diagnosis and therapy," *Clinical Imaging*, vol. 37, no. 1, pp. 28–36, 2013.

[47] P. Wang, Z. Medarova, and A. Moore, "Molecular imaging: a promising tool to monitor islet transplantation," *Journal of Transplantation*, vol. 2011, Article ID 202915, 14 pages, 2011.

[48] N. Panagiotopoulos, R. L. Duschka, M. Ahlborg et al., "Magnetic particle imaging: current developments and future directions," *International Journal of Nanomedicine*, vol. 10, pp. 3097–3114, 2015.

[49] P. Wang, P. W. Goodwill, P. Pandit et al., "Magnetic particle imaging of islet transplantation in the liver and under the kidney capsule in mouse models," *Quantitative Imaging in Medicine and Surgery*, vol. 8, no. 2, pp. 114–122, 2018.

[50] B. Zheng, T. Vazin, P. W. Goodwill et al., "Magnetic particle imaging tracks the long-term fate of *in vivo* neural cell implants with high image contrast," *Scientific Reports*, vol. 5, article 14055, 2015.

[51] B. Zheng, M. P. von See, E. Yu et al., "Quantitative magnetic particle imaging monitors the transplantation, biodistribution, and clearance of stem cells *in vivo*," *Theranostics*, vol. 6, no. 3, pp. 291–301, 2016.

[52] Y. X. J. Wáng and J.-M. Idée, "A comprehensive literatures update of clinical researches of superparamagnetic resonance iron oxide nanoparticles for magnetic resonance imaging," *Quantitative Imaging in Medicine and Surgery*, vol. 7, no. 1, pp. 88–122, 2017.

[53] A. Allegra, G. Penna, A. Alonci, V. Rizzo, S. Russo, and C. Musolino, "Nanoparticles in oncology: the new theragnostic molecules," *Anti-Cancer Agents in Medicinal Chemistry*, vol. 11, no. 7, pp. 669–686, 2011.

[54] Z. Fan, P. P. Fu, H. Yu, and P. C. Ray, "Theranostic nanomedicine for cancer detection and treatment," *Journal of Food and Drug Analysis*, vol. 22, no. 1, pp. 3–17, 2014.

[55] E. P. Papapetrou, "Patient-derived induced pluripotent stem cells in cancer research and precision oncology," *Nature Medicine*, vol. 22, no. 12, pp. 1392–1401, 2016.

[56] D. Zhu, C. S. L. Kong, J. A. Gingold, R. Zhao, and D. F. Lee, "Induced pluripotent stem cells and induced pluripotent cancer cells in cancer disease modeling," in *Advances in Experimental Medicine and Biology*, Springer, New York, NY, 2018.

[57] C. Reinshagen, D. Bhere, S. H. Choi et al., "CRISPR-enhanced engineering of therapy-sensitive cancer cells for self-targeting of primary and metastatic tumors," *Science Translational Medicine*, vol. 10, no. 449, article eaao3240, 2018.